

การสังเคราะห์และศึกษาสมบัติการจับของอนุพันธ์คาลิกซ์[4]เอรีนที่มีหมู่ไทโอยูเรีย



นางสาว กมลวรรณ ธรรมเจริญ

สถาบันวิทยบริการ

จุฬาลงกรณ์มหาวิทยาลัย

วิทยานิพนธ์นี้เป็นส่วนหนึ่งของการศึกษาตามหลักสูตรปริญญาวิทยาศาสตรดุษฎีบัณฑิต

สาขาวิชาเคมี ภาควิชาเคมี


คณะวิทยาศาสตร์ จุฬาลงกรณ์มหาวิทยาลัย

ปีการศึกษา 2546

ISBN 974-17-4615-6

ลิขสิทธิ์ของจุฬาลงกรณ์มหาวิทยาลัย

SYNTHESIS AND BINDING STUDY OF THIOUREA CALIX[4]ARENE DERIVATIVES



Miss Gamolwan Tumchareern

สถาบันวิทยบริการ  
จุฬาลงกรณ์มหาวิทยาลัย

A Dissertation Submitted in Partial Fulfillment of the Requirements  
for the Degree of Doctor of Philosophy in Chemistry

Department of Chemistry

Faculty of Science

Chulalongkorn University

Academic Year 2003

ISBN 974-17-4615-6

Thesis Title            Synthesis and Binding Study of Thiourea Calix[4]arene Derivatives  
By                         Miss Gamolwan Tumcharern  
Field of Study          Chemistry  
Thesis Advisor        Assistant Professor Thawatchai Tuntulani, Ph.D.

---

Accepted by the Faculty of Science, Chulalongkorn University in Partial  
Fulfillment of the Requirements for the Doctor's Degree

..... Dean of Faculty of Science  
(Professor Piamsak Menasveta, Ph.D)

THESIS COMMITTEE

.....Chairman  
(Professor Sophon Roengsumran, Ph.D.)

.....Thesis Advisor  
(Assistant Professor Thawatchai Tuntulani, Ph.D.)

.....Member  
(Professor Apichart Suksamran, Ph.D.)

.....Member  
(Assistant Professor Mongkol Sukwattanasinitt, Ph.D.)

.....Member  
(Assistant Professor Orawon Chailapakul, Ph.D.)

.....Member  
(Soamwadee Chaianansutcharit, Ph.D.)



# # 4172338223: MAJOR CHEMISTRY.

KEY WORDS: BIS-THIOUREA/ HETERODITOPIC RECEPTOR/ CATION/ ANION/ AMINO ACID/ ION-PAIR/ COOPERATIVE BINDING/ ALLOSTERISM/ <sup>1</sup>H-NMR TITRATION

GAMOLWAN TUMCHARERN: SYNTHESIS AND BINDING STUDY OF THIOUREA CALIX[4]ARENE DERIVATIVES. THESIS ADVISOR: ASSISTANT PROF. THAWATCHAI TUNTULANI, Ph.D. 276 pp. ISBN 974-17-4615-6

Two novel macrocyclic heteroditopic receptors **14** and **15** which were comprised of calixarene scaffolds and bis-thiourea binding sites bearing two amide or ester moieties at the lower rim were synthesized. The proper synthetic pathway for the preparation of calix[4]arene amide **14** (3.7%) and ester **15** (15%) were different. Both macromolecule **14** and its analogous **15** existed in cone conformation in either chloroform or acetonitrile solution. The x-ray structure of **14** indicated the closed flattened cone conformation. The cations, anions (both basic anions and amino acid anions) as well as cooperative binding properties of both receptors were investigated. <sup>1</sup>H-NMR titration was employed to measure the stoichiometry of the complexes, binding constants and Gibbs free energy in acetonitrile-*d*<sub>3</sub>.

Both receptors recognized alkali cations with highest selectivity towards sodium. Compared to **14**, compound **15** was found to be a more efficiency and specific host for sodium. Despite their similar structures, macromolecule **14** can selectively bind Y-shaped carboxylate anions while analogous molecule **15** displayed a good selectivity with tetrahedral phosphate type anions.

Moreover, the binding affinity of both receptors towards TBA salt of amino acids was affected by changing the amino acid side chain. Bis-thiourea **14** and **15** did not show a significant difference in binding affinity among various amino acids. However, receptor **14** showed a moderate selectivity for TBA salt of leucine whereas ester macromolecule **15** formed a remarkably strong complex with carboxylate salts of phenylalanine and asparagine. Both bis-thiourea derivatives were more selective for TBA salts of shorter amino acids (aspartic acid and asparagine) than those of longer amino acids (glutamic acid and glutamine). Additionally, ligand **14** preferentially recognized dicarboxylate amino anions (aspartic acid and glutamic acid) over monocarboxylate amino anions (asparagine and glutamine) while the inverse trend was observed for ligand **15**.

The binding efficiency of sodium bound **14** towards common carboxylate or phosphate anion could be evaluated only with diphenylphosphate as a negative allosterism. Unlike bound **14**, the sequestering by ion-pairing effect in the case of bound **15** was not predominantly observed. Both free and sodium bound **15** preferentially recognized phosphate type anions, in which the latter system was controlled by synergistic effects. The strongest binding efficiency was found in the case of dihydrogen phosphate whereas the highest cooperativity factor was discovered in the case of acetate. On the other hand, the presence of sodium cation in the amide cavity of **14** displayed the positive allosterism in the case of dicarboxylate salt of aspartic acid and negative allosterism in the case of dicarboxylate anion of glutamic acid. On the contrary, the binding affinity of the sodium bound **15** towards bis-TBA salts of aspartic acid and glutamic acid were decreased.

Department.....	Chemistry.....	Student's signature.....
Field of study .....	Chemistry.....	Advisor's signature.....
Academic year.....	2003.....	Co-advisor's signature .....

## ACKNOWLEDGEMENTS

I wish to express deepest appreciation to my thesis advisor and co-advisor, Assist. Prof. Thawatchai Tuntulani and Prof. Jeremy D. Kilburn, for their regularly close supervision, invaluable guidance, willing assistance, generous encouragement, sincere forgiveness and personal friendship throughout my postgraduate career. In addition, I would like to thank and pay my respect to Prof. Sophon Roengsumran, Prof. Apichart Suksamrarn, Assist. Prof. Mongkol Sukwattanasinitt, Assist. Prof. Orawon Chailapakul and Dr. Soamwadee Chaianansutcharit for their valuable suggestions and comments as committee members and thesis examiners. Furthermore, I would like to thank and express my gratitude to all staffs in Supramolecular Chemistry Research Unit especially Assoc. Prof. Vithaya Ruangpornvisuti, Assoc. Prof. Nuanphun Chantarasiri, Assist. Prof. Buncha Pulpoka and Dr. Boosayarat Tomapatanaget for their generous helps and useful suggestions.

Definitely, this thesis cannot be completed without kindness and helpful of many people. Firstly, I would like to thank the Scientific and Technological Research Equipment Center of Chulalongkorn University, particularly, Miss Amporn Aengpakornkaew for elemental analysis results. Absolutely, I am grateful to the University of Southampton to furnish many facilities for my research; and all staffs in the Department of Chemistry for their generous helps. I would like to thank Mrs. Joan Street and Mr. Neil Well for NMR spectra, Dr. John Langley and Ms Julie Herniman for Electrospray Ionization Mass Spectra as well as Dr. Simon Coles and Prof. Michael B. Hursthouse for an X-ray crystal structure. Finally, the Thailand Research Fund is gratefully acknowledged for the Royal Golden Jubilee grant during my Ph.D. degree.

I would like to express my highest gratitude to my family for their love, kindness, encouragement, and financial support throughout my life. Additionally, I would like to thank Mr. Thanawit Pothsree for his helps in NMR titration experiments and also his care and understanding. Finally, my appreciation would be expressed to all members in Tuntulani's and Kilburn's group as well as all my friends in Southampton in the past and present for their very nice friendship, sincere helps and encouragement throughout my doctoral course, especially when I was away from home.

## CONTENTS

	<b>Page</b>
<b>ABSTRACT IN THAI.....</b>	iv
<b>ABSTRACT IN ENGLISH.....</b>	v
<b>ACKNOWLEDGEMENTS.....</b>	vi
<b>CONTENTS.....</b>	vii
<b>LIST OF TABLES.....</b>	x
<b>LIST OF FIGURES.....</b>	xii
<b>LIST OF SCHEMES.....</b>	xvii
<b>LIST OF ABBREVIATIONS AND SIGNS.....</b>	xviii
<b>CHAPTER I INTRODUCTION.....</b>	1
1.1 Supramolecular Chemistry.....	1
1.2 Molecular Recognition .....	1
1.3 Cation Recognition .....	3
1.4 Anion Recognition.....	3
1.5 Neutral Hydrogen Bonding Receptors for Anions .....	5
1.6 Receptor for Amino Acids.....	6
1.7 Ditung Receptors .....	8
1.8 Calixarene Building Block.....	9
1.9 Thiourea-Based Receptor .....	10
1.10 Determination of Binding Constant.....	10
1.11 Literature Review.....	12
1.12 Scope of This Thesis .....	17
<b>CHAPTER II EXPERIMENTAL SECTION.....</b>	20
2.1 Synthesis of Heteroditopic Receptors.....	20
2.1.1 General Procedure.....	20
2.1.1.1 Materials.....	20
2.1.1.2 Instrumentation.....	20

**CONTENTS** (*Continued*)

	<b>Page</b>
2.1.2.1 Synthesis of 5,11,17,23-Tetra- <i>tert</i> -butyl-25,27- <i>N,N'</i> -1,3-bis(methoxyl-carbamoylpropylthioureidomethyl)benzene-26,28-bis(3-oxabutyloxy)calix[4] arene, <b>14</b> .....	21
2.1.2.2 Synthesis of 5,11,17,23-Tetra- <i>tert</i> -butyl-25,27- <i>N,N'</i> -1,3-bis(methoxyl-carbonylpropylthioureidomethyl)benzene-26,28-bis(3-oxabutyloxy)calix[4]arene, <b>15</b> .....	31
2.2 Binding Studies.....	44
2.2.1 General Procedure.....	44
2.2.1.1 Materials.....	44
2.2.1.2 Instrumentation.....	45
2.2.2 Experimental Procedure.....	45
2.2.2.1 General Procedure for Determination of Binding Constants: <sup>1</sup> H-NMR Titration .....	45
2.2.2.1.1 Cation Complexation.....	45
2.2.2.1.2 Anion Complexation.....	47
2.2.2.1.3 Binding Enhancement of Anions in the Presence of Cations	48
2.2.2.2 General Procedure for Determination of Binding Stoichiometry: Conventional Job's Plots.....	50
<b>CHAPTER III RESULTS AND DISCUSSION.....</b>	<b>52</b>
3.1 Synthesis of Heteroditopic Receptors.....	52
3.1.1 Synthesis and Characterization of Receptor <b>14</b> .....	52
3.1.2 Synthesis and Characterization of Receptor <b>15</b> .....	60
3.2 Investigation of Binding Ability.....	66
3.2.1 Binding Ability of Receptors <b>14</b> and <b>15</b> towards Cations.....	68
3.2.2 Binding Ability of Receptors <b>14</b> and <b>15</b> towards Anions.....	78
3.2.3 Binding Abilities of Receptors <b>14</b> and <b>15</b> towards Amino Acids in Anionic Forms.....	101
3.2.4 Binding Enhancement of Receptors <b>14</b> and <b>15</b> towards Anions Using Sodium Cation.....	117



**CONTENTS** (*Continued*)

	<b>Page</b>
3.2.5 Binding Ability of Chiral <b>26</b> .....	140
<b>CHAPTER IV CONCLUSION</b> .....	141
4.1 Conclusion.....	141
4.2 Suggestions for Future Work .....	143
<b>REFERENCES</b> .....	145
<b>APPENDICES</b> .....	158
<b>APPENDIX A</b> .....	159
<b>APPENDIX B</b> .....	178
<b>VITA</b> .....	276



สถาบันวิทยบริการ  
จุฬาลงกรณ์มหาวิทยาลัย

## LIST OF TABLES

<b>Table</b>	<b>Page</b>
<b>2.1</b> Amounts of alkali cations that used in cation complexation study with compounds <b>14</b> and <b>15</b> .....	45
<b>2.2</b> Volume of the guest stock solution that added in each portion.....	46
<b>2.3</b> Amounts of tetrabutylammonium salts that used in anion complexation study with compound <b>14</b> . ....	47
<b>2.4</b> Amounts of tetrabutylammonium salts that used in anion complexation study with compound <b>15</b> . ....	48
<b>2.5</b> Amounts of NaClO <sub>4</sub> and tetrabutylammonium salts that were used in case of titration with compound <b>14</b> . ....	49
<b>2.6</b> Amounts of NaClO <sub>4</sub> and tetrabutylammonium salts that were used in case of titration with compound <b>15</b> . ....	49
<b>2.7</b> Amounts of NaClO <sub>4</sub> and tetrabutylammonium salts that were used in Job's plots experiment. ....	50
<b>2.8</b> Volume of solution of hosts and anions in each NMR tube.....	51
<b>3.1</b> Product yields of the conversion of the acid <b>19</b> to the acid chloride under various conditions.....	56
<b>3.2</b> Product yields of the conversion of the amine to the thiocyanate <b>21</b> under various conditions.....	56
<b>3.3</b> Product yields of the conversion of the amine to the thiocyanate <b>25</b> under various conditions.....	63
<b>3.4</b> Product yields of the conversion of the acid chloride to bis-thiourea calix[4]arene ester <b>25</b> under various conditions.....	66
<b>3.5</b> Donor numbers and acceptor numbers of organic solvents.....	67
<b>3.6</b> The average association constants and Gibbs free energy upon the formation of <b>14</b> ·cation and <b>15</b> ·cation complexes in acetonitrile- <i>d</i> <sub>3</sub> .....	73
<b>3.7</b> A comparison of the ionic radius (Å) of isoelectronic alkali cations.....	75
<b>3.8</b> Geometry and basicity of a variation of anions.....	80
<b>3.9</b> The average association constants and Gibbs free energy upon the formation of <b>14</b> ·anion and <b>15</b> ·anion complexes.....	89
<b>3.10</b> The average association constants and Gibbs free energy upon the formation of <b>14</b> ·dicarboxylate <sup>2-</sup> and <b>15</b> ·dicarboxylate <sup>2-</sup> .....	98

**LIST OF TABLES** (*Continued*)

<b>Table</b>	<b>Page</b>
<b>3.11</b> Geometry and basicity of carboxylate anions.....	99
<b>3.12</b> The average association constants and Gibbs free energy upon the formation of <b>14</b> ·amino carboxylate and <b>15</b> ·amino carboxylate complexes.....	112
<b>3.13</b> Basicity of some amino acids in water at 25 °C.....	114
<b>3.14</b> The average association constants and Gibbs free energy upon the formation of <b>14</b> ·Na <sup>+</sup> ·anion and <b>15</b> ·Na <sup>+</sup> ·anion complexes.....	128
<b>3.15</b> The average association constants and Gibbs free energy upon the formation of <b>14</b> ·Na <sup>+</sup> ·dicarboxylate <sup>2-</sup> and <b>15</b> ·Na <sup>+</sup> ·dicarboxylate <sup>2-</sup> complexes.....	137

สถาบันวิทยบริการ  
จุฬาลงกรณ์มหาวิทยาลัย

## LIST OF FIGURES

Figure	Page
1.1 Supramolecular chemistry and molecular recognition represented by “ <i>Lock and Key</i> ” principle.....	2
1.2 Formation of hydrogen bonding in carboxylate bound urea or thiourea..	6
1.3 Twenty primary amino acids. ....	7
1.4 Two or four (thio)urea groups functionalized on <i>p-tert</i> -butylcalix[4]arene.....	13
1.5 Calix[4]arene mono(thio)urea derivatives.....	14
1.6 Effect of the chain length towards the formation of solvent separate or contact ion-pairing.....	15
1.7 Other contacted ion-pair recognitions by which the number of hydrogen bond donor controlled the stability of complex .....	15
1.8 Ion-pair recognition of tetramethylammonium sulfonate in a calixarene derivative.....	16
1.9 Chiral macrobicyclic anion receptors containing two L-alanine units as chiral center .....	17
1.10 The novel <i>p-tert</i> -butylcalix[4]arene derivatives containing <i>bis</i> -thiourea moieties <b>14</b> and <b>15</b> that were designed and synthesized in this thesis.....	19
3.1 Crystal structure of <b>14</b> with the common numbering scheme.....	59
3.2 Examples of an open (a) and a closed (b) flattened cone conformation of calix[4]arene derivatives.....	60
3.3 The complexation induced shifts of some proton signals on <sup>1</sup> H-NMR spectrum (a) <b>15</b> ·Li <sup>+</sup> (b) <b>15</b> ·Na <sup>+</sup> and (c) <b>15</b> ·K <sup>+</sup> .....	71
3.4 Job’s plots of –OCH <sub>2</sub> COO– in <b>15</b> ·Li <sup>+</sup> , <b>15</b> ·Na <sup>+</sup> and <b>15</b> ·K <sup>+</sup> complexes.....	72
3.5 Titration curves of –OCH <sub>2</sub> COO– in <b>15</b> ·Li <sup>+</sup> , <b>15</b> ·Na <sup>+</sup> and <b>15</b> ·K <sup>+</sup> complexes.....	73
3.6 The selectivity of receptors <b>14</b> and <b>15</b> towards sodium over potassium and lithium cation.....	74
3.7 From the intramolecular hydrogen bonding in amide <b>14</b> (a) or the exo-annulus carbonyl (b) in ester <b>15</b> to the proposed structure of <b>14</b> ·cation and <b>15</b> ·cation complexes (c).....	77

## LIST OF FIGURES (Continued)

Figures	Page
<b>3.8</b> The structures of anions that used in this experiment.....	81
<b>3.9</b> The complexation induced shifts of some proton signals on <sup>1</sup> H-NMR spectrum (a) <b>14</b> ·CH <sub>3</sub> COO <sup>-</sup> (b) <b>14</b> ·C <sub>6</sub> H <sub>5</sub> COO <sup>-</sup> (c) <b>14</b> ·H <sub>2</sub> PO <sub>4</sub> <sup>-</sup> , (d) <b>14</b> ·Ph(H)POO <sup>-</sup> (e) <b>14</b> ·(PhO) <sub>2</sub> PO <sub>2</sub> <sup>-</sup> .....	83
<b>3.10</b> The complexation induced shifts of some proton signals on <sup>1</sup> H-NMR spectrum (a) <b>15</b> ·CH <sub>3</sub> COO <sup>-</sup> (b) <b>15</b> ·C <sub>6</sub> H <sub>5</sub> COO <sup>-</sup> (c) <b>15</b> ·H <sub>2</sub> PO <sub>4</sub> <sup>-</sup> , (d) <b>15</b> ·Ph(H)POO <sup>-</sup> (e) <b>15</b> ·(PhO) <sub>2</sub> PO <sub>2</sub> <sup>-</sup> .....	84
<b>3.11</b> Job's plots of -CH <sub>2</sub> CH <sub>2</sub> NHCSNH- in <b>14</b> ·CH <sub>3</sub> COO <sup>-</sup> , <b>14</b> ·C <sub>6</sub> H <sub>5</sub> COO <sup>-</sup> , <b>14</b> ·H <sub>2</sub> PO <sub>4</sub> <sup>-</sup> , <b>14</b> ·Ph(H)POO <sup>-</sup> and <b>14</b> ·(PhO) <sub>2</sub> PO <sub>2</sub> <sup>-</sup> complexes.....	86
<b>3.12</b> Job's plots of -NHCSNHCH <sub>2</sub> Ar- in <b>15</b> ·CH <sub>3</sub> COO <sup>-</sup> , <b>15</b> ·C <sub>6</sub> H <sub>5</sub> COO <sup>-</sup> , as well as <b>15</b> ·H <sub>2</sub> PO <sub>4</sub> <sup>-</sup> and -CH <sub>2</sub> CH <sub>2</sub> NHCSNH- in <b>15</b> ·Ph(H)POO <sup>-</sup> as well as <b>15</b> ·(PhO) <sub>2</sub> PO <sub>2</sub> <sup>-</sup> complexes.....	86
<b>3.13</b> Titration curves of -CH <sub>2</sub> CH <sub>2</sub> NHCSNH- in <b>14</b> ·CH <sub>3</sub> COO <sup>-</sup> , <b>14</b> ·C <sub>6</sub> H <sub>5</sub> COO <sup>-</sup> , <b>14</b> ·H <sub>2</sub> PO <sub>4</sub> <sup>-</sup> , <b>14</b> ·Ph(H)POO <sup>-</sup> and <b>14</b> ·(PhO) <sub>2</sub> PO <sub>2</sub> <sup>-</sup> complexes.....	87
<b>3.14</b> Titration curves of -NHCSNHCH <sub>2</sub> Ar- in <b>15</b> ·CH <sub>3</sub> COO <sup>-</sup> , <b>15</b> ·C <sub>6</sub> H <sub>5</sub> COO <sup>-</sup> , <b>15</b> ·H <sub>2</sub> PO <sub>4</sub> <sup>-</sup> , <b>15</b> ·Ph(H)POO <sup>-</sup> and <b>15</b> ·(PhO) <sub>2</sub> PO <sub>2</sub> <sup>-</sup> complexes.....	87
<b>3.15</b> The selectivity of receptors <b>14</b> and <b>15</b> towards various anions.....	90
<b>3.16</b> Simple acyclic thiourea and cyclophane cyclic thiourea receptors.....	91
<b>3.17</b> Macrocyclic bis-urea calix[4]quinone.....	92
<b>3.18</b> X-ray structure of <b>13b</b> ·CH <sub>3</sub> COO <sup>-</sup> complex.....	93
<b>3.19</b> X-ray structure of cyclic(thiourea)·H <sub>2</sub> PO <sub>4</sub> <sup>-</sup> .....	93
<b>3.20</b> The proposed structures of 1:1 anion complexes ( <b>46-47</b> ).....	93
<b>3.21</b> The complexation induced shifts of some proton signals on <sup>1</sup> H-NMR spectrum (a) <b>14</b> ·succinate <sup>2-</sup> (b) <b>14</b> ·glutarate <sup>2-</sup> .....	95
<b>3.22</b> The complexation induced shifts of some proton signals on <sup>1</sup> H-NMR spectrum (a) <b>15</b> ·succinate <sup>2-</sup> (b) <b>15</b> ·glutarate <sup>2-</sup> .....	95
<b>3.23</b> Job's plots of -OCH <sub>2</sub> CONH- in <b>14</b> ·succinate <sup>2-</sup> and <b>14</b> ·glutarate <sup>2-</sup> complexes.....	96

## LIST OF FIGURES (Continued)

Figures	Page
<b>3.24</b> Job's plots of $-\text{NHCSNHCH}_2\text{Ar}-$ in <b>15</b> ·succinate <sup>2-</sup> and <b>15</b> ·glutarate <sup>2-</sup> complexes.....	96
<b>3.25</b> Titration curves of $-\text{OCH}_2\text{CONH}-$ in <b>14</b> ·succinate <sup>2-</sup> and <b>14</b> ·glutarate <sup>2-</sup> complexes.....	97
<b>3.26</b> Titration curves of $-\text{NHCSNHCH}_2\text{Ar}-$ in <b>15</b> ·succinate <sup>2-</sup> and <b>15</b> ·glutarate <sup>2-</sup> complexes. ....	97
<b>3.27</b> The selectivity of receptors <b>14</b> and <b>15</b> towards dicarboxylate anions compared to the monocarboxylate complexes.....	99
<b>3.28</b> Tris-guanidinium-tricarballate complex.....	100
<b>3.29</b> The proposed structures of 1:1 dicarboxylate complexes ( <b>49</b> ).....	100
<b>3.30</b> The structures of all amino acid anions in this experiment.....	103
<b>3.31</b> The complexation induced shifts of some proton signals on <sup>1</sup> H-NMR spectrum (a) <b>14</b> ·Asp <sup>2-</sup> , (b) <b>14</b> ·Glu <sup>2-</sup> , (c) <b>14</b> ·Asn <sup>-</sup> , (d) <b>14</b> ·Gln <sup>-</sup> , (e) <b>14</b> ·Phe <sup>-</sup> , (f) <b>14</b> ·Leu <sup>-</sup> , (g) <b>14</b> ·Thr <sup>-</sup> and (h) <b>14</b> ·Ser <sup>-</sup> .....	105
<b>3.32</b> The complexation induced shifts of some proton signals on <sup>1</sup> H-NMR spectrum (a) <b>15</b> ·Asp <sup>2-</sup> , (b) <b>15</b> ·Glu <sup>2-</sup> , (c) <b>15</b> ·Asn <sup>-</sup> , (d) <b>15</b> ·Gln <sup>-</sup> (e) <b>15</b> ·Phe <sup>-</sup> , (f) <b>15</b> ·Leu <sup>-</sup> , (g) <b>15</b> ·Thr <sup>-</sup> and (h) <b>15</b> ·Ser <sup>-</sup> .....	107
<b>3.33</b> Job's plots of $-\text{CH}_2\text{CH}_2\text{NHCSNHCH}_2\text{Ar}-$ in <b>14</b> ·Asp <sup>2-</sup> , <b>14</b> ·Glu <sup>2-</sup> , <b>14</b> ·Asn <sup>-</sup> , <b>14</b> ·Gln <sup>-</sup> , <b>14</b> ·Phe <sup>-</sup> , <b>14</b> ·Leu <sup>-</sup> , <b>14</b> ·Thr <sup>-</sup> , and <b>14</b> ·Ser <sup>-</sup> complexes.....	109
<b>3.34</b> Job's plots of $-\text{CH}_2\text{CH}_2\text{NHCSNHCH}_2\text{Ar}-$ in <b>15</b> ·Asp <sup>2-</sup> , <b>15</b> ·Glu <sup>2-</sup> , <b>15</b> ·Asn <sup>-</sup> , <b>15</b> ·Gln <sup>-</sup> , <b>15</b> ·Phe <sup>-</sup> , <b>15</b> ·Leu <sup>-</sup> , <b>15</b> ·Thr <sup>-</sup> , and <b>15</b> ·Ser <sup>-</sup> complexes.....	110
<b>3.35</b> Titration curves of $-\text{CH}_2\text{CH}_2\text{NHCSNHCH}_2\text{Ar}-$ in <b>14</b> ·Asp <sup>2-</sup> , <b>14</b> ·Glu <sup>2-</sup> , <b>14</b> ·Asn <sup>-</sup> , <b>14</b> ·Gln <sup>-</sup> , <b>14</b> ·Phe <sup>-</sup> , <b>14</b> ·Leu <sup>-</sup> , <b>14</b> ·Thr <sup>-</sup> , and <b>14</b> ·Ser <sup>-</sup> complexes.....	111
<b>3.36</b> Titration curves of $-\text{CH}_2\text{CH}_2\text{NHCSNHCH}_2\text{Ar}-$ in <b>15</b> ·Asp <sup>2-</sup> , <b>15</b> ·Glu <sup>2-</sup> , <b>15</b> ·Asn <sup>-</sup> , <b>15</b> ·Gln <sup>-</sup> , <b>15</b> ·Phe <sup>-</sup> , <b>15</b> ·Leu <sup>-</sup> , <b>15</b> ·Thr <sup>-</sup> , and <b>15</b> ·Ser <sup>-</sup> complexes.....	111
<b>3.37</b> The selectivity of receptors <b>14</b> and <b>15</b> towards various amino mono- and dicarboxylate anions.....	113
<b>3.38</b> Intramolecular hydrogen bonding of carboxylate anion of serine.....	115
<b>3.39</b> The selectivity of receptors <b>14</b> and <b>15</b> towards monocarboxylate, unsubstituted dicarboxylate and substituted dicarboxylate anions.....	116

## LIST OF FIGURES (Continued)

Figures	Page
<b>3.40</b> The proposed structures of 1:1 amino acid anion complexes ( <b>58</b> ).....	117
<b>3.41</b> The complexation induced shifts of some proton signals on <sup>1</sup> H-NMR spectrum (a) <b>14</b> ·Na <sup>+</sup> ·CH <sub>3</sub> COO <sup>-</sup> (b) <b>14</b> ·Na <sup>+</sup> ·C <sub>6</sub> H <sub>5</sub> COO <sup>-</sup> (c) <b>14</b> ·Na <sup>+</sup> ·H <sub>2</sub> PO <sub>4</sub> <sup>-</sup> , (d) <b>14</b> ·Na <sup>+</sup> ·Ph(H)POO <sup>-</sup> and (e) <b>14</b> ·Na <sup>+</sup> ·(PhO) <sub>2</sub> PO <sub>2</sub> <sup>-</sup> .....	120
<b>3.42</b> The complexation induced shifts of some proton signals on <sup>1</sup> H-NMR spectra (a) <b>15</b> ·Na <sup>+</sup> ·CH <sub>3</sub> COO <sup>-</sup> (b) <b>15</b> ·Na <sup>+</sup> ·C <sub>6</sub> H <sub>5</sub> COO <sup>-</sup> (c) <b>15</b> ·Na <sup>+</sup> ·H <sub>2</sub> PO <sub>4</sub> <sup>-</sup> , (d) <b>15</b> ·Na <sup>+</sup> ·Ph(H)POO <sup>-</sup> and (e) <b>15</b> ·Na <sup>+</sup> ·(PhO) <sub>2</sub> PO <sub>2</sub> <sup>-</sup> .....	121
<b>3.43</b> Job's plots of -NHCSNHCH <sub>2</sub> Ar- in <b>14</b> ·Na <sup>+</sup> ·CH <sub>3</sub> COO <sup>-</sup> , <b>14</b> ·Na <sup>+</sup> ·C <sub>6</sub> H <sub>5</sub> COO <sup>-</sup> , <b>14</b> ·Na <sup>+</sup> ·Ph(H)POO <sup>-</sup> and <b>14</b> ·Na <sup>+</sup> ·(PhO) <sub>2</sub> PO <sub>2</sub> <sup>-</sup> complexes.....	122
<b>3.44</b> Job's plots of <b>15</b> ·Na <sup>+</sup> ·CH <sub>3</sub> COO <sup>-</sup> , <b>15</b> ·Na <sup>+</sup> ·C <sub>6</sub> H <sub>5</sub> COO <sup>-</sup> , <b>15</b> ·Na <sup>+</sup> ·H <sub>2</sub> PO <sub>4</sub> <sup>-</sup> , <b>15</b> ·Na <sup>+</sup> ·Ph(H)POO <sup>-</sup> and <b>15</b> ·Na <sup>+</sup> ·(PhO) <sub>2</sub> PO <sub>2</sub> <sup>-</sup> complexes.....	123
<b>3.45</b> Titration curves of -CH <sub>2</sub> CH <sub>2</sub> NHCSNH- signals in <b>14</b> ·Na <sup>+</sup> ·CH <sub>3</sub> COO <sup>-</sup> , <b>14</b> ·Na <sup>+</sup> ·C <sub>6</sub> H <sub>5</sub> COO <sup>-</sup> , <b>14</b> ·Na <sup>+</sup> ·Ph(H)POO <sup>-</sup> and <b>14</b> ·Na <sup>+</sup> ·(PhO) <sub>2</sub> PO <sub>2</sub> <sup>-</sup> complexes.....	123
<b>3.46</b> Titration curves of -NHCSNHCH <sub>2</sub> Ar- signals in <b>15</b> ·Na <sup>+</sup> ·CH <sub>3</sub> COO <sup>-</sup> , <b>15</b> ·Na <sup>+</sup> ·C <sub>6</sub> H <sub>5</sub> COO <sup>-</sup> , <b>15</b> ·Na <sup>+</sup> ·H <sub>2</sub> PO <sub>4</sub> <sup>-</sup> , <b>15</b> ·Na <sup>+</sup> ·Ph(H)POO <sup>-</sup> and <b>15</b> ·Na <sup>+</sup> ·(PhO) <sub>2</sub> PO <sub>2</sub> <sup>-</sup> complexes.....	124
<b>3.47</b> Titration curves of -CH <sub>2</sub> CH <sub>2</sub> NHCSNHCH <sub>2</sub> Ar- in the absence and in the presence of sodium cation of (a) <b>14</b> ·CH <sub>3</sub> COO <sup>-</sup> and (b) <b>14</b> ·C <sub>6</sub> H <sub>5</sub> COO <sup>-</sup> complexes.....	125
<b>3.48</b> The selectivity of sodium bound <b>14</b> and <b>15</b> towards various anions.....	129
<b>3.49</b> The cooperativity factors of sodium bound to receptor <b>14</b> or <b>15</b> in the presence of various anions.....	130
<b>3.50</b> The proposed structures of cation enhancement anion complexes ( <b>64-65</b> ).....	132
<b>3.51</b> The complexation induced shifts of some proton signals on <sup>1</sup> H-NMR spectrum (a) <b>14</b> ·Na <sup>+</sup> ·Asp <sup>2-</sup> and (b) <b>14</b> ·Na <sup>+</sup> ·Glu <sup>2-</sup> .....	133
<b>3.52</b> The complexation induced shifts of some proton signals on <sup>1</sup> H-NMR spectrum (a) <b>15</b> ·Na <sup>+</sup> ·Asp <sup>2-</sup> and (b) <b>15</b> ·Na <sup>+</sup> ·Glu <sup>2-</sup> .....	134

**LIST OF FIGURES** (*Continued*)

<b>Figures</b>	<b>Page</b>
<b>3.53</b> Job's plots of $-\text{CH}_2\text{CH}_2\text{NHCSNHCH}_2\text{Ar}-$ in (a) <b>14</b> · $\text{Na}^+\cdot\text{Asp}^{2-}$ and (b) <b>14</b> · $\text{Na}^+\cdot\text{Glu}^{2-}$ complexes.....	135
<b>3.54</b> Job's plots of $-\text{CH}_2\text{CH}_2\text{NHCSNHCH}_2\text{Ar}-$ signal in (a) <b>15</b> · $\text{Na}^+\cdot\text{Asp}^{2-}$ and (b) <b>15</b> · $\text{Na}^+\cdot\text{Glu}^{2-}$ complexes.....	135
<b>3.55</b> Titration curves of $-\text{CH}_2\text{CH}_2\text{NHCSNHCH}_2\text{Ar}-$ in (a) <b>14</b> · $\text{Na}^+\cdot\text{Asp}^{2-}$ and (b) <b>14</b> · $\text{Na}^+\cdot\text{Glu}^{2-}$ complexes.....	136
<b>3.56</b> Titration curves of $-\text{CH}_2\text{CH}_2\text{NHCSNHCH}_2\text{Ar}-$ signal in (a) <b>15</b> · $\text{Na}^+\cdot\text{Asp}^{2-}$ and (b) <b>15</b> · $\text{Na}^+\cdot\text{Glu}^{2-}$ complexes.....	136
<b>3.57</b> The selectivity of receptors <b>14</b> and <b>15</b> towards various carboxylate anions.....	137
<b>3.58</b> The cooperativity factors of sodium bound to receptor <b>14</b> or <b>15</b> in the presence of carboxylate anions.....	138
<b>3.59</b> The proposed structures of 1:1 sodium amino acid anion complexes ( <b>66</b> ).....	139



## LIST OF SCHEMES

Scheme	Page
3.1 Synthetic scheme for calix[4]arene amide receptor <b>14</b> .....	53
3.2 Synthetic scheme of 5,11,17,23-tetra- <i>tert</i> -butyl-26,28-dihydroxy-25,27-bis(2-isothiocyanoethoxy)calix[4]arene from its amine analogue.	57
3.3 Proposed by-product during the preparation of the thiocyanate <b>21</b> .....	57
3.4 Synthetic scheme for calix[4]arene ester receptor <b>15</b> .....	61
3.5 The unexpected reaction during preparation of thiocyanate <b>25</b> .....	63
3.6 Another synthetic route to achieve ester derivative receptor <b>15</b> .....	65
3.7 Lewis theory of acids and bases.....	75
3.8 The interconversion between cone and pinched cone conformation of calix[4]arene.....	78
3.9 The effects of cation to the binding curves.....	126
3.10 Equilibrium involved in ion-pair binding.....	127

สถาบันวิทยบริการ  
จุฬาลงกรณ์มหาวิทยาลัย

## LIST OF ABBREVIATIONS AND SIGNS

AN	Acceptor Number (Acceptivity)
ACN	Acetonitrile
ADP	Adenosine Diphosphate
ATP	Adenosine Triphosphate
$\alpha$	Alpha
Å	Angstrom
Asn	Asparagine
Asp	Aspartic Acid
$^{13}\text{C-NMR}$	Carbon-13 Nuclear Magnetic Resonance
CPA	Carboxypeptidase A
$\delta$	Chemical Shift
CIS	Complexation Induced Shift
$J$	Coupling Constant
$^{\circ}\text{C}$	Degree Celcius
DNA	Deoxyribonucleic Acid
DCM	Dichloromethane
DMAP	4-(Dimethylamino)pyridine
DMF	Dimethylformamide
$\mu$	Dipole Moment
DEPT	Distortionless Enhancement of NMR Signals by Polarization Transfer
DN	Donor Number (Donicity)
d	Doublet
ddd	Doublet of Doublet of Doublet
dt	Doublet of Triplet
EPA	Electron Pair Acceptor
EPD	Electron Pair Donor
ESI-MS	Electrospray Ionization Mass Spectrometry
FT-IR	Fourier Transform Infrared Spectroscopy
$\Delta G$	Gibbs Free Energy
Glu	Glutamic Acid
Gln	Glutamine
g	Gram

**LIST OF ABBREVIATIONS AND SIGNS** (*Continued*)

HSAB	Hard-Soft Acid-Base
Hz	Hertz
HBD	Hydrogen Bond Donor
ITC	Isothermal Calorimetry
Leu	Leucine
LRMS	Low Resolution Mass Spectroscopy
m/z	Mass per Charge Ratio
MHz	Megahertz
$\mu\text{L}$	Microliter
mg	Milligram
mL	Milliliter
mmol	Millimol
X	Mole Fraction
m	Multiplet
NMR	Nuclear Magnetic Resonance
$\beta_i$	Overall Association Constant
ppm	Part per Million
$\text{M}^{-1}$	Per Molar
Phe	Phenylalanine
R	Gas Constant
$^1\text{H-NMR}$	Proton-1 Nuclear Magnetic Resonance
q	Quartet
quint	Quintet
RNA	Ribonucleic Acid
RT	Room Temperature
Ser	Serine
s-curve	Sigmoidal Curve
s	Singlet
$K_i$	Stepwise Association Constant
T	Temperature
TBA	Tetrabutylammonium
THF	Tetrahydrofuran

**LIST OF ABBREVIATIONS AND SIGNS** (*Continued*)

TLC	Thin Layer Chromatography
Thr	Threonine
TEA	Triethylamine
TFA	Trifluoroacetic Acid
t	Triplet
2D-NMR	Two-Dimensional Nuclear Magnetic Resonance
UV-VIS	Ultraviolet-Visible
VPO	Vapor Pressure Osmometry



สถาบันวิทยบริการ  
จุฬาลงกรณ์มหาวิทยาลัย

# CHAPTER I

## INTRODUCTION

### 1.1 Supramolecular Chemistry

Research in the area of supramolecular chemistry which may be defined as “*chemistry beyond the molecule*”<sup>[1]</sup> is now an interesting branch of chemistry. These molecular systems result from the association of two or more chemical species held together by intermolecular forces, not by covalent bonds. Supramolecular chemistry is thermodynamically less stable, kinetically more labile and dynamically more flexible than ordinary molecules.

Supramolecular chemistry may be divided into two broad categories, supermolecules and supramolecular assemblies. Supermolecules come from intermolecular association of a few components. Supramolecular assemblies are polymolecular entities that result from the spontaneous association of a large number of components into a specific phase having more or less well-defined microscopic organization and microscopic characteristic. The development of supramolecular chemistry has led to a growing interest in the design and synthesis of macrocyclic molecules incorporating intermolecular cavities.

### 1.2 Molecular Recognition

Molecular recognition is a critical component of intermolecular processes, including enzyme-substrate recognition, receptor-ligand binding, molecular self-assembly, and chemical sensing. The design of new hosts and/or guests is essential for providing insight into the factors governing molecular recognition and for preparing new materials with desirable properties.

Basically, molecular recognition is defined by energy and information involved in the binding and selection of substrate(s) by a given receptor molecule containing a specific function. Sometimes, this idea is described as “*Lock and Key*” principle (Figure 1.1).<sup>[2]</sup> The arrangement of binding sites in the host (lock) is complementary to the guest (key) both sterically (structurally) and electronically.

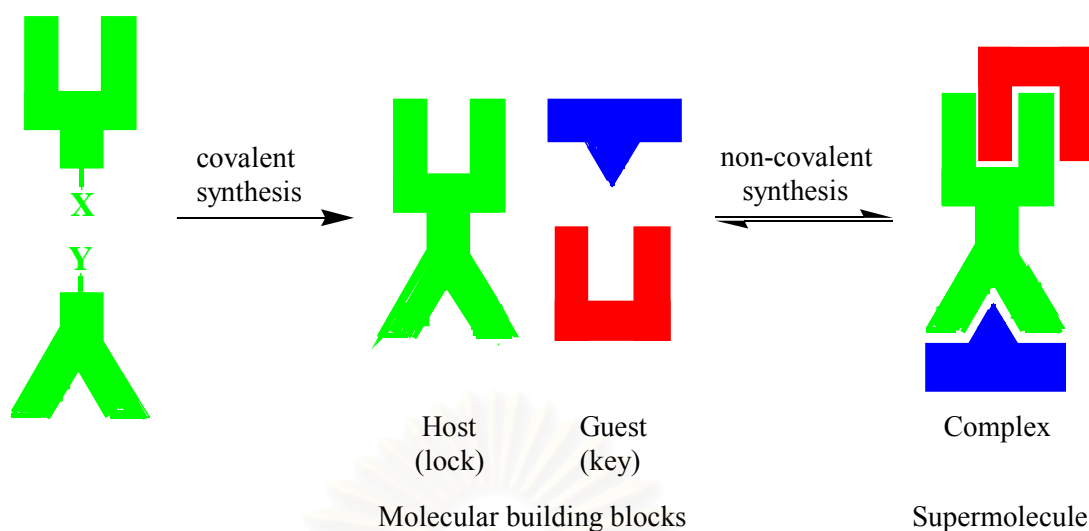


**Figure 1.1.** Supramolecular chemistry and molecular recognition represented by “Lock and Key” principle.<sup>[2]</sup>

Molecular receptors are defined as organic structures held by covalent bonds, that are able to bind ionic or molecular substrates (or both) by means of various intermolecular interactions such as electrostatic interaction, ion-dipole interaction, dipole-dipole interaction, hydrogen bonding,<sup>[3]</sup>  $\pi$ - $\pi$  stacking interaction, cation- $\pi$  interaction, hydrophobic effects and close packing in the solid state, leading to an assembly of two or more species. Design of receptor molecules depends on numerous types of complementary between host and guest such as geometry, size and electron cloud and interactions. Moreover, the large contact area and multiple interaction sites which lead to the strong overall bindings are also affected.<sup>[1]</sup> Molecular recognition can be divided into neutral substrate recognition,<sup>[4]</sup> cation recognition,<sup>[5-6]</sup> and anion recognition.<sup>[7-10]</sup>

Supramolecular chemists hope to probe fundamental aspects of molecular recognition through design and synthesis of completely artificial receptors, followed by examination of the structures and stabilities of artificial receptors and their complexes. Applications of these kinds of synthetic receptors can be used in a number of areas, such as medical analysis, detection of toxic compounds in environments, development of biosensors, separation of mixtures of compounds, including separation of enantiomers.

### 1.3 Cation Recognition

Both alkali and transition metal cations play important roles across many fields such as industry,<sup>[11]</sup> environments,<sup>[12]</sup> biology<sup>[13]</sup> and chemical therapy.<sup>[14]</sup> This thesis involves the chemistry of alkali cation recognition; therefore, solely the role of alkali cations will be briefly mentioned.

In living systems, the energy source called adenosine triphosphate (ATP) is strictly balanced its 4-ionic charge by alkali and alkaline earth metal cations. In addition, the  $\text{Na}^+/\text{K}^+$ -ATPase enzyme is an example of a transmembrane enzyme; i.e. an enzyme that exists in the phospholipid membrane of a biological cell, to transport the alkali metal cation;  $\text{Na}^+$  and  $\text{K}^+$ , against the concentration gradient from one side of the cell membrane to the other.<sup>[15]</sup> On the other hand, there is an increased interest in the development of optical sensors for the determination of clinically important metal ions such as sodium, potassium and lithium.

Cation complexation of chemistry has effectively given birth to the whole field of molecular recognition since the late 1960s. There are several kinds of cation based receptors such as podands, crown ethers, lariat crown ethers, cryptands, spherands<sup>[16]</sup> and calixarenes.<sup>[17]</sup> A principle in the design of artificial receptors is based on using the proper binding sites and the proper cavity size. The chemistry of them mainly depends on the hard-soft acid-base concept.<sup>[18]</sup> Ion-ion interactions, ion-dipole interactions and cation- $\pi$  interactions play important roles in this kind of chemistry.

### 1.4 Anion Recognition

The design of anion receptors is particularly challenging and this area of supramolecular chemistry has become a well established in the last 2 decades. There are a number of reasons for a sudden growth in this new area of coordination chemistry. Anions such as deoxyribonucleic acid (DNA) and adenosine triphosphate (ATP) are ubiquitous throughout biological systems. DNA, a polyanion containing phosphate esters along its ribose backbone, carries genetic information by transcription and translation processes.<sup>[19]</sup> The free energy of life process (ATP), made up of adenosine diphosphate (ADP) and dihydrogen phosphate ( $\text{H}_2\text{PO}_4$ ), is itself an anion bound by enzymes in order to perform many metabolic functions.

Moreover, the majority of enzyme is carboxypeptidase A (CPA), an enzyme that coordinates to the C-terminal carboxylate group of polypeptides by the formation of an arginine-aspartate salt-bridge and catalyses the hydrolysis of this residue. The salt-bridge motif is also observed in zinc finger DNA complexes and RNA (ribonucleic acid) stem loop-protein interactions. In addition, dicarboxylate anions are essential components of numerous metabolic processes in a living cell such as Krebs cycle (citric acid cycle).<sup>[20]</sup> Dicarboxylate species such as succinate, fumarate, oxaloacetate,  $\alpha$ -ketoglutarate and malate are important intermediates for generating ATP in this cycle.<sup>[20]</sup>

Chemically, anions serve as nucleophiles, bases, redox mediators and phase-transfer catalysts.<sup>[21]</sup> The chemical reactivity of some molecules can alter after coordinating to anion(s) leading to ability to separate hazardous anions or stabilization of unstable anionic species.

Anions also involve in pollution problems. In particular, nitrate<sup>[22]</sup> and phosphate that use in fertilizers on agricultural land as well as the phosphate anion that use in detergents and insecticides<sup>[23]</sup> often pollute natural water sources.

Medically, anions are of great importance in many disease pathways. Cystic fibrosis is caused by misregulation of chloride channels.<sup>[24]</sup> There is a real need for selective halide detection as established methods of chloride analysis are unsuitable for biological application. Cancer is caused by the uncontrolled replication of polyanionic DNA. Anion-binding proteins have also been implicated in the mechanism of Alzheimer's disease.<sup>[25]</sup>

Anion recognition chemistry actually grew from its beginnings in the same period as cation and neutral molecule recognition. Non-covalent interactions that used in anion-host binding can be actually categorized into 4 types; hydrogen-bondings, electrostatic interactions, metal or Lewis acid center (dipole-dipole interactions) or hydrophobic effects.<sup>[26]</sup> In comparison to cation and neutral molecule coordination chemistry, design and synthesis of anion receptors are a recent development due to a number of reasons. Firstly, the ordinary interaction is electrostatic forces. Most anion sizes are greater than isoelectronic cations, thus their charge to radius ratio are lower. This means that electrostatic binding interaction is less effective in the case of larger anions. Secondly, some anions such as



carboxylates, phosphates and sulphates exist in narrow pH window. Thus, the stability and the basicity of anions should be considered for a well-match between hosts and anions. Finally, there are wide varieties of geometry and coordination number. Therefore, a higher degree of design may be required to make receptors complementary to their anionic guests. A well-designed host molecule would gain both high selective and great sensitive binding.

### 1.5 Neutral Hydrogen Bonding Receptors for Anions

The design and synthesis of neutral anion receptors have been a subject of current interest in host-guest chemistry due to their possible applications to ion sensors such as ion-selective electrodes and optodes. The synthetic anion receptors can be actually divided into two classes: positively charged and uncharged receptors.<sup>[27]</sup> Many receptors for anion substrates reported in the first period are charged molecules for example polyammonium receptors, guanidinium based receptors, cobalticinium and ferrocinium based receptors. The particularly important anion receptor is neutral hydrogen bonding receptors, which show higher selectivity, although they are able to operate only in apolar non-competing media. Furthermore, the neutral receptor must compete with solution ion-pairing of guest leading to the lower sensitivity.

In nature, neutral anion binding proteins are known to bind anions only *via* hydrogen bonding interactions<sup>[28-29]</sup> which are the most important of all noncovalent bond types in biochemistry. Hydrogen bonds play an essential role in the formation of biological macromolecules such as the globular proteins and the DNA double helix and in the mechanism of enzyme-substrate recognition. Additionally, phosphate or sulfate binding proteins are naturally known examples that bind anions strongly and selectively *via* neutral proton-donor groups using the main chain protein *NH*-groups. Therefore, the formation of hydrogen bonds as a driving force of the molecular recognition has also been widely used in artificial receptors.<sup>[30]</sup>

Hydrogen bonds are in general significantly weaker than electrostatic interactions when the corresponding carboxylate anions are involved. The former interaction may become a dominating force in the association process if several hydrogen bond donor and acceptor sites act concertedly; for instance, the carboxylate binding pocket of the vancomycin group antibiotics in nature.<sup>[31-32]</sup> This implies that

hydrogen bonding is one of the most important recognition elements in anion sensing. Thus, the design and synthesis of hydrogen bonding receptors for biologically and/or chemically important anions are of current interest.<sup>[33-34]</sup>

The relatively strong hydrogen bonding of urea and thiourea groups has been used in the development of neutral anion receptors, because the hydrogen bond is directional in character, and correct orientation of the hydrogen bond donors can provide selective anion recognition. Urea and thiourea are particularly good hydrogen bond donors and are excellent receptors for anions such as carboxylate *via* the formation of two hydrogen bonds (Figure 1.2).



**Figure 1.2.** Formation of hydrogen bonding in carboxylate bound urea or thiourea.

In general, thiourea derivatives show stronger anion binding ability due to stronger hydrogen-bond donor capability than that of the corresponding ureas because of the higher acidity of the former.<sup>[35]</sup> The higher acidity of the thiourea hydrogens dominates the weaker hydrogen bond accepting ability of sulfur as compare to oxygen, unlikely to interfere in conformational or complexing studies involving other strong acceptor centers.<sup>[36-37]</sup>

## 1.6 Receptor for Amino Acids

Amino alcohol moieties are found in many natural products (amino polyols, amino sugars, amino acids, etc.) of biochemical and pharmacological interest.<sup>[38]</sup> In addition, the protein amino acids are the basic building blocks for all peptide chains (amino acid polymers and oligomers) and protein chains (a protein is a large polypeptide), which make up the structure of an enormous number of biological molecules. The chains are held together by peptide links (amino bonds), formed by intermolecular condensation reactions between the acid and amine parts of amino acids. Amino acids are chiral molecules, and in the living systems the range of proteins found is limited to be L- $\alpha$ -amino acids. In bacteria and fungi, a much wider

range of amino acids is found. L-amino acids are easy to synthesize or to separate from some bacteria, but the D-enantiomers must be synthesized by the different route. The precise selectivity of an effective receptor towards a kind of amino acid would be ideally to serve as an indicative of some diseases in biological system. Additionally, a particular challenge has been the enantiospecific binding of chiral species such as protonated amino acids. The twenty primary protein constituents are shown in Figure 1.3. All are  $\alpha$ -amino acids except proline which is a cyclic  $\alpha$ -amino acid.

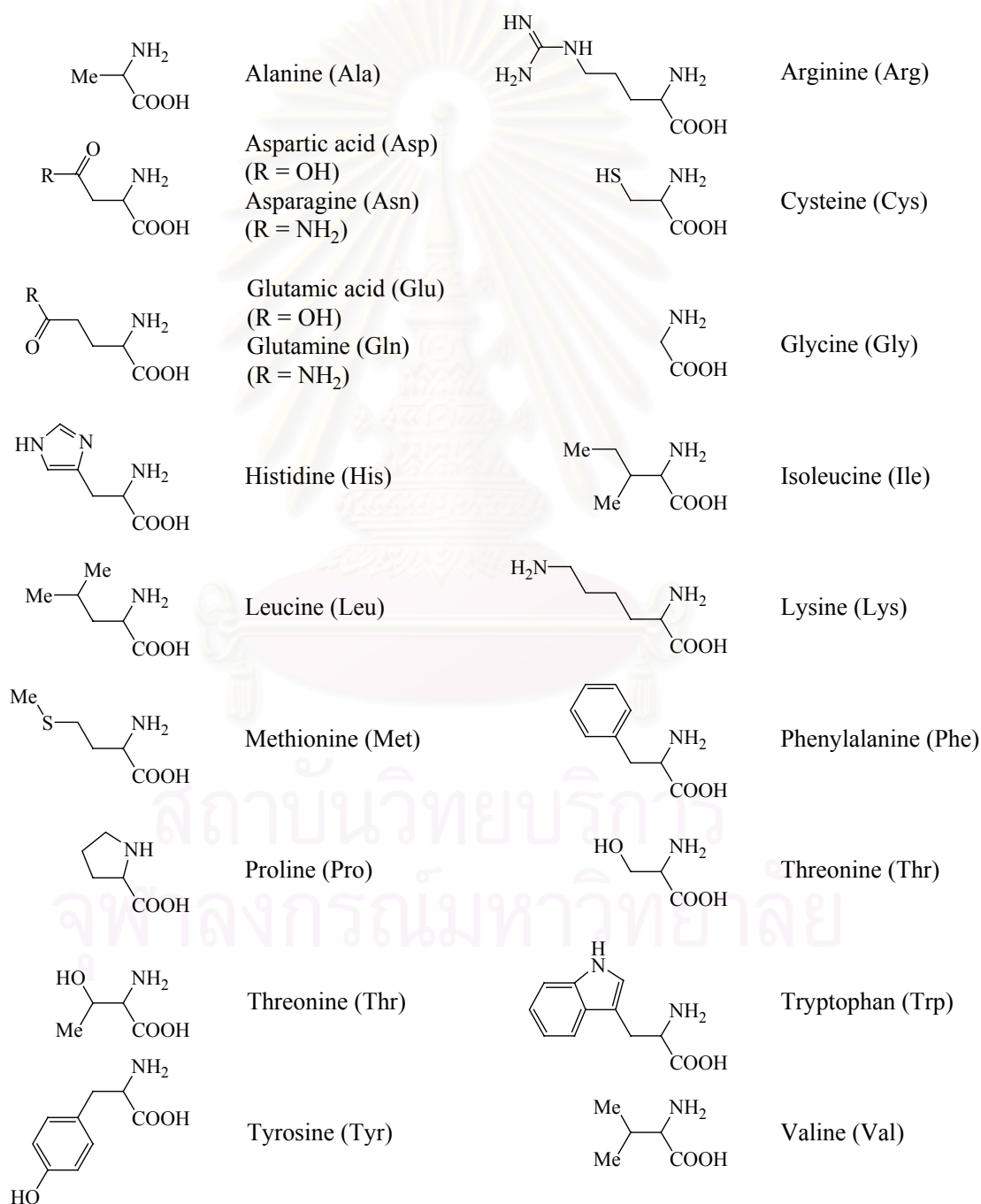


**Figure 1.3.** Twenty primary amino acids.

As a consequence of the rapid development of supramolecular chemistry, supramolecular technology has allowed the development of probes for amino acid. Artificial receptors can be tailored to bind small, biologically relevant molecules, such as models of natural receptors, carriers or enzymes.<sup>[39]</sup> Targeting guest molecules of biological importance also invite opportunities for practical applications of the hosts, e.g. as chemosensors or chemotherapeutic agents. The intermolecular interactions involved in this processes are of direct relevance to many biological events and may also lead to new biosensors, therapeutics, transport systems and separation of peptide mixtures.

### 1.7 Ditopic Receptors

The design of receptors for cations, and more recently anions, is a continuing challenge to supramolecular chemists. However, as stimulated by the needs of new selective extraction and transportation reagents for metal salt species in environmental and biological systems, ditopic receptors have been developed. As its name, a ditopic receptor contains two binding cavities. These two cavities are probably for either the same or different ions. In the case that ditopic receptors are designed for two alkali cations,<sup>[40]</sup> two transition metal cations,<sup>[41-43]</sup> or one organic salt with the same ends,<sup>[44-46]</sup> they are defined as “*homoditopic receptors*”. On the other hand, the receptors for alkaline earth cation-transition metal cation,<sup>[47]</sup> alkali cation-anion,<sup>[48-50]</sup> transition metal cation-anion<sup>[51-52]</sup> or organic ion-pairs<sup>[53]</sup> are categorized as “*heteroditopic receptors*”.<sup>[54]</sup>

The simultaneous complexation of cationic and anionic guest species by heteroditopic multisite receptors named “*ion-pair recognition*” is a new field of supramolecular chemistry which is the interface of cation and anion coordination.<sup>[55]</sup> The basic approach to develop receptors that recognize the salt as an associated ion-pair is to reduce the interference of anions during cation binding study or *vice versa*. These heteroditopic receptors consist of two recognition moieties that are either directly linked to allow a highly efficient communication or connected by a flexible spacer to ensure an optimal approaching of the ion-pair. Therefore, these bifunctional receptors can be designed to exhibit novel co-operative or allosteric behavior, which

one charged guest can enhance binding ability of another through hydrogen bonding, hydrophobic functionality, electrostatic force and conformational effects.<sup>[56-57]</sup>

In biological systems, the selective recognition of oxoanion substrates such as phosphate and sulfate often take place by a combination of hydrogen bonds and electrostatic interactions.<sup>[58-61]</sup> The effective receptors have been expected to be the artificial carriers and channels for the symport (co-transport) of inorganic and organic salts across lipophilic membranes and to the selective extraction and transportation reagents for ion-pair species of environmental importance and for zwitterion recognition. The subsequent coordination of the pairing anion has been demonstrated by a number of ditopic crown ethers functionalised boron, uranyl, polyammonium, amide, urea and amide-urea calix[4]arene based receptor systems.<sup>[55]</sup>

## 1.8 Calixarene Building Block

Calix[*n*]arenes, a family of synthetic macrocyclic receptors consisting of cyclic arrays of *n* phenol moieties linked by methylene groups,<sup>[62]</sup> were chosen as the putative hosts. This cyclic oligomer made up of phenols and formaldehydes provides new fascinating platforms.<sup>[63]</sup> The most famous calixarene is calix[4]arene because it is easiest to prepare. Calix[4]arene can adopt 4 conformations: cone, partial cone, 1,2-alternate and 1,3-alternate. Cone conformation is the most stable due to an array of hydrogen bonding between the phenolic-*OH* groups at the narrow rim of the macrocycle. This conformation is particularly useful because of its “bucket” shape leading to the rigidify cavity.

This cavity-containing molecule possesses hydroxyl groups on the lower rim and potentially free *para* position on the upper rim. The hydroxyl group provides convenient points for attachment of various moieties, as numerous other researchers have been demonstrated.<sup>[64-65]</sup> Calixarene with the appropriate appended groups are good candidates for probes because they have been shown to be highly specific ligands. In addition, their potential applications as sensing agents have received increasing interest. Indeed, the most significant feature of chemistry of these rigid macrocyclic molecules is their ability to bind selectively alkali, alkaline earth, transition metal cations<sup>[63]</sup> and a wide variety of anions inside the cavity.<sup>[66]</sup>

Their potential application in the treatment of metal rich nuclear wastes has been investigated worldwide.<sup>[67-68]</sup> Calixarene-based receptors were found to form complexes with cationic or anionic species and also a variety of organic ion or organic compounds.<sup>[69]</sup> Furthermore, calixarene derivatives can be used as more sophisticated molecules, for example, they are used as chemical sensors,<sup>[70]</sup> enzyme mimetics,<sup>[71]</sup> allosteric molecules<sup>[72]</sup> and peptide libraries.<sup>[73]</sup>

## 1.9 Thiourea-Based Receptor

In recent years, a number of molecules possessing thiourea functional groups have been designed as neutral receptors for various anions. Molecular recognition is achieved by establishing multiple hydrogen bonds with the relatively acidic *NH*-protons of these groups which are located in a well-defined position and direction with complementary acceptor groups in a specific and predictable manner. The potential for establishing highly ordered hydrogen bond networks with these functional groups is also used to construct supramolecular structures both in solution<sup>[74-75]</sup> and in solid state.<sup>[76-77]</sup> Several receptors contain thiourea functional groups with suitable spacers such as benzene and cyclohexene are particularly useful in the construction of neutral hydrogen bonding receptors.

## 1.10 Determination of Binding Constant<sup>[78-79]</sup>

In the viewpoint of molecular recognition systems, the weak chemical interaction is amplified, integrated and converted to physical signal that can readily read out and record. This data are related to complexation process. There are several methodologies to determine binding constant such as UV-VIS spectroscopy, NMR spectroscopy, bomb calorimeter, electrochemical instrument and fluorescence depending on the molecular design.

<sup>1</sup>H-NMR titration is one of the most useful techniques available to chemists for the investigation of dynamic molecular processes. Appeared NMR spectra are basically treated to display a qualitative description of reversible dynamic processes. This topic is often introduced with a discussion of simple two-site exchange systems; slow and fast exchange. It is stated that the spectrum consists of two signals under “*slow-exchange*” conditions. The binding constant can be evaluated by ratio of

integration of the NMR signals for free and bound hosts. The bound and free molecules give rise to discrete NMR signals that can be integrated to determine  $[G]$  and  $[HG]$  directly and association constant ( $\beta_i$ ) finally. Occasionally, observation of slow chemical exchange is classified as a moderately tightly bound host-guest system ( $\beta_i \approx 10^3$ ). The exchange rate of ligand does not necessarily correlate with the binding constant. There is just one signal at the population-averages chemical shift under “*fast-exchange*” conditions. Most of the host-guest equilibria are fast on the NMR time scale. Basically, the association constant ( $\beta_i$ ) of either slow or fast exchange process is represented by the following equation.

$$\beta_i = [H \cdot G_i] / [H][G]^i$$

Generally, the Job’s plot of chemical induced shift based on a series of solution containing both host and guest in varying proportions is essential to perform before any determination of  $\beta_i$ . The total concentration in each solution ( $[H]_0 + [G]_0$ ) is constant in this continuous variation analysis. Mole ratios between a host and a guest are in the range of  $0 > [H]_0 / ([H]_0 + [G]_0) < 1$ . It is worth mentioning that the data obtained to determine stoichiometry are not the best data for abstracting the association constant. Therefore, the separate experiments should be planned and executed.

In a typical fast exchange NMR titration experiment, a small aliquot of a guest may be added to a known concentration solution of a host in a deuterated solvent and the NMR spectrum is monitored as a function of the guest concentration or a host to guest ratio. Commonly, changes in chemical shift ( $\Delta\delta$ ) are noted for various atomic nuclei attributed to the influence of guest binding on their magnetic environments. As a result, two kinds of information are gained. Firstly, the location of nuclei most affected may give qualitative information about the selectivity of guest binding. More importantly, the shape of the titration curve plot of chemical induced shift ( $\delta$  or  $\Delta\delta$ ) against added guest concentration gives quantitative information about the binding constant. Such titration curves are often analyzed by modern curve fitting procedure; for instance, EQNMR, EMUL/MULTIFIT or NMRTIT. Although several methods have been developed to determine the association constant, curve fitting approaches are more widely used. Clear advantages of curve fitting treatments are that the experimental conditions are less constrained and more complex binding models (non

1:1 stoichiometry) can be accommodated. NMR based determinations of  $\beta_i$  are usually only reliable for association constants in the range of  $10$ - $10^4$   $M^{-1}$ . To maximize the reliability of NMR titration data, the experiment needs to be designed. The binding curve should cover a large range of percentage bound (ideally from 20 to 80%). For  $\beta_i \approx 1$ - $5$   $M^{-1}$ ,  $\Delta\delta_{\max}$  cannot be accurately measured. On the other hand, the graph of  $\Delta\delta$  against  $[H]_0/[G]_0$  become too steep to determine within convenient measurement times in the case of  $\beta_i \approx 10^5$   $M^{-1}$ . A more dilution condition probing by a more sensitive NMR will slightly extend the range of measurable association constants.

### 1.11 Literature Review

A few group have been devoting their research efforts towards the molecular design of *p*-*tert*-butylcalix[4]arene containing thiourea. However, it seems to be no report, to our knowledge, about the macrocyclic framework containing both of them.

Derivatives of *p*-*tert*-butylcalix[4]arene which are functionalized with two or four (thio)urea groups (Figure 1.4) reported by Scheerder *et al.* in 1994<sup>[80]</sup> were found to selectively bind spherical anions exclusively through hydrogen bonding. It was found that anions bound phenyl substituted derivatives **1a** stronger than *t*-butyl **1d**, octyl **1c** and propyl **1b** substituted which can be explained in term of steric hindrance. The larger bulky group, the less intramolecular hydrogen bonding was occurred leading to the higher binding constant. Moreover, they found that urea derivative **1a** bound anions stronger than thiourea derivative **2**. Thiourea is a better hydrogen bond donor thus it is easier to form intramolecular hydrogen bonding. In addition, *bis*-urea derivative **3** bound anions stronger than tetrakis-thiourea derivative because of more preorganization and less self-association. <sup>1</sup>H-NMR spectroscopy in CDCl<sub>3</sub> reveals a selectivity for Cl<sup>-</sup> over Br<sup>-</sup> and I<sup>-</sup>. The stoichiometry is 1:1 in all cases as confirmed by Job's plots. All receptors are not selectively bound H<sub>2</sub>PO<sub>4</sub><sup>-</sup> because this anion is too large to fit into the cavity. Moreover, hydrogen bond donor and acceptor sites of anions are not complementary with the hydrogen bond donor sites in the cavity.



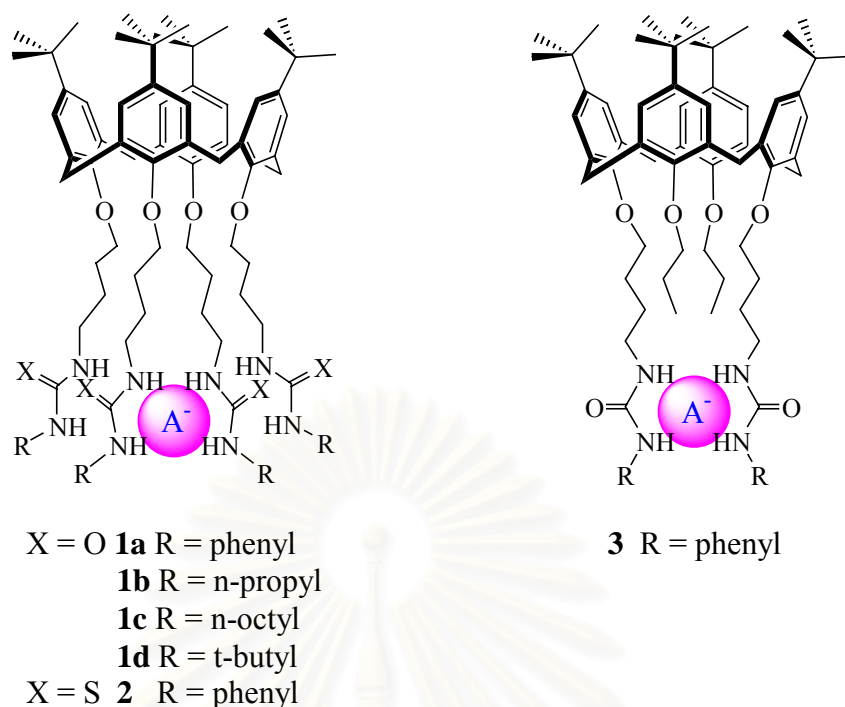


**Figure 1.4.** Two or four (thio)urea groups functionalized on *p-tert*-butylcalix[4]arene.

Four years later, calix[4]arene tetramide mono(thio)urea derivatives (Figure 1.5) were synthesized to reduce the effect of intramolecular hydrogen bonding by Pelizzi and co-worker.<sup>[81]</sup> These derivatives act as heteroditopic receptors containing amide moieties at the lower rim of calixarene as cation binding site and (thio)urea at the upper rim of calixarene as anion binding sites. These receptors were found to selectively bind Y-shape carboxylate anions over spherical anions. Receptors **5** and **6** bound acetate stronger than benzoate and formate which could be explained in term of  $pK_a$  ( $pK_a$  of acetate, benzoate and formate are 12.60, 10.90 and 10.26, respectively). Compared to urea **5b**, thiourea **5a** is a more effective ligand due to the higher degree of hydrogen bond donating. Sodium ion was encapsulated at the narrow rim in a slow exchange manner with the free ligand. The apolar cavity of the calix[4]arene building block is also rigidified by encapsulation of alkali ions. In addition, the anion coordination ability of the molecule that contains methylene linkage between the calixarene scaffold and the thiourea moiety has been affected by addition of sodium ion in the solution of the host. Receptor **6** containing thiourea group directly connected to the aromatic units is more efficient than **5a**, which has methylene spacer, because of electron-delocalization effect. Co-bound sodium ion in **5a** enhanced binding ability of anions towards receptor **4** due to intermolecular hydrogen bonding

and electrostatic interactions. Nevertheless, the cooperative binding decreases the selectivity.

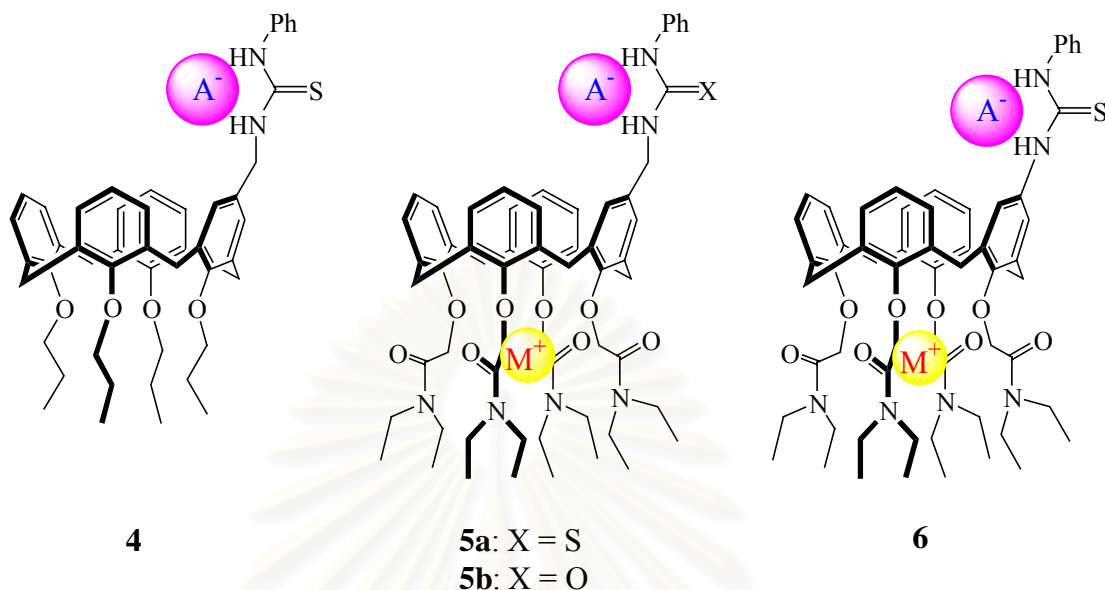


**Figure 1.5.** Calix[4]arene mono(thio)urea derivatives.

Deetz and co-worker reported an X-ray crystal structure of heteroditopic receptor **7** binding NaCl as a solvent separated ion-pair.<sup>[82]</sup> However, the binding cooperativity would be improved if the salt were bound to the receptor as a contact ion-pair. Later, they designed host **8** as a salt binding analogous of **7** but with a shorter distance between the anion and cation binding site.<sup>[83]</sup> These results suggested that macrocycle **8** is the first unambiguous example of a ditopic salt receptor that binds alkali halide as their contact ion-pair in solution more strongly than either of free ions (sodium or potassium was used as cation while chloride was served as anion). The solvent separated ion-pair of **7** and contact ion-pair of **8** are displayed in Figure 1.6. Furthermore, they also found that the significant binding enhancements were obtained in a less polar solvent like  $\text{CDCl}_3$ :DMSO- $d_6$  (85:15). The binding affinity of **8** towards chloride anion is higher in the presence of potassium, compared to sodium. When receptor **8** accommodated sodium cation, the diazacrown alters its conformation and reduced its effective binding. Even though chloride anion is located closer to the four diazacrown oxygen in  $\mathbf{8}\cdot\text{Na}^+$ , the association constant is much less than  $\mathbf{8}\cdot\text{K}^+\cdot\text{Cl}^-$ . This explained by the fact that the closer of contact ion-pair in  $\mathbf{8}\cdot\text{Na}^+$  increase ion-dipole repulsions between chloride and diazacrown oxygen.

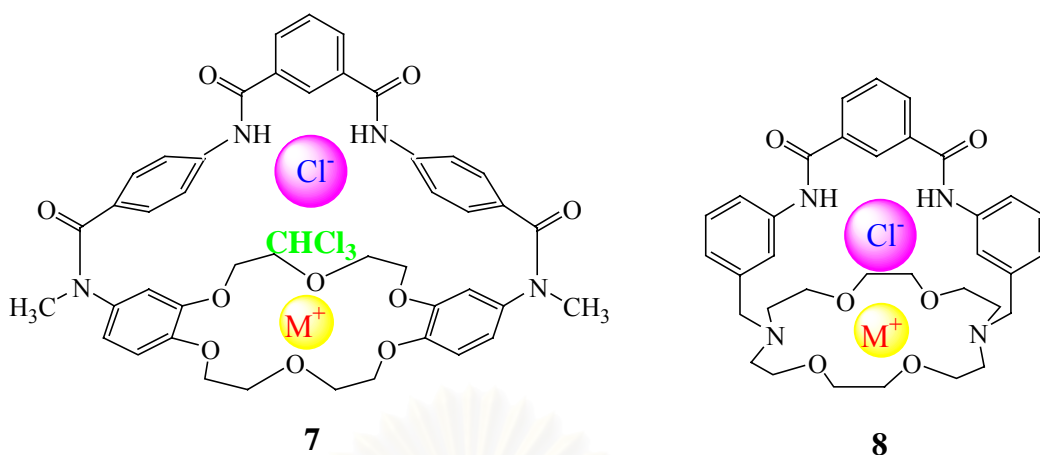


**Figure 1.6.** Effect of the chain length towards the formation of solvent separate or contact ion-pairing.

Analogous receptors have been reported by Mahoney *et al* (Figure 1.7).<sup>[84]</sup> Compared to heteroditopic **9**, bicyclic **10** was found to be a better host towards chloride anion either in the absence or the presence of an alkali cation (sodium or potassium). The crystal structure of [**10**·NaCl] was obtained. The contact ion-pair affect was found as expected. Although the x-ray structure reveals that the Na-Cl distance is shorter than Na-Cl distance in crystalline NaCl, it does not lead to the effective enhancement like KCl. This also resulted from the repulsion between chloride anion and oxygen on diazacrown. Moreover, the binding of a cation or an anion was also revealed to displace any trapped solvent molecules (water and methanol). Therefore, they did not inhibit the binding of the second counterion.

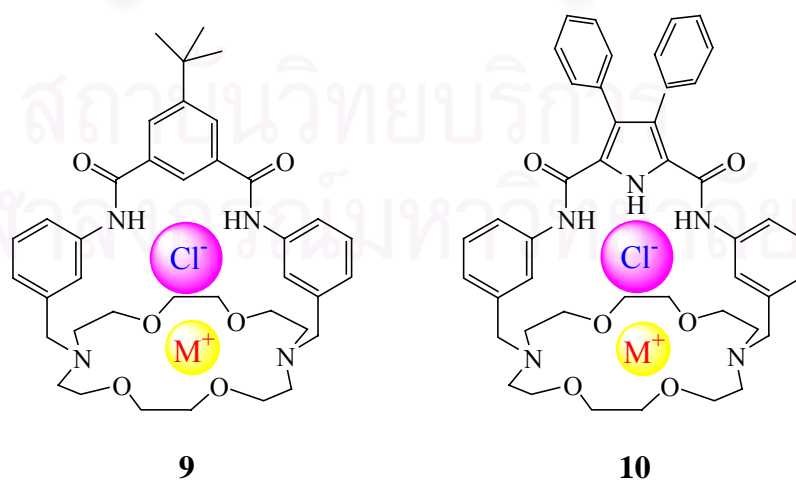


**Figure 1.7.** Other contacted ion-pair recognitions by which the number of hydrogen bond donor controlled the stability of complex.

Arduini and co-workers have found a positive allosteric effect during ion-pair binding by extended-cavity calix[4]arenes in the cone conformation.<sup>[85]</sup> In the complex, the sulfonate anion interacted with the phenolic upper rim of the calixarene by hydrogen bonds and, subsequently, the binding cavity of this macromolecule was further preorganized for complexing tetramethylammonium cation using chloroform-*d* as solvent (Figure 1.8). Therefore, sulfonate substrate was stabilized in the complex by hydrogen bonding and electrostatic forces.



**Figure 1.8.** Ion-pair recognition of tetramethylammonium sulfonate in a calixarene derivative.

Macrobicyclic anion receptors **13a** and **13b** (Figure 1.9) containing calix[4]arene as building block, two L-alanine units as chiral center and 2,6-diacetylpyridine or a phthaloyl bridge (to reduce conformational flexibility) were synthesized by Sansone *et al.*<sup>[86]</sup> Receptor **12** which is the clef like molecule without rigid spacer was found to bind anions less strongly than **13a** and **13b** which contained rigid linkages to reduce mobility. The rigid receptors showed selectivity towards Y-shaped carboxylate anions over other basic inorganic anions ( $\text{Cl}^-$ ,  $\text{I}^-$ ,  $\text{NO}_3^-$ ,  $\text{H}_2\text{PO}_4^-$ ). Moreover, all receptors prefer to bind benzoate to acetate. Both hydrogen-bonding interactions and  $\pi$ - $\pi$  stacking interactions are involved in the efficiency and the selectivity of these anion receptors.

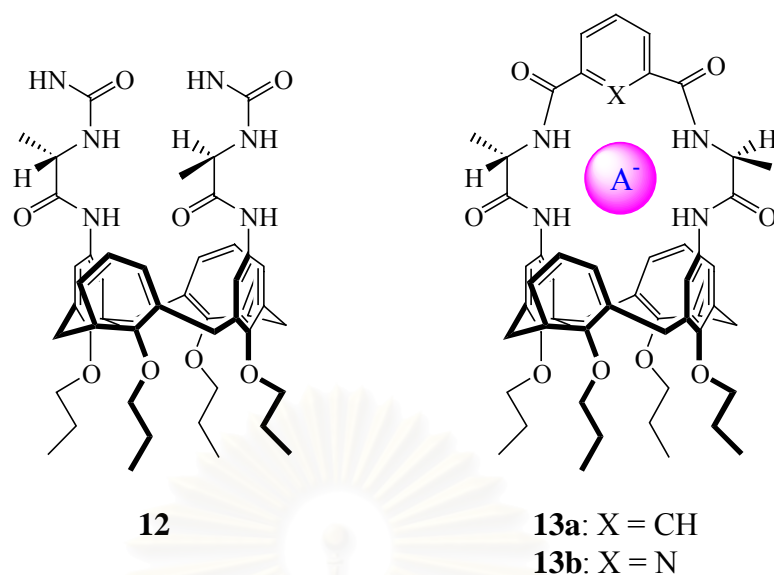


**Figure 1.9.** Chiral macrobicyclic anion receptors containing two L-alanine units as chiral center.

### 1.12 Scope of This Thesis

To gain a basic understanding of molecular recognition, synthesis of receptor molecules with a high selectivity for a particular guest molecule has been of interest to supramolecular chemists. This has been one of the driving forces for design of synthetic receptors.

In the last few years evidence has been accumulated showing that preorganization plays a fundamental role in molecular recognition by synthetic receptors. Preorganization and rigidity of host molecules are usually obtained by covalently linking binding groups or rigid spacers to suitable templates.

However, there seems to be no report, to our knowledge, on calixarene based receptors having thiourea groups as a part of macrocyclic framework, despite the fact that preorganization of the binding sites would improve the binding ability and selectivity. Our approach utilizes cyclic framework to control molecular architecture and consequently to preorganize the host molecules. Moreover, the rigid molecular components have been used to hold hydrogen-bonding groups at a fixed distance. Recently, separation of two thiourea units by 1,3-(dimethylene)benzene leads to receptors that form strong, multiple hydrogen bonded complexes with dihydrogen phosphate.<sup>[87]</sup> Thus, the novel neutral bifunctional receptors for the simultaneous

complexation of anions and cations in organic media have been developed. In these receptors, the appropriate binding sites for both anionic and cationic species are covalently combined in a neutral molecule.

The frame of this thesis aims at the understanding of molecular recognition processes involving cations and anions. According to the proposed concept, the synthesis of two *p-tert*-butylcalix[4]arene derivatives containing *bis*-thiourea moieties **14** and **15** have been developed (Figure 1.10). Their binding ability and selectivity towards several guests, cations, anions or both of them, have been investigated. The complex stoichiometry and binding association ( $\beta_1$ ) for the complexation between the receptors and several guest substrates have been determined by  $^1\text{H-NMR}$  spectroscopy in acetonitrile- $d_3$ . The target receptors are designed to contain thiourea moieties as carboxylate binding site. Calix[4]arene acts as a building block to maintain rigidity of the molecule. Amide or ester moiety is designed as a part of a flexible linkage between calixarene unit and the thiourea group to ensure an optimal approaching of them and also functions as alkali metal receptor to enhance binding ability of the receptor towards anions. The direct effect of ester and amide moieties on the binding efficiency for a wide variety of anions will also be evaluated. Both receptors possess two thiourea groups connected by 1,3-(dimethylene)benzene as a rigid spacer group. The aromatic unit which is linked between two thiourea moieties participates in the selective binding due to size-dependence and  $\pi$ - $\pi$  stacking interactions. Both receptors are expected to be the stronger salt binders with guests containing phenyl groups.

สถาบันวิทยบริการ  
จุฬาลงกรณ์มหาวิทยาลัย

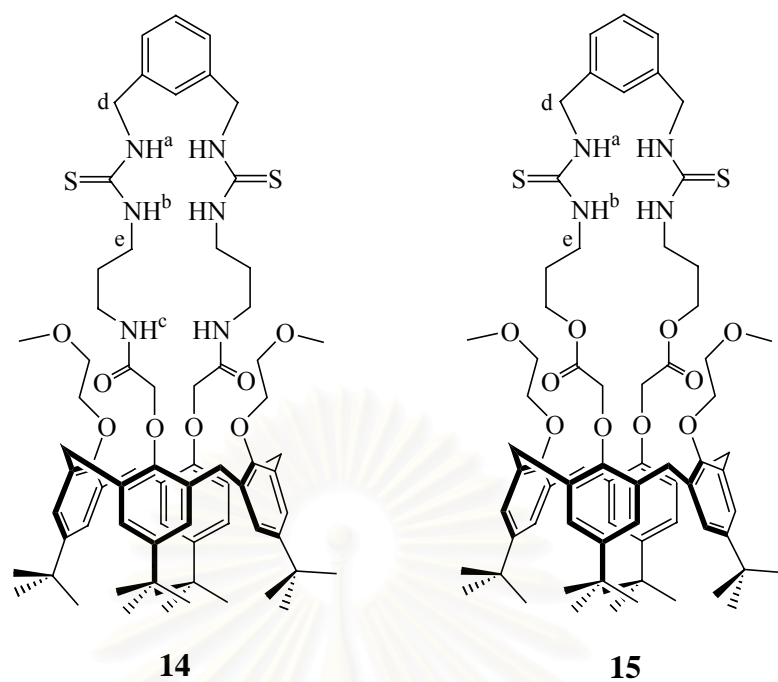


**Figure 1.10.** The novel *p*-*tert*-butylcalix[4]arene derivatives containing *bis*-thiourea moieties **14** and **15** that were designed and synthesized in this thesis.

สถาบันวิทยบริการ  
จุฬาลงกรณ์มหาวิทยาลัย

## CHAPTER II

### EXPERIMENTAL SECTION

#### 2.1 Synthesis of Heteroditopic Receptors

##### 2.1.1 General Procedure

###### 2.1.1.1 Materials

Tetrahydrofuran was dried and distilled under argon from sodium benzophenone ketyl immediately before use. Acetone was dried with anhydrous potassium carbonate and distilled.<sup>[88]</sup> Other dried reagents and solvents; acetonitrile, benzene, dichloromethane, pyridine and triethylamine, were dried and distilled from calcium hydride prior to use.<sup>[88]</sup> *p*-*tert*-Butyl calix[4]arene was prepared according to a modified literature procedure.<sup>[89]</sup> All other reagents and solvents, unless otherwise noted, were employed as purchased without further purification. Most reactions were carried out under argon atmosphere. Chromatographic separations were performed on silica gel flash column (Sorbsil C60, 40-60 mesh), small amount of triethylamine was added to neutralized silica gel if necessary. Thin Layer Chromatography was performed on aluminium backed plates coated with silica gel (0.25 mm) which contained the fluorescent indicator UV<sub>254</sub>.

###### 2.1.1.2 Instrumentation

<sup>1</sup>H-NMR spectra were obtained at 200 MHz on Brüker AC-200, at 300 MHz on Brüker AC-300, Brüker AM-300 and Brüker DPX-300 spectrometer as well as at 400 MHz on a Brüker DPX-400 spectrometer. <sup>13</sup>C-NMR spectra were recorded at 50 MHz on a Brüker AC-200, at 75.5 MHz on a Brüker AC-300 and at 100 MHz on a Brüker DPX-400 spectrometer. Two dimensional NMR spectra were obtained using Brüker DPX-400 spectrometer. Chemical shifts are reported in ppm on the  $\delta$  scale relative to the residual proton peak of the deuterated solvent. Coupling constants were given in Hertz. Assignments of <sup>1</sup>H-NMR and <sup>13</sup>C-NMR spectra were carried out using either Distortionless Enhancement by Polarization Transfer (DEPT) or two-dimensional NMR experiments.

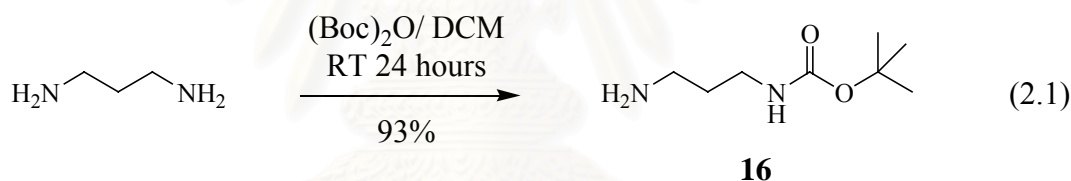


Electrospray mass spectra were determined on a Micromass Platform quadrupole mass analyser with an electrospray ion source using acetonitrile as solvent. Infrared spectra were carried out on either a Bio-Rad FT-IR spectrophotometer or a Nicolet Impact 410 FT-IR spectrophotometer. Spectra were obtained as neat films supported on sodium chloride plates for the former FT-IR spectrophotometer while the latter one afforded spectrum as potassium bromide pellet. Elemental analysis was analyzed by a Perkin Elmer CHON/S analyzer (PE2400 series II). All melting points were measured in open capillary tubes using an Electrothermal 9100 apparatus and are uncorrected.

## 2.1.2 Experimental procedure

### 2.1.2.1 Synthesis of 5,11,17,23-Tetra-*tert*-butyl-25,27-*N,N'*-1,3-bis(methoxycarbonylpropylthioureidomethyl)benzene-26,28-bis(3-oxabutyloxy)calix[4]arene, **14**

*tert*-Butyl *N*-(3-aminopropyl)carbamate,<sup>[90]</sup> **16**



This procedure was modified from the procedure reported by Muller *et al.*<sup>[90]</sup>

Di-*tert*-butyl dicarbonate (4.50 g, 20.62 mmol) in dichloromethane (400 mL) was added dropwise to a solution of excess 1,3-diaminopropane (8.00 g, 107.92 mmol) in dichloromethane (40 mL) for over a period of 12 hours with vigorous stirring. The stirring was continued for further 36 hours at room temperature. The reaction mixture was washed with aqueous sodium carbonate (2x120 mL) and water (2x100 mL). The organic layer was dried over magnesium sulfate and the solvent was evaporated under reduced pressure. The purified product was obtained from column chromatography (30% methanol in dichloromethane) as a colourless viscous liquid (3.35 g, 93%).

*Characterization data for 16*

**TLC:**  $R_f = 0.82$  (30% methanol in dichloromethane)

**IR (neat)/cm<sup>-1</sup>:** 3332 (NH), 1961 (CO)

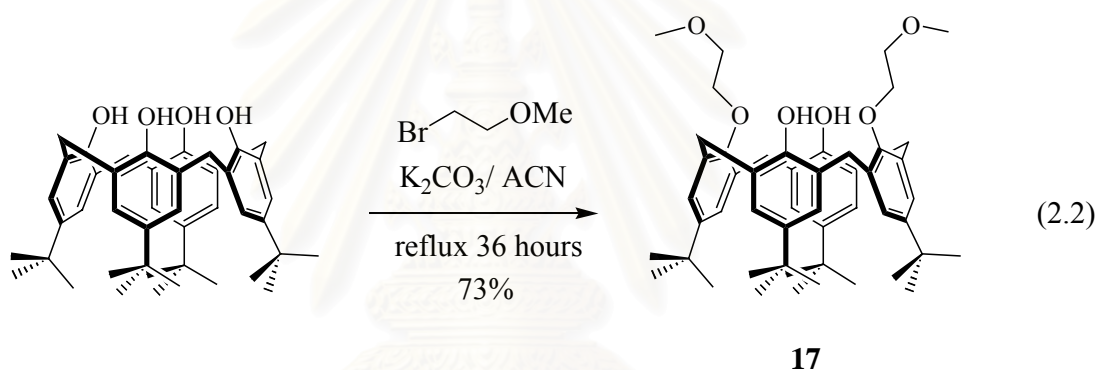
**<sup>1</sup>H-NMR (400 MHz, CDCl<sub>3</sub>):**  $\delta$  = 4.93 (broad s, 1H, -CH<sub>2</sub>NHCOO-), 3.20 (q,  $J$  = 6 Hz, 2H, -CH<sub>2</sub>CH<sub>2</sub>NH-, 2.75 (t,  $J$  = 7 Hz, 2H, H<sub>2</sub>NCH<sub>2</sub>CH<sub>2</sub>-), 1.60 (quint,  $J$  = 7 Hz, 2H, -CH<sub>2</sub>CH<sub>2</sub>CH<sub>2</sub>-), 1.43 (s, 9H, -COOC(CH<sub>3</sub>)<sub>3</sub>), 1.38 (s, 2H, H<sub>2</sub>NCH<sub>2</sub>CH<sub>2</sub>-)

**<sup>13</sup>C-NMR (75 MHz, CDCl<sub>3</sub>):**  $\delta$  = 156.30 (s, -NHCOOC(CH<sub>3</sub>)<sub>3</sub>-), 79.1 (s, -CH<sub>2</sub>CH<sub>2</sub>NH-), 39.7 (s, H<sub>2</sub>NCH<sub>2</sub>CH<sub>2</sub>-), 38.5 (s, -CH<sub>2</sub>CH<sub>2</sub>CH<sub>2</sub>-), 35.5 (s, -COOC(CH<sub>3</sub>)<sub>3</sub>), 28.5 (s, -COOC(CH<sub>3</sub>)<sub>3</sub>)

All spectroscopic data are consistent with those reported in the literatures.<sup>[91-92]</sup>

5,11,17,23-Tetra-*tert*-butyl-25,27-dihydroxy-26,28-bis(3-oxabutyloxy)calix[4]arene.

<sup>[93]</sup> **17**



This procedure was modified from the procedure reported by Wieser and co worker.<sup>[94]</sup>

A suspension of *p-tert*-butylcalix[4]arene (5.00 g, 7.70 mmol) and potassium carbonate (2.50 g, 18.09 mmol) was stirred at room temperature in dried acetonitrile (125 mL) for half an hour. Then, 2-bromoethyl methyl ether (2.68 g, 1.81 mL, 19.28 mmol) was added and the reaction mixture was heated at reflux for 36 hours under argon atmosphere. After the mixture cooled down to room temperature and the solid was filtered, the solvent was removed to dryness. The residue was dissolved in dichloromethane (100 mL) then washed with 2M HCl (2x50 mL) and subsequently with water (2x50 mL). The organic layer was dried over anhydrous magnesium sulfate and then purified by column chromatography (5% ethyl acetate in dichloromethane). After evaporation of the solvent, the purified product was obtained as a white solid (4.28 g, 73%).

*Characterization data for 17*

**TLC:**  $R_f = 0.35$  (5% ethyl acetate in dichloromethane)

**Melting point:** 221-222 °C

**IR (film)/ $\text{cm}^{-1}$ :** 3368 (broad) (OH)

**$^1\text{H-NMR}$  (400 MHz,  $\text{CDCl}_3$ ):**  $\delta = 7.80$  (s, 2H,  $-\text{ArOH}$ ), 7.23 and 7.08 (2s, 8H,  $\text{ArH}$ -calixarene), 4.58 and 3.50 (AB spin system, 8H,  $-\text{ArCH}_2\text{Ar}-$ ,  $^2J = 13$  Hz), 4.33 and 4.06 (2t, 8H,  $-\text{OCH}_2\text{CH}_2\text{O}-$ ,  $J = 5$  Hz), 3.72 (s, 6H,  $-\text{CH}_2\text{OCH}_3$ ), 1.47 and 1.23 (2s, 36H,  $-\text{ArC}(\text{CH}_3)_3$ )

**$^{13}\text{C-NMR}$  (100 MHz,  $\text{CDCl}_3$ ):**  $\delta = 150.62$ , 149.73, 146.81, 141.17, 132.64, 127.47, 125.53, 125.01 (8s, aromatic-C), 75.16 and 71.28 (2s,  $-\text{OCH}_2\text{CH}_2\text{O}-$ ), 59.06 (1s,  $-\text{CH}_2\text{OCH}_3$ ), 33.85 and 33.64 (2s,  $-\text{ArC}(\text{CH}_3)_3$ ), 31.58 and 31.00 (2s,  $-\text{ArC}(\text{CH}_3)_3$ ), 31.35 (s,  $-\text{ArCH}_2\text{Ar}-$ )

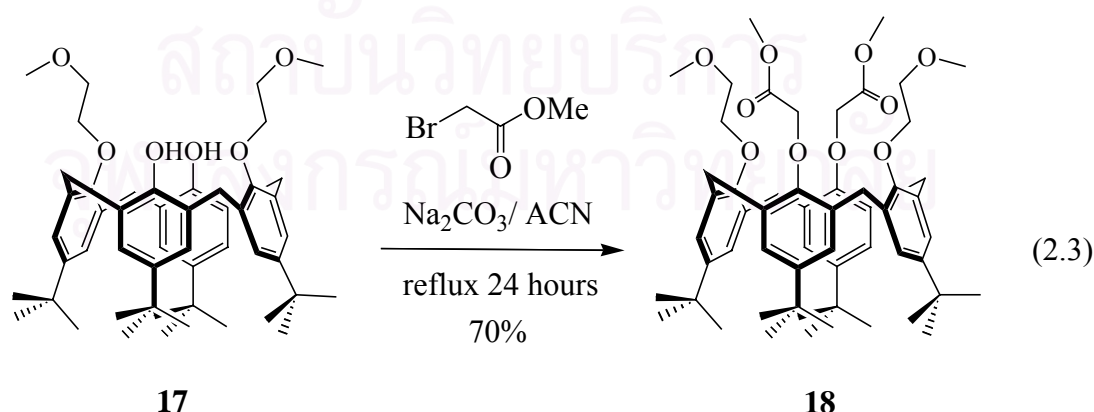
**LRMS ( $\text{ES}^+$ ):**  $m/z$  (%) = 787.6 (100)  $[\text{M}+\text{Na}]^+$

**Elemental analysis:** *Anal Calcd.* for  $\text{C}_{50}\text{H}_{68}\text{O}_6$ : C, 78.49; H, 8.96.

*Found.* C, 78.24; H, 8.96.

All spectroscopic data are consistent with those reported in the literature.<sup>[94]</sup>

5,11,17,23-Tetra-*tert*-butyl-25,27-bis(methoxycarbonylmethoxy)-26,28-bis(3-oxa-butyloxy)calix[4]arene,<sup>[95]</sup> **18**



This procedure was modified from the procedure reported by Jeunesse and co-worker.<sup>[95]</sup>

A suspension of compound **17** (1.87 g, 2.44 mmol) and sodium carbonate (0.78 g, 7.36 mmol) was stirred at room temperature in dried acetonitrile (100 mL) for half an hour. Then methyl bromoacetate (1.13 g, 0.70 mL, 7.39 mmol) was added and the reaction mixture was heated at reflux for 36 hours under argon atmosphere. After the mixture cooled to room temperature and the solid was filtered, the solvent was removed to dryness. The residue was dissolved in dichloromethane (70 mL) and washed with 2M HCl (2x30 mL) and subsequently with water (2x30 mL). The organic layer was dried over anhydrous magnesium sulfate and then purified by column chromatography (SiO<sub>2</sub>) eluting with 10% ethyl acetate in dichloromethane. The purified product was a white solid after dryness (1.56 g, 70%).

*Characterization data for 18*

**TLC:** R<sub>f</sub> = 0.33 (10% ethyl acetate in dichloromethane)

**Melting point:** 138-139 °C

**IR (film)/cm<sup>-1</sup>:** 1762 (CO)

**<sup>1</sup>H-NMR (300 MHz, CDCl<sub>3</sub>):** δ = 6.89-6.86 and 6.74-6.71 (2m, 8H, ArH-calixarene), 4.97-4.96, 4.83-4.82 and 4.75-4.74 (3m, 4H, -OCH<sub>2</sub>COO-), 4.71-4.66 and 3.20-3.16 (2m, 8H, -ArCH<sub>2</sub>Ar-), 4.12-4.07 and 3.89-3.83 (2m, 8H, -OCH<sub>2</sub>CH<sub>2</sub>O-), 3.80-3.77 (m, 6H, -CH<sub>2</sub>COOCH<sub>3</sub>), 3.45-3.44 (m, 6H, -CH<sub>2</sub>OCH<sub>3</sub>), 1.16-1.14 and 1.05-1.03 (2m, 36H, -ArC(CH<sub>3</sub>)<sub>3</sub>)

**<sup>13</sup>C-NMR (100 MHz, CDCl<sub>3</sub>):** δ = 171.09 and 165.25 (2s, -COOCH<sub>3</sub>), 153.26, 153.23, 152.97, 152.89, 145.19, 145.08, 145.06, 144.73, 133.88, 133.86, 133.81, 133.37, 133.33, 133.29, 125.41 and 124.97 (16s, aromatic-C), 73.19, 73.14, 71.92 and 71.89 (4s, -OCH<sub>2</sub>CH<sub>2</sub>O-), 70.91 and 70.53 (2s, -OCH<sub>2</sub>COO-), 60.38, 58.67 and 58.58 (3s, -CH<sub>2</sub>OCH<sub>3</sub>), 52.15 and 51.35 (2s, -CH<sub>2</sub>COOCH<sub>3</sub>), 33.86 and 33.77 (2s, -ArC(CH<sub>3</sub>)<sub>3</sub>), 31.69, 31.61, 31.03 and 30.53 (4s, -ArC(CH<sub>3</sub>)<sub>3</sub>), 31.43 and 30.36 (s, -ArCH<sub>2</sub>Ar-)

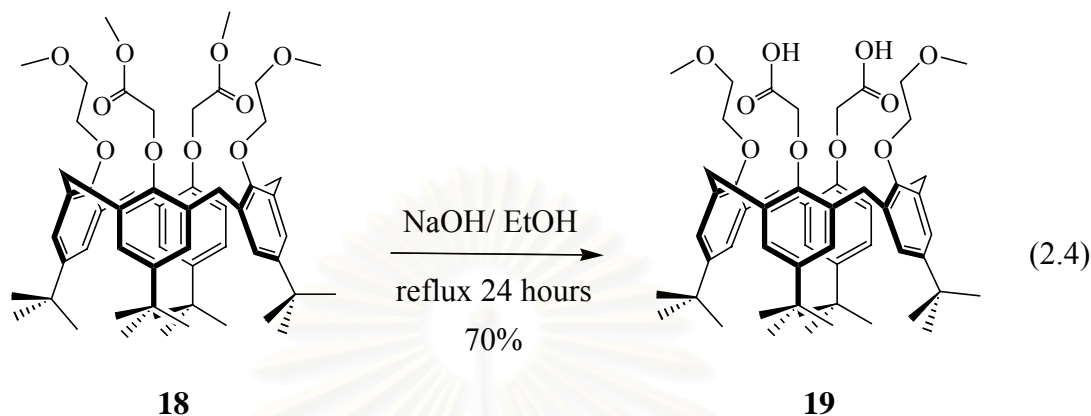
**LRMS (ES<sup>+</sup>):** m/z (%) = 931.8 (48) [M+Na]<sup>+</sup>

**Elemental analysis:** *Anal Calcd.* for C<sub>56</sub>H<sub>76</sub>O<sub>10</sub>: C, 73.98; H, 8.43.

*Found.* C, 73.95; H, 8.49.

All spectroscopic data are consistent with those reported in the literature.<sup>[95]</sup>

5,11,17,23-Tetra-*tert*-butyl-25,27-bis(hydroxycarbonylmethoxy)-26,28-bis(3-oxa-butyl-oxy)calix[4]arene,<sup>[96]</sup> **19**



This procedure was modified from the procedure reported by Araki *et al.*<sup>[97]</sup>

A mixture of compound **18** (1.79 g, 1.97 mmol) and sodium hydroxide (0.20 g, 5.00 mmol) in ethanol (100 mL) was heated at reflux for 24 hours under argon atmosphere. The solvent was then evaporated to dryness. Cold 3M HCl (50 mL) was added into the solid with vigorous stirring till pH reached 1 to afford a white precipitate. The solid was filtered off, taken up in dichloromethane (70 mL) and then washed with 3M HCl (2x50 mL) and sodium chloride solution (2x30 mL). After drying *in vacuo*, the desired product in dichloromethane was crystallized as white needle crystals (1.21 g, 70%) by adding methanol.

*Characterization data for 19*

**Melting point:** 262-263 °C

**IR (film)/cm<sup>-1</sup>:** 3252 (OH), 1758 (CO)

**<sup>1</sup>H-NMR (300 MHz, CDCl<sub>3</sub>):**  $\delta$  = 7.18 and 6.58 (2s, 8H, ArH-calixarene), 4.76 (s, 4H, -OCH<sub>2</sub>COOH), 4.42 and 3.26 (AB spin system, 8H, -ArCH<sub>2</sub>Ar-,  $J$  = 13 Hz), 3.99-3.75 (m, 8H, -OCH<sub>2</sub>CH<sub>2</sub>O-), 3.47 (s, 6H, -CH<sub>2</sub>OCH<sub>3</sub>), 1.35 and 0.84 (2s, 36H, -ArC(CH<sub>3</sub>)<sub>3</sub>)

**<sup>13</sup>C-NMR (75 MHz, CDCl<sub>3</sub>):**  $\delta$  = 170.43 (s, -OCH<sub>2</sub>COOH), 153.01, 149.96, 147.23, 145.98, 134.78, 132.10, 126.04 and 125.34 (8s, aromatic-C), 76.23 (s, -OCH<sub>2</sub>COOH),

72.00 and 70.91 (2s,  $-\text{OCH}_2\text{CH}_2\text{O}-$ ), 58.74 (s,  $-\text{CH}_2\text{OCH}_3$ ), 34.18 and 33.70 (2s,  $-\text{ArC}(\text{CH}_3)_3$ ), 31.57 and 30.94 (2s,  $-\text{ArC}(\text{CH}_3)_3$ ), 30.79 (s,  $-\text{ArCH}_2\text{Ar}-$ )

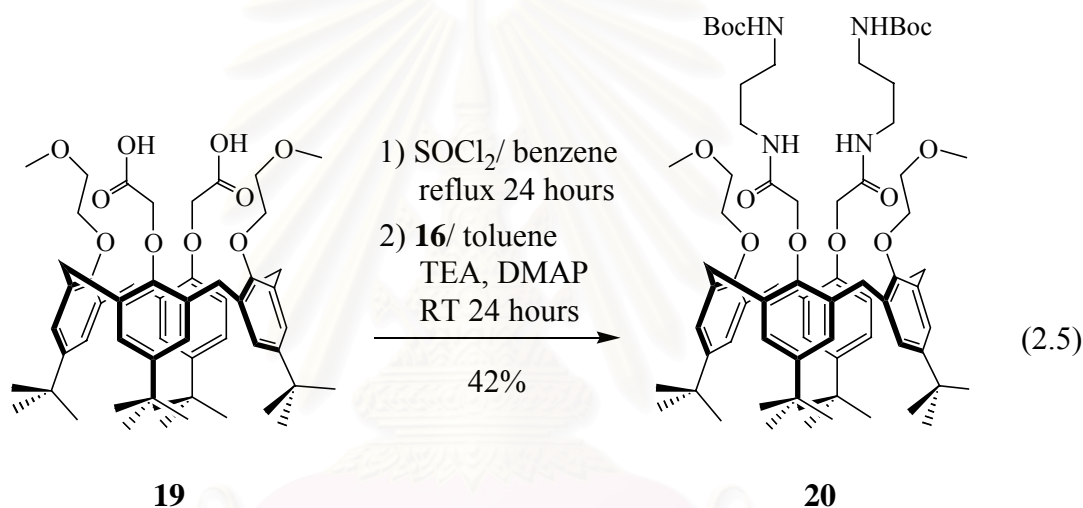
**LRMS ( $\text{ES}^+$ ):**  $m/z$  (%) = 902.8 (100)  $[\text{M}+\text{Na}]^+$

**Elemental analysis:** *Anal Calcd.* for  $\text{C}_{54}\text{H}_{72}\text{O}_{10}$ : C, 73.61; H, 8.24.

*Found.* C, 73.61; H, 8.40.

All spectroscopic data are consistent with those reported in the literature.<sup>[97]</sup>

5,11,17,23-Tetra-*tert*-butyl-25,27-bis(3-*tert*-butoxycarbonylaminopropylcarbamoyl-methoxy)-26,28-bis(3-oxabutyloxy)calix[4]arene, **20**



This procedure was modified from the procedure reported by Boehmer and his co-worker<sup>[98]</sup> as well as Kawaguchi and his co-worker.<sup>[99]</sup>

To a solution of compound **19** (1.00 g, 1.13 mmol) in benzene (50 mL), thionyl chloride (0.30 g, 0.18 mL, 2.52 mmol) was added dropwise. The reaction mixture was heated at reflux for 24 hours under argon atmosphere. After drying *in vacuo*, the white solid of 5,11,17,23-tetra-*tert*-butyl-25,27-bis(chlorocarbonyl-methoxy)-26,28-bis(3-oxa-butyloxy)calix[4]arene was used in the next step without further purification.\*

\**Characterization data for 5,11,17,23-tetra-*tert*-butyl-25,27-bis(chlorocarbonyl-methoxy)-26,28-bis(3-oxa-butyloxy)calix[4]arene*

The mixture of compound **16** (0.45 g, 2.58 mmol), triethylamine (0.25 g, 0.34 mL, 2.47 mmol) and 4-(dimethylamino)pyridine (0.02 g, 0.16 mmol) was stirred for approximately 15 minutes in toluene (20 mL) and then it was added to a solution of the previous white solid (acid chloride derivative) in toluene (40 mL). The reaction mixture was stirred at room temperature for 5 hours under argon atmosphere. After the solid was filtered, the solution was evaporated to dryness. The solid was dissolved in dichloromethane (30 mL) and washed with water (2x20 mL). The organic layer was dried over anhydrous magnesium sulfate and then purified using column chromatography (5% methanol in dichloromethane) to yield an oily yellowish compound (0.56 g, 42%).

*Characterization data for 20*

**TLC:**  $R_f = 0.28$  (10% methanol in dichloromethane)

**Melting point:** 130-131 °C

**IR (film)/ $\text{cm}^{-1}$ :** 1695 (CO), 3347 (NH)

**$^1\text{H-NMR}$  (300 MHz,  $\text{CDCl}_3$ ):**  $\delta = 8.33$  (broad s, 2H,  $-\text{CH}_2\text{NHCOOC}(\text{CH}_3)_3$ ), 7.27 and 7.05 (2s, 8H, ArH-calixarene), 6.55 (broad s, 2H,  $-\text{CH}_2\text{CONHCH}_2-$ ), 4.73 (s, 4H,  $-\text{OCH}_2\text{CONH}-$ ), 4.43 and 3.26 (AB spin system, 8H,  $-\text{ArCH}_2\text{Ar}-$ ,  $J = 13$  Hz), 4.09-4.08 and 3.46-3.44 (2 broad m, 8H,  $-\text{OCH}_2\text{CH}_2\text{O}-$ ), 3.49 (q, 4H,  $-\text{CH}_2\text{CH}_2\text{NHCOOC}(\text{CH}_3)_3$ ,  $J = 7$  Hz), 3.39 (s, 6H,  $-\text{CH}_2\text{OCH}_3$ ), 3.16 (q, 4H,  $-\text{CONHCH}_2\text{CH}_2-$ ,  $J = 4$  Hz), 1.86 (broad s,  $\text{H}_2\text{O}$ ), 1.82 (quin, 4H,  $-\text{CH}_2\text{CH}_2\text{CH}_2-$ ,  $J = 6$  Hz), 1.43 (s, 18H,  $-\text{COOC}(\text{CH}_3)_3$ ), 1.28 and 0.89 (2s, 36H,  $-\text{ArC}(\text{CH}_3)_3$ )

**$^1\text{H-NMR}$  (300 MHz,  $\text{CDCl}_3$ ):**  $\delta = 7.16$  and 6.46 (2s, 8H, ArH-calixarene), 5.47 (s, 4H,  $-\text{OCH}_2\text{COCl}$ ), 4.71 and 3.23 (AB spin system, 8H,  $-\text{ArCH}_2\text{Ar}-$ ,  $J = 13$  Hz), 3.95-3.79 (m, 8H,  $-\text{OCH}_2\text{CH}_2\text{O}-$ ), 3.55 (s, 6H,  $-\text{CH}_2\text{OCH}_3$ ), 1.37 and 0.85 (2s, 36H,  $-\text{ArC}(\text{CH}_3)_3$ )

**$^{13}\text{C-NMR}$  (75 MHz,  $\text{CDCl}_3$ ):**  $\delta = 171.63$  (s,  $-\text{OCH}_2\text{COCl}$ ), 152.75, 152.07, 146.25, 144.87, 134.93, 131.59, 126.06 and 124.61 (8s, aromatic-C), 77.86 (s,  $-\text{OCH}_2\text{COCl}$ ), 74.33 and 71.95 (2s,  $-\text{OCH}_2\text{CH}_2\text{O}-$ ), 59.11 (s,  $-\text{CH}_2\text{OCH}_3$ ), 34.04 and 33.51 (2s,  $-\text{ArC}(\text{CH}_3)_3$ ), 31.56 and 30.95 (2s,  $-\text{ArC}(\text{CH}_3)_3$ ), 31.36 (s,  $-\text{ArCH}_2\text{Ar}-$ )

All spectroscopic data are consistent with those reported in the literature.<sup>[97]</sup>

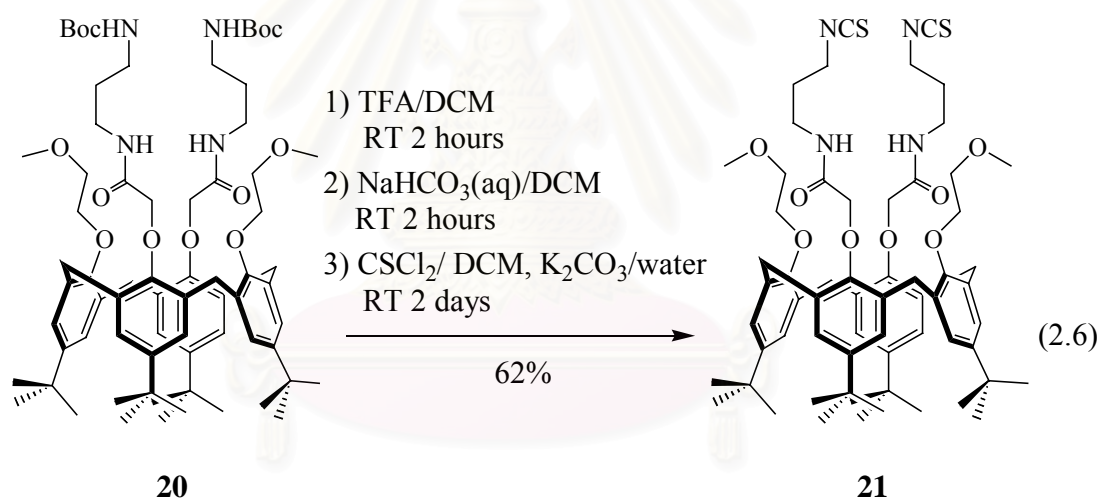
$^{13}\text{C-NMR}$  (75 MHz,  $\text{CDCl}_3$ ):  $\delta = 174.07$  (s,  $-\text{COOC}(\text{CH}_3)_3$ ), 170.91 (s,  $-\text{OCH}_2\text{CONH-}$ ), 156.20, 154.05, 150.37, 145.59, 133.55, 132.05, 126.28 and 125.04 (8s, ArC-calixarene), 78.71, 74.47, 73.83, 69.99, 37.58 and 36.76 (6s,  $-\text{OCH}_2\text{CH}_2\text{O-}$ ,  $-\text{OCH}_2\text{CONH-}$  and  $-\text{CONHCH}_2\text{CH}_2\text{CH}_2\text{NH-}$ ), 58.75 (s,  $-\text{CH}_2\text{OCH}_3$ ), 33.97 and 33.71 (2s,  $-\text{ArC}(\text{CH}_3)_3$ ), 33.71 and 31.50 (2s,  $-\text{ArC}(\text{CH}_3)_3$ ), 31.08 (s,  $-\text{COOC}(\text{CH}_3)_3$ ), 28.46 (s,  $-\text{COOC}(\text{CH}_3)_3$ )

**LRMS ( $\text{ES}^+$ ):**  $m/z$  (%) = 1215.6 (100)  $[\text{M}+\text{Na}]^+$

**Elemental analysis:** *Anal Calcd.* for  $\text{C}_{70}\text{H}_{104}\text{N}_4\text{O}_{12}\cdot 4\text{H}_2\text{O}$ : C, 66.43; H, 8.92; N, 4.43.

*Found.* C, 66.56; H, 8.78; N, 4.69.

5,11,17,23-Tetra-*tert*-butyl-25,27-bis(3-isothiocyanatopropylcarbamoylmethoxy)-26,28-bis(3-oxabutylloxy)calix[4]arene, **21**



To a solution of compound **20** (0.50 g,  $4.19 \times 10^{-1}$  mmol) in dichloromethane (20 mL), trifluoroacetic acid (5 mL) was added dropwise and the mixture was stirred at room temperature for 2 hours. After removal of the solvent in vacuum, the residue which was dissolved in dichloromethane was washed with sodium hydrogen carbonate solution (2x30 mL) and water (2x30 mL). The organic layer was dried over anhydrous magnesium sulfate and then evaporated to dryness. The yellowish liquid was used in the next step without further purification.

The above oily compound was taken up in dichloromethane (15 mL) and then stirred with potassium carbonate (0.18 g, 1.30 mmol) in water (5 mL). After that,



thiophosgene (0.10 g, 0.07 mL,  $8.70 \times 10^{-1}$  mmol) was slowly dropped into the mixture. The reaction was stirred at room temperature for 4 days. After extracting with dichloromethane (2x15 mL), the organic layer was washed with water (2x20 mL), dried over anhydrous magnesium sulfate, and then evaporated to dryness *in vacuo*. The purified product was eluted from column chromatography ( $\text{SiO}_2$ ) using 10% methanol in dichloromethane as eluent to provide a white solid (0.28 g, 62%).

*Characterization data for 21*

**TLC:**  $R_f = 0.48$  (10% methanol in dichloromethane)

**Melting point:** 185-187 °C

**IR (film)/ $\text{cm}^{-1}$ :** 1664 (CO), 2105 (NCS), 3336 (NH)

**$^1\text{H-NMR}$  (400 MHz,  $\text{CDCl}_3$ ):**  $\delta = 8.46$  (t, 2H,  $-\text{CH}_2\text{CONHCH}_2-$ ,  $J = 6$  Hz), 7.09 and 6.54 (2s, 8H, ArH-calixarene), 4.76 (s, 4H,  $-\text{OCH}_2\text{CONH}-$ ), 4.46 and 3.28 (AB spin system, 8H,  $-\text{ArCH}_2\text{Ar}-$ ,  $J = 13$  Hz), 4.11 and 3.45 (2t, 8H,  $-\text{OCH}_2\text{CH}_2\text{O}-$ ,  $J = 4$  Hz), 3.63 (t, 4H,  $-\text{CH}_2\text{CH}_2\text{NCS}$ ,  $J = 7$  Hz), 3.53 (q, 4H,  $-\text{CONHCH}_2\text{CH}_2-$ ,  $J = 7$  Hz), 3.41 (s, 6H,  $-\text{CH}_2\text{OCH}_3$ ), 2.10 (quin, 4H,  $-\text{CH}_2\text{CH}_2\text{CH}_2-$ ,  $J = 7$  Hz), 1.80 (broad s,  $\text{H}_2\text{O}$ ), 1.32 and 0.89 (2s, 36H,  $-\text{ArC}(\text{CH}_3)_3$ )

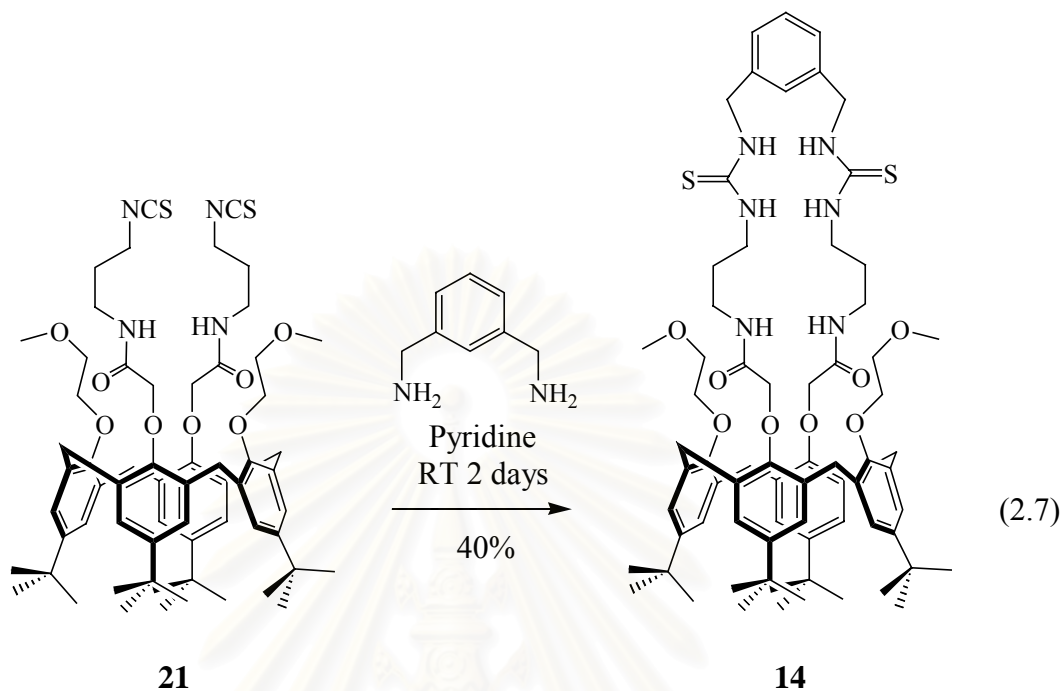
**LRMS ( $\text{ES}^+$ ):**  $m/z$  (%) = 1099.4 (100)  $[\text{M}+\text{Na}]^+$

**Elemental analysis:** *Anal Calcd.* for  $\text{C}_{62}\text{H}_{84}\text{N}_4\text{O}_8\text{S}_2 \cdot 1.5\text{H}_2\text{O}$ : C, 67.42; H, 7.94; N, 5.07.

*Found.* C, 67.43; H, 7.80; N, 5.21.

สถาบันวิทยบริการ  
จุฬาลงกรณ์มหาวิทยาลัย

5,11,17,23-Tetra-tert-butyl-25,27-N,N'-1,3-bis(methoxycarbonylpropylthioureido-methyl)benzene-26,28-bis(3-oxabutyloxy)calix[4]arene, 14



To a solution of 1,3-bis(aminomethyl)benzene (20.6 mg, 0.02 mL,  $1.51 \times 10^{-1}$  mmol) in dried pyridine (20 mL), the solution of compound **21** (100.0 mg,  $9.28 \times 10^{-2}$  mmol) in dried pyridine (5 mL) was slowly dropped for a period of 12 hours. The reaction mixture was stirred under argon atmosphere at room temperature for further 3 days. After concentrating *in vacuo*, the residue was dissolved in dichloromethane (50 mL) and washed with water (2x50 mL). The organic layer was dried over anhydrous magnesium sulfate and then evaporated under vacuum. The desired product was eluted from column chromatography ( $\text{SiO}_2$ ) using 10% methanol in dichloromethane as eluent. This product could be further purified by precipitation in methanol (45.2 mg, 40%).

*Characterization data for 14*

**TLC:**  $R_f = 0.33$  (10% methanol in dichloromethane)

**Melting point:** 158-159 °C

**IR (film)/ $\text{cm}^{-1}$ :** 1735 (CO), 2206 (NCS), 3308 (NH)

**$^1\text{H-NMR}$  (400 MHz,  $\text{CDCl}_3$ ):**  $\delta$  = 8.67 (broad s, 2H,  $-\text{CH}_2\text{CONHCH}_2-$ ), 7.58 (broad s, 2H,  $-\text{CH}_2\text{CH}_2\text{NHCSNH-}$ ), 7.36-6.50 (m, 4H, ArH-linkage), 7.14 and 6.47 (2s, 8H, ArH-calixarene), 6.66 (broad s, 2H,  $-\text{NHCSNHCH}_2\text{Ar-}$ ), 5.30 (s,  $\text{CH}_2\text{Cl}_2$ ), 4.80 (s, 4H,  $-\text{OCH}_2\text{CONH-}$ ), 4.75 (broad s, 4H,  $-\text{NHCSHNCH}_2\text{Ar-}$ ), 4.42 and 3.30 (AB spin system, 8H,  $-\text{ArCH}_2\text{Ar-}$ ,  $J = 13$  Hz), 4.07 and 3.36 (2 broad s, 8H,  $-\text{OCH}_2\text{CH}_2\text{O-}$ ), 3.61 (broad s, 4H,  $-\text{NHCSNHCH}_2\text{CH}_2-$ ), 3.43 (broad s, 4H,  $-\text{CONHCH}_2\text{CH}_2-$ ), 3.35 (s, 6H,  $-\text{CH}_2\text{OCH}_3$ ), 1.92 (broad s, 4H,  $-\text{CH}_2\text{CH}_2\text{CH}_2-$ ), 1.91 (broad s,  $\text{H}_2\text{O}$ ), 1.36 and 0.85 (2s, 4H,  $-\text{ArC}(\text{CH}_3)_3$ )

**$^{13}\text{C-NMR}$  (100 MHz,  $\text{CDCl}_3$ ):**  $\delta$  = 182.03 (s,  $-\text{NHCSNH-}$ ), 171.73 (s,  $-\text{CH}_2\text{CONH-}$ ), 154.44, 149.69, 145.85, 145.72, 133.59, 131.46, 126.63 and 124.93 (8s, aromatic-C (calixarene)), 138.49, 135.95, 128.65 and 124.93 (4s, aromatic-C (linkage)), 75.03 and 69.40 (2s,  $-\text{OCH}_2\text{CH}_2\text{O-}$ ), 73.39 (s,  $-\text{OCH}_2\text{CONH-}$ ), 58.75 (s,  $-\text{CH}_2\text{CH}_2\text{OCH}_3$ ), 47.53 (s,  $-\text{NHCSNHCH}_2\text{Ar-}$ ), 45.91 (s,  $-\text{CONHCH}_2\text{CH}_2-$ ), 41.42 (s,  $-\text{CH}_2\text{CH}_2\text{NHCSNH-}$ ), 36.68 (s,  $-\text{CH}_2\text{CH}_2\text{CH}_2-$ ), 33.99 and 33.65 (2s,  $-\text{ArC}(\text{CH}_3)_3$ ), 31.51 and 30.97 (2s,  $-\text{ArC}(\text{CH}_3)_3$ ), 29.06 (s,  $-\text{ArCH}_2\text{Ar-}$ )

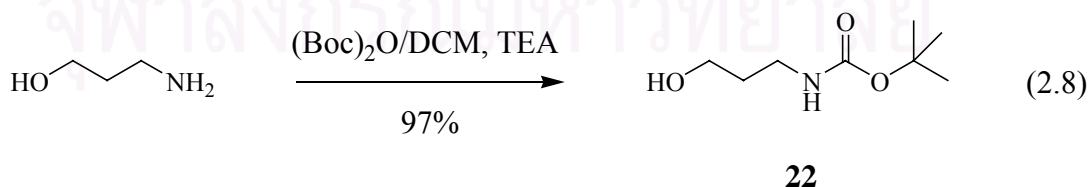
**LRMS ( $\text{ES}^+$ ):**  $m/z$  (%) = 1235.2 (100)  $[\text{M}+\text{Na}]^+$

**Elemental analysis:** *Anal Calcd.* for  $\text{C}_{70}\text{H}_{96}\text{N}_6\text{O}_8\text{S}_2 \cdot 0.5\text{CH}_2\text{Cl}_2 \cdot \text{H}_2\text{O}$ : C, 66.46; H, 7.83; N, 6.60.

*Found.* C, 66.55; H, 7.53; N, 6.37.

### 2.1.2.2 Synthesis of 5,11,17,23-Tetra-*tert*-butyl-25,27-*N,N'*-1,3-bis(methoxycarbonylpropylthioureidomethyl)benzene-26,28-bis(3-oxabutyloxy)calix[4]arene, 15

*tert*-Butyl *N*-(3-hydroxypropanol)carbamate, (22)



This procedure was modified from the procedure reported by Dubowchik *et al.*<sup>[100]</sup>

To a mixture of 3-amino-1-propanol (3.11 g, 3.17 mL, 41.41 mmol) and triethylamine (4.50g, 6.20 mL, 44.47 mmol) in dichloromethane (150 mL), the solution of di-*tert*-butyl dicarbonate (9.15 g, 41.92 mmol) in dichloromethane (50 mL) was added dropwise. The reaction mixture was stirred for further 24 hours. After that it was washed with 10% acetic acid solution (2x100 mL) and water (2x50 mL). The organic layer was dried over anhydrous magnesium sulfate and purified by column chromatography (SiO<sub>2</sub>) using 20% ethyl acetate in dichloromethane as eluent to afford a colourless oil (7.07 g, 97%).

*Characterization data for 22*

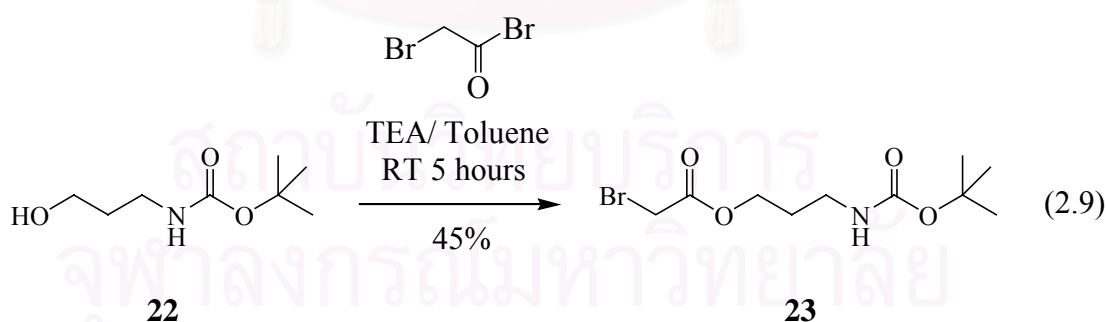
**TLC:** R<sub>f</sub> = 0.33 (50% ethyl acetate in dichloromethane)

**<sup>1</sup>H-NMR (300 MHz, CDCl<sub>3</sub>):** δ = 4.99 (broad s, 1H, -CH<sub>2</sub>NHCOO-), 3.62 (t, 2H, HOCH<sub>2</sub>CH<sub>2</sub>-, J = 6 Hz), 3.23 (broad s, 2H, -CH<sub>2</sub>CH<sub>2</sub>NH-), 3.09 (broad s, 1H, HOCH<sub>2</sub>-), 1.64 (q, 2H, -CH<sub>2</sub>CH<sub>2</sub>CH<sub>2</sub>-, J = 6 Hz), 1.41 (s, 9H, -COOC(CH<sub>3</sub>)<sub>3</sub>)

**<sup>13</sup>C-NMR (75 MHz, CDCl<sub>3</sub>):** δ = 156.90 (s, -NHCOOC(CH<sub>3</sub>)<sub>3</sub>-), 79.16 (s, HOCH<sub>2</sub>CH<sub>2</sub>-), 59.08 (s, -CH<sub>2</sub>CH<sub>2</sub>NH-), 36.90 (s, -CH<sub>2</sub>CH<sub>2</sub>CH<sub>2</sub>-), 32.38 (s, -COOC(CH<sub>3</sub>)<sub>3</sub>), 28.16 (s, -COOC(CH<sub>3</sub>)<sub>3</sub>)

All spectroscopic data are consistent with those reported in the literature.<sup>[101]</sup>

*tert*-Butyl N-(3-(bromoacetatepropyl)carbamate), 23



A solution of bromoacetyl bromide (0.70 g, 0.30 mL, 3.44 mmol) in dried toluene (50 mL) was added dropwise for a period of 2 hours to a mixture of compound **22** (0.57 g, 3.25 mmol), triethylamine (0.36 g, 0.5 mL, 3.56 mmol), a catalytic amount of 4-dimethylaminopyridine (0.04 g, 3.27 mmol) and toluene (10 mL) in an iced bath (-5 °C). The reaction mixture was stirred under argon atmosphere for 5 hours. After the solid was filtered, the solvent was removed in vacuum.

Column chromatography (SiO<sub>2</sub>) was done immediately using 10% ethyl acetate in dichloromethane as eluent to yield a yellow liquid (0.43 g, 45%).

*Characterization data for 23*

**TLC:** R<sub>f</sub> = 0.50 (10% ethyl acetate in dichloromethane)

**IR (neat)/cm<sup>-1</sup>:** 1686 (CO), 3347 (NH)

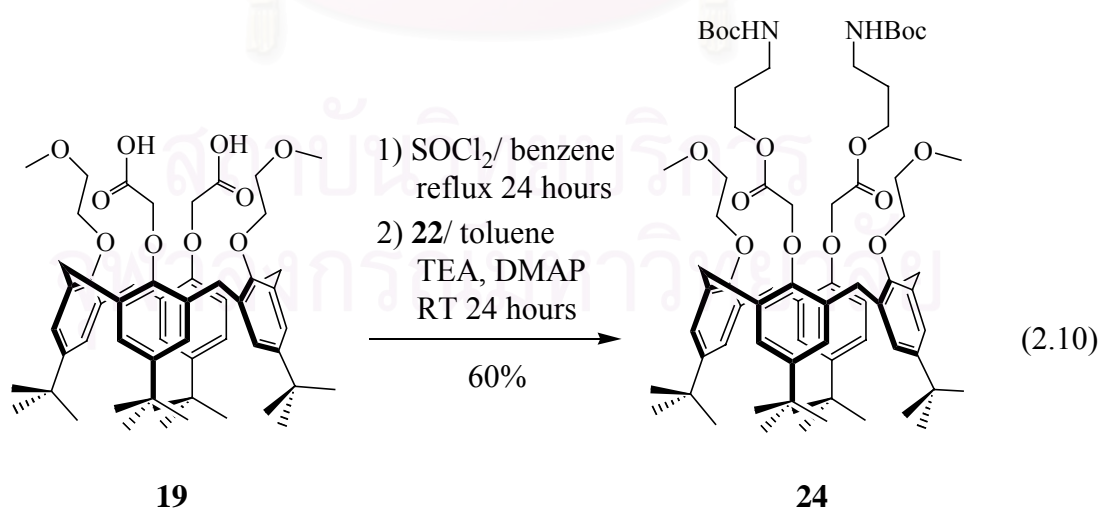
**<sup>1</sup>H-NMR (300 MHz, CDCl<sub>3</sub>):** δ = 4.80 (broad s, 1H, -CH<sub>2</sub>NHCOO-), 4.22 (t, 2H, -COOCH<sub>2</sub>CH<sub>2</sub>-, *J* = 6 Hz), 3.83 (s, 2H, BrCH<sub>2</sub>COO-), 3.20 (q, 2H, -CH<sub>2</sub>CH<sub>2</sub>NH-, <sup>1</sup>*J* = 10 Hz, <sup>2</sup>*J* = 6 Hz), 1.84 (quin, 2H, -CH<sub>2</sub>CH<sub>2</sub>CH<sub>2</sub>-, <sup>1</sup>*J* = 6 Hz, <sup>2</sup>*J* = 7 Hz), 1.41 (s, 9H, -COOC(CH<sub>3</sub>)<sub>3</sub>)

**<sup>13</sup>C-NMR (75 MHz, CDCl<sub>3</sub>):** δ = 167.48 (s, -NHCOOC(CH<sub>3</sub>)<sub>3</sub>-), 156.07 (s, -CH<sub>2</sub>COOCH<sub>2</sub>-), 79.45 (s, -COOC(CH<sub>3</sub>)<sub>3</sub>), 60.00 (s, -COOCH<sub>2</sub>CH<sub>2</sub>-), 37.37 (s, -CH<sub>2</sub>CH<sub>2</sub>NH-), 29.04 (s, -CH<sub>2</sub>CH<sub>2</sub>CH<sub>2</sub>-), 28.52 (s, -COOC(CH<sub>3</sub>)<sub>3</sub>), 25.93 (s, BrCH<sub>2</sub>COO-)

**LRMS (ES<sup>+</sup>):** m/z (%) = 295 (66) [M] and 296 (43) [M+H]<sup>+</sup>

5,11,17,23-Tetra-*tert*-butyl-25,27-bis(3-(*tert*-butoxycarbonylamino)propylcarbonyl-methoxy)-26,28-bis(3-oxabutyloxy)calix[4]arene, **24**

*Method I*

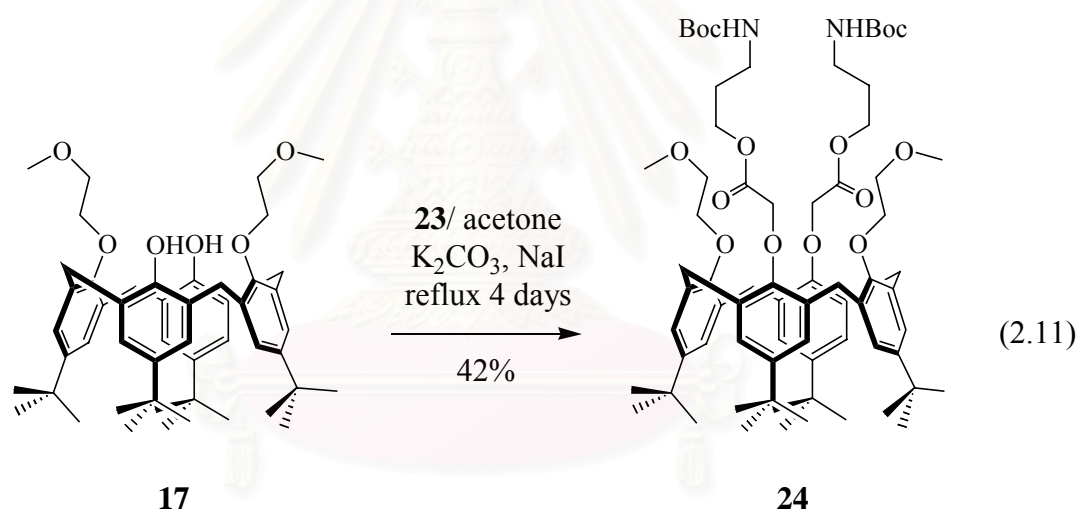


To a solution of compound **19** (0.50 g, 5.67x10<sup>-1</sup> mmol) in benzene (25 mL), thionyl chloride (0.16 g, 0.10 mL, 1.34 mmol) was added. The reaction mixture was

heated at reflux for 24 hours under argon atmosphere. After drying *in vacuo*, the white solid was used in the next step without further purification.

The mixture of compound **22** (0.22 g, 1.26 mmol), triethylamine (0.15 g, 0.20 mL, 1.48 mmol) and 4-(dimethylamino)pyridine (0.02 g, 1.64 mmol) was stirred for 15 minutes in toluene (10 mL) and then it was added to a solution of the previous white solid (acid chloride derivative) in toluene (20 mL). The reaction mixture was stirred under argon atmosphere for further 20 hours at room temperature. After filtration, the solution was dried *in vacuo*, dissolved in dichloromethane (20 mL) and washed with water (2x15 mL). The organic layer was dried over anhydrous magnesium sulfate and then purified by column chromatography (SiO<sub>2</sub>) using 5% methanol in dichloromethane as eluent to provide an off-white solid **24** (0.34 g, 60%)

#### Method II



A suspension of compound **17** (1.00 g, 1.31 mmol), potassium carbonate (0.42 g, 3.04 mmol) and a catalytic amount of sodium iodide (0.05 g, 0.33 mmol) in dried acetone (15 mL) was stirred at room temperature for half an hour. Then a solution of compound **23** (0.83 g, 2.80 mmol) in dried acetone (10 mL) was added dropwise for half an hour. The reaction mixture was heated at reflux for 24 hours. After allowing to cool to room temperature, the solid was filtered off and the solution was evaporated to dryness. The residue was taken up in dichloromethane (30 mL) and washed with water (2x25 mL). The organic layer was dried over anhydrous magnesium sulfate. Compound **24** was purified by column chromatography using 5% methanol in dichloromethane as eluent to provide an off-white solid as a product (0.55 g, 42%).

*Characterization data for 24*

**TLC:**  $R_f = 0.28$  (10% methanol in dichloromethane)

**Melting point:** 77-78 °C

**IR (film)/ $\text{cm}^{-1}$ :** 1695 (CO), 3337 (NH)

**$^1\text{H-NMR}$  (400 MHz,  $\text{CDCl}_3$ ):**  $\delta = 6.85$  and  $6.69$  (2s, 8H, ArH-calixarene), 5.32 (s,  $\text{CH}_2\text{Cl}_2$ ), 5.07 (broad s, 2H,  $-\text{CH}_2\text{NHCOOC}(\text{CH}_3)_3$ ), 4.81 (s, 4H,  $-\text{OCH}_2\text{COO}-$ ), 4.63 and 3.16 (AB spin system, 8H,  $-\text{ArCH}_2\text{Ar}-$ ,  $J = 13$  Hz), 4.23 (t, 4H,  $-\text{COOCH}_2\text{CH}_2-$ ,  $J = 6$  Hz), 4.07 and 3.85 (2t, 8H,  $-\text{OCH}_2\text{CH}_2\text{O}-$ ,  $J = 5$  Hz), 3.44 (s, 6H,  $-\text{CH}_2\text{OCH}_3$ ), 3.14 (broad s, 4H,  $-\text{CH}_2\text{CH}_2\text{NH}-$ ), 2.53 (q,  $\text{N}(\text{CH}_2\text{CH}_3)_3$ ), 1.84 (quin, 4H,  $-\text{CH}_2\text{CH}_2\text{CH}_2-$ ,  $J = 6$  Hz), 1.43 (s, 18H,  $-\text{COOC}(\text{CH}_3)_3$ ), 1.32 (t,  $\text{N}(\text{CH}_2\text{CH}_3)_3$ ), 1.13 and 1.01 (2s, 36H,  $-\text{ArC}(\text{CH}_3)_3$ )

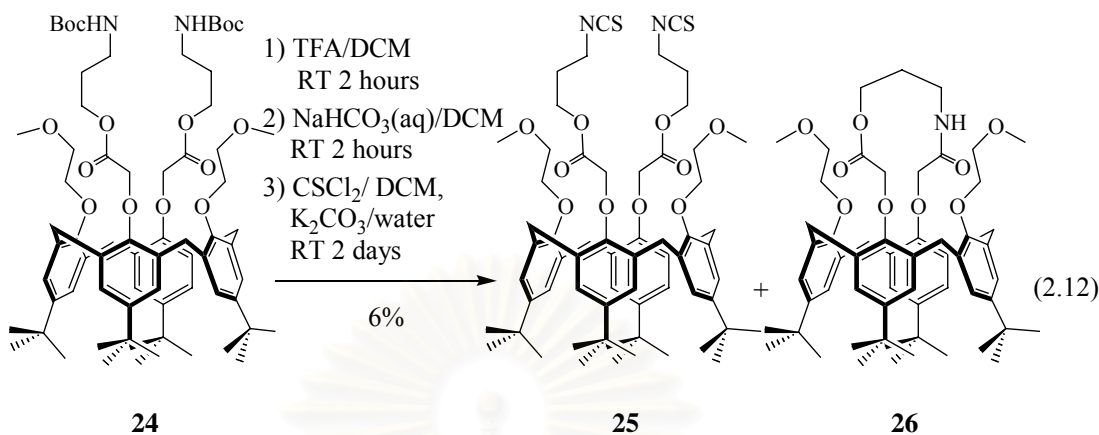
**$^{13}\text{C-NMR}$  (100 MHz,  $\text{CDCl}_3$ ):**  $\delta = 170.69$  (s,  $-\text{NHCOOC}(\text{CH}_3)_3$ ), 155.96 (s,  $-\text{CH}_2\text{COOCH}_2-$ ), 153.07, 152.78, 145.08, 144.72, 133.79, 133.13, 125.34 and 124.88 (8s, aromatic-C), 79.48, 79.06, 72.98, 71.75, 70.84 and 61.72 (6s,  $-\text{OCH}_2\text{CH}_2\text{O}-$  and  $-\text{OCH}_2\text{COOCH}_2\text{CH}_2\text{CH}_2\text{NH}-$ ), 58.50 (s,  $-\text{CH}_2\text{OCH}_3$ ), 33.80 and 33.78 (2s,  $-\text{ArC}(\text{CH}_3)_3$ ), 33.69 (s,  $-\text{ArCH}_2\text{Ar}-$ ), 31.36 and 31.33 (2s,  $-\text{ArC}(\text{CH}_3)_3$ ), 28.92 (s,  $-\text{NHCOOC}(\text{CH}_3)_3$ ), 28.40 (s,  $-\text{NHCOOC}(\text{CH}_3)_3$ )

**LRMS ( $\text{ES}^+$ ):**  $m/z$  (%) = 1217.8 (100)  $[\text{M}+\text{Na}^+]$

**Elemental analysis:** *Anal Calcd.* for  $\text{C}_{70}\text{H}_{102}\text{N}_2\text{O}_{14}\cdot\text{CH}_2\text{Cl}_2\cdot\text{N}(\text{CH}_2\text{CH}_3)_3$ : C, 66.93; H, 8.68; N, 3.04.

*Found.* C, 67.27; H, 8.72; N, 2.95.

5,11,17,23-Tetra-*tert*-butyl-25,27-bis((3-isothiocyanatopropyl)carbonylmethoxy)-26,28-bis(3-oxabutyloxy)calix[4]arene, **25**



To a solution of compound **24** (203 mg,  $2.04 \times 10^{-1}$  mmol) in dichloromethane (10 mL), trifluoroacetic acid (2.5 mL) was added dropwise and the mixture was stirred at room temperature for 2 hours. After the solution was concentrated in vacuum, the residue was dissolved in dichloromethane was washed with sodium hydrogen carbonate solution (2x15 mL) and water (2x15 mL). The organic layer was dried over anhydrous magnesium sulfate and then evaporated to dryness. The yellowish oil was used in the next step without further purification.

The above oily compound was taken up in dichloromethane (7 mL) and then stirred with potassium carbonate (56 mg,  $4.05 \times 10^{-4}$  mol) in water (3 mL). After that, thiophosgene was slowly dropped into the mixture. The reaction was stirred at room temperature for 3 days. After extracting with dichloromethane (2x10 mL), the organic layer was washed with water (2x10 mL), dried over magnesium sulfate, and then the solvent was evaporated to dryness *in vacuo*. Products were obtained by precipitation in methanol. Then they were purified by column chromatography (SiO<sub>2</sub>) using 10% methanol in dichloromethane as eluent to provide two white solids, compound **25** (13 mg, 6%) and compound **26** (5,11,17,23-tetra-*tert*-butyl-25,27-(3-carbonyl-9-carbamoyl-4-propyl-1,11-dimethoxy)-26,28-bis(3-oxabutyloxy)calix[4]arene) (50.2 mg, 27%).

*Characterization data for 25*

**TLC:** R<sub>f</sub> = 0.43 (10% methanol in dichloromethane)



**Melting point:** 118-119 °C (decomposed)

**IR (film)/cm<sup>-1</sup>:** 2092 (NCS), 1758 (CO)

**<sup>1</sup>H-NMR (400 MHz, CDCl<sub>3</sub>):**  $\delta$  = 6.94 and 6.65 (2s, 8H, ArH-calixarene), 4.91 (s, 4H, -OCH<sub>2</sub>COO-), 4.63 and 3.18 (AB spin system, 8H, -ArCH<sub>2</sub>Ar-,  $J$  = 13 Hz), 4.29 (t, 4H, -COOCH<sub>2</sub>CH<sub>2</sub>-,  $J$  = 6 Hz), 4.05 and 3.83 (2t, 8H, -OCH<sub>2</sub>CH<sub>2</sub>O-,  $J$  = 5 Hz), 3.51 (t, 4H, -CH<sub>2</sub>CH<sub>2</sub>NCS,  $J$  = 7 Hz), 3.44 (s, 6H, -CH<sub>2</sub>OCH<sub>3</sub>), 2.01 (quin, 4H, -CH<sub>2</sub>CH<sub>2</sub>CH<sub>2</sub>-,  $J$  = 6 Hz), 1.20 and 0.98 (2s, 36H, -ArC(CH<sub>3</sub>)<sub>3</sub>)

**<sup>13</sup>C-NMR (100 MHz, CDCl<sub>3</sub>):**  $\delta$  = 179.60 (s, -CH<sub>2</sub>NCS), 170.50 (s, -CH<sub>2</sub>COOCH<sub>2</sub>-), 155.96, 152.92, 145.30, 144.78, 134.23, 132.81, 125.53 and 124.88 (8s, aromatic-C), 73.33, 71.92, 70.66, 60.64, 45.97 and 41.85 (6s, -OCH<sub>2</sub>CH<sub>2</sub>O-, -OCH<sub>2</sub>COO- and -COOCH<sub>2</sub>CH<sub>2</sub>CH<sub>2</sub>NCS-), 58.64 (s, -CH<sub>2</sub>OCH<sub>3</sub>), 33.93 and 33.71 (2s, -ArC(CH<sub>3</sub>)<sub>3</sub>), 31.48 and 31.26 (2s, -ArC(CH<sub>3</sub>)<sub>3</sub>), 29.22 (s, -ArCH<sub>2</sub>Ar-)

**LRMS (ES<sup>+</sup>): m/z (%) =** 1101.4 (100) [M+Na]<sup>+</sup>

**Elemental analysis:** *Anal Calcd.* for C<sub>62</sub>H<sub>82</sub>N<sub>2</sub>O<sub>10</sub>S<sub>2</sub>: C, 68.99; H, 7.66; N, 2.60.

*Found.* C, 68.96; H, 7.74; N, 2.62.

*Characterization data for 26*

**TLC:** R<sub>f</sub> = 0.70 (10% methanol in dichloromethane)

**Melting point:** 260-261 °C

**IR (KBr pellet)/cm<sup>-1</sup>:** 1697 (CO), 3343 (NH)

**<sup>1</sup>H-NMR (400 MHz, CDCl<sub>3</sub>):**  $\delta$  = 8.65 (t, 1H, -CH<sub>2</sub>CONHCH<sub>2</sub>-), 7.14 and 7.11 (2s, 4H, ArH-calixarene), 6.50 (dt, 4H, -ArH-,  $^1J$  = 6 Hz,  $^2J$  = 2 Hz), 4.96 (s, 2H, -OCH<sub>2</sub>COO-), 4.91 (s, 2H, -OCH<sub>2</sub>CONH-), 4.74, 4.48, 3.22 and 3.20 (ddd, 8H, -ArCH<sub>2</sub>Ar-,  $J$  = 13 Hz), 4.55 (t, 2H, -COOCH<sub>2</sub>CH<sub>2</sub>-,  $J$  = 5 Hz), 4.17 and 3.61 (ddd, 2H, -OCH<sub>a</sub>H<sub>b</sub>CH<sub>c</sub>H<sub>d</sub>O-,  $^1J$  = 12 Hz,  $^2J$  = 8 Hz,  $^3J$  = 4 Hz), 3.87 and 3.53 (dt, 2H, -OCH<sub>a</sub>H<sub>b</sub>CH<sub>c</sub>H<sub>d</sub>O-,  $^1J$  = 12 Hz,  $^2J$  = 4 Hz), 3.78 (q, 2H, -CH<sub>2</sub>CH<sub>2</sub>CONH-,  $J$  = 5 Hz), 3.41 (s, 6H, -CH<sub>2</sub>OCH<sub>3</sub>), 2.19 (quin, 2H, -CH<sub>2</sub>CH<sub>2</sub>CH<sub>2</sub>-,  $J$  = 5 Hz), 1.36, 1.35 and 0.83 (3s, 36H, -ArC(CH<sub>3</sub>)<sub>3</sub>)

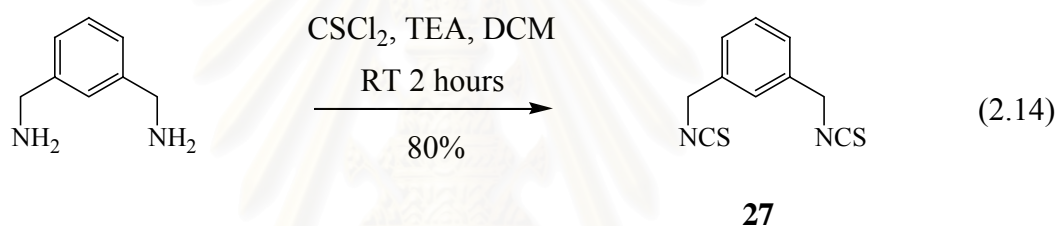
**$^{13}\text{C-NMR}$  (100 MHz,  $\text{CDCl}_3$ ):**  $\delta = 171.77$  (s,  $-\text{CH}_2\text{CONHCH}_2-$ ), 171.93 (s,  $-\text{CH}_2\text{COOCH}_2-$ ), 156.37, 155.84, 151.81, 145.43, 135.03, 134.50, 132.22 and 132.08 (8s, aromatic-C), 126.64, 126.41, 125.59 and 124.72 (4s, aromatic-CH), 75.30 and 71.42 (2s,  $-\text{OCH}_2\text{CH}_2\text{O}-$ ), 74.98 (s,  $-\text{OCH}_2\text{CONH}-$ ), 73.19 (s,  $-\text{OCH}_2\text{COO}-$ ), 65.28 (s,  $-\text{COOCH}_2\text{CH}_2-$ ), 59.39 (s,  $-\text{CH}_2\text{OCH}_3$ ), 40.41 (s,  $-\text{CH}_2\text{CH}_2\text{CONH}-$ ), 34.49, 34.40 and 34.05 (3s,  $-\text{ArC}(\text{CH}_3)_3$ ), 32.08, 32.05 and 31.50 (2s,  $-\text{ArC}(\text{CH}_3)_3$ ), 31.89 (s,  $-\text{ArCH}_2\text{Ar}-$ ), 27.73 (s,  $-\text{CH}_2\text{CH}_2\text{CH}_2-$ )

**LRMS ( $\text{ES}^+$ ):**  $m/z$  (%) = 920.5 (100)  $[\text{M}+\text{H}^+]$  and 942.5 (37)  $[\text{M}+\text{Na}^+]$

**Elemental analysis:** *Anal Calcd.* for  $\text{C}_{57}\text{H}_{77}\text{NO}_9$ : C, 74.40; H, 8.43; N, 1.52.

*Found.* C, 74.26; H, 8.21; N, 1.39.

1,3-Bis(isothiocyanatomethyl)benzene,<sup>[102]</sup> **27**



This procedure was modified from the procedure reported by Gross *et al.*<sup>[102]</sup>

To a mixture of 1,3-bis(aminomethyl)benzene (1.03 g, 1.0 mL, 7.56 mmol) and triethylamine (1.82 g, 2.5 mL, 17.99 mmol) which was stirred in dried dichloromethane (30 mL) for about 15 minutes, the solution of thiophosgene (1.96 g, 1.3 mL, 17.05 mmol) in dried dichloromethane (10 mL) was added dropwise. The reaction mixture was stirred at room temperature for further 2 hours, then the solution was heated at boiling for 1 hour. After evaporating to dryness, the residue was dissolved in dichloromethane and washed with water (2x30 mL). The purified product was eluted from column chromatography ( $\text{SiO}_2$ ) using 20% ethyl acetate in petroleum ethers as eluent to afford a yellow oil (1.34 g, 80%)

*Characterization data for 27*

**TLC:**  $R_f = 0.40$  (20% ethyl acetate in petroleum ethers)

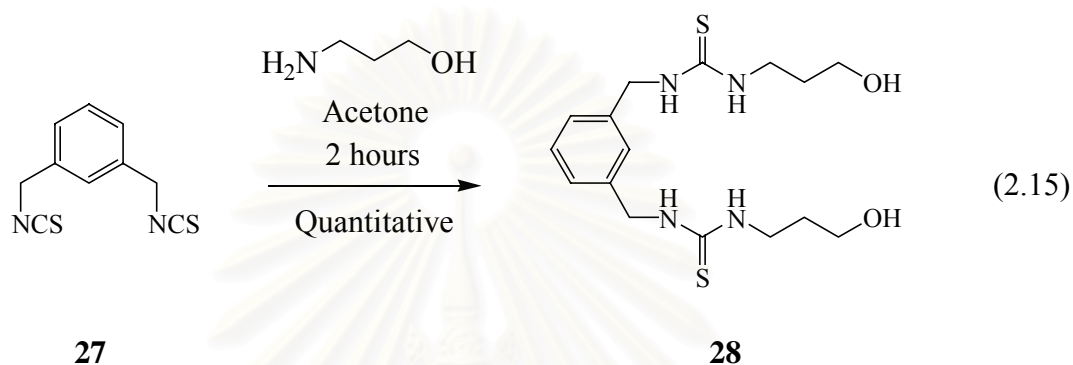
**$^1\text{H-NMR}$  (300 MHz,  $\text{CDCl}_3$ ):**  $\delta = 7.47$ -7.26 (m, 4H,  $-\text{ArH}-$ ), 4.76 (s, 4H,  $-\text{ArCH}_2\text{NCS}$ )

$^{13}\text{C-NMR}$  (75 MHz,  $\text{CDCl}_3$ ):  $\delta = 171.12$  (s,  $-\text{CH}_2\text{NCS}$ ), 135.14, 129.66, 126.78 and 125.20 (4s, aromatic-C), 48.38 (s,  $-\text{ArCH}_2\text{NCS}$ )

**LRMS (ES<sup>+</sup>):**  $m/z$  (%) = 440.9 (4)  $[2\text{M}+\text{H}]^+$

All spectroscopic data are consistent with those reported in the literature.<sup>[103]</sup>

1,3-Bis(*N'*-hydroxypropylthioureidomethyl)benzene, **28**



This procedure was modified from the procedure reported by Benito and co-worker.<sup>[104]</sup>

To a solution of 3-aminopropanol (0.88 g, 0.9 mL, 11.72 mmol) in dried acetone, the solution of compound **27** (1.16 g, 5.27 mmol) was added dropwise. While the reaction mixture was stirred for 2 hours, the white solid precipitated. The solid was filtered off and dried (1.95 g, 100%).

*Characterization data for 28*

**Melting point:** 122-123 °C

**IR (film)/cm<sup>-1</sup>:** 2129 (NCS), 3268 (NH), 3391 (OH)

**$^1\text{H-NMR}$  (400 MHz,  $\text{DMSO-}d_6$ ):**  $\delta = 7.92$  (broad s, 2H,  $-\text{NHCSNHCH}_2\text{Ar-}$ ), 7.58 (broad s, 2H,  $-\text{CH}_2\text{CH}_2\text{NHCSNH-}$ ), 7.41-7.26 (m, 4H,  $\text{ArH-linkage}$ ), 4.74 (broad s, 4H,  $-\text{NHCSNHCH}_2\text{Ar-}$ ), 4.61 (t, 2H,  $-\text{CH}_2\text{CH}_2\text{OH}$ ,  $J = 5$  Hz), 3.55 (t, 4H,  $-\text{CH}_2\text{CH}_2\text{OH}$ ,  $J = 6$  Hz), 3.54 (t, 4H,  $-\text{CH}_2\text{CH}_2\text{NHCSNH-}$ ,  $J = 6$  Hz), 1.75 (quin, 4H,  $-\text{CH}_2\text{CH}_2\text{CH}_2-$ ,  $J = 7$  Hz)

$^{13}\text{C-NMR}$  (100 MHz,  $\text{DMSO-}d_6$ ):  $\delta = 180.70$  (s,  $-\text{HNCSNH}-$ ), 137.52, 126.33, 124.34 and 123.90 (4s, aromatic-C), 56.62 (s,  $-\text{NHCSNHCH}_2\text{Ar}-$ ), 45.06 (s,  $-\text{CH}_2\text{CH}_2\text{OH}$ ), 39.11 (s,  $-\text{CH}_2\text{CH}_2\text{NHCSNH}-$ ), 30.04 (s,  $-\text{CH}_2\text{CH}_2\text{CH}_2-$ )

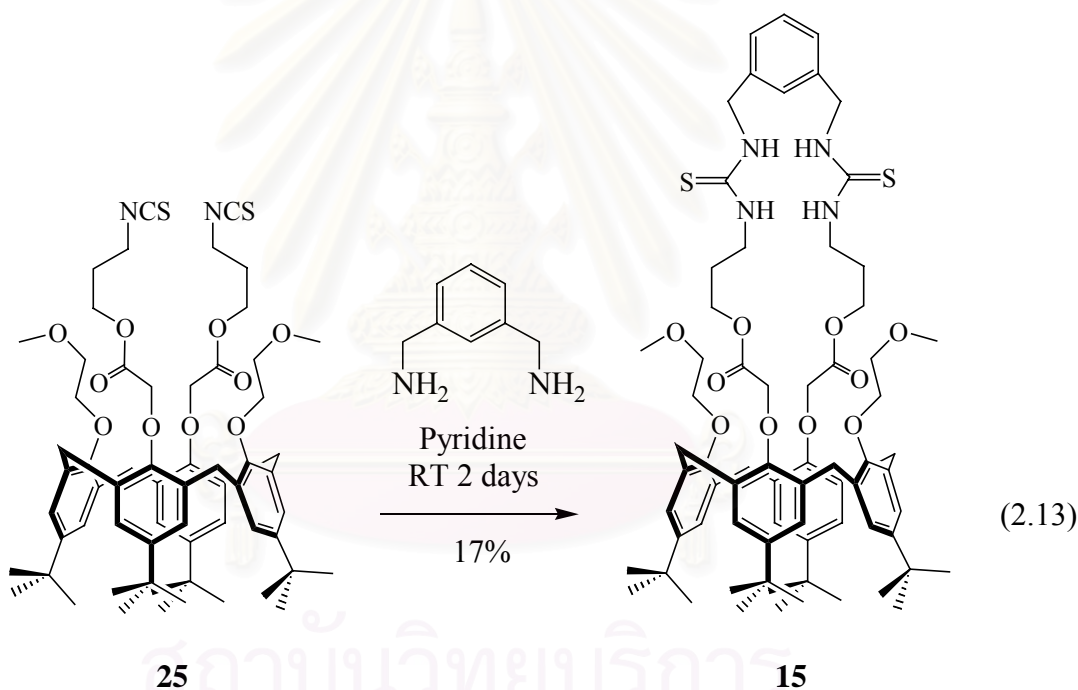
**LRMS ( $\text{ES}^+$ ):**  $m/z$  (%) = 371.1 (22)  $[\text{M}+\text{H}]^+$

**Elemental analysis:** *Anal Calcd.* for  $\text{C}_{16}\text{H}_{26}\text{N}_4\text{O}_2\text{S}_2$ : C, 51.86; H, 7.07; N, 15.12.

*Found.* C, 51.49; H, 7.24; N, 14.79.

5,11,17,23-Tetra-*tert*-butyl-25,27-N,N'-1,3-bis(methoxycarbonylpropylthioureido-methyl)benzene-26,28-bis(3-oxabutyloxy)calix[4]arene, 15

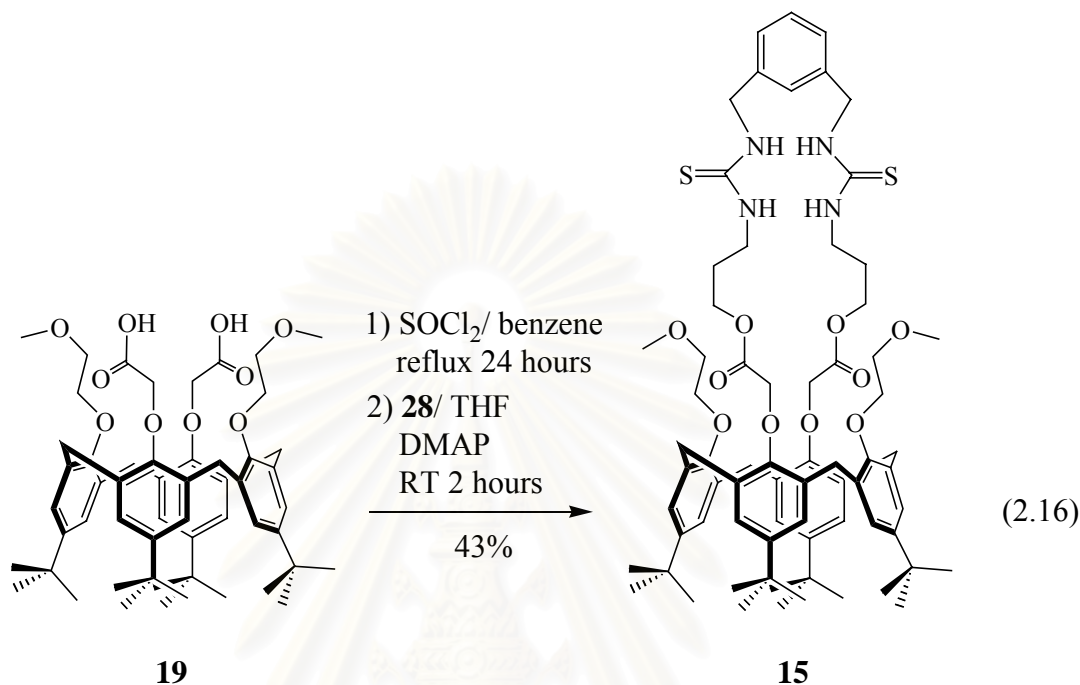
*Method I*



To a solution of 1,3-bis(aminomethyl)benzene (7.2 mg, 7  $\mu\text{L}$ ,  $5.30 \times 10^{-2}$  mmol) in dried pyridine (10 mL), the solution of compound **25** (52 mg,  $4.82 \times 10^{-2}$  mmol) in dried pyridine (5 mL) was slowly dropped for over a period of 12 hours. The reaction mixture was stirred under argon atmosphere at room temperature for further 3 days. After evaporation *in vacuo*, the residue was dissolved in dichloromethane (30 mL) and washed with water (2x30 mL). The organic layer was dried over anhydrous magnesium sulfate and then evaporated under vacuum. The designed product was

purified from column chromatography (SiO<sub>2</sub>) using 10% methanol in dichloromethane as eluent to yield the off-white solid (10.1 mg, 17%).

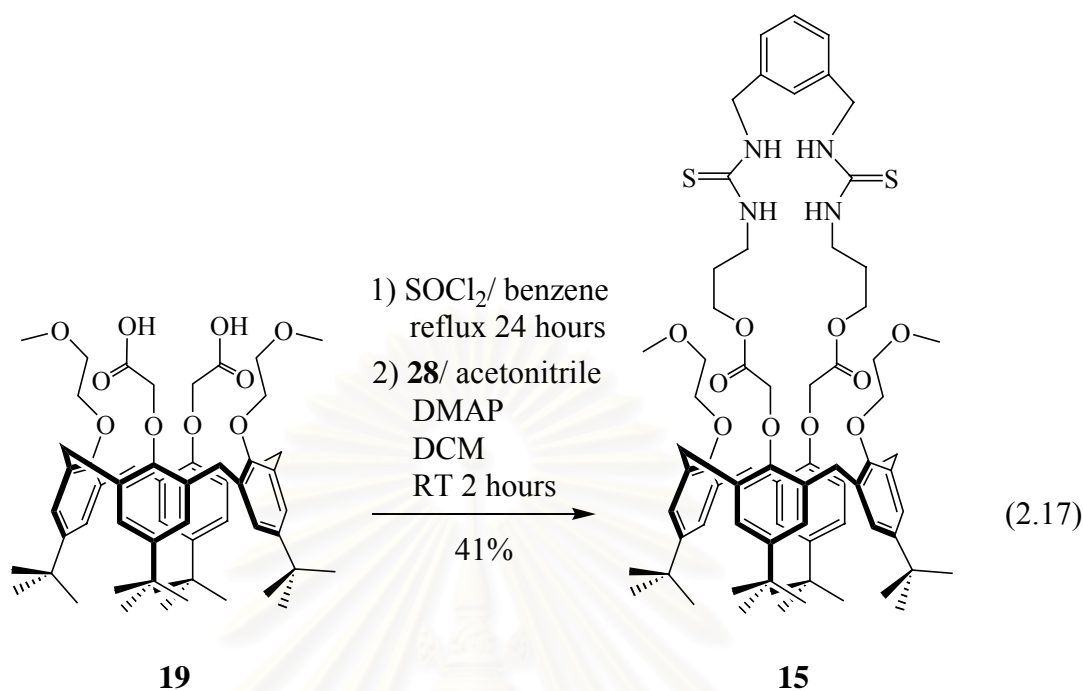
*Method II*



To a solution of compound **19** (50.2 mg,  $5.70 \times 10^{-2}$  mmol) in benzene (2 mL), thionyl chloride (16.3 mg, 10  $\mu$ L,  $1.37 \times 10^{-1}$  mmol) was added. The reaction mixture was heated at reflux for 20 hours under argon atmosphere. After drying *in vacuo*, the white solid was used in the next step without further purification.

To a mixture of compound **28** (23.1 mg,  $6.23 \times 10^{-2}$  mmol) and 4-(dimethylamino)pyridine (15.1 mg,  $1.24 \times 10^{-1}$  mmol) in dried tetrahydrofuran (3 mL), the solution of previous white solid (acid chloride derivative) in dried tetrahydrofuran (2 mL) was added dropwise. The reaction mixture was further stirred under argon atmosphere for 5 hours. After the solid was filtered, the solution was evaporated to dryness. The product was carried out as a white solid from column chromatography (SiO<sub>2</sub>) using 10% methanol in dichloromethane as eluent (29.7 mg, 43%).

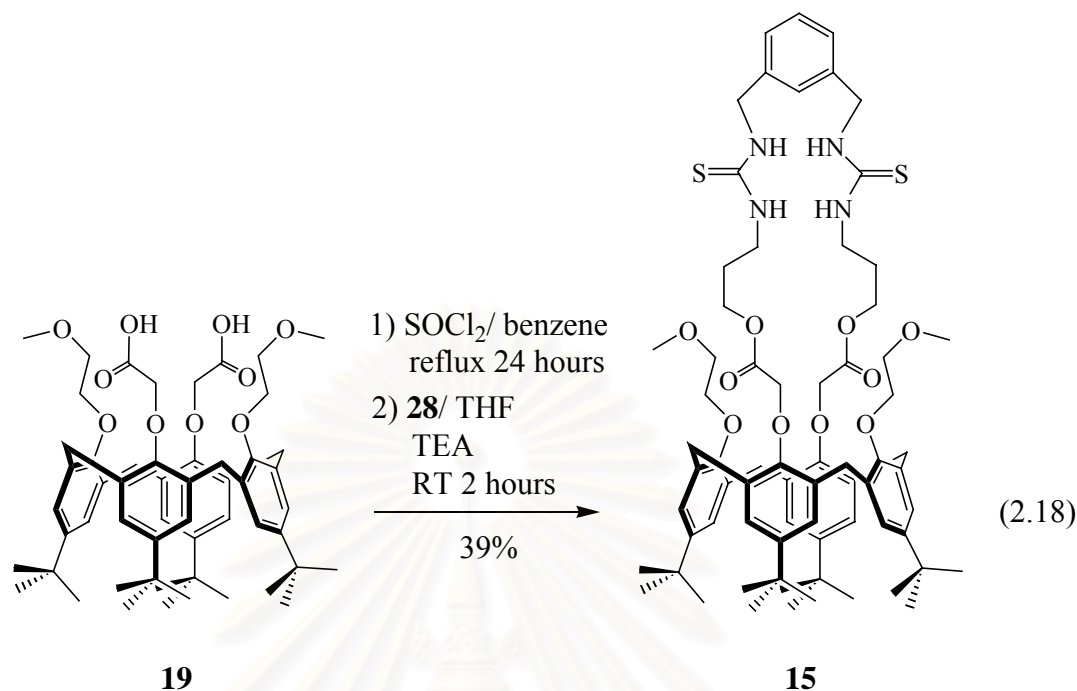
## Method III



To a solution of compound **19** (51.1 mg,  $5.80 \times 10^{-2}$  mmol) in benzene (2 mL), thionyl chloride (16.3 mg, 10  $\mu\text{L}$ ,  $1.37 \times 10^{-1}$  mmol) was added. The reaction mixture was heated at reflux for 20 hours under argon atmosphere. After drying *in vacuo*, the white solid was used in the next step without further purification.

To a warm solution of compound **28** (22.9 mg,  $6.18 \times 10^{-2}$  mmol) and 4-(dimethylamino)pyridine (15.0 mg,  $1.23 \times 10^{-1}$  mmol) in dried acetonitrile (2 mL), the solution of the above white solid (acid chloride derivative) in dried dichloromethane (2 mL) was added dropwise. Then the reaction mixture was stirred for 5 hours. After drying *in vacuo*, the product was obtained as a white solid from column chromatography ( $\text{SiO}_2$ ) using 10% methanol in dichloromethane as eluent (28.9 mg, 41%).

## Method IV



To a solution of compound **19** (50.8 mg,  $5.77 \times 10^{-2}$  mmol) in benzene (2 mL), thionyl chloride (16.3 mg, 10  $\mu$ L,  $1.37 \times 10^{-1}$  mmol) was added. The reaction mixture was heated at reflux for 20 hours under argon. After drying *in vacuo*, the white solid was used in the next step without further purification.

To a mixture of compound **28** (22.7 mg,  $6.13 \times 10^{-2}$  mmol) and triethylamine (14.5 mg, 20  $\mu$ L,  $1.43 \times 10^{-1}$  mmol) in dried tetrahydrofuran (2 mL), the solution of the above white solid (acid chloride derivative) in dried tetrahydrofuran (2 mL) was added dropwise. The reaction mixture was further stirred under argon atmosphere for 5 hours. After the solid was filtered off, the solution was evaporated to dryness. The product was obtained as a white solid from column chromatography (SiO<sub>2</sub>) using 10% methanol in dichloromethane as eluent (27.3 mg, 39%).

*Characterization data for 15*

**TLC:** R<sub>f</sub> = 0.45 (10% methanol in dichloromethane)

**Melting point:** 193-194 °C

**IR (film)/cm<sup>-1</sup>:** 1739 (CO), 2206 (NSC), 3262 (NH)

**$^1\text{H-NMR}$  (400 MHz,  $\text{CDCl}_3$ ):**  $\delta$  = 8.21 (broad s, 2H,  $-\text{CH}_2\text{CH}_2\text{NHCSNH-}$ ), 8.01 (broad s, 2H,  $-\text{NHCSNHCH}_2\text{Ar-}$ ), 7.70-7.09 (m, 4H, ArH-linkage), 7.15 and 7.05 (2s, 8H, ArH-calixarene), 5.31 (s,  $\text{CH}_2\text{Cl}_2$ ), 4.78 (d, 4H,  $-\text{NHCSNHCH}_2\text{Ar-}$ ,  $J = 4$  Hz), 4.65 (t, 4H,  $-\text{COOCH}_2\text{CH}_2-$ ,  $J = 7$  Hz), 4.49 (s, 4H,  $-\text{OCH}_2\text{COO-}$ ), 4.35 and 3.35 (AB spin system, 18H,  $-\text{ArCH}_2\text{Ar-}$ ,  $J = 12$  Hz), 4.08 and 3.55 (2m, 8H,  $-\text{OCH}_2\text{CH}_2\text{O-}$ ), 3.76 (q, 4H,  $-\text{CH}_2\text{CH}_2\text{NHCSNH-}$ ,  $J = 6$  Hz), 3.35 (s, 6H,  $-\text{CH}_2\text{OCH}_3$ ), 2.18 (quin, 4H,  $-\text{CH}_2\text{CH}_2\text{CH}_2-$ ,  $J = 6$  Hz), 1.86 (broad s,  $\text{H}_2\text{O}$ ), 1.18 and 1.10 (2s, 36H,  $-\text{ArC}(\text{CH}_3)_3$ )

**$^{13}\text{C-NMR}$  (100 MHz,  $\text{CDCl}_3$ ):**  $\delta$  = 183.36 (s,  $-\text{NHCSNH-}$ ), 171.23 (s,  $-\text{CH}_2\text{COOCH}_2-$ ), 148.81, 148.71, 148.18, 147.84, 138.37, 138.29, 134.54, 134.39, 128.42, 126.96, 126.42 and 125.91 (12s, aromatic-C (calixarene and linkage)), 75.92 and 69.95 (2s,  $-\text{OCH}_2\text{CH}_2\text{O-}$ ), 72.60 (s,  $-\text{OCH}_2\text{COO-}$ ), 65.02 (s,  $-\text{COOCH}_2\text{CH}_2-$ ), 58.79 (s,  $-\text{CH}_2\text{OCH}_3$ ), 49.13 (s,  $-\text{NHCSNHCH}_2\text{Ar-}$ ), 40.32 (s,  $-\text{CH}_2\text{CH}_2\text{NHCSNH-}$ ), 34.21 and 34.06 (2s,  $-\text{ArC}(\text{CH}_3)_3$ ), 31.27 and 31.15 (2s,  $-\text{ArC}(\text{CH}_3)_3$ ), 29.42 (s,  $-\text{ArCH}_2\text{Ar-}$ ), 27.76 (s,  $-\text{CH}_2\text{CH}_2\text{CH}_2-$ )

**LRMS ( $\text{ES}^+$ ):**  $m/z$  (%) = 1237.3 (100)  $[\text{M}+\text{Na}]^+$

**Elemental analysis:** *Anal Calcd.* for  $\text{C}_{70}\text{H}_{94}\text{N}_4\text{O}_{10}\text{S}_2 \cdot 2\text{H}_2\text{O} \cdot \text{CH}_2\text{Cl}_2$ : C, 63.80;

H, 7.54; N, 4.19

*Found.* C, 64.07; H, 7.86; N, 4.28.

## 2.2 Binding Studies

### 2.2.1 General Procedure

#### 2.2.1.1 Materials

Deuterated acetonitrile was purchased from Apollo<sup>®</sup> and stored over molecular sieves (4 Å). All cations, lithium, sodium and potassium perchlorate, were dried in an oven at 105 °C prior to use. All tetra-*n*-butylammonium (TBA) salts were prepared under normal atmosphere and dried using either a freeze dryer or a rotary evaporator. All compounds were dried *in vacuo* over both silica gel and phosphorus pentoxide prior to use.



### 2.2.1.2 Instrumentation

<sup>1</sup>H-NMR titration experiments were carried out at 200 MHz on a Bruker AC-200 and at 300 MHz on either Bruker AC-300 or Bruker DPX-300. All titration experiments were recorded in acetonitrile-*d*<sub>3</sub> and using a residual proton signal as internal standard.

## 2.2.2 Experimental Procedure

### 2.2.2.1 General Procedure for Determination of Binding Constants: <sup>1</sup>H-NMR Titration

#### 2.2.2.1.1 Cation Complexation

In a typical titration experiment, a stock solution of 0.0025 g (0.0021 mmol) of a host in CD<sub>3</sub>CN (1.1 mL) was prepared. Then, a 600 μL aliquot was transferred to a 5 mm NMR tube. The initial NMR spectrum was recorded. A solution of the alkali salt in the previous host solution was prepared (Table 2.1) and then added *via* microsyringe in 5 μL portions into the NMR tube (Table 2.2). The <sup>1</sup>H-NMR spectrum of each solution was recorded and the chemical shifts of the diagnostic protons obtained at 12-21 different host-guest concentration ratios were plotted against the equivalents of guest added, then the binding constants were calculated using Christopher A. Hunter's 1:1 complexation model program (Department of Chemistry, University of Sheffield, UK).<sup>[105]</sup> In the case of complexation with compound **14**, the binding constant was calculated using integration data<sup>[79]</sup> processing in microsoft excel instead of chemical shift data in the program.

**Table 2.1.** Amounts of alkali cations that used in cation complexation study with compounds **14** and **15**.

Cations	
Name	Weight (g)
Li <sup>+</sup>	0.0010
Na <sup>+</sup>	0.0011
K <sup>+</sup>	0.0013

**Table 2.2.** Volume of the guest stock solution that added in each portion.

Total volume of added alkali ( $\mu\text{L}$ )	Total volume in NMR tube ( $\mu\text{L}$ )	Mole of alkali (mmol)	Mole ratio of alkali:host
0	600	0.00000	0.00
5	605	0.00009	0.08
10	610	0.00019	0.16
20	620	0.00037	0.32
30	630	0.00056	0.48
40	640	0.00075	0.63
50	650	0.00093	0.77
60	660	0.00112	0.91
70	670	0.00131	1.04
80	680	0.00150	1.18
90	690	0.00168	1.30
100	700	0.00187	1.43
120	720	0.00224	1.67
140	740	0.00262	1.89
160	760	0.00299	2.11
180	780	0.00337	2.31
200	800	0.00374	2.50
250	850	0.00467	2.94
300	900	0.00561	3.33
350	950	0.00654	3.68
400	1000	0.00748	4.00

### 2.2.2.1.2 Anion Complexation

Typically, a stock solution of 0.0025 g (0.0021 mmol)\* of a host in  $\text{CD}_3\text{CN}$  (1.1 mL) was prepared (Table 2.3 and Table 2.4). Then, a 600  $\mu\text{L}$  aliquot was transferred to a 5 mm NMR tube. The initial NMR spectrum was recorded. A solution of the guest in the previous host solution was prepared and then added *via* microsyringe in 5  $\mu\text{L}$  portions into the NMR tube. These amounts were increased until completion of complexation of the host. The  $^1\text{H}$ -NMR spectrum of each solution

was recorded and the chemical shifts of the diagnostic protons obtained at 21 different host-guest concentration ratios were plotted against the equivalents of guest added, then the binding constants were calculated using Christopher A. Hunter's 1:1 complexation model program (Department of Chemistry, University of Sheffield, UK).<sup>[105]</sup>

**Table 2.3.** Amounts of tetrabutylammonium salts that used in anion complexation study with compound **14**.

Hosts	Anions	
	Name	Weight (g)
<b>14</b>	CH <sub>3</sub> COO <sup>-</sup>	0.0028
	C <sub>6</sub> H <sub>5</sub> COO <sup>-</sup>	0.0034
	H <sub>2</sub> PO <sub>4</sub> <sup>-</sup>	0.0032
	Ph(H)POO <sup>-</sup>	0.0036
	(PhO) <sub>2</sub> PO <sub>2</sub> <sup>-</sup>	0.0046
	<sup>-</sup> OOC(CH <sub>2</sub> ) <sub>2</sub> COO <sup>-</sup>	0.0056
	<sup>-</sup> OOC(CH <sub>2</sub> ) <sub>3</sub> COO <sup>-</sup>	0.0058
	<sup>-</sup> OOCCH <sub>2</sub> CH(NH <sub>2</sub> )COO <sup>-</sup>	0.0058
	<sup>-</sup> OOC(CH <sub>2</sub> ) <sub>2</sub> CH(NH <sub>2</sub> )COO <sup>-</sup>	0.0059
	H <sub>2</sub> NOCCH <sub>2</sub> CH(NH <sub>2</sub> )COO <sup>-</sup>	0.0035
	H <sub>2</sub> NOC(CH <sub>2</sub> ) <sub>2</sub> CH(NH <sub>2</sub> )COO <sup>-</sup>	0.0036
	C <sub>6</sub> H <sub>5</sub> CH <sub>2</sub> CH(NH <sub>2</sub> )COO <sup>-</sup>	0.0038
	(CH <sub>3</sub> ) <sub>2</sub> CHCH <sub>2</sub> CH(NH <sub>2</sub> )COO <sup>-</sup>	0.0035
	(CH <sub>3</sub> )CH(OH)CH(NH <sub>2</sub> )COO <sup>-</sup>	0.0034
	HOCH <sub>2</sub> CH(NH <sub>2</sub> )COO <sup>-</sup>	0.0033

**Table 2.4.** Amounts of tetrabutylammonium salts that used in anion complexation study with compound **15**.

Hosts	Anions	
	Name	Weight (g)
<b>15</b>	CH <sub>3</sub> COO <sup>-</sup>	0.0056*
	C <sub>6</sub> H <sub>5</sub> COO <sup>-</sup>	0.0034
	H <sub>2</sub> PO <sub>4</sub> <sup>-</sup>	0.0032
	Ph(H)POO <sup>-</sup>	0.0072*
	(PhO) <sub>2</sub> PO <sub>2</sub> <sup>-</sup>	0.0046
	<sup>-</sup> OOC(CH <sub>2</sub> ) <sub>2</sub> COO <sup>-</sup>	0.0056
	<sup>-</sup> OOC(CH <sub>2</sub> ) <sub>3</sub> COO <sup>-</sup>	0.0058
	<sup>-</sup> OOCCH <sub>2</sub> CH(NH <sub>2</sub> )COO <sup>-</sup>	0.0058
	<sup>-</sup> OOC(CH <sub>2</sub> ) <sub>2</sub> CH(NH <sub>2</sub> )COO <sup>-</sup>	0.0059
	H <sub>2</sub> NOCCH <sub>2</sub> CH(NH <sub>2</sub> )COO <sup>-</sup>	0.0035
	H <sub>2</sub> NOC (CH <sub>2</sub> ) <sub>2</sub> CH(NH <sub>2</sub> )COO <sup>-</sup>	0.0036
	C <sub>6</sub> H <sub>5</sub> CH <sub>2</sub> CH(NH <sub>2</sub> )COO <sup>-</sup>	0.0038
	(CH <sub>3</sub> ) <sub>2</sub> CHCH <sub>2</sub> CH(NH <sub>2</sub> )COO <sup>-</sup>	0.0035
	(CH <sub>3</sub> )CH(OH)CH(NH <sub>2</sub> )COO <sup>-</sup>	0.0034
	HOCH <sub>2</sub> CH(NH <sub>2</sub> )COO <sup>-</sup>	0.0032

\*0.0050 g of compound **15** was used in the case of titration with either phenylphosphinate or acetate anion.

### 2.2.2.1.3 Binding Enhancement of Anions in the Presence of Cations

In a typical titration experiment, a stock solution of 0.0025 g (0.0021 mmol) of host and 1 equivalent of NaClO<sub>4</sub> in CD<sub>3</sub>CN (1.1 mL) was prepared (Table 2.5 and Table 2.6). Then, a 600 μL aliquot was transferred to a 5 mm NMR tube. The initial NMR spectrum was recorded. A solution of the guest in the previous host solution was prepared and then added *via* microsyringe in 5 μL portions into the NMR tube. These amounts were increased until completion of complexation of the host. The <sup>1</sup>H-NMR spectrum of each solution was recorded and the chemical shifts of the diagnostic protons obtained at 21 different host-guest concentration ratios were plotted against the equivalents of guest added, then the binding constants were

calculated using Christopher A. Hunter's 1:1 complexation model program (Department of Chemistry, University of Sheffield, UK).<sup>[105]</sup>

**Table 2.5.** Amounts of NaClO<sub>4</sub> and tetrabutylammonium salts that were used in the case of titration with compound **14**.

Host	Guests			
	Cations		Anions	
	Name	Weight (g)	Name	Weight (g)
<b>14</b>	Na <sup>+</sup>	0.00024	CH <sub>3</sub> COO <sup>-</sup>	0.0028
	Na <sup>+</sup>	0.00024	C <sub>6</sub> H <sub>5</sub> COO <sup>-</sup>	0.0034
	Na <sup>+</sup>	0.00024	H <sub>2</sub> PO <sub>4</sub> <sup>-</sup>	0.0032
	Na <sup>+</sup>	0.00024	Ph(H)POO <sup>-</sup>	0.0036
	Na <sup>+</sup>	0.00024	(PhO) <sub>2</sub> PO <sub>2</sub> <sup>-</sup>	0.0046
	Na <sup>+</sup>	0.00024	<sup>-</sup> OOCCH <sub>2</sub> CH(NH <sub>2</sub> )COO <sup>-</sup>	0.0058
	Na <sup>+</sup>	0.00024	<sup>-</sup> OOC(CH <sub>2</sub> ) <sub>2</sub> CH(NH <sub>2</sub> )COO <sup>-</sup>	0.0059

**Table 2.6.** Amounts of NaClO<sub>4</sub> and tetrabutylammonium salts that were used in the case of titration with compound **15**.

Host	Guests			
	Cations		Anions	
	Name	Weight (g)	Name	Weight (g)
<b>15</b>	Na <sup>+</sup>	0.00025	CH <sub>3</sub> COO <sup>-</sup>	0.0028
	Na <sup>+</sup>	0.00025	C <sub>6</sub> H <sub>5</sub> COO <sup>-</sup>	0.0034
	Na <sup>+</sup>	0.00025	H <sub>2</sub> PO <sub>4</sub> <sup>-</sup>	0.0032
	Na <sup>+</sup>	0.00025	Ph(H)POO <sup>-</sup>	0.0036
	Na <sup>+</sup>	0.00025	(PhO) <sub>2</sub> PO <sub>2</sub> <sup>-</sup>	0.0046
	Na <sup>+</sup>	0.00025	<sup>-</sup> OOCCH <sub>2</sub> CH(NH <sub>2</sub> )COO <sup>-</sup>	0.0058
	Na <sup>+</sup>	0.00025	<sup>-</sup> OOC(CH <sub>2</sub> ) <sub>2</sub> CH(NH <sub>2</sub> )COO <sup>-</sup>	0.0059

### 2.2.2.2 General Procedure for Determination of Binding Stoichiometry: Conventional Job's Plots<sup>[106]</sup>

Stock solution of host (0.0050 g) and tetrabutylammonium anion salts in 1.1 mL of CD<sub>3</sub>CN was prepared separately (Table 2.7). In the case of binding enhancement, 1 equivalent of NaClO<sub>4</sub> was added with a solution of a host in this step. Six NMR tubes were filled with 300 μL mixtures of the host and guest solutions in various ratios (Table 2.8). The <sup>1</sup>H-NMR spectrum were recorded and the complex concentrations were calculated as follows:

$$[\text{Host}\cdot\text{Guest}] = [\text{Host}]_{\text{total}} \cdot (\delta_{\text{obs}} - \delta_{\text{host}}) / (\delta_{\text{host-guest}} - \delta_{\text{host}})$$

where  $[\text{Host}]_{\text{total}}$  is the total concentration of the host in solution

$\delta_{\text{obs}}$  is the observed chemical shift

$\delta_{\text{host}}$  is the chemical shift of the observed protons of the host

$\delta_{\text{host-guest}}$  is the chemical shift of the observed protons of the complex

**Table 2.7.** Amounts of NaClO<sub>4</sub> and tetrabutylammonium salts that were used in the Job's plot experiment.

Host	Guests			
	Cations		Anions	
	Name	Weight (g)	Name	Weight (g)
<b>14</b>	Na <sup>+</sup>	0.00050	CH <sub>3</sub> COO <sup>-</sup>	0.00124
<b>15</b>	-	-	HOCH <sub>2</sub> CH(NH <sub>2</sub> )COO <sup>-</sup>	0.00154
<b>15</b>	-	-	H <sub>2</sub> NOCCH <sub>2</sub> CH(NH <sub>2</sub> )COO <sup>-</sup>	0.00159
<b>15</b>	-	-	(CH <sub>3</sub> )CH(OH)CH(NH <sub>2</sub> )COO <sup>-</sup>	0.00148
<b>15</b>	-	-	C <sub>6</sub> H <sub>5</sub> CH <sub>2</sub> CH(NH <sub>2</sub> )COO <sup>-</sup>	0.00167
<b>15</b>	Na <sup>+</sup>	0.00050	Ph(H)POO <sup>-</sup>	0.00158

**Table 2.8.** Volume of solution of hosts and anions in each NMR tube.

Host		Anion		Mole ratio host: anion
Volume ( $\mu\text{L}$ )	Mole (mmol)	Volume ( $\mu\text{L}$ )	Mole (mmol)	
300	0.00124	0	0.00000	1.00:0.00
240	0.00090	60	0.00022	1.00:0.24
180	0.00067	120	0.00045	1.00:0.67
150	0.00056	150	0.00056	1.00:1.00
120	0.00045	180	0.00067	0.67:1.00
60	0.00022	240	0.00090	0.24:1.00
0	0.00000	300	0.00124	0.00:1.00



สถาบันวิทยบริการ  
จุฬาลงกรณ์มหาวิทยาลัย

## CHAPTER III

### RESULTS AND DISCUSSION

#### 3.1 Synthesis of Heteroditopic Receptors

It is our interest to combine a *p-tert*-butylcalix[4]arene framework with a cage constructing unit to form an interesting compound that can simultaneously bind metal ions and anions. Ligands **14** and **15** are ditopic ion receptors possessing a cavity of phenolic oxygen donors similar to a cryptand<sup>[107]</sup> providing a cage to accommodate an alkali cation *via* ion-dipole interactions. In addition, both macromolecules contain thiourea moieties as neutral anion receptors which are well-known to bind anions especially Y-shaped carboxylate anion by means of hydrogen bonding interactions. Thus both receptors **14** and **15** can possibly exhibit appealing host-guest binding with both cations and anions. All calix[4]arenes containing thiourea that mentioned in Chapter I<sup>[80-81]</sup> are not cyclic compounds. The cyclic molecule is expected to display an advantage in terms of selectivity. Therefore, compounds **14** and **15** were synthesized and their binding abilities with cations and anions were investigated.

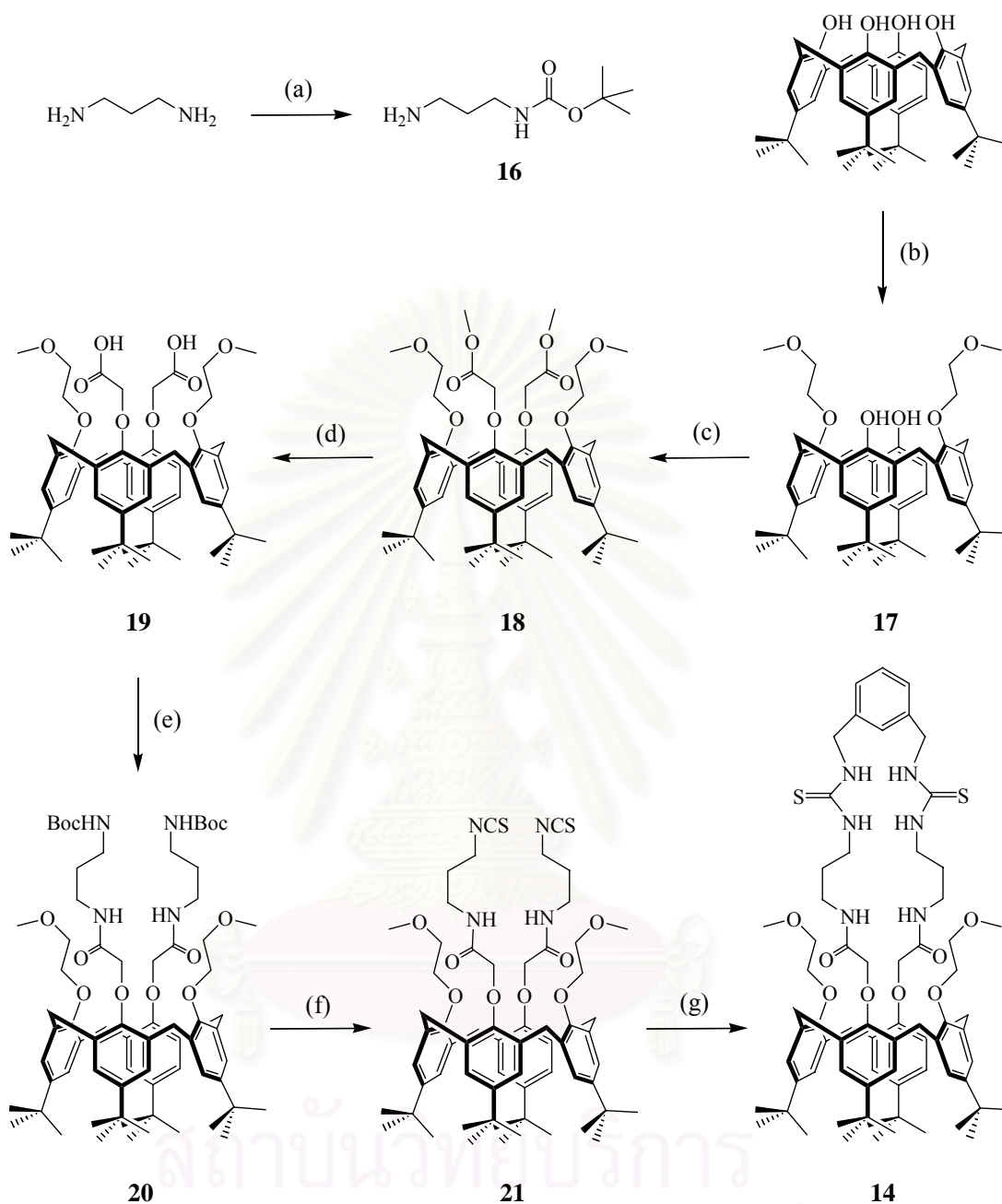
##### 3.1.1 Synthesis and Characterization of Receptor 14

The synthesis of host **14** was carried out *via* 6 steps from *p-tert*-butylcalix[4]arene in 3.7% overall yield as shown in Scheme 3.1.

สถาบันวิทยบริการ  
จุฬาลงกรณ์มหาวิทยาลัย



**Scheme 3.1.** Synthetic scheme for calix[4]arene amide receptor **14**.\*



\*Reagents and conditions: (a) di-*tert*-butyl dicarbonate, DCM, RT, 24 hours, 93%; (b) 2-bromoethyl methyl ether,  $K_2CO_3$ , ACN, reflux, 36 hours, 73%; (c) methyl bromoacetate,  $Na_2CO_3$ , ACN, reflux, 24 hours, 70%; (d) NaOH, EtOH, reflux, 24 hours, 70%; (e) i.  $SOCl_2$ , benzene, reflux, 24 hours, ii. **16**, TEA, DMAP, toluene, RT, 24 hours, 42%; (f) i. TFA, DCM, RT, 2 hours, ii.  $NaHCO_3$  (aq), DCM, RT, 2 hours, iii.  $CSCl_2$ ,  $K_2CO_3$  (aq), DCM, RT, 2 days, 62%; (g) 1,3-bis(aminomethyl)-benzene, pyridine, RT, 2 days, 40%.

In the first step, disubstituted compound **17** was prepared by a nucleophilic substitution of *p*-*tert*-butylcalix[4]arene and 2.5 equivalents of 2-bromoethyl methyl ether using potassium carbonate as base in acetonitrile at reflux for 36 hours. The product was purified by column chromatography using 5% ethyl acetate in dichloromethane as eluent to gain 73% yield of the product. The condition that used 2-ethoxyethyl tosylate as a reagent and refluxed for a longer time would improve the yield up to 82%.<sup>[108]</sup> The formation of derivative **17** was indicated by the arising of two triplet of  $-OCH_2CH_2O-$  signals at 4.06 and 4.33 ppm and one singlet of  $-CH_2OCH_3$  at 3.72 ppm. Moreover, the spectrum also displayed typical signals of disubstituted *p*-*tert*-butylcalix[4]arene at the opposite phenol units (two singlets with an equal of integration (4H:4H) at 7.08 and 7.23 ppm belonging to *ArH*-calixarene and two singlets with an integral of 18H:18H corresponding to  $-ArC(CH_3)_3$  at 1.23 and 1.47 ppm). Additionally, the doublet of doublet signals at 3.50 and 4.58 ppm owing to the methylene bridge protons on the lower rim with a coupling constant of 13 Hz indicated that this compound oriented in a cone conformation.<sup>[109-110]</sup>

The excess of methyl bromoacetate was reacted with the rest of phenolic-*OH* moieties of **17** in the presence of sodium carbonate as a base in acetonitrile at reflux for a day. After the residue was purified by column chromatography using 10% ethyl acetate in dichloromethane, the tetrasubstituted compound **18** was obtained in 70% yield. According to the literature, other bases and solvents such as sodium hydride in tetrahydrofuran,<sup>[111]</sup> sodium hydride in dimethylformamide,<sup>[112-113]</sup> sodium hydride in tetrahydrofuran and dimethylformamide,<sup>[97]</sup> sodium butoxide ( $NaOBu^t$ ) in tetrahydrofuran and dimethylformamide<sup>[94]</sup> could be used to produce this product. Compared to other conditions using different bases and solvents, the condition that used in this experiment was easy to work up and resulted in high yield of the desired product. <sup>1</sup>H-NMR data of derivative **18** displayed signals of  $-CH_2COOCH_3$  at 3.77-3.80 ppm and  $-OCH_2COO-$  at 4.74-4.75, 4.82-4.83 and 4.96-4.97 ppm in place of the  $-ArOH$  signal. In addition, the infrared spectra exhibited the absence of broad OH and the arising of sharp CO at  $1762\text{ cm}^{-1}$ . Even though the <sup>1</sup>H-NMR and <sup>13</sup>C-NMR spectra of compound **18** showed complicated spectra due to the mixed conformation in chloroform-*d* solution, the structure of this product was confirmed by electrospray mass spectrometry, infrared spectrophotometry, melting point and elemental analysis. Moreover, acid derivative **19**, which was afforded from treating **18** with sodium

hydroxide in ethanol at reflux for 24 hours, was in a cone conformation. This was signified by the coupling constant of the methylene bridge signal ( $J = 13$  Hz).<sup>[109-110]</sup> The structure of **19** was easily diagnosed by the typical symmetry pattern for *p*-*tert*-butylcalix[4]arene derivatives in <sup>1</sup>H-NMR spectra. The absence of  $-\text{CH}_2\text{COOCH}_3$  signal in <sup>1</sup>H-NMR spectra and the appearance of broad OH signal at  $3252\text{ cm}^{-1}$  in the infrared spectra supported the existence of product. Compared to tetrasubstituted calixarene derivative **18**, either its starting material **17** or subsequent product **19** showed well-defined <sup>1</sup>H-NMR spectra of cone conformation. This may be stemmed from the disappearance of intramolecular hydrogen bonding in macromolecule **18**. In addition, the ethyl methyl ether chains were probably not steric enough for protecting the rotation of aromatic unit on calixarene building block. Therefore, the unexpected conformational behavior was observed in both <sup>1</sup>H- and <sup>13</sup>C-NMR spectra of tetrasubstituted calixarene **18**.

The acid derivative **19** was then transformed to acid chloride derivative using thionyl chloride in benzene at reflux for 24 hours. Previously, this reaction was carried out with other reagents and solvents (Table 3.1) but thionyl chloride and benzene yielded a better product in the case of quantity and quality due to the strongest vigorous condition (highest temperature). In spite of a broad NMR spectra, the intermediate compound was assigned by the downfield shift of  $-\text{OCH}_2\text{COCl}$  signal (from 4.76 to 5.47 ppm) affecting by the presence of the acid chloride group instead of the carboxylic acid ( $-\text{OCH}_2\text{COOH}$ ). Attributed to the unstable property of this intermediate, only characteristic <sup>1</sup>H-NMR and <sup>13</sup>C-NMR spectrum were used as tools for characterization and this step must be done immediately prior to use.<sup>[114]</sup> After that, this acid chloride was condensed with boc-protecting diaminopropane **16** which prepared in toluene using triethylamine as organic base and 4-(dimethylamino)pyridine as a catalyst at room temperature for 24 hours according to the procedure reported in the literature.<sup>[98-99]</sup> The purified product **20** was obtained in 42% yield. In the absence of 4-(dimethylamino)pyridine, only 23% of the product was received. This implied that, 4-(dimethylamino)pyridine acted as a catalyst in this reaction. The <sup>1</sup>H-NMR spectrum showed a broad signal of  $-\text{CH}_2\text{CONHCH}_2-$  at 6.55 ppm and  $-\text{CH}_2\text{NHCOOC}(\text{CH}_3)_3$  at 8.33 ppm which were confirmed by COSY and deuterium exchanged experiment as well as an additional signal of boc-protecting moiety ( $-\text{COOC}(\text{CH}_3)_3$ ) at 1.43 ppm accompanied with two *t*-butyl signal of the

calixarene scaffold (0.89 and 1.28 ppm). In addition, the infrared spectra displayed the signal of CO (1695  $\text{cm}^{-1}$ ) and NH (3347  $\text{cm}^{-1}$ ).

**Table 3.1.** Product yields of the conversion of the acid **19** to the acid chloride under various conditions.

Conditions		Percentage yield of acid chloride derivative (%)
Reagents	Solvents	
(COCl) <sub>2</sub>	DCM and DMF	57
(COCl) <sub>2</sub>	-	55
SOCl <sub>2</sub>	DCM	85
SOCl <sub>2</sub>	benzene	99

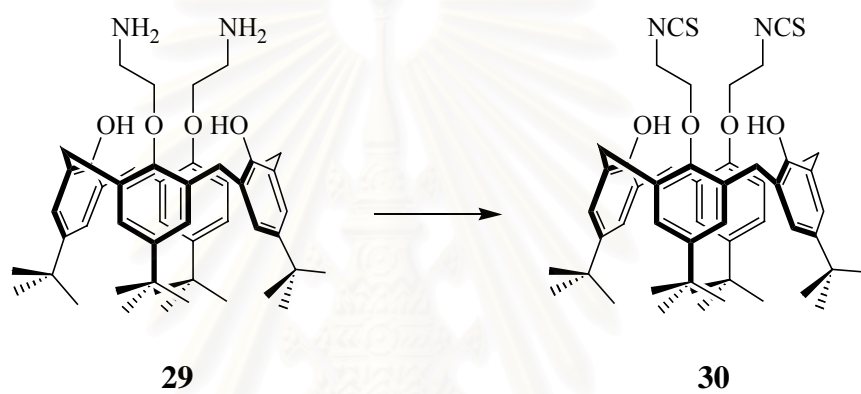
In the next step, the protecting group was deprotected by trifluoroacetic acid at room temperature for 2 hours to obtain trifluoroacetate salt. Then the salt was extracted with sodium hydrogen carbonate solution and dichloromethane. After removal of the solvent, amine **31** was obtained. It was further reacted with thiophosgene using potassium carbonate in aqueous solution as a base to afford thiocyanate **21** in 62% yield after purification by a column chromatography (10% methanol in dichloromethane). Other bases as shown in Table 3.2 were also used. Barium carbonate gave a low percent yield while sodium hydrogencarbonate did not give the desired product at all. This could be ascribed by the basicity of inorganic base ( $\text{K}_2\text{CO}_3 > \text{Ba}_2\text{CO}_3 > \text{NaHCO}_3$ ). The product had characteristic signals of  $-\text{CH}_2\text{NCS}$  in the infrared spectra (2105  $\text{cm}^{-1}$ ) and a highest molecular mass at 1099.4 according to  $[\text{M}+\text{Na}]^+$  species.

**Table 3.2.** Product yields of the conversion of the amine to the thiocyanate **21** under various conditions.

Base	Percentage yield (%)
NaHCO <sub>3</sub>	0
Ba <sub>2</sub> CO <sub>3</sub>	40
K <sub>2</sub> CO <sub>3</sub>	62

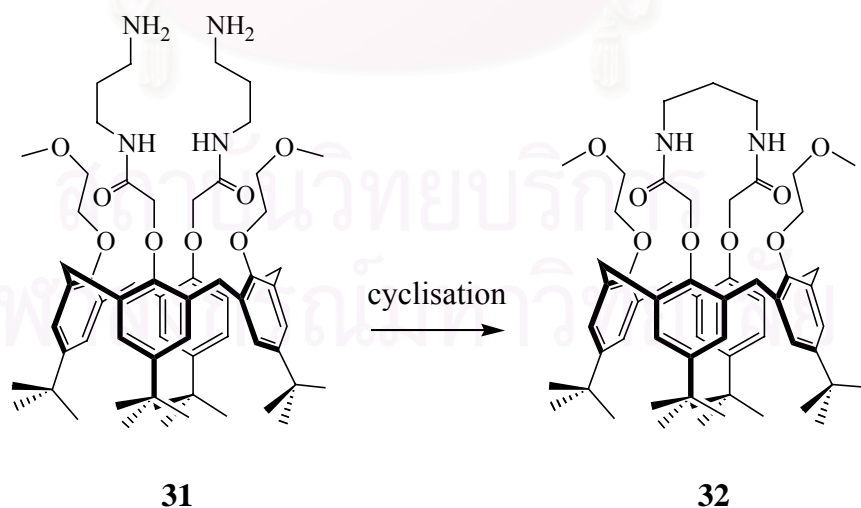
Compared to thiocyanate **30** (Scheme 3.2) which prepared from compound **29** using potassium carbonate as base, a much lower yield was obtained in our case.<sup>[115]</sup> The unstable primary amine in intermediate **31** could attack the carbonyl group of the opposite substituent. Thus, after deprotecting, some of compound **31** was cyclised to gain a cyclic compound **32** (Scheme 3.3) and 1,3-diaminopropane before treating with thiophosgene. The existence of compound **26** is an evidence to support this assumption (*see* Section 3.1.2).

**Scheme 3.2.** Synthetic scheme of 5,11,17,23-tetra-*tert*-butyl-26,28-dihydroxy-25,27-bis(2-isothiocyanoethoxy)calix[4]arene from its amine analogue.\*



\*Reagent and condition:  $\text{CSCl}_2$ ,  $\text{BaCO}_3$ , DCM, RT, 24 hours, 96%.<sup>[115]</sup>

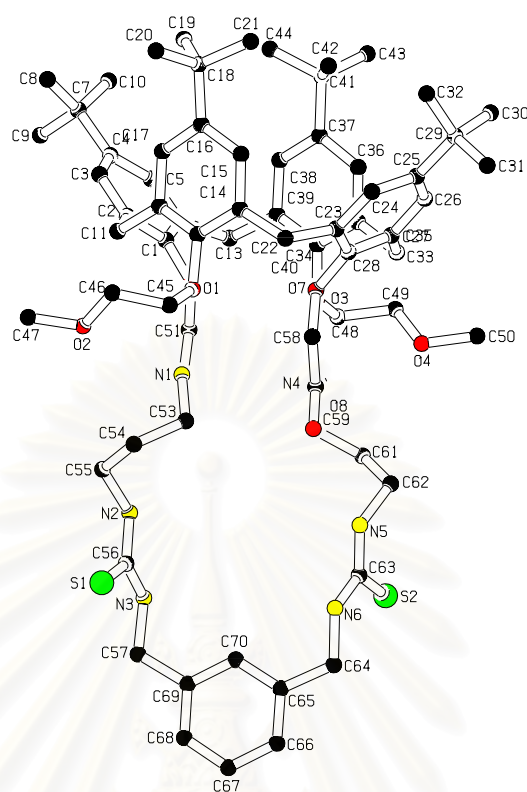
**Scheme 3.3.** Proposed by-product during the preparation of the thiocyanate **21**.



From the literature, the isothiocyanates were readily transformed to the corresponding symmetric  $N,N'$ -disubstituted thioureas by a simple treatment with pyridine-water.<sup>[116]</sup> Therefore, the last step was carried out by treating compound **21**

with 1,3-bis(aminomethyl)benzene in pyridine at room temperature for 2 days. Separation of the desired product by a column chromatography using 10% methanol in dichloromethane as an eluent gave bis-thiourea calix[4]arene amide **14** in 40% yield. The symmetrical structure of molecule **14** resulted in a well-defined  $^1\text{H-NMR}$  spectra. The spectrum showed broad singlets of both  $-\text{NHCSNHCH}_2\text{Ar}-$  at 6.66 ppm and  $-\text{CH}_2\text{CH}_2\text{NHCSNH}-$  at 7.58 ppm. The signal of  $-\text{CH}_2\text{CH}_2\text{NHCSNH}-$  at 3.61 ppm and the signal of  $-\text{HNCSNHCH}_2\text{Ar}-$  at 4.75 ppm as well as signals of  $\text{ArH}$ -linkage in aromatic region indicating by the integration were observed in the spectrum. The characteristic signal of thiourea appeared at 182.03 ppm in the  $^{13}\text{C-NMR}$  spectrum and  $2206\text{ cm}^{-1}$  in the infrared spectrum.

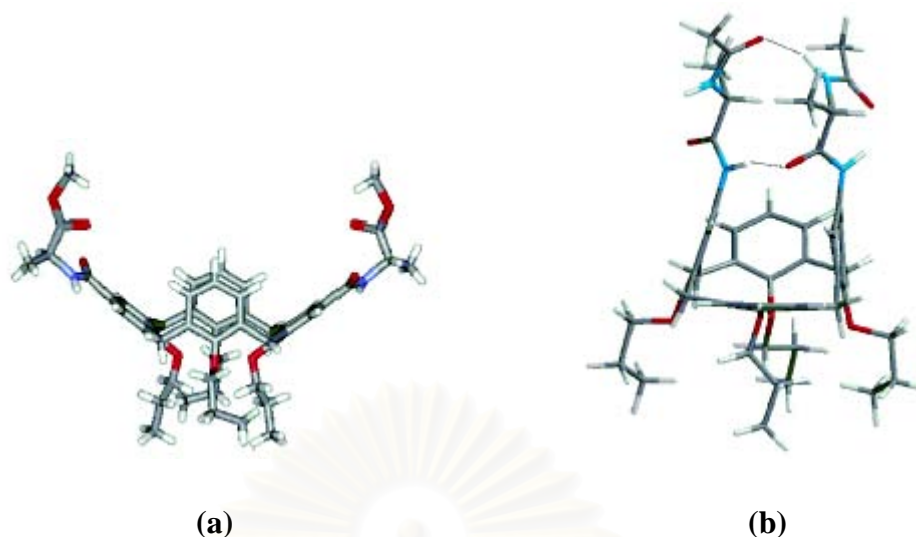
This reaction was also done at  $60\text{ }^\circ\text{C}$ , compound **14** was obtained in higher yield (60%) but it existed as a mixture of at least two conformations in either chloroform-*d* or methanol-*d*<sub>4</sub> solution. Nevertheless, a rod crystal of size  $0.26 \times 0.08 \times 0.06$  mm was obtained from this condition. Crystal of ligand **14** was clear and colorless. Single rod crystal of receptor **14** was obtained by rapidly cooling a methanol solution to gain a small crystal and consequently by slowly cooling this solution to grow the crystal. X-ray crystallographic analysis produced the crystal structure shown in Figure 3.1.



**Figure 3.1.** Crystal structure of **14** with the common numbering scheme.

The hydrogen atoms are omitted for clarity. The structure is solvated by one molecule of methanol and two molecules of pyridine. The x-ray structure of this desired product **14** is in  $C_2$  symmetry. The crystal data and details of data collection together with structure refinement are displayed in Appendix A.

The crystal structure indicates that compound **14** adopts a closed flattened cone conformation<sup>[117]</sup> which is a type of the pinch cone conformations to reduce the steric strain of the macromolecule. The closed flattened cone conformation is defined as the pinched cone conformation that 2 aromatic units of the calixarene building block which contain larger substituted group are parallel while other 2 units composed of smaller substituents are flattened. *Vice versa*, two aromatic units with the larger substituents are flattened while the rest of them are parallel in an open flattened cone conformation (Figure 3.2). Receptor **14** hardly exists in an open flattened cone conformation due to the presence of bis-thiourea linkage.

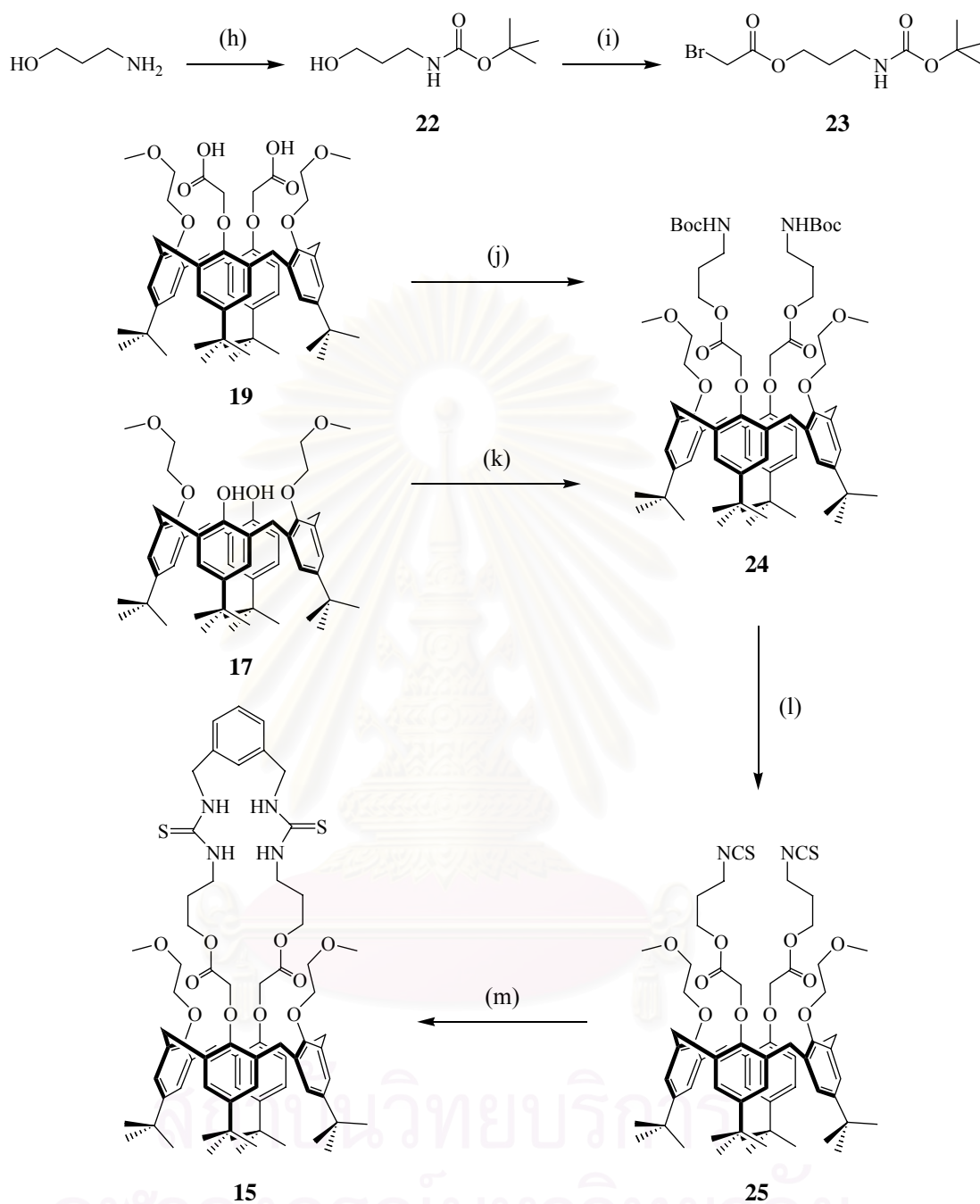


**Figure 3.2.** Examples of an open (a) and a closed (b) flattened cone conformation of calix[4]arene derivatives.<sup>[117]</sup>

### 3.1.2 Synthesis and Characterization of Receptor 15

The analogous derivative **15** was synthesized by the similar procedure as host **14** *via* either 6 steps (0.2%) or 4 steps (0.3%) (Scheme 3.4). The aim of this synthesis is to compare the functional group specificity towards the interaction between the ester donor and cations with the interaction between the amide donor and cations in the case of derivative **14**.



**Scheme 3.4.** Synthetic scheme for calix[4]arene ester receptor **15**.\*

\*Reagents and conditions: (h) di-*tert*-butyl dicarbonate, TEA, DCM, RT, 24 hours, 97%; (i) bromoacetyl bromide, TEA, toluene, RT, 5 hours, 45%; (j) i. SOCl<sub>2</sub>, benzene, reflux, 24 hours, ii. **22**, TEA, DMAP, toluene, RT, 24 hours, 59%; (k) **23**, K<sub>2</sub>CO<sub>3</sub>, NaI, acetone, reflux, 4 days, 42%; (l) i. TFA, DCM, RT, 2 hours, ii. NaHCO<sub>3</sub>(aq), DCM, RT, 2 hours, iii. CSeCl<sub>2</sub>, K<sub>2</sub>CO<sub>3</sub>(aq), DCM, RT, 4 days, 6%; (m) 1,3-bis(aminomethyl)benzene, pyridine, RT, 2 days, 17%.

First, the starting material for compound **24** was the acid chloride derivative which was prepared by the same procedure as previously mentioned. After that, this acid chloride was coupled with compound **22** which was prepared according to the literature<sup>[100]</sup> in toluene using triethylamine as an organic base and 4-(dimethylamino)pyridine as a catalyst. After purifying by column chromatography using 5% methanol in dichloromethane as eluent, product **24** was obtained in 59% yield. Column chromatography in this step needed to be neutralized by a few drops of triethylamine and the product needed to be separated immediately. Otherwise the desired product was transformed to another compound such as polymer. The <sup>1</sup>H-NMR spectrum showed a broad singlet of  $-\text{CH}_2\text{NHCOOC}(\text{CH}_3)_3$  at 5.07 ppm, a triplet of  $-\text{COOCH}_2\text{CH}_2-$  at 4.23 ppm, a broad singlet of  $-\text{CH}_2\text{CH}_2\text{NH}-$  at 3.14 ppm, a quintet of  $-\text{CH}_2\text{CH}_2\text{CH}_2-$  at 1.84 ppm and a singlet of  $-\text{COOC}(\text{CH}_3)_3$  at 1.43 ppm as well as the typical signals of *p-tert*-butylcalix[4]arene molecule.

Alternatively, compound **24** was able to prepare from a substitution reaction of compound **17** and compound **23** using 2.3 equivalents of base, potassium carbonate, and a catalytic amount of sodium iodide. The same product which was characterized by <sup>1</sup>H-NMR spectroscopy and electrospray mass spectroscopy was separated by column chromatography in 42% yield. Although this step gave the lower yield, the total yield was higher (old route: 21%, new route: 31%). The second procedure was thus the optimum condition and was used to prepare **24**.

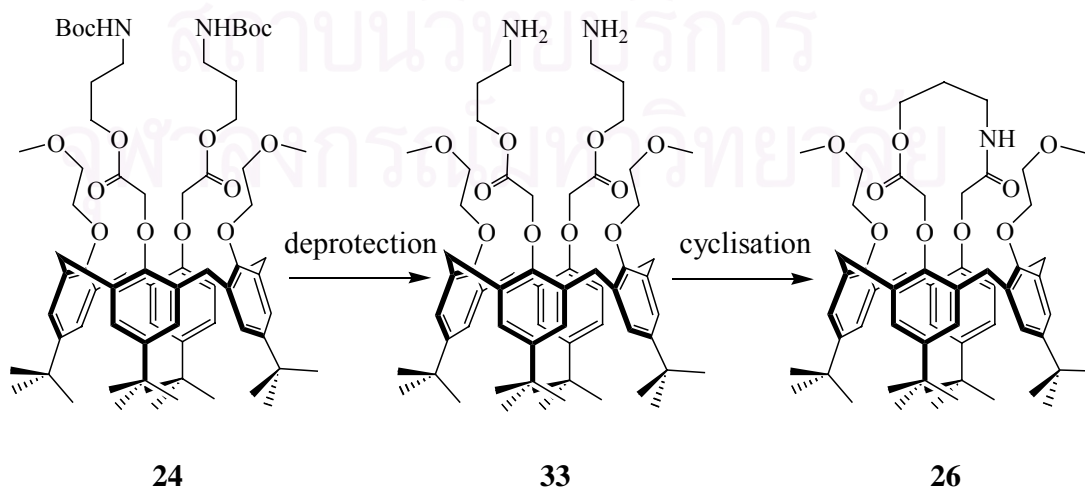
Subsequently, the trifluoroacetate salt was yielded by treating the boc-protecting compound **24** with trifluoroacetic acid at room temperature for 2 hours. After that, the salt was extracted with sodium hydrogen carbonate solution and dichloromethane to yield amine derivative **33**. Then, it was reacted with thiophosgene using potassium carbonate in an aqueous solution as base to yield thiocyanate derivative **25**. After separation by column chromatography (10% methanol in dichloromethane), the desired product was obtained in only 6% yield. Unfortunately, the much lower yield was obtained in this step compared to that of compound **21**. This can be explained in the similar manner as compound **31** and **32**. The reactive primary amine moiety in compound **33** led to a chiral compound **26** (Scheme 3.5). Chiral molecule **26** was eluted from column chromatography before compound **25** due to its less polarity. In the case of di-thiocyanate macromolecule **25**, the signals of  $-\text{CH}_2\text{NHCOO}(\text{CH}_3)_3$  in <sup>1</sup>H-NMR spectra disappeared while the characteristic signal

of  $-\text{CH}_2\text{NCS}$  was found at 179.60 ppm in  $^{13}\text{C}$ -NMR spectra. The absorption band at  $2092\text{ cm}^{-1}$  according to NCS functionality in the infrared spectrum supported the proposed structure. Chiral compound **26** was fully characterized by all techniques to support the structure. Compared to derivative **25**,  $^1\text{H}$ -NMR and  $^{13}\text{C}$ -NMR spectrum of compound **26** was more complicated owing to the chirality playing a role to the symmetry of its molecule. The NMR spectrum contained a signal of  $-\text{CH}_2\text{CONHCH}_2-$  at 8.65 ppm with integration for only one proton in the proton type. There was no  $-\text{CH}_2\text{NCS}$  signal in the spectra but a signal of  $-\text{CH}_2\text{CONHCH}_2-$  at 177.77 and a signal of  $-\text{CH}_2\text{COOCH}_2-$  at 171.93 ppm were found in the  $^{13}\text{C}$ -NMR spectrum. The structure of both compounds **25** and **26** were confirmed by LRMS and elemental analysis. Unlike compound **25** or the others, the major peak in the electrospray mass spectra of chiral **26** was the molecular mass of monomer and proton  $[\text{M}+\text{H}]^+$ , not the molecular mass of monomer and sodium ion  $[\text{M}+\text{Na}]^+$ . Another base was also used to improve the yield of compound **25** (Table 3.3), but potassium carbonate produced a better percentage yield because of the stronger basicity.

**Table 3.3.** Product yields of the conversion of the amine to the thiocyanate **25** under various conditions.

Base	Percentage yield (%)
$\text{Ba}_2\text{CO}_3$	0
$\text{K}_2\text{CO}_3$	6

**Scheme 3.5.** The unexpected reaction during preparation of thiocyanate **25**.



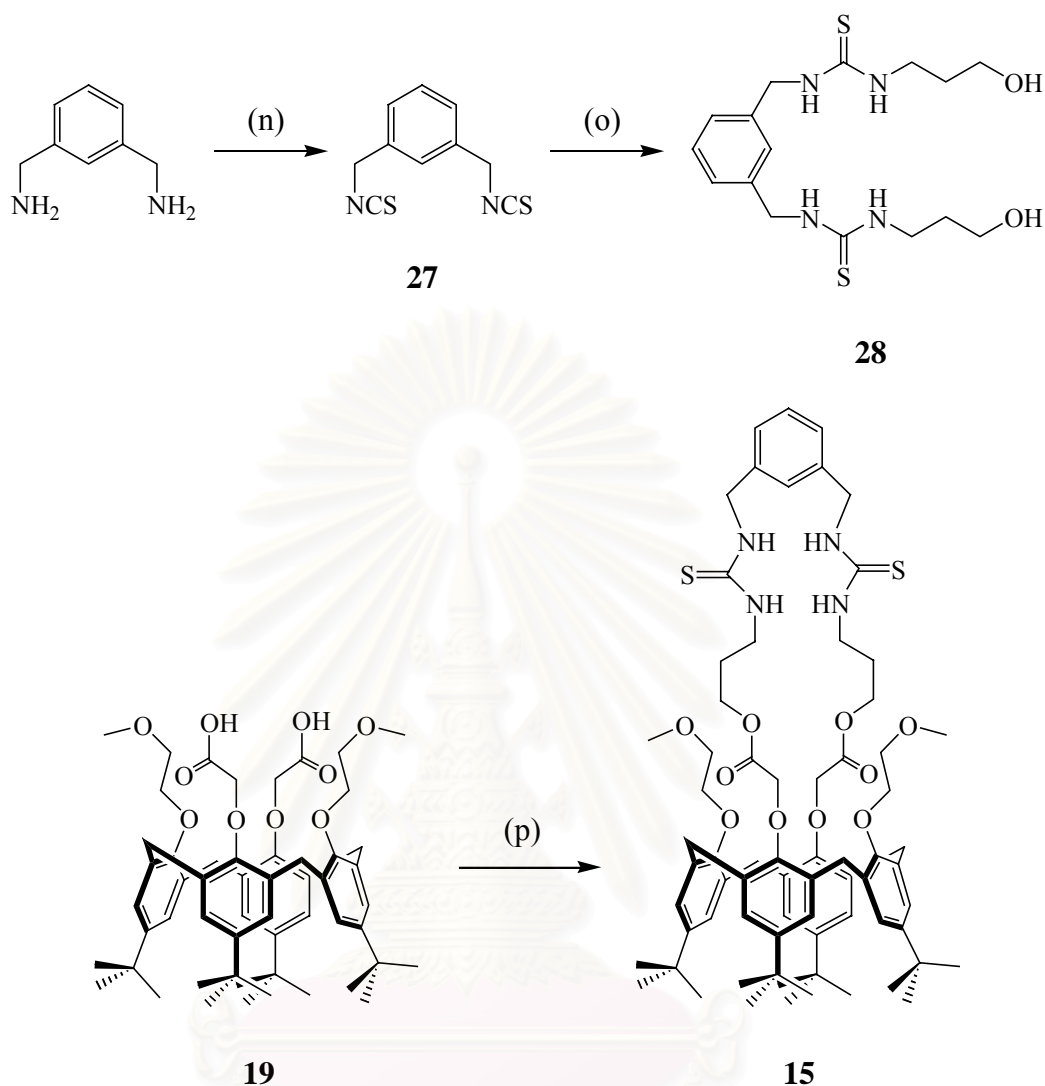
Finally, the last step was carried on by converting di-thiocyanate **25** to host **15** by stirring with 1,3-bis(aminomethyl)benzene in pyridine at room temperature for 2 days. The desired product was eluted in 17% yield from column chromatography using 10% methanol in dichloromethane as eluent. The  $^1\text{H-NMR}$  spectra of receptor **15** displayed two broad singlets of  $-\text{NHCSNHCH}_2\text{Ar}-$  and  $-\text{CH}_2\text{CH}_2\text{NHCSNH}-$  signals at 8.01 and 8.21 ppm, respectively. Their NMR data also consisted with a doublet of  $-\text{NHCSNHCH}_2\text{Ar}-$  at 4.78 ppm, a triplet of  $-\text{COOCH}_2\text{CH}_2-$  at 4.65 ppm, a quartet of  $-\text{CH}_2\text{CH}_2\text{NHCSNH}-$  at 3.76 ppm, a quintet of  $-\text{CH}_2\text{CH}_2\text{CH}_2-$  at 2.18 ppm as well as multiplet signal of  $\text{ArH}$ -linkage in aromatic region. The spectrum was also composed of typical signals for calix[4]arene in cone conformation.

In summary, bis-thiourea calix[4]arene ester **15** was able to prepare by the same procedure as amide receptor **14**, but the overall percent yield was much lower. In order to improve the yields of ligand **15**, an alternative strategy was developed and carried out *via* 4 steps. Receptor **15** was efficiently prepared by the procedure shown in Scheme 3.6 (15%).



สถาบันวิทยบริการ  
จุฬาลงกรณ์มหาวิทยาลัย

**Scheme 3.6.** Another synthetic route to achieve ester derivative receptor **15**.\*



\*Reagents and conditions:(n)  $\text{CSCl}_2$ , TEA, DCM, RT, 2 hours, 80%; (o) 3-aminopropanol, acetone, RT, 2 hours, quantitative; (p) i.  $\text{SOCl}_2$ , benzene, reflux, 24 hours, ii. **28**, DMAP, THF, RT, 2 hours, 43%.

Compound **27** was prepared according to the literature.<sup>[102]</sup> The quantitative yield of bis-thiourea linkage **28** was obtained from treating **27** with 2.2 equivalents of 3-aminopropanol in acetone at room temperature for 2 hours. Then, the reaction mixture was stirred with acid chloride in dry tetrahydrofuran using 4-(dimethylamino)pyridine as a base to obtain bis-thiourea calix[4]arene ester **15**. This reaction was carried out using different bases and solvents as shown in Table 3.4 to find out the best condition. The higher yield under the condition of 4-

(dimethylamino)pyridine and tetrahydrofuran could be explained by a stronger basicity of base and a higher polarity of solvent.

**Table 3.4.** Product yields of the conversion of the acid chloride to bis-thiourea calix[4]arene ester **25** under various conditions.

Condition		Percentage yield
Base	Solvent	(%)
DMAP	THF	43
DMAP	ACN and DCM	41
TEA	THF	39
TEA	ACN and DCM	0
TEA	DMF and DCM	0
TEA	DCM	0

The latter route was discovered to be the optimum procedure to obtain compound **15** because it gave much higher overall yield and also took less time. Moreover, this methodology gave access to study the binding property because enough material was obtained (>100 mg).

### 3.2 Investigation of Binding Ability

Both synthetic molecules **14** and **15** are heteroditopic receptors which are expected to encapsulate both cations and anions simultaneously. As previously mentioned in Chapter 1, the binding ability of this kind of receptors towards anions should be enhanced by electrostatic forces between cations and anions.<sup>[56-57]</sup> Thus the binding efficacy of receptors will be investigated towards cations, anions as well as ion-pairs.

The solvent used in the binding recognition study is very important because the stability of the host-guest adducts is strongly dependent on the polarity of the media. In fact, salts are present as ion pairs or as aggregates of ion pairs in apolar media. Compared to a chloroform-*d* solution, the ion-pairs exist as the free species in more polar solvents such as methanol-*d*<sub>4</sub>, dimethylsulfoxide-*d*<sub>6</sub> or acetonitrile-*d*<sub>3</sub>. The free species will give an advantage in binding study compared to the aggregated ion-pairs.

The solubility of a host and a guest is the main criteria in recognition study. Receptor **14**, receptor **15** as well as tetrabutylammonium anions were able to dissolve in chloroform-*d* while the cation perchlorate salts were hardly soluble in this media. Thus, other solvents will be considered to use in this experiment.

The electron pair donor (EPD) and electron pair acceptor (EPA) solvent are also one of the main criteria for complexation in supramolecular chemistry area. Some solvents mainly act as donors while some solvents prefer to serve as acceptors. However, all solvents are amphoteric. A measurement of the nucleophilicity of EPD solvents is provided by the donor number *DN* (or donicity) whereas a quantity for characterization of the electrophilicity is the acceptor number *AN* (acceptivity).<sup>[118]</sup> EPD solvents are particularly important for cation complexation. Reciprocally, EPA solvents play a particular important role for anion complexation. Table 3.5 exhibits the donor or acceptor numbers of some organic solvents. The higher *DN* and *AN* reflect the stronger interaction of solvents towards cations and anions, respectively. Therefore, acetonitrile-*d*<sub>3</sub> was the solvent of choice for the whole experiment.

**Table 3.5.** Donor numbers and acceptor numbers of organic solvents.<sup>[118]</sup>

Solvents	<i>DN</i> / (kcal·mol <sup>-1</sup> )	<i>AN</i>
Acetone	17.0	12.5
Acetonitrile	14.1	18.9
Dimethyl sulfoxide	29.8	19.3
Dichloromethane	-	20.4
Chloroform	-	23.1
Methanol	-	41.5
Water	-	54.8

<sup>1</sup>H-NMR spectroscopy has been widely employed to investigate receptor-substrate interactions. This technique allows access to the detail of the interaction between a host and a guest molecule. Therefore the binding ability of the novel multidentate thiourea receptors based on calix[4]arene building block in acetonitrile-*d*<sub>3</sub> was investigated by <sup>1</sup>H-NMR titration technique to determine the stoichiometry of the complexes, association constant and Gibbs free energy. The concentration of hosts in this experiment is ~0.0018 mol/L while the stock solution of guests is 10

fold-higher in concentration. No effort was made to maintain a constant pH, but care was taken to avoid water absorption from the atmosphere. The calculated association constants for the different curves were within 10% of the error.

Both receptors exist in cone conformation in acetonitrile- $d_3$ ; like in chloroform- $d$ , which could be observed from a pair of doublet<sup>[109-110]</sup> at 4.4861 and 3.2986 ppm for **14** ( $^2J = 13$  Hz) and a pair of doublet at 3.4423 and 4.3514 ppm for **15** ( $^2J = 12$  Hz). Compared to other conformations of calix[4]arene, cone is the most steric conformation but it is stabilized in polar solvents due to the higher dipole moment ( $\mu$ ).<sup>[109-110]</sup> In the non-polar solvent, a mixture of conformations is observed.

### 3.2.1 Binding Ability of Receptors **14** and **15** towards Cations

Basically, a proper cation for investigating the enhancement of anion binding should be found out before the cation enhancement anion recognition study. To reduce the effect of ion pair, perchlorate or hexafluorophosphate should be used as counter anions. For this purpose, compounds **14** and **15** were titrated with perchlorate salts of lithium, sodium and potassium to evaluate binding constants.

Addition of cations, lithium, sodium and potassium, caused a decrease in intensity of most signals in the  $^1\text{H-NMR}$  spectra of **14** upon addition of successive aliquots of guests. In addition, a new set of signals was found to appear which became well resolved after the addition of 1 equivalent of sodium perchlorate. This result suggested that a new species was formed upon the addition of sodium. The simultaneous decrease in intensity of the unbound calixarene and increase in intensity of the host-guest complex indicated the relatively slow of the recognition process on the NMR time scale. For lithium and potassium perchlorate, the broadened spectrum were not well resolved at any equivalent of the guests added. The integration ratios of bound and unbound receptor were stable at 1.7 and 1.0 equivalents of lithium and potassium, respectively. Unlike the sodium case, the spectrum without unbound species was not monitored in both lithium and potassium cases. Therefore, receptor **14** exhibited changeable binding kinetics, showing the slower chemical exchange for lithium and potassium compared to sodium ion. This is supported by the more complicated spectrum of  $\mathbf{14}\cdot\text{Li}^+$  and  $\mathbf{14}\cdot\text{K}^+$ , compared to  $\mathbf{14}\cdot\text{Na}^+$ .



In the case of  $\mathbf{14}\cdot\text{Na}^+$ , slow interconversion between free ligand and the complex was shown by two sets of  $-\text{ArCH}_2\text{Ar}-$  signals (4 doublets),  $-\text{OCH}_2\text{CONH}-$  (2 singlets),  $-\text{OCH}_2\text{CH}_2\text{OCH}_3$  (4 triplets),  $-\text{CH}_2\text{CH}_2\text{NHCSNH}-$  (2 broad singlets),  $-\text{NHCSNHCH}_2\text{Ar}-$  (2 broad singlets),  $-\text{CH}_2\text{ArHCH}_2-$  (4 singlets) and  $-\text{ArC}(\text{CH}_3)_3$  (3 singlets). After 1 equivalent of sodium perchlorate was added, only one set of all previously mentioned signals appeared in the  $^1\text{H-NMR}$  spectrum of  $\mathbf{14}$  at the higher magnetic field (upfield) as compared to those of free ligand. Moreover, these complicated signals might be induced by the calixarene based molecule. The similar change to  $\mathbf{14}\cdot\text{Na}^+$  was observed in the system of lithium and potassium perchlorate, but the spectrum was not as well-resolved as in the sodium case.

The stoichiometry of  $\mathbf{14}\cdot\text{Na}^+$  complex was 1:1 as judged by the disappearance of the old set of signals as well as the rise of the new set of NMR peaks at 1 equivalent of sodium perchlorate in the  $^1\text{H-NMR}$  spectrum. Indeed, it was not possible to measure an association constant by monitoring the change in the peak positions of any proton signal. However, the stability constants could be easily determined from the variation of the integration ratio between complex and ligand at various amount of the cationic salt. When a 1:1 complex formation between receptor  $\mathbf{14}$  and each cation takes place, the stability constant ( $\beta_1$ ) for the equilibrium is expressed as:<sup>[79]</sup>

$$\beta_1 = \frac{[\text{HG}]}{([\text{H}]_0 - [\text{HG}])([\text{G}]_0 - [\text{HG}])}$$

$$\beta_1 = \frac{n_{\text{hg}}/[\text{H}]_0}{(1 - n_{\text{hg}})(\text{R} - n_{\text{hg}})}$$

where  $[\text{H}]_0$  represents initial concentration of the host

$[\text{G}]_0$  represents initial concentration of the guest

$[\text{HG}]$  represents concentration of the complex

$$[\text{HG}] = n_{\text{hg}}[\text{H}]_0$$

$$n_{\text{hg}} = \frac{I_{\text{hg}}}{I_{\text{hg}} + I_{\text{h}}}$$

where  $I_{\text{hg}}$  represents integration of the complex

$I_{\text{h}}$  represents integration of the host

$$\text{and } \text{R} = [\text{G}]_0/[\text{H}]_0$$

On the other hand, the complexation of receptor **15** towards alkali cations, was a fast process on the NMR time scale, and accordingly a singlet set of time-averaged signals was observed for both free ligand and complexed species of the host and the guest. Upon addition of increasing amounts of lithium perchlorate (up to 4 equivalents) in an acetonitrile- $d_3$  solution of **15**, the triplet signal of  $-\text{COOCH}_2\text{CH}_2-$  moved upfield from 4.5077 to 4.4801 ppm ( $\Delta\delta = -0.0276$  ppm) and the quartet signal of  $-\text{CH}_2\text{CH}_2\text{NHCSNH}-$  also moved upfield from 3.6694 to 3.6658 ppm ( $\Delta\delta = -0.0036$  ppm). The signal at 4.5419 ppm which belonged to  $-\text{OCH}_2\text{CO}-$  moved to the downfield region with  $\Delta\delta = +0.0056$  ppm. Concomitantly, the downfield shifts were observed with  $-\text{OCH}_2\text{CH}_2\text{OCH}_3$  shifting  $+0.0276$  ppm (from 4.0647 to 4.0923 ppm) at 3.68 equivalents. The  $-\text{CH}_2\text{CH}_2\text{NHCSNHCH}_2\text{Ar}-$  and  $-\text{CH}_2\text{CH}_2\text{NHCSNHCH}_2\text{Ar}-$  signals underwent the upfield complexation induced shift of respective  $-0.3709$  and  $-0.2902$  ppm (from 8.1811 and 8.1004 to 7.8102 ppm). Changes in the  $-\text{OCH}_2\text{CH}_2\text{OCH}_3$ ,  $-\text{ArCH}_2\text{Ar}-$  and  $-\text{CH}_2\text{ArHCH}_2-$  of receptor **15** with lithium cation were also monitored. The singlet signal of  $-\text{OCH}_2\text{CH}_2\text{OCH}_3$  was deshielded from 3.3173 to 3.3191 ( $\Delta\delta = +0.0018$  ppm). The  $-\text{ArCH}_2\text{Ar}-$  and  $-\text{CH}_2\text{ArHCH}_2-$  signals moved downfield from 4.3797 to 4.3814 ( $\Delta\delta = +0.0017$  ppm) and from 7.3707 to 7.3726 ( $\Delta\delta = +0.0019$  ppm), respectively.

In the system of sodium or potassium, the similar complexation induced shifts in the spectrum of **15** upon the NMR titration were observed (Figure 3.3). The greater effect towards most signals was shown in both sodium and potassium cases compared to the lithium one. Unless otherwise noted, all data are presented at 4 equivalents of added cation. The positive sign in the following figure reflects the downfield shift while the negative sign indicates the upfield shift.

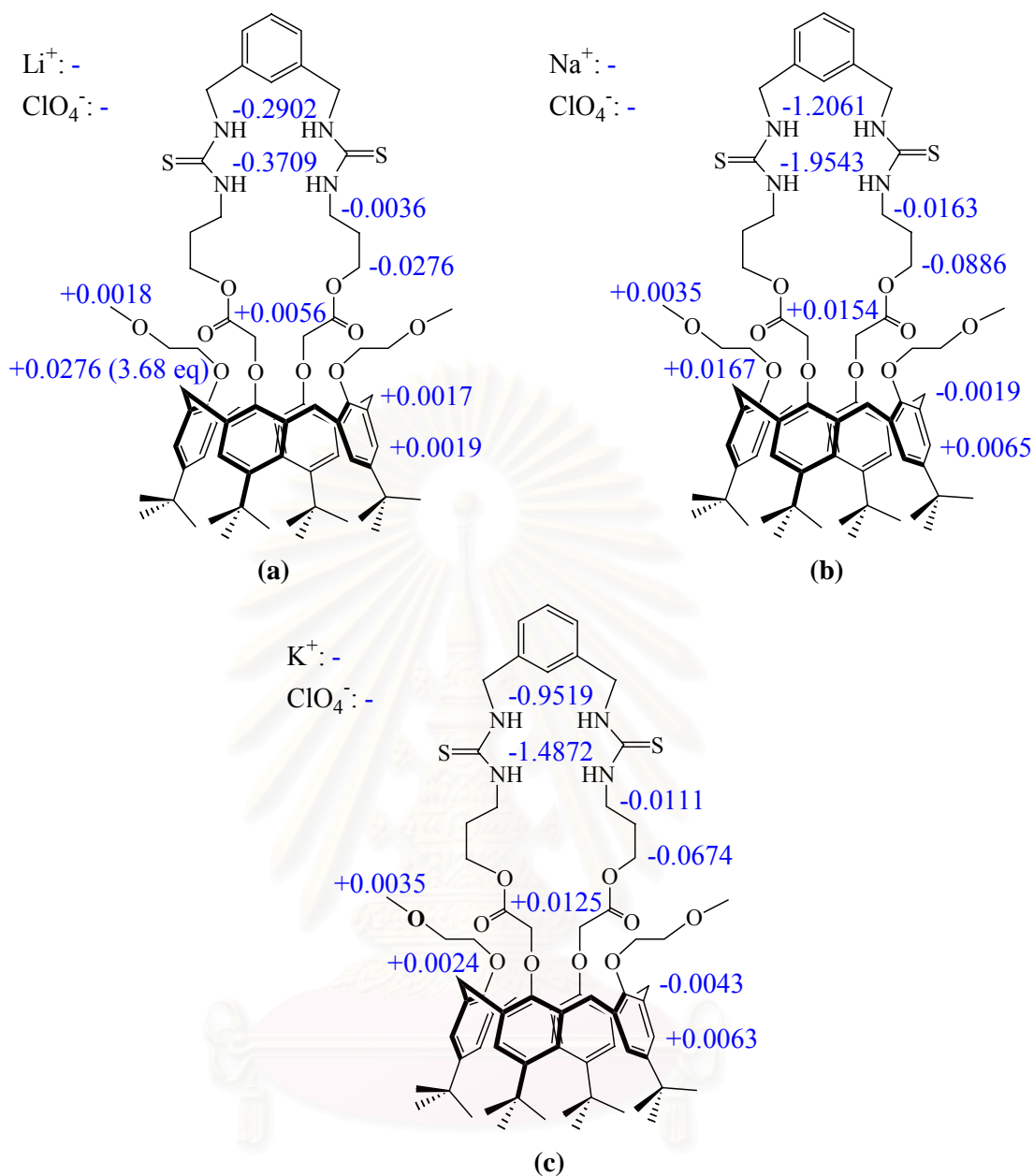


**Figure 3.3.** The complexation induced shifts of some proton signals on  $^1\text{H}$ -NMR spectrum (a)  $15 \cdot \text{Li}^+$  (b)  $15 \cdot \text{Na}^+$  and (c)  $15 \cdot \text{K}^+$ .

The downfield shift of  $-\text{OCH}_2\text{COO}-$  and the upfield shift of  $-\text{COOCH}_2\text{CH}_2-$  can be explained by the  $\alpha$ -H and the normal cation complexation, respectively. It is still not clear why *NH*-thiourea and their adjacent methylene protons continuously shift to the highfield region. The upfield shift of *NH*-thiourea signals is probably a consequence of encapsulation of cationic substrate at the ester and crown cavity which enlarges the size of cavity until the intramolecular hydrogen bonding between both *NH*-thiourea groups are broken.<sup>[119]</sup> The breaking of any hydrogen bond interactions was indicated by the upfield movement of that proton signal in NMR

spectrum. The shift to the highfield region of both *NH*-thiourea signals was also observed in the system of receptor **14**.

The association stoichiometry of **15**·cation complexes indicated by the titration curves were confirmed by the continuous variation method (Job's plots). The bell-shaped Job's plots which obtained from the modified data of <sup>1</sup>H-NMR titration of receptor **15** with 0-100 μL of cationic solution added in acetonitrile-*d*<sub>3</sub> showed the symmetry curve with maxima for mole ratio  $[G]_t / \{[G]_t + [H]_t\}$  about 0.5 or  $[G]_t/[H]_t$  of 1 indicating a 1:1 complex.  $\Delta\delta(1-X)$  is the supramolecular complex concentration as determined by the chemical shift changes ( $\Delta\delta$ ) for the corresponding protons multiplied by their inverse mole fractions (1-*X*). These were supported by the titration curve for all signals which were fitted well to a 1:1 binding model. Figures 3.4 and 3.5 show the Job's plots and titration curves, respectively, for only –OCH<sub>2</sub>COO– signals in all complexes due to the closest of this proton to the binding site as well as its clearly resolved signal in the <sup>1</sup>H-NMR spectrum. For the case of any 1:1 complexes which display the faster exchange rate than the NMR time scale, the association constant can be calculated using NMRTit\_HG program.<sup>[105]</sup>

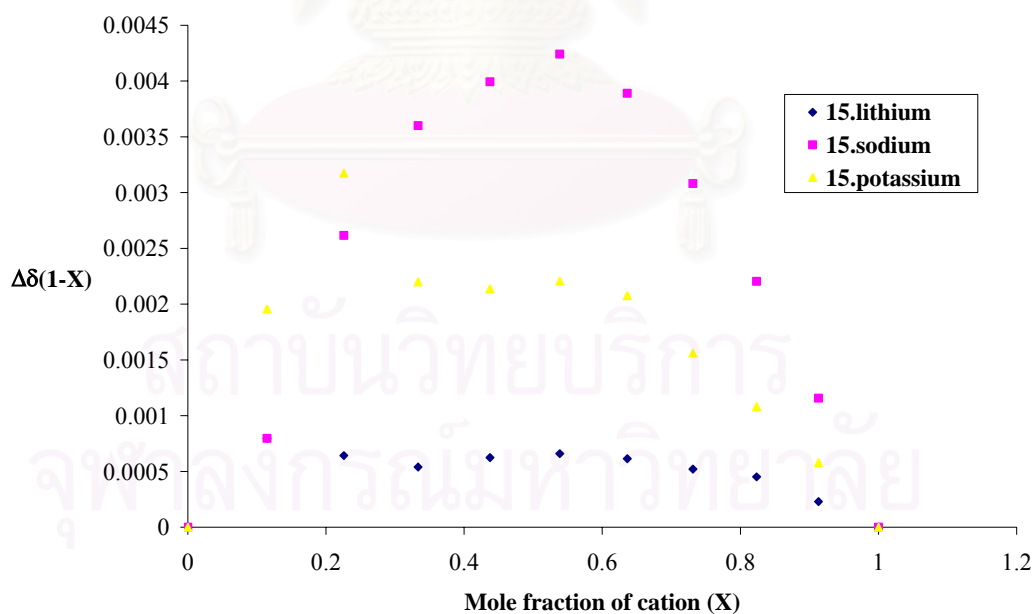


**Figure 3.4.** Job's plots of –OCH<sub>2</sub>COO– in **15**·Li<sup>+</sup>, **15**·Na<sup>+</sup> and **15**·K<sup>+</sup> complexes.

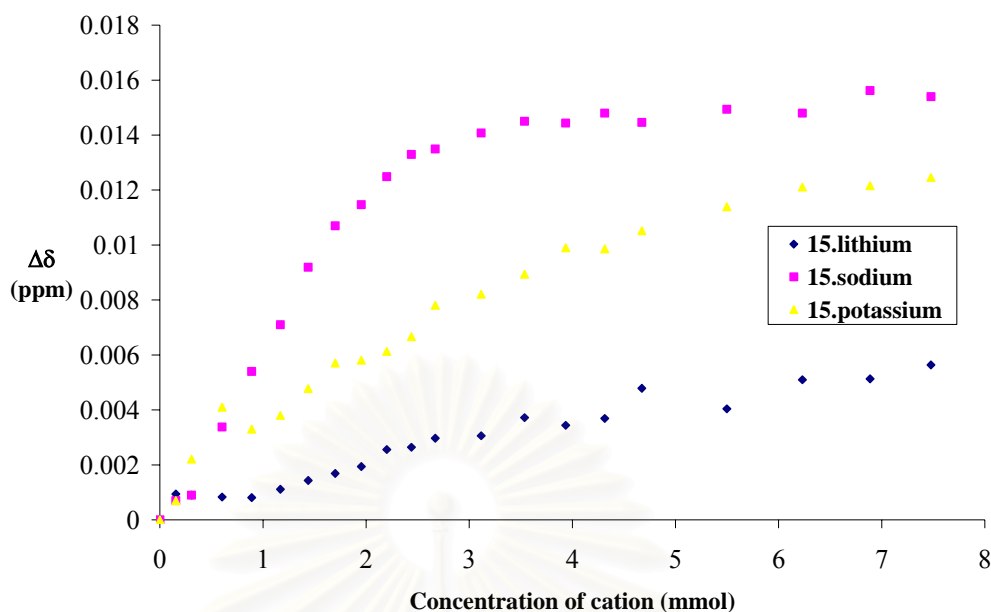


**Figure 3.5.** Titration curves of  $-OCH_2COO^-$  in  $15 \cdot Li^+$ ,  $15 \cdot Na^+$  and  $15 \cdot K^+$  complexes.

It was revealed that either **14** or **15** bound lithium, sodium as well as potassium perchlorate with the association constants and Gibbs free energies in acetonitrile- $d_3$  as shown in Table 3.6. The binding data of all **14**-cation complexes were calculated from the integration of  $-ArCH_2Ar-$  signal plus  $-OCH_2CONH-$  signal according to their clear change. On the other hand,  $\beta_1$  and  $\Delta G$  values of the **15**-cation complexes were obtained by the complexation induced shift (CIS) of the  $-OCH_2COO^-$ ,  $-COOCH_2CH_2-$  and  $-OCH_2CH_2OCH_3$ . It should be noted that  $\Delta G$  is calculated from  $\Delta G = -RT \ln \beta_1$  when  $R = 8.314 \text{ J} \cdot \text{mol}^{-1} \cdot \text{K}^{-1}$  and  $T = 298 \text{ K}$ .

**Table 3.6.** The average association constants and Gibbs free energies upon the formation of **14**-cation and **15**-cation complexes in acetonitrile- $d_3$ .

Complex		Association Constant	Gibbs free energy
Type	Stoichiometry	( $M^{-1}$ )	( $\text{kJ} \cdot \text{Mol}^{-1}$ )
<b>14</b> · $Li^+$	1:1	914	-16.9
<b>14</b> · $Na^+$	1:1	5531	-21.4
<b>14</b> · $K^+$	1:1	617	-15.9
<b>15</b> · $Li^+$	1:1	371	-14.7
<b>15</b> · $Na^+$	1:1	15500	-23.9
<b>15</b> · $K^+$	1:1	688	-16.2

Both novel calixarene compounds **14** and **15**, which contained the cation binding site closed to a lower rim of calixarene building block showed strong binding towards sodium. The binding recognition of lithium and potassium afford slightly different in the systems of either **14** or **15**. However, bis-thiourea **14** exhibited a slightly more selective to lithium over potassium. *Vice versa*, analogous **15** showed a particularly more selective to potassium over lithium (Figure 3.6). Additionally, calix[4]arene ester **15** appeared to be more efficient and more selective for alkali cation complexation. This could be rationalized by hard-soft acid-base (HSAB) concept and size complementary.

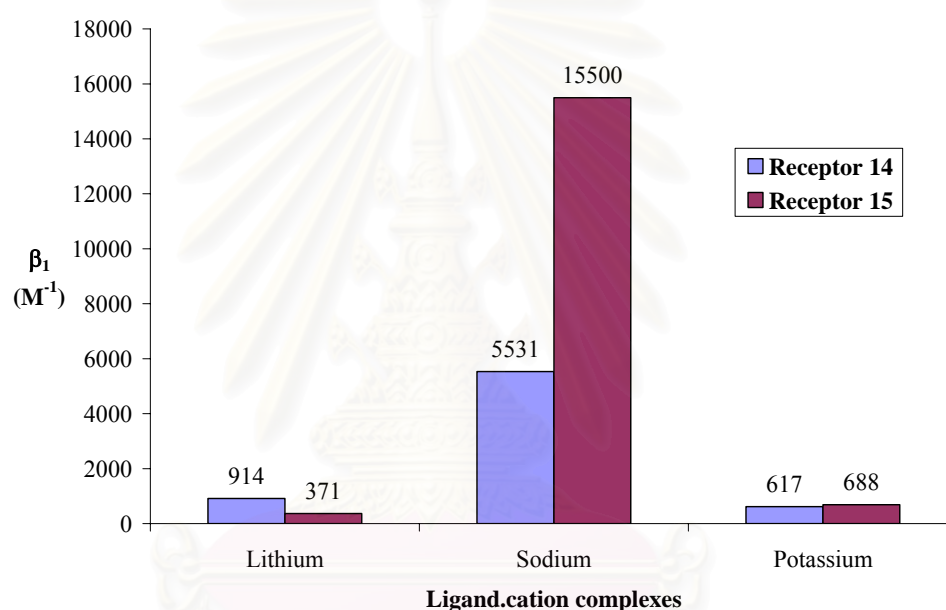
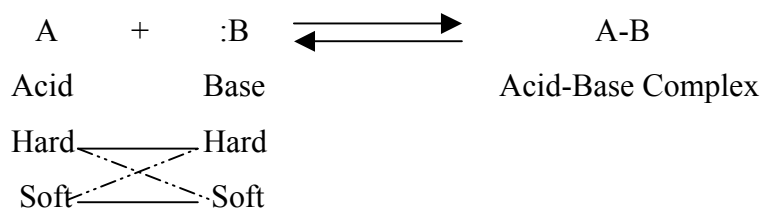


**Figure 3.6.** The selectivity of receptors **14** and **15** towards sodium over potassium and lithium cation.

The main idea of HSAB concept is shown in Scheme 3.7.<sup>[18]</sup> Oxygen donor atoms in receptors **14** and **15** are hard bases because of their high electronegativity. Alkali cations are hard acid due to their non-polarisable sphere. Receptor **15** contains 10 hard bases (10 oxygen atoms) whereas compound **14** contains 8 hard bases (8 oxygen atoms) as cationic binding site. Thus, it was reasonable that the complex formation constant of **15**·Na<sup>+</sup> was larger than that of **14**·Na<sup>+</sup> and the kinetic of complexation of the former was faster than the latter. It is worth mentioning that the amide<sup>[40, 120-123]</sup> and ester<sup>[55, 124]</sup> cavity on the lower rim of calix[4]arene always afford the slow and the fast exchange on NMR time scale, respectively.

**Scheme 3.7.** Lewis theory of acids and bases (————— favorable combination and - - - - - unfavorable combination).<sup>[18]</sup>



The hard acid of alkali cations is in the order  $\text{Li}^+ > \text{Na}^+ > \text{K}^+$  owing to their sizes. Thus, the selectivity trend did not absolutely control by HSAB concept. If we consider the size of alkali cations, potassium ion is larger than sodium and lithium (Table 3.7). Among the three ions, the size of sodium cation probably has the most proper size to fit into the cavity of ligands **14** and **15**. The lithium cation is too small to be bound tightly with the ligands while potassium cation is too large to bind with the receptors without causing significant strain in the calixarene scaffold.

**Table 3.7.** A comparison of the ionic radius (Å) of isoelectronic alkali cations.<sup>[125]</sup>

Alkali Cations	r (Å)
$\text{Li}^+$	0.69
$\text{Na}^+$	1.02
$\text{K}^+$	1.38

For **14**-cation complexes, the result suggested that alkali cation was encapsulated in the cavity by cleaving the intramolecular hydrogen bonding between two amide groups using the ion-dipole interaction between two *CO*-amide groups and a cation as previously discovered in the literature.<sup>[120]</sup> Murakami and Shinkai proposed the closed form of calix[4]arene amide before complexation due to the intramolecular hydrogen bonding (Figure 3.7 (a)). Their structures were confirmed by IR spectroscopy and the more downfield shift of *-CONH-* signals in the <sup>1</sup>H-NMR spectrum, compared to their analogous non-intramolecular hydrogen bonding *-CONH-* signal. Moreover, they also found that the encapsulation of a cation induced an opened form of the receptors (Figure 3.7 (c)).<sup>[121, 126]</sup> The <sup>1</sup>H-NMR and IR data in this experiment could not compare to those reported in the literatures due to the different solvent system. Furthermore, the *NH*-thiourea in our receptor interfered with the *-CONH-* signal in the IR spectrum. However, if we have a look back at our

experimental data (Chapter II),  $-CONH-$  signals in bisprotected diamine **20**, bisisothiocyanate **21** and cyclic receptor **14** were identified at 6.55, 8.46 and 8.67 ppm, respectively. The more deshielding of  $NH$ -amide signals in compounds **21** and **14** as compared to those in **20** might be arisen from the hydrogen bonding which could be either intra- or intermolecular hydrogen bonding. The dilution experiment is the best method to differentiate the hydrogen bonding interaction.  $^1H$ -NMR spectra of 1.87 mmol/L and 3.75 mmol/L of receptor **14** in  $CD_3CN$  showed virtually the same position of  $-CONH-$  signal ( $\delta$  at 7.5307 and 7.5298 ppm, respectively) implying the insignificant intermolecular hydrogen bonding.

The complexation of cation in the cavity of host **14** broke the intramolecular hydrogen bonding and induced the rearrangement of calixarene building block. The former was evidenced by the upfield shift of  $-CONH-$  signal while the latter was supported by a new set of nearly all signals, especially  $-ArCH_2Ar-$ ,  $-CH_2ArHCH_2-$  and  $-ArC(CH_3)_3$  which are not likely to directly interact with the alkali cation. The appearance of new  $-OCH_2CH_2OCH_3$  in **14**·cation spectrum can be attributed to the involving of both oxygen atoms in the cation recognition.

The two carbonyl groups in free calix[4]arene ester **15** were turned outward to reduce electrostatic repulsion among carbonyl oxygens, while bound  $Na^+$  mechanically changed from the exo-annulus carbonyls (Figure 3.7 (b)) to the endo-annulus carbonyls (Figure 3.7 (c)) for the oxygen carbonyls to trap  $Na^+$  ion. X represents of NH and O in the case of receptor **14** and **15**, respectively.



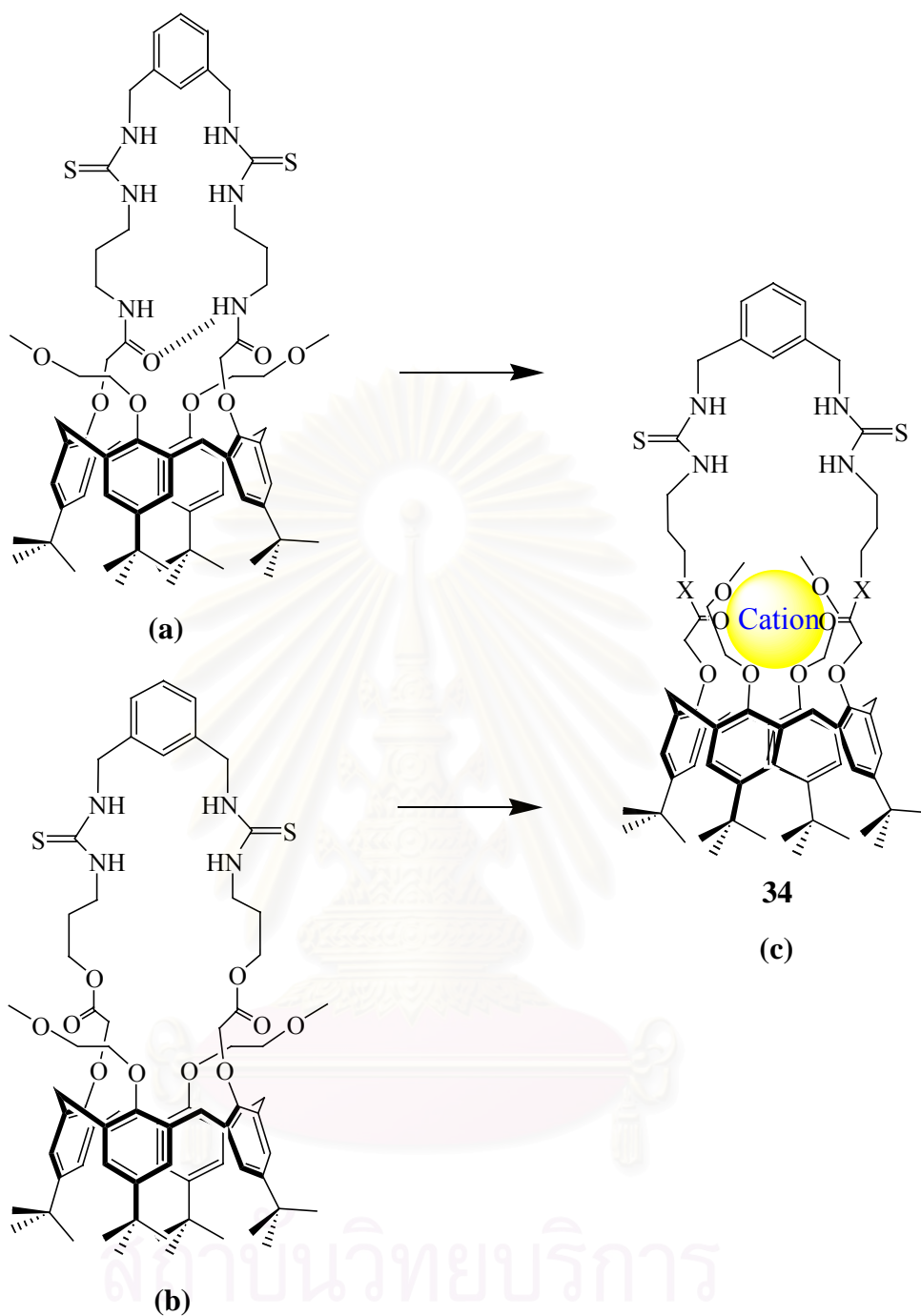
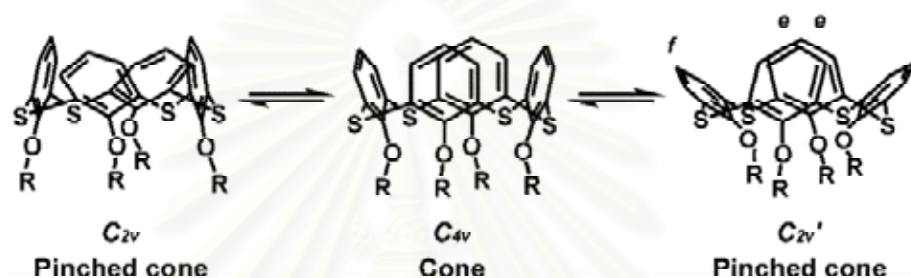


**Figure 3.7.** From the intramolecular hydrogen bonding in amide **14** (a) or the exo-annulus carbonyl (b) in ester **15** to the proposed structure of **14**·cation and **15**·cation complexes (c).

Major resources of these changing might stem from the rearrangement of the molecule to exist in the most stable conformation during complexation. All of these cation complexes existed in the cone conformation, which was determined by two singlets for *tert*-butyl groups, two singlets for *ArH*-calixarene and a doublet of

doublet signal of AB system which belonged to the bridging methylene on calixarene skeleton with coupling constant  ${}^2J \approx 12\text{-}13\text{ Hz}$  in the  ${}^1\text{H-NMR}$  spectrum. In addition, the closer of two  $-\text{CH}_2\text{Ar}H\text{CH}_2-$  signals as well as the closer of two  $-\text{ArC}(\text{CH}_3)_3$  signals in complexes upon the addition of metal perchlorates implied that the pinched cone conformation of free ligand **14** or **15** adopted to a nearly cone conformation after an inclusion of an alkali cation into their cavities (Scheme 3.8).<sup>[127]</sup>

**Scheme 3.8.** The interconversion between cone and pinched cone conformation of calix[4]arene.<sup>[128]</sup>



This observation allowed us to study the effect of sodium ion complexation on the anion binding because of the well-resolved  ${}^1\text{H-NMR}$  spectrum of **14**· $\text{Na}^+$  complex and a pretty high stable complex of **15**· $\text{Na}^+$ . Hereby, it was possible to saturate the cationic binding site, by adding one equivalent of sodium perchlorate, and then evaluate the association constants with anions.

### 3.2.2 Binding Ability of Receptors **14** and **15** towards Anions

To minimize possible effects of ion-pair formation on the determination of the association constants as well as to solubilize anions into organic solvents, the bulky tetrabutylammonium ion was chosen as a counter ion for all anions. There are a variety of tetrabutylammonium anions in which the geometry, basicity and branched chain (substituted unit) determine the selectivity. In this case, the branched alkyl ammonium cation ( $n\text{-Bu}_4\text{N}^+$ ) is hardly approach the cationic binding site and consequently forms exclusively exo-complexes.

A solid-liquid extraction was performed for selecting proper anions for titration experiments. To a solution of ligand **14** or **15** in chloroform-*d*, the solid of a wide variety of the excess amount of sodium and potassium salts (about 50 mg of chloride, bromide, nitrate, hydrogen sulfate, acetate, benzoate, hydrogen phosphate, dihydrogen phosphate, phenylphosphate, diphenylphosphate, phenylphosphinate,

hydrogen phenylphosphonate and phenylphosphonate) was added, shaken at room temperature overnight, and then centrifuged for 15 minutes. The solution phase was carefully removed and filtered through a pasteur pipet with cotton wool. Extraction of anionic salts into the complex species which are soluble in organic phase can be detected by peak shifts in the  $^1\text{H-NMR}$  spectrum.

Generally, the thiourea group in the receptors acts as acid site for base (anion). The preliminary results revealed that receptor **14** bound phenylphosphinate and diphenylphosphate preferentially that can be observed from the peak shifts in the  $^1\text{H-NMR}$  spectrum. Acetate also bound substantially with this host. On the other hand, the spectrum of bis-thiourea **15** was predominantly changed in the presence of benzoate, dihydrogen phosphate or phenylphosphinate. The observed selectivity for phosphate and carboxylate type could be rationalized based on the sum of the guest basicity (Table 3.8) and the complementary structure. The oxyanions like tetrahedron  $\text{HSO}_4^-$  and trigonal planar  $\text{NO}_3^-$  could bind the hosts in a similar manner to  $\text{H}_2\text{PO}_4^-$  and  $\text{CH}_3\text{COO}^-$  but much weaker complexes would be formed due to much stronger hydrogen bond acceptor. The low basicity spherical inorganic anions like chloride and bromide did not display any significant different from the free host molecules. Compared to phenylphosphinate, the less binding was found in the case of hydrogen phenylphosphonate. This was probably due to the higher  $\text{p}K_a$  as well as the smaller size of phenylphosphinate.

สถาบันวิทยบริการ  
จุฬาลงกรณ์มหาวิทยาลัย

**Table 3.8.** Geometry and basicity of various anions.

Anions	Geometry	$pK_a$ at 25 °C in water <sup>[129-130]</sup>	$pK_a$ at 25 °C in DMSO <sup>[81]</sup>
Chloride	Spherical	< -2	-
Bromide	Spherical	< -2	-
Nitrate	Trigonal planar	-1.64	-
Hydrogen sulphate	Tetrahedral	< -2	-
Acetate	Trigonal planar	4.75	12.60
Benzoate	Trigonal planar	4.20	10.90
Hydrogen phosphate	Tetrahedral	7.21	-
Dihydrogen phosphate	Tetrahedral	2.12	-
Phenylphosphate	Tetrahedral	-	-
Diphenylphosphate,	Tetrahedral	-	-
Phenylphosphinate	Tetrahedral	2.1	-
Hydrogen phenylphosphonate	Tetrahedral	1.83	-
Phenylphosphonate	Tetrahedral	7.07	-

These receptors formed remarkably strong complexes with carboxylate and phosphate. Therefore, <sup>1</sup>H-NMR titration experiments of receptors **14** and **15** would be done with acetate (**35**), benzoate (**36**), dihydrogen phosphate (**37**), phenylphosphinate (**38**) and diphenylphosphate (**39**) (Figure 3.8) to determine the effect of geometry and the benzene substituent upon complexation process. Additionally, the two different unsubstituted dicarboxylate anions like succinate (**40**) and glutarate (**41**) (Figure 3.8) were chosen aiming to discriminate the effect of the second carboxylate functionality and the length of guest molecules. In the presence of the low basicity anions, the *NH*-protons of thiourea functionality were hardly shifted and these affects were too small to determine either the association constant or the stoichiometry using this spectroscopy. However, the association constants of weakly bound anions in some cases would be intensively enhanced when they are in ion-pairing system. Thus determination of stability constants of some of the above anions like hydrogen sulfate or nitrate would be worth trying by other techniques such as calorimetry. This might be suitable to do as a future work because the calorimetric titration has recently been

exploited in the evaluation of weakly binding small molecular systems to widely apply in biological complexation.<sup>[131]</sup>

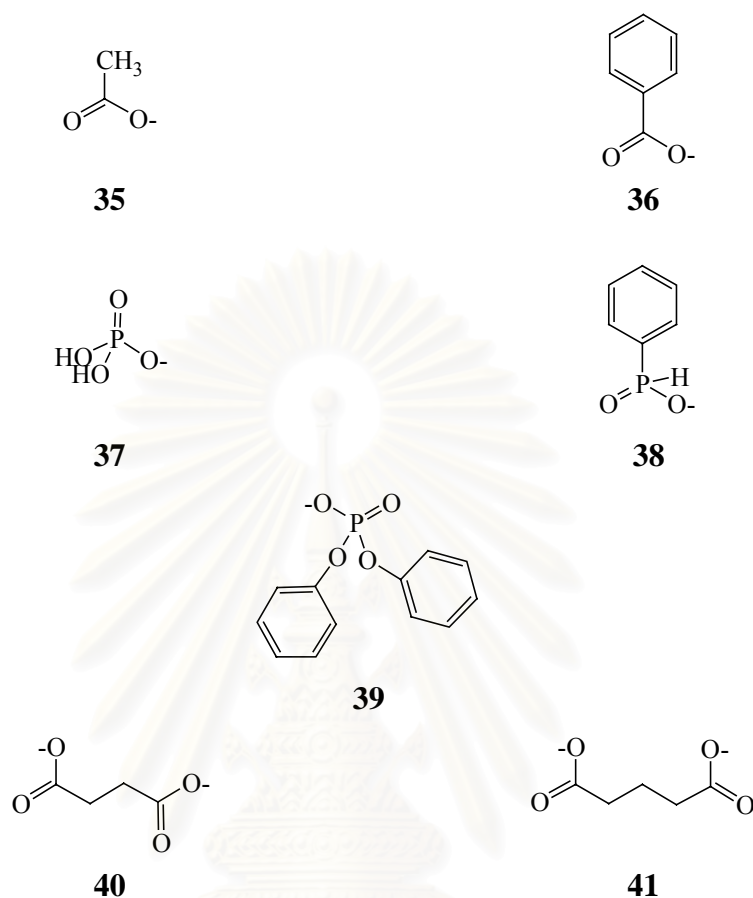


**Figure 3.8.** The structures of anions that used in this experiment.

The quantitative anion binding ability of the novel bidentate thiourea receptors **14** and **15** was investigated by titrated with the aliquots of TBA salts of acetate, benzoate, dihydrogen phosphate, phenylphosphinate and diphenylphosphate. NMR titrations were performed and changes in chemical shifts that occurred in several signals of ligand **14** or **15** upon complexation were monitored. The continuous movement of signals indicated the faster exchange of complexation processes than the NMR time scale

The binding of compound **14** using acetate anion was initially investigated. This anion has been known to form strong directional hydrogen bonding with a thiourea due to its basicity.<sup>[87, 132-134]</sup> Moreover, the carboxylate itself is a functional group of great biological relevance which leads to a wide application in biotechnology.<sup>[135]</sup> The addition of one equivalent of tetrabutylammonium acetate

resulted in large downfield shifts in the  $^1\text{H-NMR}$  spectrum of ligand **14**. The lower field of thiourea proton  $-\text{CH}_2\text{CH}_2\text{NHCSNHCH}_2\text{Ar-}$ , the higher field of thiourea signal  $-\text{CH}_2\text{CH}_2\text{NHCSNHCH}_2\text{Ar-}$  and amide hydrogen atoms  $-\text{OCH}_2\text{CONHCH}_2-$  strongly shifted downfield ( $\Delta\delta = +2.1438$ ,  $+1.3852$  and  $+0.7329$  ppm, respectively). Moreover, the hydrogen atoms at  $-\text{NHCSNHCH}_2\text{Ar-}$  and  $-\text{CH}_2\text{CH}_2\text{NHCSNH-}$  shifted downfield with  $\Delta\delta = +0.0532$  and  $+0.0321$  ppm, respectively. This clearly indicates that all thiourea *NH*-protons are involved in anion binding. A similar behavior was observed for  $-\text{OCH}_2\text{CH}_2\text{OCH}_3$ ,  $-\text{OCH}_2\text{CH}_2\text{OCH}_3$  and  $-\text{OCH}_2\text{CH}_2\text{OCH}_3$  as well as  $-\text{OCH}_2\text{CONH-}$  hydrogen atoms  $+0.0137$ ,  $+0.0634$ ,  $-0.0125$  and  $+0.0603$  ppm. The shift of signals which were not closed to hydrogen bond donor site ( $-\text{OCH}_2\text{CH}_2\text{OCH}_3$  and  $-\text{OCH}_2\text{CONH-}$  signals) was probably derived from the preorganization of molecule. This also supported by the upfield shift of  $-\text{ArCH}_2\text{Ar-}$  ( $\Delta\delta = +0.0203$  ppm) and  $-\text{CH}_2\text{ArHCH}_2-$  ( $\Delta\delta = -0.0215$  ppm) signals which were the outstanding signals of calixarene unit. Additionally, both  $-\text{CH}_2\text{ArHCH}_2-$  signals were continuously shifted close to each other to propose the interconversion from pinched cone to cone conformation. Unless the movement of building block, the hydrogen signals which are far from the *NH*-thiourea should not be changed.

$^1\text{H-NMR}$  spectra of **14** $\cdot\text{C}_6\text{H}_5\text{COO}^-$ , **14** $\cdot\text{H}_2\text{PO}_4^-$ , **14** $\cdot\text{Ph(H)POO}^-$  and **14** $\cdot(\text{PhO})_2\text{PO}_2^-$  were shifted in the similar manner as **14** $\cdot\text{CH}_3\text{COO}^-$  but different amount of effect as shown in Figure 3.9. Such chemical shift changes for intracavity interactions and effect of all **15** $\cdot$ anion complexes are shown in Figure 3.10.

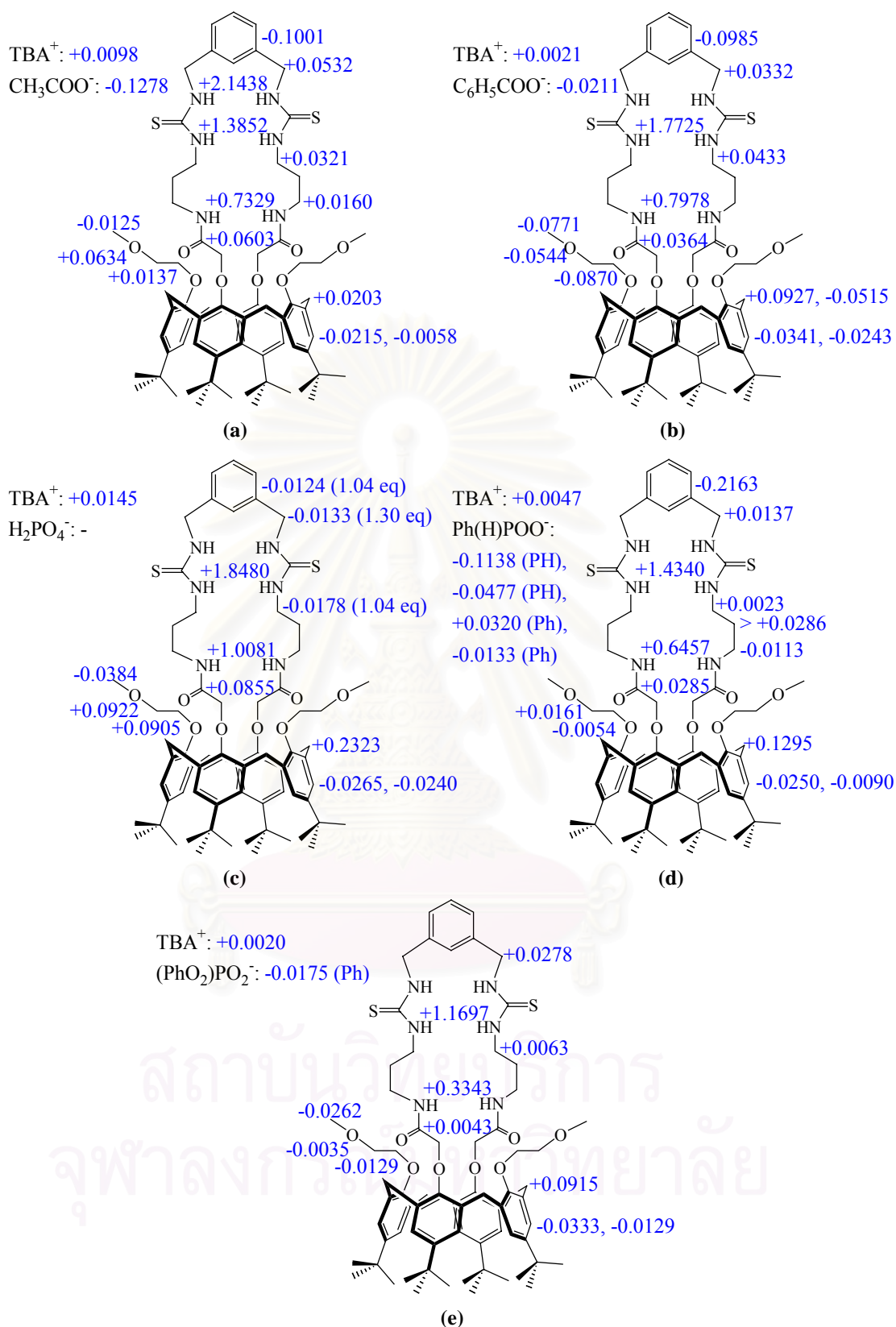


**Figure 3.9.** The complexation induced shifts of some proton signals on  $^1\text{H}$ -NMR spectrum (a)  $\mathbf{14}\cdot\text{CH}_3\text{COO}^-$  (b)  $\mathbf{14}\cdot\text{C}_6\text{H}_5\text{COO}^-$  (c)  $\mathbf{14}\cdot\text{H}_2\text{PO}_4^-$ , (d)  $\mathbf{14}\cdot\text{Ph(H)POO}^-$  (e)  $\mathbf{14}\cdot(\text{PhO})_2\text{PO}_2^-$ .

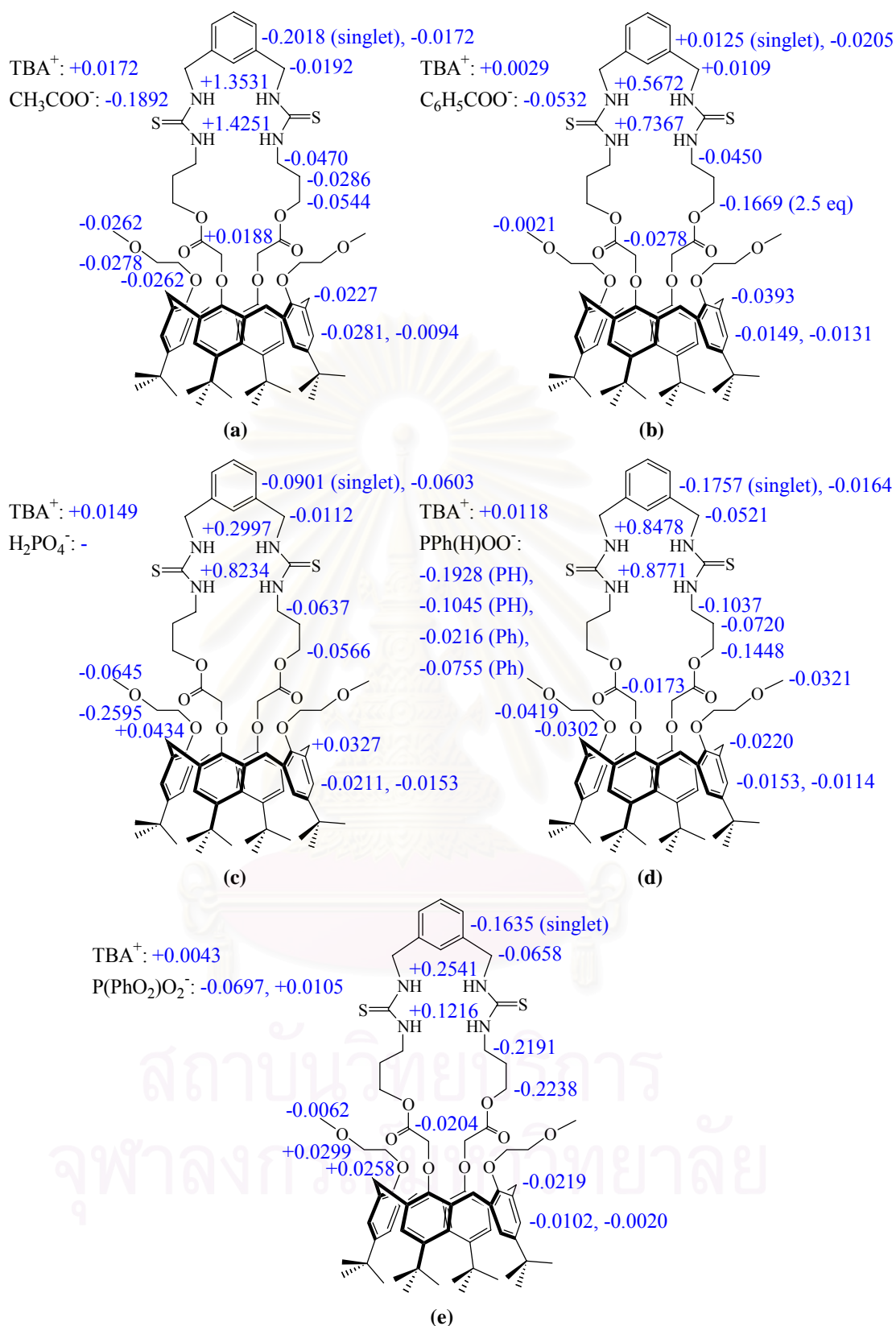


**Figure 3.10.** The complexation induced shifts of some proton signals on  $^1\text{H-NMR}$  spectrum (a)  $15 \cdot \text{CH}_3\text{COO}^-$  (b)  $15 \cdot \text{C}_6\text{H}_5\text{COO}^-$  (c)  $15 \cdot \text{H}_2\text{PO}_4^-$ , (d)  $15 \cdot \text{Ph(H)POO}^-$  (e)  $15 \cdot (\text{PhO})_2\text{PO}_2^-$ .



Compared to the CIS of any signals of  $\mathbf{14}\cdot\text{H}_2\text{PO}_4^-$  in chloroform-*d* in the preliminary experiment, the shift in acetonitrile-*d*<sub>3</sub> solution was much easier to observe. This could be ascribed to the effect of solvents. The halohydrocarbon solvent like chloroform is classified as Lewis acid due to its acidic C-H bond. Hence, anion (such as  $\text{H}_2\text{PO}_4^-$ ) is able to form hydrogen bonding to the thiourea functionality of receptor **14** and the acidic C-H of chloroform. The halohydrocarbon solvents are able to break the hydrogen bonding leading to the less stable complex. This phenomenon is also found in living organisms. For instance, the anaesthetic properties of some halogen-containing solvents have been connected with their ability to hinder the formation of biologically important hydrogen bonds.<sup>[118]</sup>

The broadened and the large (>1 ppm) changes in the chemical shifts of thiourea and amide *NH*-protons were the evidence for the presence of hydrogen bonding in anion complexation. In addition, the upfield shifts for *CH*<sub>2</sub>-protons adjacent to hydrogen bonded *NH* groups in the presence of anions were usually observed.<sup>[136]</sup> This might be attributed to the more basicity at methylene protons compared to *NH*-thiourea, the through space effect from electron density of anions or the anisotropic effect of carbonyl or phosphonyl group.

The Job's plots of all  $\mathbf{14}\cdot$ anion complexes corresponded to an association stoichiometry of 1:1 (Figure 3.11). The Job's analysis for the anion complexation by **15** which composed of two ester moieties instead of amide groups indicated that **15** favored binding acetate, phenylphosphinate and diphenylphosphate anion in a simple 1:1 complex (Figure 3.12). For benzoate and dihydrogen phosphate anion, the distorted bell-shaped curves with a maximum at  $X \approx 0.66$  had been shown in Job's plots (Figure 3.12). This indicated a 1:2 host-guest stoichiometry.

จุฬาลงกรณ์มหาวิทยาลัย

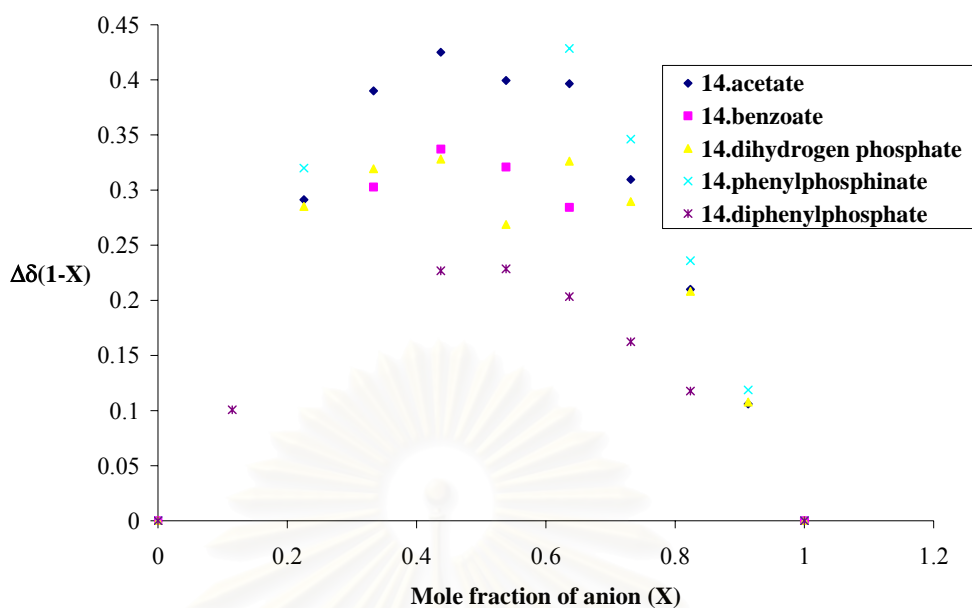


**Figure 3.11.** Job's plots of  $-\text{CH}_2\text{CH}_2\text{NHCSNH}-$  in  $14 \cdot \text{CH}_3\text{COO}^-$ ,  $14 \cdot \text{C}_6\text{H}_5\text{COO}^-$ ,  $14 \cdot \text{H}_2\text{PO}_4^-$ ,  $14 \cdot \text{Ph}(\text{H})\text{POO}^-$  and  $14 \cdot (\text{PhO})_2\text{PO}_2^-$  complexes.

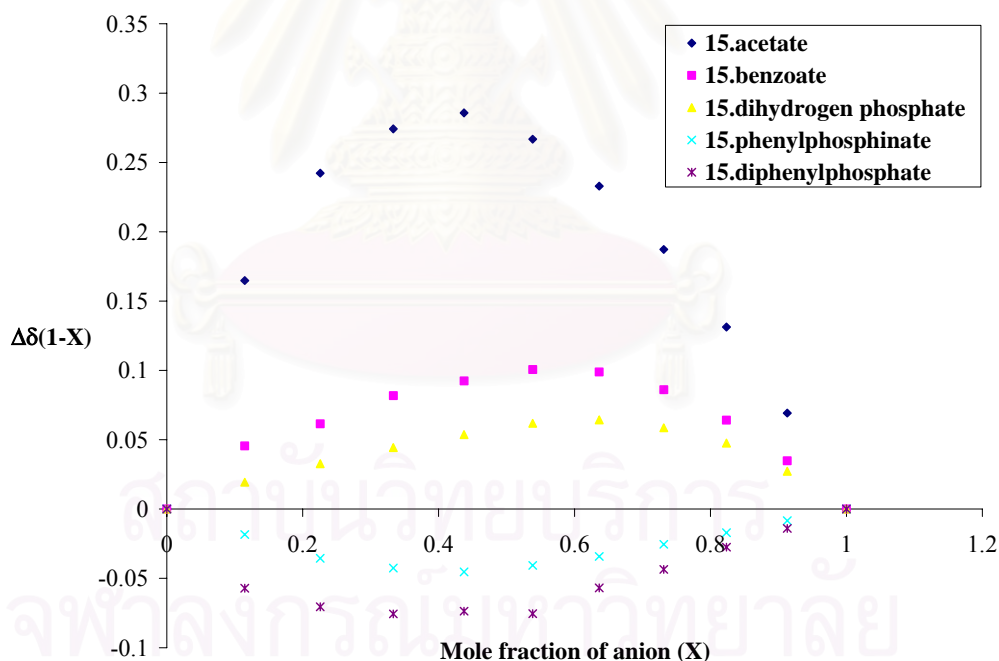


**Figure 3.12.** Job's plots of  $-\text{NHCSNHCH}_2\text{Ar}-$  in  $15 \cdot \text{CH}_3\text{COO}^-$ ,  $15 \cdot \text{C}_6\text{H}_5\text{COO}^-$ , as well as  $15 \cdot \text{H}_2\text{PO}_4^-$  and  $-\text{CH}_2\text{CH}_2\text{NHCSNH}-$  in  $15 \cdot \text{Ph}(\text{H})\text{POO}^-$  as well as  $15 \cdot (\text{PhO})_2\text{PO}_2^-$  complexes.

The titration curves of **14**·anion and **15**·anion complexes are shown in Figure 3.13 and Figure 3.14, respectively. The chemical shifts of some other signals were also plotted against the equivalent of added TBA anion (*see* Appendix B).

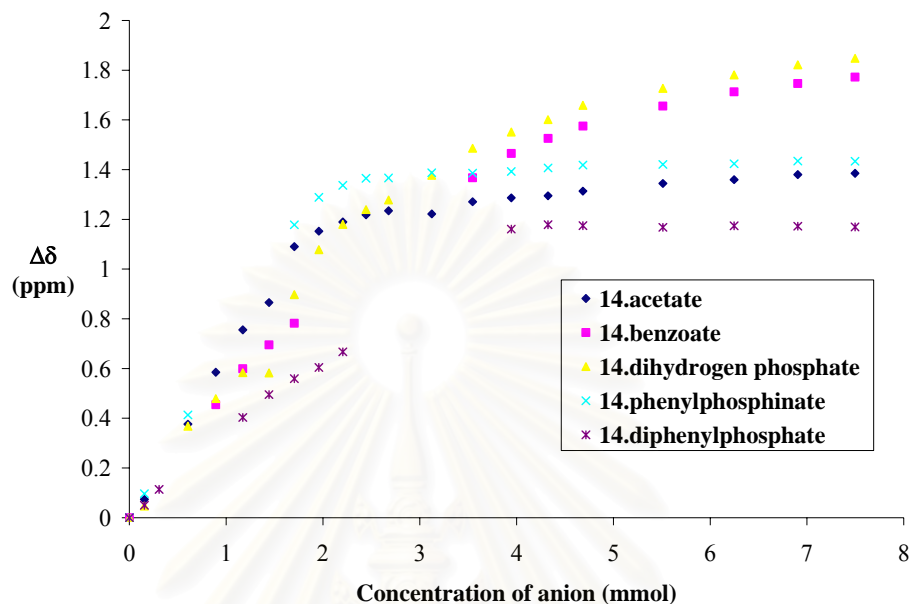


**Figure 3.13.** Titration curves of  $-\text{CH}_2\text{CH}_2\text{NHCSNH}-$  in **14**· $\text{CH}_3\text{COO}^-$ , **14**· $\text{C}_6\text{H}_5\text{COO}^-$ , **14**· $\text{H}_2\text{PO}_4^-$ , **14**· $\text{Ph}(\text{H})\text{POO}^-$  and **14**· $(\text{PhO})_2\text{PO}_2^-$  complexes.

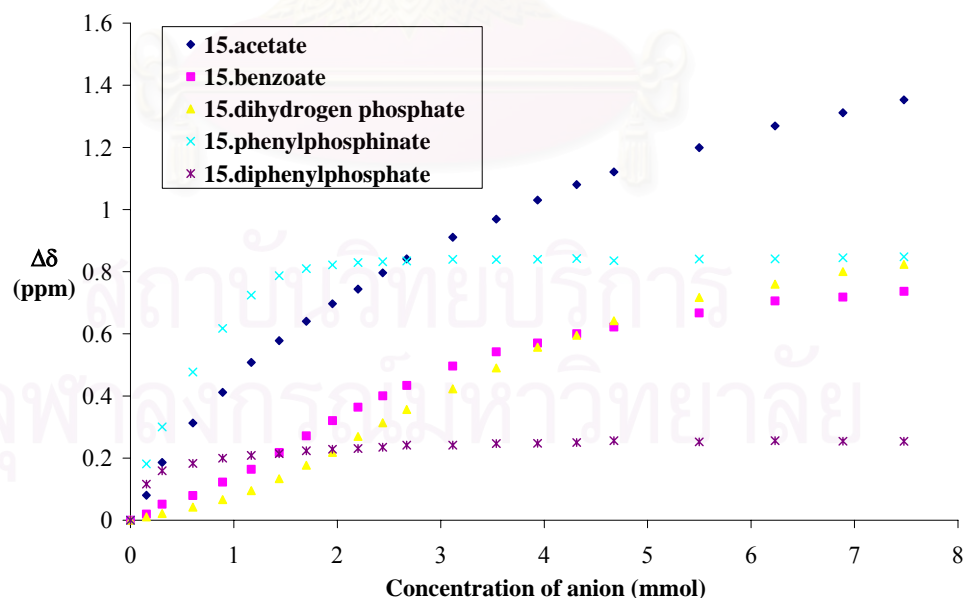


**Figure 3.14.** Titration curves of  $-\text{NHCSNHCH}_2\text{Ar}-$  in **15**· $\text{CH}_3\text{COO}^-$ , **15**· $\text{C}_6\text{H}_5\text{COO}^-$ , **15**· $\text{H}_2\text{PO}_4^-$ , **15**· $\text{Ph}(\text{H})\text{POO}^-$  and **15**· $(\text{PhO})_2\text{PO}_2^-$  complexes.

The normal looking titration curves of **14**·anion complexes (Figure 3.13), **15**·CH<sub>3</sub>COO<sup>-</sup>, **15**·Ph(H)POO<sup>-</sup> and **15**·(PhO)<sub>2</sub>PO<sub>2</sub><sup>-</sup> (Figure 3.14) supported a 1:1 association stoichiometry. In the case of **15**·C<sub>6</sub>H<sub>5</sub>COO<sup>-</sup> and **15**·H<sub>2</sub>PO<sub>4</sub><sup>-</sup>, both titration curves displayed a small variation of sigmoidal curve which was a characteristic of an association of more than two species.<sup>[137]</sup> Unfortunately attempts to relate these 1:2 complexes with their molecular mass in ESI-MS (Electrospray Ionization Mass Spectrometry) have so far been unsuccessful as it was not possible to obtain the correct mass of **15** and anions.<sup>[138]</sup> Electrospray ionization is served as one of the softest ionization methods to date and this technique has rapidly gained momentum to study noncovalently bound complexes. However, the study of hydrogen bond in supramolecular aggregates from smaller organic building blocks by ESI-MS is relatively rare.<sup>[139]</sup> This is presumably according to the lower binding constants of these species when compared to, for example, the protein-substrate complex. Another technique that can be used to support this formation is molecular weight determination by means of Vapor Pressure Osmometry (VPO).<sup>[140]</sup>

The  $\Delta\delta$  of the more sensitive  $-\text{CH}_2\text{CH}_2\text{NHCSNH}-$ ,  $-\text{NHCSNHCH}_2\text{Ar}-$  and  $-\text{OCH}_2\text{CONH}-$  (in the system of **14**) as well as adjacent methylene signals which located next to the thiourea moiety were used to evaluate binding efficacy. The association constants ( $\beta_1$ ) in acetonitrile-*d*<sub>3</sub> of all **14**·anion complexes as well as **15**·CH<sub>3</sub>COO<sup>-</sup>, **15**·Ph(H)POO<sup>-</sup> and **15**·(PhO)<sub>2</sub>PO<sub>2</sub><sup>-</sup> complexes were evaluated from a 1:1 curve fitting binding model provided by Hunter's NMRTit\_HG program.<sup>[105]</sup> On the other hand, the degree of complexation selectivity of **15**·C<sub>6</sub>H<sub>5</sub>COO<sup>-</sup> and **15**·H<sub>2</sub>PO<sub>4</sub><sup>-</sup> could be calculated using NMRTit\_HGG program.<sup>[105]</sup> The average binding abilities and Gibbs free energies are displayed in Table 3.9. The good fit between experimental data and calculation of the titration curves in NMRTit\_HGG program supported that compound **15** forms stable 1:2 complexes with both benzoate and dihydrogen phosphate.

**Table 3.9.** The average association constants and Gibbs free energies upon the formation of **14**·anion and **15**·anion complexes.

Complex		Association Constant (M <sup>-1</sup> )	Gibbs free energy (kJ·Mol <sup>-1</sup> )
Type	Stoichiometry		
<b>14</b> ·CH <sub>3</sub> COO <sup>-</sup>	1:1	30400	-25.6
<b>14</b> ·C <sub>6</sub> H <sub>5</sub> COO <sup>-</sup>	1:1	3290	-20.1
<b>14</b> ·H <sub>2</sub> PO <sub>4</sub> <sup>-</sup>	1:1	858	-16.7
<b>14</b> ·Ph(H)POO <sup>-</sup>	1:1	17100	-24.1
<b>14</b> ·(PhO) <sub>2</sub> PO <sub>2</sub> <sup>-</sup>	1:1	2330	-19.2
<b>15</b> ·CH <sub>3</sub> COO <sup>-</sup>	1:1	2010	-18.8
<b>15</b> ·C <sub>6</sub> H <sub>5</sub> COO <sup>-</sup>	1:2	8300	-22.4
		286350000 (M <sup>-2</sup> )	-48.2
<b>15</b> ·H <sub>2</sub> PO <sub>4</sub> <sup>-</sup>	1:2	9710	-22.7
		10583900 (M <sup>-2</sup> )	-40.1
<b>15</b> ·Ph(H)POO <sup>-</sup>	1:1	14300	-23.7
<b>15</b> ·(PhO) <sub>2</sub> PO <sub>2</sub> <sup>-</sup>	1:1	3240	-20.0

In order to compared to the others, only  $\beta_1$  of **15**·C<sub>6</sub>H<sub>5</sub>COO<sup>-</sup> and **15**·H<sub>2</sub>PO<sub>4</sub><sup>-</sup> are shown in Figure 3.15. The amide **14** recognizes acetate better than phenylphosphinate, benzoate, diphenylphosphate and dihydrogen phosphate while the analogous ester **15** binds phenylphosphinate slightly stronger than dihydrogen phosphate ( $\beta_1$ ), benzoate ( $\beta_1$ ), diphenylphosphate and acetate. The  $\beta_1$  value does not follow the amount of complexation induced shifts. Sometimes the titration data with smaller  $\Delta\delta$  could yield the higher  $\beta_1$  than the larger  $\Delta\delta$  data, for example, in the case of **14**·CH<sub>3</sub>COO<sup>-</sup> and **14**·C<sub>6</sub>H<sub>5</sub>COO<sup>-</sup>.<sup>[141]</sup> Hence, the binding constant depends on the characteristic of curve not the shifting values. The more the curve bends, the higher the binding constant is.

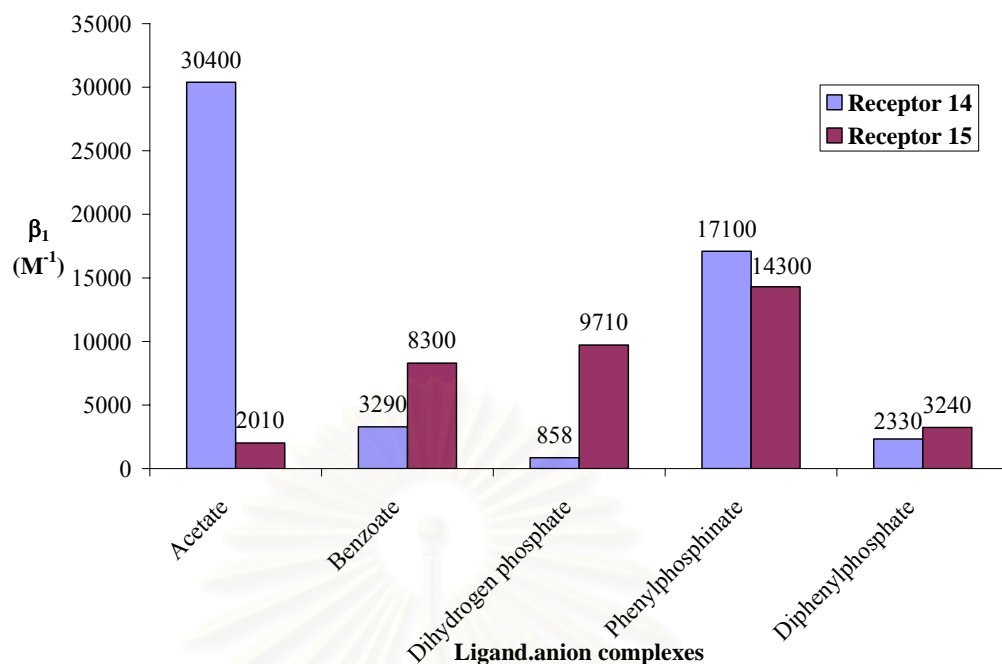


**Figure 3.15.** The selectivity of receptors **14** and **15** towards various anions.

The binding data of **14**-anion and **15**-anion complexes does not undergo the same trend. The replacement of the amide group in compound **14** with the ester moiety yields the decrease in selectivity, change in stoichiometry of association and binding affinity trend as well as increase in the association constant when complexing with phenyl substituted anions. These selectivity trends are explained by basicity, complementary structure,  $\pi$ - $\pi$  interaction and  $O^{\delta-}$ - $\pi$  repulsion. Compared to macromolecule **15**, compound **14** displayed a stronger acidity and consequently from a more stable complex with a stronger base. Thus, host **14** recognized acetate better than benzoate and dihydrogen phosphate. The opposite trend ( $H_2PO_4^- > C_6H_5COO^- > CH_3COO^-$ ) was observed in the system of **15**.

The complementary structure between the host and the guest molecule is another factor to control selectivity. For the thiourea base receptor, this type of ligand was discovered to bind guests *via* hydrogen bonding which is a directional interaction. Presumably, the arrangement of the directional hydrogen bond donor on *NH*-thiourea in both receptors might be different attributed to the number of lone pair on  $-CONH-$  in **14** and  $-COO-$  atom in **15**. This preorganization led to the preferential of receptor **14** to Y-shaped carboxylate and the preferential of ligand **15** to tetrahedral phosphate anion. A number of reports showed the binding ability of simple acyclic thiourea (**42a-42c**)<sup>[87, 132, 142]</sup> and cyclophane based cyclic thiourea (**43a-43c**)<sup>[143]</sup>

towards both dihydrogen phosphate and acetate over other anions, with preferentially to the former over the latter (Figure 3.16). The selectivity trend of these receptors was found to be against basicity due to the lack of additional acid site. Like receptor **15**, the structure complementary dominated the other effects.

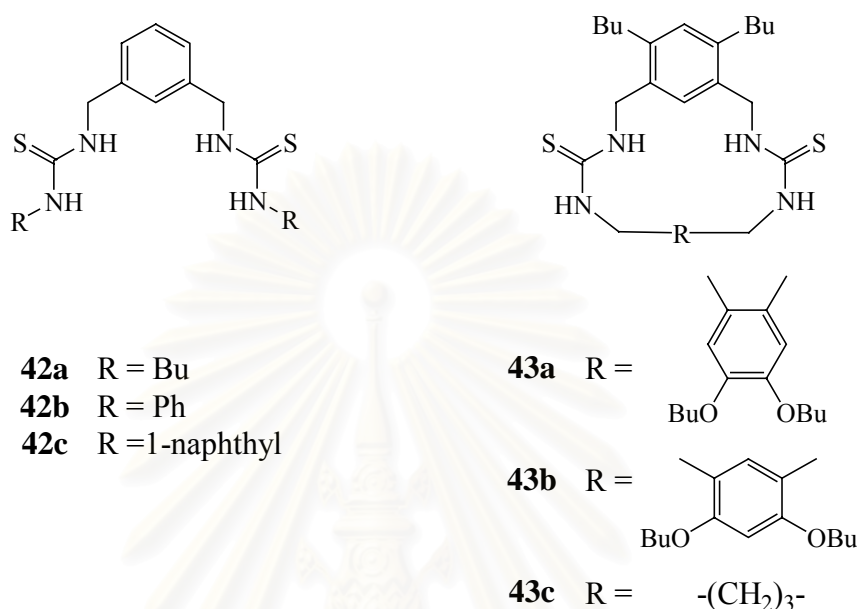


**Figure 3.16.** Simple acyclic thiourea and cyclophane cyclic thiourea receptors.

In the case of less acidic molecule like compound **15**, the solvent also plays a role in complexation. There are some examples about the effect of media through the selectivity trend.<sup>[144, 145]</sup> This interrelation between solvation effects and receptor structure is also used to achieve anion binding selectivity in nature.<sup>[146]</sup> The more steric hindrance around the central atom of anion resulted in the less effective of the binding of solvents towards anions. Therefore, it is easier for acetonitrile to donate electron to central C of acetate compared to P of dihydrogen phosphate yielding  $\beta_1$  ( $\mathbf{15} \cdot \text{CH}_3\text{COO}^-$ ) <  $\beta_1$  ( $\mathbf{15} \cdot \text{H}_2\text{PO}_4^-$ ).

Compared to  $\mathbf{14} \cdot \text{H}_2\text{PO}_4^-$  and  $\mathbf{15} \cdot \text{H}_2\text{PO}_4^-$ , the higher affinity of receptors **14** and **15** towards phenylphosphinate was aided by size and shape complementary as well as  $\pi$ - $\pi$  interaction. In contrast to phenylphosphinate, the diminished binding strength of diphenylphosphate is likely explained by steric effect and the negative-negative repulsion between oxygen-ester of host and the electron-rich-aromatic guest.

As previously mentioned, the chemical shift of  $-\text{OCH}_2\text{CONH}-$  of receptor **14** displayed a large downfield shift in all cases indicating that two *NH*-amide moieties

might be incorporated in hydrogen bonding for complexation. Although the *NH*-amide donor atoms are far from the main binding site (thiourea), they could involve in anion recognition. Recently, Nam and *co-worker* attached the similar bis-urea linkage on the narrow rim of calix[4]arene **44** (Figure 3.17).<sup>[147]</sup> The negative effect of quinone units; which are far from urea function in nearly the same length as compound **14**, on the calixarene scaffold towards anion recognition due to the ion-dipole repulsion was reported.

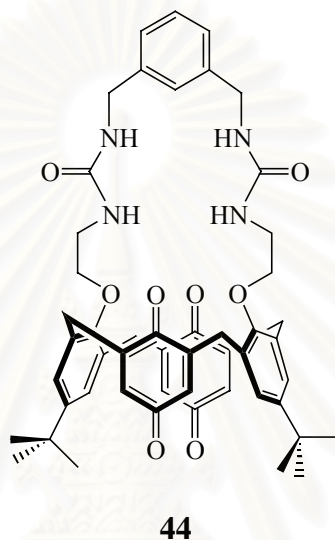


**Figure 3.17.** Macrocyclic bis-urea calix[4]quinone.<sup>[147]</sup>

Attempt to grow crystals suitable for x-ray analysis produced inappropriate single crystals. Therefore, the **14**·anion and **15**·anion complexes are proposed based on the x-ray structures of **13b**·CH<sub>3</sub>COO<sup>-</sup><sup>[117]</sup> (Figure 3.18) and cyclic(thiourea)·H<sub>2</sub>PO<sub>4</sub><sup>-</sup><sup>[148]</sup> (Figure 3.19) as well as the proposed structures of bis(guanidinium)·H<sub>2</sub>PO<sub>4</sub><sup>-</sup><sup>[149]</sup> and bis(thiourea)·H<sub>2</sub>PO<sub>4</sub><sup>-</sup><sup>[132]</sup> as well as bis(thiourea)·C<sub>6</sub>H<sub>5</sub>COO<sup>-</sup> complexes.<sup>[132]</sup> Generally, the stability of these complexes are aided by CH<sub>3</sub>- $\pi$  and  $\pi$ - $\pi$  interaction. The proposed structures of anion complexes are shown in Figure 3.20. X represents of NH and O in the case of compounds **14** and **15**, respectively. R<sub>1</sub>, R<sub>2</sub> and R<sub>3</sub> refer to the substituted group on acetate, benzoate, dihydrogen phosphate, phenylphosphate and diphenylphosphate as presented in Figure 3.8.



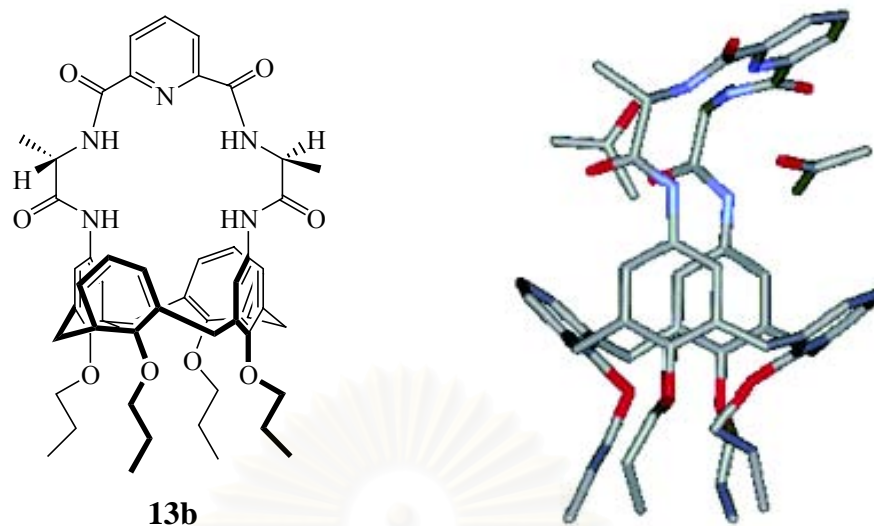


**Figure 3.18.** X-ray structure of **13b**·CH<sub>3</sub>COO<sup>-</sup> complex.<sup>[117]</sup>

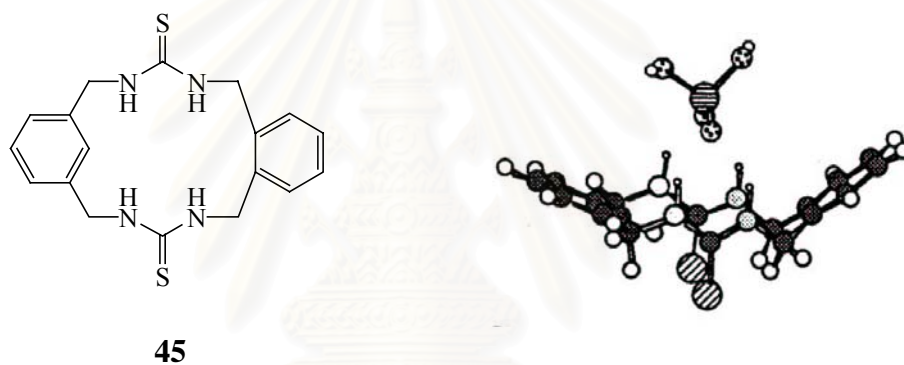


**Figure 3.19.** X-ray structure of cyclic(thiourea)·H<sub>2</sub>PO<sub>4</sub><sup>-</sup>.<sup>[148]</sup>

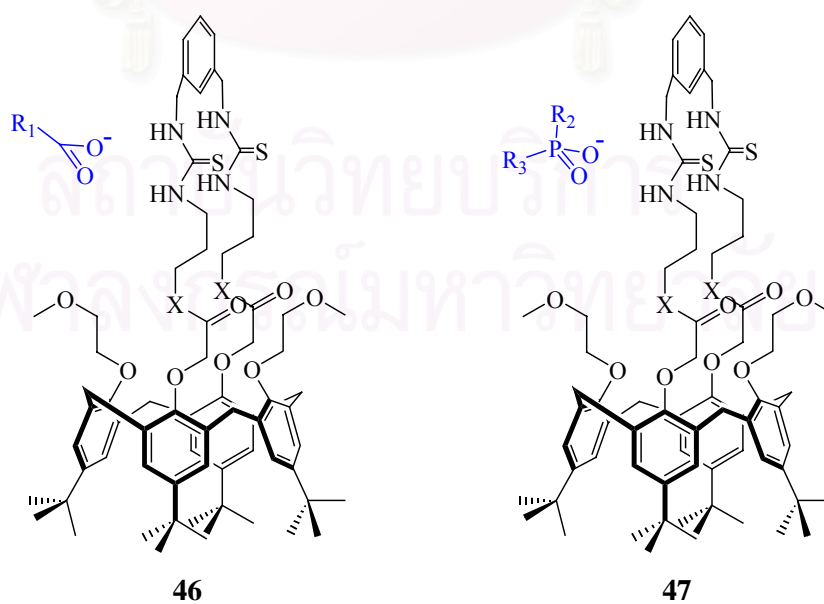


**Figure 3.20.** The proposed structures of 1:1 anion complexes (**46-47**).

Owing to the important role of dicarboxylate in our biological system as well as the high and moderate association constant of respective  $\mathbf{14}\cdot\text{CH}_3\text{COO}^-$  and  $\mathbf{15}\cdot\text{CH}_3\text{COO}^-$  complexes, recognition studies of both receptors towards some dicarboxylate anions are worth performing. Succinate and glutarate which employed as their bis-TBA salts were used in the titration experiment because the numbers of carbons between two carboxylate groups correspond to the chosen amino acid in Section 3.2.3. These dicarboxylate titration results will be compared to monocarboxylate recognition.

When a complex is formed, various protons display signal shifts to indicate a rapid exchange behavior. Chemical shifts of all the *NH*-signals of the receptor in the mixture of  $\mathbf{14}$  and succinate anion shifted much larger downfield compared to the remaining signals (+0.8825 ppm for  $-\text{CH}_2\text{CH}_2\text{NHCSNHCH}_2\text{Ar}-$  and +0.4228 ppm for  $-\text{OCH}_2\text{CONH}-$ ). The adjacent signals were slightly shifted downfield. For instance, the  $-\text{NHCSNHCH}_2\text{Ar}-$  signal moved +0.0482 ppm and the  $-\text{CH}_2\text{CH}_2\text{NHCSNH}-$  proton shifted +0.0344 ppm. The aromatic linkage moved downfield with  $\Delta\delta = +0.1445$  ppm. The  $-\text{OCH}_2\text{CH}_2\text{OCH}_3$ ,  $-\text{OCH}_2\text{CH}_2\text{OCH}_3$  as well as  $-\text{OCH}_2\text{CH}_2\text{OCH}_3$  moved to the lower magnetic field (downfield) by complexation with succinate anion for +0.0423, +0.0236 and +0.0059 ppm, respectively. NMR titration analysis also showed the downfield shift of the  $-\text{OCH}_2\text{CONH}-$  signal from +4.4636 to +4.5204 ppm. The aromatic protons of calixarene unit on thiourea  $\mathbf{14}$  shifted upfield with  $\Delta\delta = -0.0192$  and  $-0.0261$  ppm upon addition of 4 equivalents of succinate whereas the  $-\text{ArCH}_2\text{Ar}-$  protons shifted downfield about +0.0981 ppm. This result supports the preorganization of the receptor molecule. The aromatic unit on calixarene scaffold was probably changed from pinched cone to cone conformation. Thus, two phenyl units were presumably moved close to each other and caused the anisotropic effect to occur. Although the shifts of some signals seem to be very small but their titration curves are in a normal shape (*see* Appendix B).

Changes in the peak positions during the formation of  $\mathbf{14}\cdot\text{glutarate}^{2-}$  (Figure 3.21),  $\mathbf{15}\cdot\text{succinate}^{2-}$  and  $\mathbf{15}\cdot\text{glutarate}^{2-}$  complexes (Figure 3.22) were found in the similar manner as  $\mathbf{14}\cdot\text{succinate}^{2-}$ . However, greater shifts were observed in the case of glutarate compared to succinate. The superscript <sup>a</sup> is denoted as the sigmoidal titration curves and superscript <sup>b</sup> is referred to the inverse titration curves.

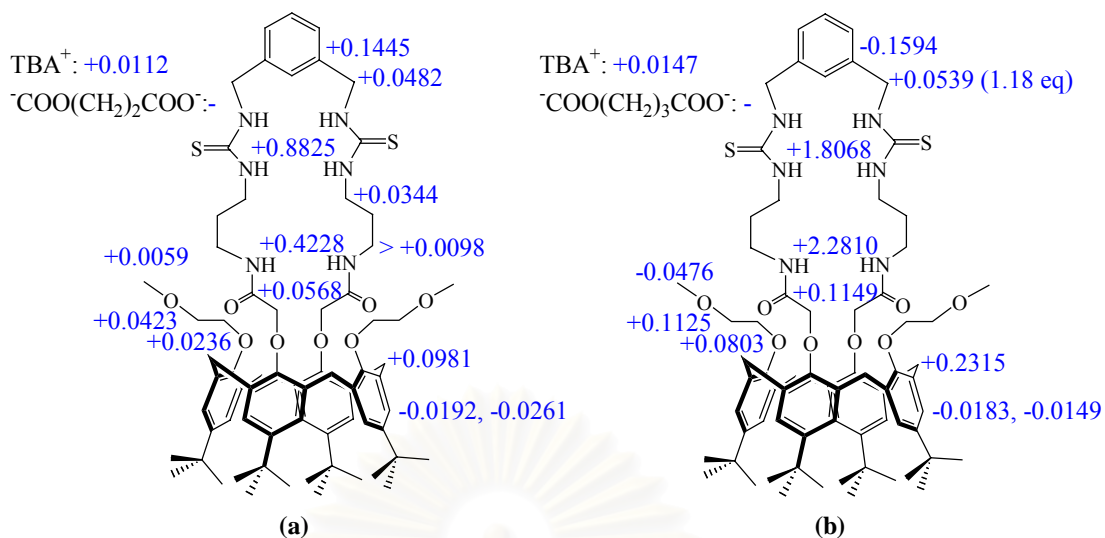


**Figure 3.21.** The complexation induced shifts of some proton signals on  $^1\text{H-NMR}$  spectrum (a) **14**·succinate $^{2-}$  (b) **14**·glutarate $^{2-}$ .

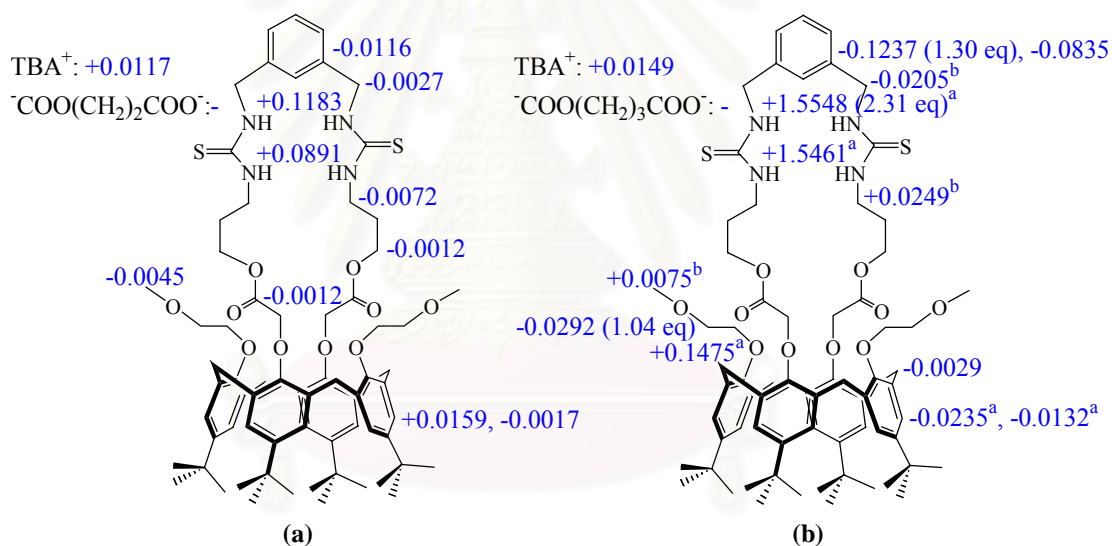


**Figure 3.22.** The complexation induced shifts of some proton signals on  $^1\text{H-NMR}$  spectrum (a) **15**·succinate $^{2-}$  (b) **15**·glutarate $^{2-}$ .

Data sets from the titration experiments verified the bell-shaped curve with a maximum point at  $X \approx 0.5$  indicating a 1:1 stoichiometry for all complexes in Job's analysis (Figure 3.23 and Figure 3.24).

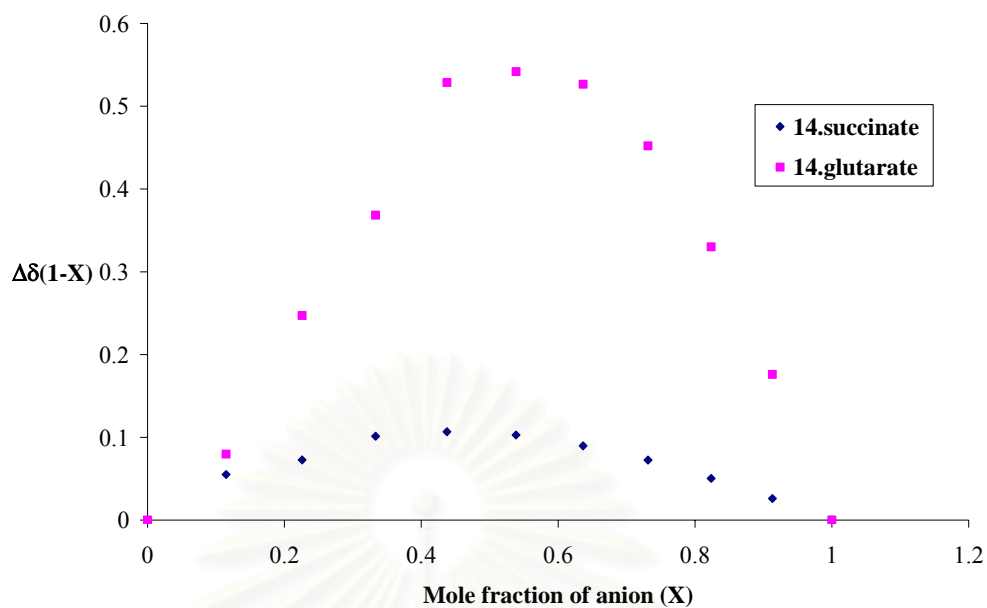


**Figure 3.23.** Job's plots of  $-\text{OCH}_2\text{CONH}-$  in  $\mathbf{14}\cdot\text{succinate}^{2-}$  and  $\mathbf{14}\cdot\text{glutarate}^{2-}$  complexes.

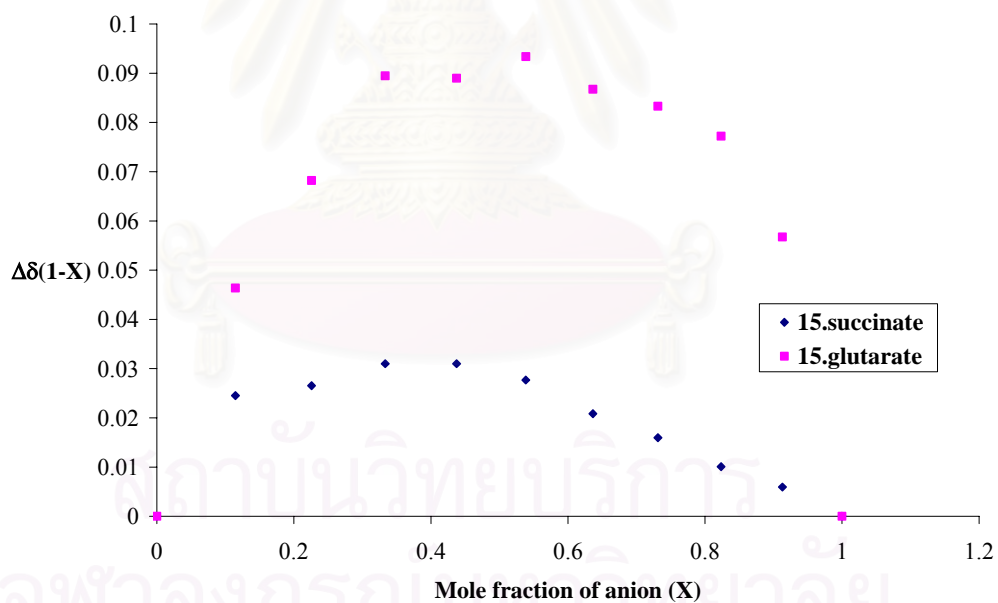


**Figure 3.24.** Job's plots of  $-\text{NHCSNHCH}_2\text{Ar}-$  in  $\mathbf{15}\cdot\text{succinate}^{2-}$  and  $\mathbf{15}\cdot\text{glutarate}^{2-}$  complexes.

The titration curves of  $\mathbf{14}\cdot\text{succinate}^{2-}$ ,  $\mathbf{14}\cdot\text{glutarate}^{2-}$  and  $\mathbf{15}\cdot\text{succinate}^{2-}$  complexes correlated well with a 1:1 binding model whereas the titration curve of  $\mathbf{15}\cdot\text{glutarate}^{2-}$  did not agree with that model at all (Figures 3.25 and 3.26).

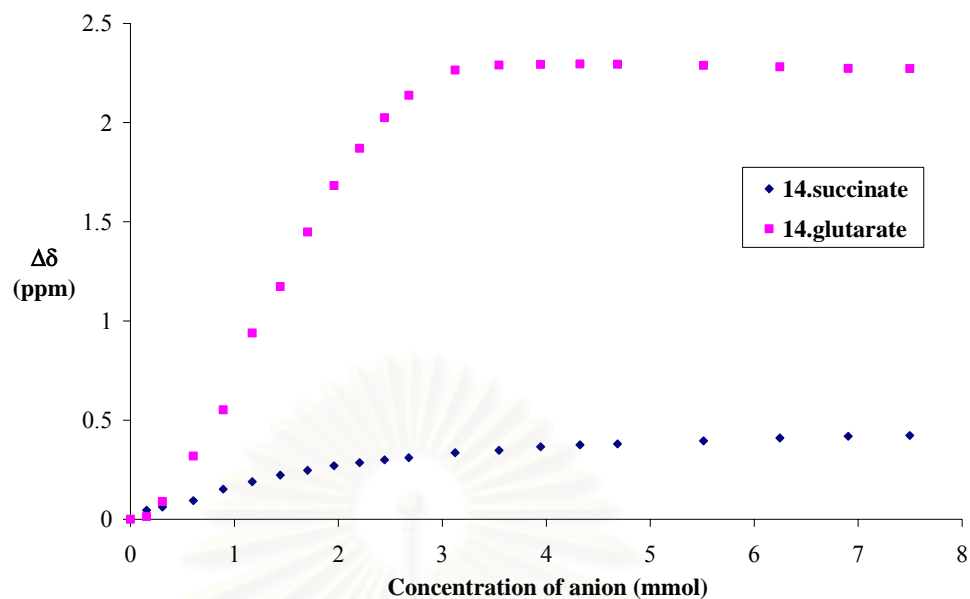


**Figure 3.25.** Titration curves of  $-\text{OCH}_2\text{CONH}-$  in  $14\cdot\text{succinate}^{2-}$  and  $14\cdot\text{glutarate}^{2-}$  complexes.

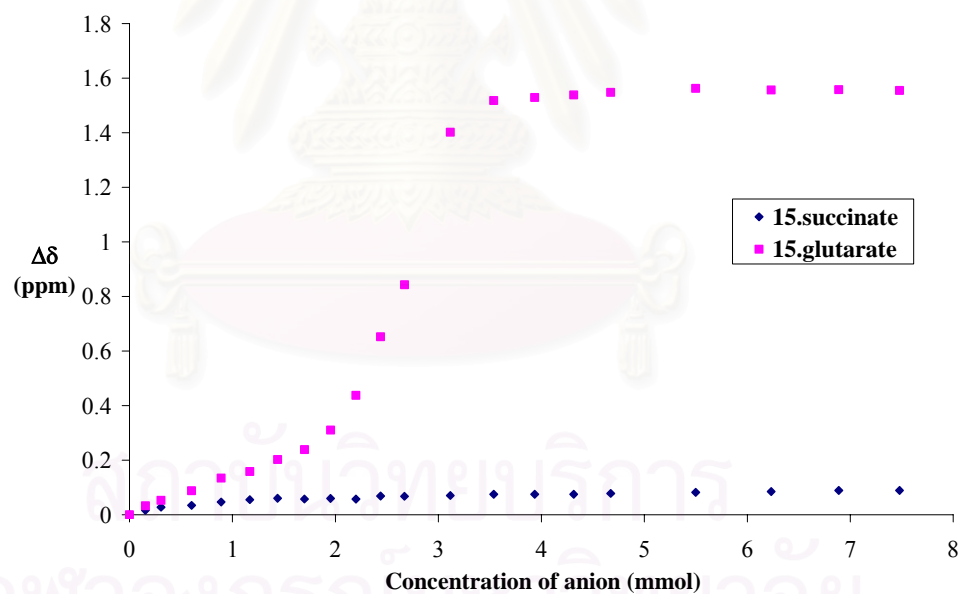


**Figure 3.26.** Titration curves of  $-\text{NHCSNHCH}_2\text{Ar}-$  in  $15\cdot\text{succinate}^{2-}$  and  $15\cdot\text{glutarate}^{2-}$  complexes.

The titration curve of  $15\cdot\text{glutarate}^{2-}$  complex featured a slow shifting until 1 equivalent of TBA glutarate was added, after that the shifting was accelerated until stable at about 1.5 equivalents of anion. This sigmoidal curve was observed for  $-\text{CH}_2\text{CH}_2\text{NHCSNHCH}_2\text{Ar}-$ ,  $-\text{CH}_2\text{CH}_2\text{NHCSNHCH}_2\text{Ar}-$  (see Appendix B) as well as -

$\text{OCH}_2\text{CH}_2\text{OCH}_3$  signals. The ArH-calixarene was also shifted in this pattern but in the opposite direction (upfield). Interestingly, the titration curves of  $-\text{NHCSNHCH}_2\text{Ar}-$ ,  $-\text{CH}_2\text{CH}_2\text{NHCSNH}-$  and  $-\text{OCH}_2\text{CH}_2\text{OCH}_3$  showed the upfield shift immediately before the inverse shift at about 1 equivalent. From the literatures, the normal titration curve could be either 1:1<sup>[150]</sup> or 1:2<sup>[144]</sup> host-guest stoichiometry. The sigmoidal or inverse curve have been reported only in the case of a 1:2 association.<sup>[131, 144]</sup> However, the Job's plots in **15**·glutarate<sup>2-</sup> did not show a maximum at  $X \approx 0.66$ . Therefore, it is impossible to assign this interaction to a discrete 1:2 complex. Consequently, the association constant has not been calculated in **15**·glutarate<sup>2-</sup> case. The sigmoidal curve could be originated the negative ion-pair effect of its counter cation ( $n\text{-Bu}_4\text{N}^+$ ). Table 3.10 displays the average association constants and Gibbs free energies which belongs to **14**·succinate<sup>2-</sup>, **14**·glutarate<sup>2-</sup> and **15**·succinate<sup>2-</sup>. The average calculated  $\beta_1$  of dicarboxylate complexes are compared as shown in Figure 3.27.

**Table 3.10.** The average association constants and Gibbs free energies upon the formation of **14**·dicarboxylate<sup>2-</sup> and **15**·dicarboxylate<sup>2-</sup>.

Complex		Association Constant	Gibbs free energy
Type	Stoichiometry	( $\text{M}^{-1}$ )	( $\text{kJ}\cdot\text{Mol}^{-1}$ )
<b>14</b> ·succinate <sup>2-</sup>	1:1	11000	-23.1
<b>14</b> ·glutarate <sup>2-</sup>	1:1	42900	-26.4
<b>15</b> ·succinate <sup>2-</sup>	1:1	2020	-18.9
<b>15</b> ·glutarate <sup>2-</sup>	1:1	-	-

สถาบันวิทยบริการ  
จุฬาลงกรณ์มหาวิทยาลัย

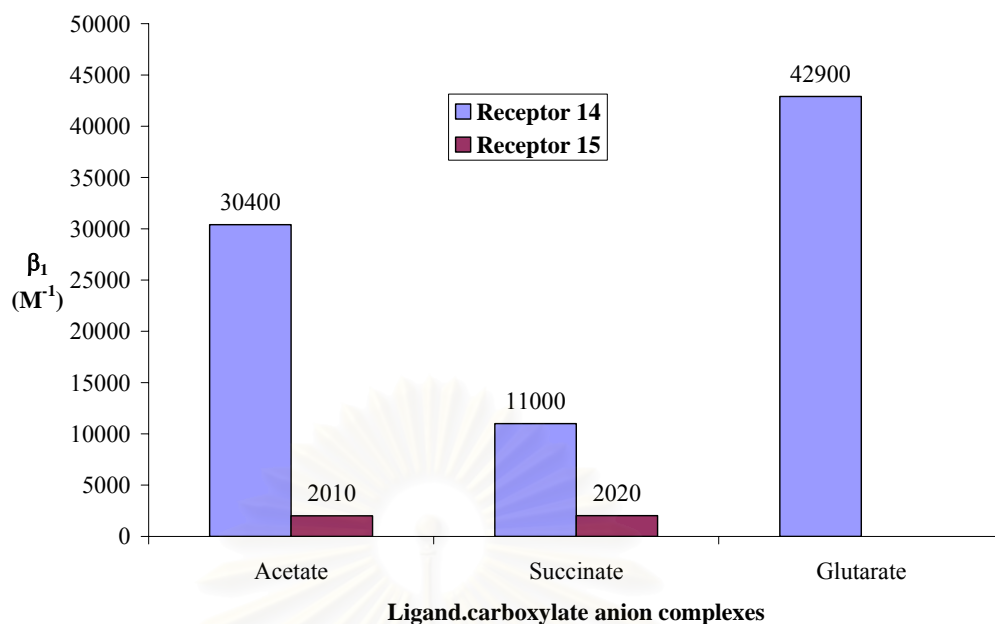


**Figure 3.27.** The selectivity of receptors **14** and **15** towards dicarboxylate anions compared to the monocarboxylate complexes.

Receptor **14** was found to bind succinate weaker and to recognize glutarate slightly better than acetate while compound **15** showed the moderate stability constants with acetate and succinate with similar binding abilities. The selectivity trend of both receptors towards succinate and glutarate could not be explained by basicity (Table 3.11). Therefore, there should be other effects such as size or length of anions to control the selectivity.

**Table 3.11.** Geometry and basicity of carboxylate anions.

Anions	Geometry	pK at 25 °C in water <sup>[130]</sup>	pK at 25 °C in DMSO <sup>[81]</sup>
Acetate	Trigonal planar	4.75	12.60
Succinate	Trigonal planar	4.21	-
Glutarate	Trigonal planar	3.77	-

The sizes of cavities between two thiourea functions in either **14** or **15**, which are rigidified by the aromatic linkage and the calixarene scaffold, are probably too small to bind both carboxylate ending sites simultaneously. Compared to receptor **15**, the amide group in compound **14** can be served as an additional anionic binding site.<sup>[151]</sup> From our result, the length of cavities in macromolecules **14** (from thiourea

to amide moiety) are well-match with the length of longer dicarboxylate anion like glutarate, but not with shorter dicarboxylate anion like succinate. In the system of compound **15**, insignificant preferential recognition were observed due to the lack of amide group. Therefore, the selectivity of these receptors highly depends on the number of hydrogen bonding interactions. The more involving hydrogen bonding interactions resulted in larger binding constants.<sup>[141]</sup> For instance, the crystal structure of tris-guanidinium·tricarballate complex which reported by Anslyn and co-workers showed the involvement of all guanidinium moieties to three carboxylate groups in the guest (Figure 3.28).<sup>[152]</sup>

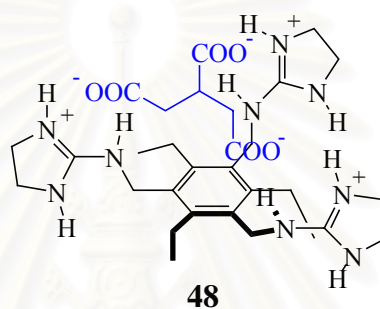


**Figure 3.28.** Tris-guanidinium·tricarballate complex.<sup>[152]</sup>

From the x-ray structure of tris-guanidinium·tricarballate complex and proposed structures of amide-carboxylate<sup>[151]</sup> association, the structures of dicarboxylate anion complexes are proposed in Figure 3.29 (X= NH or O; n = 2 or 3).

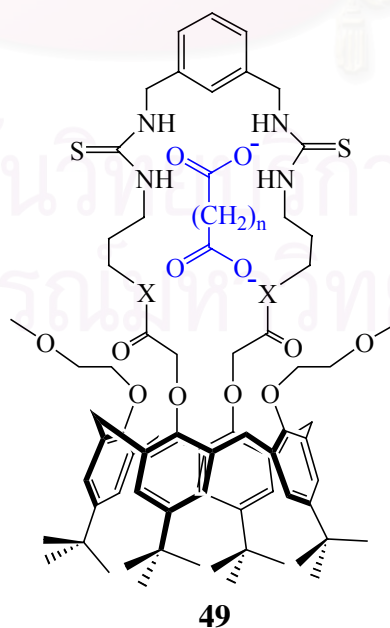


**Figure 3.29.** The proposed structures of 1:1 dicarboxylate complexes (**49**).



### 3.2.3 Binding Ability of Receptors **14** and **15** towards Amino Acids in Anionic Forms

The effective receptors for biorelevant oxoanions such as amino acids have recently received attention in the development of ion-selective electrodes or the carriers for drug delivery because amino acids are the most important substrates in living organisms. A well-designed receptor for amino acid should be able to dissolve in aqueous solution and comprises of at least two main recognition sites under neutral condition: ammonium and carboxylate groups. In addition, host should contain stereochemically active site. Accordingly, amino acids do actually exist as chiral zwitterions in blood system.

Although our receptors (**14** and **15**) are not specifically designed for amino acids, a good selectivity for either mono- or dicarboxylate anions over other inorganic anions have been found. Therefore, it is worth studying the binding ability of both receptors towards a wide range of underivatized amino acids. Basically, common amino acids provide a rich variety of side chains. To achieve a good selectivity for each amino acid, another moiety should be incorporated in the receptor. The aromatic linkage between two thiourea moieties which mainly used to preorganize receptor **14** and **15** is predicted to serve as an additional site for the side chain of aromatic containing amino acids. The chiral recognition is not expected due to the lack of stereochemically dependent. All amino acids are used as their optically pure L-enantiomer due to their importance species and cheaper cost.

The solid-liquid extraction was performed for some amino acids (glycine, L-alanine, D-alanine,  $\beta$ -alanine, 4-aminobutyric acid, L-phenylalanine, L-aspartic acid and L-glutamic acid). The excess amount of amino acids (about 50 mg) were added into acetonitrile- $d_3$  and dimethylsulfoxide- $d_6$  solutions of either **14** or **15**. The mixtures were shaken overnight and centrifuged for 15 minutes to precipitate the solid. A small amount of organic layer was collected and characterized by the complexation induced shift in  $^1\text{H-NMR}$  spectrum. There was no peak shift observing in the spectrum at all. This reflected that none of the association between solid amino acids and receptors because amino acids would not exist as their zwitterionic form in acetonitrile- $d_3$  or dimethylsulfoxide- $d_6$ . Consequently, the dipole-dipole repulsion between *NH*-thiourea and *OH*-carboxylic acid hydrogen bond donor inhibited the

complexation. Although some common amino acids are able to solvate and display as zwitterions in methanol in which both host molecules **14** and **15** are hardly soluble prohibiting the preliminary extraction experiment in methanol-*d*<sub>4</sub>.

Generally, artificial receptors for amino acids have been synthesized using single charged substrate, under either acidic (amino acid or amino ester salts) or basic (carboxylate salts or N-protected amino acid) condition.<sup>[153]</sup> Most receptors based on positively and negatively charged binding sites are able to collapse internally or aggregate into dimers or oligomers. Both bis-thiourea calix[4]arene amide **14** and ester **15** can serve as receptors for basic amino acids like carboxylate salts. Therefore, instead of the neutral zwitterions, amino acids are modified to their tetrabutylammonium carboxylate anions to dissolve in acetonitrile-*d*<sub>3</sub> and to reduce ion-pair effect.

A number of model receptors for recognition of unsubstituted dicarboxylate anion have been prepared and evaluated. Examples of suitable ligands for the selective complexation of mono- and dicarboxylate anions of amino acids are scarce. Consequently, the binding properties of supramolecules **14** and **15** were investigated towards various TBA salts of amino acids. The aspartic acid (**50**) and glutamic acid (**51**) were chosen due to their dicarboxylate groups and the equivalent of carbon to succinate (**40**) and glutarate (**41**) anion as previously discussed in Section 3.2.2. To probe the chain length and effect of functional side chain of amino acid, binding properties of receptors **14** and **15** towards a wide range of amino acid in anionic form; asparagine (**52**), glutamine (**53**), phenylalanine (**54**), leucine (**55**), threonine (**56**) and serine (**57**), were also investigated. The structures of all substituted mono- and dicarboxylate anions that used in this experiment are displayed in Figure 3.30.

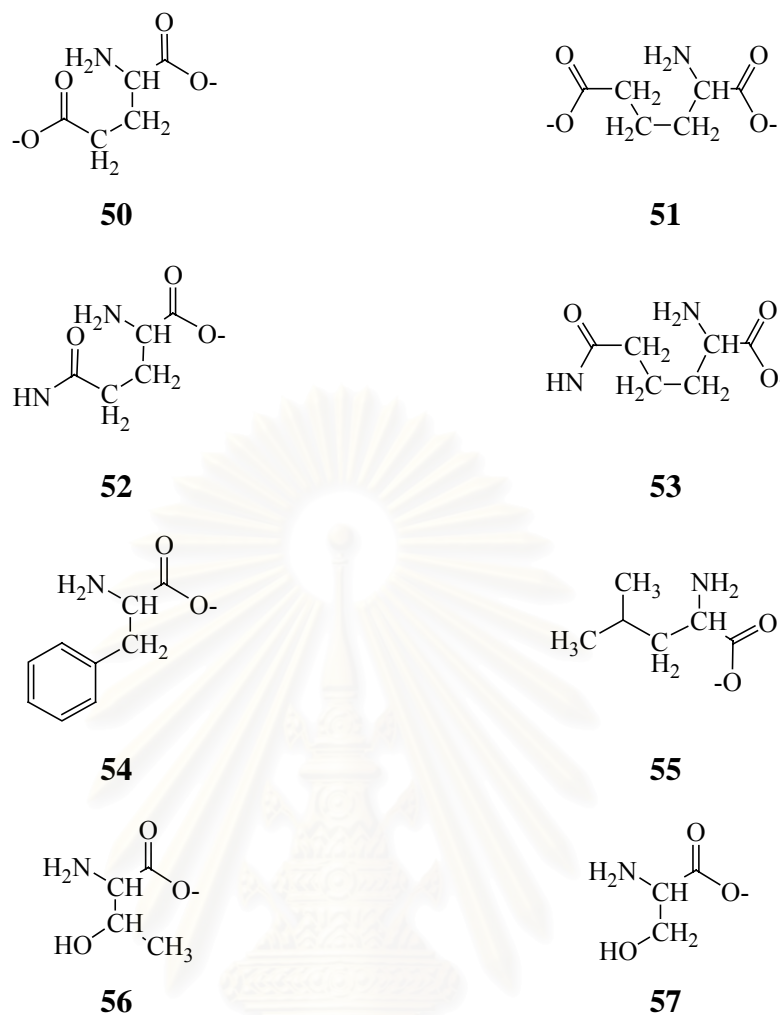
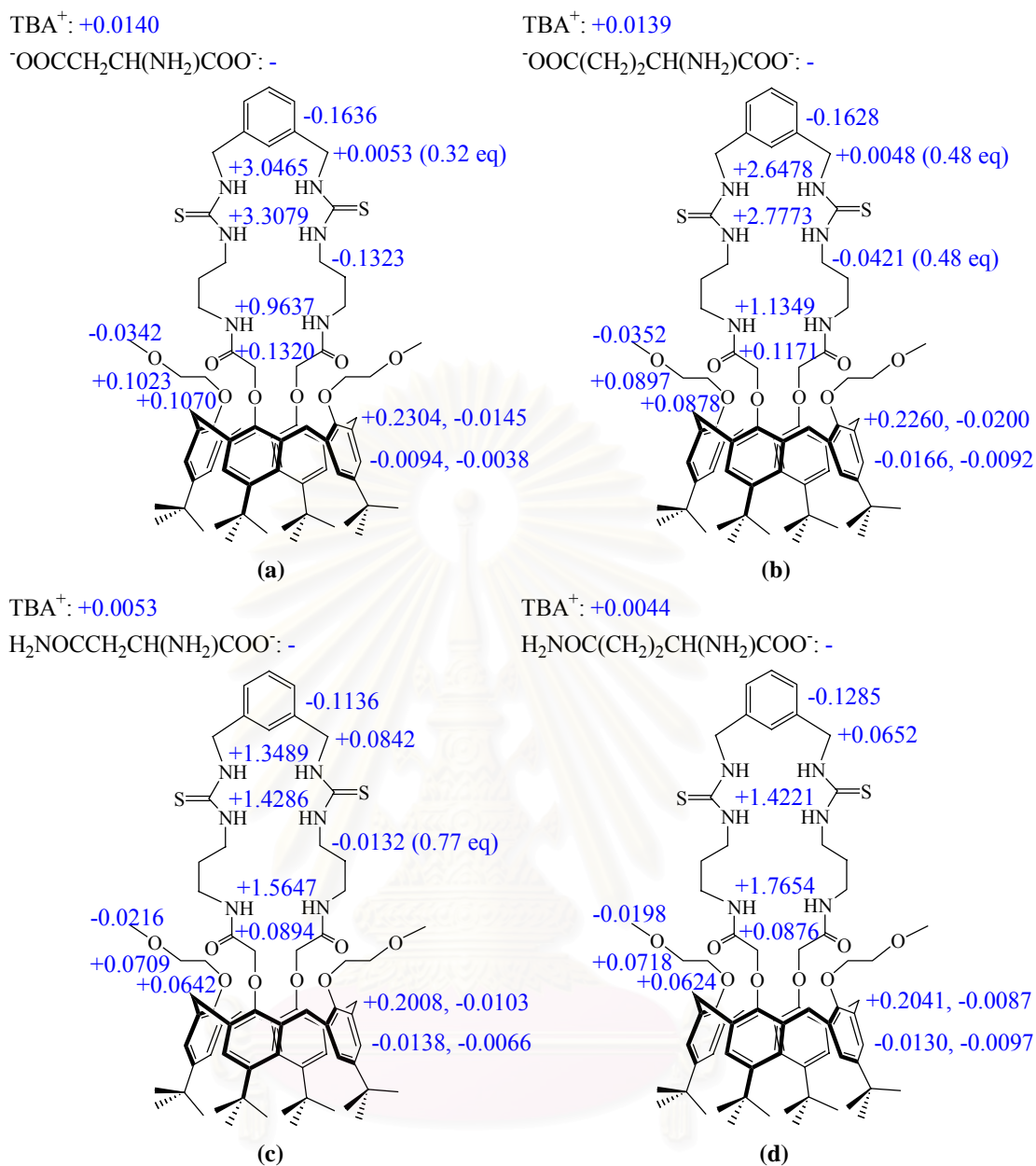


**Figure 3.30.** The structures of all amino acid anions in this experiment.

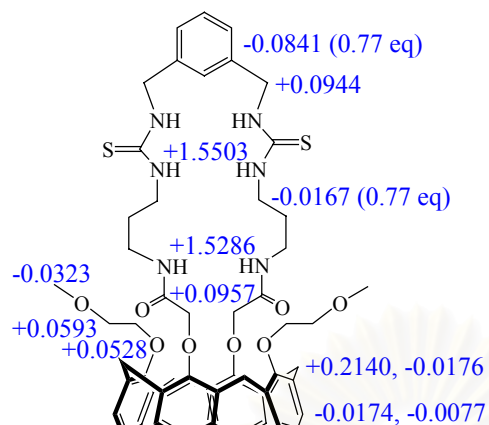
$^1\text{H-NMR}$  spectra of free and bound receptors **14** and **15** showed only one set of signals corresponding to the faster exchange rate compared to the NMR time scale which was the same as observed in the carboxylate and phosphate anion recognition. The binding property of compound **14** towards the bis-TBA salt of aspartic acid was firstly investigated. The association of host **14** and this substituted dicarboxylate anion was supported by the partial separation of the overlapping *NH*-thiourea signals in the  $^1\text{H-NMR}$  spectrum of **14**·Asp $^{2-}$ . The acetonitrile- $d_3$  solution of the complex displayed a magnificent downfield shift with  $\Delta\delta = +3.3079$  ppm due to the  $-\text{CH}_2\text{CH}_2\text{NHCSNHCH}_2\text{Ar}-$  protons and with  $\Delta\delta = +3.0465$  ppm owing to  $-\text{CH}_2\text{CH}_2\text{NHCSNHCH}_2\text{Ar}-$  protons. In addition,  $-\text{CH}_2\text{CH}_2\text{NHCSNH}-$  signal experienced the upfield shift ( $\Delta\delta = -0.1323$  ppm), while the  $-\text{NHCSNHCH}_2\text{Ar}-$  signals tended to broaden until disappear after shifting to a lower magnetic field (from 4.6817 to 4.6870 ppm,  $\Delta\delta = +0.0053$  ppm) in the presence of 0.32 equivalent of the

bis-TBA salt of aspartic acid. Another significant downfield shift for this association process was discovered at 7.5617 ppm belonging to the *NH*-amide protons ( $\Delta\delta = 0.9637$  ppm). One of the aromatic linkage protons was moved to the higher magnetic field with  $\Delta\delta = -0.1636$  ppm. Moreover, the downfield shift from 4.4630 to 4.5950 ppm ( $\Delta\delta = +0.1320$  ppm) of the  $-\text{OCH}_2\text{CONH}-$  signal was observed. Other downfield shifts were also revealed for  $-\text{OCH}_2\text{CH}_2\text{OCH}_3$  ( $\Delta\delta = +0.1070$  ppm) and  $-\text{OCH}_2\text{CH}_2\text{OCH}_3$  ( $\Delta\delta = +0.1023$  ppm) signals in  $^1\text{H-NMR}$  titration data whereas the changing of  $-\text{OCH}_2\text{CH}_2\text{OCH}_3$  was observed as an upfield shift,  $\Delta\delta = -0.0342$  ppm. The downfield shift of  $n\text{-Bu}_4\text{N}^+$  signal ( $\Delta\delta = +0.0140$  ppm) suggested that this bulky cation was situated in the close proximity to the anionic substrate. In addition, the changing in the peak position of both  $-\text{ArCH}_2\text{Ar}-$  ( $\Delta\delta = +0.2304, -0.0145$  ppm) and  $-\text{CH}_2\text{ArHCH}_2-$  ( $\Delta\delta = -0.0094, -0.0038$  ppm) which were characteristic signals of the calixarene building block were also monitored.

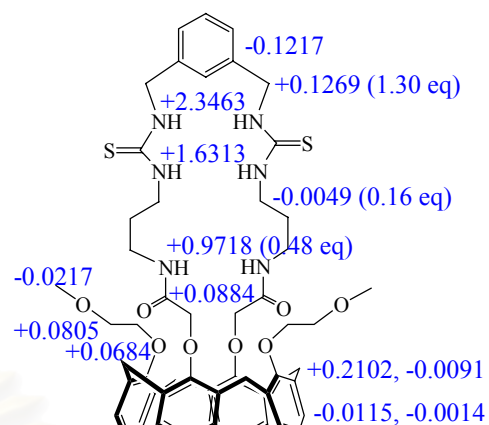
Titration of an acetonitrile- $d_3$  solution of either **14** or **15** with aliquots of substituted mono- and dicarboxylate guests resulted in several shifts as displayed in Figure 3.31 and Figure 3.32.



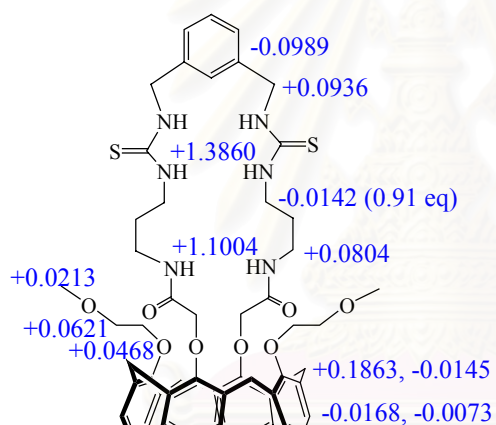
**Figure 3.31.** The complexation induced shifts of some proton signals on <sup>1</sup>H-NMR spectrum (a) **14**·Asp<sup>2-</sup>, (b) **14**·Glu<sup>2-</sup>, (c) **14**·Asn<sup>-</sup>, (d) **14**·Gln<sup>-</sup>, (e) **14**·Phe<sup>-</sup>, (f) **14**·Leu<sup>-</sup>, (g) **14**·Thr<sup>-</sup> and (h) **14**·Ser<sup>-</sup>.

TBA<sup>+</sup>: +0.0040C<sub>6</sub>H<sub>5</sub>CH<sub>2</sub>CH(NH<sub>2</sub>)COO<sup>-</sup>: -

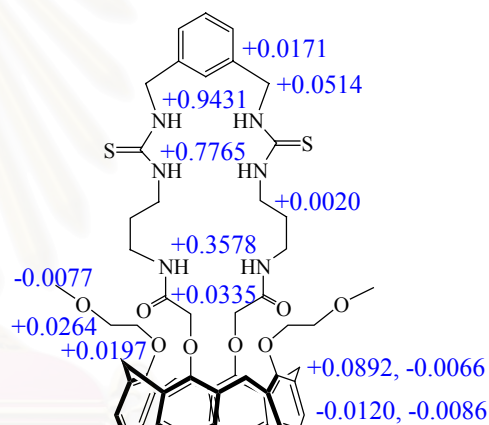
(e)

TBA<sup>+</sup>: +0.0370(CH<sub>3</sub>)<sub>2</sub>CHCH<sub>2</sub>CH(NH<sub>2</sub>)COO<sup>-</sup>: -

(f)

TBA<sup>+</sup>: +0.0058CH<sub>3</sub>CH(OH)CH(NH<sub>2</sub>)COO<sup>-</sup>: -

(g)

TBA<sup>+</sup>: +0.0027HOCH<sub>2</sub>CH(NH<sub>2</sub>)COO<sup>-</sup>: -

(h)

Figure 3.31. *Continued.*

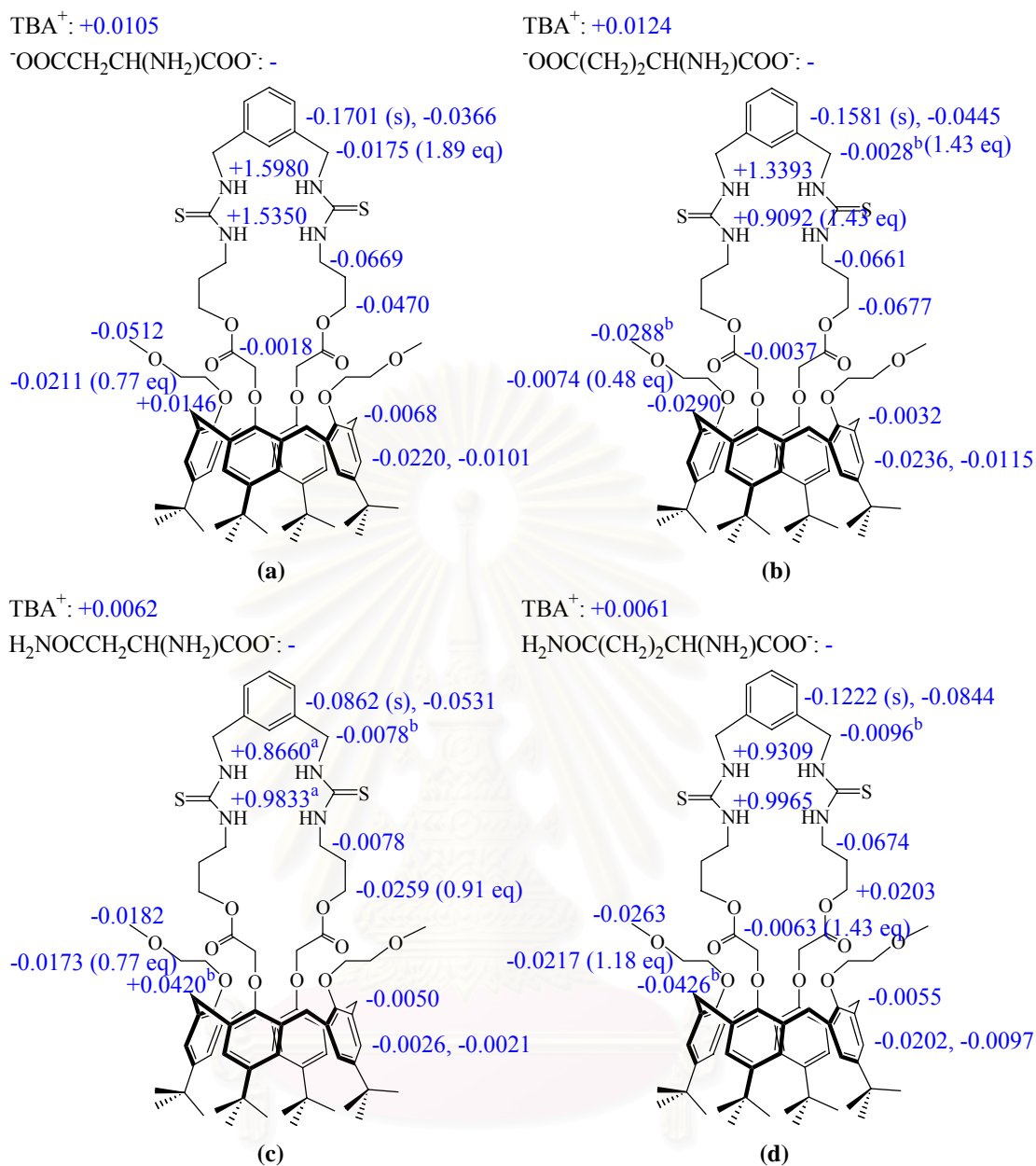


**Figure 3.32.** The complexation induced shifts of some proton signals on <sup>1</sup>H-NMR spectrum (a) **15**·Asp<sup>2-</sup>, (b) **15**·Glu<sup>-</sup>, (c) **15**·Asn<sup>-</sup>, (d) **15**·Gln<sup>-</sup> (e) **15**·Phe<sup>-</sup>, (f) **15**·Leu<sup>-</sup>, (g) **15**·Thr<sup>-</sup> and (h) **15**·Ser<sup>-</sup>.

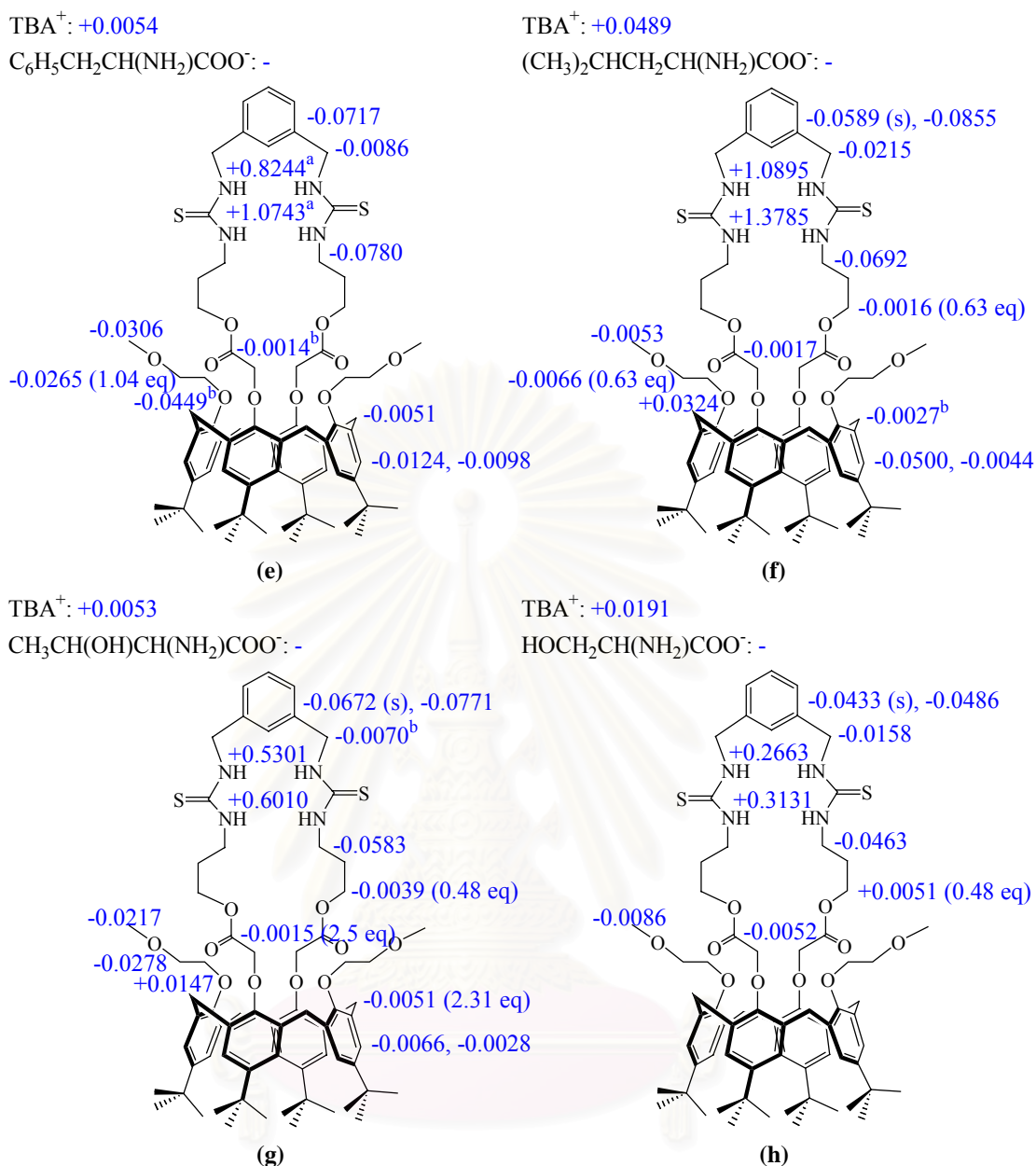


**Figure 3.32.** *Continued.*

The downfield shift observed for the signals corresponding to the *NH*-thiourea moiety of all complexes in the presence of TBA salt of amino acid is an indicative of the intermolecular hydrogen bonding. In some cases (glutamine, phenylalanine and threonine), the signal for the  $-\text{CH}_2\text{CH}_2\text{NHCSNHCH}_2\text{Ar}-$  of host **14** could not be followed because the *NH*-resonance disappears after coalesce in the aromatic signal region upon adding 0.05 equivalents of the anion. However, the strong hydrogen bonding in complexes was indicated by the significant downfield shift before completely disappearing.



The complex stoichiometry in an acetonitrile- $d_3$  solution was judged by Job's plot consistent with the titration curve of the  $^1\text{H-NMR}$  binding data. The formation of simple 1:1 complexes in cases of all **14**·amino carboxylate complexes (Figure 3.33) and **15**· $\text{Asp}^{2-}$ , **15**· $\text{Glu}^{2-}$ , **15**· $\text{Leu}^-$  as well as **15**· $\text{Ser}^-$  (Figure 3.34) was evidence by the symmetric bell-shaped ( $X \approx 0.5$ ) in Job's analysis. In contrast, Job's plots of amino monocarboxylate anions such as asparagine, glutamine, phenylalanine and threonine were asymmetrical and exhibited a maximum point when the mole fraction was  $\sim 0.66$  (Figure 3.34), which reflected the formation of an unexpected 1:2 stoichiometry.

Bis-thiourea calix[4]arene amide **14** was found to bind anions in 1:1 fashions whereas analogous ester **15** was able to recognize these guests in either 1:1 or 1:2 fashions. Theoretically, a 1:2 binding fashion is possible to confirm by ESI-MS<sup>[138-139]</sup> or VPO.<sup>[140]</sup> Our attempts to observe the molecular peak in ESI<sup>+</sup>/ESI<sup>-</sup> mass spectra of this complex were unsuccessful because the complex was probably not stable enough under MS conditions.

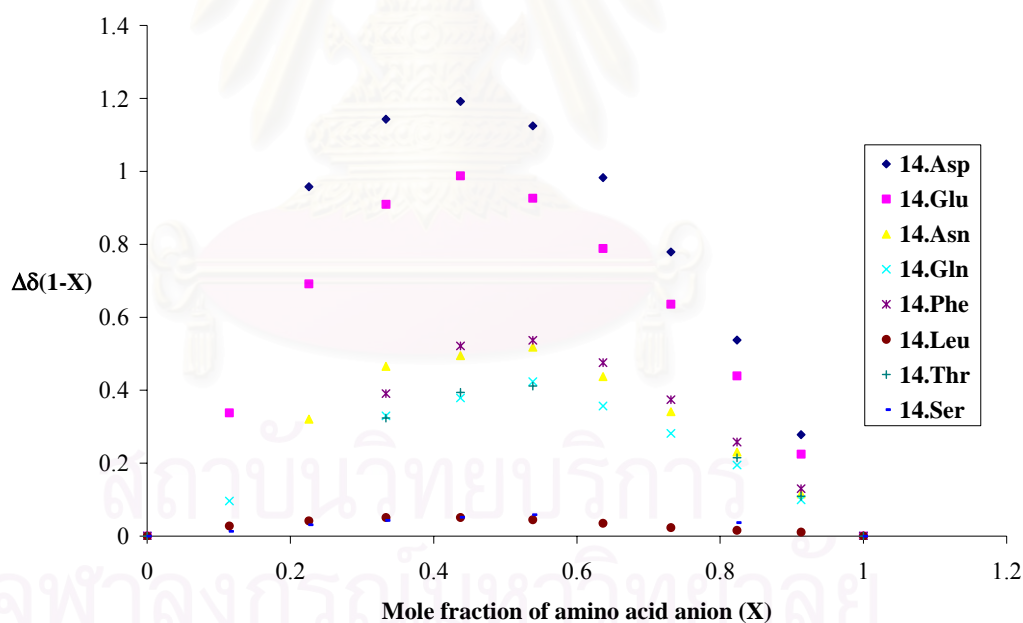


**Figure 3.33.** Job's plots of  $-\text{CH}_2\text{CH}_2\text{NHCSNHCH}_2\text{Ar}-$  in **14**· $\text{Asp}^{2-}$ , **14**· $\text{Glu}^{2-}$ , **14**· $\text{Asn}^-$ , **14**· $\text{Gln}^-$ , **14**· $\text{Phe}^-$ , **14**· $\text{Leu}^-$ , **14**· $\text{Thr}^-$ , and **14**· $\text{Ser}^-$  complexes (using  $-\text{NHCSNHCH}_2\text{Ar}-$  signal in case of **14**· $\text{Leu}^-$ ).

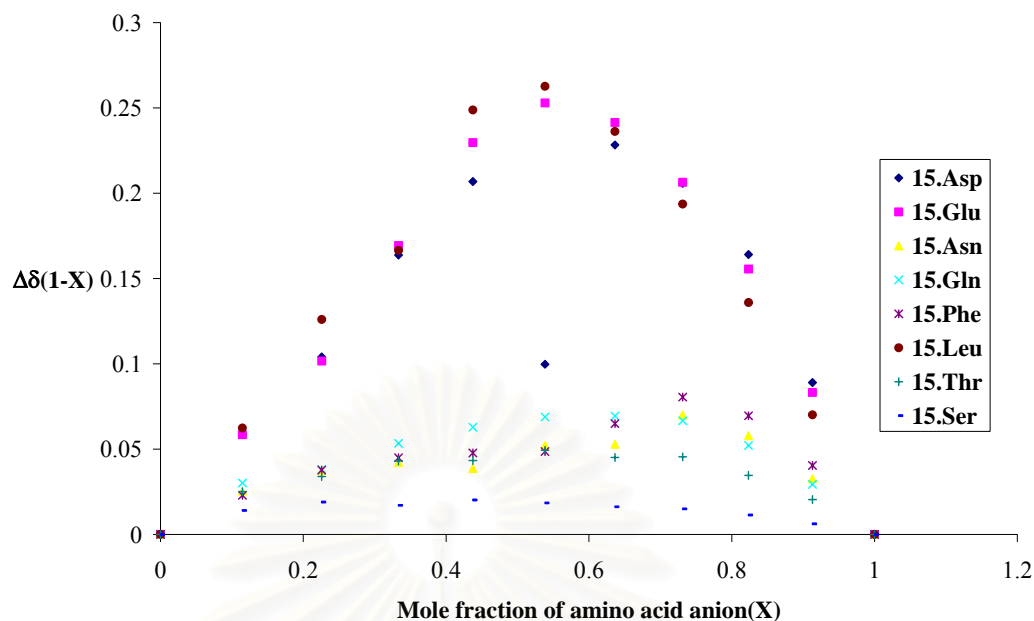


**Figure 3.34.** Job's plots of  $-\text{CH}_2\text{CH}_2\text{NHCSNHCH}_2\text{Ar}-$  in  $15\cdot\text{Asp}^-$ ,  $15\cdot\text{Glu}^{2-}$ ,  $15\cdot\text{Asn}^-$ ,  $15\cdot\text{Gln}^-$ ,  $15\cdot\text{Phe}^-$ ,  $15\cdot\text{Leu}^-$ ,  $15\cdot\text{Thr}^-$ , and  $15\cdot\text{Ser}^-$  complexes.

Generally, the shape of titration curves is dependent on types of complexation. The titration plots of all **14**·amino acid anion (Figure 3.35) as well as receptor **15** in the presence of TBA salt of aspartic acid, glutamic acid or leucine (Figure 3.36) exhibited the normal looking curve for the 1:1 stoichiometry complex. In the presence of carboxylate salt of serine, the straight lines of titration curves were displayed in both systems (**14** or **15**) and subsequently, no equilibrium was observed (Figures 3.35 and 3.36). The titration curve of the remaining cases ( $15\cdot\text{Asn}^-$ ,  $15\cdot\text{Gln}^-$ ,  $15\cdot\text{Phe}^-$ , and  $15\cdot\text{Thr}^-$ ) indicated the successive binding of two anions (Figure 3.36). This singly and doubly bound in each case were nearly coincident leading to two indistinguishable events.<sup>[131]</sup> Such a behavior was more clearly displayed in the case of TBA salt of phenylalanine. The suitable technique to observe these multiple binding equilibria is the calorimetric titration due to the distinct nature of the enthalpy of the alternate complexes.

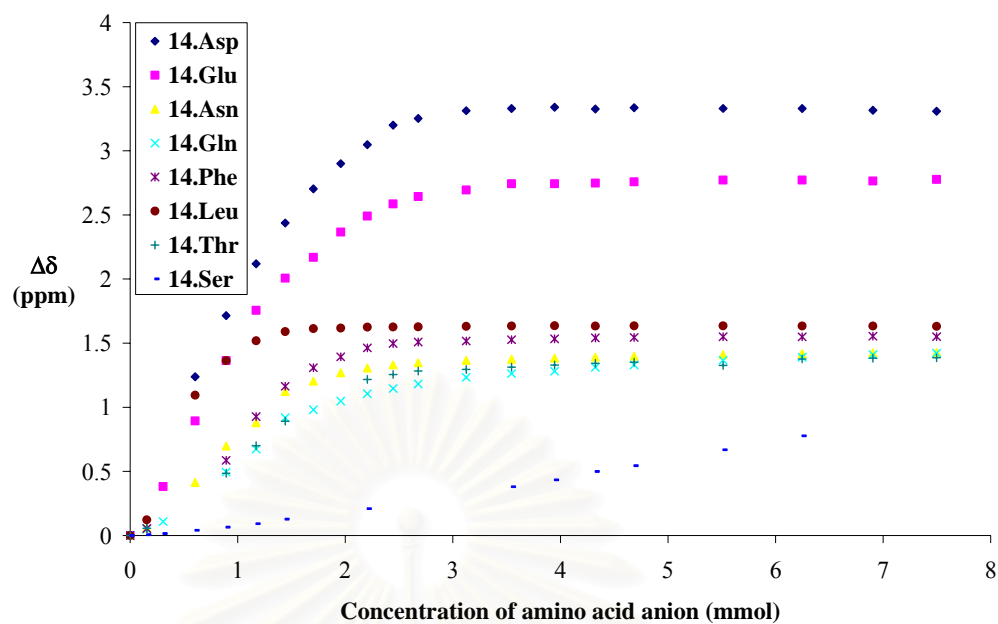


**Figure 3.35.** Titration curves of  $-\text{CH}_2\text{CH}_2\text{NHCSNHCH}_2\text{Ar}-$  in  $14\cdot\text{Asp}^{2-}$ ,  $14\cdot\text{Glu}^{2-}$ ,  $14\cdot\text{Asn}^-$ ,  $14\cdot\text{Gln}^-$ ,  $14\cdot\text{Phe}^-$ ,  $14\cdot\text{Leu}^-$ ,  $14\cdot\text{Thr}^-$ , and  $14\cdot\text{Ser}^-$  complexes.

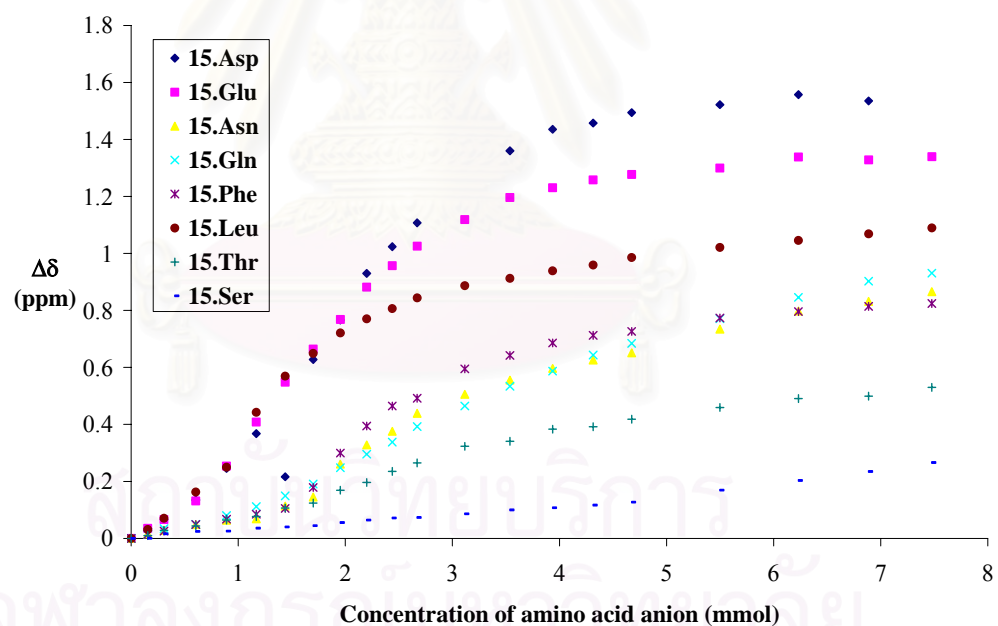


**Figure 3.36.** Titration curves of  $-\text{CH}_2\text{CH}_2\text{NHCSNHCH}_2\text{Ar}-$  in  $15\cdot\text{Asp}^{2-}$ ,  $15\cdot\text{Glu}^{2-}$ ,  $15\cdot\text{Asn}^-$ ,  $15\cdot\text{Gln}^-$ ,  $15\cdot\text{Phe}^-$ ,  $15\cdot\text{Leu}^-$ ,  $15\cdot\text{Thr}^-$ , and  $15\cdot\text{Ser}^-$  complexes.

Having verified the 1:1 and 1:2 stoichiometry for the associations by means of continuous variation method, the stability constants were determined by NMRTit\_HG and NMRTit\_HGG program, respectively.<sup>[105]</sup> The average association constants and Gibbs free energies which are based on monitoring of both *NH*-thiourea and their

adjacent methylene protons as well as the *NH*-amide signals (in the case of ligand **14**) are displayed in Table 3.12. Binding curves of **15**·Asp<sup>-</sup>, **15**·Glu<sup>-</sup>, **15**·Phe<sup>-</sup> and **15**·Thr<sup>-</sup> were fitted well in NMRTit\_HGG program. Clearly, formation of the 1:2 fashion of these complexes can be observed from the sigmoidal curve. The binding data of **15**·Asp<sup>-</sup> and **15**·Phe<sup>-</sup> complexes gave the association constants at the upper limit of detectability using NMR titrations ( $>10^4$  M<sup>-1</sup>) whereas the binding data of **14**·Ser<sup>-</sup> and **15**·Ser<sup>-</sup> complexes are at the lower limit of this techniques ( $<10$  M<sup>-1</sup>), thus the binding constants have been reported approximately.<sup>[78, 154-155]</sup>

**Table 3.12.** The average association constants and Gibbs free energies upon the formation of **14**·amino carboxylate and **15**·amino carboxylate complexes.

Complex		Association Constant	Gibbs free energy
Type	Stoichiometry	(M <sup>-1</sup> )	(kJ·Mol <sup>-1</sup> )
<b>14</b> ·Asp <sup>2-</sup>	1:1	21200	-24.7
<b>14</b> ·Glu <sup>-</sup>	1:1	15500	-23.9
<b>14</b> ·Asn <sup>-</sup>	1:1	19600	-24.5
<b>14</b> ·Gln <sup>-</sup>	1:1	8270	-22.3
<b>14</b> ·Phe <sup>-</sup>	1:1	24800	-25.1
<b>14</b> ·Leu <sup>-</sup>	1:1	49600	-26.8
<b>14</b> ·Thr <sup>-</sup>	1:1	10300	-22.9
<b>14</b> ·Ser <sup>-</sup>	1:1	< 10	-
<b>15</b> ·Asp <sup>2-</sup>	1:1	17700	-24.2
<b>15</b> ·Glu <sup>2-</sup>	1:1	11900	-23.3
<b>15</b> ·Asn <sup>-</sup>	1:2	$> 10^4$	-
		$> 10^7$ (M <sup>-2</sup> )	-
<b>15</b> ·Gln <sup>-</sup>	1:2	39100	-26.2
		28269300 (M <sup>-2</sup> )	-42.5
<b>15</b> ·Phe <sup>-</sup>	1:2	$>10^4$	-
		$> 10^7$ (M <sup>-2</sup> )	-
<b>15</b> ·Leu <sup>-</sup>	1:1	10200	-22.9
<b>15</b> ·Thr <sup>-</sup>	1:2	17100	-24.1
		31122000 (M <sup>-2</sup> )	-42.7
<b>15</b> ·Ser <sup>-</sup>	1:1	< 10	-

The binding data in Table 3.12 implied that the association constants of the singly bound complexes ( $K_1$ ) of  $15 \cdot \text{Asn}^-$ ,  $15 \cdot \text{Gln}^-$ ,  $15 \cdot \text{Phe}^-$  and  $15 \cdot \text{Thr}^-$  are much larger than the doubly bound complexes ( $K_2$ ). This can be rationalized by the anion-anion repulsion.  $K_1$  and  $K_2$  are stepwise formation constants which define by the following equations.

$$K_1 = \frac{[\text{HG}]}{[\text{H}][\text{G}]}$$

$$K_2 = \frac{[\text{HGG}]}{[\text{HG}][\text{G}]}$$

The association constants of all amino carboxylate complexes are displayed in Figure 3.37. In the case of 1:2 association, the first bound association constant ( $\beta_1$ ) are shown.

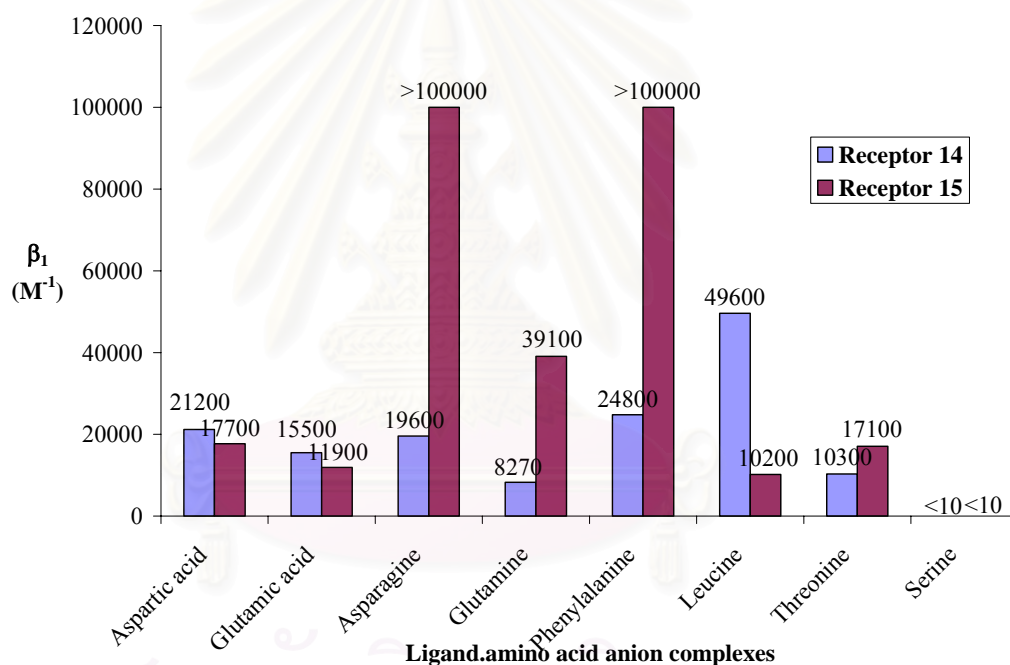


**Figure 3.37.** The selectivity of receptors **14** and **15** towards various amino mono- and dicarboxylate anions.

Like the anion recognition study, receptors **14** and **15** did not display the same stoichiometry ratio and trend of selectivity in the presence of TBA salt of amino acids. Macromolecule **15** displayed the higher efficiency and selectivity than compound **14**. Presumably, either amide or ester function played a role in partially controlling the recognition process by means of the complementary structure and the acid-base property.

The binding constants of amide compound **14** towards all amino acid anions suggested the following order of affinity: leucine > phenylalanine > aspartic acid > asparagine > glutamic acid > threonine > glutamine >> serine. On the other hand, the binding efficiency of ester **15** was as follows: phenylalanine  $\approx$  asparagine > glutamine > aspartic acid > threonine > glutamic acid > leucine > glutamine >> serine. Generally, the design of a receptor for selective recognition of the amino acid side chain is a difficult task.<sup>[153]</sup> Therefore, it is reasonable that the association constant of all complexes is  $\sim 10^4$ .

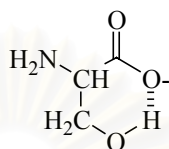
Except for **14**·Leu<sup>-</sup> and **15**·Asn<sup>-</sup>, both receptors displayed the largest affinity towards TBA salt of phenylalanine. This can originate from  $\pi$ - $\pi$  interaction in the similar manner as phenylphosphinate complexes. The strongest affinity of host **14** towards TBA salt of leucine compared to other amino acid anions (especially TBA salt of threonine) as well as the preference of macromolecule **15** to carboxylate anion of threonine over leucine might be attributed to acid-base property (Table 3.13). The more acidic receptor like **14** preferred the more base like TBA salt of leucine. *Vice versa*, the less acidic host like **15** better recognized the less base like carboxylate anion of threonine. The effect of acid-base in the system of **14**·Leu<sup>-</sup> was strong enough to override the complementary structure in **14**·Phe<sup>-</sup>.

**Table 3.13.** Basicity of some amino acids in water at 25 °C.<sup>[130]</sup>

Amino acid	Type of anion	p <i>K</i> <sub>a1</sub>	p <i>K</i> <sub>a2</sub>
D-Aspartic acid	Dicarboxylate	-	3.87
L-Glutamic acid	Dicarboxylate	2.13	4.31
L-Asparagine	Carboxylate	-	8.80
L-Glutamine	Carboxylate	2.15	9.00
L-Phenylalanine	Carboxylate	2.16	9.31
L-Leucine	Carboxylate	2.328	9.744
L-Threonine	Carboxylate	2.088	9.100
L-Serine	Carboxylate	2.186	9.208

The <sup>1</sup>H-NMR data of either **14**·Ser<sup>-</sup> or **15**·Ser<sup>-</sup> showed moderate spectral changes, however, their calculated association constants displayed a very low stability complex. Presumably, the OH group on serine was able to form the intramolecular

hydrogen bonding (Figure 3.38) which was more stable than the intermolecular hydrogen bonding. This led to a generally unfavorable interaction between host and TBA salt of serine. The presence of methyl group on the carboxylate anion of threonine gave an advantage in preventing the rotation of OH moiety to form a six-membered ring. Hence, the host-guest interaction in the system of TBA salt of threonine displayed four orders of magnitude larger than serine.



57

**Figure 3.38.** Intramolecular hydrogen bonding of carboxylate anion of serine.

Ligand **14** bound TBA salt of aspartic acid stronger than asparagines and TBA salt of glutamic acid stronger than glutamine. Conversely, macromolecule **15** recognized carboxylate anion of asparagine better than aspartic acid and carboxylate anion of glutamine better than glutamic acid. Receptor **14** preferred to bind amino dicarboxylate anions whereas host **15** preferred to encapsulate amino monocarboxylate anions which had the same length. This could be rationalized based on the complementary of hydrogen bond donors and acceptors. In addition to the *NH*-thiourea, compound **14** contained amide as a hydrogen bond donor to an acceptor like carboxylate group of dicarboxylate salt of aspartic or glutamic acid<sup>[151]</sup> whereas the ester moiety in macromolecule **15** acted as a hydrogen bond acceptor for a donor like amide group of monocarboxylate salt of asparagine or glutamine. The selectivity trend of these amino mono and dicarboxylate anion complexations seemed to be a combination of two binding sites.

The ability of either receptor **14** or **15** towards TBA salts of aspartic acid, glutamic acid, asparagine and glutamine also clearly depended on the chain length *n* of amino acid anions. The order of binding ability are aspartic acid ( $n = 2$ ) > glutamic acid ( $n = 3$ ) and asparagine ( $n = 2$ ) > glutamine ( $n = 3$ ) when *n* is defined as number of carbon between two carboxylate end sites. A slightly lower efficiency of both receptors towards longer amino acids ( $n = 3$ ) was observed. This could be ascribed to the compensation of the steric hindrance by hydrogen bonding.

The binding efficacies of **14** and **15** towards unsubstituted and substituted dicarboxylate anions are displayed in Figure 3.39. In most cases, receptor **14** preferred to bind acetate stronger than dicarboxylate while ligand **15** recognized dicarboxylate better than acetate.

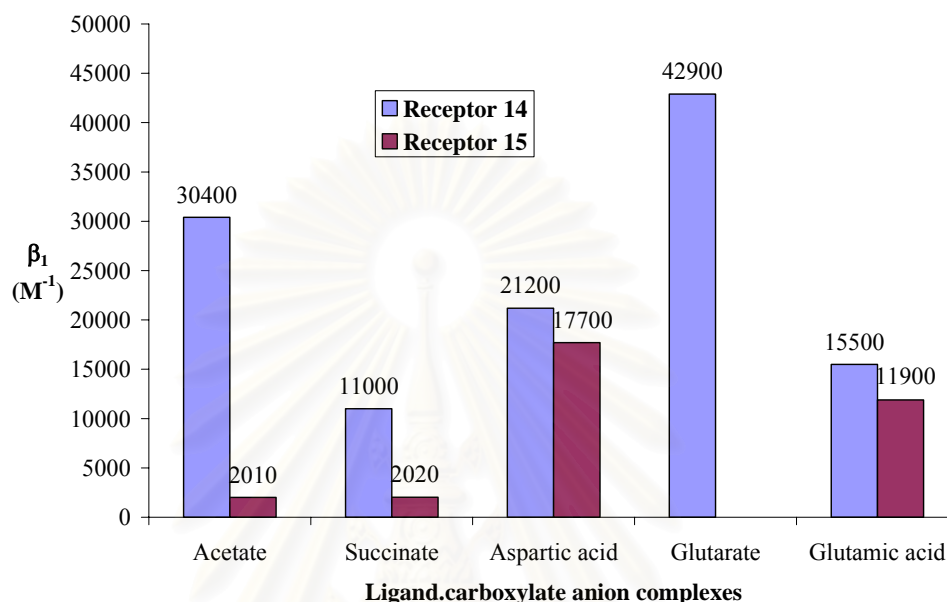


**Figure 3.39.** The selectivity of receptors **14** and **15** towards monocarboxylate anion (acetate), unsubstituted dicarboxylate anion (succinate and glutamine) and substituted dicarboxylate anion (aspartic acid and glutamic acid).

Bis-thiourea **14** is the more effective receptor for the longer unsubstituted dicarboxylate like glutarate compared to the shorter one like succinate. Conversely, the shorter substituted dicarboxylate anion such as bis-TBA salt of aspartic acid is better recognized by either **14** or **15** compared to the longer one like bis-TBA salt of glutamic acid. The different in affinity trend could be described in terms of the more rigid of the side chains of substituted dicarboxylates. Compared to receptor **15**, the greater recognition ability of host **14** towards either unsubstituted or substituted dicarboxylate was supported by the preference of ligand **14** to encapsulate acetate. The observed selectivity order demonstrated the importance of complementary between the substituted unit of guests and the binding site of the hosts as well as the acid-base property. The most stabilized complex occurred when this match is optimized. Although it is not able to indicate the exact position of the guest, the structure of amino acid anion complexes are proposed based on our  $^1H$ -NMR titration



data and the structures reported in literature<sup>[34, 151, 156]</sup> (Figure 3.40). X represents of NH and O in the case of compounds **14** and **15**, respectively. R refers to the substituted group on TBA salts of aspartic acid, glutamic acid, asparagine, glutamine, phenylalanine, threonine, leucine and serine as presented in Figure 3.30.

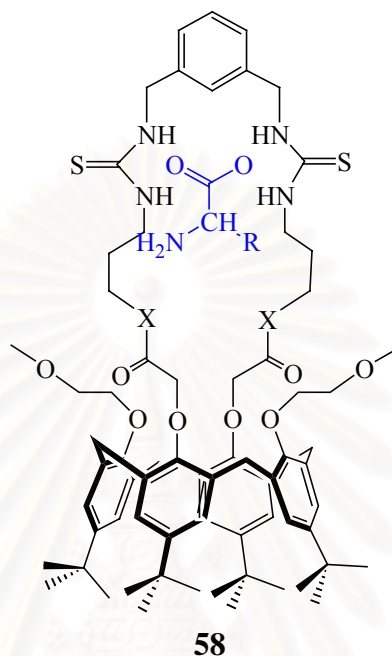


**Figure 3.40.** The proposed structures of 1:1 amino acid anion complexes (**58**).

### 3.2.4 Binding Enhancement of Receptors **14** and **15** towards Anions Using Sodium Cation

Moving to the realm of allosteric system, a new approach for the specific design of a receptor is very important in the allosteric study. To design a positively heteroditopic system, the first guest binding must make the remote site more suitable for the second guest binding. In order to complex an ion-pair successfully, the receptor should design to complex cation and anion species as either contact ion-pairs<sup>[83, 157]</sup> or solvent separated ion-pair ( $C^+$ -solvent- $A^-$ )<sup>[82, 157]</sup>

Calixarenes are attractive host molecules to construct recognition sites for target guests. Although calix[4]arene structural framework has been widely modified at the lower rim for the recognition of cations or anions, the design and synthesis of ditopic calix[4]arene to simultaneously bind cations and anions is still relatively rare. Receptors **14** and **15** which contain a potential cation binding site and an effective anion binding site are well designed for ion-pair recognition. Ion-pair recognition can

be achieved based on the sum of weak interactions. Generally, favourable electrostatic forces are strong, but not directional; hydrogen bonding is directional, but usually not strong enough to compete with multiple solvation effects in polar protic media. The combination of both types of interactions and preorganization effect would enhance the binding efficiency, both ability (quantity) and selectivity (quality).

Macromolecules **14** and **15** were found to strongly bind cations and anions separately; therefore, the ability to bind an ion-pair of both receptors was able to achieve in two ways. One equivalent of cation was encapsulated in calix[4]arene amide or ester and followed by evaluating anion binding affinity. Alternatively, one or two equivalents molar of anions (depends on the previous data in anion recognition) were added to the acetonitrile solution of host and then titrated with a cation. The former choice was employed in this thesis, since the latter could form either 1:1 or 1:2 complexes. Sodium cation was added as its perchlorate salt whereas anions are used as their tetrabutylammonium salts. Anions used in this binding study are carboxylate and phosphate type anion (acetate (**37**), benzoate (**38**), dihydrogen phosphate (**39**), phenylphosphinate (**40**) and diphenylphosphate (**41**)) as well as dicarboxylate anions of aspartic acid (**52**) and glutamic acid (**53**) as the representative of essential amino acids. The binding of either receptor **14** or **15** to cation make a room for anion at the thiourea cavity. This enabled us to study the effect of cation-calixarene complex on the stability of anion complexes. The fact that both cations and anions are involved in many biochemistry processes, the detection of the anion binding ability of these cation bound receptors maybe important for better understanding of interactions with the important anion bearing a large number of cations.

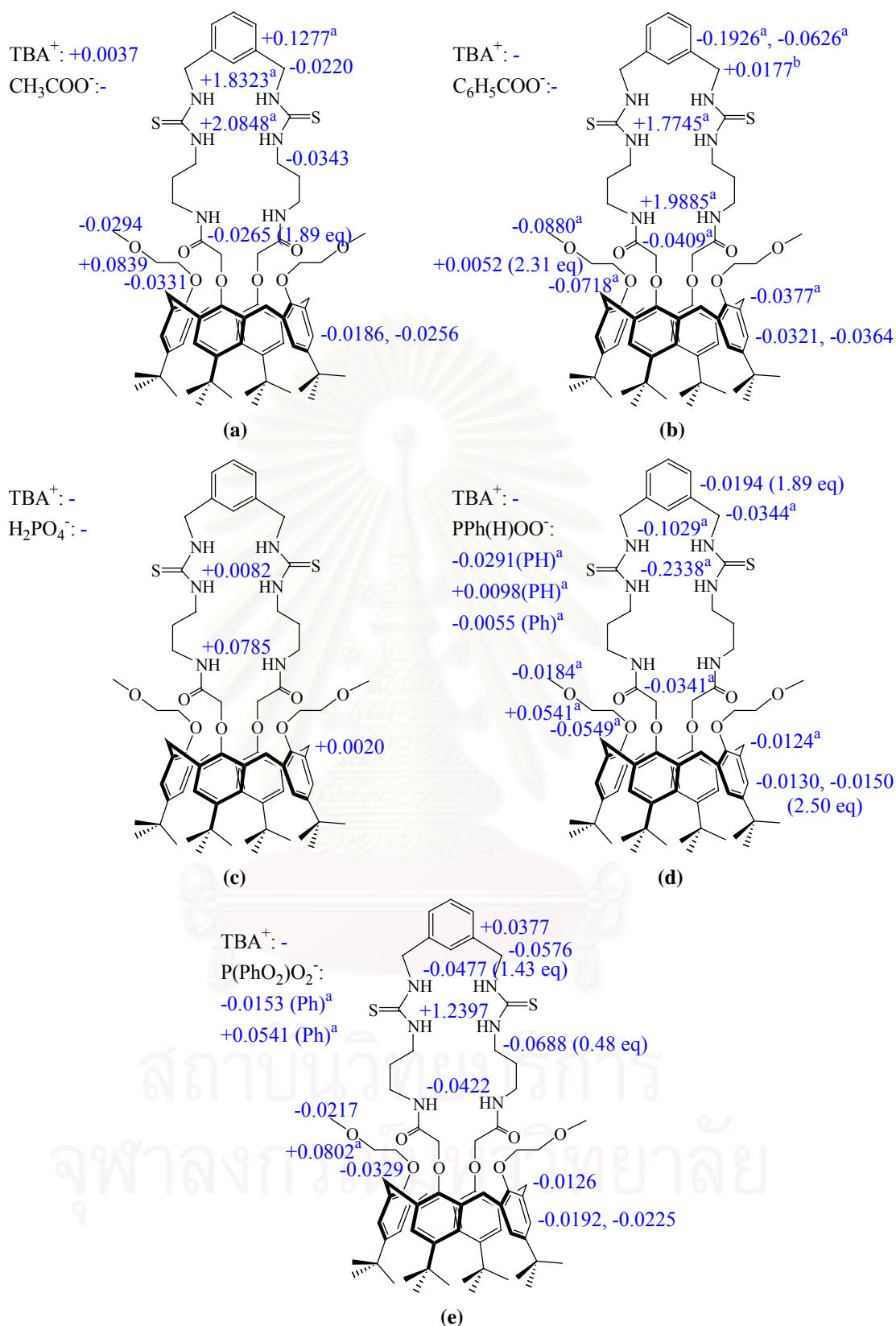
The exchange rates of either anions or amino acid anions in the presence of sodium were observed as the time-averaged signals. The  $^1\text{H-NMR}$  spectra of the mixture of host **14** and one equivalent of sodium perchlorate with various amount of acetate were obtained. The spectra of bound receptor **14** exhibited a markedly downfield shift of broaden signal of  $-\text{CH}_2\text{CH}_2\text{NHCSNHCH}_2\text{Ar}-$  with  $\Delta\delta = +1.8323$  ppm and of  $-\text{CH}_2\text{CH}_2\text{NHCSNHCH}_2\text{Ar}-$  with  $\Delta\delta = +2.0848$  ppm due to the intermolecular hydrogen bonding towards the carboxylate group of the guest. The upfield shift of the adjacent methylene protons  $-\text{NHCSNHCH}_2\text{Ar}-$  and  $-$

$\text{CH}_2\text{CH}_2\text{NHCSNH-}$  were found from 4.6808 to 4.6588 ppm ( $\Delta\delta = -0.0220$  ppm) and from 3.6334 to 3.5991 ppm ( $\Delta\delta = -0.0343$  ppm), respectively. Proton signals of aromatic linkage shifted to the higher magnetic field with  $\Delta\delta = +0.1277$  ppm. Addition of  $\text{Bu}_4\text{N}^+\text{CH}_3\text{COO}^-$  also caused considerable upfield shifts of the signals at  $\delta$  4.1290, 3.3189 and 4.3956 ppm, which attributed to  $-\text{OCH}_2\text{CH}_2\text{OCH}_3-$  ( $\Delta\delta = -0.0331$  ppm),  $-\text{OCH}_2\text{CH}_2\text{OCH}_3-$  ( $\Delta\delta = -0.0294$  ppm) and  $-\text{OCH}_2\text{CONH-}$  ( $\Delta\delta = -0.0265$  ppm), respectively, and a downfield shift of the signals at  $\delta$  3.4970 ppm, which was attributed to  $-\text{OCH}_2\text{CH}_2\text{OCH}_3-$  ( $\Delta\delta = +0.0839$  ppm). Both aromatic signals of calix[4]arene building block were shielded with  $\Delta\delta = -0.0186$  and  $-0.0256$  ppm.

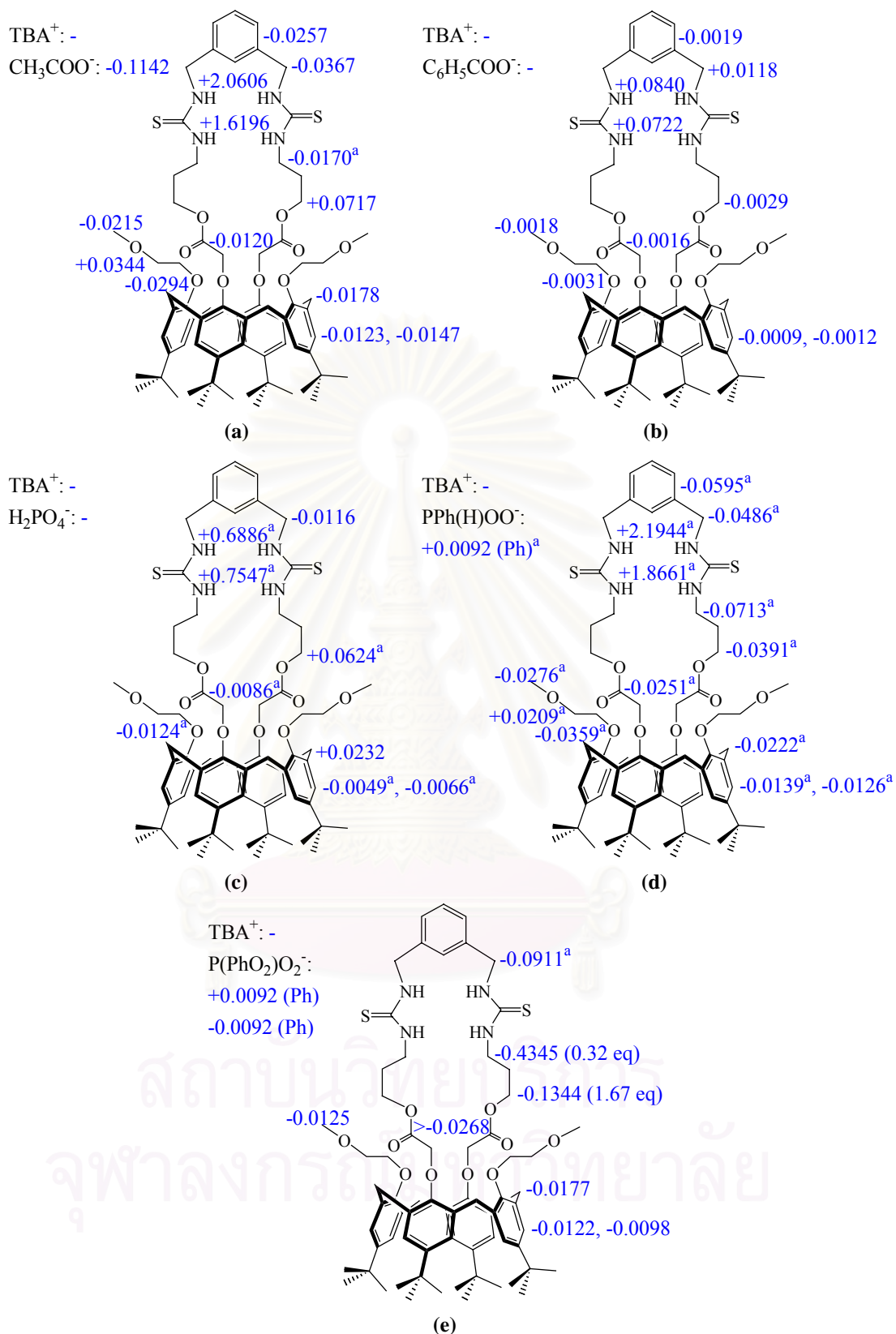
The addition of  $\text{Bu}_4\text{N}^+\text{X}^-$ ;  $\text{X} = \text{CH}_3\text{COO}^-$ ,  $\text{C}_6\text{H}_5\text{COO}^-$ ,  $\text{H}_2\text{PO}_4^-$ ,  $\text{Ph(H)POO}^-$  and  $(\text{PhO})_2\text{PO}_2^-$ , into the acetonitrile- $d_3$  solution of sodium trapped **14** or **15** caused the similar shifting as shown in Figure 3.41 and Figure 3.42.



สถาบันวิทยบริการ  
จุฬาลงกรณ์มหาวิทยาลัย



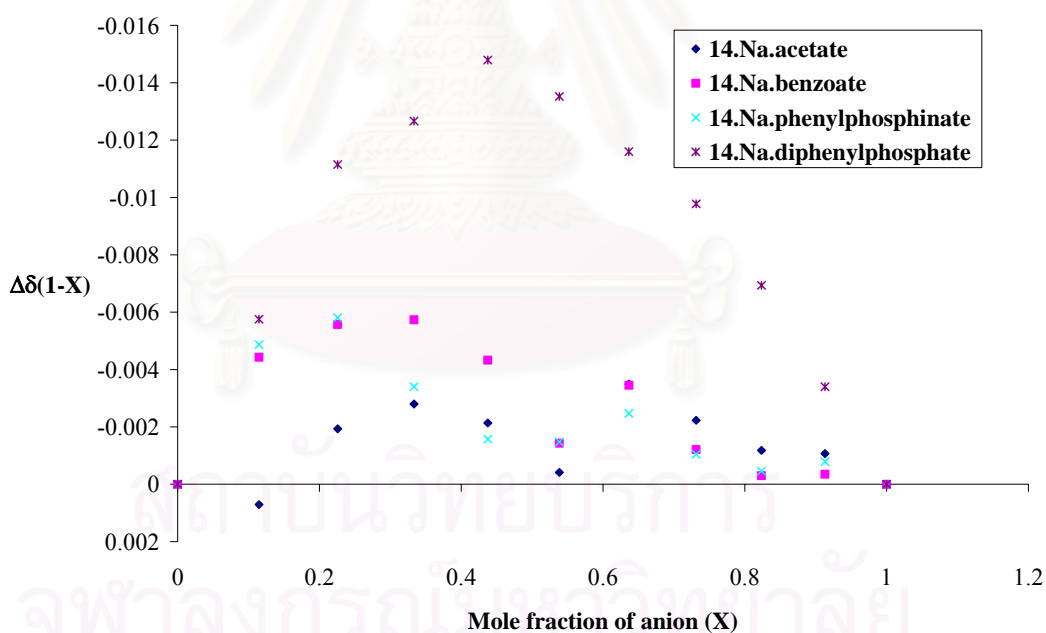
**Figure 3.41.** The complexation induced shifts of some proton signals on <sup>1</sup>H-NMR spectrum (a) **14**·Na<sup>+</sup>·CH<sub>3</sub>COO<sup>-</sup> (b) **14**·Na<sup>+</sup>·C<sub>6</sub>H<sub>5</sub>COO<sup>-</sup> (c) **14**·Na<sup>+</sup>·H<sub>2</sub>PO<sub>4</sub><sup>-</sup>, (d) **14**·Na<sup>+</sup>·Ph(H)POO<sup>-</sup> and (e) **14**·Na<sup>+</sup>·(PhO)<sub>2</sub>PO<sub>2</sub><sup>-</sup>.



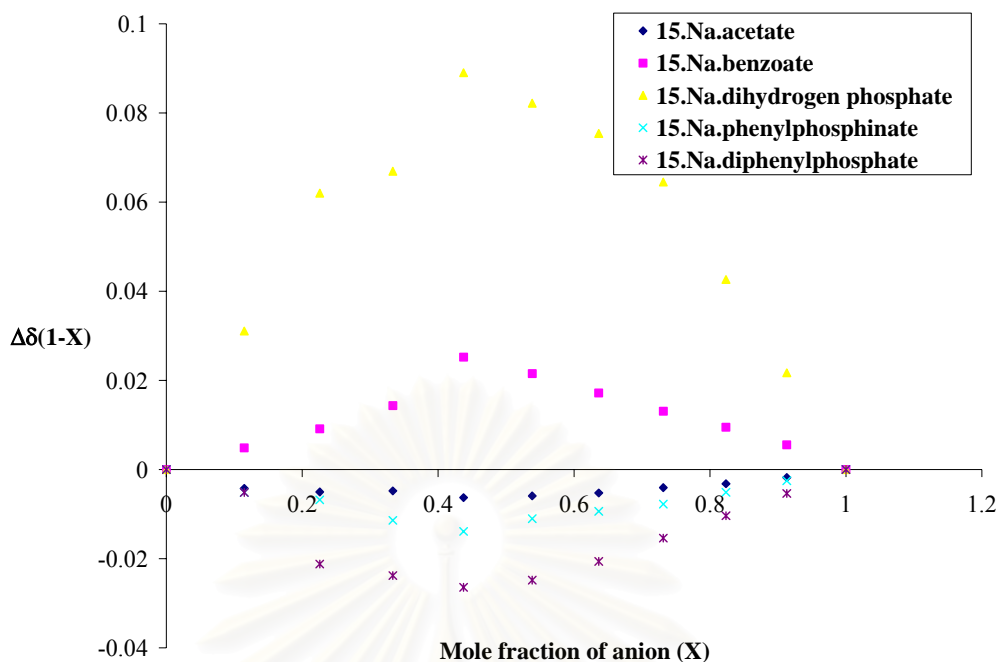
**Figure 3.42.** The complexation induced shifts of some proton signals on <sup>1</sup>H-NMR spectra (a) **15**·Na<sup>+</sup>·CH<sub>3</sub>COO<sup>-</sup> (b) **15**·Na<sup>+</sup>·C<sub>6</sub>H<sub>5</sub>COO<sup>-</sup> (c) **15**·Na<sup>+</sup>·H<sub>2</sub>PO<sub>4</sub><sup>-</sup>, (d) **15**·Na<sup>+</sup>·Ph(H)POO<sup>-</sup> and (e) **15**·Na<sup>+</sup>·(PhO)<sub>2</sub>PO<sub>2</sub><sup>-</sup>.

Upon addition of tetrabutylammonium dihydrogen phosphate, the observed peak positions of nearly all signals, except for  $-\text{CH}_2\text{CH}_2\text{NHCSNHCH}_2\text{Ar}-$ ,  $-\text{OCH}_2\text{CONH}-$  and  $-\text{ArCH}_2\text{Ar}-$ , did not show any change compared to the parent molecule ( $\mathbf{14}\cdot\text{Na}^+$ ). However, the binding constant could not be calculated from these three signals because of the unverified Job's analysis (Figure 3.43). These proton signals were closed to the cationic binding site, thus the shifting were probably attributed to the rearrangement around the sodium cation. This indicated that the presence of sodium in amide cavity inhibited the binding of bis-thiourea  $\mathbf{14}$  towards dihydrogen phosphate owing to the uncomplimentary hydrogen bonding.

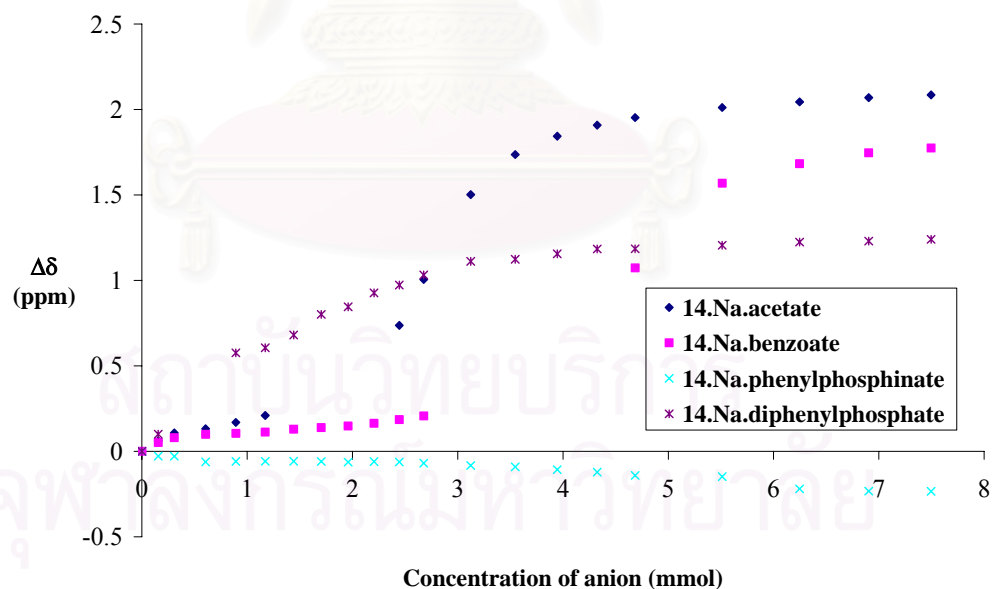
The 1:1 stoichiometry ratios of the  $\mathbf{14}\cdot\text{Na}^+\cdot(\text{PhO})_2\text{PO}_2^-$  and all  $\mathbf{15}\cdot\text{Na}^+$ ·anion complexes were suggested by the Job's plots (Figures 3.43 and 3.44). The titration curves of  $\mathbf{14}\cdot\text{Na}^+\cdot(\text{PhO})_2\text{PO}_2^-$ ,  $\mathbf{15}\cdot\text{Na}^+\cdot\text{CH}_3\text{COO}^-$ ,  $\mathbf{15}\cdot\text{Na}^+\cdot\text{C}_6\text{H}_5\text{COO}^-$  and  $\mathbf{15}\cdot\text{Na}^+\cdot(\text{PhO})_2\text{PO}_2^-$  are almost normal looking and correlate well with the 1:1 binding model (Figures 3.45 and 3.46).



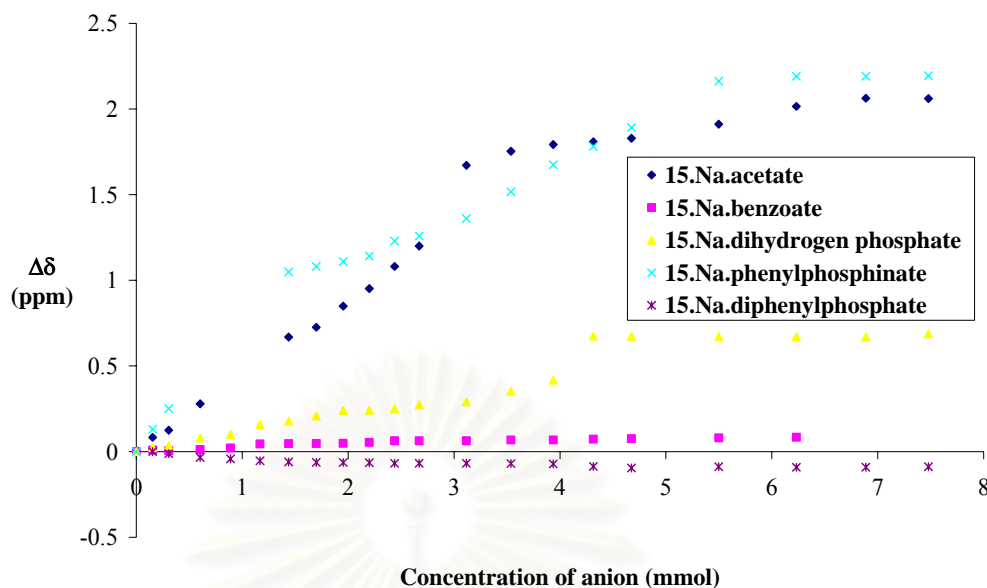
**Figure 3.43.** Job's plots of  $-\text{NHCSNHCH}_2\text{Ar}-$  in  $\mathbf{14}\cdot\text{Na}^+\cdot\text{CH}_3\text{COO}^-$ ,  $\mathbf{14}\cdot\text{Na}^+\cdot\text{C}_6\text{H}_5\text{COO}^-$ ,  $\mathbf{14}\cdot\text{Na}^+\cdot\text{Ph(H)POO}^-$  and  $\mathbf{14}\cdot\text{Na}^+\cdot(\text{PhO})_2\text{PO}_2^-$  complexes.



**Figure 3.44.** Job's plots of  $15 \cdot \text{Na}^+ \cdot \text{CH}_3\text{COO}^-$ ,  $15 \cdot \text{Na}^+ \cdot \text{C}_6\text{H}_5\text{COO}^-$ ,  $15 \cdot \text{Na}^+ \cdot \text{H}_2\text{PO}_4^-$ ,  $15 \cdot \text{Na}^+ \cdot \text{Ph}(\text{H})\text{POO}^-$  and  $15 \cdot \text{Na}^+ \cdot (\text{PhO})_2\text{PO}_2^-$  complexes (\* using  $-\text{NHCSNHCH}_2\text{Ar}$ - signal and  $^{\S}$  using  $-\text{NHCSNHCH}_2\text{Ar}$ - signal).



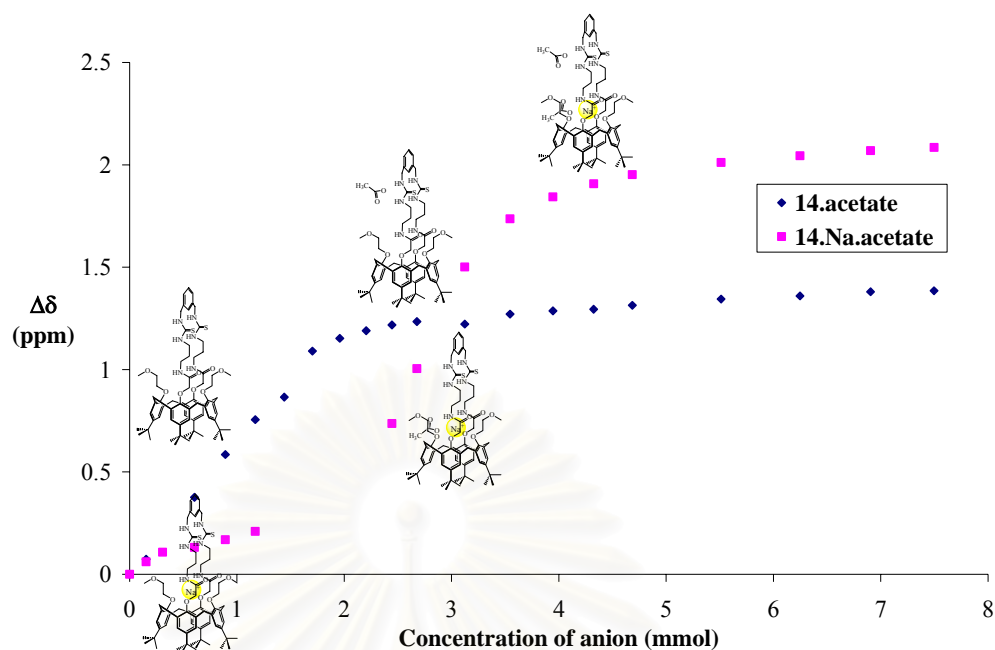
**Figure 3.45.** Titration curves of  $-\text{CH}_2\text{CH}_2\text{NHCSNH}-$  signals in  $14 \cdot \text{Na}^+ \cdot \text{CH}_3\text{COO}^-$ ,  $14 \cdot \text{Na}^+ \cdot \text{C}_6\text{H}_5\text{COO}^-$ ,  $14 \cdot \text{Na}^+ \cdot \text{Ph}(\text{H})\text{POO}^-$  and  $14 \cdot \text{Na}^+ \cdot (\text{PhO})_2\text{PO}_2^-$  complexes (\* using  $-\text{NHCSNHCH}_2\text{Ar}$ - signal).



**Figure 3.46.** Titration curves of  $-\text{NHCSNHCH}_2\text{Ar}-$  signals in  $15\cdot\text{Na}^+\cdot\text{CH}_3\text{COO}^-$ ,  $15\cdot\text{Na}^+\cdot\text{C}_6\text{H}_5\text{COO}^-$ ,  $15\cdot\text{Na}^+\cdot\text{H}_2\text{PO}_4^-$ ,  $15\cdot\text{Na}^+\cdot\text{Ph(H)POO}^-$  and  $15\cdot\text{Na}^+\cdot(\text{PhO})_2\text{PO}_2^*$  complexes (\* using  $-\text{NHCSNHCH}_2\text{Ar}-$  signal).

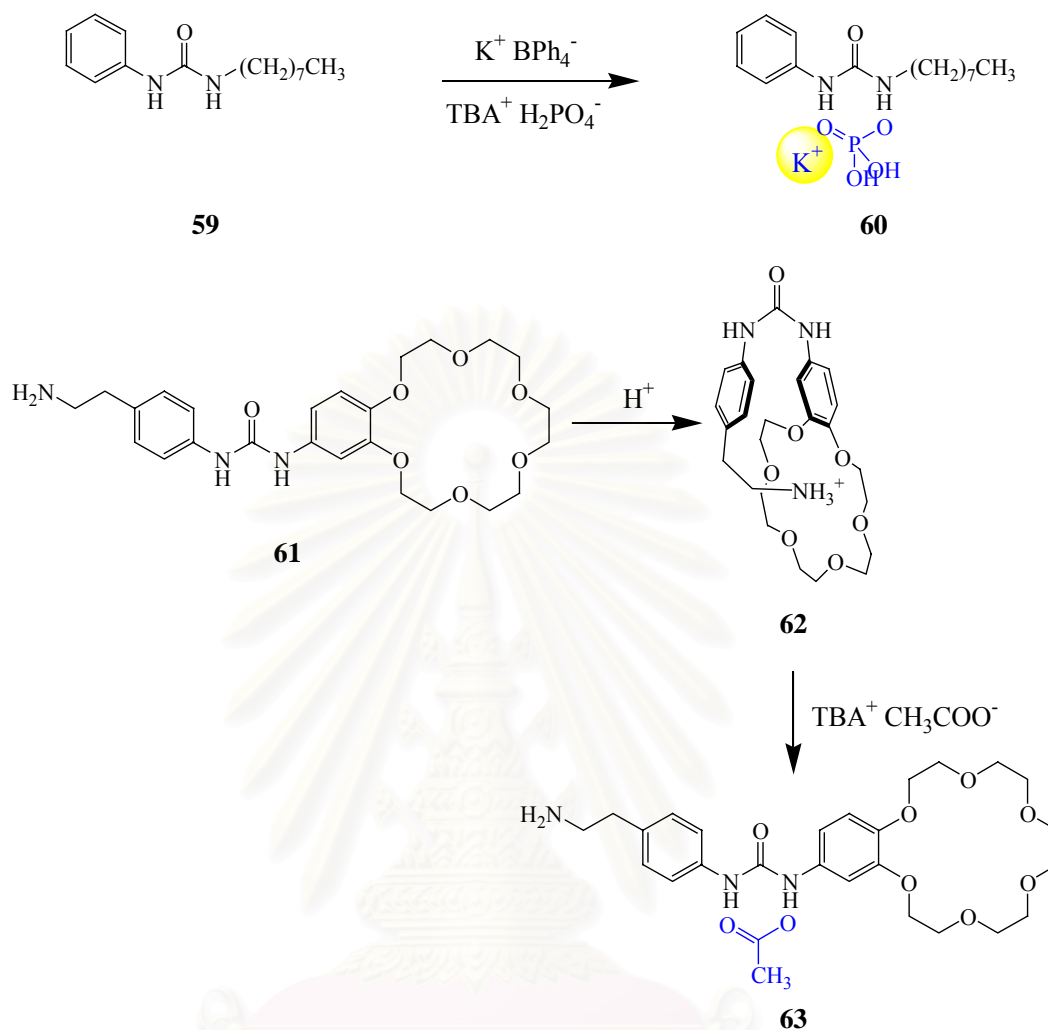
In the case of  $14\cdot\text{Na}^+\cdot\text{CH}_3\text{COO}^-$ ,  $14\cdot\text{Na}^+\cdot\text{C}_6\text{H}_5\text{COO}^-$  and  $14\cdot\text{Na}^+\cdot\text{Ph(H)POO}^-$ , the stoichiometric ratios could not be verified by Job's analysis and the titration curves existed as sigmoidal curves (Figures 3.45 and 3.46). Compared to the titration curve of unbound **14** with acetate, the plotting of initial host containing sodium perchlorate was different (Figure 3.47). It seemed to be no affinity of *NH*-thiourea in  $14\cdot\text{Na}^+$  to acetate until 1 equivalent of this anion was added. The subsequent addition reactivated the host as evidence by the sudden downfield shift of *NH*-thiourea signals. Sodium can stoichiometrically sequester acetate and the hydrogen bond recognition site is reactivated in response to the excess amount of guest. The binding curves of  $14\cdot\text{Na}^+\cdot\text{C}_6\text{H}_5\text{COO}^-$  and  $14\cdot\text{Na}^+\cdot\text{Ph(H)POO}^-$  displayed the similar events. This sequestering effect by negative ion-pairing in the system of a heteroditopic receptor was recently reported by Gale *et al.*<sup>[158]</sup> The species during the titration of anions are also proposed in Figure 3.47.





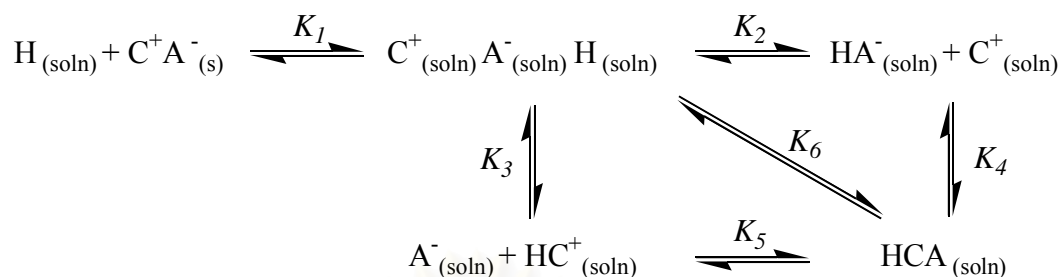
**Figure 3.47.** Titration curves of  $-\text{CH}_2\text{CH}_2\text{NHCSNHCH}_2\text{Ar}-$  in  $\mathbf{14}\cdot\text{Na}^+\cdot\text{CH}_3\text{COO}^-$  compared to  $\mathbf{14}\cdot\text{CH}_3\text{COO}^-$  complex.

The similar titration curves were previously reported by Shukla *et al.*<sup>[159]</sup> and Al-Sayah *et al.*<sup>[160]</sup> Both research groups reported the sigmoidal curves which did not arise from the 1:2 stoichiometry complex. The former case was rooted from the ion-pair effect of its counter cation in anion recognition study (Scheme 3.9 (**59-60**)). The latter report was stemmed from the intramolecular hydrogen bonding at the cationic binding site of the heteroditopic receptor by another end side of its molecule (Scheme 3.9 (**61-63**)). Both articles displayed the replacements of anion-host interactions by cations.

**Scheme 3.9.** The effects of cation on the binding curves.

The salts of alkali cations do not usually exist as free ions in most organic solvents. Instead, they present as solvent separated ion-pairs, contact ion-pairs, and/or aggregated contact ion-pairs.<sup>[159]</sup> Hereby, the difficulty in investigating simultaneous cation and anion binding is that there are a number of competing equilibria involved (Scheme 3.10).<sup>[55]</sup> The predominant equilibria is judged by types of cation, anion and ion-pair species as well as the medium. The precipitation of ion-pair salt which is not soluble in the solvent will be the major event to compete with anion binding by the bound receptor.

**Scheme 3.10.** Equilibrium involved in ion-pair binding (H = host, C = cation and A = anion).<sup>[55]</sup>



Basically, a heteroditopic host is designed in order to inhibit the negative ion-pairing association between anions and its counter cations. However, the sequestering effect in our result can be discussed by two explanations. First, the sodium presenting in solution, in our experiment, was assumed to bind host **14** or **15** completely. It is possible that the unbound cation presenting in the solution associates with anion then leading to the decrease or inhibit in strength of anion binding during the first period of titration. Second, the bound sodium could associate with anion leading to the ion-pairing species.

The replacement of amide in **14** with ester moiety in **15** intensively changed the affinity of these receptors for ion-pair recognition. On the other hand, the ester calix[4]arene compound is known to strongly complex alkali metal cations,<sup>[161]</sup> thus ligand **15** will minimize competing negative ion-pairing interactions more effectively than host **14**. The stronger interaction of ester moiety in **15** towards sodium compared to the amide donor in **14** confirms by the larger  $\beta_1$  of the former. This explanation is supported by an article by Olmstead *et al* which reported the effective elimination of the negative ion-pairing effect of sodium and  $[\text{CH}_3\text{COCHCOCH}_3]^-$  by addition of a cryptand (1 equivalent)<sup>[162]</sup> which is a well-known receptor for sodium cation. Generally, the ion-pair association constant of alkali or alkaline earth cation towards various anions in a number of dipolar aprotic solvents is greater in the presence of the more effective electron donor (anions). Sodium has been reported to be the largest ion-pairing cation among the alkali metal cations (sodium, potassium and cesium).<sup>[159]</sup> In the absence of sodium, macromolecule **14** displayed a more acidic property than compound **15**. The acidity of host **14** was enhanced by the entrapped sodium. Hence, anions were able to compete with the solvent molecules for a site in the coordination sphere of the sodium.<sup>[163]</sup> The negative ion-pair effect was found in the system of host

**14**, but not in the case of receptor **15**. The weakest ion-pairing effect of  $\mathbf{14}\cdot\text{Na}^+\cdot(\text{PhO})_2\text{PO}_2^-$  complex can be rationalized by the lowest basicity of diphenylphosphate.<sup>[130]</sup>

For the systems of  $\mathbf{15}\cdot\text{Na}^+\cdot\text{H}_2\text{PO}_4^-$  and  $\mathbf{15}\cdot\text{Na}^+\cdot\text{Ph}(\text{H})\text{POO}^-$ , NMR evidences displayed the sigmoidal titration curves despite of their 1:1 stoichiometry ratio from Job's analysis. This could be explained by the stepwise formation of complex from  $\mathbf{15}\cdot\text{Na}^+\cdot\text{A}^-$  to  $\mathbf{15}\cdot\text{Na}^+\cdot 2\text{A}^-$  ( $\text{A}^-$ :  $\text{H}_2\text{PO}_4^-$  or  $\text{Ph}(\text{H})\text{POO}^-$ ). Thus, the association constants of  $\mathbf{15}\cdot\text{Na}^+\cdot\text{H}_2\text{PO}_4^-$  and  $\mathbf{15}\cdot\text{Na}^+\cdot\text{Ph}(\text{H})\text{POO}^-$  were evaluated using the data range from 0-2 equivalents of anions by 1:1 binding model. The quantitative evaluation of average association constants and Gibbs free energies of  $\mathbf{14}\cdot\text{Na}^+\cdot(\text{PhO})_2\text{PO}_2^-$  as well as all  $\mathbf{15}\cdot\text{Na}^+\cdot\text{anion}$  complexes are listed in Table 3.14 and Figure 3.48.

**Table 3.14.** The average association constants and Gibbs free energies upon the formation of  $\mathbf{14}\cdot\text{Na}^+\cdot\text{anion}$  and  $\mathbf{15}\cdot\text{Na}^+\cdot\text{anion}$  complexes.

Complex		Association Constant	Gibbs free energy
Type	Stoichiometry	( $\text{M}^{-1}$ )	( $\text{kJ}\cdot\text{Mol}^{-1}$ )
$\mathbf{14}\cdot\text{Na}^+\cdot(\text{PhO})_2\text{PO}_2^-$	1:1	1790	-18.6
$\mathbf{15}\cdot\text{Na}^+\cdot\text{CH}_3\text{COO}^-$	1:1	28000	-25.4
$\mathbf{15}\cdot\text{Na}^+\cdot\text{C}_6\text{H}_5\text{COO}^-$	1:1	982	-17.1
$\mathbf{15}\cdot\text{Na}^+\cdot\text{H}_2\text{PO}_4^-$	1:1	53900	-27.0
$\mathbf{15}\cdot\text{Na}^+\cdot\text{Ph}(\text{H})\text{POO}^-$	1:1	45800	-26.6
$\mathbf{15}\cdot\text{Na}^+\cdot(\text{PhO})_2\text{PO}_2^-$	1:1	11100	-23.1

สถาบันวิทยบริการ  
จุฬาลงกรณ์มหาวิทยาลัย

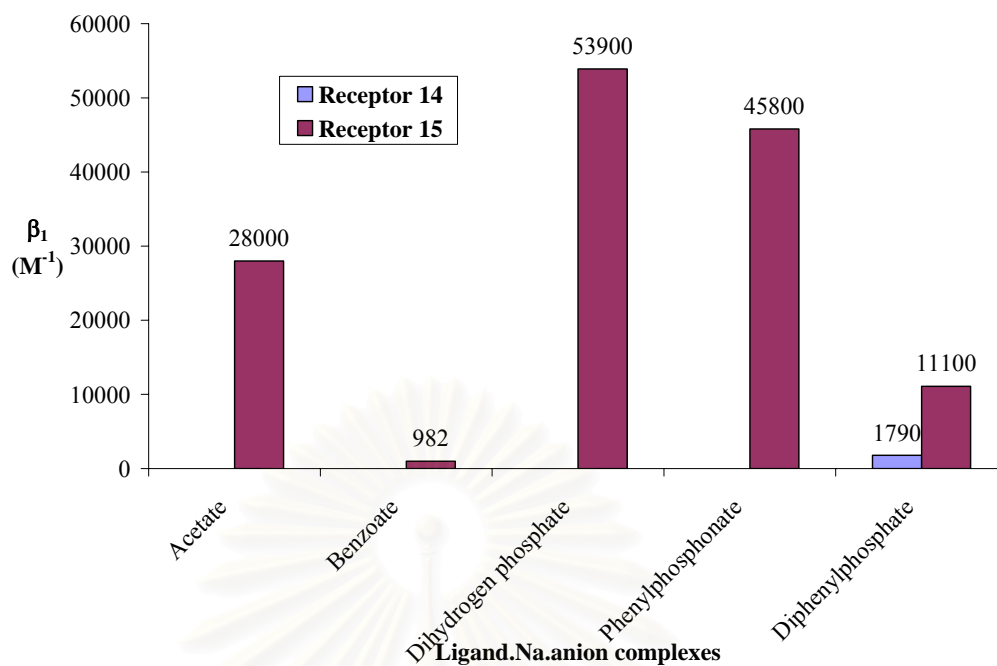


**Figure 3.48.** The selectivity of sodium bound **14** and **15** towards various anions.

The sodium bound **14** selectively recognized diphenylphosphate while the sodium trapped **15** bound dihydrogen phosphate more tightly than phenylphosphinate, acetate, diphenylphosphate and benzoate. The sodium bound **15** exhibited remarkable selectivity towards tetrahedral dihydrogen phosphate whereas it tended to form weaker complex towards Y-shaped acetate in spite of the substantially higher basicity of the latter. This trend is similar to the previously result of the unbound **15**. The binding ability of  $\mathbf{15} \cdot \text{Na}^+$  towards carboxylate and phosphate anions can be explained in terms of complexation geometry<sup>[132]</sup> and coordinated solvent.

The phenyl containing anions play a positive role in the system of unbound **15** while these anions play a negative role in the system of  $\mathbf{15} \cdot \text{Na}^+$ . This could be ascribed by the larger  $pK_a$  of acetate over benzoate and dihydrogen phosphate over phenylphosphinate because the basicity plays an important role in the ion-pair recognition. The weakest complex of  $\mathbf{15} \cdot \text{Na}^+ \cdot (\text{PhO})_2\text{PO}_2$ <sup>[164]</sup> among other phosphate anions is explained by the lowest basicity and the largest steric hindrance of diphenylphosphate. From our results, the complementary interactions between donor and acceptor sites determine selectivity whereas both steric hindrance and basicity determine the binding efficiency.

The cooperativity factors which generate from the ratio of anion association constant in the presence of cation to the anion binding ability in the absence of

cation<sup>[159]</sup> are displayed in Figure 3.49. Sodium enhances anion recognition of receptor **15** towards acetate, dihydrogen phosphate, phenylphosphinate and diphenylphosphate (cooperativity factor > 1); thus, they are termed as positively heterotropic allosterism. On the contrary, the presence of sodium in  $\mathbf{14}\cdot\text{Na}^+\cdot(\text{PhO})_2\text{PO}_2^-$  and  $\mathbf{15}\cdot\text{Na}^+\cdot\text{C}_6\text{H}_5\text{COO}^-$  reduces the anion binding efficacy (cooperativity factor < 1); therefore, they are classified as negatively heterotropic allosterism.

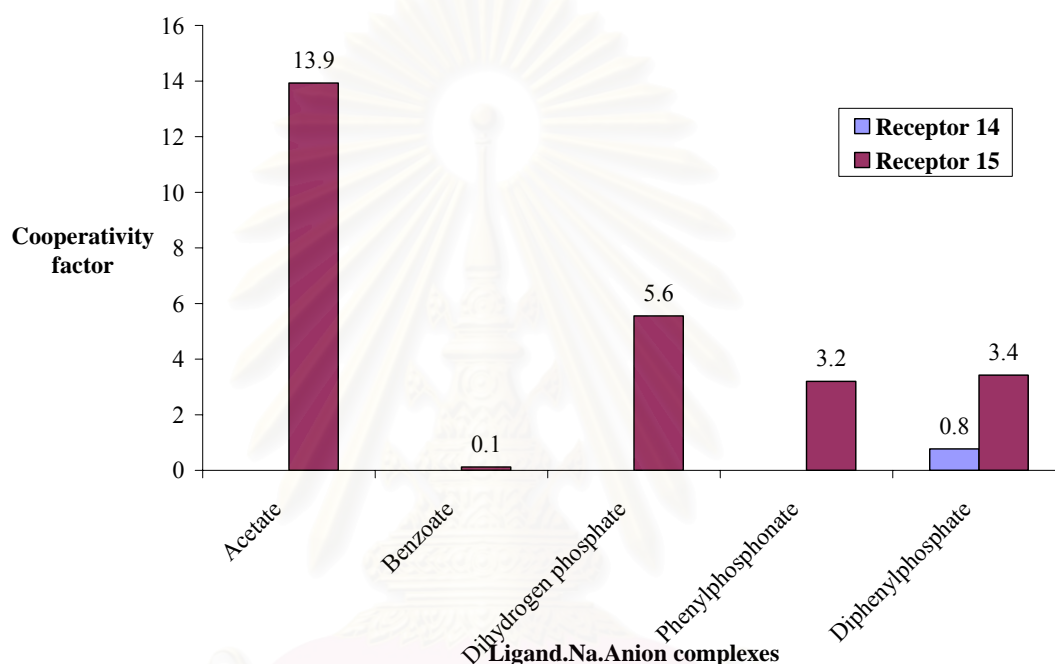


**Figure 3.49.** The cooperativity factors of sodium bound to receptor **14** or **15** in the presence of various anions.

The lower association constant of  $\mathbf{14}\cdot\text{Na}^+\cdot(\text{PhO})_2\text{PO}_2^-$  compared to  $\mathbf{14}\cdot(\text{PhO})_2\text{PO}_2^-$  complex can be explained by the less number of intermolecular hydrogen bonding. Only two  $-\text{CH}_2\text{CH}_2\text{NHCSNHCH}_2\text{Ar}-$  donor protons are involving in ion-pairing complex but another *NH*-thiourea and *NH*-amide are inactive which evidences by a slightly upfield shift. However, the association constant of  $\mathbf{14}\cdot\text{Na}^+\cdot(\text{PhO})_2\text{PO}_2^-$  does not show much lower ability. The stability of this complex can be compensated by the  $\pi$ - $\pi$  and  $\text{Na}^+\cdot\pi$ <sup>[165]</sup> interaction.

The cooperativity trend of ditopic receptor **15** was found to be slightly different from ion-pair recognition selectivity. The addition of sodium perchlorate changed the molecule into a conformation that demonstrated the interestingly greatest enhancement towards acetate (cooperativity factor = 13.9) but totally inhibited

inclusion of benzoate (cooperativity factor = 0.1). The largest effective of entrapped  $\text{Na}^+$  towards acetate in the system of **15** can be explained by the highest  $\text{p}K_a$  of acetate. Sodium cation is thus a positive effector that can activate the molecule recognition event of host **15**. Presumably, the negative allosterism in the presence of benzoate arises from the uncomplimentary hydrogen bonding. This present system is a rare example which features both positively and negatively heteroditopic allosterisms between metal ions and anions in a calix[4]arene host.

The positive allosteric property can generally be explained by two possible reasons. Firstly, the ditopic receptor **15** in the presence of sodium has a stronger affinity for anion leading to an additional coulombic force. Secondly, the receptor has the same affinity for anions, but sodium binds one anion stronger than other anions. However, these two explanations refer to the complementary hydrogen bonding (thiourea-anion) and the cooperative acting of the electrostatic component (sodium-anion). In addition, the positive allosterism of heteroditopic **15** in the presence of sodium can be discussed by the enthalpy effect.<sup>[57, 131]</sup> This explanation should be supported by thermodynamic data by either variable-temperature  $^1\text{H-NMR}$  titration method<sup>[57]</sup> or isothermal titration calorimetry (ITC).<sup>[166]</sup>

The presence of phenyl group in phosphate anion led to the decrease in positive allosteric effect. In contrast, it induced the negative allosterism in the case of carboxylate anions. The stability of  $\mathbf{15}\cdot\text{Na}^+\cdot\text{PhP(H)OO}^-$  can be compensated by  $\pi$ - $\pi$  and electrostatic interactions whereas the steric hindrance in  $\mathbf{15}\cdot\text{Na}^+\cdot(\text{PhO})_2\text{PO}_2^-$  can be compensated by  $\pi$ - $\pi$ ,  $\text{Na}^+$ - $\pi$  and electrostatic interactions. The effective ion-pair recognition can be achieved based on the sum of weak interactions.

Based on the NMR titration data, the proposed structure of cation and anion complexes as well as the literatures<sup>[54, 157, 167-168]</sup> of ion-pair complexes, the structure of the 1:1 ion-pair complexes are proposed in Figure 3.50. X represents of NH and O in the case of compounds **14** and **15**, respectively.  $\text{R}_1$ ,  $\text{R}_2$  and  $\text{R}_3$  refer to the substituted group on acetate, benzoate, dihydrogen phosphate, phenylphosphinate and diphenylphosphate as presented in Figure 3.8.

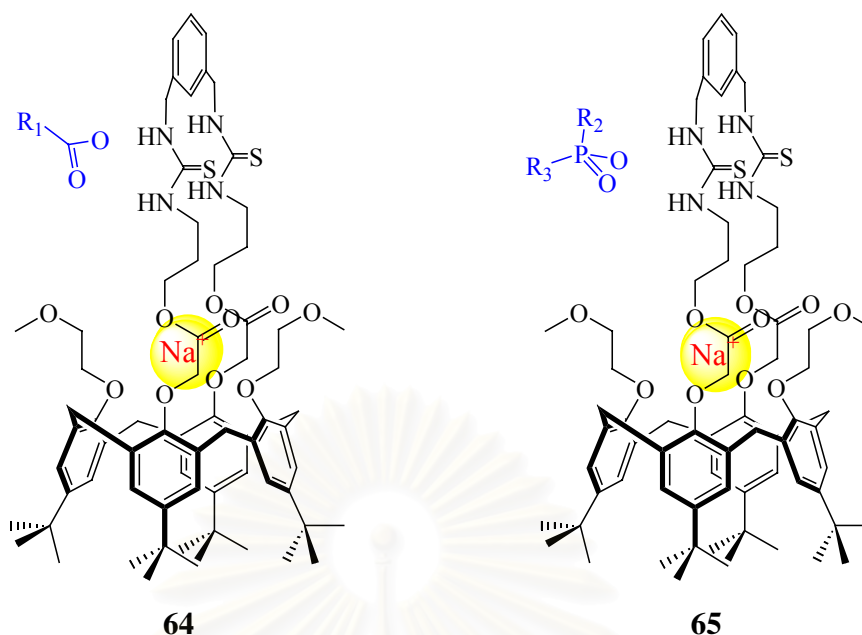
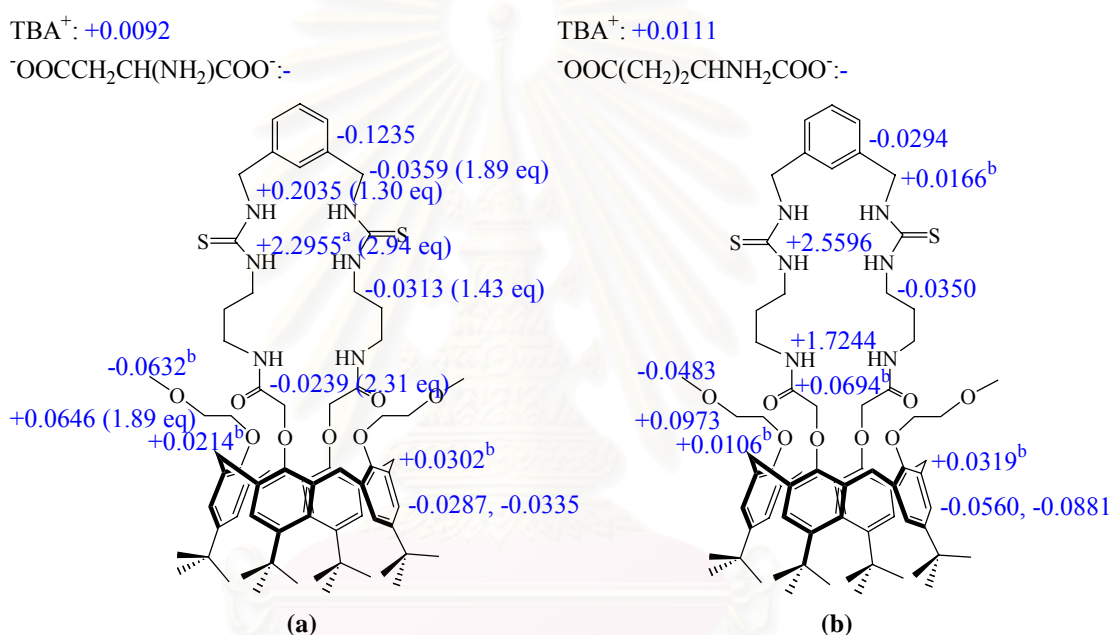


**Figure 3.50.** The proposed structures of cation enhancement anion complexes (**64-65**).

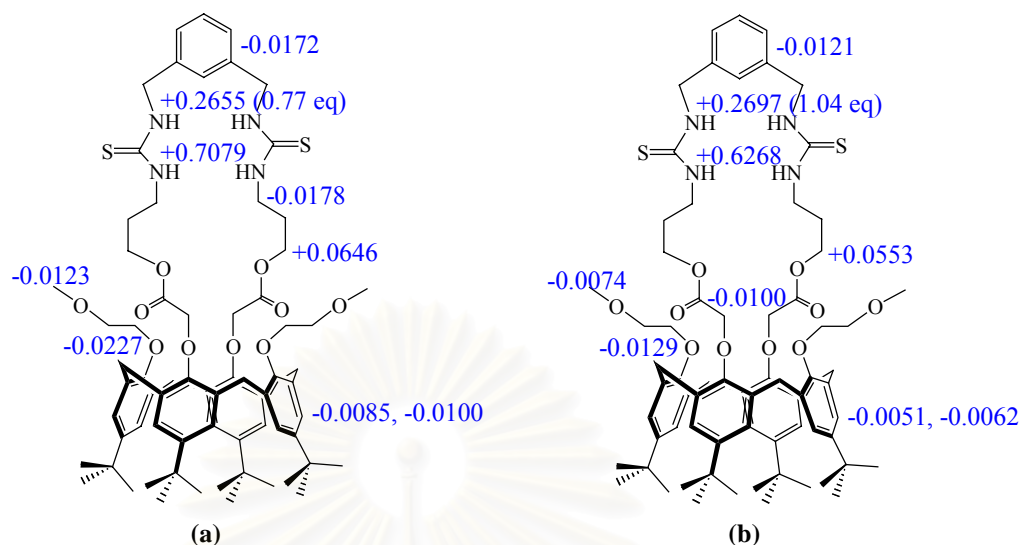
Moving on from common carboxylate and phosphate anions to amino carboxylate anion, bis-TBA salts of aspartic acid and glutamic acid were chosen as the substrates to investigate the ion-pairing binding ability of the ditopic bis-thiourea calix[4]arene **14** and **15**. Addition of the dicarboxylate salts of aspartic acid caused either downfield or upfield shift depend upon the complexation induced effects. The predominantly large downfield shift from 6.9235 to 9.2190 ppm ( $\Delta\delta = +2.2955$  ppm) upon adding 2.94 equivalents of the anion was found in the case of  $-\text{CH}_2\text{CH}_2\text{NHCSNHCH}_2\text{Ar}-$  signal. This signal could not be followed after 3 equivalents because it was broaden and disappeared. Another *NH*-thiourea signal ( $-\text{CH}_2\text{CH}_2\text{NHCSNHCH}_2\text{Ar}-$ ) coalesced with other peaks in the aromatic region after displayed a movement to the lower magnetic field ( $\Delta\delta = +0.2035$  ppm). However, both *NH*-thiourea chemical shifts intensively changed in the presence of TBA salt of aspartic acid. These results signified that **14** interacted with dicarboxylate anion of aspartic acid *via* hydrogen bonding like other anion systems. The typical upfield shift experienced by the  $-\text{NHCSNHCH}_2\text{Ar}-$  and  $-\text{CH}_2\text{CH}_2\text{NHCSNH}-$  protons were found at 1.89 and 1.43 equivalents, respectively. The shift of the former protons was observed from 4.6802 to 4.6443 ppm ( $\Delta\delta = -0.0359$  ppm) whereas the latter one was shifted from 3.6327 to 3.6014 ppm ( $\Delta\delta = -0.0313$  ppm). One of the aromatic linkage signal moved to the higher magnetic field with  $\Delta\delta = -0.1235$  ppm. The protons on



methyl ethyl ether substituted chain were moved with  $\Delta\delta = +0.0214$ ,  $+0.0646$  (1.89 eq) and  $-0.0632$  ppm; they were attributed to  $-\text{OCH}_2\text{CH}_2\text{OCH}_3$ ,  $-\text{OCH}_2\text{CH}_2\text{OCH}_3$  and  $-\text{OCH}_2\text{CH}_2\text{OCH}_3$ , respectively. The  $-\text{OCH}_2\text{CONH}-$  protons which absorbed at around 4.3931 ppm shifted upfield with  $\Delta\delta = -0.0239$  ppm in the present of 2.31 equivalent of anion. One of the  $-\text{ArCH}_2\text{Ar}-$  protons shifted downfield with  $\Delta\delta +0.0302$  ppm while the  $-\text{CH}_2\text{ArHCH}_2-$  signals shifted upfield with  $\Delta\delta = -0.0287$  and  $-0.0335$  ppm causing by the  $\pi$  cloud of the aromatic rings. The addition of dicarboxylate salt of aspartic or glutamic acid to bis-thiourea **14** or **15** depicted the similar shifting as shown in Figure 3.51 and Figure 3.52.



**Figure 3.51.** The complexation induced shifts of some proton signals on <sup>1</sup>H-NMR spectrum (a) **14**·Na<sup>+</sup>·Asp<sup>2-</sup> and (b) **14**·Na<sup>+</sup>·Glu<sup>2-</sup>.

TBA<sup>+</sup>: +0.0012<sup>-</sup>OOCCH<sub>2</sub>CH(NH<sub>2</sub>)COO<sup>-</sup>:TBA<sup>+</sup>: -<sup>-</sup>OOC(CH<sub>2</sub>)<sub>2</sub>CHNH<sub>2</sub>COO<sup>-</sup>:

**Figure 3.52.** The complexation induced shifts of some proton signals on <sup>1</sup>H-NMR spectrum (a) **15**·Na<sup>+</sup>·Asp<sup>2-</sup> and (b) **15**·Na<sup>+</sup>·Glu<sup>2-</sup>.

NMR evidence showed the formation of a 1:2 complexes of **14**·Na<sup>+</sup>·Asp<sup>2-</sup> ( $X \approx 0.66$ ) whereas the 1:1 fashion of **14**·Na<sup>+</sup>·Glu<sup>2-</sup>, **15**·Na<sup>+</sup>·Asp<sup>2-</sup> and **15**·Na<sup>+</sup>·Glu<sup>2-</sup> ( $X \approx 0.5$ ) were verified by means of Job's analysis (Figures 3.53 and 3.54). The different in the type of formation between **14**·Na<sup>+</sup>·Asp<sup>2-</sup> and **15**·Na<sup>+</sup>·Asp<sup>2-</sup> can be ascribed to the difference in the hydrogen bond donor site of each thiourea in the host molecule. Job's plots of all systems corresponded with their titration curves (Figures 3.55 and 3.56). The determination of a 1:2 complex from binding curve were verified by two sudden change points during titration which belonged to two binding equilibrium like in the system of **14**·Na<sup>+</sup>·Asp<sup>2-</sup>. The titration curve of the remaining systems generated only one sudden change point as a normal looking titration curve like other 1:1 cases. No negative ion-pairing effect presented in ion-pair recognition of either receptor **14** or **15** towards both amino dicarboxylate anions in spite of the use of sodium as cation bound substrate. This could be ascribed to the lower basicity of both dicarboxylate anions of aspartic acid and glutamic acid compared to acetate and benzoate as well as the effect of entrapped sodium. These amino acid anions comprised of two carboxylate ending sites and their chains were long enough to stabilize by *NH*-thiourea and bound sodium.

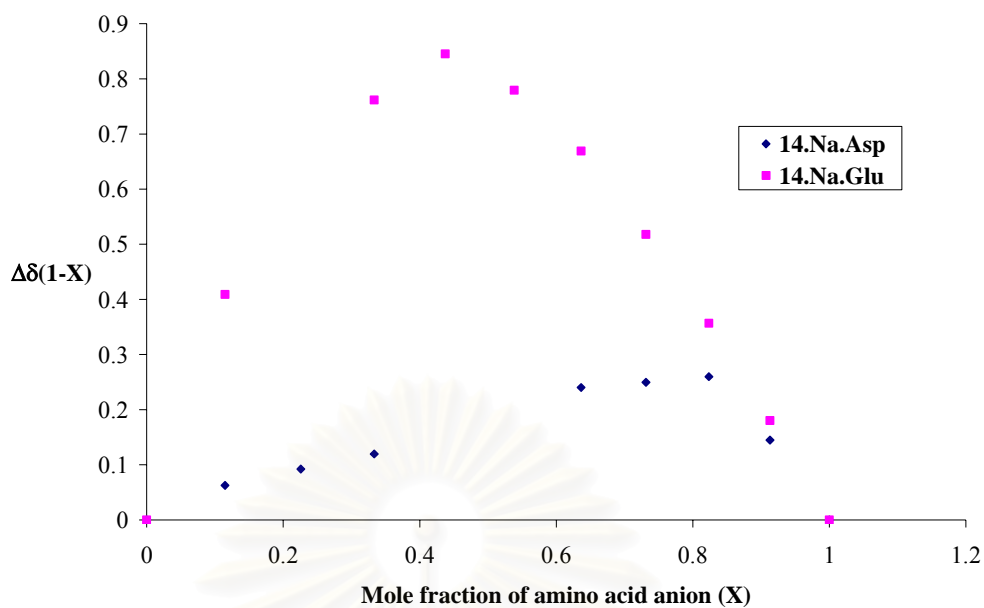


**Figure 3.53.** Job's plots of  $-\text{CH}_2\text{CH}_2\text{NHCSNHCH}_2\text{Ar}-$  in (a)  $14 \cdot \text{Na}^+ \cdot \text{Asp}^{2-}$  and (b)  $14 \cdot \text{Na}^+ \cdot \text{Glu}^{2-}$  complexes.

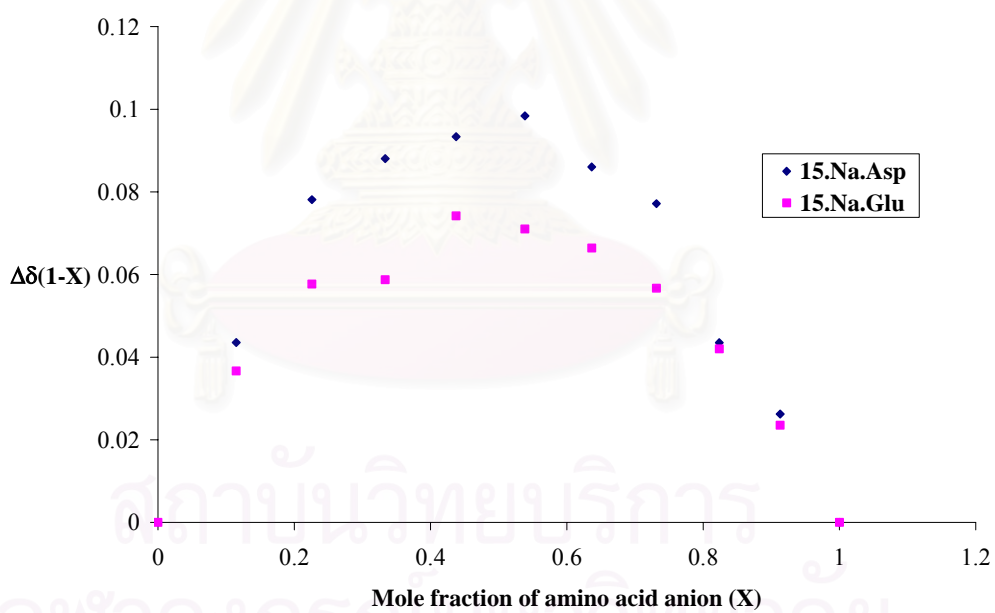


**Figure 3.54.** Job's plots of  $-\text{CH}_2\text{CH}_2\text{NHCSNHCH}_2\text{Ar}-$  signal in (a)  $15 \cdot \text{Na}^+ \cdot \text{Asp}^{2-}$  and (b)  $15 \cdot \text{Na}^+ \cdot \text{Glu}^{2-}$  complexes.

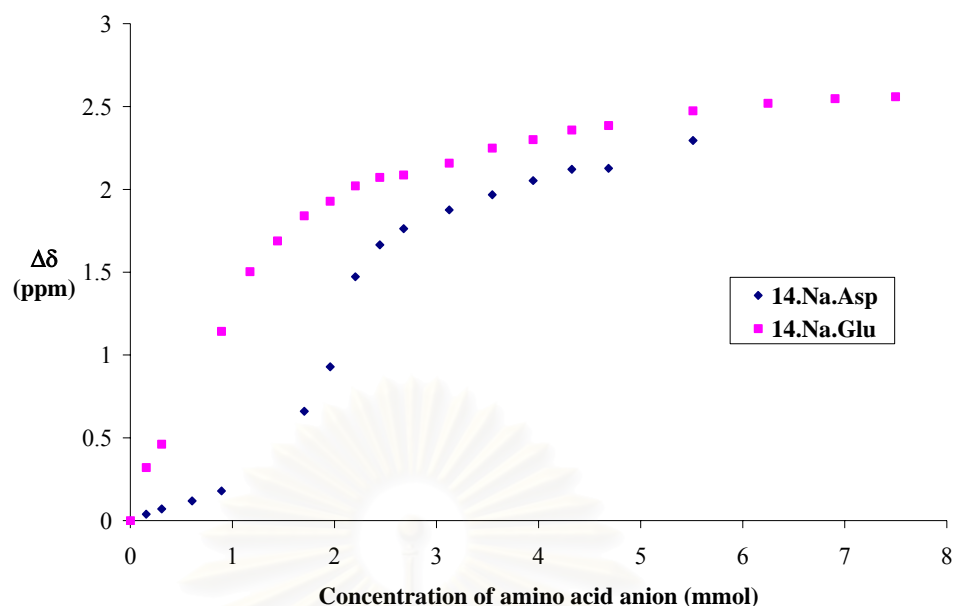


**Figure 3.55.** Titration curves of  $-\text{CH}_2\text{CH}_2\text{NHCSNHCH}_2\text{Ar}-$  in (a)  $14\cdot\text{Na}^+\cdot\text{Asp}^{2-}$  and (b)  $14\cdot\text{Na}^+\cdot\text{Glu}^{2-}$  complexes.

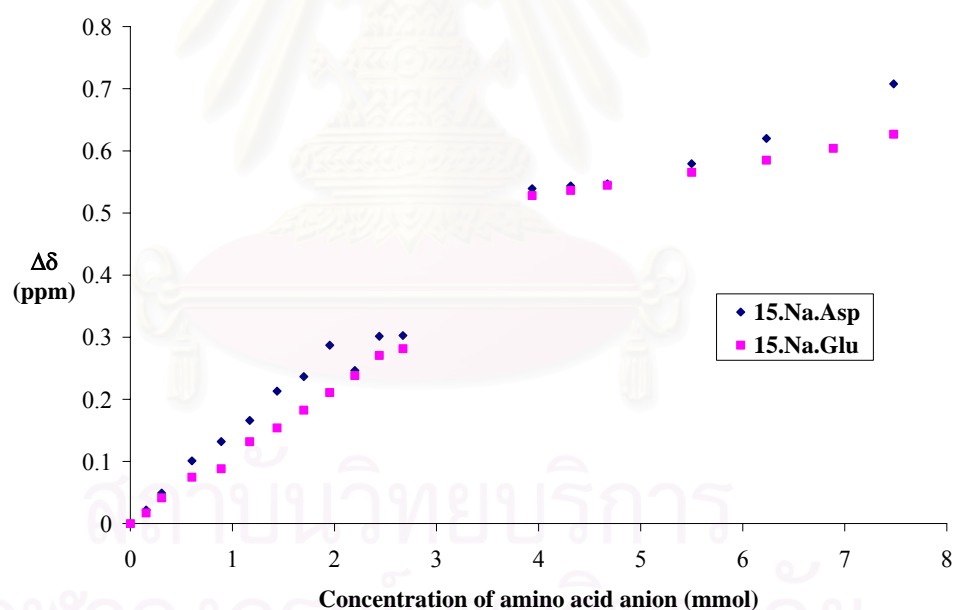


**Figure 3.56.** Titration curves of  $-\text{CH}_2\text{CH}_2\text{NHCSNHCH}_2\text{Ar}-$  signal in (a)  $15\cdot\text{Na}^+\cdot\text{Asp}^{2-}$  and (b)  $15\cdot\text{Na}^+\cdot\text{Glu}^{2-}$  complexes.

Association constants and Gibbs free energies of all sodium amino dicarboxylate are shown in Table 3.15. The quantitative binding efficiencies were calculated by an iterative curve fitting method by the use of NMRTit\_HG and NMRTit\_HGG program for 1:1 and 1:2 complexes, respectively.<sup>[105]</sup>

**Table 3.15.** The average association constants and Gibbs free energies upon the formation of  $14 \cdot \text{Na}^+ \cdot \text{dicarboxylate}^{2-}$  and  $15 \cdot \text{Na}^+ \cdot \text{dicarboxylate}^{2-}$  complexes.

Complex		Association Constant	Gibbs free energy
Type	Stoichiometry	( $\text{M}^{-1}$ )	( $\text{kJ} \cdot \text{Mol}^{-1}$ )
$14 \cdot \text{Na}^+ \cdot \text{Asp}^{2-}$	1:2	$> 10^4$	-
		$> 10^8 (\text{M}^{-2})$	-
$14 \cdot \text{Na}^+ \cdot \text{Glu}^{2-}$	1:1	5370	-21.3
$15 \cdot \text{Na}^+ \cdot \text{Asp}^{2-}$	1:1	162	-12.6
$15 \cdot \text{Na}^+ \cdot \text{Glu}^{2-}$	1:1	93.6	-11.2

The binding constants of both sodium bound receptors towards TBA salts of aspartic acid and glutamic acid compared to common carboxylate anions like acetate are shown in Figure 3.57. In order to compare to the others, only  $\beta_1$  of  $14 \cdot \text{Na}^+ \cdot \text{Asp}^{2-}$  is displayed.

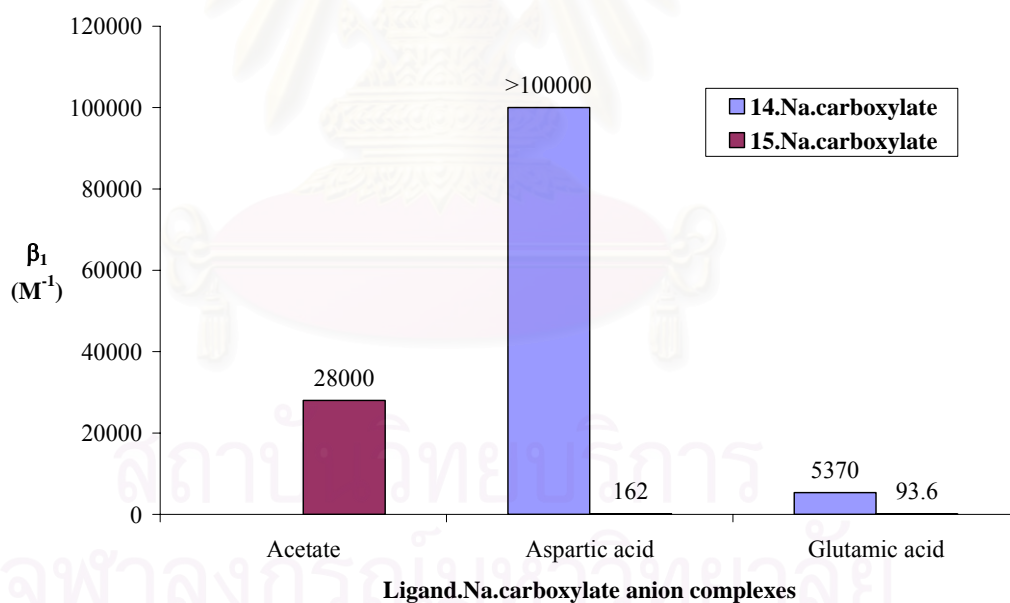


**Figure 3.57.** The selectivity of receptors **14** and **15** towards various carboxylate anions.

The entrapped sodium in the lower rim cavity of **14** and **15** seems to introduce the new site for recognizing the carboxylate anions indicating by either the higher or lower affinity compared to efficiency of the free receptor. Both receptors in the absence or presence of sodium tend to display the size-complementary with

dicarboxylate anion of aspartic acid over glutamic acid. Based on the same geometry of guests, the length of alkyl chain determines the selectivity. The cavity of ligands **14** and **15** are too short for dicarboxylate anion of glutamic acid despite of the presence of sodium cation.

The positive or negative allosteric effect of encapsulated sodium in cavity of **14** or **15** towards substituted dicarboxylate anions is quantitatively displayed by the cooperativity factor (Figure 3.58).

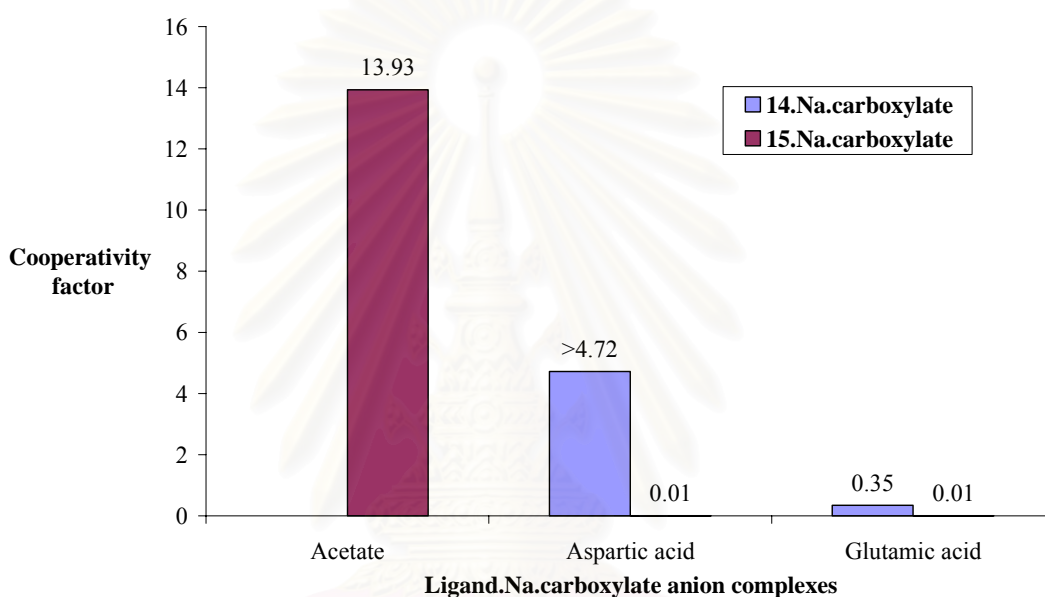


**Figure 3.58.** The cooperativity factors of sodium bound to receptor **14** or **15** in the presence of carboxylate anions.

The binding ability of receptor **14** towards the bis-TBA salt of aspartic acid was activated by the entrapped sodium whereas the selectivity towards the bis-TBA salt of glutamic acid was inhibited by the same cation. The binding efficacy of host **15** towards both dicarboxylate anions poorly recognized in the presence of sodium. Presumably, the preorganization of receptor **15** after including sodium in the cavity leads to the mismatch between the hydrogen bond donor site in the host and the acceptor site in the guest.

The sodium bound **14** was recognized dicarboxylate anion especially dicarboxylate anion of aspartic acid while the presence of sodium in compound **15** afforded the much greater selectivity with monocarboxylate anion like acetate. This

could be ascribed to the presence of amide and ester moiety in macromolecules **14** and **15**, respectively. The amide function is widely served as anionic binding site,<sup>[151, 169]</sup> therefore, it is possible to interact with the second carboxylate in dicarboxylate salt of aspartic acid and stabilized ion-pair complexes.

In summary, the presence of sodium cation in the system of macromolecule **14** was effective both in the enhancement of amino acid anion binding site using a cation and in the differentiation of dicarboxylate salts of aspartic acid and glutamic acid. The unbound receptor **14** displayed a small ability in differentiating these two substituted dicarboxylate anions.

The structures of ion-pair complexes between sodium bound molecules **14** and **15** towards substituted dicarboxylate anions are proposed based on our NMR data, structure of amino acid anion complexes<sup>[34, 151, 156]</sup> and ion-pair complexes<sup>[54, 152, 157, 167]</sup> (Figure 3.59). R represents side chains of dicarboxylate anions of aspartic acid and glutamic acid.

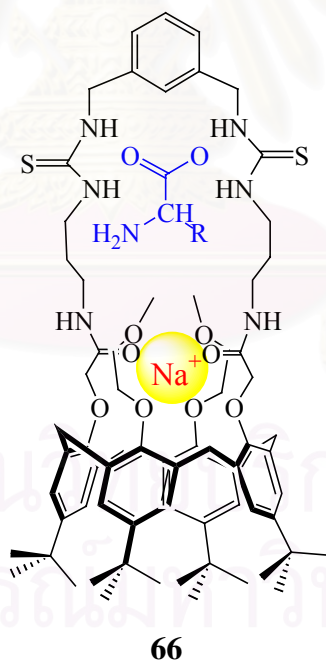


**Figure 3.59.** The proposed structures of 1:1 sodium amino acid anion complexes (**66**).

### 3.2.5 Binding Ability of Chiral **26**

There is no chiral center in compound **26** which is cyclised from compound **24**, however, it is a chiral molecule. Macrocyclic molecule **26** can act as traditional hydrogen bond donor like amide moiety which is known to form stable complexes with anions. Therefore, it is worth testing the efficacy in chiral recognition. The amino carboxylate binding studies were conducted by solid-liquid extraction with compound **26** as a preliminary screening. Interactions of chiral molecule **26** with some TBA salts of amino acids were investigated by  $^1\text{H-NMR}$  spectroscopy.

Chiral **26** displayed poor solubility in DMSO or methanol, but it was found to be soluble in chloroform-*d* in which the guest substrates were not soluble. Therefore, acetonitrile-*d*<sub>3</sub> was again the choice of solvent owing to the well-resolved  $^1\text{H-NMR}$  spectrum of compound **26** in this media. The difference in amino acid side chains and configuration (L and D) were expected to give difference in selectivity. The solid of mono- or dicarboxylate anions (L-phenylalanine, L-alanine and D-alanine) were added into an acetonitrile-*d*<sub>3</sub> solution of compound **26** and they were shaken at room temperature overnight. After that the mixtures were centrifuged for 15 minutes and consequently filtered through a pasteur pipet with cotton. The clear solutions were measured by the NMR technique. Attempts to study the complexation of all guests with **26** in acetonitrile-*d*<sub>3</sub> were unsuccessful. By monitoring the complexation induced shift (CIS) of the *NH*-amide or any other signals, the  $^1\text{H-NMR}$  spectra showed negligible shift of the *NH*-amide signal for all salts probably because of the less flexible and too small cavity of receptor **26**.



## CHAPTER IV

### CONCLUSION

#### 4.1 Conclusion

The synthesis of U-shaped macrocyclic receptor **14** was carried out from *p*-*tert*-butylcalix[4]arene in 3.7% overall yield. A nucleophilic substitution reaction of *p*-*tert*-butylcalix[4]arene with 2-bromoethyl methyl ether using potassium carbonate as base in acetonitrile yielded **17** (73%), then followed by a substitution reaction with methyl bromoacetate in the presence of sodium carbonate as base in acetonitrile to afford **18** (70%). After that **18** was treated with sodium hydroxide in ethanol to gain **19** (70%). The acid derivative **19** was transformed to acid chloride using thionyl chloride in benzene and subsequently by a condensation reaction with boc-protecting diaminopropane **16** in toluene in the presence of triethylamine as base and 4-(dimethylamino)pyridine as catalyst to give product **20** (42%). In the next step, the protecting group was deprotected by trifluoroacetic acid and consequently extracted with sodium hydrogen carbonate solution. Then it was immediately reacted with thiophosgene using potassium carbonate as base to afford thiocyanate derivative **21** (62%). Compound **14** was obtained by treating compound **21** with 1,3-bis(aminomethyl)benzene in pyridine (40%). The crystal structure of compound **14** showed the closed flattened cone conformation of the calix[4]arene unit. Compound **15** was synthesized by treating the acid chloride derivative with bis-thiourea linkage **28** using 4-(dimethylamino)pyridine as base in dry tetrahydrofuran (43%). This method gave calix[4]arene ester **15** in 15% overall yield. Except for tetrasubstituted calix[4]arene **18**, other derivatives clearly existed in cone conformation.

Binding recognition of both receptors in acetonitrile-*d*<sub>3</sub> was investigated towards cations, anions (common and amino acid anion) and ion-pairs using <sup>1</sup>H-NMR titration technique. The alkali cations were used as their perchlorate salts while either common or amino acid anions were prepared as mono- or di-tetrabutylammonium salts. The exchange rate between the complexed and uncomplexed cationic guest in the inner cavity of macromolecule **14** was slower than the <sup>1</sup>H-NMR time scales, giving rise to new separate NMR peaks assignable to the **14**-cation complex. However, the exchange rate of the **15**-cation complexes was faster than the NMR time scale affording the

time-average signals. From either integral intensity ratio or chemical induced shift, stoichiometry of complexes, binding constants and Gibbs free energies were evaluated.

Both receptors showed the selective recognition towards sodium; however, receptor **15** displayed the more sensitive and selective to this alkali cation [**14**·sodium ( $5531 \text{ M}^{-1}$ ) > **14**·lithium ( $914 \text{ M}^{-1}$ ) > **14**·potassium ( $617 \text{ M}^{-1}$ ) and **15**·sodium ( $15500 \text{ M}^{-1}$ ) > **15**·potassium ( $688 \text{ M}^{-1}$ ) > **15**·lithium ( $371 \text{ M}^{-1}$ )]. The selectivity and affinity trend could be ascribed to the HSAB concept and size complementary.

The anion recognition at the thiourea binding site of calix[4]arene amide **14** and ester **15** displayed the different complex stoichiometry and selectivity trend. Macromolecule **14** preferred to bind trigonal planar carboxylate anion over tetrahedral phosphate anion [glutarate ( $42900 \text{ M}^{-1}$ ) > acetate ( $30400 \text{ M}^{-1}$ ) > succinate ( $11000 \text{ M}^{-1}$ ) > phenylphosphinate ( $17100 \text{ M}^{-1}$ ) > benzoate ( $3290 \text{ M}^{-1}$ ) > diphenylphosphate ( $2330 \text{ M}^{-1}$ ) > dihydrogen phosphate ( $858 \text{ M}^{-1}$ )]. On the other hand, compound **15** bound phosphate type anions stronger than carboxylate anions [phenylphosphinate ( $14300 \text{ M}^{-1}$ ) > dihydrogen phosphate ( $9710 \text{ M}^{-1}$ ) > benzoate ( $8300 \text{ M}^{-1}$ ) > diphenylphosphate ( $3240 \text{ M}^{-1}$ ) > succinate ( $2020 \text{ M}^{-1}$ ) > acetate ( $2010 \text{ M}^{-1}$ )]. These selectivity trends can be rationalized by the complementary structure, the acid-base property and the solvent effect.

Receptor **14** was discovered to bind anionic form of leucine stronger than other amino acids [leucine ( $49600 \text{ M}^{-1}$ ) > phenylalanine ( $24800 \text{ M}^{-1}$ ) > aspartic acid ( $21200 \text{ M}^{-1}$ ) > asparagine ( $19600 \text{ M}^{-1}$ ) > glutamic acid ( $15500 \text{ M}^{-1}$ ) > threonine ( $10300 \text{ M}^{-1}$ ) > glutamine ( $8270 \text{ M}^{-1}$ ) >> serine ( $<10 \text{ M}^{-1}$ )] while analogous **15** was selectively recognized TBA salt of phenylalanine and asparagine [phenylalanine ~ asparagine ( $>10^4 \text{ M}^{-1}$ ) > glutamine ( $39100 \text{ M}^{-1}$ ) > aspartic acid ( $17700 \text{ M}^{-1}$ ) > threonine ( $17100 \text{ M}^{-1}$ ) > glutamic acid ( $11900 \text{ M}^{-1}$ ) > leucine ( $10200 \text{ M}^{-1}$ ) >> serine ( $<10 \text{ M}^{-1}$ )]. Both hosts **14** and **15** had the greatest recognition towards TBA salt of phenylalanine. Both macrocyclic compounds **14** and **15** had the lowest stability constant towards carboxylate anion of serine. Interestingly, the ability of both receptors towards TBA salts of aspartic acid, glutamic acid, asparagine and glutamine clearly depended on the chain length  $n$  of amino acids. The order of binding ability was aspartic acid ( $n = 2$ ) > glutamic acid ( $n = 3$ ) and asparagine ( $n = 2$ ) > glutamine ( $n = 3$ ). Either the amide function in **14** or ester group **15** acted as alkali cation binding sites and as a remote

anion binding sites to discriminate anion and ion-pair binding. The bis-thiourea **14** preferred to bind carboxylate anion of aspartic acid over asparagine and carboxylate salt of glutamic acid over glutamine. On the other hand, analogous **15** afforded the better recognition towards TBA salt of asparagine over aspartic acid and TBA salt of glutamine over glutamic acid. The binding efficacy towards amino carboxylate anions could be explained in terms of acid-base property and complementary structure from additional moiety.

After bound with sodium cation, calix[4]arene amide **14** did not associate with dihydrogen phosphate. Only the binding efficacy upon the addition of TBA salts of diphenylphosphate, aspartic acid and glutamic acid could be evaluated attributed to the negative ion-pairing effect in the remaining systems [aspartic acid ( $>10^4 \text{ M}^{-1}$ ) > glutamic acid ( $5370 \text{ M}^{-1}$ ) > diphenylphosphate ( $1790 \text{ M}^{-1}$ )]. The presence of sodium cation enhanced the binding recognition of dicarboxylate anion of aspartic acid due to the combination of hydrogen bonding and electrostatic effects but retarded the association process in the case of TBA salts of glutamic acid and diphenylphosphate. Comparison to unbound **14**, the bound receptor displayed much higher ability in differentiating these two amino acid anions.

Relative stabilities for receptor **15** towards anions were as follow: dihydrogen phosphate ( $53900 \text{ M}^{-1}$ ) > phenylphosphinate ( $45800 \text{ M}^{-1}$ ) > acetate ( $28000 \text{ M}^{-1}$ ) > diphenylphosphate ( $11100 \text{ M}^{-1}$ ) > benzoate ( $982 \text{ M}^{-1}$ ) > aspartic acid ( $162 \text{ M}^{-1}$ ) > glutamic acid ( $94 \text{ M}^{-1}$ ). The  $\mathbf{15}\cdot\text{Na}^+$  receptor served as a positive allosteric system in the presence of dihydrogen phosphate, phenylphosphinate, acetate or diphenylphosphate while it acted as a negative allsoterism in the presence of benzoate, aspartic acid or glutamic acid. The acid-base property as well as the complementary of donor-acceptor binding sites determined the selectivity.

#### 4.2 Suggestions for Future Work

The host-guest association of these complexes could be studied by other techniques such as infrared spectroscopy,<sup>[170]</sup> UV-VIS spectroscopy<sup>[171]</sup> or calorimetry.<sup>[166]</sup> Furthermore, attempts to recrystallize each complex to obtain a crystal structure should be carried out to reveal the solid state structure of the complexes.

Generally, anions, especially, carboxylate, dicarboxylate and phosphate play an important role in chemical and biological process.<sup>[172]</sup> Our receptors are able to bind these anions well in different detail, so it might be valuable to modify our receptor to be an electrochemical<sup>[173-174]</sup> or naked-eye<sup>[175-176]</sup> sensors that are able to response a specific anion by giving an electrochemical response or color changes. After that the high sensitive and selective electrochemical response receptor should be incorporated in an electrode membrane and used as an ion selective electrode.<sup>[177]</sup> A covalent attachment of these receptors to solid-phase HPLC is another possible application for separation of anions.<sup>[178]</sup>

An introduction of pendent arms of amino acid or a short chain of peptide on a part of any substituted unit<sup>[179-180]</sup> would afford a higher specific ligand for an oligopeptide. An attachment of this oligopeptide receptor to a polystyrene resin will provide a peptide library based on calix[4]arene which is a powerful tool for investigation of host-guest interactions.<sup>[73, 181]</sup>



สถาบันวิทยบริการ  
จุฬาลงกรณ์มหาวิทยาลัย

## REFERENCES

1. Lehn, J-M. *Supramolecular Chemistry: Concepts and Perspectives*, VCH, Weinheim, **1995**, pp.5.
2. Beer P. D.; Gale, P. A.; Smith, D. K. *Supramolecular Chemistry*, Oxford University Press, Oxford, **1999**, pp.2.
3. Jeffrey, G. A. *An Introduction to Hydrogen Bonding*, Oxford University Press, Oxford, **1997**, p.2-3.
4. Arduini, A.; Secchi, A.; Pochini, A. *J. Org. Chem.* **2000**, 65(26), 9085-9091.
5. Bodenant, B.; Weil, T.; Businelli-Pourcel, M.; Fages, F.; Barbe, B.; Pianet, I.; Laguerre, M. *J. Org. Chem.* **1999**, 64(19), 7034-7039.
6. Ikeda, A.; Shinkai, S. *Chem. Rev.* **1997**, 97, 1713-1734.
7. Kral, V.; Sessler, J. L.; Shishkanova, T. V.; Gale, P. A.; Volf, R. *J. Am. Chem. Soc.* **1999**, 121, 8771-8775.
8. Lee, D. H.; Lee, H. Y.; Lee, K. H.; Hong, J-I. *J. Chem. Soc., Chem. Commun.* **2002**, 1188-1189.
9. Lee, D. H.; Lee, K. H.; Hong, J-I. *Org. Lett.* **2001**, 3, 5-8.
10. Hennrich, G.; Sonnenschein, H.; Resch-Genger, U. *Tetrahedron Lett.* **2001**, 42, 2805-2808.
11. Darensbourg, D. J.; Joó, F.; Kannisto, M.; Kathó, A.; Reibenspies, J. H.; Dailage, D. J. *Inorg. Chem.* **1994**, 33(2), 200-208.
12. Costa, J; Delgado, R; Drew, M. G. B.; Felix, V.; Saint-Maurice, A. *J. Chem. Soc., Dalton Trans.* **2000**, 12, 1907-1916.
13. Lippard, S. J.; Berg, A. *Principles of Bioinorganic Chemistry* California: University Science Books, **1994**, pp.3.

14. Dilworth, J.; Parrott, S. *Chem. Soc. Rev.* **1998**, 27(1), 43-55.
15. Steed, J. W.; Atwood, J. L. *Supramolecular Chemistry* John Wiley & Sons, Chichester, **2000**, p.36-38.
16. Vögtle, F. *Supramolecular Chemistry: An Introduction* Chichester, John Wiley & Sons, **1991**, p.27-76.
17. Danil de Namor, A. F.; Kowalska, D.; Marcus, Y.; Villanueva-Salas, J. *J. Phys. Chem. B* **2001**, 105, 7542-7549.
18. Shriver, D. F.; Atkins, P. W.; Langford, C. H. *Inorganic Chemistry* 3<sup>rd</sup> ed, W. H. Freeman, New York, **1990**, p.173-176.
19. Calladine, C. R.; Drew, H. R. *Understanding DNA: The molecule and how it works* 2<sup>nd</sup> ed. New York: Academic Press, **1997**, 281 pp.
20. Stryer, L. *Biochemistry* 4<sup>th</sup> ed, W. H. Freeman, New York, **2000**, p.509-528.
21. Beer, P. D. *J. Chem. Soc., Chem. Commun.* **1996**, 6, 689-696.
22. Harrison, R. M. *Pollution: Causes Effects and Control.* 3<sup>rd</sup> ed, London, Royal Society of Chemistry, **1996**, 480 pp.
23. Stetter, J.; Lieb, F. *Angew. Chem., Int. Ed. Engl.* **2000**, 39, 1724-1744.
24. Quinton, P. M. *FASEB J.* **1990**, 4, 2709-2717.
25. Renkawek, K.; Bosman, G. J. C. G. M. *Neuroreport* **1995**, 6(6), 929-932.
26. Beer, P. D.; Gale, P. A. *Angew. Chem., Int. Ed. Engl.* **2002**, 40, 486-516.
27. Scheerder, J.; Engbersen, J. F. J.; Reinhoudt, D. N. *Recl. Trav. Chim. Pays-Bas.* **1996**, 115(6), 307-320.
28. Quioco, F. A., Sack, J. S.; Vyas, N. K. *Nature* **1987**, 329, 561-564.
29. Pflugrath, J. W., Quioco, F. A. *J. Biol. Chem.* **1988**, 263, 163-180.

30. Pinkhassik, E.; Sidorov, V.; Stibor, I. *J. Org. Chem.* **1998**, *63*, 9644-9651.
31. Loll, P. J.; Bevivino, B. D.; Korty, B. D.; Axelsen, P. H. *J. Am. Chem. Soc.* **1997**, *119*, 1516-1522.
32. Sharman, G. J.; Williams, D. H. *J. Chem. Soc., Chem. Commun.* **1997**, 723-724.
33. Linton, B. R.; Goodman, M. S.; Hamilton, A. D. *Chem. Eur. J.* **2000**, *6*, 2449-2455.
34. Pernía, G. J.; Kilburn, J. D.; Essex, J. W.; Mortishire-Smith, R. J.; Rowley, M. J. *Am. Chem. Soc.* **1996**, *118*, 10220-10227.
35. Bordwell, F. G.; Algrim, D. J.; Harrelson, J. A., Jr. *J. Am. Chem. Soc.* **1988**, *110*, 5903-5904.
36. Molina, M. T.; Yáñez, M.; Mó, O.; Notario, R.; Abboud, J.-L. M. In *Supplement A3, The Chemistry of Double-Bonded Functional Groups, Part 2*; Patai, S., Ed.; John Wiley & Sons: Chichester, **1997**, 1355-1496.
37. Rienäcker, C. M.; Klapötke, T. In *Supplement A3, The Chemistry of Double-Bonded Functional Groups, Part 1*; Patai, S., Ed.; John Wiley & Sons: Chichester, **1997**, 341-365.
38. Kabalka, G.W.; Li, N.-S.; Pace, R.D. *Synth. Commun.*, **1995**, *25(14)*, 2135-2143.
39. Bell, T.W.; Hext, N.M.; Khasanov, A. B. *Pure & Appl. Chem.* **1998**, *70(12)*, 2371-2377.
40. Koh, K. N.; Imada, T.; Nagasaki, T.; Shinkai, S. *Tetrahedron Lett.* **1994**, *35(24)*, 4157-4160.
41. Chartres, J. D.; Groth, A. M.; Lindoy, L. F.; Lowe, M. P.; Meehan, G. V. *J. Chem. Soc., Perkin Trans. 1* **2000**, 3444-3450.
42. Fabbriizzi, L.; Montagna, L.; Poggi, A. *J. Chem. Soc., Dalton Trans.* **1987**, 2631-2634.

43. Fages, F.; Desvergne, J.-P.; Bouas-Laurent, H. *J. Org. Chem.* **1994**, *59*, 5264-5271.
44. Fages, F.; Desvergne, J.-P.; Bouas-Laurent, H.; Lehn, J.-M.; Konopelski, J.P.; Marsau, P.; Barrans, Y. *J. Chem. Soc., Chem. Commun.* **1990**, 655-658.
45. Sutherland, I.O. *Pure & Appl. Chem.* **1989**, *61*(9), 1547-1554.
46. Ray, J.K.; Gupta, S.; Pan, D.; Kar, G. K. *Tetrahedron* **2001**, *57*, 7213-7219.
47. Graf, E.; Hosseini, W.; Ruppert, R. *Tetrahedron Lett.* **1994**, *35*(42), 7779-7782.
48. Rudkevich, D. M.; Mercer-Chalmers, J. D.; Verboom, W.; Ungaro, R.; de Jong, F.; Reinhoudt, D. N. *J. Am. Chem. Soc.* **1995**, *117*, 6124-6125.
49. Beer, P. D.; Dent, S. W. *J. Chem. Soc., Chem. Commun.* **1998**, 825-826.
50. Nabeshima, T.; Hanami, T. *Heterocycles* **1999**, *50*(2), 1091-1096.
51. Love, J. B.; Vere, J. M.; Glenny, M. W.; Blake, A. J.; Schröder, M. *J. Chem. Soc., Chem. Commun.* **2001**, 2678-2679.
52. Liu, X.; Kilner, C. A.; Halcrow, M. A. *J. Chem. Soc., Chem. Commun.* **2002**, 704-705.
53. Park, C. E.; Jung, Y.-G.; Hong, J.-I. *Tetrahedron Lett.* **1998**, *39*, 2353-2356.
54. Kirkovits, G. J.; Shriver, J. A.; Gale, P. A.; Sessler, J. L. *J. Inclus.* **2001**, *41*, 69-75.
55. Cooper, J. B.; Drew, M. G. B.; Beer, P. D. *J. Chem. Soc., Dalton Trans.* **2001**, 392-401.
56. Beer, P. D.; Dent, S. W. *J. Chem. Soc., Chem. Commun.* **1998**, 825-826.
57. Nishizawa, S.; Shigemori, K.; Teramae, N. *Chem. Lett.* **1999**, 1185-1186.
58. Luecke, H.; Quioco, F. A. *Nature* **1990**, *347*, 402-406.
59. Mangani, S.; Ferraroni, M.; Orioli, P. *Inorg. Chem.* **1994**, *33*, 3421-3423.



60. Malashkevich, V.; Kammerer, R. A.; Efimov, V. P.; Schulthess, T.; Engel, J. *Science* **1996**, *274*, 761-765.
61. Kanyo, Z. F.; Christianson, D. W. *J. Biol. Chem.* **1991**, *266*, 4246-4268.
62. Asfari, Z.; Böhmer, V.; Harrowfield, J.; Vicens, J. *Calixarenes 2001* Kluwer Academic Publishers, Dordrecht, 2001, p.1-2.
63. Wieser, C.; Dieleman, D. B.; Matt, D. *Coord. Chem. Rev.* **1997**, *165*, 93-161.
64. Wolbers, M. P. O.; van Veggel, F. C. J. M.; Peters, F. G. A.; van Beelen, E. S. E.; Hofstraat, J. W.; Geurts, F. A. J.; Reinhoudt, D. N. *Chem. Eur. J.* **1998**, *4*(5), 772-780.
65. Cuevas, F.; Stefano, S. D.; Magrans, J. O.; Prados, P.; Mandolini, L.; de Mendoza, J. *Chem. Eur. J.* **2000**, *6*(17), 3228-3234.
66. Collins, E. M.; McKervey, M. A.; Madigan, E.; Moran, M. B.; Owens, M.; Ferguson, G.; Harris, S. J. *J. Chem. Soc., Perkin Trans. 1* **1991**, 3137-3142.
67. Arnaud-Neu, F.; Browne, J. k.; Byrne, D.; Marrs, D. J. McKervey, M. A.; O'Hagan, P. Schwing-Weill, M. J. Walker, A. *Chem. Eur. J.* **1999**, *5*(1), 175-186.
68. Ludwig, R.; Kunogi, K.; Dung, N.; Tachimori, S. *J. Chem. Soc., Chem. Commun.* **1997**, *20*, 1985-1986.
69. Tuntulani, T.; Tumcharern, G.; Ruangpornvisuti, V. *J. Inclus. Phenom.* **2001**, *39*, 47-53.
70. Diamond, D.; Nolan, K. *Anal. Chem.* **2001**, 22A-29A.
71. Molenveld, P.; Engbersen, J. F. J.; Kooijman, H. J.; Spek, A. L.; Reinhoudt, D. N. *J. Am. Chem. Soc.* **1998**, *120*(27), 6726-6737.
72. Haino, T.; Akii, H.; Fukazawa, Y. *Synth. Lett.* **1998**, *9*, 1016-1018.

73. Hioki, H.; Yamada, T.; Fujioka, C.; Kodama, M. *Tetrahedron Lett.* **1999**, *40*, 6821-6825.
74. Mogck, O.; Böhmer, V.; Vogt, W. *Tetrahedron* **1996**, *52*, 8489-8496.
75. Harmann, B. C.; Shimizu, K. D.; Rebek, J., Jr. *Angew. Chem., Int. Ed. Engl.* **1996**, *35*, 1326-1329.
76. Zhao, X.; Chang, Y-L.; Fowler, F.W.; Lauher, J. W. *J. Am. Chem. Soc.* **1990**, *112*, 6627-6634.
77. Kane, J. J.; Liao, R.-F.; Lauher, J. W.; Fowler, F. W. *J. Am. Chem. Soc.* **1995**, *117*, 12003-12004.
78. Fielding, L. *Tetrahedron* **2000**, *56*, 6151-6170.
79. Macomber, R.S. *J. Chem., Ed.* **1992**, *69(5)*, 375-378.
80. Scheerder, J.; Fochi, M.; Engbersen, J. F. J.; Reinhoudt, D. N. *J. Org. Chem.* **1994**, *59*, 7815-7820.
81. Pelizzi, N.; Casnati, A.; Friggeri, A.; Ungaro, R. *J. Chem. Soc., Perkin Trans. 2* **1998**, 1307-1311.
82. Deetz, M. J.; Shang, M.; Smith, B. D. *J. Am. Chem. Soc.* **2000**, *122*, 6201-6207.
83. Mahoney, J. M.; Beatty, A. M.; Smith, B. D. *J. Am. Chem. Soc.* **2001**, *123*, 5847-5848.
84. Mahoney, J. M.; Marshall, R. A.; Beatty, A. M.; Smith, B. D.; Salvatore, C.; Gale, P. A. *J. Supra. Chem. 1*, **2001**, 289-292.
85. Arduini, A.; Giorgi, G.; Pochini, A.; Secchi, A.; Ugozzoli, F. *J. Org. Chem.* **2001**, *66*, 8302-8308.
86. Sansone, F.; Baldini, L.; Castani, A.; Lazzarotto, M.; Ugozzoli, F.; Ungaro, R. *Proc. Natl. Acad. Sci.*, **2002**, *99*, 4842-4847.

87. Bühlmann, P.; Nishizawa, S.; Xiao, K.P.; Umezawa, Y. *Tetrahedron* **1997**, *53*(5), 1647-1654.
88. Perrin, D. D.; Armarego, W. L. F. *Purification of Laboratory Chemicals* Pergamon, Oxford, **1988**.
89. Gutsche, C. D.; Iqbal, M. *Org. Synth.* **1990**, *68*, 234-237.
90. Muller, D; Zeltser, I; Bitan, G.; Gilon, C. *J. Org. Chem.* **1997**, *62*, 411-416.
91. Houssin, R.; Bernier, J-L.; Hénichart, J-P. *Synthesis* **1988**, 259-261.
92. Hu, W.; Hesse, M. *Helv. Chim. Acta* **1996**, *79*, 548-559.
93. Guelzim, A.; Khrifi, S.; Baert, F.; Asfari, Z.; Vicens, J.; *Acta Crystallogr. Sect.C: Cryst. Struct. Commun.* **1993**, *49*(12), 2121-2124.
94. Wieser, C.; Matt, D.; Fischer, J.; Harriman, A. *J. Chem. Soc., Dalton Trans.* **1997**, 2391-2402.
95. Jeunesse, C.; Dieleman, C.; Steyer, S.; Matt, D. *J. Chem. Soc., Dalton Trans.* **2001**, 881-892.
96. Thuery, P.; Nierlich, M.; Asfari, Z.; Vicens, J. *Acta Crystallogr. Sect.C.: Cryst. Struct. Commun.* **2000**, *56*(3), 343-344.
97. Araki, K.; Nakamura, R.; Otsuka, H.; Shinkai, S. *J. Chem. Soc., Chem. Commun.* **1995**, *20*, 2121-2122.
98. Boehmer, V.; Ferguson, G.; Gallagher, J.F.; Lough, A.J. McKervey, M.A. *J. Chem. Soc., Perkin Trans. I* **1993**, *13*, 1521-1527.
99. Kawaguchi, M.; Ikeda, A.; Hamachi, I.; Shinkai, S. *Tetrahedron Lett.* **1999**, *40*, 8245-8249.
100. Dubowchik, G.M.; Ditta, J.L.; Herbst, J.J.; Bollini, S.; Vinitzky, A. *Bioorg. Med. Chem. Lett.* **2000**, *10*, 559-562.

101. Chaubet, F.; Duong, M.N.V.; Courtieu, J.; Gaudemer, A. *Can. J. Chem.* **1991**, *69*, 1107-1116.
102. Gross, R.; Dürner, G.; Göbel, M.W. *Liebigs Ann. Chem.* **1994**, 49-58.
103. Tobe, Y.; Sasaki, S-i.; Mizuno, M; Hirose, K.; Naemura, K. *J. Org. Chem.* **1998**, *63*, 7481-7489.
104. Benito, J. M.; Gomez-Garcia, M.; Blanco, J. L. J.; Mellet, C. O.; Fernandez, J. M. *G. J. Org. Chem.* **2001**, *66(4)*, 1366-1372.
105. Bisson, A. P.; Hunter, C. A.; Morales, J. C.; Young, K. *Chem. Eur. J.* **1998**, *4*, 845-851.
106. Homer, J.; Perry, M. C. *J. Chem. Soc., Faraday Trans. 1* **1986**, *82*, 533-543.
107. Ding, Z. N.; Ellis, D. E.; Sigmund, E.; Halperin, W. P.; Shriver, D. F. *Phys. Chem. Chem. Phys.* **2003**, *5(10)*, 2072-2081.
108. Verboom, W.; Datta, S.; Asfari, Z.; Harkema, S.; Reinhoudt, D. N. *J. Org. Chem.* **1992**, *57(20)*, 5394-5398.
109. Shinkai, S.; Iwamoto, K.; Araki, K.; Matsuda, T. *Chem. Lett.* **1990**, 1263-1266.
110. Iwamoto, K.; Ikeda, A.; Araki, K.; Harada, T.; Shinkai, S. *Tetrahedron* **1993**, *49(44)*, 9937-9946.
111. Ohseto, F.; Shinkai, S. *J. Chem. Soc., Perkin. Trans. 2* **1995**, *6*, 1103-1110.
112. Kawaguchi, M.; Ikeda, A.; Shinkai, S. *J. Chem. Soc., Perkin. Trans. 1* **1998**, *2*, 179-184.
113. Peña, M. S.; Zhang, Y.; Thibodeaux, S.; McLaughlin, M. L.; de la Peña, A. M.; Warner, I. M. *Tetrahedron Lett.* **1996**, *37(33)*, 5841-5844.
114. Mogck, O.; Parzuchowski, P.; Nissinen, M.; Böhmer, V.; Rokicki, G.; Rissanen, K. *Tetrahedron*, **1998**, *54*, 10053-10068

115. Fernández, J. M.; Mellet, C. O.; Fuentes, J. *J. Org. Chem.* **1993**, *58*(19), 5192-5199.
116. Blanco, J. L.; Barria, C. S.; Benito, J. M.; Mellet, C. O.; Fuentes, J.; Santoyo-González, F.; Fernández, J. M. *Synthesis* **1999**, *11*, 1907-1914.
117. Casnati, A.; Sansone, F.; Ungaro, R. *Acc. Chem. Res.* **2003**, *36*, 246-254.
118. Reichardt, C. *Solvents and Solvents Effects in Organic Chemistry*, **1988**, VCH publishers, Weinheim, p. 16-17.
119. Scheerder, J.; van Duynhoven, J. P. M.; Engbersen, J. F. J.; Reinhoudt, D. N. *Angew. Chem., Int. Ed. Engl.* **1996**, *35*(10), 1090-1093.
120. Calestani, G.; Ugozzoli, F.; Arduini, A.; Ghidini, E.; Ungaro, R. *J. Chem. Soc., Chem. Commun.*, **1987**, 344-346.
121. Murakami, H.; Shinkai, S. *Tetrahedron Lett.* **1993**, *34*(26), 4237-4240.
122. Beer, P. D.; Drew, M. G. B.; Knubley, R. J.; Ogden, M. I. *J. Chem. Soc., Dalton Trans.* **1995**, 3117-3123.
123. Nomura, E.; Takagaki, M.; Nakaoka, C.; Uchida, M.; Taniguchi, H. *J. Org. Chem.* **1999**, *64*, 3151-3156.
124. Cooper, J. B.; Drew, M. G. B., Beer, P. D. *J. Chem. Soc., Dalton Trans.* **2000**, 2721-2728.
125. Schmidtchen, F. P.; Berger, M. *Chem. Rev.*, **1997**, *97*, 1609-1646.
126. Murakami, H.; Shinkai, S. *J. Chem. Soc., Chem. Commun.*, **1993**, *20*, 1533-1535.
127. Nomura, E.; Takagaki, M.; Nakaoka, C.; Taniguchi, H.; *J. Org. Chem.* **2000**, *65*, 5932-5936.
128. Čajan, M.; Lhoták, P.; Lang, J.; Dvořáková, H.; Stibor, I.; Koča, J. *J. Chem. Soc., Perkin Trans. 2* **2002**, 1922-1929.

129. Gordon, A. J.; Ford, R. A. *The Chemist's Companion: A Handbook of Practical Data, Techniques and References* **1972**, John Wiley & Sons, New York, p. 58-62.
130. Dean, J. A. *Handbook of Organic Chemistry* 1987, Mc Graw-Hill, New York, p. 8-2 - 8-65.
131. Linton, B. R.; Goodman, M. S.; Fan, E.; van Arman, S. A.; Hamilton, A. D. *J. Org. Chem.* **2001**, 66, 7313-7319.
132. Nishizawa, S.; Bühlmann, P.; Iwao, M.; Umezawa, Y. *Tetrahedron Lett.* **1995**, 36, 6483-6486.
133. Nishizawa, S.; Teramae, N. *Anal. Sci.* **1997**, 13 (supplement), 485-488.
134. Nishizawa, S.; Kato, R.; Hayashita, T.; Teramae, N. *Anal. Sci.* **1998**, 14, 595-597.
135. Pernía, G. J.; Kilburn, J. D.; Rowley, M. *J. Chem. Soc., Chem. Commun.* **1995**, 305-306.
136. Werner, F.; Schneider, H.-J. *Helv. Chim. Acta.* **2000**, 83, 465-478.
137. Takeuchi, D.; Shioya, T.; Swager, T. M. *Angew. Chem., Int. Ed. Engl.* **2001**, 40(18), 3372-3376.
138. Schalley, C. A.; Castellano, R. K.; Brody, M. S.; Rudkevich, D. M.; Siuzdak, G.; Rebek, Jr. *J. Am. Chem. Soc.* **1999**, 121, 4568-4579.
139. Smith, R. D.; Bruce, J. E.; Wu, Q.; Lei, Q. P. *Chem. Soc. Rev.* **1997**, 26, 191-202.
140. Kikuchi, Y.; Tanaka, Y.; Sutarto, S.; Kobayashi, K.; Toi, H.; Aoyama, Y. *J. Am. Chem. Soc.* **1992**, 114, 10302-10306.
141. Albrecht, M.; Zauner, J.; Burgert, R.; Röttele, H.; Fröhlich, R. *Mat. Sci. Eng. C* **2001**, 18, 185-190.
142. Fan, E.; Van Arman, S. A.; Kincaid, S.; Hamilton, A. D. *J. Am. Chem. Soc.* **1993**, 115, 369-370.

143. Sasaki, S-i.; Mizuno, M.; Naemura, K.; Tobe, Y. *J. Org. Chem.* **2000**, *65*(2), 275-283.
144. Godoy-Alcántar, C.; Rivera, I. L.; Yatsimirsky, A. K. *Bioorg. Med. Chem. Lett.* **2001**, *11*, 651-654.
145. Beer, P. D.; Shade, M. *J. Chem. Soc., Chem. Commun.* **1997**, 2377-2378.
146. Gale, P. A. *Coord. Chem. Rev.*, **2000**, *199*, 181-233.
147. Yang, Y. S., Ko, S. W.; Song, I. H.; Ryu, B. J.; Nam, K. C. *Bull. Korean Chem. Soc.* **2003**, *24*(5), 681-683.
148. Tobe, Y; Sasaki, S-i.; Mizuno, M; Naemura, K. *Chem. Lett.* **1998**, 835-836.
149. Dixon, R.P.; Geib, S. J.; Hamilton, A.D. *J. Am. Chem. Soc.* **1992**, *114*, 365-366.
150. Gunnlaugsson, T.; Davis, A. P.; Glynn, M. *J. Chem. Soc., Chem. Commun.* **2001**, 2556-2557.
151. Fitzmaurice, R. J.; Kyne, G. M.; Douheret, D.; Kilburn, J. D. *J. Chem. Soc., Perkin Trans. 1*, **2002**, 841-864.
152. Metzger, A.; Lynch, V. M.; Anslyn, E. V. *Angew. Chem., Int. Ed. Engl.* **1997**, *36*, 862-865.
153. Breccia, P.; Gool, M. V.; Pérez-Fernández, R.; Martín-Santamaría, S.; Gago, F.; Prados, P.; de Mendoza, J. *J. Am. Chem. Soc.* **2003**, *125*, 8270-8284.
154. Wilcox, C. S. *Frontiers in Supramolecular Organic Chemistry and Photochemistry* (Eds.: H.-J. Schneider, H. Dürr), VCH, Weinheim, **1991**, p. 123-143.
155. Weber, G.; Anderson, S. R. *Biochemistry*, **1965**, *4*, 1942-1947.
156. Kyne, G. M.; Light, M. E.; Hursthouse, M. B.; de Mendoza, J.; Kilburn, J. D. *J. Chem. Soc., Perkin Trans. 1* **2001**, 1258-1263.

157. Gale, P. A. *Coord. Chem. Rev.* **2003**, *240*, 191-221.
158. Camiolo, S.; Coles, S. J.; Gale, P. A. Hursthouse, M. B.; Tizzard, G. J. *Supramol. Chem.* **2003**, *15(3)*, 231-234.
159. Shukla, R.; Kida, T.; Smith, B. D. *Org. Lett.* **2000**, *20(2)*, 3099-3102.
160. Al-Sayah, M. H.; Branda, N. R. *Org. Lett.* **2002**, *4(6)*, 881-884.
161. Arnaud-Neu, F.; Collins, E. M.; Deasy, M.; Ferguson, G.; Harris, S. J.; Kaitner, B.; Lough, A. J.; Mckerverey, M. A.; Marques, E.; Ruhl, B. L.; Schwing-Weill, M. J.; Seward, E. M. *J. Am. Chem. Soc.* **1989**, *111*, 8681-8691.
162. Olmstead, W. N.; Bordwell, F. G. *J. Org. Chem.* **1980**, *45*, 3299-3305.
163. Krestov, G. A.; Novosyolov, N. P.; Perelygin, I. S.; Kolker, A. M.; Safonova, L. P.; Ovchinnikova, V. D.; Trostin, V. N. *Ionic Solvation*; Ellis Horwood: Chichester, **1994**, p. 159-161.
164. Tozawa, T.; Misawa, Y.; Tokita, S.; Kubo, Y. *Tetrahedron Lett.* **2000**, *41*, 5219-5223.
165. Gokel, G. W.; Barbour, L. J.; Ferdani, R.; Hu, J. *Acc. Chem. Res.* **2002**, *35*, 878-886.
166. Wadsö, I. *Chem. Soc. Rev.* **1997**, 79-86.
167. Arduini, A.; Brindani, E.; Giorgi, G.; Pochini, A.; Secchi, A. *J. Org. Chem.* **2002**, *67*, 6188-6194.
168. Sénèque, O.; Giorgi, M.; Reinaud, O. *Supramol. Chem.* **2003**, *15(7-8)*, 573-580.
169. Beer, P. D.; Gale, P. A.; Heseck, D. *Tetrahedron Lett.* **1995**, *36(5)*, 767-770.
170. Nissink, J. W. M.; Boerrigter, H.; Verboom, W.; Reinhoudt, D. N.; van der Maas, J. H. *J. Chem. Soc., Perkin Trans. 2*, **1998**, 2617-2622.
171. Xie, H.; Yi, S.; Wu, S. *J. Chem. Soc., Perkin Trans. 2*, **1999**, 2751-2754.



172. Mei, M.; Wu, S. *New J. Chem.*, **2001**, 25, 471-475.
173. Kang, S. K.; Chung, T. D.; Kim, H. *Electrochim. Acta* **2000**, 45(18), 2939-2943.
174. Kuo, L-J.; Liao, J-H.; Chen, C-T.; Huang, C-H.; Chen, C-S.; Fang, J-M. *Org. Lett.* **2003**, 5(11), 1821-1824.
175. Kato, R.; Nishizawa, S.; Hayashita, T.; Teramae, N. *Tetrahedron Lett.* **2001**, 42, 5053-5056.
176. Jiménez, D.; Martínez-Máñez, R.; Sancenón, F.; Soto, J. *Tetrahedron Lett.* **2002**, 43, 2823-2825.
177. Sasaki, S-i.; Hashizume, A.; Ozawa, S.; Citterio, D.; Iwasawa, N.; Suzuki, K. *Chem. Lett.* **2001**, 382-383.
178. Sessler, J. L.; Gale, P. A.; Genge, J. W. *Chem. Eur. J.* **1998**, 4(6), 1095-1099.
179. Molard, Y.; Bureau, C.; Parrot-Lopez, H.; Lamartine, R.; Regnouf-de-Vains, J-B. *Tetrahedron Lett.* **1999**, 40, 6383-6387.
180. Yuan, H-S.; Zhang, Y.; Hou, Y-J.; Zhang, X-Y.; Yang, X-Z.; Huang, Z-T. *Tetrahedron*, **2000**, 56, 9611-9617.
181. Shuker, S. B.; Esterbrook, J.; Gonzalez, J. *Synth. Lett.* **2001**, 2, 210-213.



**APPENDICES**

สถาบันวิทยบริการ  
จุฬาลงกรณ์มหาวิทยาลัย



**APPENDIX A**

สถาบันวิทยบริการ  
จุฬาลงกรณ์มหาวิทยาลัย

**Table 1.** Crystal data and structure refinement.

Identification code	<b>01sot145</b>	
Empirical formula	$C_{72}H_{104}N_6O_{10}S_2$	
Formula weight	1277.73	
Temperature	120(2) K	
Wavelength	0.71073 Å	
Crystal system	Orthorhombic	
Space group	$Pna2_1$	
Unit cell dimensions	$a = 23.8484(9)$ Å	$\alpha = 90^\circ$
	$b = 20.3212(6)$ Å	$\beta = 90^\circ$
	$c = 15.0907(4)$ Å	$\gamma = 90^\circ$
Volume	7313.4(4) Å <sup>3</sup>	
Z	4	
Density (calculated)	1.160 Mg / m <sup>3</sup>	
Absorption coefficient	0.131 mm <sup>-1</sup>	
$F(000)$	2760	
Crystal	Rod; colourless	
Crystal size	0.26 × 0.08 × 0.06 mm <sup>3</sup>	
$\theta$ range for data collection	2.96 – 24.40°	
Index ranges	–27 ≤ $h$ ≤ 27, –23 ≤ $k$ ≤ 21, –17 ≤ $l$ ≤ 16	
Reflections collected	25269	
Independent reflections	11335 [ $R_{int} = 0.0646$ ]	
Completeness to $\theta = 24.40^\circ$	99.1 %	
Absorption correction	Semi-empirical from equivalents	
Max. and min. transmission	0.9922 and 0.9667	
Refinement method	Full-matrix least-squares on $F^2$	
Data / restraints / parameters	11335 / 1 / 851	
Goodness-of-fit on $F^2$	1.010	
Final $R$ indices [ $F^2 > 2\sigma(F^2)$ ]	$R1 = 0.0530$ , $wR2 = 0.1214$	
$R$ indices (all data)	$R1 = 0.0864$ , $wR2 = 0.1389$	
Absolute structure parameter	0.75(9)	
Extinction coefficient	0.0017(3)	
Largest diff. peak and hole	0.358 and –0.227 e Å <sup>-3</sup>	

**Diffraction:** *Enraf Nonius KappaCCD* area detector ( $\phi$  scans and  $\omega$  scans to fill Ewald sphere). **Data collection and cell refinement:** *Denzo* (Z. Otwinowski & W. Minor, *Methods in Enzymology* (1997) Vol. **276**: *Macromolecular Crystallography*, part A, pp. 307–326; C. W. Carter, Jr. & R. M. Sweet, Eds., Academic Press). **Absorption correction:** *SORTAV* (R. H. Blessing, *Acta Cryst.* **A51** (1995) 33–37; R. H. Blessing, *J. Appl. Cryst.* **30** (1997) 421–426). **Program used to solve structure:** *SHELXS97* (G. M. Sheldrick, *Acta Cryst.* (1990) **A46** 467–473). **Program used to refine structure:** *SHELXL97* (G. M. Sheldrick (1997), University of Göttingen, Germany).

**Further information:** <http://www.soton.ac.uk/~xservice/strat.htm>

**Special details:**

**Table 2.** Atomic coordinates [ $\times 10^4$ ], equivalent isotropic displacement parameters [ $\text{\AA}^2 \times 10^3$ ] and site occupancy factors.  $U_{eq}$  is defined as one third of the trace of the orthogonalized  $U^{ij}$  tensor.

Atom	<i>x</i>	<i>y</i>	<i>z</i>	$U_{eq}$	<i>S.o.f.</i>
C71	9287(2)	5117(2)	8285(3)	54(1)	1
C72	9383(2)	4777(2)	1810(3)	50(1)	1
O9	9311(1)	4444(1)	8047(2)	44(1)	1
O10	9316(1)	5441(2)	2054(2)	50(1)	1
C1	7550(2)	3935(2)	6290(2)	30(1)	1
C2	7338(1)	3359(2)	5909(2)	29(1)	1
C3	6914(2)	3028(2)	6365(3)	32(1)	1
C4	6694(2)	3256(2)	7159(3)	32(1)	1
C5	6898(2)	3851(2)	7478(2)	35(1)	1
C6	7324(2)	4205(2)	7051(2)	33(1)	1
C7	6232(2)	2870(2)	7656(3)	40(1)	1
C8	5940(6)	2382(8)	7213(7)	70(4)	0.50
C9	6529(4)	2539(5)	8520(7)	54(3)	0.50
C8'	5752(5)	2712(8)	6871(9)	75(4)	0.50
C9'	6455(4)	2225(5)	7868(8)	63(3)	0.50
C10	5887(3)	3311(3)	8250(4)	93(2)	1
C11	7518(2)	3126(2)	5000(3)	34(1)	1
C12	7218(2)	3531(2)	4302(3)	32(1)	1
C13	7490(2)	3965(2)	3724(2)	31(1)	1
C14	7184(2)	4400(2)	3195(2)	31(1)	1
C15	6598(2)	4352(2)	3193(3)	38(1)	1
C16	6315(2)	3886(2)	3695(3)	40(1)	1
C17	6634(2)	3501(2)	4265(3)	37(1)	1
C18	5679(2)	3773(2)	3625(3)	45(1)	1
C19	5413(2)	3691(2)	4537(3)	56(1)	1
C20	5581(2)	3136(2)	3076(3)	58(1)	1
C21	5387(2)	4343(2)	3139(3)	54(1)	1
C22	7459(2)	4933(2)	2639(2)	34(1)	1
C23	7304(2)	5616(2)	2965(2)	30(1)	1
C24	6877(2)	5966(2)	2522(2)	33(1)	1
C25	6667(2)	6563(2)	2820(3)	33(1)	1
C26	6885(2)	6805(2)	3600(3)	33(1)	1
C27	7306(2)	6486(2)	4074(2)	29(1)	1
C28	7527(2)	5906(2)	3731(2)	28(1)	1
C29	6209(2)	6934(2)	2291(3)	38(1)	1
C30	5920(3)	7437(4)	2825(5)	143(4)	1
C31	6498(3)	7263(4)	1497(5)	128(3)	1
C32	5789(3)	6468(3)	1898(6)	115(3)	1
C33	7470(2)	6710(2)	5002(2)	31(1)	1
C34	7455(2)	4903(2)	7372(2)	34(1)	1
C35	7175(2)	6272(2)	5668(2)	29(1)	1
C36	6596(2)	6210(2)	5601(3)	36(1)	1
C37	6291(2)	5751(2)	6084(3)	36(1)	1
C38	6585(2)	5354(2)	6664(3)	39(1)	1
C39	7166(2)	5395(2)	6775(2)	33(1)	1
C40	7451(2)	5873(2)	6281(2)	31(1)	1
C41	5654(2)	5688(2)	5924(3)	47(1)	1
C42	5552(2)	5620(3)	4918(3)	81(2)	1

C43	5369(2)	6296(2)	6272(4)	65(1)	1
C44	5413(2)	5064(2)	6375(3)	57(1)	1
C45	8278(2)	3568(2)	2927(3)	39(1)	1
C46	8202(2)	2843(2)	3024(3)	43(1)	1
C47	8536(3)	1907(2)	3792(4)	75(2)	1
C48	8190(2)	6338(2)	7148(3)	35(1)	1
C49	8057(2)	7052(2)	7060(3)	41(1)	1
C50	8272(3)	8008(2)	6244(4)	71(2)	1
C51	8483(2)	4341(2)	6350(3)	38(1)	1
C52	9018(2)	4242(2)	5837(3)	35(1)	1
C53	9480(2)	4118(2)	4399(3)	37(1)	1
C54	9779(2)	3466(2)	4275(3)	43(1)	1
C55	10068(2)	3213(2)	5105(3)	41(1)	1
C56	11048(2)	3637(2)	5233(3)	37(1)	1
C57	11997(2)	3959(2)	5710(3)	47(1)	1
C58	8467(2)	5538(2)	3699(3)	32(1)	1
C59	8992(2)	5712(2)	4221(2)	30(1)	1
C60	9426(2)	5930(2)	5645(3)	35(1)	1
C61	9666(2)	6608(2)	5746(3)	41(1)	1
C62	9946(2)	6879(2)	4922(3)	40(1)	1
C63	10951(2)	6568(2)	4860(3)	37(1)	1
C64	11935(2)	6289(2)	4471(4)	54(1)	1
C65	12237(2)	5682(2)	4761(3)	35(1)	1
C66	12823(2)	5687(2)	4723(3)	45(1)	1
C67	13126(2)	5129(3)	4951(3)	49(1)	1
C68	12848(2)	4575(2)	5231(3)	44(1)	1
C69	12271(2)	4567(2)	5316(3)	38(1)	1
C70	11969(2)	5122(2)	5074(3)	37(1)	1
N1	8984(1)	4102(2)	4985(2)	36(1)	1
N2	10501(1)	3658(2)	5456(2)	37(1)	1
N3	11390(1)	3979(2)	5766(2)	39(1)	1
N4	8939(1)	5871(2)	5059(2)	32(1)	1
N5	10418(1)	6486(2)	4602(2)	36(1)	1
N6	11330(1)	6228(2)	4370(2)	42(1)	1
O1	8077(1)	3953(1)	3672(2)	32(1)	1
O2	8575(1)	2599(1)	3682(2)	47(1)	1
O3	8035(1)	5944(1)	6385(2)	31(1)	1
O4	8404(1)	7334(1)	6396(2)	46(1)	1
O5	7991(1)	4242(1)	5829(2)	33(1)	1
O6	9468(1)	4330(1)	6246(2)	38(1)	1
O7	7962(1)	5606(1)	4197(2)	31(1)	1
O8	9445(1)	5672(1)	3822(2)	36(1)	1
S1	11285(1)	3220(1)	4349(1)	50(1)	1
S2	11134(1)	7054(1)	5715(1)	51(1)	1

---

**Table 3.** Bond lengths [Å] and angles [°].

C71–O9	1.415(5)
C71–H71A	0.9800
C71–H71B	0.9800
C71–H71C	0.9800
C72–O10	1.408(5)
C72–H72A	0.9800
C72–H72B	0.9800
C72–H72C	0.9800
O9–H9	0.8400
O10–H10	0.8400
C1–C6	1.382(5)
C1–C2	1.399(5)
C1–O5	1.407(4)
C2–C3	1.395(5)
C2–C11	1.513(5)
C3–C4	1.388(5)
C3–H3	0.9500
C4–C5	1.390(5)
C4–C7	1.545(5)
C5–C6	1.401(5)
C5–H5	0.9500
C6–C34	1.531(5)
C7–C8	1.385(12)
C7–C9'	1.450(11)
C7–C10	1.511(7)
C7–C9	1.629(9)
C7–C8'	1.680(12)
C8–H8A	0.9800
C8–H8B	0.9800
C8–H8C	0.9800
C9–H9A	0.9800
C9–H9B	0.9800
C9–H9C	0.9800
C8'–H8'1	0.9800
C8'–H8'2	0.9800
C8'–H8'3	0.9800
C9'–H9'1	0.9800
C9'–H9'2	0.9800
C9'–H9'3	0.9800
C10–H10A	0.9800
C10–H10B	0.9800
C10–H10C	0.9800
C11–C12	1.517(5)
C11–H11A	0.9900
C11–H11B	0.9900
C12–C17	1.394(5)
C12–C13	1.399(5)
C13–C14	1.397(5)
C13–O1	1.403(4)

C14–C15	1.402(6)
C14–C22	1.518(5)
C15–C16	1.387(6)
C15–H15	0.9500
C16–C17	1.390(5)
C16–C18	1.539(6)
C17–H17	0.9500
C18–C19	1.525(6)
C18–C21	1.537(6)
C18–C20	1.554(6)
C19–H19A	0.9800
C19–H19B	0.9800
C19–H19C	0.9800
C20–H20A	0.9800
C20–H20B	0.9800
C20–H20C	0.9800
C21–H21A	0.9800
C21–H21B	0.9800
C21–H21C	0.9800
C22–C23	1.519(5)
C22–H22A	0.9900
C22–H22B	0.9900
C23–C28	1.403(5)
C23–C24	1.411(5)
C24–C25	1.387(5)
C24–H24	0.9500
C25–C26	1.377(6)
C25–C29	1.549(6)
C26–C27	1.392(5)
C26–H26	0.9500
C27–C28	1.392(5)
C27–C33	1.523(5)
C28–O7	1.392(4)
C29–C30	1.473(7)
C29–C32	1.501(7)
C29–C31	1.537(7)
C30–H30A	0.9800
C30–H30B	0.9800
C30–H30C	0.9800
C31–H31A	0.9800
C31–H31B	0.9800
C31–H31C	0.9800
C32–H32A	0.9800
C32–H32B	0.9800
C32–H32C	0.9800
C33–C35	1.515(5)
C33–H33A	0.9900
C33–H33B	0.9900
C34–C39	1.512(5)
C34–H34A	0.9900
C34–H34B	0.9900



C35–C36	1.392(5)
C35–C40	1.395(5)
C36–C37	1.389(5)
C36–H36	0.9500
C37–C38	1.382(6)
C37–C41	1.546(6)
C38–C39	1.398(6)
C38–H38	0.9500
C39–C40	1.400(5)
C40–O3	1.409(4)
C41–C43	1.505(6)
C41–C42	1.543(7)
C41–C44	1.549(6)
C42–H42A	0.9800
C42–H42B	0.9800
C42–H42C	0.9800
C43–H43A	0.9800
C43–H43B	0.9800
C43–H43C	0.9800
C44–H44A	0.9800
C44–H44B	0.9800
C44–H44C	0.9800
C45–O1	1.450(4)
C45–C46	1.492(6)
C45–H45A	0.9900
C45–H45B	0.9900
C46–O2	1.423(5)
C46–H46A	0.9900
C46–H46B	0.9900
C47–O2	1.419(5)
C47–H47A	0.9800
C47–H47B	0.9800
C47–H47C	0.9800
C48–O3	1.451(4)
C48–C49	1.491(5)
C48–H48A	0.9900
C48–H48B	0.9900
C49–O4	1.419(5)
C49–H49A	0.9900
C49–H49B	0.9900
C50–O4	1.425(5)
C50–H50A	0.9800
C50–H50B	0.9800
C50–H50C	0.9800
C51–O5	1.427(4)
C51–C52	1.505(5)
C51–H51A	0.9900
C51–H51B	0.9900
C52–O6	1.251(4)
C52–N1	1.320(5)
C53–N1	1.477(5)

C53-C54	1.518(5)
C53-H53A	0.9900
C53-H53B	0.9900
C54-C55	1.519(6)
C54-H54A	0.9900
C54-H54B	0.9900
C55-N2	1.471(5)
C55-H55A	0.9900
C55-H55B	0.9900
C56-N3	1.339(5)
C56-N2	1.349(5)
C56-S1	1.679(4)
C57-N3	1.449(5)
C57-C69	1.520(6)
C57-H57A	0.9900
C57-H57B	0.9900
C58-O7	1.427(4)
C58-C59	1.521(5)
C58-H58A	0.9900
C58-H58B	0.9900
C59-O8	1.238(4)
C59-N4	1.311(5)
C60-N4	1.465(5)
C60-C61	1.500(5)
C60-H60A	0.9900
C60-H60B	0.9900
C61-C62	1.515(6)
C61-H61A	0.9900
C61-H61B	0.9900
C62-N5	1.462(5)
C62-H62A	0.9900
C62-H62B	0.9900
C63-N5	1.340(5)
C63-N6	1.358(5)
C63-S2	1.682(4)
C64-N6	1.455(5)
C64-C65	1.493(6)
C64-H64A	0.9900
C64-H64B	0.9900
C65-C70	1.388(5)
C65-C66	1.399(6)
C66-C67	1.390(6)
C66-H66	0.9500
C67-C68	1.373(6)
C67-H67	0.9500
C68-C69	1.382(6)
C68-H68	0.9500
C69-C70	1.386(6)
C70-H70	0.9500
N1-H1	0.8800
N2-H2	0.8800

N3-H3A	0.8800
N4-H4	0.8800
N5-H5A	0.8800
N6-H6	0.8800

O9-C71-H71A	109.5
O9-C71-H71B	109.5
H71A-C71-H71B	109.5
O9-C71-H71C	109.5
H71A-C71-H71C	109.5
H71B-C71-H71C	109.5
O10-C72-H72A	109.5
O10-C72-H72B	109.5
H72A-C72-H72B	109.5
O10-C72-H72C	109.5
H72A-C72-H72C	109.5
H72B-C72-H72C	109.5
C71-O9-H9	109.5
C72-O10-H10	109.5
C6-C1-C2	122.2(3)
C6-C1-O5	121.8(3)
C2-C1-O5	116.0(3)
C3-C2-C1	117.5(4)
C3-C2-C11	120.1(3)
C1-C2-C11	122.1(3)
C4-C3-C2	122.7(4)
C4-C3-H3	118.7
C2-C3-H3	118.7
C3-C4-C5	117.1(3)
C3-C4-C7	121.3(3)
C5-C4-C7	121.6(3)
C4-C5-C6	122.8(4)
C4-C5-H5	118.6
C6-C5-H5	118.6
C1-C6-C5	117.5(3)
C1-C6-C34	123.4(3)
C5-C6-C34	118.6(3)
C8-C7-C9'	69.1(9)
C8-C7-C10	115.8(7)
C9'-C7-C10	127.2(6)
C8-C7-C4	119.2(5)
C9'-C7-C4	107.8(5)
C10-C7-C4	112.0(4)
C8-C7-C9	108.0(8)
C9'-C7-C9	44.8(6)
C10-C7-C9	90.4(6)
C4-C7-C9	106.8(4)
C8-C7-C8'	34.8(8)
C9'-C7-C8'	103.5(8)
C10-C7-C8'	99.2(7)
C4-C7-C8'	103.9(5)

C9-C7-C8'	141.4(7)
C7-C8-H8A	109.4
C7-C8-H8B	109.5
C7-C8-H8C	109.5
C7-C9-H9A	109.5
C7-C9-H9B	109.5
C7-C9-H9C	109.5
C7-C8'-H8'1	109.5
C7-C8'-H8'2	109.5
H8'1-C8'-H8'2	109.5
C7-C8'-H8'3	109.5
H8'1-C8'-H8'3	109.5
H8'2-C8'-H8'3	109.5
C7-C9'-H9'1	109.5
C7-C9'-H9'2	109.5
H9'1-C9'-H9'2	109.5
C7-C9'-H9'3	109.5
H9'1-C9'-H9'3	109.5
H9'2-C9'-H9'3	109.5
C7-C10-H10A	109.5
C7-C10-H10B	109.5
H10A-C10-H10B	109.5
C7-C10-H10C	109.5
H10A-C10-H10C	109.5
H10B-C10-H10C	109.5
C2-C11-C12	109.0(3)
C2-C11-H11A	109.9
C12-C11-H11A	109.9
C2-C11-H11B	109.9
C12-C11-H11B	109.9
H11A-C11-H11B	108.3
C17-C12-C13	117.8(3)
C17-C12-C11	118.3(3)
C13-C12-C11	123.8(3)
C14-C13-C12	120.9(3)
C14-C13-O1	120.0(3)
C12-C13-O1	119.1(3)
C13-C14-C15	118.5(4)
C13-C14-C22	122.8(4)
C15-C14-C22	118.6(3)
C16-C15-C14	122.1(4)
C16-C15-H15	119.0
C14-C15-H15	119.0
C15-C16-C17	117.2(4)
C15-C16-C18	122.9(4)
C17-C16-C18	119.9(4)
C16-C17-C12	123.1(4)
C16-C17-H17	118.5
C12-C17-H17	118.5
C19-C18-C21	108.9(3)
C19-C18-C16	111.4(3)

C21-C18-C16	111.5(4)
C19-C18-C20	109.1(4)
C21-C18-C20	107.8(4)
C16-C18-C20	108.0(3)
C18-C19-H19A	109.5
C18-C19-H19B	109.5
H19A-C19-H19B	109.5
C18-C19-H19C	109.5
H19A-C19-H19C	109.5
H19B-C19-H19C	109.5
C18-C20-H20A	109.5
C18-C20-H20B	109.5
H20A-C20-H20B	109.5
C18-C20-H20C	109.5
H20A-C20-H20C	109.5
H20B-C20-H20C	109.5
C18-C21-H21A	109.5
C18-C21-H21B	109.5
H21A-C21-H21B	109.5
C18-C21-H21C	109.5
H21A-C21-H21C	109.5
H21B-C21-H21C	109.5
C14-C22-C23	111.6(3)
C14-C22-H22A	109.3
C23-C22-H22A	109.3
C14-C22-H22B	109.3
C23-C22-H22B	109.3
H22A-C22-H22B	108.0
C28-C23-C24	116.9(3)
C28-C23-C22	123.9(3)
C24-C23-C22	118.9(3)
C25-C24-C23	123.2(4)
C25-C24-H24	118.4
C23-C24-H24	118.4
C26-C25-C24	117.0(4)
C26-C25-C29	122.3(4)
C24-C25-C29	120.8(4)
C25-C26-C27	123.0(4)
C25-C26-H26	118.5
C27-C26-H26	118.5
C26-C27-C28	118.5(3)
C26-C27-C33	121.2(3)
C28-C27-C33	119.8(3)
O7-C28-C27	117.7(3)
O7-C28-C23	121.0(3)
C27-C28-C23	121.2(3)
C30-C29-C32	110.0(5)
C30-C29-C31	109.6(6)
C32-C29-C31	105.5(6)
C30-C29-C25	112.6(4)
C32-C29-C25	111.6(4)

C31-C29-C25	107.3(3)
C29-C30-H30A	109.5
C29-C30-H30B	109.5
H30A-C30-H30B	109.5
C29-C30-H30C	109.5
H30A-C30-H30C	109.5
H30B-C30-H30C	109.5
C29-C31-H31A	109.5
C29-C31-H31B	109.5
H31A-C31-H31B	109.5
C29-C31-H31C	109.5
H31A-C31-H31C	109.5
H31B-C31-H31C	109.5
C29-C32-H32A	109.5
C29-C32-H32B	109.5
H32A-C32-H32B	109.5
C29-C32-H32C	109.5
H32A-C32-H32C	109.5
H32B-C32-H32C	109.5
C35-C33-C27	108.5(3)
C35-C33-H33A	110.0
C27-C33-H33A	110.0
C35-C33-H33B	110.0
C27-C33-H33B	110.0
H33A-C33-H33B	108.4
C39-C34-C6	109.3(3)
C39-C34-H34A	109.8
C6-C34-H34A	109.8
C39-C34-H34B	109.8
C6-C34-H34B	109.8
H34A-C34-H34B	108.3
C36-C35-C40	117.7(3)
C36-C35-C33	117.7(3)
C40-C35-C33	124.2(3)
C37-C36-C35	122.7(4)
C37-C36-H36	118.6
C35-C36-H36	118.6
C38-C37-C36	117.4(4)
C38-C37-C41	123.4(4)
C36-C37-C41	119.2(4)
C37-C38-C39	123.0(4)
C37-C38-H38	118.5
C39-C38-H38	118.5
C38-C39-C40	117.3(4)
C38-C39-C34	118.9(3)
C40-C39-C34	123.7(4)
C35-C40-C39	121.8(3)
C35-C40-O3	118.8(3)
C39-C40-O3	119.4(3)
C43-C41-C42	110.3(4)
C43-C41-C37	108.7(4)

C42-C41-C37	108.4(4)
C43-C41-C44	110.6(4)
C42-C41-C44	107.5(4)
C37-C41-C44	111.4(3)
C41-C42-H42A	109.5
C41-C42-H42B	109.5
H42A-C42-H42B	109.5
C41-C42-H42C	109.5
H42A-C42-H42C	109.5
H42B-C42-H42C	109.5
C41-C43-H43A	109.5
C41-C43-H43B	109.5
H43A-C43-H43B	109.5
C41-C43-H43C	109.5
H43A-C43-H43C	109.5
H43B-C43-H43C	109.5
C41-C44-H44A	109.5
C41-C44-H44B	109.5
H44A-C44-H44B	109.5
C41-C44-H44C	109.5
H44A-C44-H44C	109.5
H44B-C44-H44C	109.5
O1-C45-C46	114.6(3)
O1-C45-H45A	108.6
C46-C45-H45A	108.6
O1-C45-H45B	108.6
C46-C45-H45B	108.6
H45A-C45-H45B	107.6
O2-C46-C45	109.7(3)
O2-C46-H46A	109.7
C45-C46-H46A	109.7
O2-C46-H46B	109.7
C45-C46-H46B	109.7
H46A-C46-H46B	108.2
O2-C47-H47A	109.5
O2-C47-H47B	109.5
H47A-C47-H47B	109.5
O2-C47-H47C	109.5
H47A-C47-H47C	109.5
H47B-C47-H47C	109.5
O3-C48-C49	114.4(3)
O3-C48-H48A	108.7
C49-C48-H48A	108.7
O3-C48-H48B	108.7
C49-C48-H48B	108.7
H48A-C48-H48B	107.6
O4-C49-C48	109.4(3)
O4-C49-H49A	109.8
C48-C49-H49A	109.8
O4-C49-H49B	109.8
C48-C49-H49B	109.8

H49A-C49-H49B	108.2
O4-C50-H50A	109.5
O4-C50-H50B	109.5
H50A-C50-H50B	109.5
O4-C50-H50C	109.5
H50A-C50-H50C	109.5
H50B-C50-H50C	109.5
O5-C51-C52	113.3(3)
O5-C51-H51A	108.9
C52-C51-H51A	108.9
O5-C51-H51B	108.9
C52-C51-H51B	108.9
H51A-C51-H51B	107.7
O6-C52-N1	124.3(4)
O6-C52-C51	117.0(3)
N1-C52-C51	118.6(3)
N1-C53-C54	115.5(3)
N1-C53-H53A	108.4
C54-C53-H53A	108.4
N1-C53-H53B	108.4
C54-C53-H53B	108.4
H53A-C53-H53B	107.5
C53-C54-C55	114.0(3)
C53-C54-H54A	108.7
C55-C54-H54A	108.7
C53-C54-H54B	108.7
C55-C54-H54B	108.7
H54A-C54-H54B	107.6
N2-C55-C54	114.0(3)
N2-C55-H55A	108.7
C54-C55-H55A	108.7
N2-C55-H55B	108.7
C54-C55-H55B	108.7
H55A-C55-H55B	107.6
N3-C56-N2	115.1(3)
N3-C56-S1	122.3(3)
N2-C56-S1	122.6(3)
N3-C57-C69	115.5(3)
N3-C57-H57A	108.4
C69-C57-H57A	108.4
N3-C57-H57B	108.4
C69-C57-H57B	108.4
H57A-C57-H57B	107.5
O7-C58-C59	113.6(3)
O7-C58-H58A	108.8
C59-C58-H58A	108.8
O7-C58-H58B	108.8
C59-C58-H58B	108.8
H58A-C58-H58B	107.7
O8-C59-N4	124.8(3)
O8-C59-C58	116.7(3)



N4-C59-C58	118.5(3)
N4-C60-C61	116.1(3)
N4-C60-H60A	108.3
C61-C60-H60A	108.3
N4-C60-H60B	108.3
C61-C60-H60B	108.3
H60A-C60-H60B	107.4
C60-C61-C62	114.8(3)
C60-C61-H61A	108.6
C62-C61-H61A	108.6
C60-C61-H61B	108.6
C62-C61-H61B	108.6
H61A-C61-H61B	107.5
N5-C62-C61	114.3(3)
N5-C62-H62A	108.7
C61-C62-H62A	108.7
N5-C62-H62B	108.7
C61-C62-H62B	108.7
H62A-C62-H62B	107.6
N5-C63-N6	114.2(4)
N5-C63-S2	122.8(3)
N6-C63-S2	122.9(3)
N6-C64-C65	116.0(3)
N6-C64-H64A	108.3
C65-C64-H64A	108.3
N6-C64-H64B	108.3
C65-C64-H64B	108.3
H64A-C64-H64B	107.4
C70-C65-C66	118.7(4)
C70-C65-C64	123.7(4)
C66-C65-C64	117.6(4)
C67-C66-C65	120.2(4)
C67-C66-H66	119.9
C65-C66-H66	119.9
C68-C67-C66	119.6(4)
C68-C67-H67	120.2
C66-C67-H67	120.2
C67-C68-C69	121.2(4)
C67-C68-H68	119.4
C69-C68-H68	119.4
C68-C69-C70	119.0(4)
C68-C69-C57	118.3(4)
C70-C69-C57	122.7(4)
C69-C70-C65	121.1(3)
C69-C70-H70	119.4
C65-C70-H70	119.4
C52-N1-C53	122.0(3)
C52-N1-H1	119.0
C53-N1-H1	119.0
C56-N2-C55	124.8(3)
C56-N2-H2	117.6

C55–N2–H2	117.6
C56–N3–C57	124.0(4)
C56–N3–H3A	118.0
C57–N3–H3A	118.0
C59–N4–C60	121.7(3)
C59–N4–H4	119.1
C60–N4–H4	119.1
C63–N5–C62	124.4(3)
C63–N5–H5A	117.8
C62–N5–H5A	117.8
C63–N6–C64	124.0(4)
C63–N6–H6	118.0
C64–N6–H6	118.0
C13–O1–C45	112.5(3)
C47–O2–C46	112.8(4)
C40–O3–C48	113.4(3)
C49–O4–C50	111.9(4)
C1–O5–C51	113.9(3)
C28–O7–C58	113.9(3)

---

Symmetry transformations used to generate equivalent atoms:

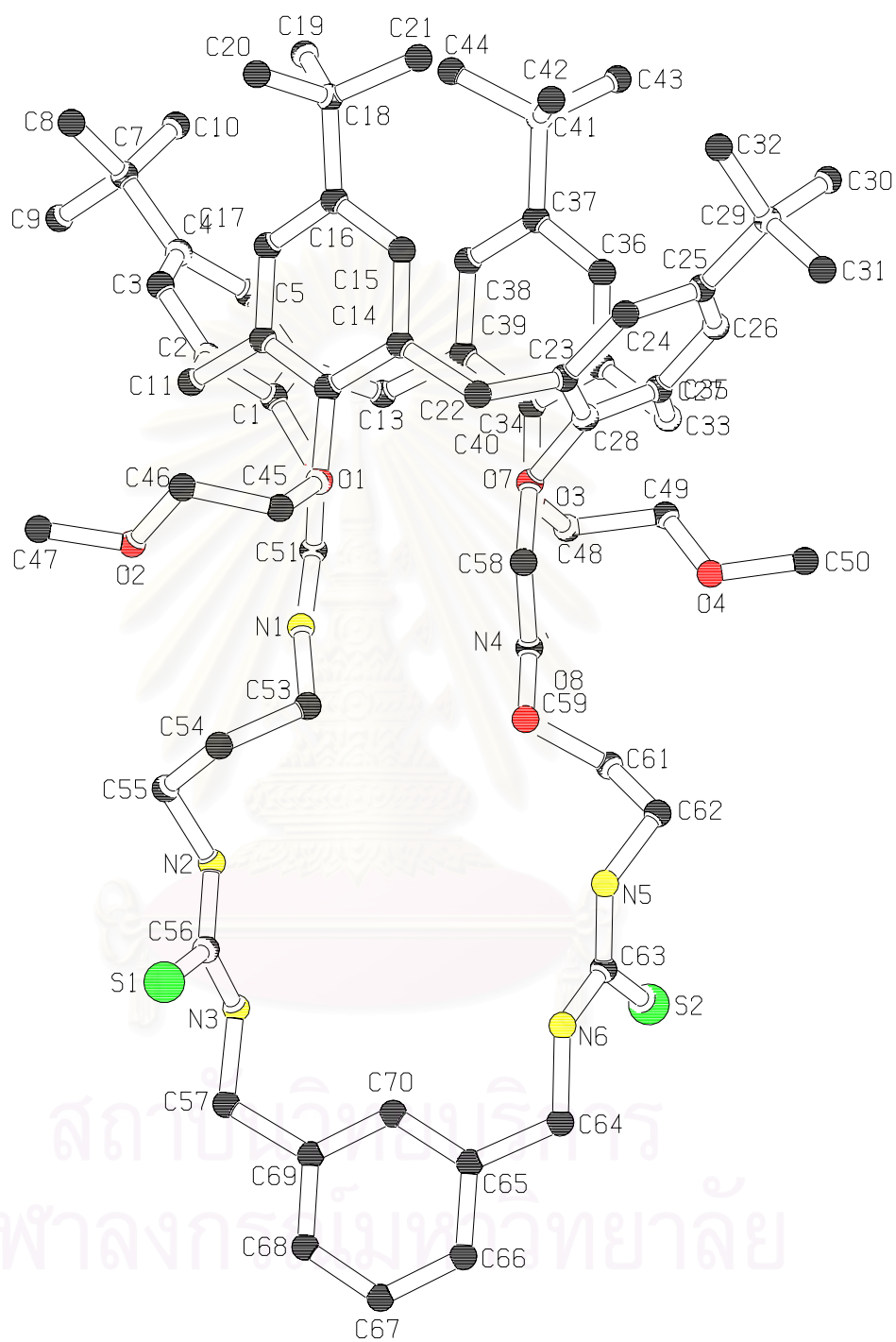


สถาบันวิทยบริการ  
จุฬาลงกรณ์มหาวิทยาลัย

**Table 4.** Anisotropic displacement parameters [ $\text{\AA}^2 \times 10^3$ ]. The anisotropic displacement factor exponent takes the form:  $-2\pi^2[h^2a^{*2}U^{11} + \dots + 2hk a^* b^* U^{12}]$ .

Atom	$U^{11}$	$U^{22}$	$U^{33}$	$U^{23}$	$U^{13}$	$U^{12}$
C71	66(3)	59(3)	37(3)	-1(2)	-4(2)	-1(3)
C72	66(3)	47(3)	38(3)	-4(2)	3(2)	6(2)
O9	50(2)	53(2)	30(2)	0(1)	-2(2)	1(2)
O10	57(2)	63(2)	31(2)	-1(1)	0(2)	6(2)
C1	26(2)	36(2)	27(2)	7(2)	-2(2)	0(2)
C2	27(2)	33(2)	28(2)	5(2)	-5(2)	2(2)
C3	33(2)	30(2)	33(2)	2(2)	-6(2)	0(2)
C4	29(2)	36(2)	31(2)	7(2)	-4(2)	-4(2)
C5	37(2)	41(3)	27(2)	2(2)	4(2)	-3(2)
C6	32(2)	37(2)	29(2)	3(2)	-2(2)	-5(2)
C7	34(2)	35(3)	50(3)	2(2)	10(2)	-3(2)
C8	74(9)	118(12)	18(6)	-7(6)	7(5)	-63(9)
C9	47(6)	70(7)	45(6)	42(5)	-4(5)	-15(5)
C8'	38(7)	139(14)	49(8)	3(7)	-5(5)	-51(8)
C9'	52(6)	69(8)	68(7)	36(6)	18(6)	2(5)
C10	88(4)	87(5)	103(5)	-22(4)	58(4)	-43(4)
C11	39(2)	33(2)	30(2)	0(2)	-1(2)	-1(2)
C12	34(2)	29(2)	32(2)	-5(2)	-6(2)	-2(2)
C13	32(2)	36(2)	24(2)	-2(2)	-5(2)	-2(2)
C14	36(2)	35(2)	22(2)	-3(2)	-3(2)	2(2)
C15	47(3)	34(2)	31(2)	0(2)	-9(2)	4(2)
C16	39(2)	40(2)	40(2)	-7(2)	-8(2)	4(2)
C17	39(2)	37(2)	36(2)	5(2)	-2(2)	-5(2)
C18	42(2)	49(3)	45(2)	0(2)	-4(2)	8(2)
C19	48(3)	54(3)	65(3)	7(2)	2(2)	2(2)
C20	52(3)	53(3)	68(3)	2(2)	-23(2)	-6(2)
C21	45(3)	54(3)	62(3)	1(2)	-9(2)	9(2)
C22	39(2)	42(3)	22(2)	0(2)	-3(2)	9(2)
C23	28(2)	38(2)	24(2)	5(2)	4(2)	4(2)
C24	30(2)	40(2)	28(2)	5(2)	3(2)	-1(2)
C25	29(2)	37(2)	33(2)	3(2)	-1(2)	1(2)
C26	35(2)	32(2)	32(2)	4(2)	6(2)	2(2)
C27	29(2)	25(2)	32(2)	2(2)	3(2)	-3(2)
C28	28(2)	32(2)	25(2)	9(2)	1(2)	3(2)
C29	33(2)	43(3)	38(2)	2(2)	-4(2)	5(2)
C30	147(6)	182(8)	99(5)	-74(5)	-72(5)	142(6)
C31	61(4)	192(8)	131(6)	113(6)	9(4)	43(5)
C32	88(5)	90(5)	168(7)	-16(5)	-86(5)	26(4)
C33	30(2)	31(2)	32(2)	1(2)	-1(2)	0(2)
C34	35(2)	37(3)	30(2)	1(2)	4(2)	-8(2)
C35	30(2)	32(2)	24(2)	-2(2)	2(2)	-1(2)
C36	37(2)	39(2)	33(2)	-6(2)	5(2)	1(2)
C37	30(2)	43(2)	36(2)	-1(2)	8(2)	-4(2)
C38	40(3)	42(3)	35(2)	-1(2)	7(2)	-4(2)
C39	39(3)	31(2)	28(2)	0(2)	6(2)	-4(2)
C40	31(2)	34(2)	27(2)	-7(2)	1(2)	2(2)
C41	38(2)	56(3)	48(3)	8(2)	5(2)	0(2)

C42	54(3)	129(5)	60(3)	10(3)	-11(3)	-34(3)
C43	42(3)	54(3)	99(4)	23(3)	21(3)	2(2)
C44	37(3)	56(3)	77(3)	-1(3)	6(2)	-11(2)
C45	48(3)	44(3)	25(2)	-6(2)	2(2)	7(2)
C46	47(3)	47(3)	35(2)	-6(2)	-4(2)	3(2)
C47	105(5)	45(3)	76(4)	9(3)	5(3)	12(3)
C48	37(2)	42(3)	27(2)	-5(2)	-1(2)	-6(2)
C49	43(2)	46(3)	35(2)	-16(2)	-2(2)	3(2)
C50	109(4)	32(3)	73(4)	1(2)	-31(3)	-4(3)
C51	32(2)	50(3)	33(2)	1(2)	-1(2)	-6(2)
C52	37(2)	35(2)	33(2)	5(2)	-4(2)	-3(2)
C53	28(2)	46(3)	35(2)	4(2)	4(2)	6(2)
C54	37(2)	47(3)	45(3)	-8(2)	1(2)	0(2)
C55	45(3)	33(2)	45(3)	0(2)	-4(2)	3(2)
C56	39(2)	39(2)	31(2)	9(2)	2(2)	11(2)
C57	43(3)	42(3)	56(3)	4(2)	-10(2)	4(2)
C58	29(2)	42(2)	26(2)	-2(2)	2(2)	4(2)
C59	31(2)	31(2)	27(2)	5(2)	2(2)	1(2)
C60	32(2)	43(2)	29(2)	-2(2)	0(2)	0(2)
C61	34(2)	50(3)	39(2)	-10(2)	-1(2)	1(2)
C62	38(2)	33(2)	49(3)	-3(2)	-6(2)	0(2)
C63	44(3)	29(2)	36(2)	8(2)	-3(2)	-4(2)
C64	40(3)	44(3)	77(3)	7(2)	6(2)	-3(2)
C65	37(2)	37(2)	33(2)	-5(2)	4(2)	-2(2)
C66	41(3)	62(3)	31(2)	-6(2)	2(2)	-12(2)
C67	29(2)	78(3)	39(2)	-3(2)	2(2)	5(2)
C68	38(3)	55(3)	38(2)	0(2)	-8(2)	10(2)
C69	39(2)	49(3)	27(2)	-7(2)	-4(2)	-2(2)
C70	31(2)	43(2)	38(2)	-2(2)	1(2)	-1(2)
N1	30(2)	43(2)	33(2)	4(2)	-4(2)	0(2)
N2	40(2)	35(2)	35(2)	0(1)	-2(2)	5(2)
N3	43(2)	34(2)	41(2)	-1(2)	-1(2)	-3(2)
N4	28(2)	40(2)	28(2)	-1(1)	-2(1)	0(2)
N5	43(2)	31(2)	34(2)	0(1)	-1(2)	-2(2)
N6	40(2)	38(2)	48(2)	-5(2)	0(2)	1(2)
O1	30(2)	38(2)	28(1)	-2(1)	-1(1)	1(1)
O2	53(2)	40(2)	48(2)	2(1)	-5(2)	4(1)
O3	30(2)	34(2)	29(1)	-1(1)	-1(1)	-1(1)
O4	64(2)	34(2)	41(2)	-3(1)	-4(2)	-2(1)
O5	29(1)	45(2)	25(1)	6(1)	-3(1)	-5(1)
O6	27(2)	49(2)	38(2)	-1(1)	-10(1)	1(1)
O7	22(1)	40(2)	31(2)	6(1)	1(1)	5(1)
O8	32(2)	44(2)	32(2)	-1(1)	-1(1)	5(1)
S1	54(1)	54(1)	44(1)	-8(1)	-1(1)	15(1)
S2	53(1)	48(1)	52(1)	-9(1)	-9(1)	-11(1)





**APPENDIX B**

สถาบันวิทยบริการ  
จุฬาลงกรณ์มหาวิทยาลัย

a) NMR titration data for lithium with receptor **14** in CD<sub>3</sub>CN

Solvent:	CD <sub>3</sub> CN
Starting volume of host solution:	600μL
Concentration of host solution:	1.87 mM
Concentration of guest solution:	18.7 mM
Association constant:	9.14x10 <sup>2</sup> M <sup>-1</sup> (ave)

Volume added /μL	Integration signal of –ArCH <sub>2</sub> Ar- and –OCH <sub>2</sub> CONH-/mm	
	Unbound receptor	Bound receptor
0	1.80	0.00
5	1.95	0.00
10	2.00	0.40
20	1.75	0.50
30	1.55	0.45
40	1.40	0.70
50	1.40	0.80
60	1.15	0.85
70	1.10	1.15
80	0.85	1.25
90	0.90	1.30
100	0.60	1.30
120	0.60	1.60
<b><i>K<sub>I</sub></i></b>	<b>9.14x10<sup>2</sup></b>	

สถาบันวิทยบริการ  
จุฬาลงกรณ์มหาวิทยาลัย

b) NMR titration data for sodium with receptor **14** in CD<sub>3</sub>CN

Solvent:	CD <sub>3</sub> CN
Starting volume of host solution:	600μL
Concentration of host solution:	1.87 mM
Concentration of guest solution:	18.7 mM
Association constant:	5.53x10 <sup>3</sup> M <sup>-1</sup> (ave)

Volume added /μL	Integration signal of –ArCH <sub>2</sub> Ar- and –OCH <sub>2</sub> CONH-/mm	
	Unbound receptor	Bound receptor
0	2.05	0.00
5	2.10	0.55
10	2.15	0.80
20	1.70	0.65
30	1.30	0.90
40	1.05	1.20
50	0.75	1.65
60	0.40	1.85
<b>K<sub>I</sub></b>	<b>5.53x10<sup>3</sup></b>	

สถาบันวิทยบริการ  
จุฬาลงกรณ์มหาวิทยาลัย



c) NMR titration data for potassium with receptor **14** in CD<sub>3</sub>CN

Solvent:	CD <sub>3</sub> CN
Starting volume of host solution:	600 μL
Concentration of host solution:	1.87 mM
Concentration of guest solution:	18.7 mM
Association constant:	6.17 × 10 <sup>2</sup> M <sup>-1</sup> (ave)

Volume added /μL	Integration signal of –ArCH <sub>2</sub> Ar- and –OCH <sub>2</sub> CONH-/mm	
	Unbound receptor	Bound receptor
0	2.10	0.00
5	1.95	0.00
10	2.20	0.45
20	1.95	0.50
30	1.80	0.65
40	1.55	0.80
50	1.65	1.15
60	1.50	1.10
70	1.10	1.10
80	1.00	1.15
90	1.00	1.45
100	1.00	1.45
120	1.00	1.35
140	0.60	1.55
160	0.60	1.90
180	0.60	1.50
<b><i>K<sub>I</sub></i></b>	<b>6.17 × 10<sup>2</sup></b>	

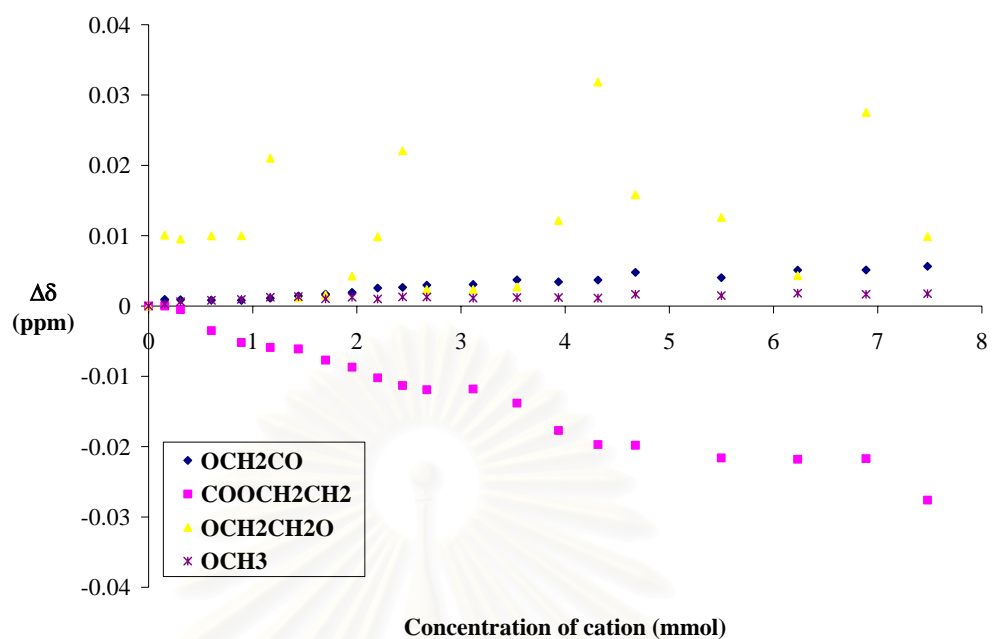
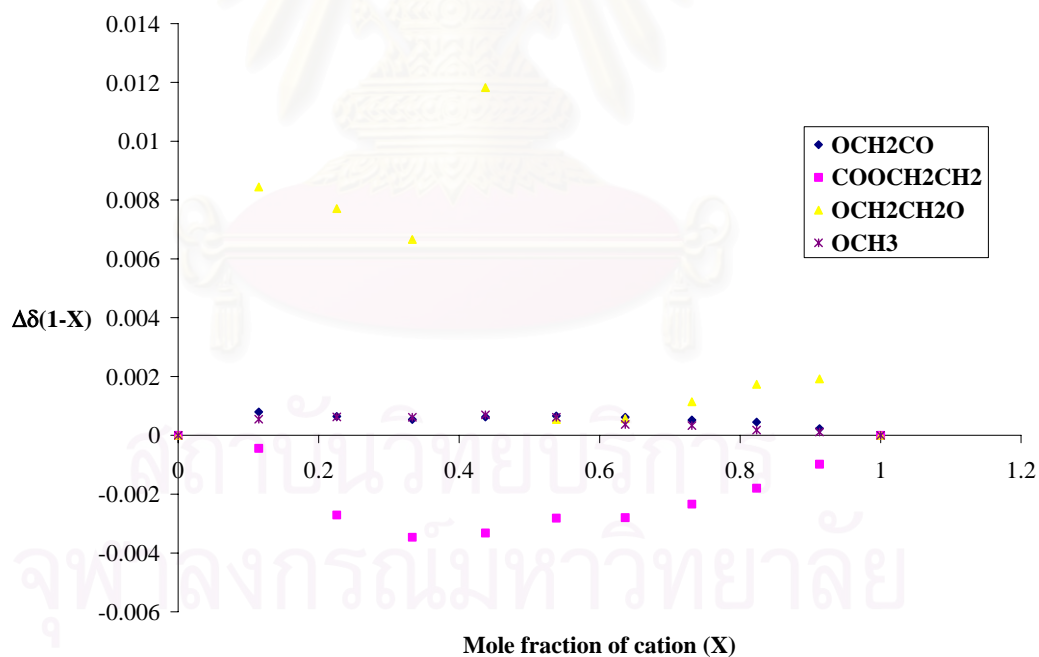
สถาบันวิทยบริการ  
จุฬาลงกรณ์มหาวิทยาลัย

d) NMR titration data for lithium with receptor **15** in CD<sub>3</sub>CN

Solvent:	CD <sub>3</sub> CN
Starting volume of host solution:	600 μL
Concentration of host solution:	1.87 mM
Concentration of guest solution:	18.7 mM
Association constant:	3.71x10 <sup>2</sup> M <sup>-1</sup> (ave)

Volume added	-OCH <sub>2</sub> COO-	-COOCH <sub>2</sub> -	-CH <sub>2</sub> CH <sub>2</sub> OCH <sub>3</sub>	-OCH <sub>3</sub>
/μL	/ppm	/ppm	/ppm	/ppm
0	4.5419	4.5077	4.0647	3.3173
5	4.5428	4.5077	4.0748	3.3176
10	4.5428	4.5072	4.0743	3.3180
20	4.5427	4.5042	4.0747	3.3182
30	4.5427	4.5025	4.0747	3.3183
40	4.5430	4.5018	4.0857	3.3186
50	4.5433	4.5016	4.0659	3.3187
60	4.5436	4.5000	4.0663	3.3184
70	4.5438	4.4990	4.0690	3.3186
80	4.5444	4.4975	4.0746	3.3183
90	4.5445	4.4964	4.0868	3.3186
100	4.5448	4.4958	4.0671	3.3186
120	4.5449	4.4959	4.0671	3.3185
140	4.5456	4.4939	4.0674	3.3185
160	4.5453	4.4900	4.0769	3.3186
180	4.5456	4.4880	4.0966	3.3185
200	4.5467	4.4879	4.0806	3.3190
250	4.5459	4.4861	4.0773	3.3188
300	4.5470	4.4859	4.0691	3.3192
350	4.5470	4.4860	4.0923	3.3190
400	4.5475	4.4801	4.0746	3.3191
<b>K<sub>I</sub></b>	<b>1.03x10<sup>1</sup></b>	<b>1.26x10<sup>2</sup></b>	-	<b>9.78x10<sup>2</sup></b>

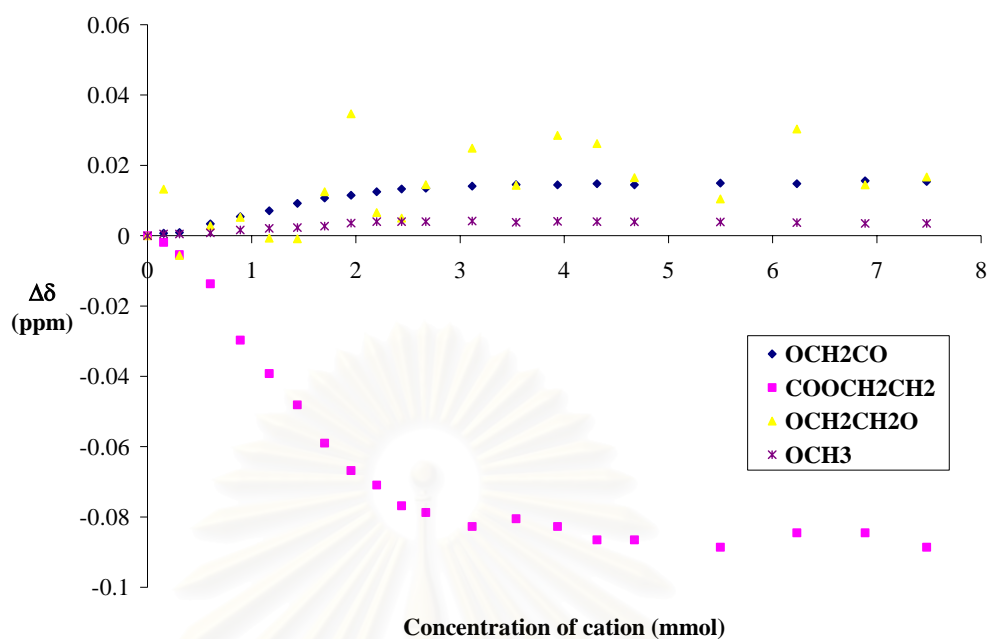
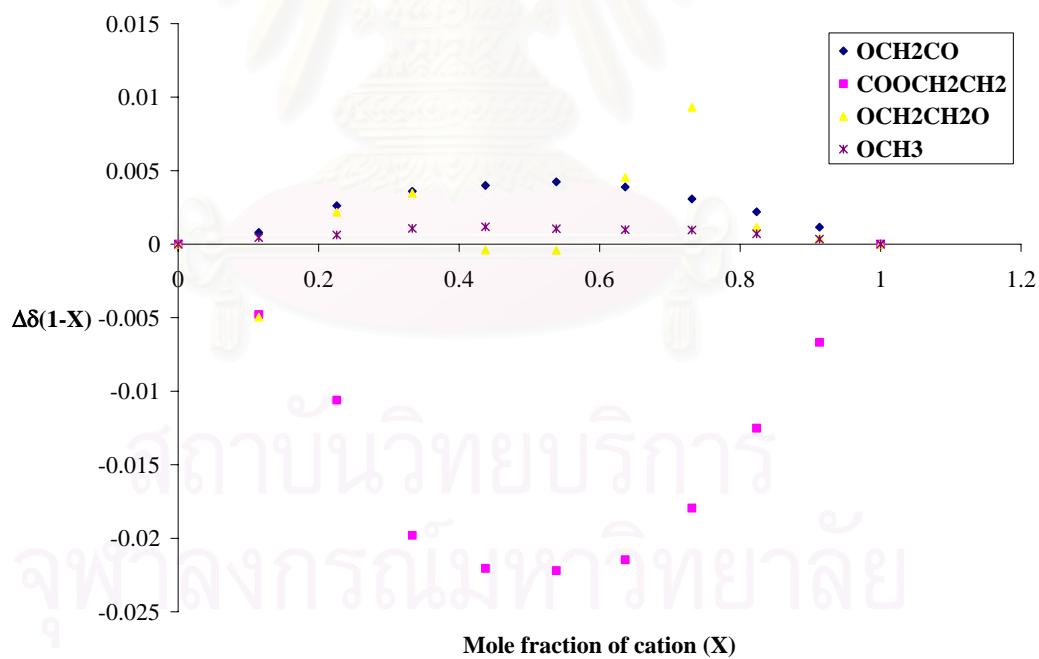
จุฬาลงกรณ์มหาวิทยาลัย

Titration curves for lithium with receptor **15** in  $\text{CD}_3\text{CN}$ Job's plots for lithium with receptor **15** in  $\text{CH}_3\text{CN}$ 

e) NMR titration data for sodium with receptor **15** in CD<sub>3</sub>CN

Solvent:	CD <sub>3</sub> CN
Starting volume of host solution:	600 μL
Concentration of host solution:	1.87 mM
Concentration of guest solution:	14.7 mM
Association constant:	1.55x10 <sup>4</sup> M <sup>-1</sup> (ave)

Volume added /μL	-OCH <sub>2</sub> CO- /ppm	-COOCH <sub>2</sub> - /ppm	-CH <sub>2</sub> CH <sub>2</sub> OCH <sub>3</sub> /ppm	-OCH <sub>3</sub> /ppm
0	4.5414	4.5076	4.0720	3.3172
5	4.5421	4.5057	4.0852	3.3177
10	4.5423	4.5022	4.0664	3.3177
20	4.5448	4.4939	4.0748	3.3180
30	4.5468	4.4779	4.0772	3.3188
40	4.5485	4.4684	4.0713	3.3193
50	4.5506	4.4595	4.0711	3.3195
60	4.5521	4.4486	4.0845	3.3199
70	4.5529	4.4408	4.1067	3.3208
80	4.5539	4.4367	4.0786	3.3212
90	4.5547	4.4308	4.0770	3.3212
100	4.5549	4.4289	4.0865	3.3212
120	4.5555	4.4249	4.0969	3.3214
140	4.5559	4.4271	4.0863	3.3210
160	4.5558	4.4249	4.1005	3.3213
180	4.5562	4.4211	4.0982	3.3212
200	4.5559	4.4211	4.0885	3.3212
250	4.5563	4.4190	4.0824	3.3211
300	4.5562	4.4231	4.1023	3.3209
350	4.5570	4.4231	4.0865	3.3207
400	4.5568	4.4190	4.0887	3.3207
<b>K<sub>I</sub></b>	<b>9.85x10<sup>3</sup></b>	<b>2.66x10<sup>4</sup></b>	-	<b>9.95x10<sup>3</sup></b>

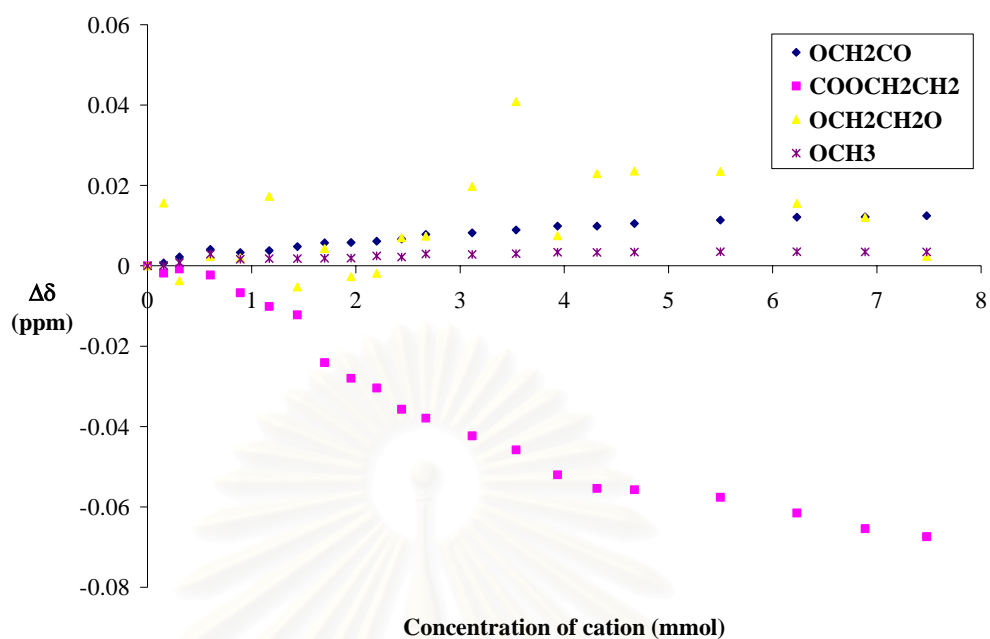
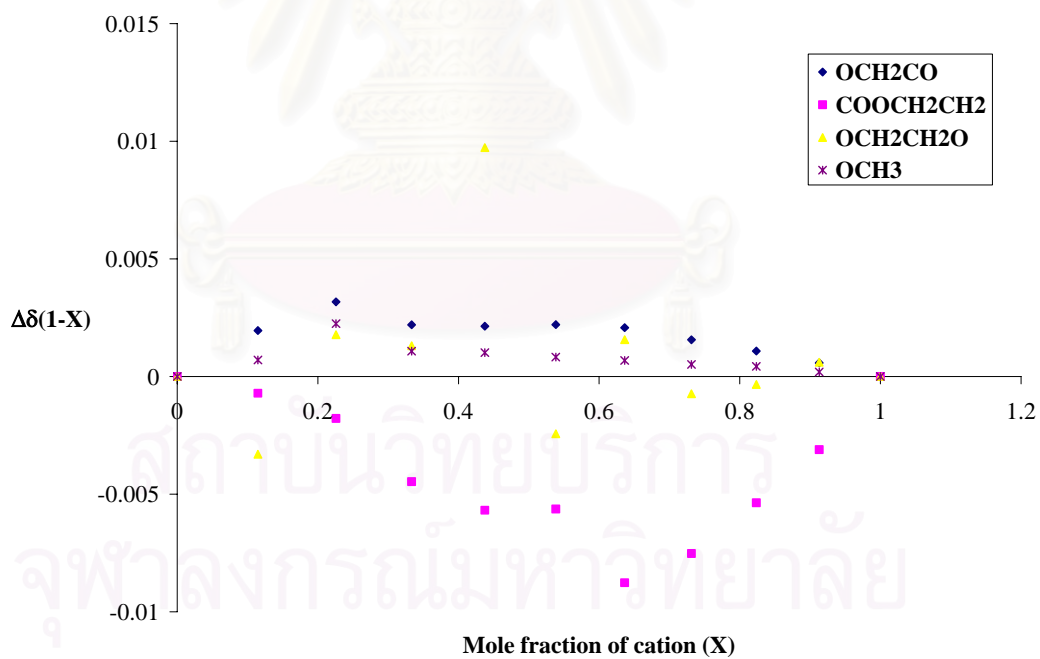
Titration curves for sodium with receptor **15** in CD<sub>3</sub>CNJob's plots for sodium with receptor **15** in CH<sub>3</sub>CN

f) NMR titration data for potassium with receptor **15** in CD<sub>3</sub>CN

Solvent:	CD <sub>3</sub> CN
Starting volume of host solution:	600 μL
Concentration of host solution:	1.87 mM
Concentration of guest solution:	18.7 mM
Association constant:	6.88x10 <sup>2</sup> M <sup>-1</sup> (ave)

Volume added /μL	-OCH <sub>2</sub> CO- /ppm	-COOCH <sub>2</sub> - /ppm	-CH <sub>2</sub> CH <sub>2</sub> OCH <sub>3</sub> /ppm	-OCH <sub>3</sub> /ppm
0	4.5411	4.5062	4.0730	3.3156
5	4.5418	4.5044	4.0886	3.3157
10	4.5433	4.5054	4.0693	3.3164
20	4.5452	4.5039	4.0753	3.3185
30	4.5444	4.4995	4.0750	3.3172
40	4.5449	4.4961	4.0903	3.3174
50	4.5459	4.4940	4.0677	3.3174
60	4.5468	4.4821	4.0773	3.3175
70	4.5469	4.4782	4.0703	3.3175
80	4.5472	4.4758	4.0711	3.3181
90	4.5478	4.4705	4.0800	3.3178
100	4.5489	4.4683	4.0803	3.3186
120	4.5493	4.4639	4.0928	3.3184
140	4.5500	4.4604	4.1139	3.3186
160	4.5510	4.4542	4.0805	3.3190
180	4.5510	4.4508	4.0959	3.3189
200	4.5516	4.4505	4.0966	3.3190
250	4.5525	4.4486	4.0965	3.3191
300	4.5532	4.4447	4.0885	3.3191
350	4.5533	4.4408	4.0850	3.3191
400	4.5536	4.4388	4.0754	3.3191
<b>K<sub>I</sub></b>	<b>5.01x10<sup>2</sup></b>	<b>8.74x10<sup>2</sup></b>	-	-

จุฬาลงกรณ์มหาวิทยาลัย

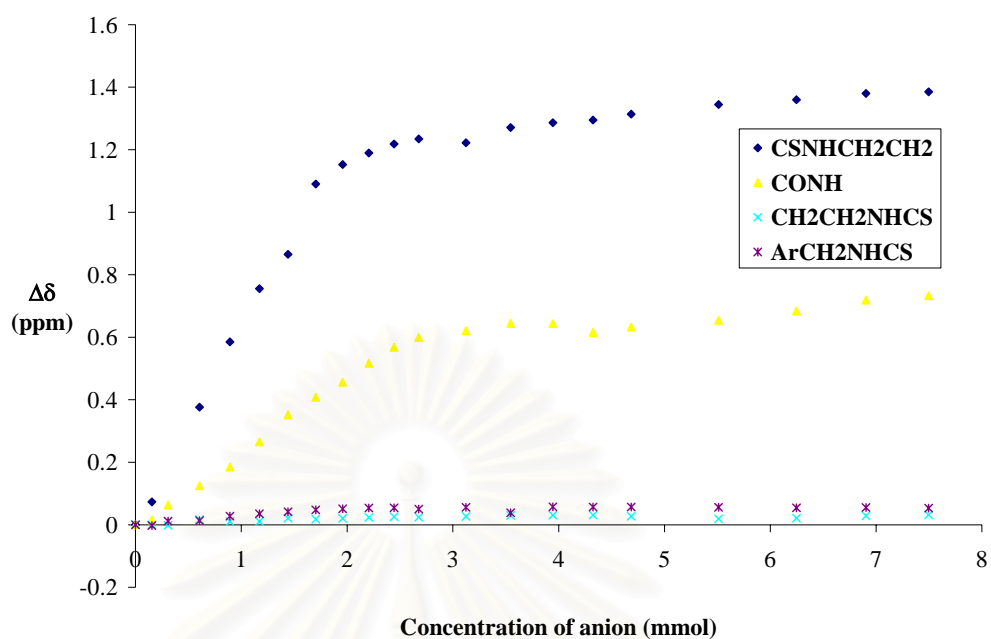
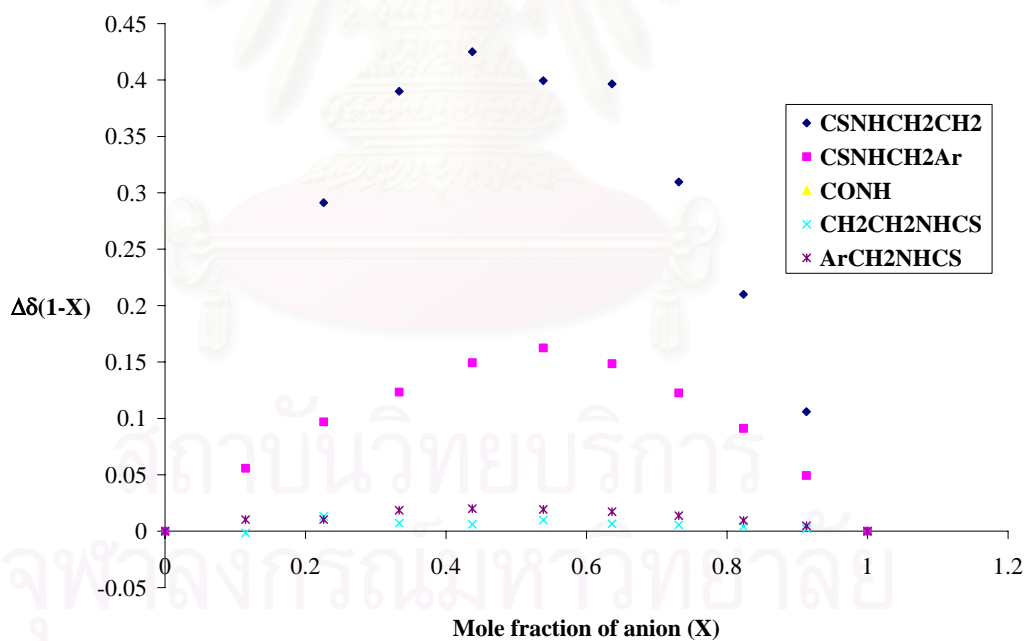
Titration curves for potassium with receptor **15** in  $\text{CD}_3\text{CN}$ Job's for potassium with receptor **15** in  $\text{CH}_3\text{CN}$ 

g) NMR titration data for acetate with receptor **14** in CD<sub>3</sub>CN

Solvent:	CD <sub>3</sub> CN
Starting volume of host solution:	600 μL
Concentration of host solution:	1.87 mM
Concentration of guest solution:	18.7 mM
Association constant:	3.04 × 10 <sup>4</sup> M <sup>-1</sup> (ave)

Volume added /μL	-NH <sup>b</sup> CH <sub>2</sub> - /ppm	-CONH <sup>c</sup> - /ppm	-CH <sub>2</sub> <sup>e</sup> NH- /ppm	-CH <sub>2</sub> <sup>d</sup> NH- /ppm
0	7.0188	7.5221	3.5344	4.6849
5	7.0923	7.5378	3.5344	4.6822
10	-	7.5851	3.5328	4.6966
20	7.3950	7.6473	3.5512	4.6982
30	7.6038	7.7070	3.5453	4.7127
40	7.7744	7.7876	3.5453	4.7205
50	7.8842	7.8741	3.5555	4.7268
60	8.1091	7.9304	3.5524	4.7326
70	8.1713	7.9785	3.5551	4.7361
80	8.2084	8.0387	3.5579	4.7389
90	8.2370	8.0899	3.5602	4.7393
100	8.2534	8.1216	3.5586	4.7353
120	8.2410	8.1431	3.5614	4.7412
140	8.2898	8.1666	3.5641	4.7232
160	8.3054	8.1658	3.5653	4.7424
180	8.3136	8.1380	3.5657	4.7420
200	8.3324	8.1545	3.5618	4.7420
250	8.3633	8.1764	3.5535	4.7412
300	8.3786	8.2061	3.5555	4.7393
350	8.3989	8.2409	3.5633	4.7401
400	8.4040	8.2550	3.5665	4.7381
<b>K<sub>I</sub></b>	<b>1.11 × 10<sup>4</sup></b>	-	-	<b>4.97 × 10<sup>4</sup></b>



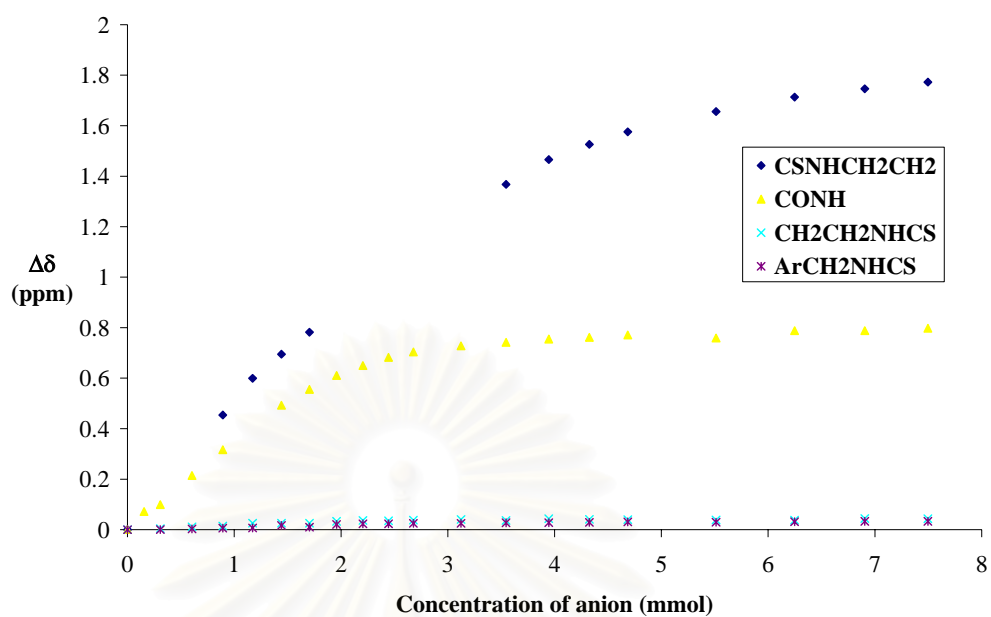
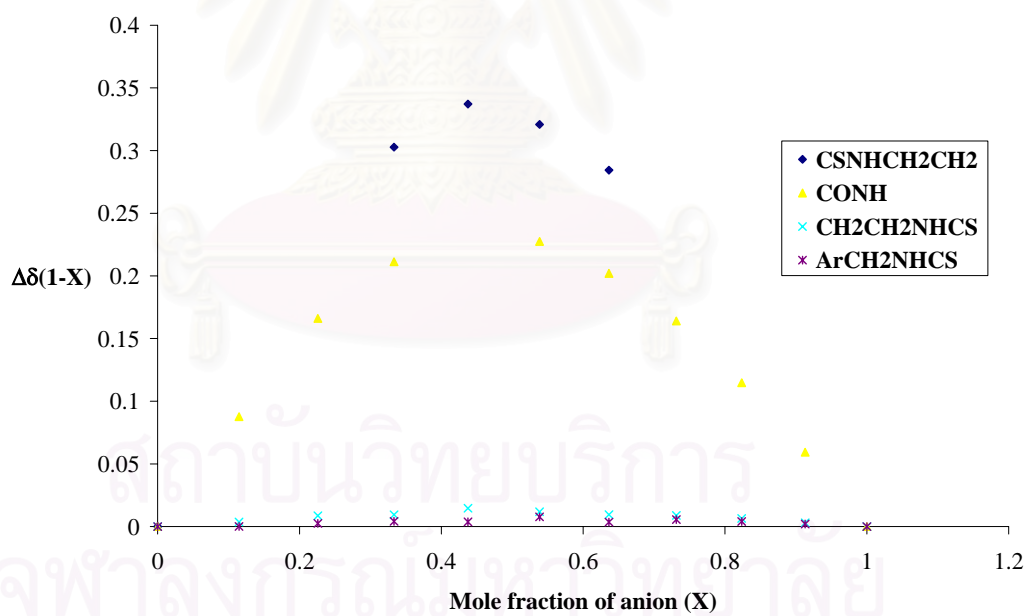
Titration curves for acetate with receptor **14** in  $\text{CD}_3\text{CN}$ Job's plots for acetate with receptor **14** in  $\text{CH}_3\text{CN}$ 

h) NMR titration data for benzoate with receptor **14** in CD<sub>3</sub>CN

Solvent:	CD <sub>3</sub> CN
Starting volume of host solution:	600 μL
Concentration of host solution:	1.87 mM
Concentration of guest solution:	18.7 mM
Association constant:	3.29x10 <sup>3</sup> M <sup>-1</sup> (ave)

Volume added /μL	-NH <sup>b</sup> CH <sub>2</sub> - /ppm	-CONH <sup>c</sup> - /ppm	-CH <sub>2</sub> <sup>e</sup> NH- /ppm	-CH <sub>2</sub> <sup>d</sup> NH- /ppm
0	7.0381	7.5209	3.5327	4.6850
5	-	7.5930	-	-
10	-	7.6199	3.5368	4.6852
20	-	7.7354	3.5439	4.6882
30	7.4922	7.8378	3.5469	4.6912
40	7.6374	-	3.5586	4.6916
50	7.7332	8.0139	3.5582	4.7018
60	7.8201	8.0765	3.5588	4.6949
70	-	8.1316	3.5658	4.7059
80	-	8.1711	3.5693	4.7080
90	-	8.2030	3.5680	4.7080
100	-	8.2250	3.5705	4.7099
120	-	8.2493	3.5732	4.7102
140	8.4056	8.2626	3.5693	4.7123
160	8.5036	8.2758	3.5759	4.7126
180	8.5641	8.2824	3.5735	4.7136
200	8.6136	8.2923	3.5724	4.7154
250	8.6939	8.2800	3.5715	4.7147
300	8.7512	8.3088	3.5703	4.7164
350	8.7842	8.3088	3.5771	4.7180
400	8.8106	8.3187	3.5760	4.7182
<b>K<sub>I</sub></b>	<b>5.66x10<sup>2</sup></b>	<b>5.42x10<sup>3</sup></b>	<b>5.02x10<sup>3</sup></b>	<b>2.11x10<sup>3</sup></b>

จุฬาลงกรณ์มหาวิทยาลัย

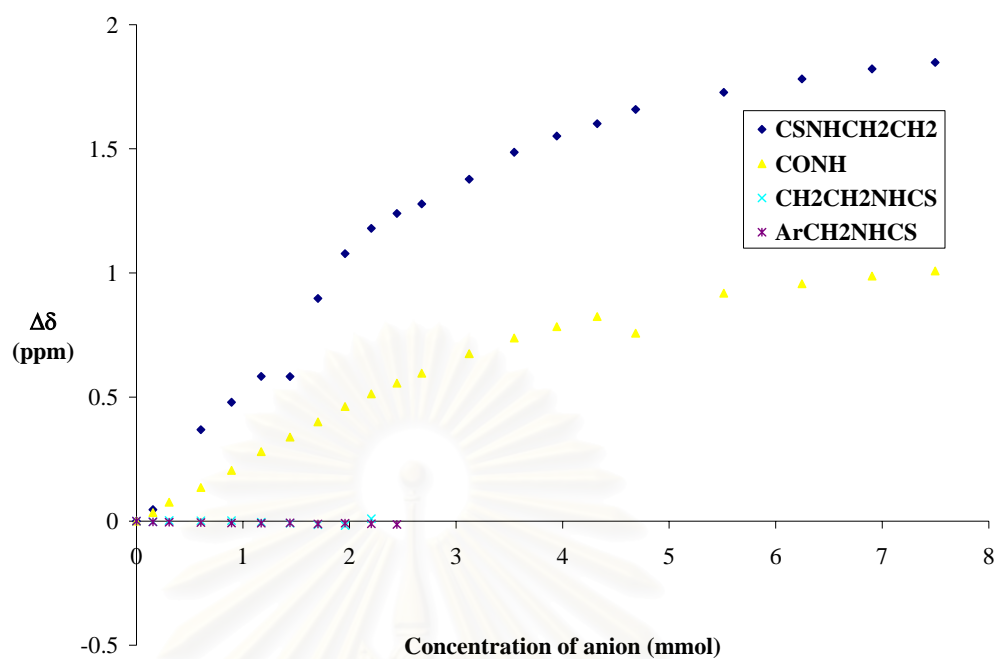
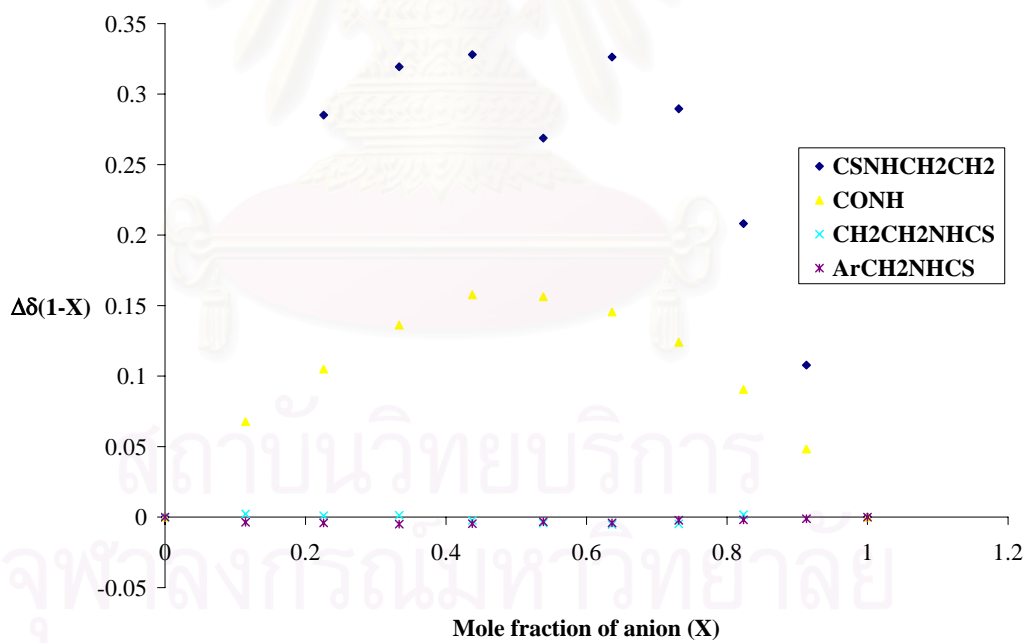
Titration curves for benzoate with receptor **14** in  $\text{CD}_3\text{CN}$ Job's plots for benzoate with receptor **14** in  $\text{CH}_3\text{CN}$ 

i) NMR titration data for dihydrogen phosphate with receptor **14** in CD<sub>3</sub>CN

Solvent:	CD <sub>3</sub> CN
Starting volume of host solution:	600 μL
Concentration of host solution:	1.87 mM
Concentration of guest solution:	18.7 mM
Association constant:	8.58x10 <sup>2</sup> M <sup>-1</sup> (ave)

Volume added /μL	-NH <sup>b</sup> CH <sub>2</sub> - /ppm	-CONH <sup>c</sup> - /ppm	-CH <sub>2</sub> <sup>e</sup> NH- /ppm	-CH <sub>2</sub> <sup>d</sup> NH- /ppm
0	7.0301	7.5273	3.5338	4.6870
5	7.0768	7.5616	3.5317	4.6836
10	-	7.6038	3.5363	4.6828
20	7.3984	7.6629	3.5350	4.6816
30	7.5091	7.7315	3.5358	4.6795
40	7.6133	7.8076	3.5296	4.6787
50	7.6125	7.8658	3.5247	4.6799
60	7.9274	7.9274	3.5193	4.6758
70	8.1080	7.9890	3.5160	4.6787
80	8.2097	8.0403	3.5434	4.6762
90	8.2697	8.0832	-	4.6737
100	8.3081	8.1233	-	-
120	8.4077	8.2015	-	-
140	8.5160	8.2647	-	-
160	8.5813	8.3110	-	-
180	8.6313	8.3515	-	-
200	8.6888	8.2846	-	-
250	8.7574	8.4453	-	-
300	8.8115	8.4838	-	-
350	8.8520	8.5148	-	-
400	8.8781	8.5354	-	-
<b>K<sub>I</sub></b>	<b>8.76x10<sup>2</sup></b>	<b>8.40x10<sup>2</sup></b>	-	-

จุฬาลงกรณ์มหาวิทยาลัย

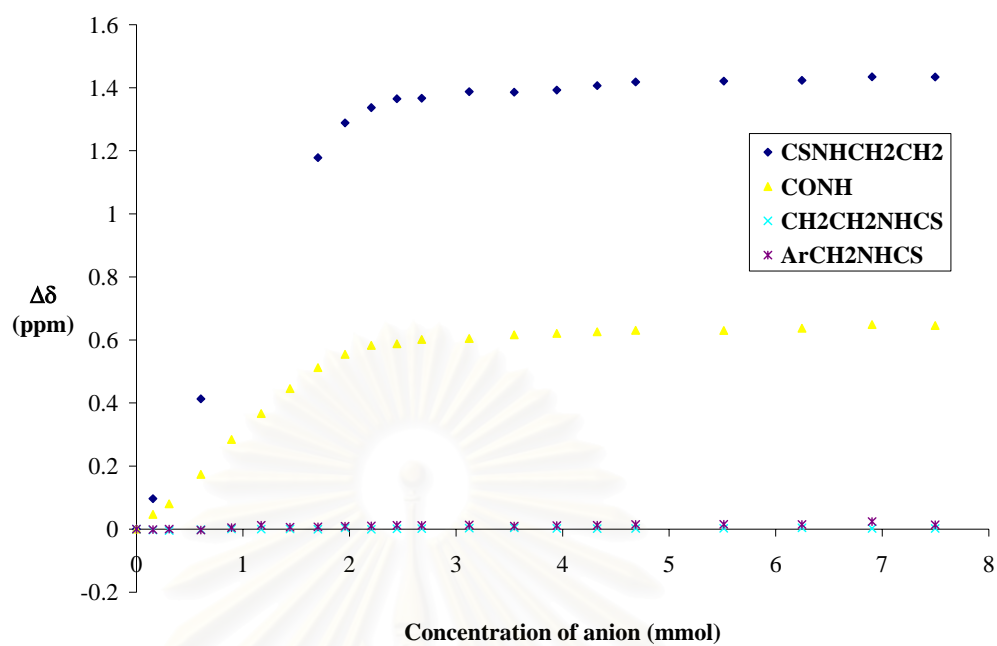
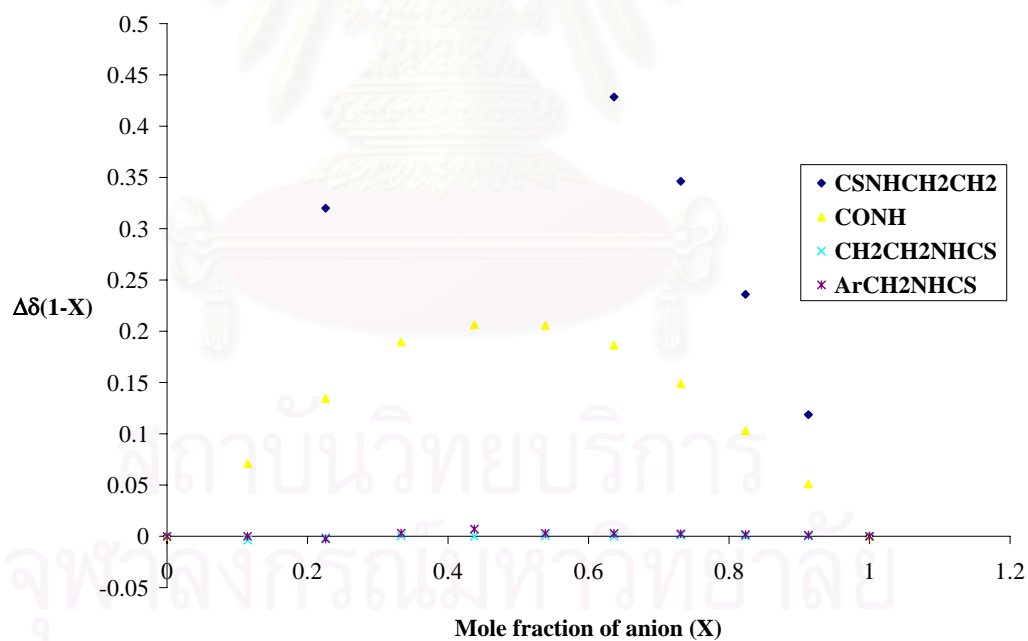
Titration curves for dihydrogen phosphate with receptor **14** in CD<sub>3</sub>CNJob's plots for dihydrogen phosphate with receptor **14** in CH<sub>3</sub>CN

j) NMR titration data for phenylphosphinate with receptor **14** in CD<sub>3</sub>CN

Solvent:	CD <sub>3</sub> CN
Starting volume of host solution:	600 μL
Concentration of host solution:	1.87 mM
Concentration of guest solution:	18.7 mM
Association constant:	1.71×10 <sup>4</sup> M <sup>-1</sup> (ave)

Volume added /μL	-NH <sup>b</sup> CH <sub>2</sub> - /ppm	-CONH <sup>c</sup> - /ppm	-CH <sub>2</sub> <sup>e</sup> NH- /ppm	-CH <sub>2</sub> <sup>d</sup> NH- /ppm
0	7.0024	7.5205	3.5340	4.6861
5	7.0990	7.5671	3.5309	4.6845
10	-	7.6007	3.5297	4.6861
20	7.4157	7.6942	3.5324	4.6830
30	-	7.8049	3.5344	4.6908
40	-	7.8874	3.534	4.6986
50	-	7.9664	3.5344	4.6923
60	8.1807	8.0328	3.5336	4.6935
70	8.2910	8.0747	3.5379	4.6955
80	8.3394	8.1036	3.5336	4.6963
90	8.3676	8.1087	3.5352	4.6982
100	8.3692	8.1220	3.5356	4.6978
120	8.3899	8.1251	3.5371	4.6994
140	8.3883	8.1369	3.5379	4.6959
160	8.3950	8.1412	3.5363	4.6970
180	8.4091	8.1467	3.5356	4.6986
200	8.4208	8.1510	3.5363	4.7009
250	8.4235	8.1506	3.5367	4.7013
300	8.4259	8.1576	3.5379	4.7009
350	8.4368	8.1693	3.5363	4.7103
400	8.4364	8.1662	3.5363	4.6998
<b>K<sub>I</sub></b>	<b>3.08x10<sup>4</sup></b>	<b>1.70x10<sup>4</sup></b>	-	<b>3.63x10<sup>3</sup></b>

จุฬาลงกรณ์มหาวิทยาลัย

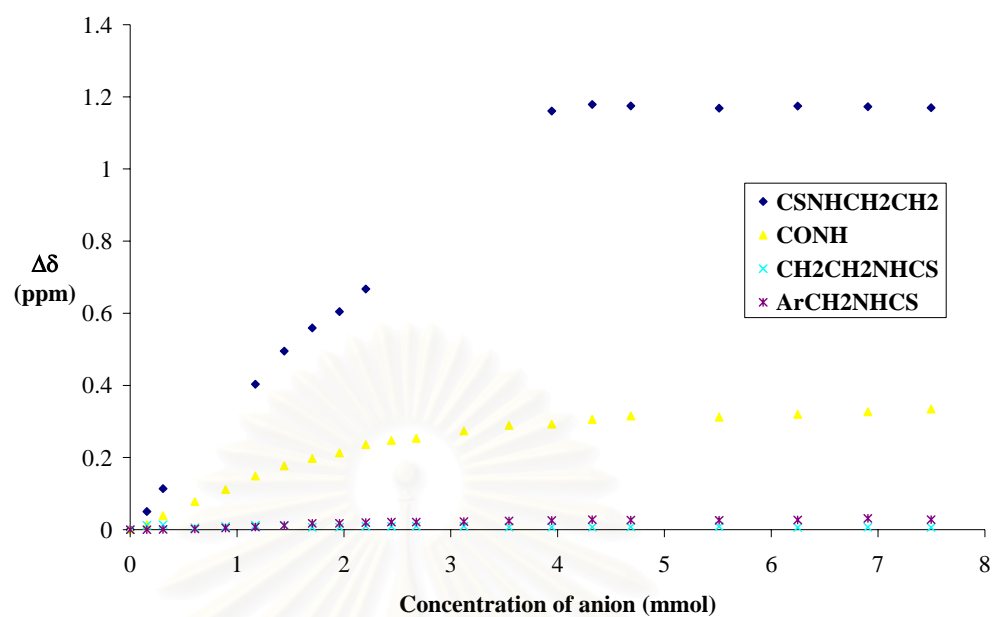
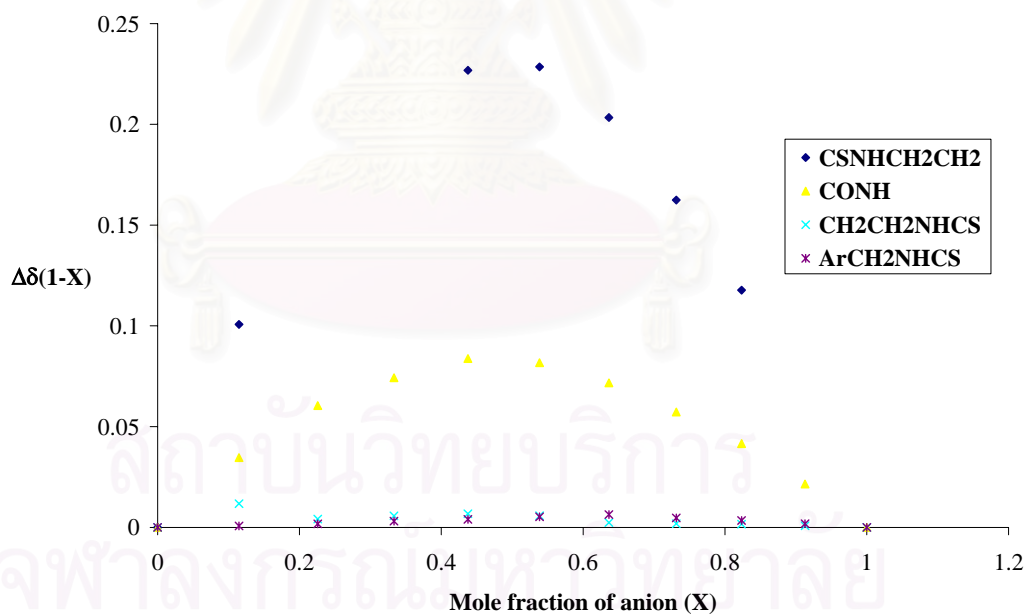
Titration curves for phenylphosphinate with receptor **14** in  $\text{CD}_3\text{CN}$ Job's plots for phenylphosphinate with receptor **14** in  $\text{CH}_3\text{CN}$ 

k) NMR titration data for diphenylphosphate with receptor **14** in CD<sub>3</sub>CN

Solvent:	CD <sub>3</sub> CN
Starting volume of host solution:	600 μL
Concentration of host solution:	1.87 mM
Concentration of guest solution:	18.7 mM
Association constant:	2.33×10 <sup>3</sup> M <sup>-1</sup> (ave)

Volume added /μL	-NH <sup>b</sup> CH <sub>2</sub> - /ppm	-CONH <sup>c</sup> - /ppm	-CH <sub>2</sub> <sup>e</sup> NH- /ppm	-CH <sub>2</sub> <sup>d</sup> NH- /ppm
0	7.0086	7.5202	3.5340	4.6849
5	7.0587	7.5335	3.5465	4.6849
10	7.1224	7.5593	3.5473	4.6857
20	-	7.5983	3.5394	4.6872
30	-	7.6316	3.5426	4.6896
40	7.4118	7.6692	3.5461	4.6920
50	7.5037	7.6973	3.5465	4.6963
60	7.5679	7.7176	3.5406	4.7025
70	7.6132	7.7333	3.5410	4.7025
80	7.6758	7.756	3.5434	4.7045
90	-	7.7677	3.5430	4.7060
100	-	7.7732	3.5438	4.7060
120	-	7.7939	3.5438	4.7072
140	-	7.8092	3.5410	4.7092
160	8.1693	7.8127	3.5410	4.7103
180	8.1873	7.8260	3.5410	4.7127
200	8.1834	7.8354	3.5414	4.7115
250	8.1768	7.8322	3.5426	4.7111
300	8.1830	7.8401	3.5403	4.7119
350	8.1811	7.8471	3.5410	4.7162
400	8.1783	7.8545	3.5403	4.7127
<b>K<sub>I</sub></b>	-	<b>1.84x10<sup>3</sup></b>	-	<b>2.81x10<sup>3</sup></b>



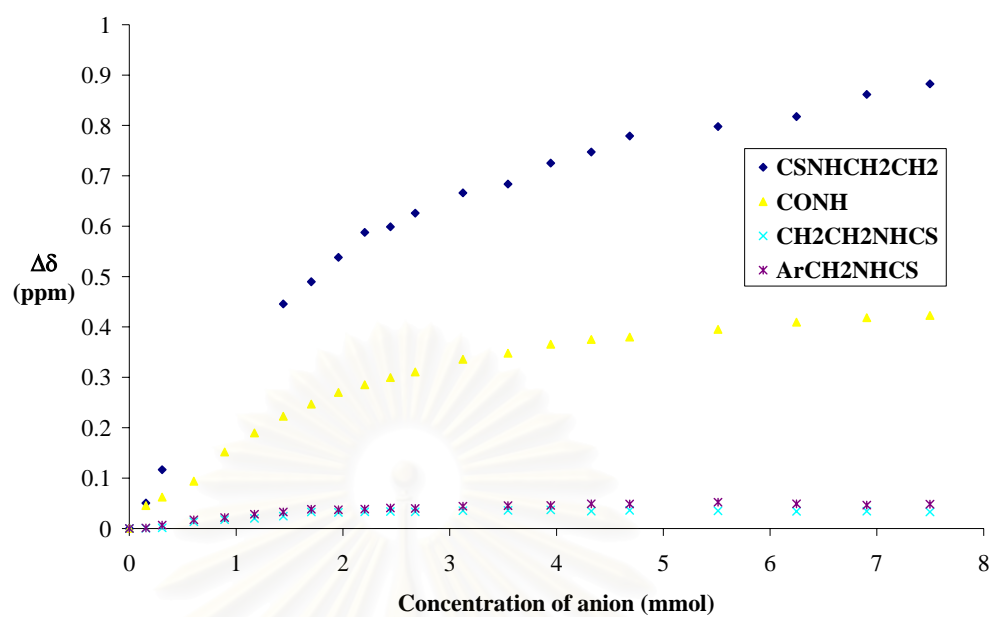
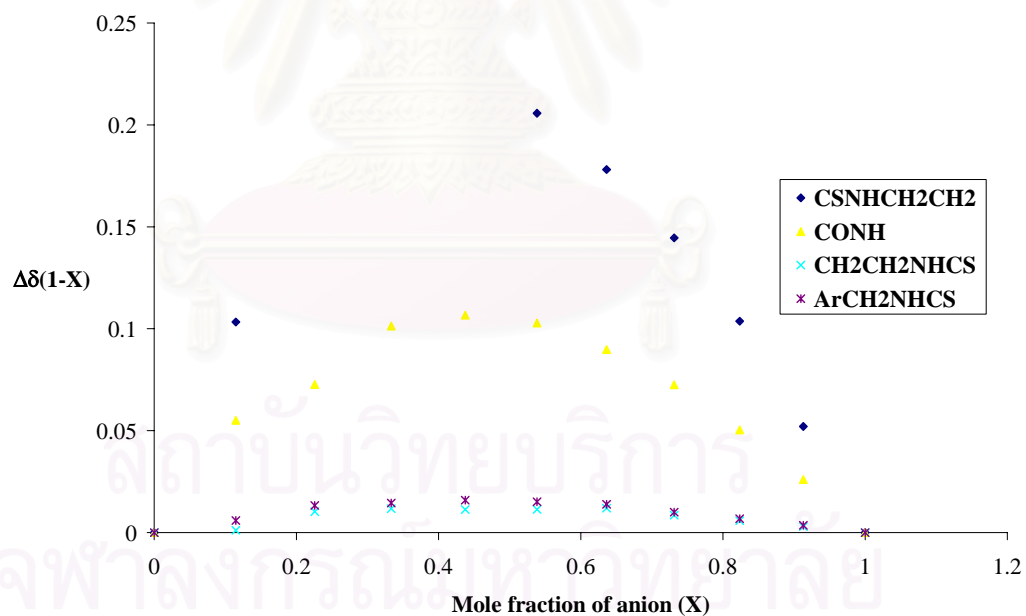
Titration curves for diphenylphosphate with receptor **14** in  $\text{CD}_3\text{CN}$ Job's for diphenylphosphate plots with receptor **14** in  $\text{CH}_3\text{CN}$ 

1) NMR titration data for succinate with receptor **14** in CD<sub>3</sub>CN

Solvent:	CD <sub>3</sub> CN
Starting volume of host solution:	600 μL
Concentration of host solution:	1.87 mM
Concentration of guest solution:	18.7 mM
Association constant:	1.10x10 <sup>4</sup> M <sup>-1</sup> (ave)

Volume added /μL	-NH <sup>b</sup> CH <sub>2</sub> - /ppm	-CONH <sup>c</sup> - /ppm	-CH <sub>2</sub> <sup>e</sup> NH- /ppm	-CH <sub>2</sub> <sup>d</sup> NH- /ppm
0	7.0244	7.5303	3.5326	4.6785
5	7.0749	7.5758	3.5332	4.6795
10	7.1411	7.5925	3.5339	4.6852
20	-	7.6242	3.5459	4.6957
30	-	7.6823	3.5502	4.7003
40	-	7.7200	3.5527	4.7068
50	7.4701	7.7531	3.5572	4.7113
60	7.5141	7.7773	3.5655	4.7167
70	7.5625	7.8003	3.5646	4.7159
80	7.6120	7.8157	3.5658	4.7172
90	7.6232	7.8299	3.5665	4.7193
100	7.6504	7.8412	3.5658	4.7183
120	7.6905	7.8663	3.5680	4.7226
140	7.7079	7.8782	3.5685	4.7239
160	7.7497	7.8960	3.5694	4.7243
180	7.7717	7.9055	3.5671	4.7277
200	7.8036	7.9103	3.5688	4.7271
250	7.8222	7.9256	3.5676	4.7309
300	7.8420	7.9399	3.5666	4.7276
350	7.8860	7.9487	3.567	4.7249
400	7.9069	7.9531	3.5655	4.7267
<b>K<sub>I</sub></b>	<b>1.23x10<sup>3</sup></b>	<b>1.38x10<sup>3</sup></b>	<b>3.53x10<sup>4</sup></b>	<b>6.09x10<sup>3</sup></b>

จุฬาลงกรณ์มหาวิทยาลัย

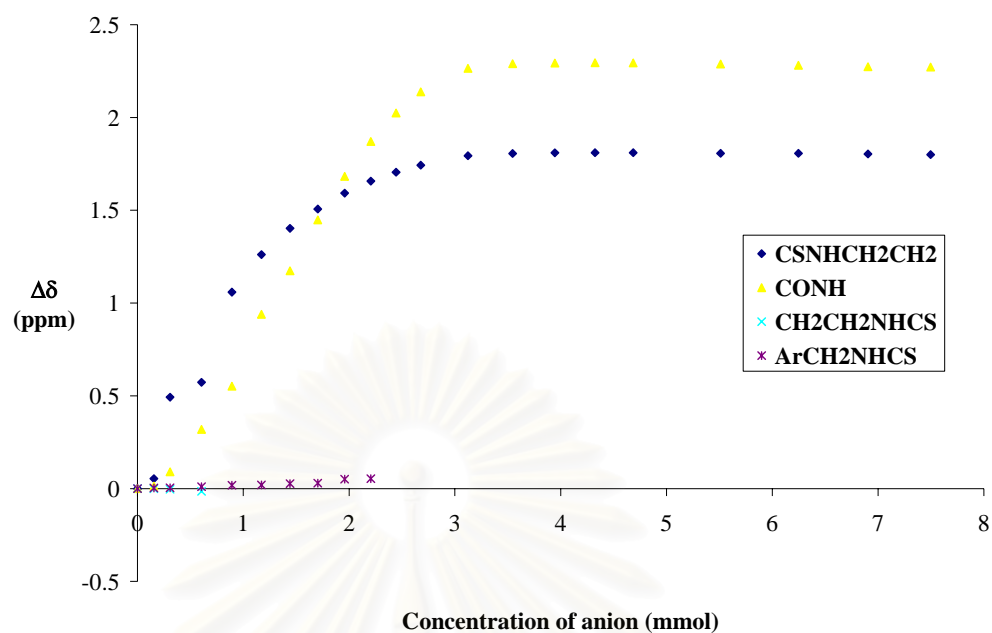
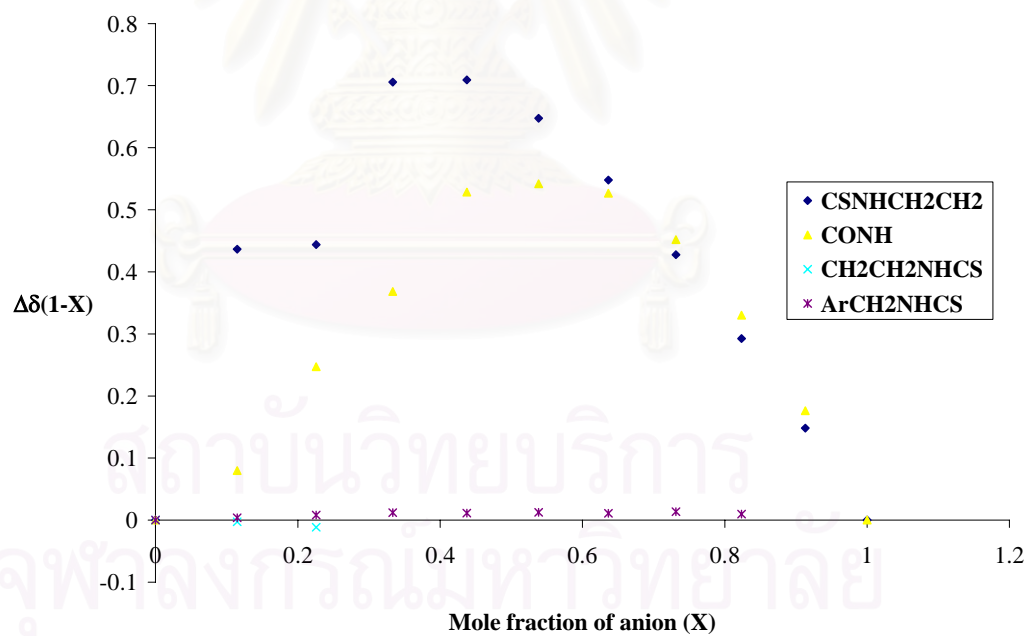
Titration curves for succinate with receptor **14** in CD<sub>3</sub>CNJob's plots for succinate with receptor **14** in CH<sub>3</sub>CN

m) NMR titration data for glutarate with receptor 14 in CD<sub>3</sub>CN

Solvent:	CD <sub>3</sub> CN
Starting volume of host solution:	600μL
Concentration of host solution:	1.87 mM
Concentration of guest solution:	18.7 mM
Association constant:	4.29x10 <sup>4</sup> M <sup>-1</sup> (ave)

Volume added	-NH <sup>b</sup> CH <sub>2</sub> -	-CONH <sup>c</sup> -	-CH <sub>2</sub> <sup>e</sup> NH-	-CH <sub>2</sub> <sup>d</sup> NH-
/μL	/ppm	/ppm	/ppm	/ppm
0	7.0247	7.5309	3.5330	4.6795
5	7.0784	7.5452	3.5327	4.6828
10	7.5177	7.6211	3.5299	4.6838
20	7.5980	7.8500	3.5181	4.6900
30	8.0833	8.0833	-	4.6975
40	8.2857	8.4705	-	4.6996
50	8.4275	8.7048	-	4.7065
60	8.5315	8.9790	-	4.7092
70	8.6166	9.2133	-	4.7301
80	8.6816	9.4015	-	4.7334
90	8.7292	9.5554	-	-
100	8.7676	9.6688	-	-
120	8.8183	9.7956	-	-
140	8.8303	9.8208	-	-
160	8.8342	9.8241	-	-
180	8.8348	9.8262	-	-
200	8.8345	9.8252	-	-
250	8.8314	9.8188	-	-
300	8.8315	9.8119	-	-
350	8.8281	9.8041	-	-
400	8.8246	9.8027	-	-
<b>K<sub>I</sub></b>	<b>6.89x10<sup>3</sup></b>	<b>7.90x10<sup>4</sup></b>	-	-

จุฬาลงกรณ์มหาวิทยาลัย

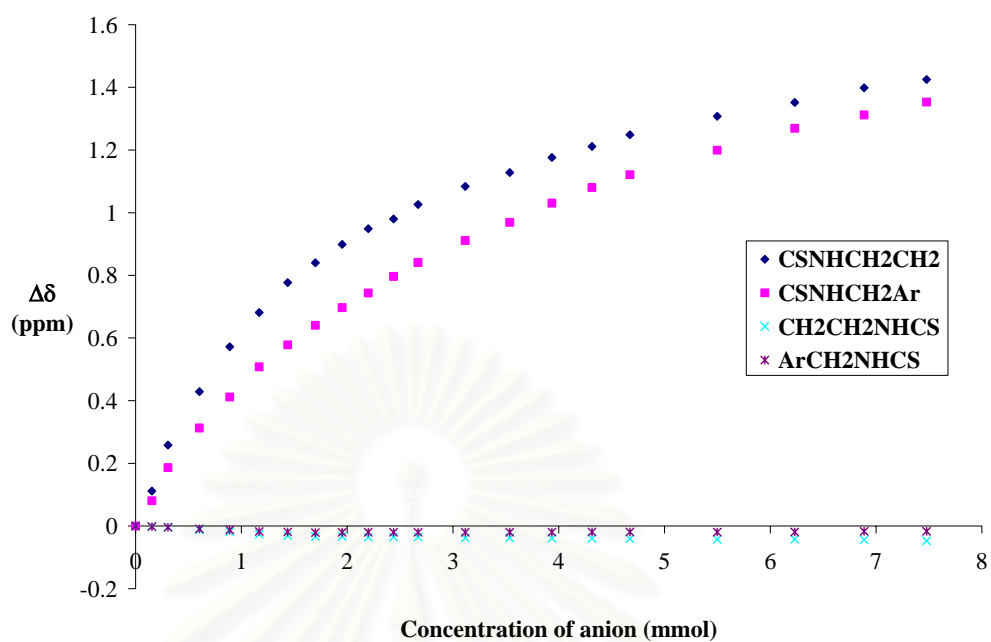
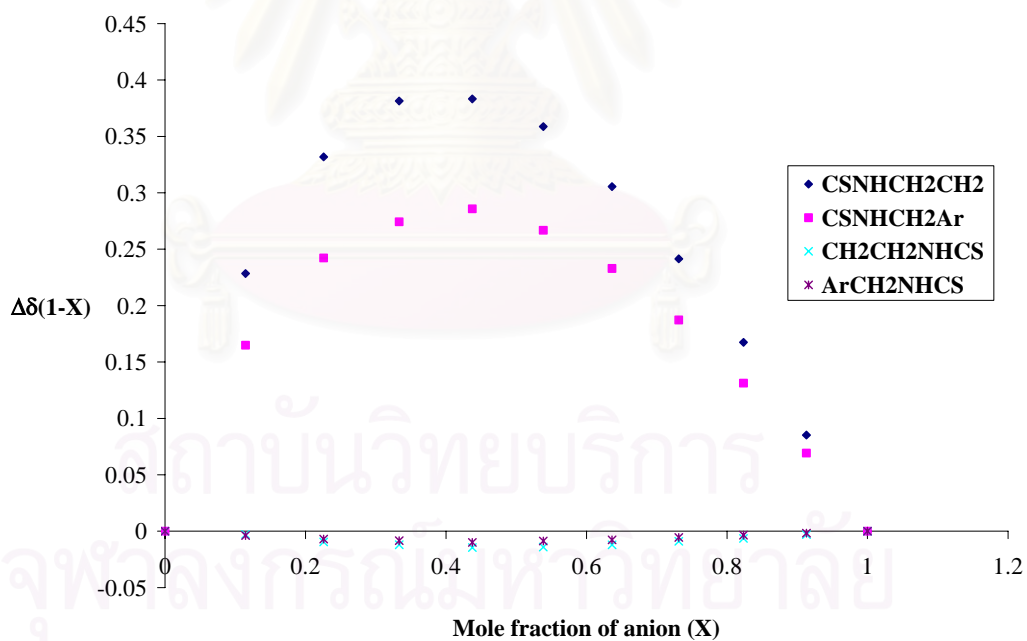
Titration curves for glutarate with receptor **14** in  $\text{CD}_3\text{CN}$ Job's plots for glutarate with receptor **14** in  $\text{CH}_3\text{CN}$ 

n) NMR titration data for acetate with receptor **15** in CD<sub>3</sub>CN

Solvent:	CD <sub>3</sub> CN
Starting volume of host solution:	600 μL
Concentration of host solution:	3.74 mM
Concentration of guest solution:	37.4 mM
Association constant:	2.01 × 10 <sup>3</sup> M <sup>-1</sup> (ave)

Volume added /μL	-NH <sup>b</sup> CH <sub>2</sub> - /ppm	-NH <sup>a</sup> CH <sub>2</sub> - /ppm	-CH <sub>2</sub> <sup>e</sup> NH- /ppm	-CH <sub>2</sub> <sup>d</sup> NH- /ppm
0	8.1353	8.0727	3.6979	4.6822
5	8.2468	8.1533	3.6971	4.6802
10	8.3934	8.2589	3.6947	4.6779
20	8.5639	8.3856	3.6857	4.6732
30	8.7074	8.4841	3.6799	4.6697
40	8.8166	8.5807	3.6720	4.6646
50	8.9124	8.6507	3.6674	4.6634
60	8.9753	8.7133	3.6646	4.6611
70	9.0340	8.7696	3.6646	4.6618
80	9.0840	8.8166	3.6619	4.6622
90	9.1153	8.8690	3.6630	4.6618
100	9.1615	8.9139	3.6630	4.6618
120	9.2190	8.9835	3.6599	4.6618
140	9.2635	9.0418	3.6603	4.6622
160	9.3116	9.1032	3.6591	4.6626
180	9.3468	9.1529	3.6584	4.6630
200	9.3840	9.1939	3.6572	4.6630
250	9.4427	9.2721	3.6552	4.6626
300	9.4872	9.3418	3.6560	4.6634
350	9.5338	9.3844	3.6541	4.6650
400	9.5604	9.4258	3.6509	4.6654
<b>K<sub>I</sub></b>	<b>4.96x10<sup>2</sup></b>	<b>2.41x10<sup>2</sup></b>	<b>5.30x10<sup>3</sup></b>	-

จุฬาลงกรณ์มหาวิทยาลัย

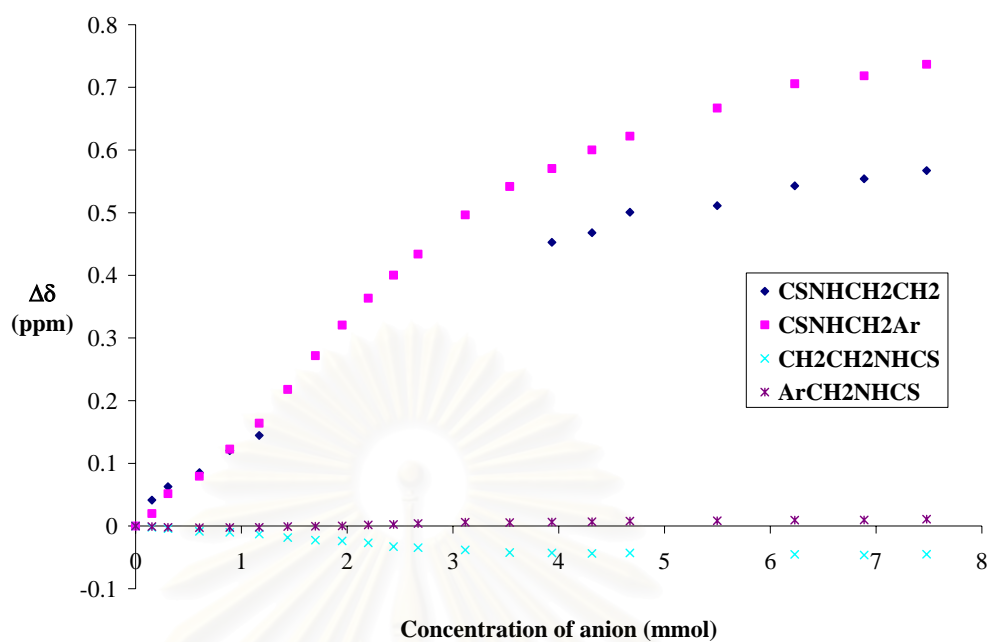
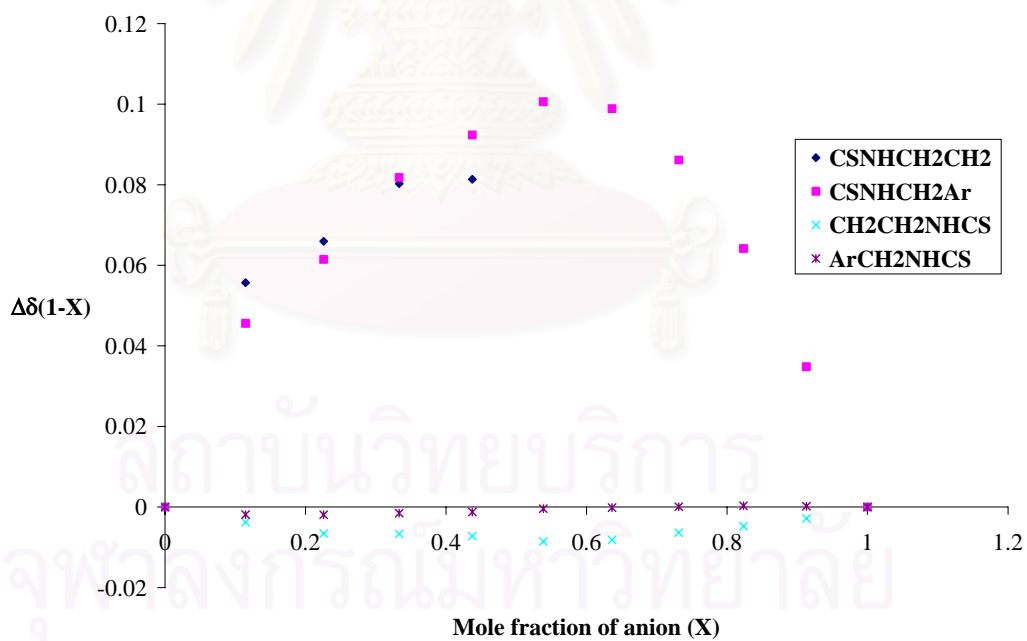
Titration curves for acetate with receptor **15** in CD<sub>3</sub>CNJob's plots for acetate with receptor **15** in CH<sub>3</sub>CN

o) NMR titration data for benzoate with receptor **15** in CD<sub>3</sub>CN

Solvent:	CD <sub>3</sub> CN
Starting volume of host solution:	600 μL
Concentration of host solution:	3.74 mM
Concentration of guest solution:	37.4 mM
Association constant:	$K_1$ : $8.30 \times 10^3 \text{ M}^{-1}$ (ave) $K_2$ : $3.45 \times 10^4 \text{ M}^{-1}$ (ave)

Volume added /μL	-NH <sup>b</sup> CH <sub>2</sub> - /ppm	-NH <sup>a</sup> CH <sub>2</sub> - /ppm	-CH <sub>2</sub> <sup>c</sup> NH- /ppm	-CH <sub>2</sub> <sup>d</sup> NH- /ppm
0	8.1868	8.1133	3.6736	4.6640
5	8.2281	8.1332	3.6714	4.6631
10	8.2497	8.1648	3.6693	4.6619
20	8.2720	8.1927	3.6651	4.6615
30	8.3072	8.2360	3.6636	4.6617
40	8.3314	8.2775	3.6607	4.6618
50	-	8.3313	3.6551	4.6631
60	-	8.3852	3.6512	4.6636
70	-	8.4339	3.6499	4.6643
80	-	8.4769	3.6467	4.6658
90	-	8.5137	3.6407	4.6664
100	-	8.5472	3.6390	4.6680
120	-	8.6098	3.6354	4.6701
140	-	8.6551	3.6313	4.6694
160	8.6396	8.6837	3.6307	4.6703
180	8.6549	8.7134	3.6299	4.6707
200	8.6874	8.7355	3.6306	4.6719
250	8.6979	8.7803	-	4.6725
300	8.7297	8.8190	3.6284	4.6734
350	8.7408	8.8317	3.6272	4.6738
400	8.7540	8.8500	3.6286	4.6749
$K_1$	$3.78 \times 10^3$	$1.13 \times 10^4$	$9.81 \times 10^3$	-
$K_2$	$1.48 \times 10^3$	$2.06 \times 10^3$	$1.00 \times 10^5$	-

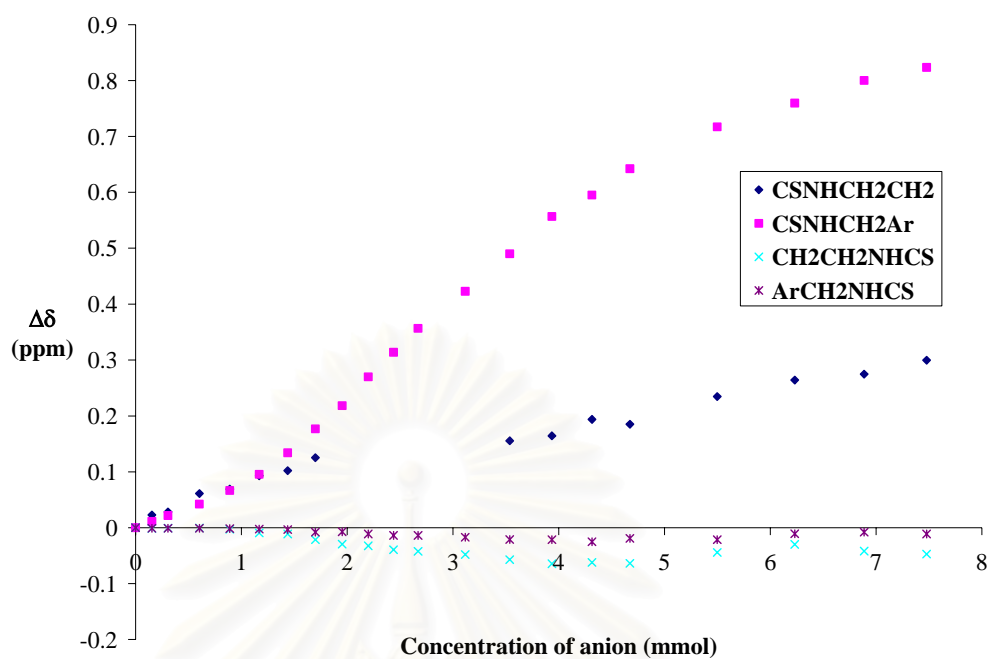
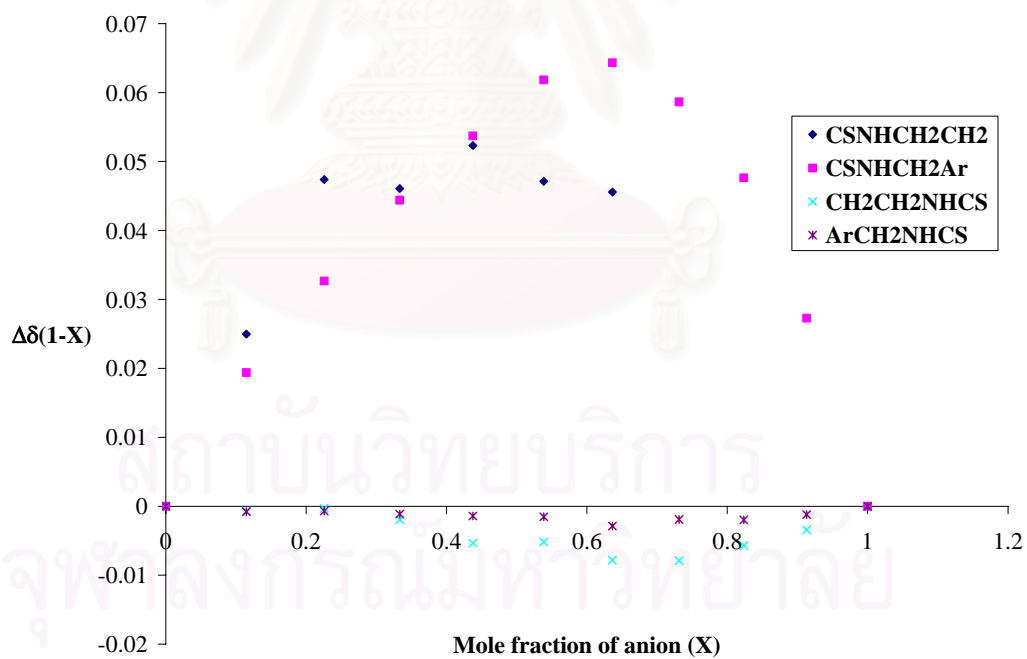


Titration curves for benzoate with receptor **15** in  $\text{CD}_3\text{CN}$ Job's plots for benzoate with receptor **15** in  $\text{CH}_3\text{CN}$ 

p) NMR titration data for dihydrogen phosphate with receptor **15** in CD<sub>3</sub>CN

Solvent:	CD <sub>3</sub> CN
Starting volume of host solution:	600 μL
Concentration of host solution:	3.74 mM
Concentration of guest solution:	37.4 mM
Association constant:	$K_1$ : $9.71 \times 10^3 \text{ M}^{-1}$ (ave)
	$K_2$ : $1.09 \times 10^3 \text{ M}^{-1}$ (ave)

Volume added /μL	-NH <sup>b</sup> CH <sub>2</sub> - /ppm	-NH <sup>a</sup> CH <sub>2</sub> - /ppm	-CH <sub>2</sub> <sup>e</sup> NH- /ppm	-CH <sub>2</sub> <sup>d</sup> NH- /ppm
0	8.2353	8.1576	3.7016	4.6688
5	8.2581	8.1688	3.7003	4.6679
10	8.2635	8.1795	3.7008	4.6679
20	8.2965	8.1998	3.7012	4.6679
30	8.3044	8.2242	3.6987	4.6671
40	8.3283	8.2531	3.6921	4.6663
50	8.3374	8.2916	3.6904	4.6655
60	8.3606	8.3345	3.6801	4.6609
70	-	8.3759	3.6722	4.6617
80	-	8.4275	3.6693	4.6576
90	-	8.4714	3.6623	4.6551
100	-	8.5143	3.6594	4.6551
120	-	8.5805	3.6536	4.6518
140	8.3908	8.6478	3.6446	4.6477
160	8.3998	8.7144	3.6371	4.6473
180	8.4292	8.7528	3.6396	4.6436
200	8.4205	8.7999	3.6379	4.6498
250	8.4701	8.8748	3.6574	4.6473
300	8.4995	8.9173	3.6718	4.6580
350	8.5102	8.9578	3.6598	4.6609
400	8.5350	8.9810	3.6545	4.6576
$K_1$	-	$9.84 \times 10^3$	$9.64 \times 10^3$	$9.65 \times 10^3$
$K_2$	-	$1.25 \times 10^3$	$1.02 \times 10^3$	$9.93 \times 10^2$

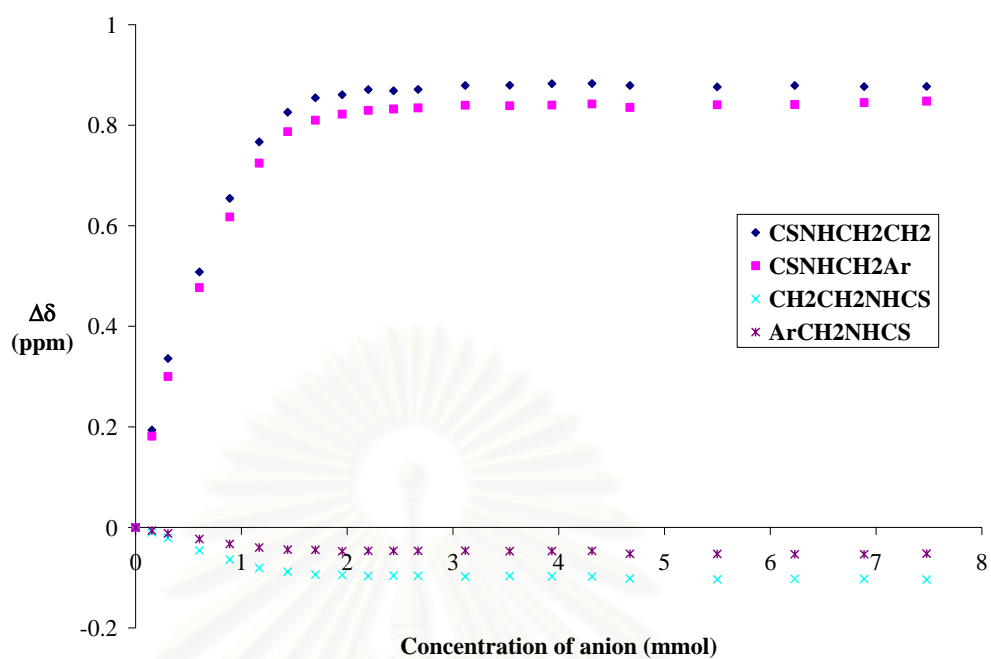
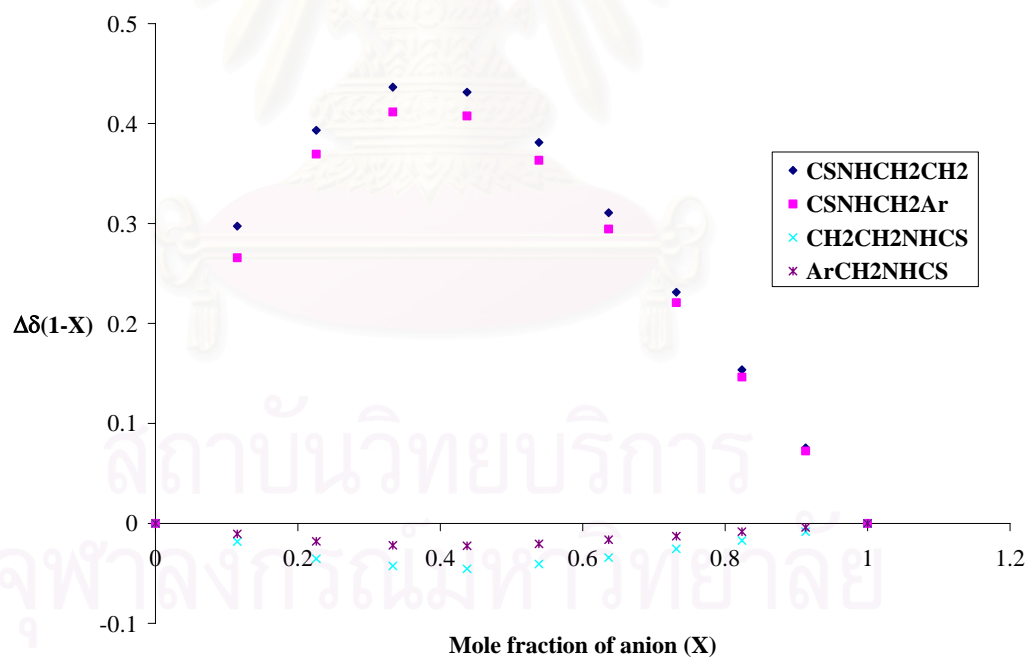
Titration curves for dihydrogen phosphate with receptor **15** in  $\text{CD}_3\text{CN}$ Job's plots for dihydrogen phosphate with receptor **15** in  $\text{CH}_3\text{CN}$ 

q) NMR titration data for phenylphosphinate with receptor **15** in CD<sub>3</sub>CN

Solvent:	CD <sub>3</sub> CN
Starting volume of host solution:	600 μL
Concentration of host solution:	3.34 mM
Concentration of guest solution:	50.4 mM
Association constant:	1.43 × 10 <sup>4</sup> M <sup>-1</sup> (ave)

<b>Volume added</b> /μL	<b>-NH<sup>b</sup>CH<sub>2</sub>-</b> /ppm	<b>-NH<sup>a</sup>CH<sub>2</sub>-</b> /ppm	<b>-CH<sub>2</sub><sup>e</sup>NH-</b> /ppm	<b>-CH<sub>2</sub><sup>d</sup>NH-</b> /ppm
0	8.1279	8.0571	3.6963	4.6822
5	8.3215	8.2386	3.6865	4.6759
10	8.4638	8.3574	3.6756	4.6704
20	8.6359	8.5342	3.6505	4.6591
30	8.7825	8.6746	3.6325	4.6493
40	8.8948	8.7817	3.6157	4.6423
50	8.9538	8.8443	3.6083	4.6380
60	8.9824	8.8670	3.6024	4.6376
70	8.9886	8.8791	3.6017	4.6349
80	8.9988	8.8866	3.5997	4.6356
90	8.9964	8.8893	3.6005	4.6356
100	8.9992	8.8916	3.6001	4.6356
120	9.0070	8.8967	3.5985	4.6360
140	9.0074	8.8959	3.5997	4.6349
160	9.0105	8.8971	3.5989	4.6352
180	9.0109	8.8995	3.5985	4.6356
200	9.0069	8.8924	3.5946	4.6297
250	9.0042	8.8978	3.5930	4.6293
300	9.0069	8.8982	3.5938	4.6289
350	9.0046	8.9021	3.5938	4.6289
400	9.0050	8.9049	3.5926	4.6301
<b>K<sub>I</sub></b>	<b>2.28 × 10<sup>4</sup></b>	<b>1.84 × 10<sup>4</sup></b>	<b>6.37 × 10<sup>3</sup></b>	<b>9.65 × 10<sup>3</sup></b>

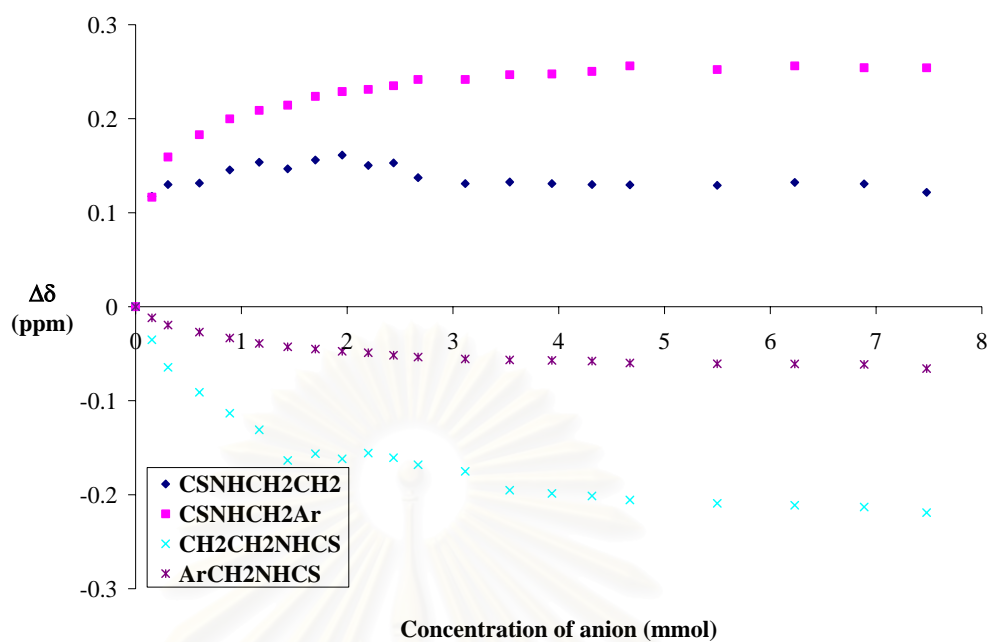
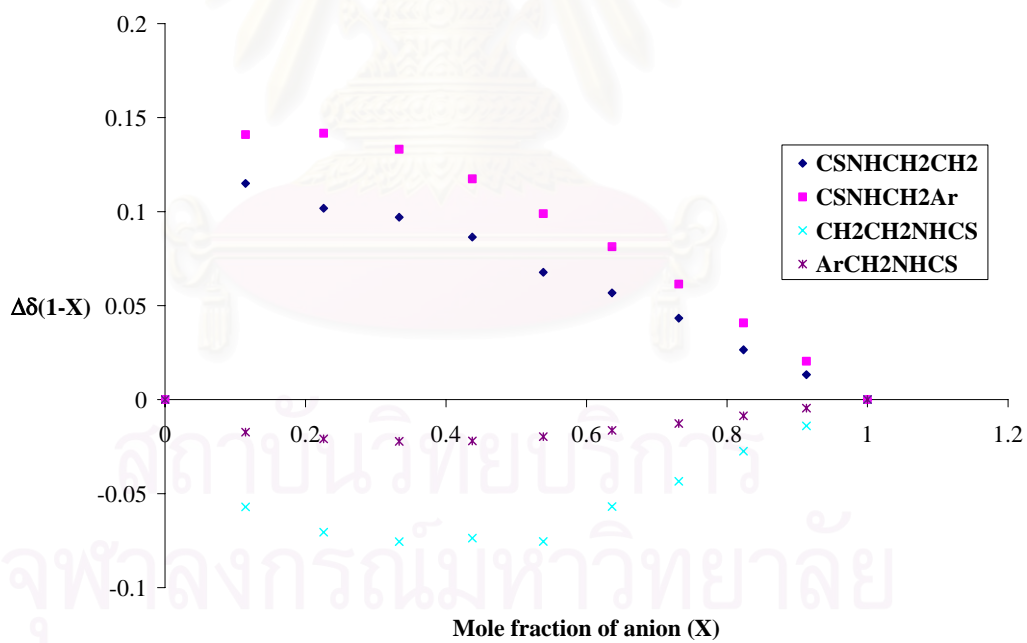
จุฬาลงกรณ์มหาวิทยาลัย

Titration curves for phenylphosphinate with receptor **15** in  $\text{CD}_3\text{CN}$ Job's plots for phenylphosphinate with receptor **15** in  $\text{CH}_3\text{CN}$ 

r) NMR titration data for diphenylphosphate with receptor **15** in CD<sub>3</sub>CN

Solvent:	CD <sub>3</sub> CN
Starting volume of host solution:	600 μL
Concentration of host solution:	1.87 mM
Concentration of guest solution:	29.7 mM
Association constant:	3.24 × 10 <sup>3</sup> M <sup>-1</sup> (ave)

Volume added /μL	-NH <sup>b</sup> CH <sub>2</sub> - /ppm	-NH <sup>a</sup> CH <sub>2</sub> - /ppm	-CH <sub>2</sub> <sup>e</sup> NH- /ppm	-CH <sub>2</sub> <sup>d</sup> NH- /ppm
0	8.1251	8.0575	3.6963	4.6826
5	8.2425	8.1740	3.6611	4.6708
10	8.2550	8.2167	3.6318	4.6630
20	8.2565	8.2405	3.6052	4.6556
30	8.2706	8.2573	3.5829	4.6493
40	8.2788	8.2663	3.5653	4.6435
50	8.2718	8.2718	3.5328	4.6399
60	8.2812	8.2812	3.5399	4.6376
70	8.2863	8.2863	3.5344	4.6352
80	8.2753	8.2886	3.5406	4.6337
90	8.2780	8.2925	3.5356	4.6309
100	8.2624	8.2992	3.5281	4.6290
120	8.2561	8.2992	3.5211	4.6270
140	8.2577	8.3043	3.5011	4.6259
160	8.2561	8.3050	3.4976	4.6255
180	8.2550	8.3078	3.4949	4.6247
200	8.2546	8.3136	3.4906	4.6227
250	8.2542	8.3097	3.4871	4.6219
300	8.2573	8.3136	3.4851	4.6216
350	8.2558	8.3117	3.4832	4.6212
400	8.2467	8.3116	3.4772	4.6168
<b>K<sub>I</sub></b>	-	<b>6.93 × 10<sup>3</sup></b>	<b>1.46 × 10<sup>3</sup></b>	<b>1.34 × 10<sup>3</sup></b>

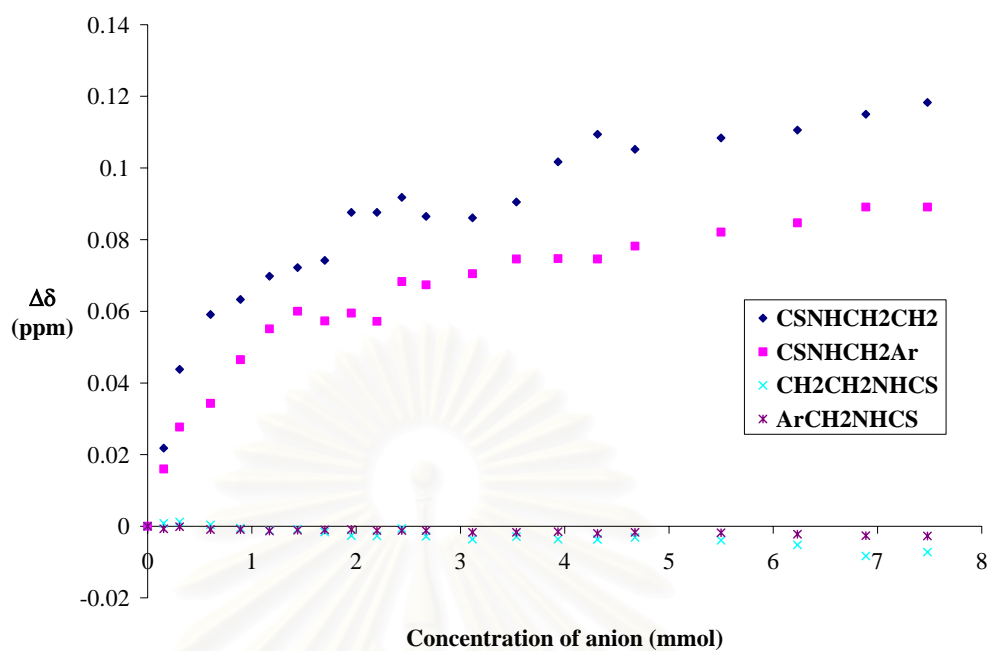
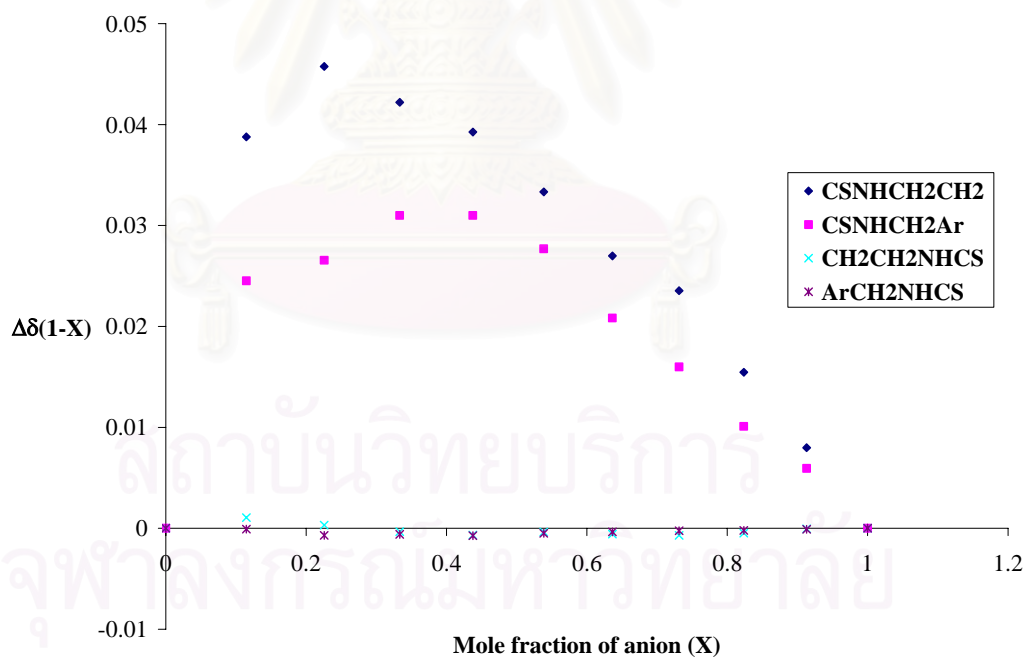
Titration curves for diphenylphosphate with receptor **15** in  $\text{CD}_3\text{CN}$ Job's for diphenylphosphate plots with receptor **15** in  $\text{CH}_3\text{CN}$ 

s) NMR titration data for succinate with receptor **15** in CD<sub>3</sub>CN

Solvent:	CD <sub>3</sub> CN
Starting volume of host solution:	600 μL
Concentration of host solution:	3.74 mM
Concentration of guest solution:	37.4 mM
Association constant:	2.02x10 <sup>3</sup> M <sup>-1</sup> (ave)

Volume added /μL	-NH <sup>b</sup> CH <sub>2</sub> - /ppm	-NH <sup>a</sup> CH <sub>2</sub> - /ppm	-CH <sub>2</sub> <sup>e</sup> NH- /ppm	-CH <sub>2</sub> <sup>d</sup> NH- /ppm
0	8.2574	8.1755	3.6940	4.6780
5	8.2792	8.1915	3.6948	4.6773
10	8.3012	8.2032	3.6952	4.6779
20	8.3165	8.2098	3.6944	4.6771
30	8.3207	8.2220	3.6935	4.6771
40	8.3272	8.2306	3.6928	4.6767
50	8.3296	8.2355	3.6932	4.6769
60	8.3316	8.2328	3.6924	4.6770
70	8.3450	8.2350	3.6914	4.6771
80	8.3450	8.2327	3.6913	4.6768
90	8.3492	8.2438	3.6934	4.6768
100	8.3439	8.2429	3.6912	4.6768
120	8.3435	8.2460	3.6904	4.6763
140	8.3479	8.2501	3.6911	4.6763
160	8.3591	8.2502	3.6904	4.6765
180	8.3668	8.2501	3.6903	4.6760
200	8.3626	8.2537	3.6909	4.6763
250	8.3658	8.2576	3.6901	4.6762
300	8.3680	8.2602	3.6888	4.6758
350	8.3724	8.2646	3.6857	4.6754
400	8.3757	8.2646	3.6868	4.6753
<b>K<sub>I</sub></b>	-	<b>2.02x10<sup>3</sup></b>	-	-



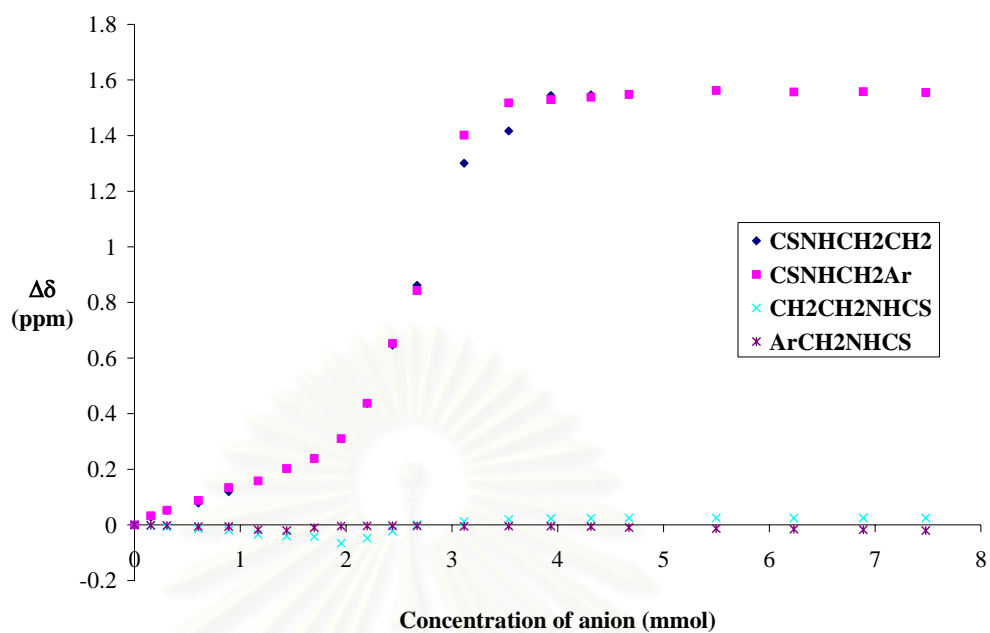
Titration curves for succinate with receptor **15** in CD<sub>3</sub>CNJob's plots for succinate with receptor **15** in CH<sub>3</sub>CN

t) NMR titration data for glutarate with receptor **15** in CD<sub>3</sub>CN

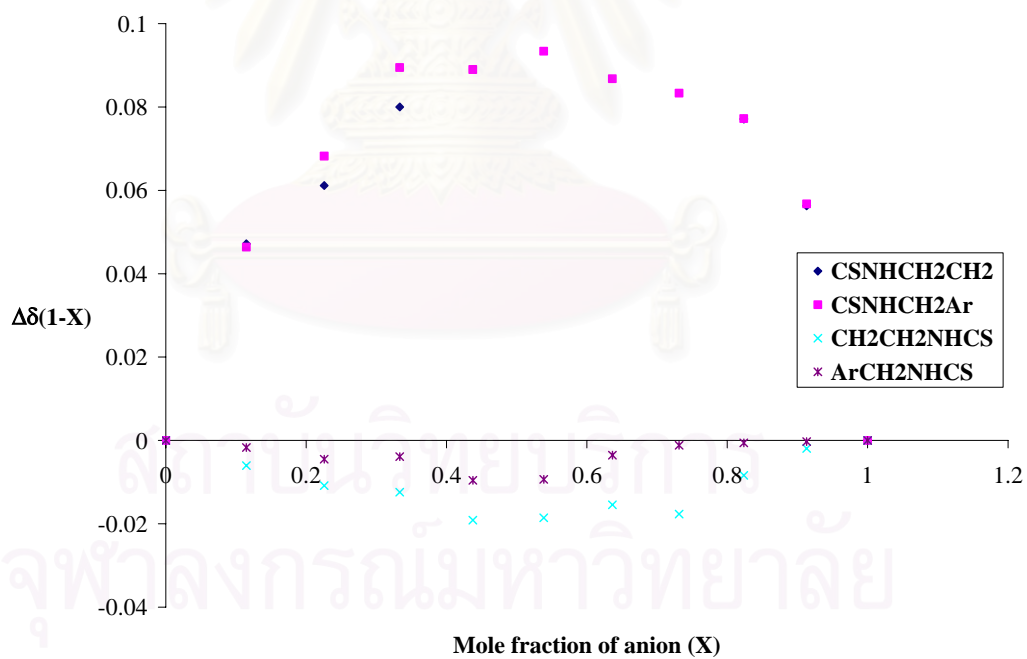
Solvent:	CD <sub>3</sub> CN
Starting volume of host solution:	600 μL
Concentration of host solution:	3.74 mM
Concentration of guest solution:	37.4 mM
Association constant:	-

Volume added /μL	-NH <sup>b</sup> CH <sub>2</sub> - /ppm	-NH <sup>a</sup> CH <sub>2</sub> - /ppm	-CH <sub>2</sub> <sup>c</sup> NH- /ppm	-CH <sub>2</sub> <sup>d</sup> NH- /ppm
0	8.2690	8.1680	3.6951	4.6778
5	8.2979	8.2006	3.6921	4.6764
10	8.3223	8.2204	3.6883	4.6759
20	8.3480	8.2561	3.6811	4.6720
30	8.3890	8.3022	3.6765	4.6720
40	-	8.3262	3.6611	4.6608
50	-	8.3703	3.6549	4.6576
60	-	8.4066	3.6527	4.6681
70	-	8.4781	3.6294	4.6735
80	8.7059	8.6056	3.6477	4.6746
90	8.9163	8.8205	3.6729	4.6749
100	9.1306	9.0108	3.6952	4.6746
120	9.5698	9.5698	3.7071	4.6721
140	9.6859	9.6859	3.7154	4.6736
160	9.8129	9.6973	3.7180	4.6732
180	9.8151	9.7061	3.7190	4.6718
200	-	9.7160	3.7195	4.6685
250	-	9.7304	3.7201	4.6644
300	-	9.7249	3.7200	4.6624
350	-	9.7260	3.7201	4.6604
400	-	9.7228	3.7200	4.6573
<b>K<sub>I</sub></b>	-	-	-	-

Titration curves for glutarate with receptor **15** in  $\text{CD}_3\text{CN}$



Job's plots for glutarate with receptor **15** in  $\text{CH}_3\text{CN}$

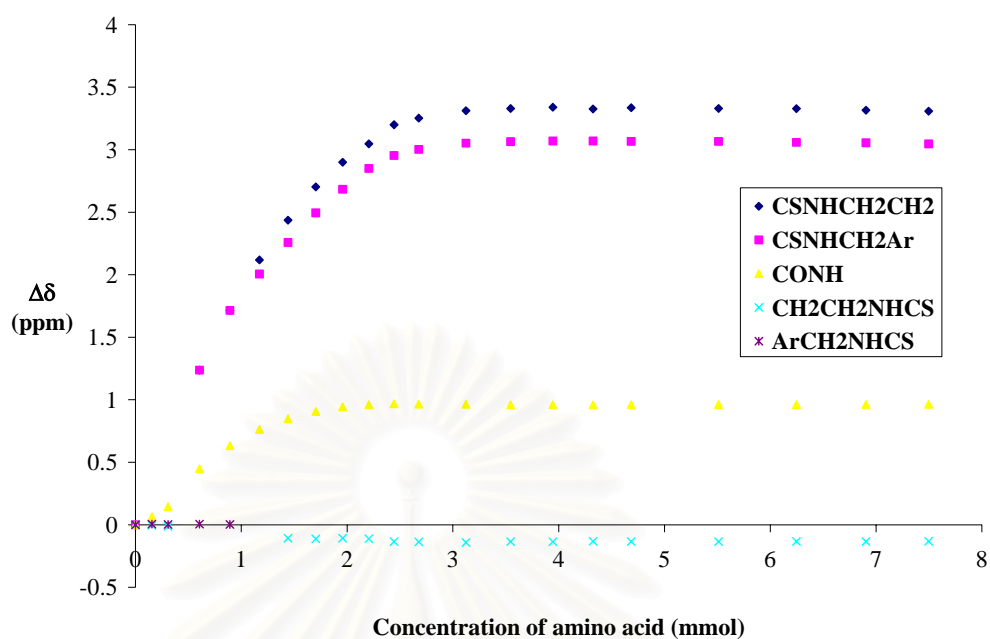


u) NMR titration data for carboxylate anion of aspartic acid with receptor **14** in  $\text{CD}_3\text{CN}$

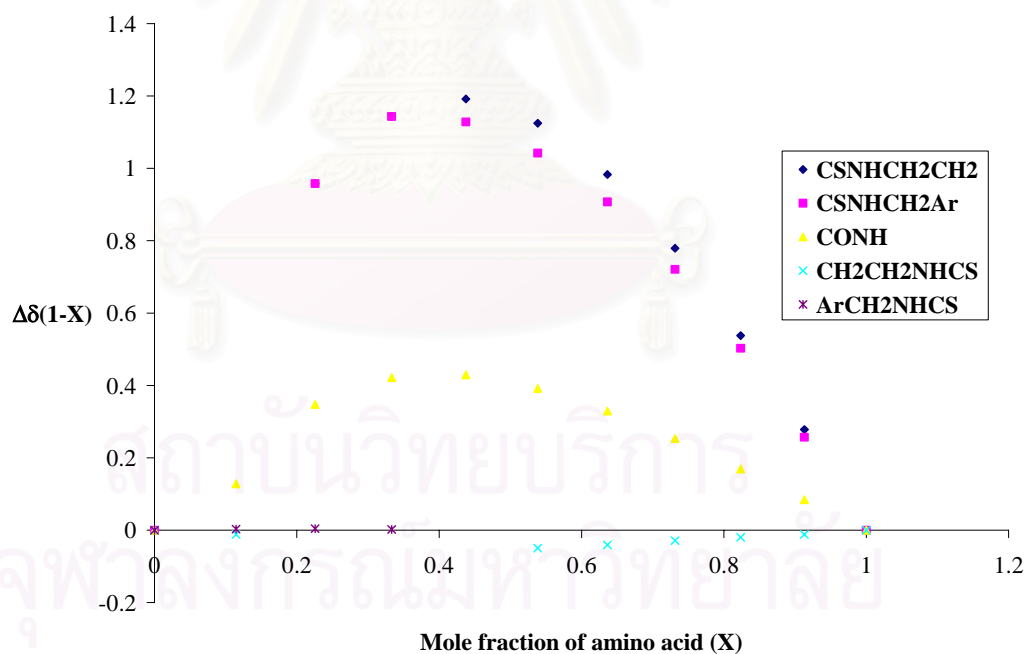
Solvent:	$\text{CD}_3\text{CN}$
Starting volume of host solution:	600 $\mu\text{L}$
Concentration of host solution:	1.87 mM
Concentration of guest solution:	18.7 mM
Association constant:	$2.12 \times 10^4 \text{ M}^{-1}$ (ave)

Volume added / $\mu\text{L}$	$-\text{NH}^b\text{CH}_2-$ /ppm	$-\text{NH}^a\text{CH}_2-$ /ppm	$-\text{CONH}^c-$ /ppm	$-\text{CH}_2^e\text{NH}-$ /ppm	$-\text{CH}_2^d\text{NH}-$ /ppm
0	7.0396	7.0396	7.5617	3.5329	4.6817
5	-	-	7.6253	3.5289	4.6875
10	-	-	7.7066	3.5196	4.6850
20	8.2768	8.2768	8.0107	-	4.6870
30	8.7544	8.7544	8.1947	-	4.6851
40	9.1582	9.0451	8.3250	-	-
50	9.4763	9.2978	8.4103	3.4256	-
60	9.7426	9.5346	8.4681	3.4212	-
70	9.9395	9.7227	8.5054	3.4258	-
80	10.0868	9.8891	8.5223	3.4213	-
90	10.2395	9.9935	8.5296	3.3988	-
100	10.2920	10.0420	8.5271	3.3964	-
120	10.3517	10.0917	8.5255	3.3914	-
140	10.3690	10.1037	8.5212	3.3989	-
160	10.3788	10.1091	8.5223	3.3975	-
180	10.3654	10.1091	8.5213	3.4007	-
200	10.3753	10.1056	8.5226	3.3996	-
250	10.3698	10.1061	8.5242	3.3987	-
300	10.3687	10.0979	8.5233	3.4003	-
350	10.3555	10.0951	8.5244	3.3997	-
400	10.3475	10.0861	8.5254	3.4006	-
$K_I$	$2.00 \times 10^4$	$2.14 \times 10^4$	$2.29 \times 10^4$	$2.06 \times 10^4$	-

Titration curves for carboxylate anion of aspartic acid with receptor **14** in  $\text{CD}_3\text{CN}$



Job's plots for carboxylate anion of aspartic acid with receptor **14** in  $\text{CH}_3\text{CN}$

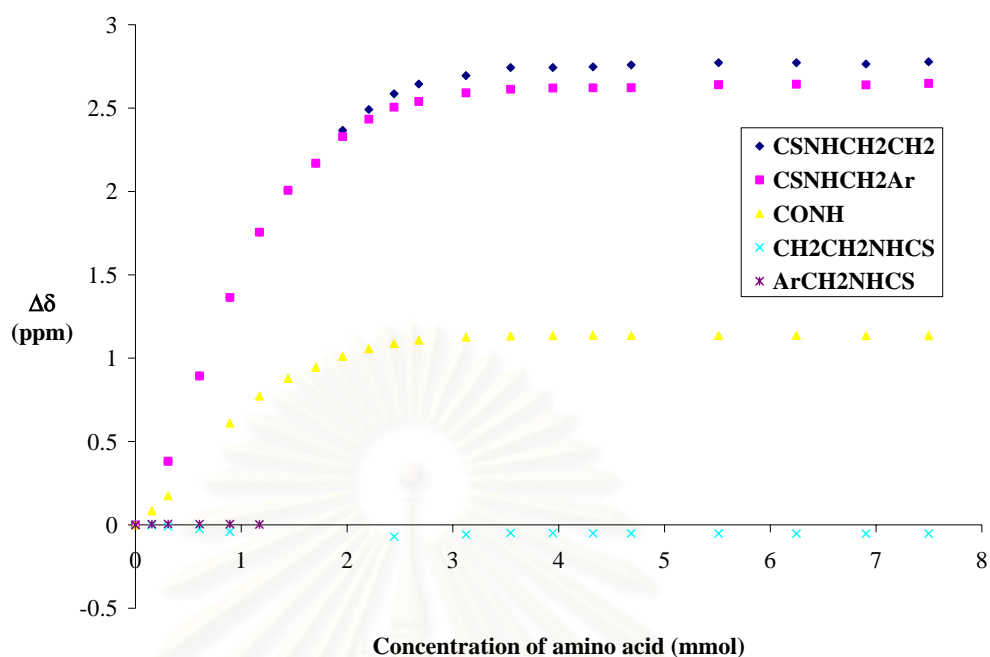


v) NMR titration data for carboxylate anion of glutamic acid with receptor **14** in  $\text{CD}_3\text{CN}$

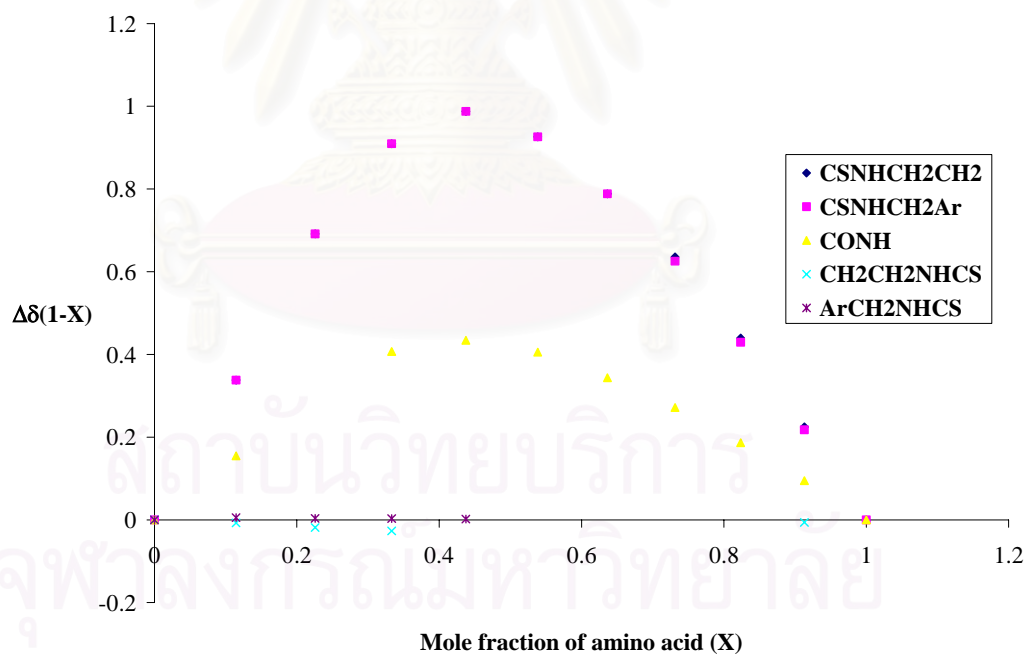
Solvent:	$\text{CD}_3\text{CN}$
Starting volume of host solution:	600 $\mu\text{L}$
Concentration of host solution:	1.87 mM
Concentration of guest solution:	18.7 mM
Association constant:	$1.55 \times 10^4 \text{ M}^{-1}$ (ave)

Volume added / $\mu\text{L}$	$-\text{NH}^b\text{CH}_2-$ /ppm	$-\text{NH}^a\text{CH}_2-$ /ppm	$-\text{CONH}^c-$ /ppm	$-\text{CH}_2^e\text{NH}-$ /ppm	$-\text{CH}_2^d\text{NH}-$ /ppm
0	7.0403	7.0403	7.5297	3.5322	4.6827
5	-	-	7.6140	3.5306	4.6870
10	7.4221	7.4221	7.7044	3.5237	4.6888
20	7.9336	7.9336	-	3.5084	4.6874
30	8.4045	8.4045	8.1404	3.4921	4.6875
40	8.7962	8.7962	8.3017	-	4.6860
50	9.0472	9.0472	8.4085	-	-
60	9.2089	9.2089	8.4752	-	-
70	9.4070	9.3685	8.5405	-	-
80	9.5314	9.4733	8.5862	-	-
90	9.6260	9.5456	8.6174	3.4624	-
100	9.6843	9.5797	8.6370	-	-
120	9.7350	9.6314	8.6555	3.4745	-
140	9.7834	9.6532	8.6629	3.4844	-
160	9.7834	9.6604	8.6643	3.4834	-
180	9.7878	9.6615	8.6669	3.4825	-
200	9.7989	9.6622	8.6662	3.4820	-
250	9.8121	9.6805	8.6657	3.4806	-
300	9.8121	9.6830	8.6664	3.4800	-
350	9.8044	9.6791	8.6638	3.4797	-
400	9.8176	9.6881	8.6646	3.4794	-
$K_I$	$1.57 \times 10^4$	$1.41 \times 10^4$	$1.67 \times 10^4$	-	-

Titration curves for carboxylate anion of glutamic acid with receptor **14** in  $\text{CD}_3\text{CN}$



Job's plots for carboxylate anion of glutamic acid with receptor **14** in  $\text{CH}_3\text{CN}$



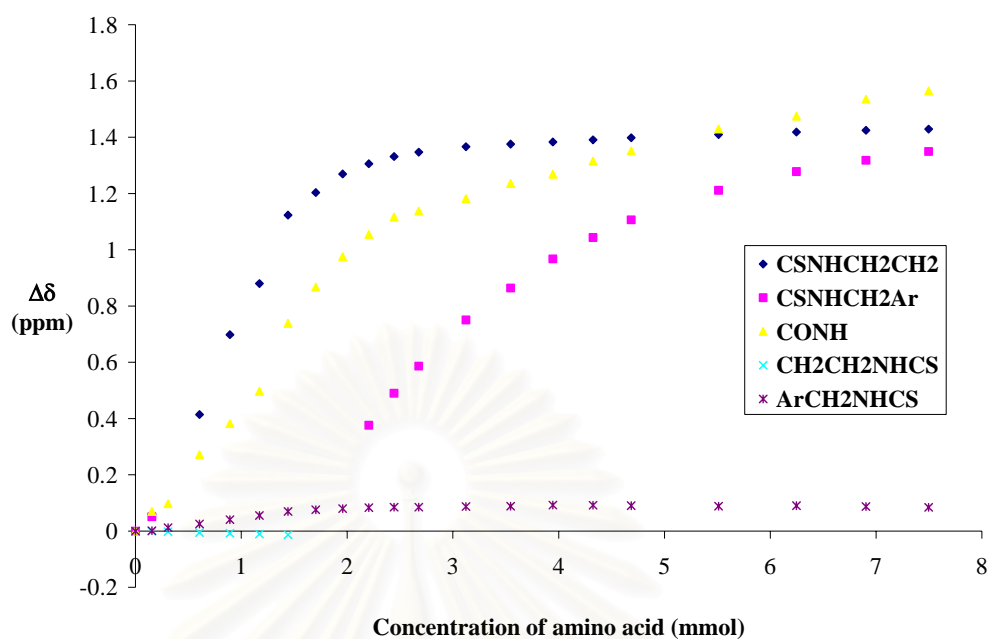
w) NMR titration data for carboxylate anion of asparagine with receptor **14** in CD<sub>3</sub>CN

Solvent:	CD <sub>3</sub> CN
Starting volume of host solution:	600 μL
Concentration of host solution:	1.87 mM
Concentration of guest solution:	18.7 mM
Association constant:	1.96x10 <sup>4</sup> M <sup>-1</sup> (ave)

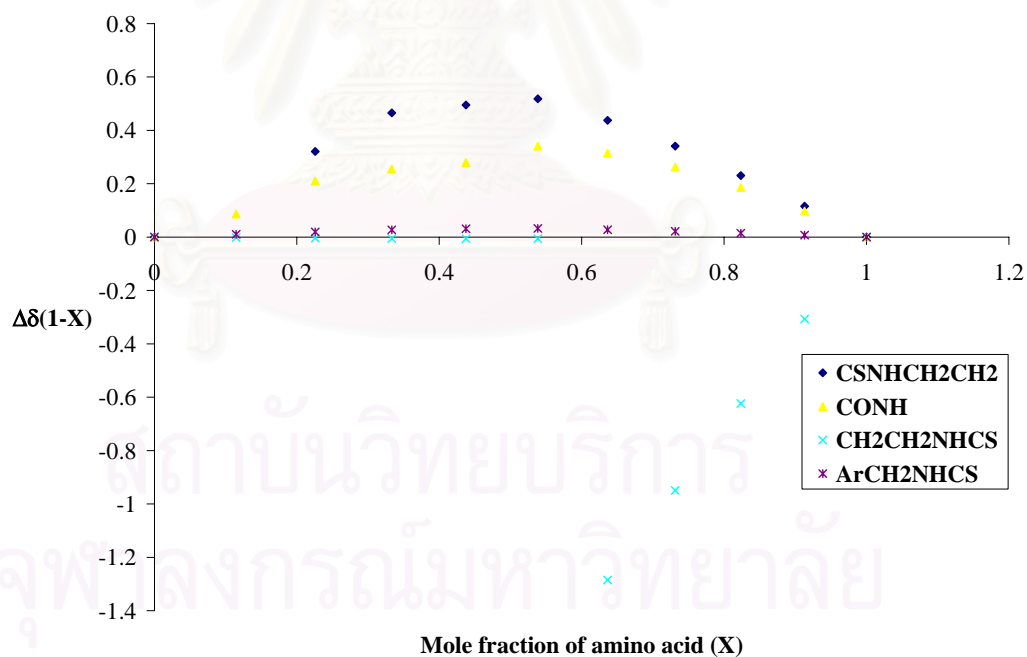
Volume added /μL	-NH <sup>b</sup> CH <sub>2</sub> - /ppm	-NH <sup>a</sup> CH <sub>2</sub> - /ppm	-CONH <sup>c</sup> - /ppm	-CH <sub>2</sub> <sup>e</sup> NH- /ppm	-CH <sub>2</sub> <sup>d</sup> NH- /ppm
0	7.0273	6.9695	7.522	3.5329	4.6838
5	7.0866	7.0202	7.5914	3.5322	4.6850
10	-	-	7.6198	3.5309	4.6957
20	7.4416	-	7.7938	3.5277	4.7092
30	7.7255	-	7.9038	3.5251	4.7244
40	7.9071	-	8.0191	3.5221	4.7394
50	8.1502	-	8.2604	3.5197	4.7534
60	8.2307	-	8.3890	-	4.7596
70	8.2967	-	8.4971	-	4.7637
80	8.3331	7.3453	8.5761	-	4.7671
90	8.3583	7.4593	8.6382	-	4.7687
100	8.3740	7.5557	8.6595	-	4.7688
120	8.3936	7.7199	8.7037	-	4.7709
140	8.4026	7.8334	8.7575	-	4.7720
160	8.4105	7.9369	8.7902	-	4.7762
180	8.4181	8.0130	8.8369	-	4.7756
200	8.4253	8.0756	8.8732	-	4.7742
250	8.4370	8.1809	8.9512	-	4.7724
300	8.4455	8.2471	8.9970	-	4.7742
350	8.4518	8.2872	9.0568	-	4.7710
400	8.4559	8.3184	9.0867	-	4.7680
<b>K<sub>I</sub></b>	<b>1.93x10<sup>4</sup></b>	<b>1.36x10<sup>3</sup></b>	-	-	<b>1.99x10<sup>4</sup></b>



Titration curves for carboxylate anion of asparagine with receptor **14** in  $\text{CD}_3\text{CN}$



Job's plots for carboxylate anion of asparagine with receptor **14** in  $\text{CH}_3\text{CN}$

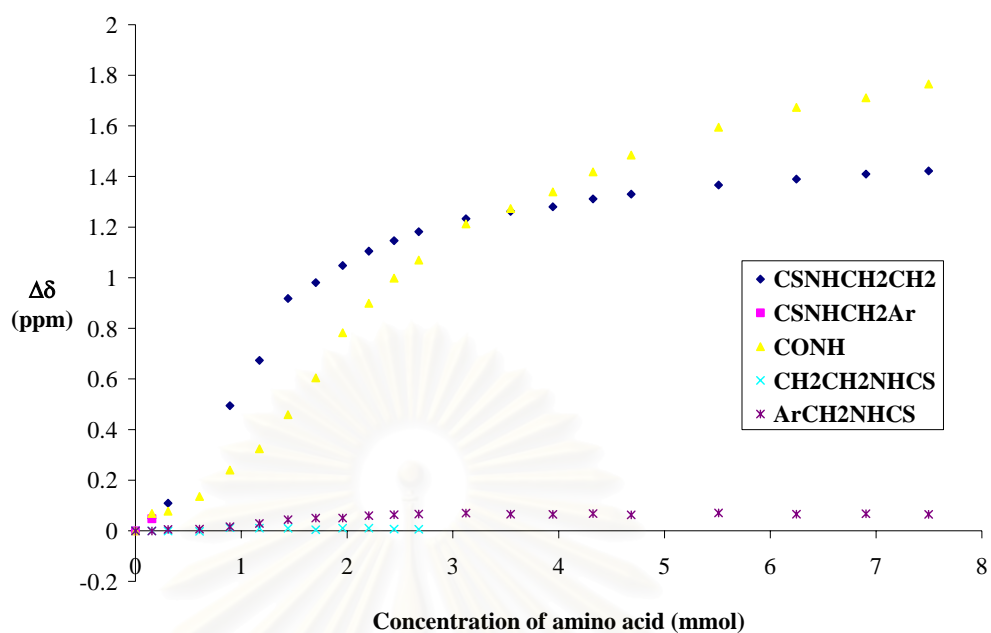


x) NMR titration data for carboxylate anion of glutamine with receptor **14** in CD<sub>3</sub>CN

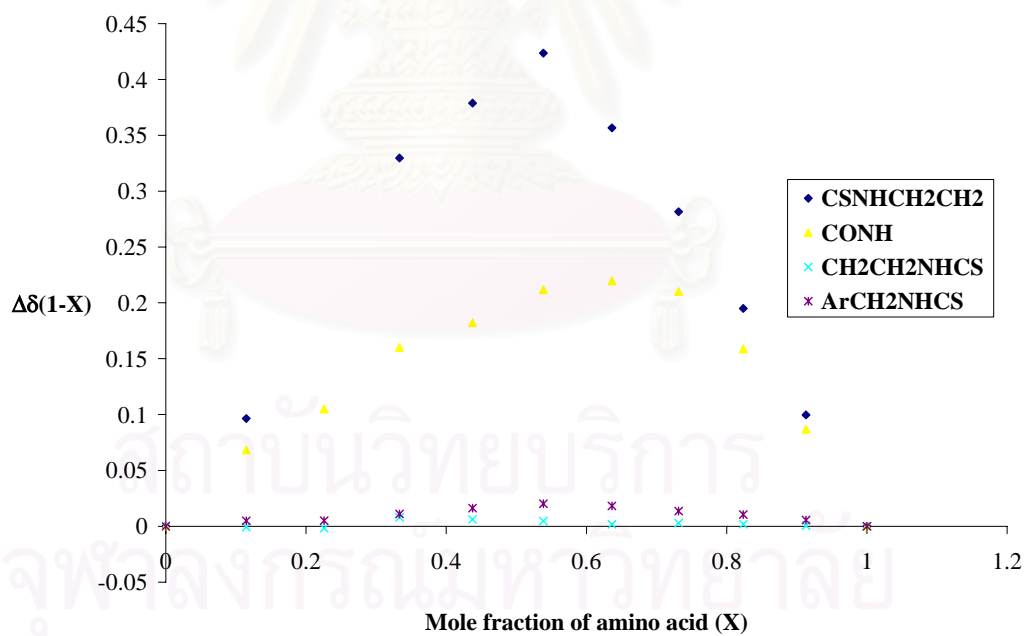
Solvent:	CD <sub>3</sub> CN
Starting volume of host solution:	600 μL
Concentration of host solution:	1.87 mM
Concentration of guest solution:	18.7 mM
Association constant:	8.27x10 <sup>3</sup> M <sup>-1</sup> (ave)

Volume added /μL	-NH <sup>b</sup> CH <sub>2</sub> - /ppm	-NH <sup>a</sup> CH <sub>2</sub> - /ppm	-CONH <sup>c</sup> - /ppm	-CH <sub>2</sub> <sup>e</sup> NH- /ppm	-CH <sub>2</sub> <sup>d</sup> NH- /ppm
0	7.0268	6.9651	7.5196	3.5329	4.6842
5	7.0760	7.0126	7.5881	3.5328	4.6834
10	7.1358	-	7.5969	3.5321	4.6897
20	-	-	7.6552	3.5306	4.6907
30	7.5213	-	7.7597	3.5450	4.7007
40	7.7002	-	7.8435	3.5439	4.7130
50	7.9446	-	7.9786	3.5431	4.7279
60	8.0076	-	8.1239	3.5375	4.7344
70	8.0751	-	8.3022	3.5435	4.7348
80	8.1318	-	8.4188	3.5435	4.7440
90	8.1732	-	8.5178	3.5398	4.7477
100	8.2087	-	8.5894	3.5387	4.7507
120	8.2601	-	8.7324	-	4.7542
140	8.2890	-	8.7930	-	4.7499
160	8.3073	-	8.8591	-	4.7492
180	8.3383	-	8.9382	-	4.7520
200	8.3571	-	9.0043	-	4.7472
250	8.3934	-	9.1143	-	4.7545
300	8.4166	-	9.1925	-	4.7500
350	8.4365	-	9.2310	-	4.7513
400	8.4489	-	9.2850	-	4.7494
<b>K<sub>I</sub></b>	<b>4.37x10<sup>3</sup></b>	<b>-</b>	<b>1.03x10<sup>3</sup></b>	<b>-</b>	<b>1.94x10<sup>4</sup></b>

Titration curves for carboxylate anion of glutamine with receptor **14** in  $\text{CD}_3\text{CN}$



Job's plots for carboxylate anion of glutamine with receptor **14** in  $\text{CH}_3\text{CN}$

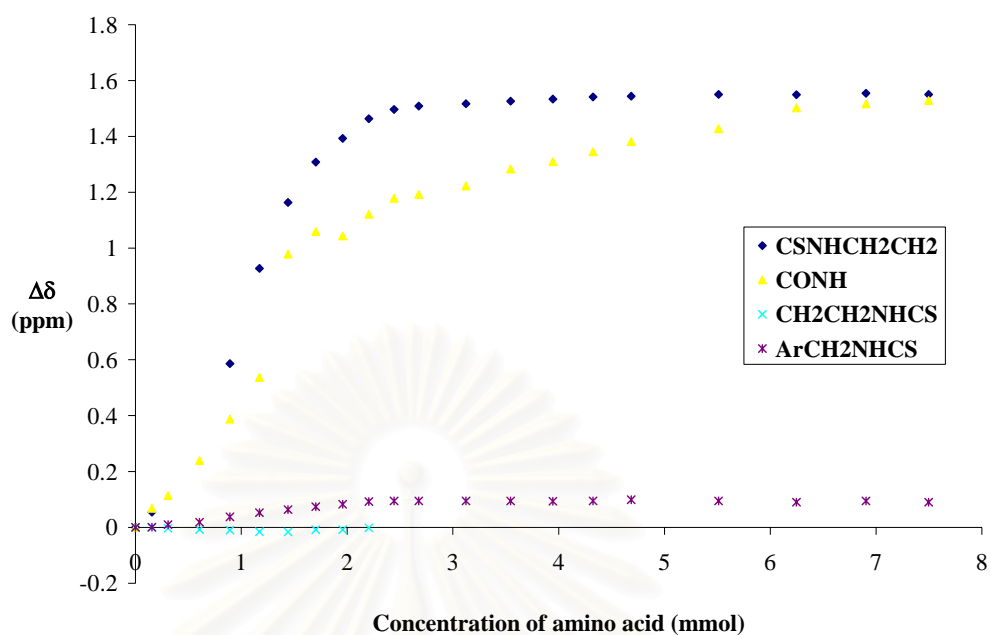


y) NMR titration data for carboxylate anion of phenylalanine with receptor **14** in  $\text{CD}_3\text{CN}$

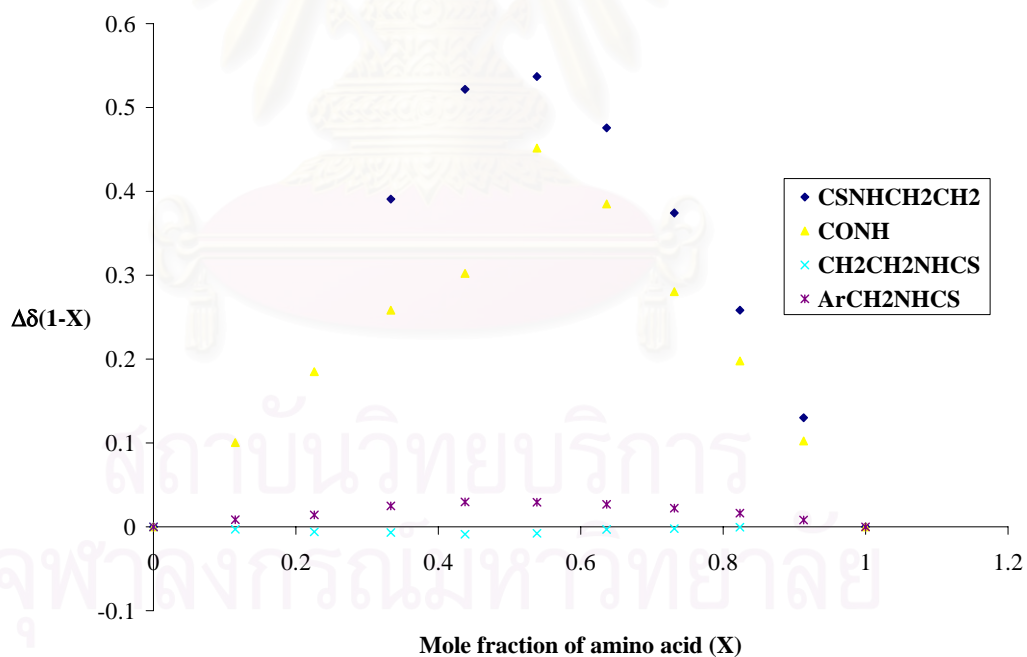
Solvent:	$\text{CD}_3\text{CN}$
Starting volume of host solution:	600 $\mu\text{L}$
Concentration of host solution:	1.87 mM
Concentration of guest solution:	18.7 mM
Association constant:	$2.48 \times 10^4 \text{ M}^{-1}$ (ave)

Volume added / $\mu\text{L}$	$-\text{NH}^b\text{CH}_2-$ /ppm	$-\text{NH}^a\text{CH}_2-$ /ppm	$-\text{CONH}^c-$ /ppm	$-\text{CH}_2^e\text{NH}-$ /ppm	$-\text{CH}_2^d\text{NH}-$ /ppm
0	7.0185	-	7.5088	3.5331	4.6809
5	7.0732	-	7.5772	3.5320	4.6817
10	-	-	7.6223	3.5299	4.6906
20	-	-	7.7479	3.5254	4.6992
30	7.6047	-	7.8963	3.5229	4.7184
40	7.9458	-	8.0461	3.5174	4.7336
50	8.1817	-	8.4873	3.5164	4.7444
60	8.3266	-	8.5676	3.5247	4.7547
70	8.4114	-	8.5522	3.5252	4.7635
80	8.4816	-	8.6301	3.5311	4.7733
90	8.5151	-	8.6872	-	4.7754
100	8.5271	-	8.7009	-	4.7755
120	8.5353	-	8.7315	-	4.7753
140	8.5447	-	8.7923	-	4.7754
160	8.5519	-	8.8185	-	4.7745
180	8.5597	-	8.8540	-	4.7755
200	8.5624	-	8.8900	-	4.7797
250	8.5686	-	8.9363	-	4.7755
300	8.5677	-	9.0110	-	4.7710
350	8.5729	-	9.0253	-	4.7753
400	8.5688	-	9.0374	-	4.7709
$K_I$	$4.00 \times 10^4$	-	$2.77 \times 10^3$	-	$3.16 \times 10^4$

Titration curves for carboxylate anion of phenylalanine with receptor **14** in  $\text{CD}_3\text{CN}$



Job's plots for carboxylate anion of phenylalanine with receptor **14** in  $\text{CH}_3\text{CN}$



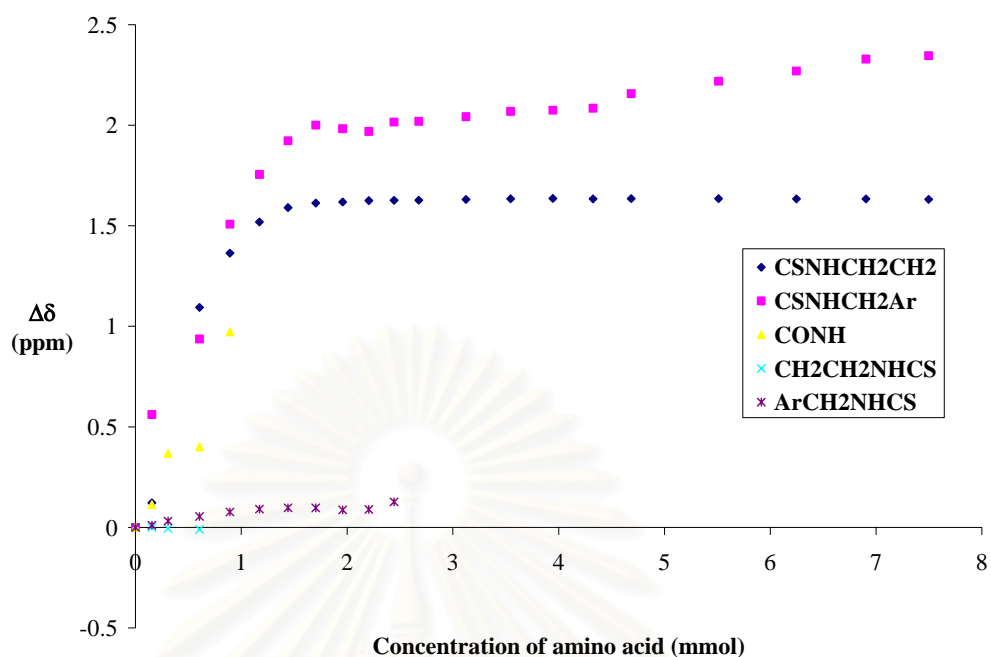
z) NMR titration data for carboxylate anion of leucine with receptor **14** in CD<sub>3</sub>CN

Solvent:	CD <sub>3</sub> CN
Starting volume of host solution:	600 μL
Concentration of host solution:	1.87 mM
Concentration of guest solution:	18.7 mM
Association constant:	4.96x10 <sup>4</sup> M <sup>-1</sup> (ave)

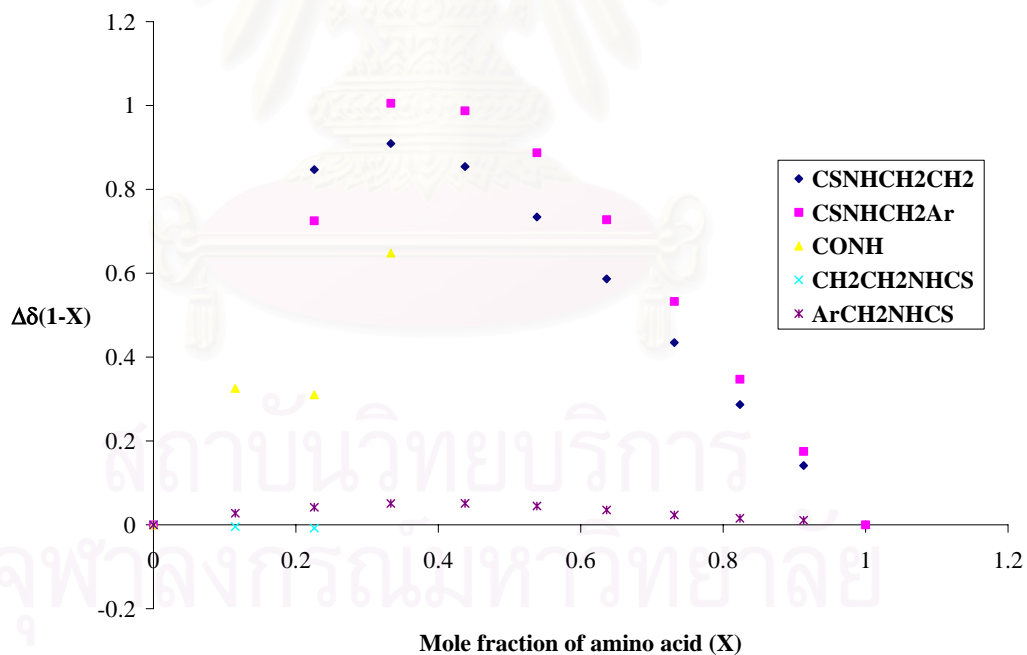
Volume added	-NH <sup>b</sup> CH <sub>2</sub> -	-NH <sup>a</sup> CH <sub>2</sub> -	-CONH <sup>c</sup> -	-CH <sub>2</sub> <sup>e</sup> NH-	-CH <sub>2</sub> <sup>d</sup> NH-
/μL	/ppm	/ppm	/ppm	/ppm	/ppm
0	7.0245	6.9662	7.5021	3.5329	4.6801
5	7.1468	7.5276	7.6156	3.5328	4.6910
10	-	-	7.8696	3.5280	4.7114
20	8.1185	7.9028	7.9028	3.5229	4.7342
30	8.3882	8.4739	8.4739	-	4.7565
40	8.5434	8.7213	-	-	4.7711
50	8.6149	8.8887	-	-	4.7775
60	8.6376	8.9669	-	-	4.7773
70	8.6424	8.9490	-	-	4.7674
80	8.6498	8.9350	-	-	4.7697
90	8.6508	8.9821	-	-	4.8070
100	8.6514	8.9856	-	-	-
120	8.6554	9.0085	-	-	-
140	8.6585	9.0352	-	-	-
160	8.6602	9.0407	-	-	-
180	8.6580	9.0506	-	-	-
200	8.6596	9.1232	-	-	-
250	8.6596	9.1848	-	-	-
300	8.6582	9.2355	-	-	-
350	8.6580	9.2949	-	-	-
400	8.6558	9.3125	-	-	-
<b>K<sub>I</sub></b>	<b>8.64x10<sup>4</sup></b>	<b>1.27x10<sup>4</sup></b>	-	-	-

จุฬาลงกรณ์มหาวิทยาลัย

Titration curves for carboxylate anion of leucine with receptor **14** in  $\text{CD}_3\text{CN}$



Job's plots for carboxylate anion of leucine with receptor **14** in  $\text{CH}_3\text{CN}$



aa) NMR titration data for carboxylate anion of threonine with receptor **14** in CD<sub>3</sub>CN

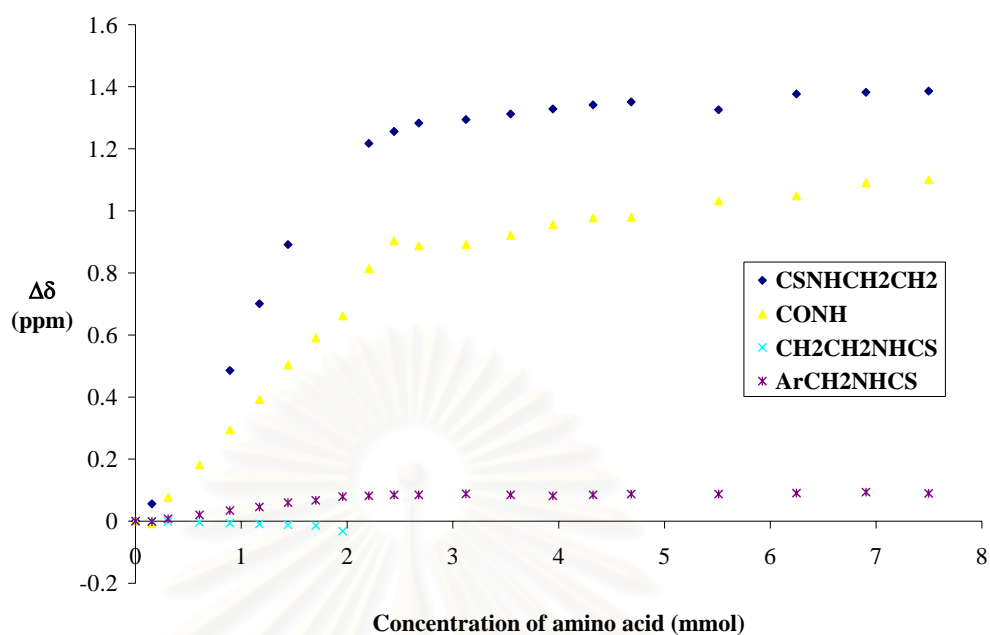
Solvent:	CD <sub>3</sub> CN
Starting volume of host solution:	600 μL
Concentration of host solution:	1.87 mM
Concentration of guest solution:	18.7 mM
Association constant:	1.03x10 <sup>4</sup> M <sup>-1</sup> (ave)

Volume added /μL	-NH <sup>b</sup> CH <sub>2</sub> - /ppm	-NH <sup>a</sup> CH <sub>2</sub> - /ppm	-CONH <sup>c</sup> - /ppm	-CH <sub>2</sub> <sup>e</sup> NH- /ppm	-CH <sub>2</sub> <sup>d</sup> NH- /ppm
0	7.0191	-	7.5265	3.5330	4.6841
5	7.0751	-	7.5182	3.5324	4.6830
10	-	-	7.6027	3.5316	4.6916
20	-	-	7.7080	3.5295	4.7043
30	7.5047	-	7.8205	3.5265	4.7184
40	7.7197	-	7.9189	3.5237	4.7298
50	7.9106	-	8.0306	3.5212	4.7435
60	-	-	8.1166	3.5188	4.7512
70	-	-	8.1880	3.5009	4.7630
80	8.2364	-	8.3409	-	4.7655
90	8.2749	-	8.4300	-	4.7687
100	8.3017	-	8.4135	-	4.7691
120	8.3135	-	8.4179	-	4.7721
140	8.3314	-	8.4476	-	4.7691
160	8.3475	-	8.4819	-	4.7656
180	8.3608	-	8.5041	-	4.7689
200	8.3702	-	8.5064	-	4.7715
250	8.3448	-	8.5583	-	4.7712
300	8.3956	-	8.5745	-	4.7746
350	8.4013	-	8.6169	-	4.7777
400	8.4051	-	8.6269	-	4.7736
<b>K<sub>I</sub></b>	<b>1.18x10<sup>4</sup></b>	-	<b>1.90x10<sup>3</sup></b>	-	<b>1.71x10<sup>4</sup></b>

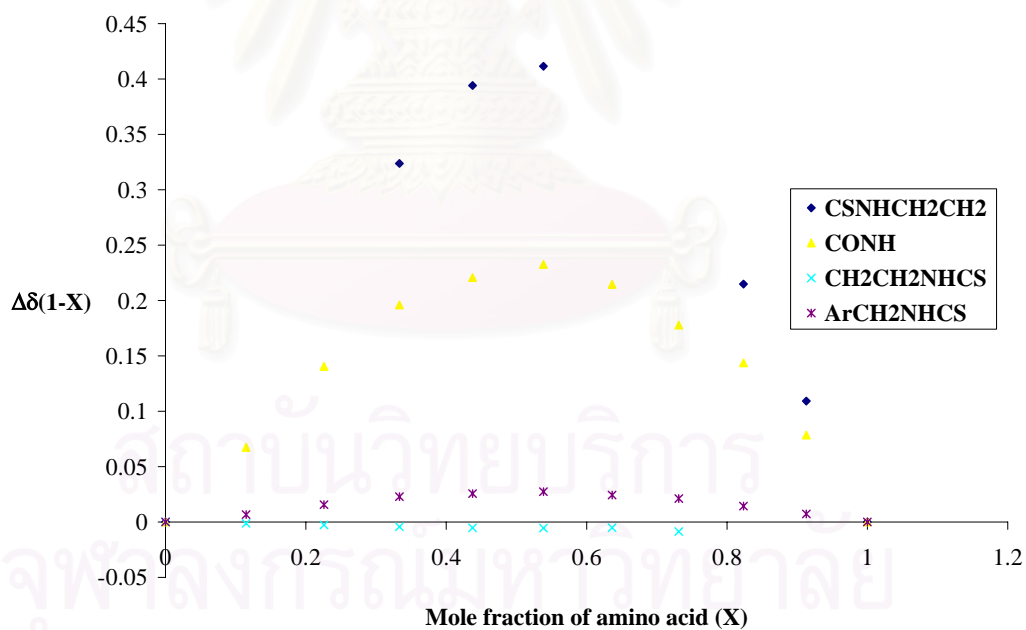
จุฬาลงกรณ์มหาวิทยาลัย



Titration curves for carboxylate anion of threonine with receptor **14** in  $\text{CD}_3\text{CN}$



Job's plots for carboxylate anion of threonine with receptor **14** in  $\text{CH}_3\text{CN}$



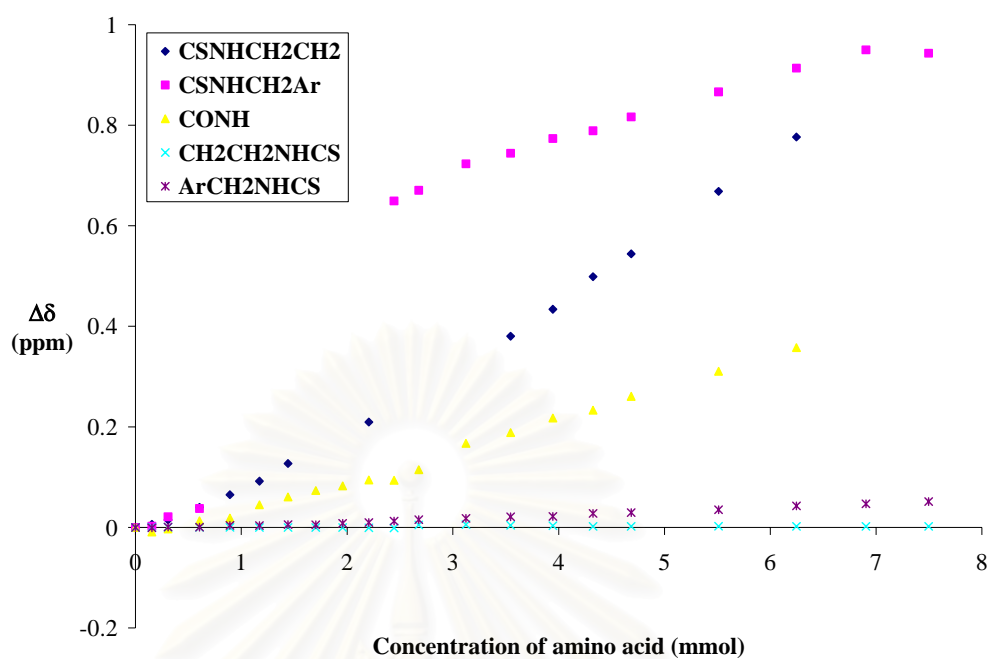
ab) NMR titration data for carboxylate anion of serine with receptor **14** in CD<sub>3</sub>CN

Solvent:	CD <sub>3</sub> CN
Starting volume of host solution:	600 μL
Concentration of host solution:	1.87 mM
Concentration of guest solution:	18.7 mM
Association constant:	0.95x10 <sup>0</sup> M <sup>-1</sup> (ave)

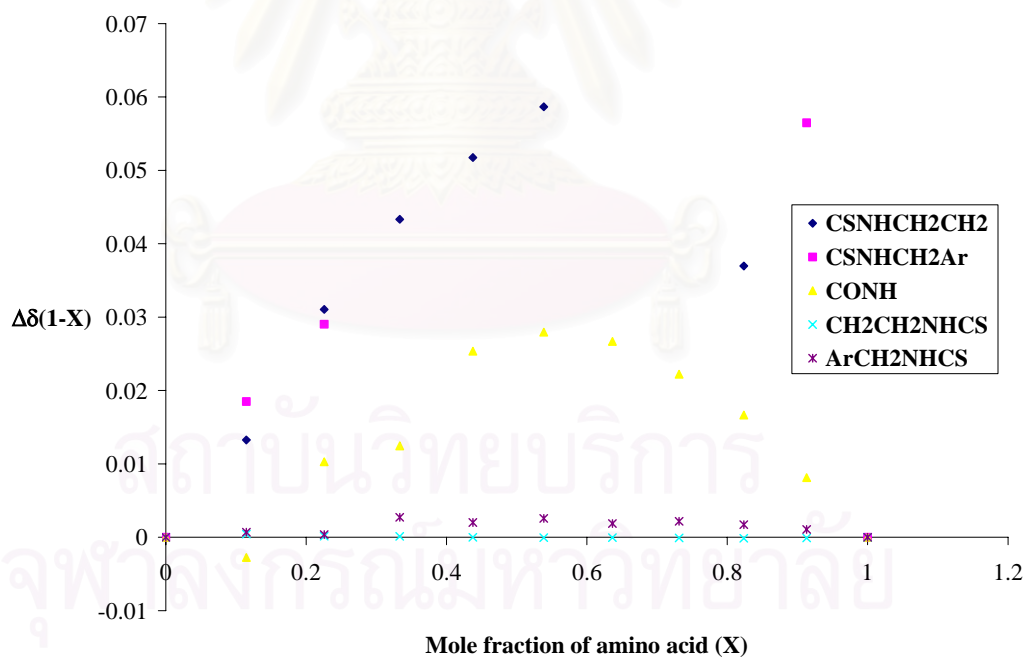
Volume added /μL	-NH <sup>b</sup> CH <sub>2</sub> - /ppm	-NH <sup>a</sup> CH <sub>2</sub> - /ppm	-CONH <sup>c</sup> - /ppm	-CH <sub>2</sub> <sup>e</sup> NH- /ppm	-CH <sub>2</sub> <sup>d</sup> NH- /ppm
0	7.0219	6.9751	7.5308	3.5331	4.6829
5	7.0280	6.9773	7.5218	3.5336	4.6821
10	7.0369	6.9960	7.5277	3.5336	4.6837
20	7.0620	7.0126	7.5441	3.5333	4.6834
30	7.0869	-	7.5495	3.5333	4.6870
40	7.1139	-	7.5759	3.5331	4.6865
50	7.1490	-	7.5914	3.5330	4.6885
60	-	-	7.6042	3.5330	4.6881
70	-	-	7.6135	3.5328	4.6910
80	7.2314	-	7.6253	3.5324	4.6927
90	-	7.6245	7.6245	3.5320	4.6953
100	-	7.6456	7.6456	3.5380	4.6981
120	-	7.6983	7.6983	3.5385	4.7009
140	7.4022	7.7193	7.7193	3.5374	4.7041
160	7.4557	7.7486	7.7486	3.5364	4.7047
180	7.5207	7.7641	7.7641	3.5350	4.7106
200	7.5661	7.7915	7.7915	3.5351	4.7125
250	7.6904	7.8414	7.8414	3.5354	4.7182
300	7.7984	7.8886	7.8886	3.5352	4.7259
350	-	7.9249	-	3.5352	4.7297
400	-	7.9182	-	3.5351	4.7343
<b>K<sub>I</sub></b>	-	-	<b>1.28x10<sup>0</sup></b>	-	<b>1.29x10<sup>0</sup></b>

จุฬาลงกรณ์มหาวิทยาลัย

Titration curves for carboxylate anion of serine with receptor **14** in  $\text{CD}_3\text{CN}$



Job's plots for carboxylate anion of serine with receptor **14** in  $\text{CH}_3\text{CN}$

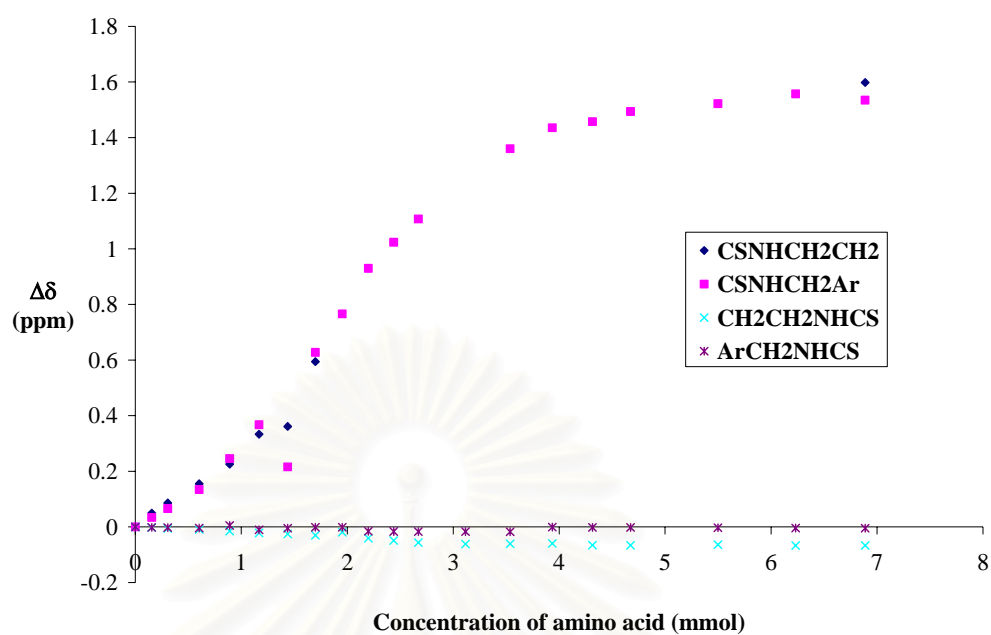


ac) NMR titration data for carboxylate anion of aspartic acid with receptor **15** in  $\text{CD}_3\text{CN}$

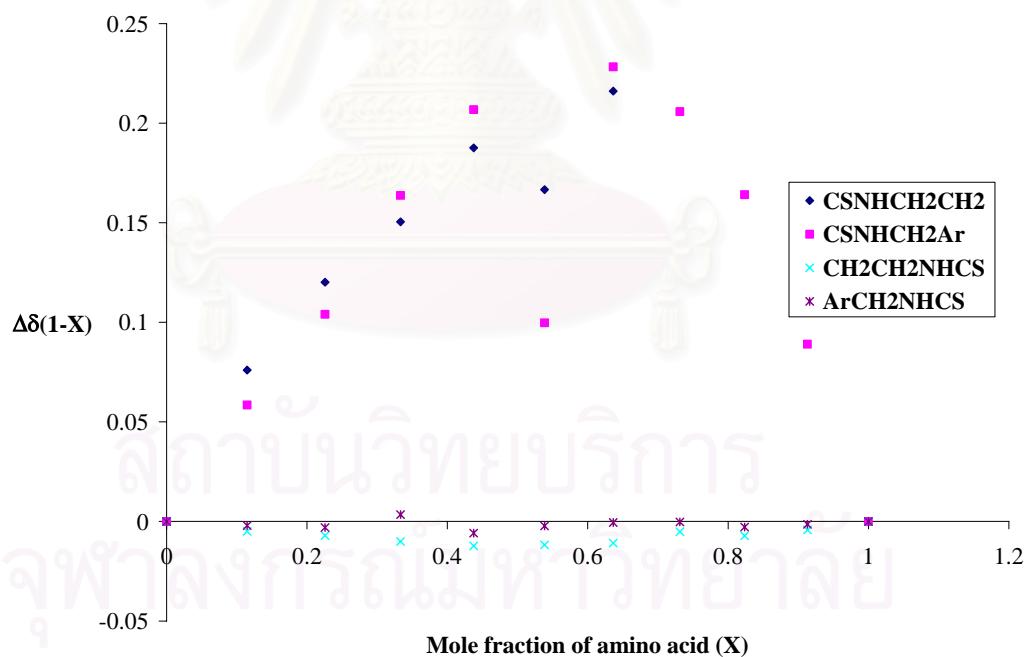
Solvent:	$\text{CD}_3\text{CN}$
Starting volume of host solution:	600 $\mu\text{L}$
Concentration of host solution:	3.74 mM
Concentration of guest solution:	37.4 mM
Association constant:	$1.77 \times 10^4 \text{ M}^{-1}$ (ave)

Volume added / $\mu\text{L}$	$-\text{NH}^{\text{b}}\text{CH}_2-$ /ppm	$-\text{NH}^{\text{a}}\text{CH}_2-$ /ppm	$-\text{CH}_2^{\text{c}}\text{NH}-$ /ppm	$-\text{CH}_2^{\text{d}}\text{NH}-$ /ppm
0	8.1638	8.1066	3.6732	4.6647
5	8.2133	8.1407	3.6710	4.6628
10	8.2497	8.1727	3.6676	4.6624
20	8.3190	8.2410	3.6641	4.6608
30	8.3895	8.3522	3.6581	4.6699
40	8.4973	8.4743	3.6514	4.6543
50	8.5248	8.3227	3.6478	4.6599
60	8.7581	8.7344	3.6433	4.6633
70	-	8.8726	3.6541	4.6637
80	-	9.0365	3.6325	4.6489
90	-	9.1304	3.6244	4.6483
100	-	9.2139	3.6167	4.6479
120	-	-	3.6116	4.6479
140	-	9.4668	3.6124	4.6472
160	-	9.5423	3.6137	4.6639
180	-	9.5642	3.6078	4.6630
200	-	9.6006	3.6071	4.6628
250	-	9.6286	3.6093	4.6618
300	-	9.6638	3.6060	4.6608
350	9.7618	9.6416	3.6063	4.6602
400	-	-	-	-
$K_I$	-	$1.93 \times 10^4$	$8.85 \times 10^3$	-

Titration curves for carboxylate anion of aspartic acid with receptor **15** in  $\text{CD}_3\text{CN}$



Job's plots for carboxylate anion of aspartic acid with receptor **15** in  $\text{CH}_3\text{CN}$

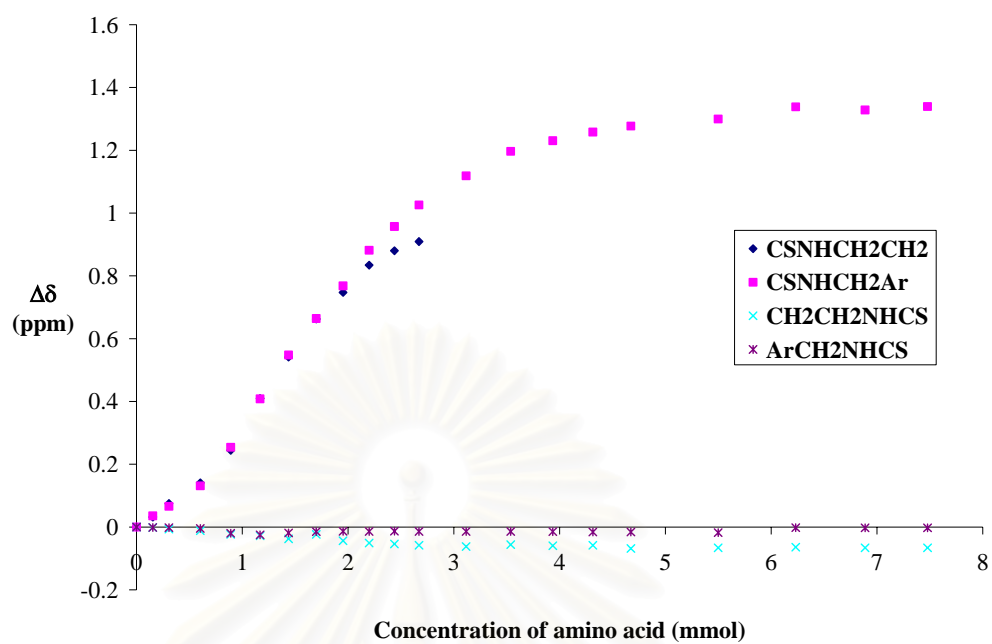


ad) NMR titration data for carboxylate anion of glutamic acid with receptor 15 in CD<sub>3</sub>CN

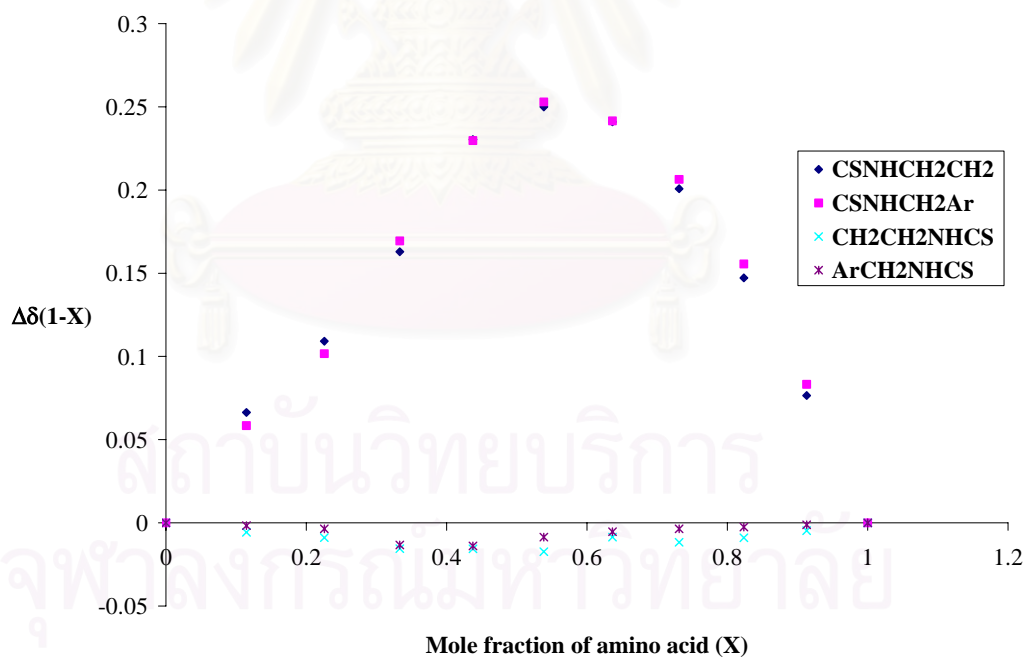
Solvent: CD<sub>3</sub>CN  
 Starting volume of host solution: 600 μL  
 Concentration of host solution: 3.74 mM  
 Concentration of guest solution: 37.4 mM  
 Association constant: 1.19x10<sup>4</sup> M<sup>-1</sup> (ave)

Volume added /μL	-NH <sup>b</sup> CH <sub>2</sub> - /ppm	-NH <sup>a</sup> CH <sub>2</sub> - /ppm	-CH <sub>2</sub> <sup>e</sup> NH- /ppm	-CH <sub>2</sub> <sup>d</sup> NH- /ppm
0	8.1882	8.1112	3.6930	4.6778
5	8.2201	8.1468	3.6915	4.6766
10	8.2632	8.1772	3.6866	4.6759
20	8.3292	8.2425	3.6815	4.6732
30	8.4326	8.3653	3.6698	4.6579
40	8.5977	8.5195	3.6653	4.6532
50	8.7297	8.6592	3.6555	4.6592
60	8.8508	8.7754	3.6695	4.6632
70	8.9355	8.8794	3.6494	4.6644
80	9.0224	8.9927	3.6424	4.6637
90	9.0683	9.0683	3.6393	4.6647
100	9.0974	9.1369	3.6351	4.6638
120	-	9.2297	3.6308	4.6637
140	-	9.3076	3.6369	4.6634
160	-	9.3417	3.6335	4.6630
180	-	9.3691	3.6349	4.6619
200	-	9.3882	3.6247	4.6621
250	-	9.4109	3.6270	4.6601
300	-	9.4494	3.6288	4.6757
350	-	9.4395	3.6269	4.6751
400	-	9.4505	3.6269	4.6750
<b>K<sub>I</sub></b>	-	<b>1.06x10<sup>4</sup></b>	<b>1.55x10<sup>4</sup></b>	<b>9.67x10<sup>3</sup></b>

Titration curves for carboxylate anion of glutamic acid with receptor **15** in  $\text{CD}_3\text{CN}$



Job's plots for carboxylate anion of glutamic acid with receptor **15** in  $\text{CH}_3\text{CN}$



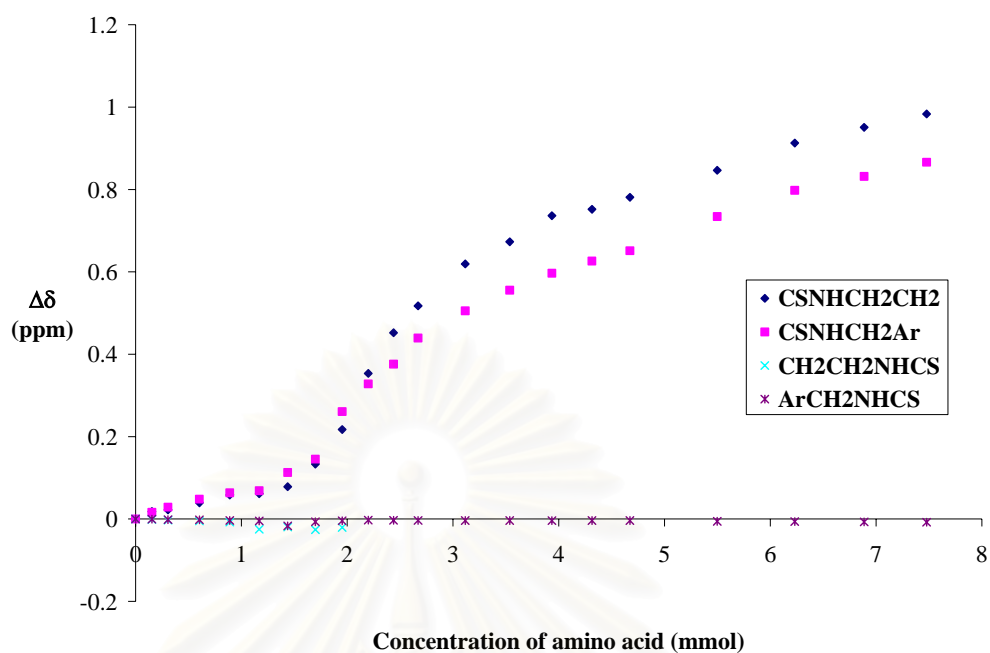
ae) NMR titration data for carboxylate anion of asparagine with receptor 15 in CD<sub>3</sub>CN

Solvent:	CD <sub>3</sub> CN
Starting volume of host solution:	600 μL
Concentration of host solution:	3.74 mM
Concentration of guest solution:	37.4 mM
Association constant:	$K_1$ : $8.90 \times 10^5 \text{ M}^{-1}$ (ave)
	$K_2$ : $1.49 \times 10^3 \text{ M}^{-1}$ (ave)

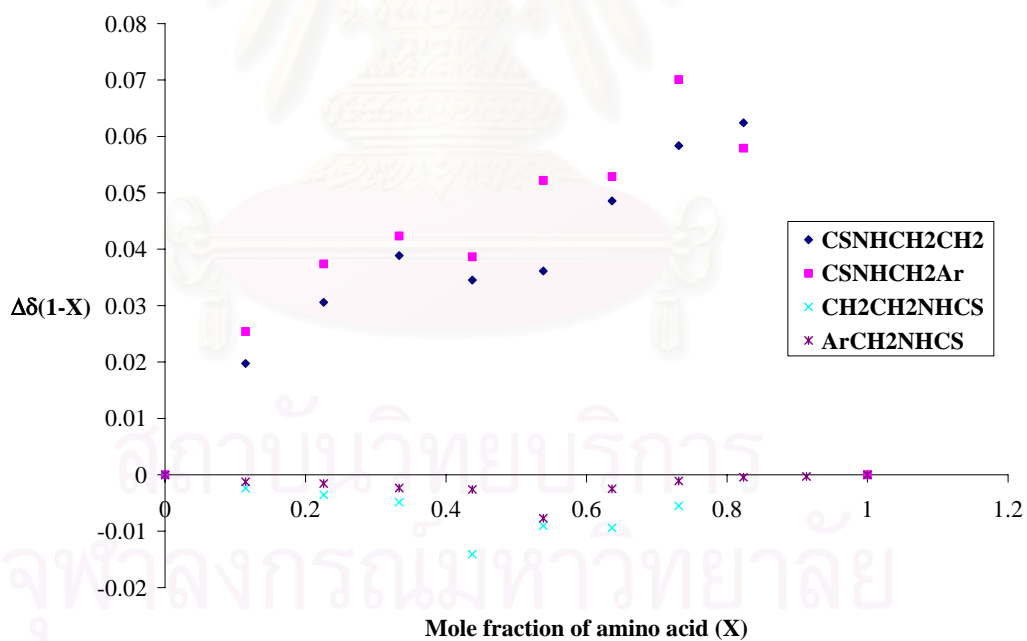
Volume added /μL	-NH <sup>b</sup> CH <sub>2</sub> - /ppm	-NH <sup>a</sup> CH <sub>2</sub> - /ppm	-CH <sub>2</sub> <sup>e</sup> NH- /ppm	-CH <sub>2</sub> <sup>d</sup> NH- /ppm
0	8.2701	8.1637	3.6955	4.6766
5	8.2881	8.1799	3.6942	4.6761
10	8.2924	8.1924	3.6928	4.6752
20	8.3096	8.2120	3.6909	4.6746
30	8.3284	8.2272	3.6882	4.6731
40	8.3315	8.2324	3.6705	4.6720
50	8.3484	8.2768	3.6759	4.6599
60	8.4036	8.3091	3.6696	4.6698
70	8.4873	8.4245	3.6759	4.6726
80	8.6237	8.4918	-	4.6741
90	8.7222	8.5397	-	4.6733
100	8.7876	8.6039	-	4.6731
120	8.8893	8.6692	-	4.6729
140	8.9431	8.7193	-	4.6730
160	9.0064	8.7603	-	4.6728
180	9.0229	8.7899	-	4.6730
200	9.0512	8.8159	-	4.6729
250	9.1167	8.8979	-	4.6709
300	9.1827	8.9617	-	4.6706
350	9.2209	8.9954	-	4.6695
400	9.2534	9.0297	-	4.6688
<b><math>K_1</math></b>	<b><math>1.75 \times 10^6</math></b>	<b><math>3.09 \times 10^4</math></b>	-	-
<b><math>K_2</math></b>	<b><math>8.01 \times 10^2</math></b>	<b><math>2.17 \times 10^3</math></b>	-	-



Titration curves for carboxylate anion of asparagine with receptor **15** in  $\text{CD}_3\text{CN}$



Job's plots for carboxylate anion of asparagine with receptor **15** in  $\text{CH}_3\text{CN}$

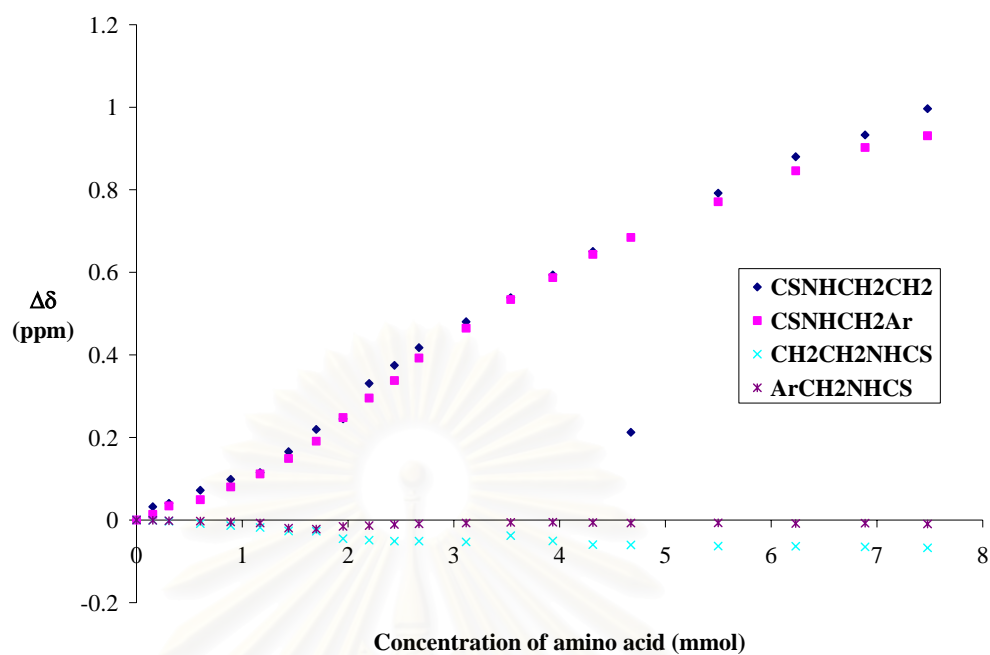


af) NMR titration data for carboxylate anion of glutamine with receptor **15** in CD<sub>3</sub>CN

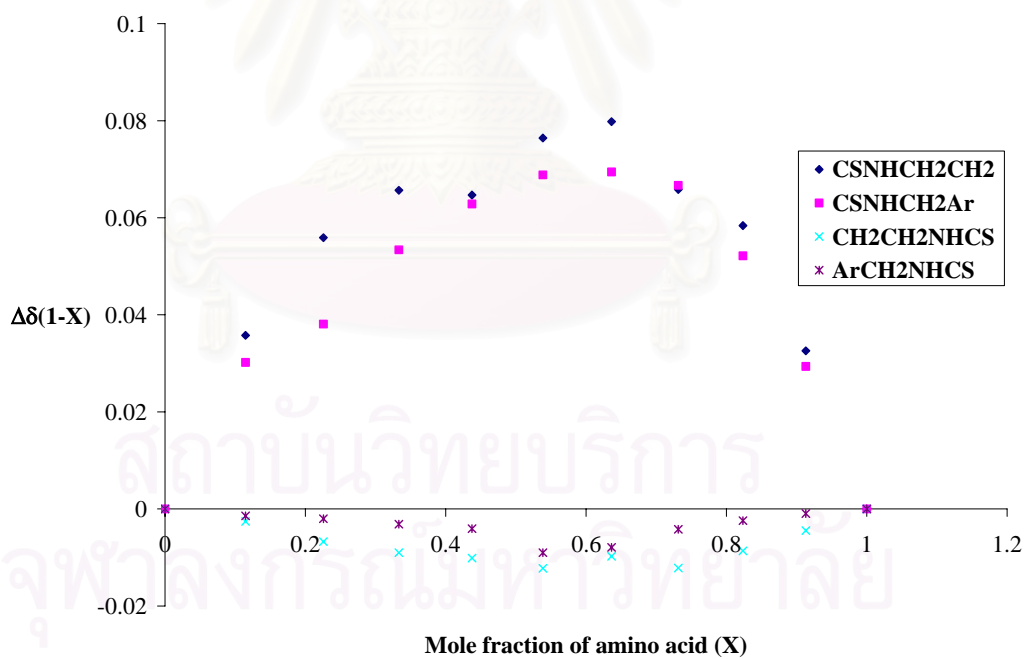
Solvent:	CD <sub>3</sub> CN
Starting volume of host solution:	600 μL
Concentration of host solution:	3.74 mM
Concentration of guest solution:	37.4 mM
Association constant:	$K_1$ : $3.91 \times 10^4 \text{ M}^{-1}$ (ave)
	$K_2$ : $7.23 \times 10^2 \text{ M}^{-1}$ (ave)

Volume added /μL	-NH <sup>b</sup> CH <sub>2</sub> - /ppm	-NH <sup>a</sup> CH <sub>2</sub> - /ppm	-CH <sub>2</sub> <sup>c</sup> NH- /ppm	-CH <sub>2</sub> <sup>d</sup> NH- /ppm
0	8.2554	8.1696	3.6949	4.6771
5	8.2876	8.1834	3.6940	4.6762
10	8.2958	8.2037	3.6920	4.6755
20	8.3276	8.2188	3.6862	4.6745
30	8.3539	8.2497	3.6814	4.6724
40	8.3704	8.2813	3.6769	4.6699
50	8.4210	8.3187	3.6684	4.6576
60	8.4749	8.3605	3.6681	4.6553
70	8.5004	8.4178	3.6497	4.6615
80	8.5862	8.4651	3.6460	4.6635
90	8.6302	8.5075	3.6438	4.6663
100	8.6730	8.5620	3.6438	4.6680
120	8.7358	8.6342	3.6417	4.6697
140	8.7942	8.7037	3.6572	4.6712
160	8.8492	8.7568	3.6444	4.6718
180	8.9061	8.8130	3.6353	4.6711
200	8.9667	8.8541	3.6346	4.6698
250	9.0472	8.9405	3.6317	4.6703
300	9.1354	9.0156	3.6313	4.6687
350	9.1882	9.0721	3.6298	4.6693
400	9.2519	9.1005	3.6275	4.6675
$K_1$	$9.46 \times 10^3$	$1.10 \times 10^4$	$9.69 \times 10^4$	-
$K_2$	$4.29 \times 10^2$	$6.99 \times 10^2$	$1.04 \times 10^3$	-

Titration curves for carboxylate anion of glutamine with receptor **15** in  $\text{CD}_3\text{CN}$



Job's plots for carboxylate anion of glutamine with receptor **15** in  $\text{CH}_3\text{CN}$

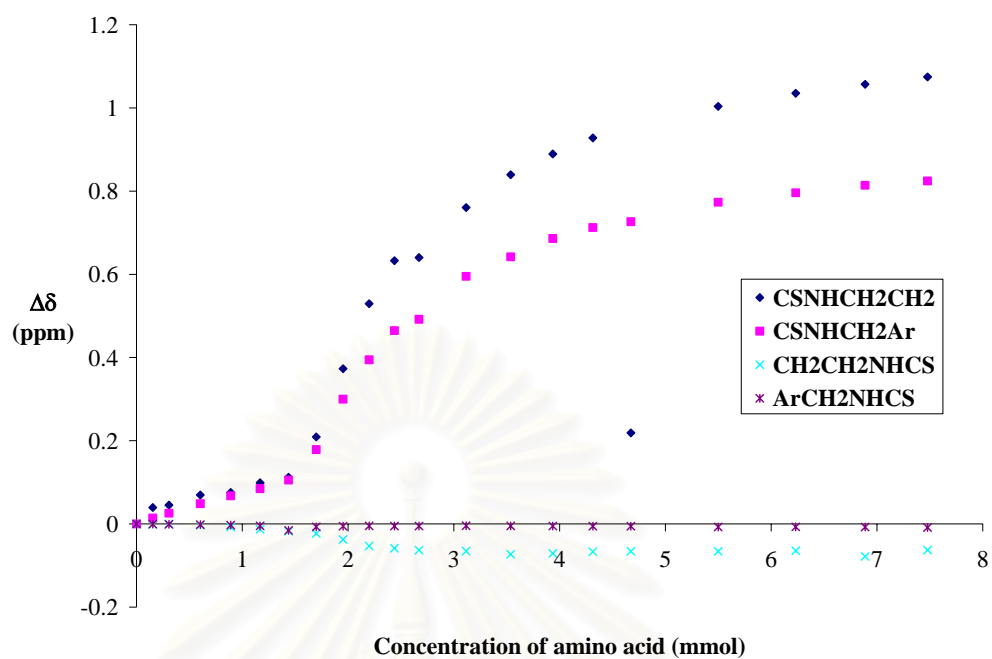


ag) NMR titration data for carboxylate anion of phenylalanine with receptor **15** in  $CD_3CN$

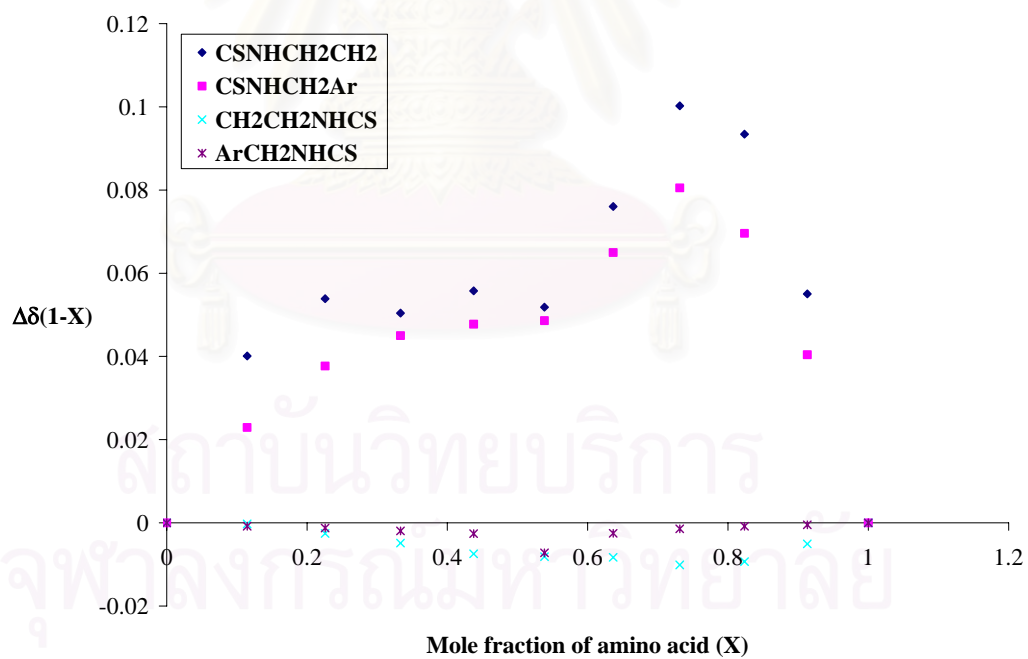
Solvent:	$CD_3CN$
Starting volume of host solution:	600 $\mu$ L
Concentration of host solution:	3.74 mM
Concentration of guest solution:	37.4 mM
Association constant:	$K_1$ : $1.48 \times 10^7 M^{-1}$ (ave) $K_2$ : $2.94 \times 10^3 M^{-1}$ (ave)

Volume added / $\mu$ L	$-NH^bCH_2-$ /ppm	$-NH^aCH_2-$ /ppm	$-CH_2^cNH-$ /ppm	$-CH_2^dNH-$ /ppm
0	8.2515	8.1719	3.6956	4.6784
5	8.2909	8.1860	3.6945	4.6777
10	8.2968	8.1978	3.6953	4.6775
20	8.3211	8.2206	3.6923	4.6768
30	8.3271	8.2394	3.6883	4.6755
40	8.3506	8.2568	3.6824	4.6738
50	8.3638	8.2772	3.6780	4.6628
60	8.4606	8.3506	3.6728	4.6715
70	8.6246	8.4716	3.658	4.6731
80	8.7809	8.5663	3.6428	4.6737
90	8.8843	8.6366	3.6373	4.6732
100	8.8919	8.6638	3.6325	4.6732
120	9.0121	8.7670	3.6303	4.6740
140	9.0909	8.8140	3.6228	4.6737
160	9.1408	8.8579	3.6247	4.6735
180	9.1792	8.8845	3.6288	4.6729
200	9.2098	8.8984	3.6299	4.6727
250	9.2552	8.9452	3.6299	4.6710
300	9.2866	8.9679	3.6312	4.6712
350	9.3081	8.9859	3.6176	4.6709
400	9.3258	8.9963	3.6327	4.6698
$K_1$	$4.43 \times 10^7$	$4.24 \times 10^3$	$2.34 \times 10^5$	-
$K_2$	$3.28 \times 10^3$	$5.37 \times 10^3$	$1.83 \times 10^2$	-

Titration curves for carboxylate anion of phenylalanine with receptor **15** in  $\text{CD}_3\text{CN}$



Job's plots for carboxylate anion of phenylalanine with receptor **15** in  $\text{CH}_3\text{CN}$



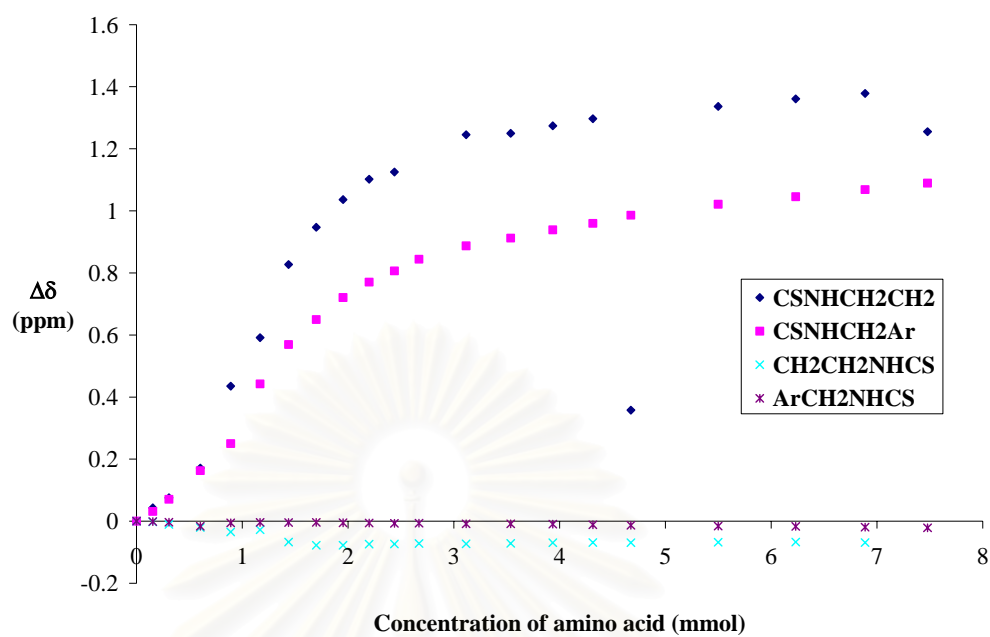
ah) NMR titration data for carboxylate anion of leucine with receptor **15** in CD<sub>3</sub>CN

Solvent:	CD <sub>3</sub> CN
Starting volume of host solution:	600 μL
Concentration of host solution:	3.74 mM
Concentration of guest solution:	37.4 mM
Association constant:	1.02x10 <sup>4</sup> M <sup>-1</sup> (ave)

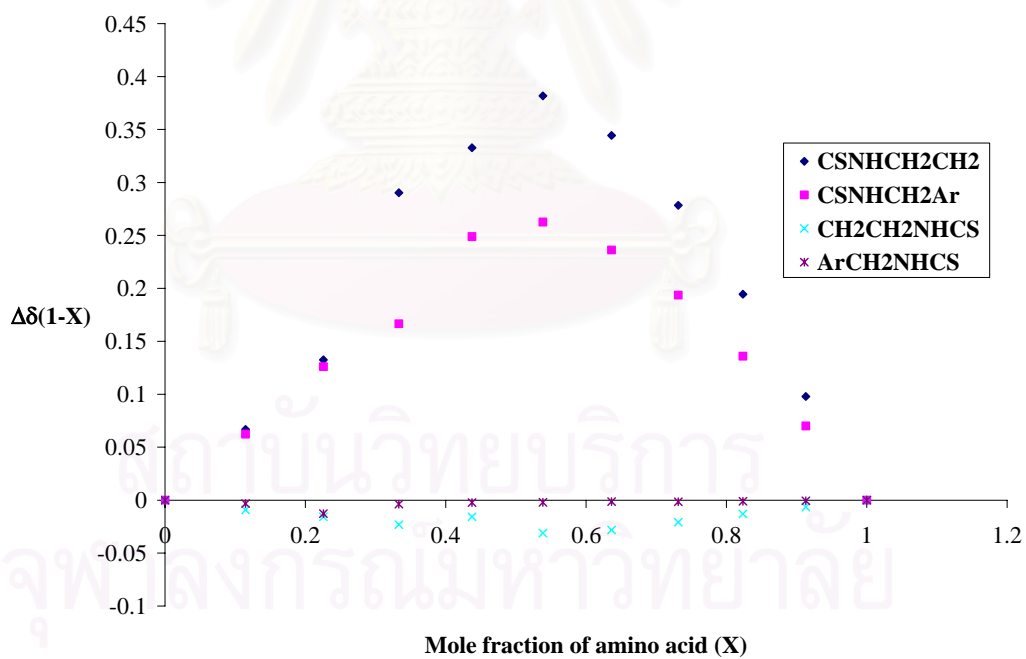
Volume added /μL	-NH <sup>b</sup> CH <sub>2</sub> - /ppm	-NH <sup>a</sup> CH <sub>2</sub> - /ppm	-CH <sub>2</sub> <sup>e</sup> NH- /ppm	-CH <sub>2</sub> <sup>d</sup> NH- /ppm
0	8.2543	8.1647	3.6962	4.6785
5	8.2969	8.1958	3.6938	4.6772
10	8.3298	8.2352	3.6859	4.6749
20	8.4254	8.3275	3.6760	4.6621
30	8.6896	8.4145	3.6615	4.6729
40	8.8458	8.6070	3.6683	4.6745
50	9.0814	8.7338	3.6289	4.6741
60	9.2013	8.8142	3.6188	4.6747
70	9.2905	8.8855	3.6188	4.6732
80	9.3565	8.9350	3.6222	4.6727
90	9.3796	8.9713	3.6225	4.6713
100	-	9.0088	3.6243	4.6718
120	9.4996	9.0517	3.6231	4.6697
140	9.5040	9.0770	3.6246	4.6697
160	9.5282	9.1034	3.6265	4.6685
180	9.5513	9.1243	3.6273	4.6668
200	9.5766	9.1507	3.6268	4.6653
250	9.5908	9.1858	3.6283	4.6627
300	9.6152	9.2102	3.6289	4.6615
350	9.6328	9.2334	3.6270	4.6591
400	9.5095	9.2542	-	4.6570
<b>K<sub>I</sub></b>	<b>6.35x10<sup>3</sup></b>	<b>1.90x10<sup>3</sup></b>	<b>2.22x10<sup>4</sup></b>	-

จุฬาลงกรณ์มหาวิทยาลัย

Titration curves for carboxylate anion of leucine with receptor **15** in  $\text{CD}_3\text{CN}$



Job's plots for carboxylate anion of leucine with receptor **15** in  $\text{CH}_3\text{CN}$



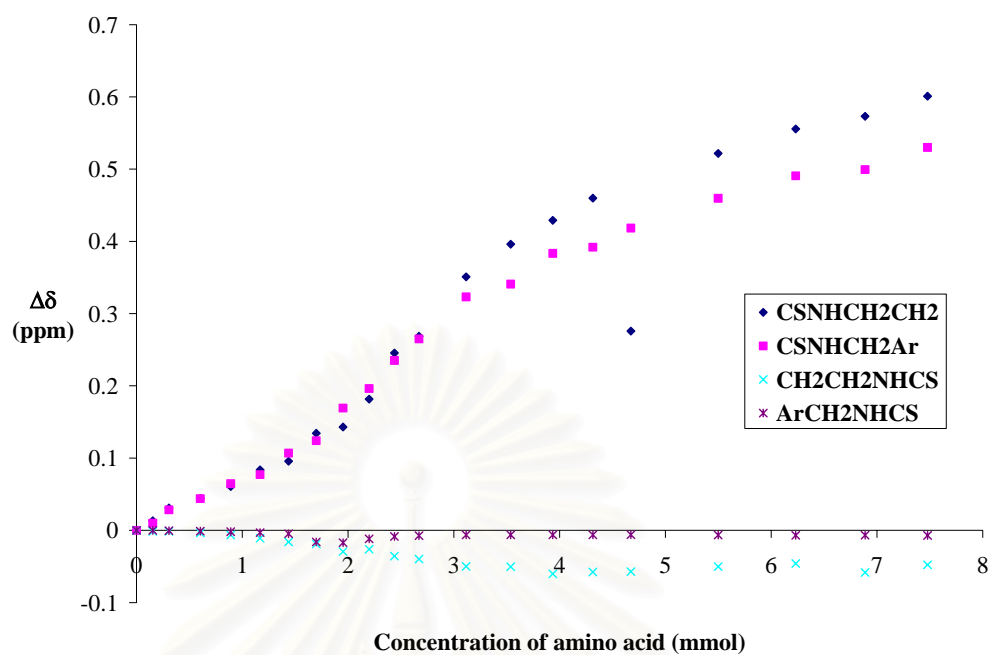
ai) NMR titration data for carboxylate anion of threonine with receptor **15** in CD<sub>3</sub>CN

Solvent:	CD <sub>3</sub> CN
Starting volume of host solution:	600 μL
Concentration of host solution:	3.74 mM
Concentration of guest solution:	37.4 mM
Association constant:	$K_1$ : $1.71 \times 10^4 \text{ M}^{-1}$ (ave) $K_2$ : $1.82 \times 10^3 \text{ M}^{-1}$ (ave)

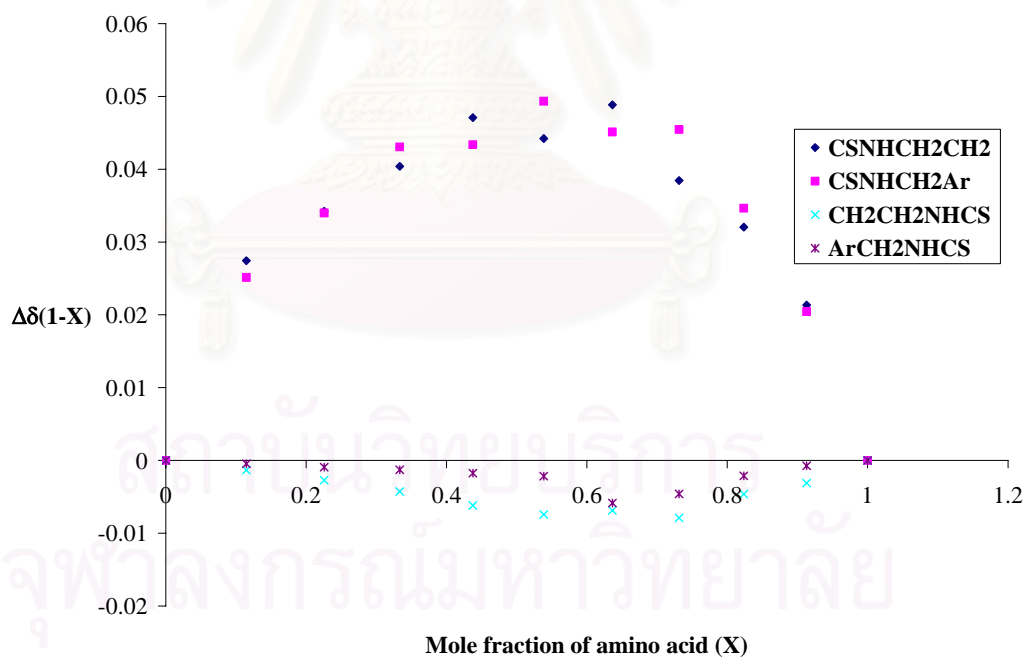
Volume added /μL	-NH <sup>b</sup> CH <sub>2</sub> - /ppm	-NH <sup>a</sup> CH <sub>2</sub> - /ppm	-CH <sub>2</sub> <sup>e</sup> NH- /ppm	-CH <sub>2</sub> <sup>d</sup> NH- /ppm
0	8.2592	8.1682	3.6959	4.6780
5	8.2724	8.1780	3.6945	4.6781
10	8.2902	8.1966	3.6944	4.6775
20	8.3034	8.2121	3.6924	4.6768
30	8.3198	8.2328	3.6895	4.6761
40	8.3429	8.2453	3.6849	4.6749
50	8.3550	8.2751	3.6798	4.6733
60	8.3935	8.2923	3.6770	4.6619
70	8.4023	8.3374	3.6665	4.6609
80	8.4408	8.3645	3.6697	4.6661
90	8.5047	8.4034	3.6602	4.6695
100	8.5278	8.4331	3.6561	4.6707
120	8.6102	8.4913	3.6461	4.6717
140	8.6553	8.5091	3.6456	4.6719
160	8.6883	8.5515	3.6356	4.6717
180	8.7190	8.5601	3.6382	4.6719
200	8.7457	8.5865	3.6387	4.6720
250	8.7809	8.6278	3.6457	4.6715
300	8.8149	8.6589	3.6499	4.6711
350	8.8324	8.6676	3.6376	4.6714
400	8.8602	8.6983	3.6483	4.6710
<b><math>K_1</math></b>	<b><math>2.02 \times 10^4</math></b>	<b><math>2.18 \times 10^4</math></b>	<b><math>9.18 \times 10^3</math></b>	-
<b><math>K_2</math></b>	<b><math>2.68 \times 10^3</math></b>	<b><math>1.82 \times 10^3</math></b>	<b><math>9.61 \times 10^2</math></b>	-



Titration curves for carboxylate anion of threonine with receptor **15** in  $\text{CD}_3\text{CN}$



Job's plots for carboxylate anion of threonine with receptor **15** in  $\text{CH}_3\text{CN}$

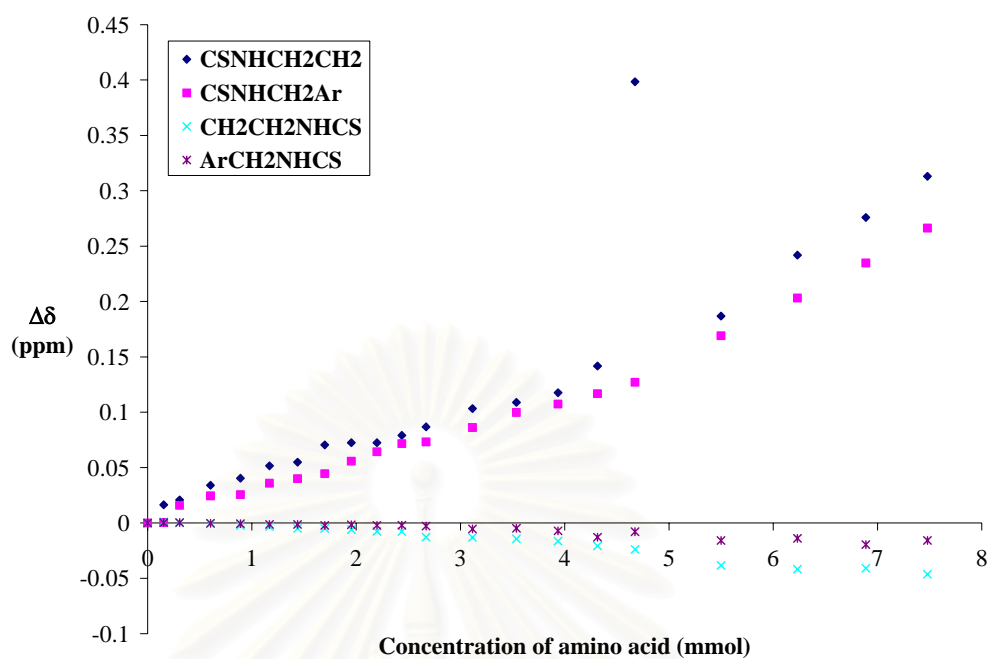


aj) NMR titration data for carboxylate anion of serine with receptor **15** in CD<sub>3</sub>CN

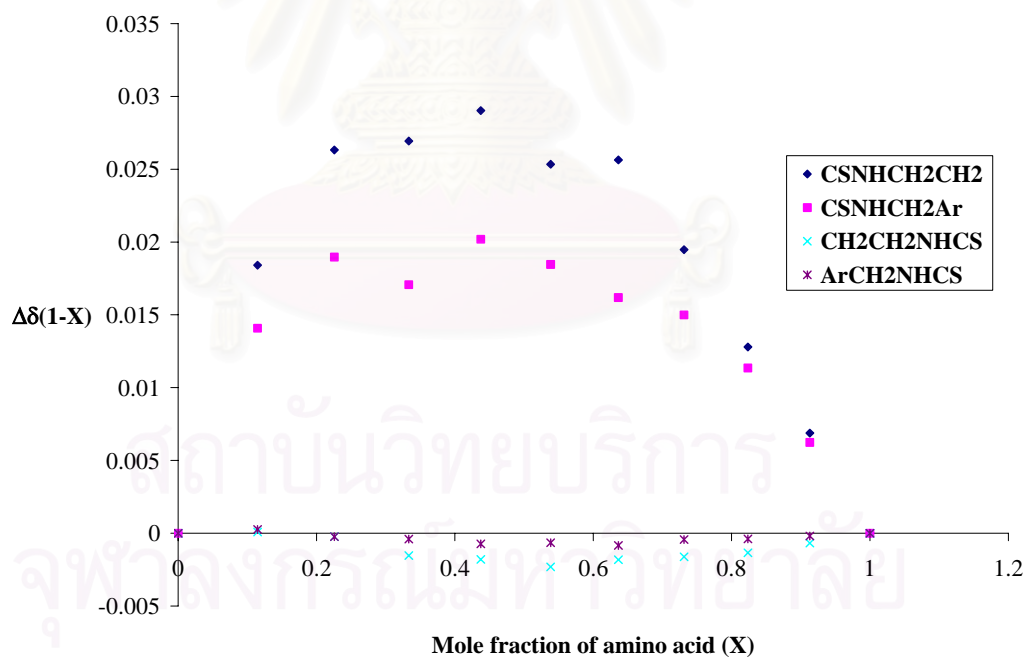
Solvent:	CD <sub>3</sub> CN
Starting volume of host solution:	600 μL
Concentration of host solution:	3.74 mM
Concentration of guest solution:	37.4 mM
Association constant:	1.22x10 <sup>1</sup> M <sup>-1</sup> (ave)

Volume added /μL	-NH <sup>b</sup> CH <sub>2</sub> - /ppm	-NH <sup>a</sup> CH <sub>2</sub> - /ppm	-CH <sub>2</sub> <sup>c</sup> NH- /ppm	-CH <sub>2</sub> <sup>d</sup> NH- /ppm
0	8.2518	8.1674	3.6957	4.6779
5	8.2682	8.1678	3.6966	4.6782
10	8.2726	8.1833	3.6958	4.6782
20	8.2858	8.1919	3.6954	4.6776
30	8.2922	8.1930	3.6934	4.6773
40	8.3034	8.2033	3.6925	4.6766
50	8.3067	8.2074	3.6907	4.6765
60	8.3223	8.2119	3.6907	4.6756
70	8.3243	8.2232	3.6897	4.6763
80	8.3243	8.2317	3.6881	4.6757
90	8.3309	8.2391	3.6879	4.6758
100	8.3386	8.2406	3.6829	4.6751
120	8.3551	8.2536	3.6826	4.6725
140	8.3607	8.2672	3.6813	4.6731
160	8.3695	8.2748	3.6793	4.6708
180	8.3935	8.2842	3.6750	4.6650
200	8.4024	8.2945	3.6718	4.6700
250	8.4386	8.3365	3.6574	4.6620
300	8.4937	8.3705	3.6541	4.6640
350	8.5277	8.4022	3.6548	4.6584
400	8.5649	8.4337	3.6494	4.6621
<b>K<sub>I</sub></b>	<b>1.13x10<sup>1</sup></b>	<b>1.31x10<sup>1</sup></b>	-	-

Titration curves for carboxylate anion of serine with receptor **15** in  $\text{CD}_3\text{CN}$



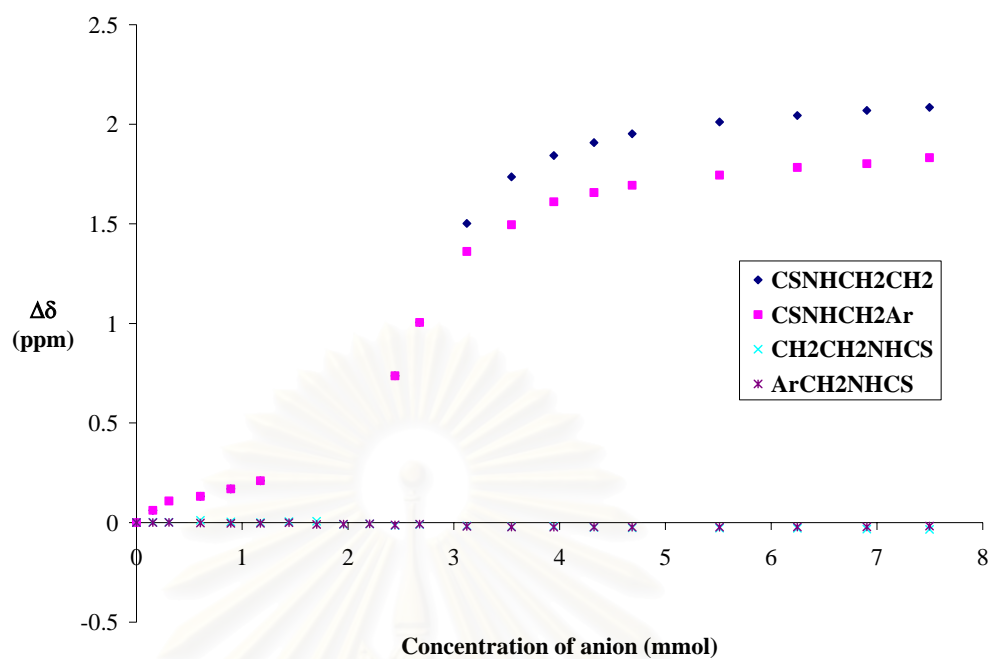
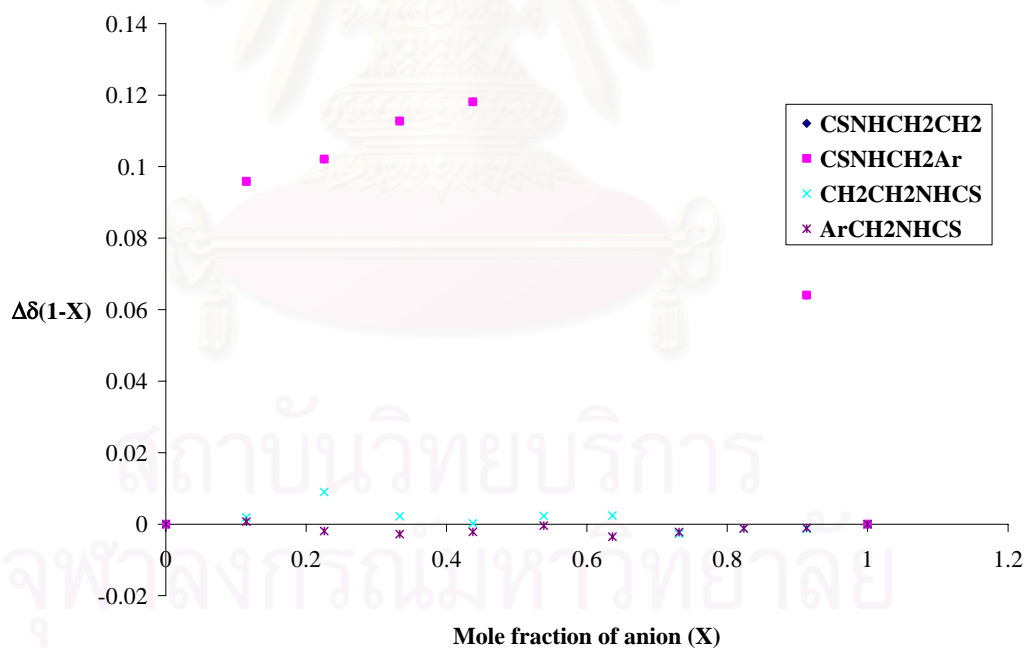
Job's plots for carboxylate anion of serine with receptor **15** in  $\text{CH}_3\text{CN}$



ak) NMR titration data for acetate with 14·Na<sup>+</sup> in CD<sub>3</sub>CN

Solvent:	CD <sub>3</sub> CN
Starting volume of host solution:	600 μL
Concentration of host solution:	1.87 mM
Concentration of guest solution:	18.7 mM
Association constant:	-

Volume added /μL	-NH <sup>b</sup> CH <sub>2</sub> - /ppm	-NH <sup>a</sup> CH <sub>2</sub> - /ppm	-CH <sub>2</sub> <sup>e</sup> NH- /ppm	-CH <sub>2</sub> <sup>d</sup> NH- /ppm
0	6.9007	6.9007	3.6334	4.6808
5	6.9623	6.9623	3.6355	4.6808
10	7.0090	7.0090	3.6355	4.6816
20	7.0326	7.0326	3.6450	4.6783
30	7.0698	7.0698	3.6367	4.6766
40	7.1107	7.1107	3.6338	4.6770
50	-	-	3.6384	4.6799
60	-	-	3.6400	4.6712
70	-	-	3.6235	4.6725
80	-	-	3.6264	4.6741
90	7.6374	7.6374	3.6182	4.6685
100	7.9055	7.9055	3.6235	4.6729
120	8.2618	8.4023	3.6169	4.6613
140	8.3961	8.6367	3.6131	4.6580
160	8.5114	8.7437	3.6136	4.6576
180	8.5577	8.8086	3.6090	4.6580
200	8.5945	8.8533	3.6065	4.6576
250	8.6454	8.9120	3.6057	4.6576
300	8.6838	8.9446	3.6049	4.6584
350	8.7028	8.9698	3.6007	4.6588
400	8.7330	8.9855	3.5991	4.6630
<b>K<sub>I</sub></b>	-	-	-	-

Titration curves for acetate with  $14 \cdot \text{Na}^+$  in  $\text{CD}_3\text{CN}$ Job's plots for acetate with  $14 \cdot \text{Na}^+$  in  $\text{CH}_3\text{CN}$ 

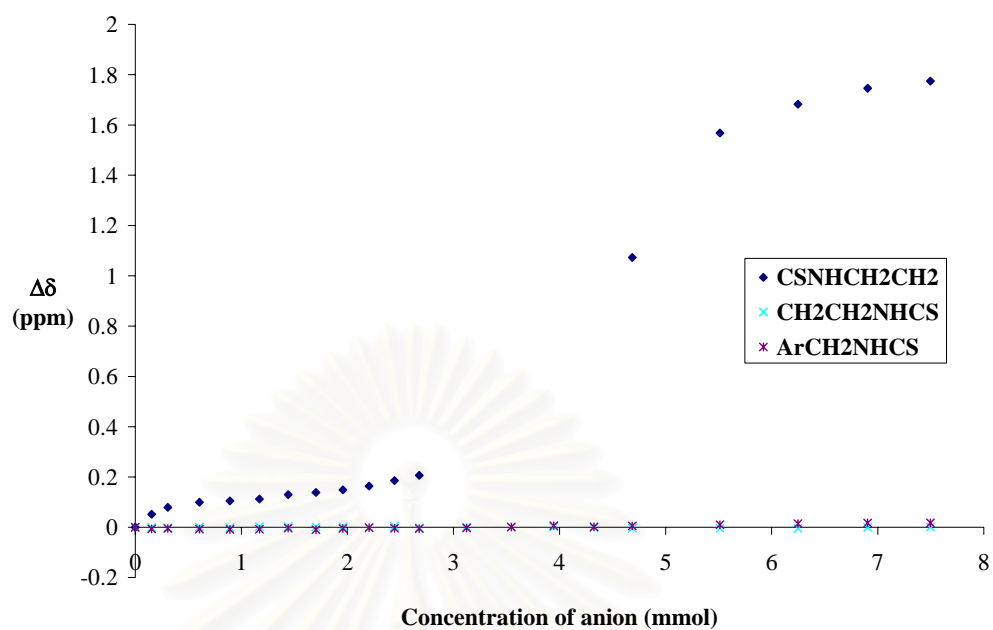
a) NMR titration data for benzoate with **14**·Na<sup>+</sup> in CD<sub>3</sub>CN

Solvent: CD<sub>3</sub>CN  
 Starting volume of host solution: 600 μL  
 Concentration of host solution: 1.87 mM  
 Concentration of guest solution: 18.7 mM  
 Association constant: -

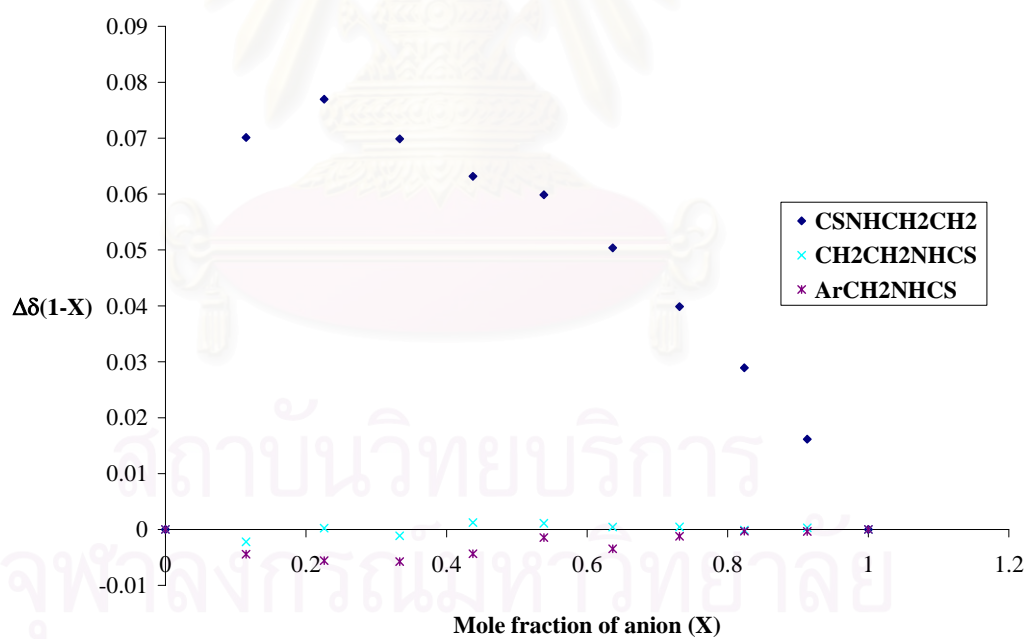
Volume added /μL	-NH <sup>b</sup> CH <sub>2</sub> - /ppm	-CONH <sup>c</sup> - /ppm	-CH <sub>2</sub> <sup>e</sup> NH- /ppm	-CH <sub>2</sub> <sup>d</sup> NH- /ppm
0	6.9652	6.7512	3.6336	4.6847
5	7.0168	6.8099	3.6329	4.6783
10	7.0444	6.8535	3.6311	4.6797
20	7.0646	6.8816	3.6339	4.6775
30	7.0700	6.8804	3.6319	4.6761
40	7.0775	6.8848	3.6358	4.6770
50	7.0949	6.8913	3.6360	4.6816
60	7.1037	6.8947	3.6348	4.6752
70	7.1136	-	3.6353	4.6802
80	7.1291	-	3.6330	4.6830
90	7.1510	-	3.6370	4.6807
100	7.1719	-	3.6318	4.6794
120	-	-	3.6346	4.6819
140	-	-	3.6346	4.6858
160	-	-	3.6359	4.6907
180	-	-	3.6310	4.6861
200	8.0382	8.0382	3.6306	4.6906
250	8.5334	8.5334	3.6293	4.6949
300	8.6478	8.6478	3.6290	4.6990
350	8.7114	8.7114	3.6336	4.7016
400	8.7397	8.7397	3.6344	4.7024
<b>K<sub>I</sub></b>	-	-	-	-

จุฬาลงกรณ์มหาวิทยาลัย

Titration curves for benzoate with  $14 \cdot \text{Na}^+$  in  $\text{CD}_3\text{CN}$



Job's plots for benzoate with  $14 \cdot \text{Na}^+$  in  $\text{CH}_3\text{CN}$



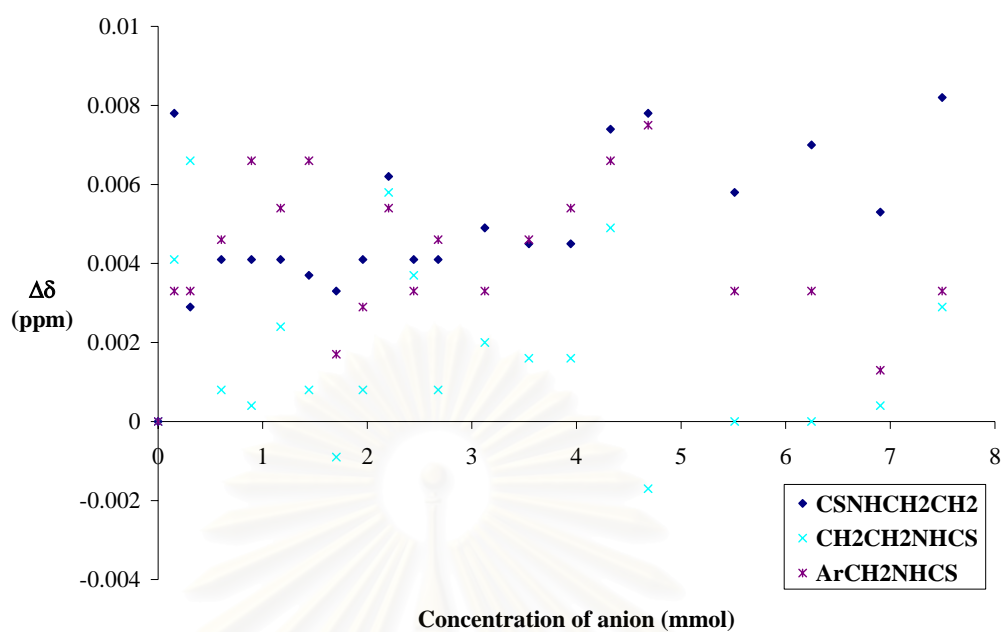
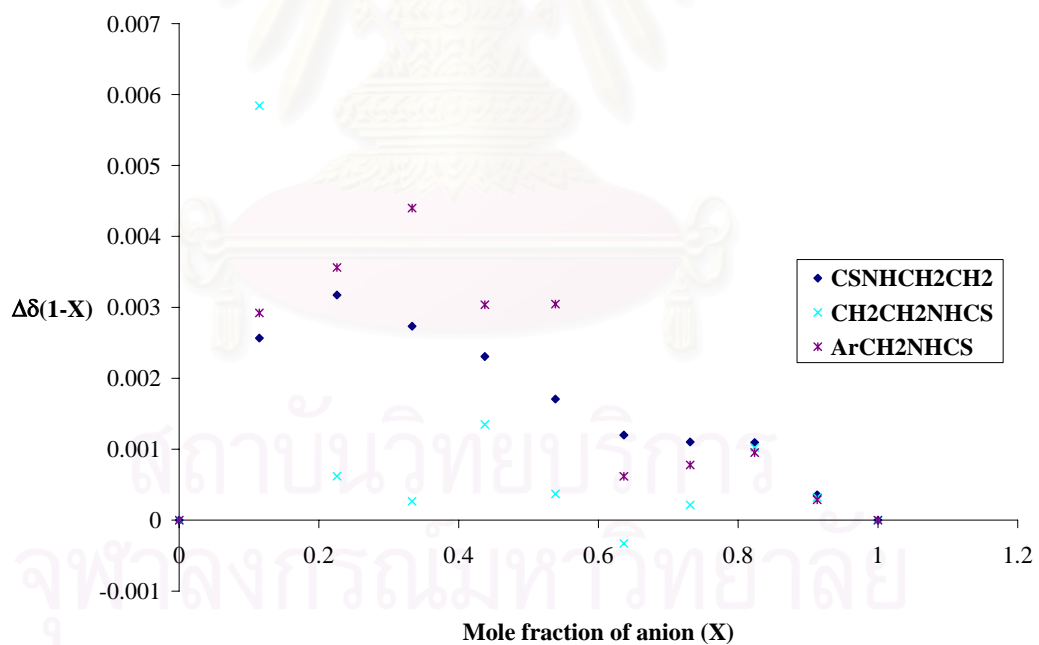
am) NMR titration data for dihydrogen phosphate with **14**·Na<sup>+</sup> in CD<sub>3</sub>CN

Solvent: CD<sub>3</sub>CN  
 Starting volume of host solution: 600 μL  
 Concentration of host solution: 1.87 mM  
 Concentration of guest solution: 18.7 mM  
 Association constant: -

Volume added /μL	-NH <sup>b</sup> CH <sub>2</sub> - /ppm	-CONH <sup>c</sup> - /ppm	-CH <sub>2</sub> <sup>e</sup> NH- /ppm	-CH <sub>2</sub> <sup>d</sup> NH- /ppm
0	6.9086	6.6784	3.6388	4.6795
5	6.9164	6.6949	3.6429	4.6828
10	6.9115	6.7106	3.6454	4.6828
20	6.9127	6.6974	3.6396	4.6841
30	6.9127	6.6895	3.6392	4.6861
40	6.9127	6.6812	3.6412	4.6849
50	6.9123	6.6891	3.6396	4.6861
60	6.9119	6.6854	3.6379	4.6812
70	6.9127	6.6912	3.6396	4.6824
80	6.9148	6.6974	3.6446	4.6849
90	6.9127	6.6850	3.6425	4.6828
100	6.9127	6.6866	3.6396	4.6841
120	6.9135	6.6908	3.6408	4.6828
140	6.9131	6.6994	3.6404	4.6841
160	6.9131	6.6990	3.6404	4.6849
180	6.9160	6.7069	3.6437	4.6861
200	6.9164	6.7015	3.6371	4.6870
250	6.9144	6.7213	3.6388	4.6828
300	6.9156	6.7284	3.6388	4.6828
350	6.9139	6.7366	3.6392	4.6808
400	6.9168	6.7569	3.6417	4.6828
<b>K<sub>I</sub></b>	-	-	-	-

จุฬาลงกรณ์มหาวิทยาลัย

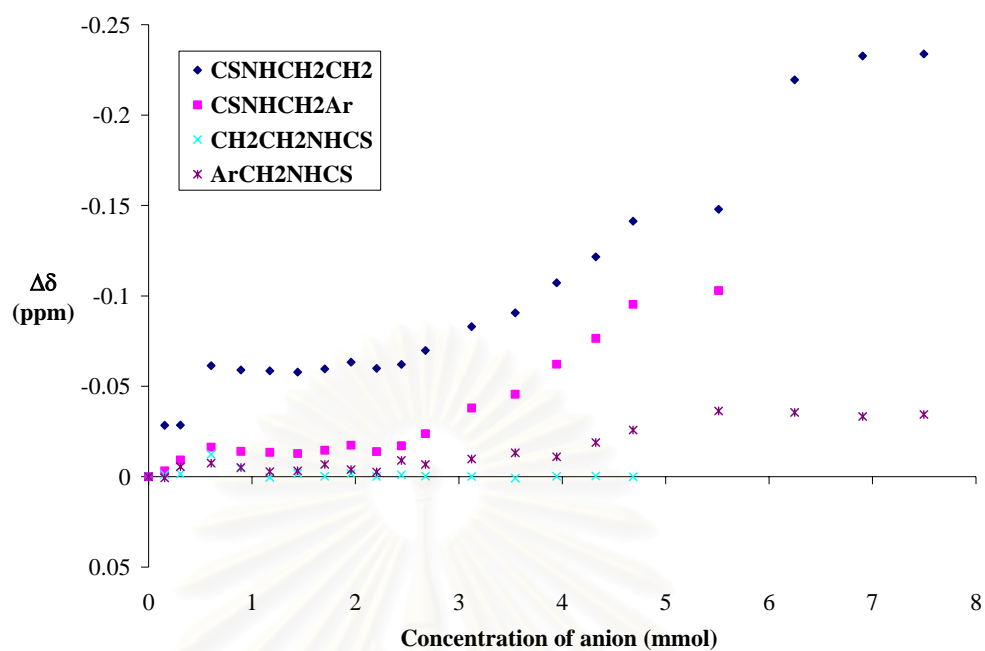
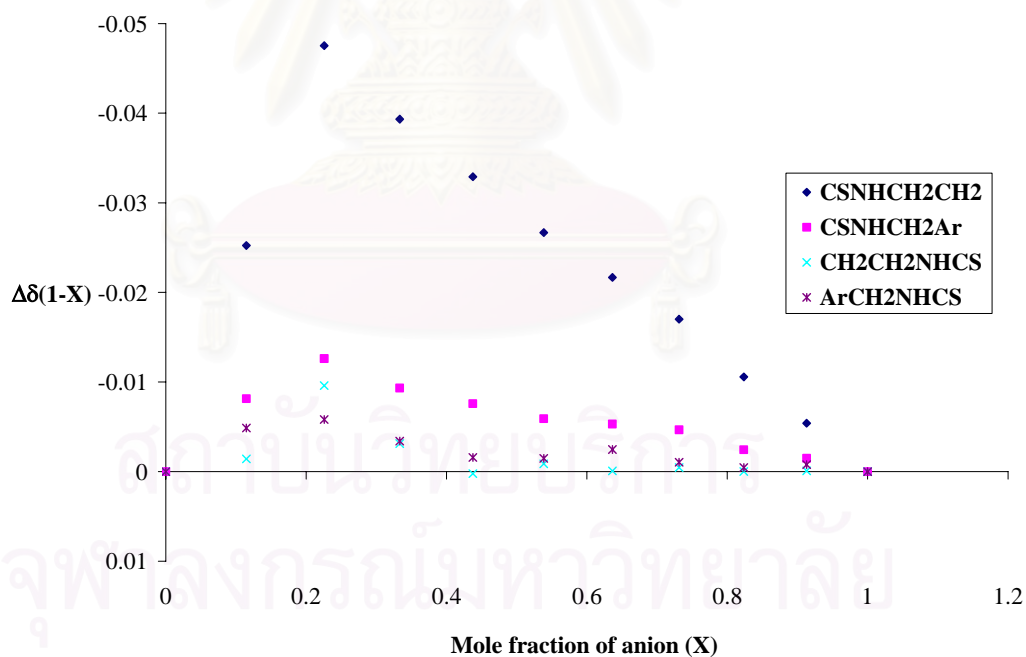


Titration curves for dihydrogen phosphate with  $14 \cdot \text{Na}^+$  in  $\text{CD}_3\text{CN}$ Job's plots for dihydrogen phosphate with  $14 \cdot \text{Na}^+$  in  $\text{CH}_3\text{CN}$ 

an) NMR titration data for phenylphosphinate with **14**·Na<sup>+</sup> in CD<sub>3</sub>CN

Solvent:	CD <sub>3</sub> CN
Starting volume of host solution:	600 μL
Concentration of host solution:	1.87 mM
Concentration of guest solution:	18.7 mM
Association constant:	-

Volume added /μL	-NH <sup>b</sup> CH <sub>2</sub> - /ppm	-NH <sup>a</sup> CH <sub>2</sub> - /ppm	-CH <sub>2</sub> <sup>c</sup> NH- /ppm	-CH <sub>2</sub> <sup>d</sup> NH- /ppm
0	6.9662	6.9207	3.6404	4.6821
5	6.9378	6.9175	3.6392	4.6828
10	6.9377	6.9115	3.6388	4.6766
20	6.9048	6.9044	3.6280	4.6746
30	6.9072	6.9067	3.6357	4.6770
40	6.9077	6.9072	3.6408	4.6793
50	6.9084	6.9079	3.6385	4.6789
60	6.9066	6.9061	3.6402	4.6753
70	6.9029	6.9033	3.6387	4.6782
80	6.9063	6.9068	3.6403	4.6795
90	6.9041	6.9036	3.6394	4.6731
100	6.8964	6.8969	3.6401	4.6753
120	6.8832	6.8827	3.6403	4.6723
140	6.8756	6.8751	3.6412	4.6689
160	6.8590	6.8585	3.6402	4.6711
180	6.8446	6.8442	3.6400	4.6632
200	6.8249	6.8254	3.6404	4.6563
250	6.8183	6.8178	-	4.6458
300	6.7467	-	-	4.6466
350	6.7335	-	-	4.6488
400	6.7324	-	-	4.6477
<b>K<sub>I</sub></b>	-	-	-	-

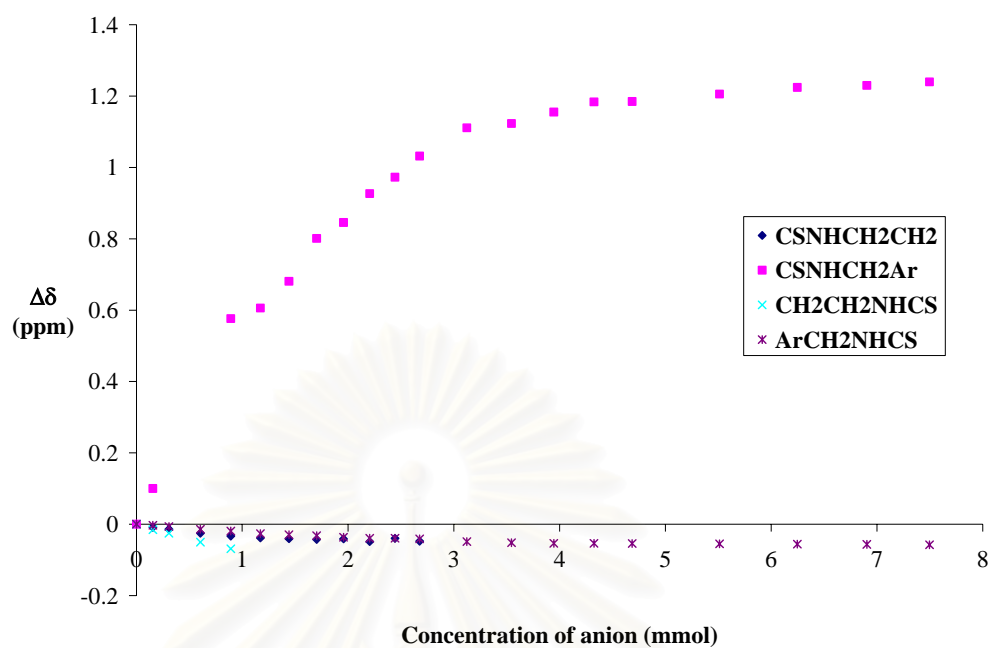
Titration curves for phenylphosphinate with  $14 \cdot \text{Na}^+$  in  $\text{CD}_3\text{CN}$ Job's plots for phenylphosphinate with  $14 \cdot \text{Na}^+$  in  $\text{CH}_3\text{CN}$ 

ao) NMR titration data for diphenylphosphate with  $14 \cdot \text{Na}^+$  in  $\text{CD}_3\text{CN}$

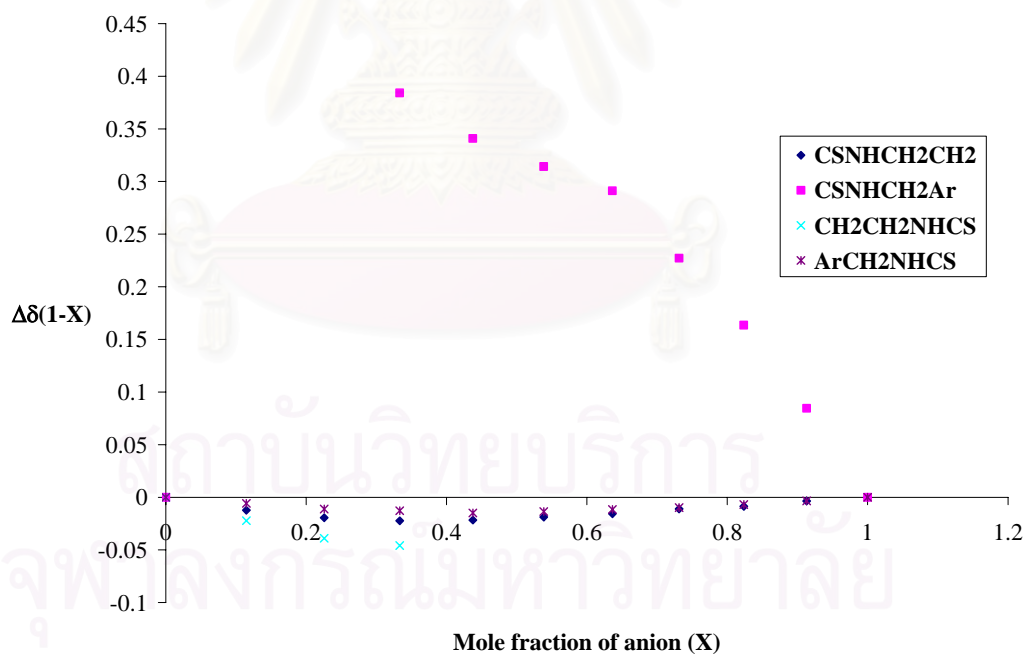
Solvent:	$\text{CD}_3\text{CN}$
Starting volume of host solution:	600 $\mu\text{L}$
Concentration of host solution:	1.87 mM
Concentration of guest solution:	18.7 mM
Association constant:	$1.79 \times 10^3 \text{ M}^{-1}$ (ave)

Volume added / $\mu\text{L}$	$-\text{NH}^{\text{b}}\text{CH}_2-$ /ppm	$-\text{NH}^{\text{a}}\text{CH}_2-$ /ppm	$-\text{CH}_2^{\text{e}}\text{NH}-$ /ppm	$-\text{CH}_2^{\text{d}}\text{NH}-$ /ppm
0	6.9206	6.9206	3.6398	4.6796
5	7.0206	6.9122	3.6243	4.6769
10	-	6.9067	3.6147	4.6731
20	-	6.8955	3.5895	4.6652
30	7.4968	6.8871	3.5710	4.6606
40	7.5266	6.8821	-	4.6533
50	7.6014	6.8799	-	4.6503
60	7.7214	6.8778	-	4.6477
70	7.7662	6.8793	-	4.6432
80	7.8472	6.8719	-	4.6403
90	7.8931	6.8809	-	4.6405
100	7.9524	6.8729	-	4.6387
120	8.0315	-	-	4.6310
140	8.0437	-	-	4.6279
160	8.0756	-	-	4.6260
180	8.1042	-	-	4.6262
200	8.1052	-	-	4.6256
250	8.1262	-	-	4.6246
300	8.1448	-	-	4.6235
350	8.1504	-	-	4.6230
400	8.1603	-	-	4.6220
<b><math>K_I</math></b>	<b><math>2.15 \times 10^3</math></b>	-	-	<b><math>1.42 \times 10^3</math></b>

Titration curves for diphenylphosphate with  $14 \cdot \text{Na}^+$  in  $\text{CD}_3\text{CN}$



Job's for diphenylphosphate plots with  $14 \cdot \text{Na}^+$  in  $\text{CH}_3\text{CN}$

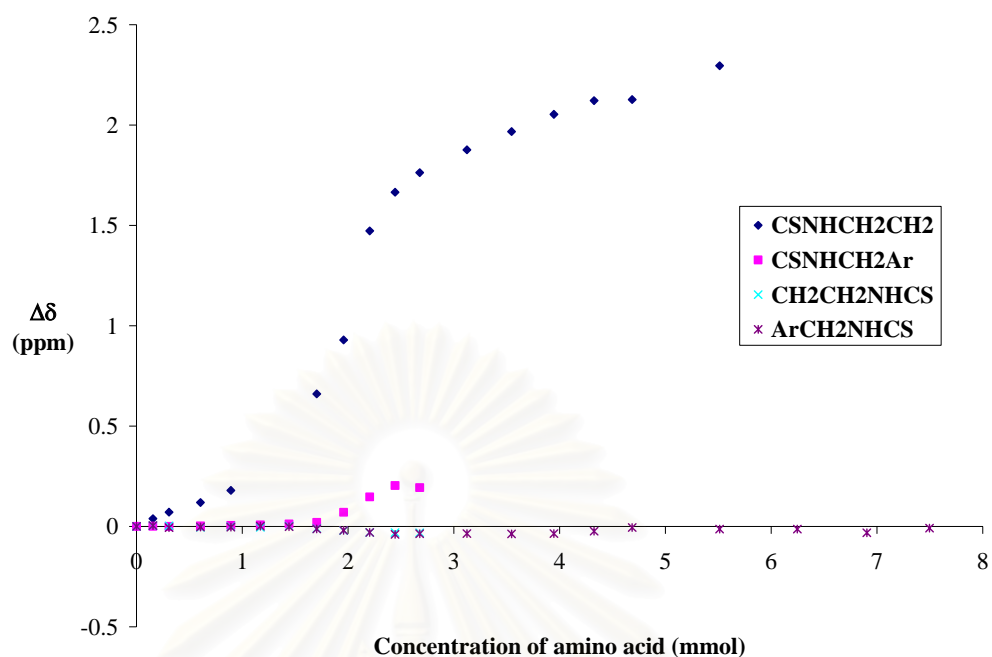


ap) NMR titration data for carboxylate anion of aspartic acid with **14**·Na<sup>+</sup> in CD<sub>3</sub>CN

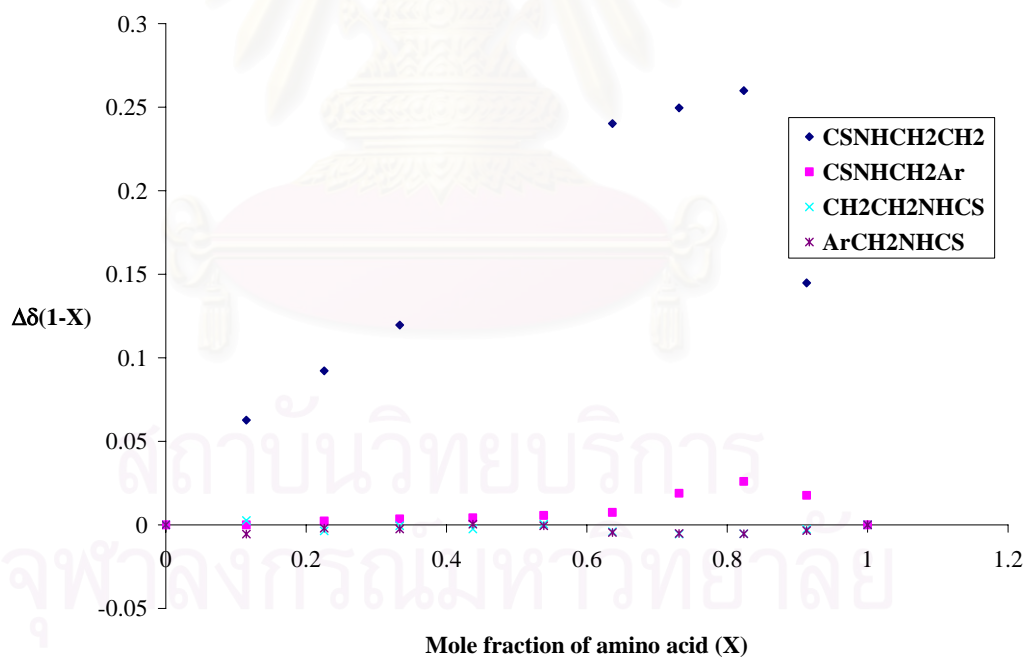
Solvent:	CD <sub>3</sub> CN
Starting volume of host solution:	600μL
Concentration of host solution:	1.87 mM
Concentration of guest solution:	18.7 mM
Association constant:	$K_1$ : $1.74 \times 10^5 \text{ M}^{-1}$ (ave)
	$K_2$ : $1.84 \times 10^4 \text{ M}^{-1}$ (ave)

Volume added /μL	-NH <sup>b</sup> CH <sub>2</sub> - /ppm	-NH <sup>a</sup> CH <sub>2</sub> - /ppm	-CH <sub>2</sub> <sup>c</sup> NH- /ppm	-CH <sub>2</sub> <sup>d</sup> NH- /ppm
0	6.9235	6.9128	3.6327	4.6802
5	6.9624	6.9138	3.6360	4.6845
10	6.9943	6.9128	3.6357	4.6740
20	7.0426	6.9158	3.6281	4.6776
30	7.1029	6.9182	3.6319	4.6764
40	-	6.9203	3.6282	4.6809
50	-	6.9251	3.6337	4.6790
60	7.5839	6.9333	3.6215	4.6677
70	7.8525	6.9831	3.6121	4.6610
80	8.3960	7.0601	3.6028	4.6500
90	8.5887	7.1163	3.6021	4.6407
100	8.6865	7.1063	3.6014	4.6434
120	8.7997	-	-	4.6447
140	8.8909	-	-	4.6431
160	8.9766	-	-	4.6443
180	9.0450	-	-	4.6565
200	9.0505	-	-	4.6749
250	9.2190	-	-	4.6670
300	-	-	-	4.6667
350	-	-	-	4.6489
400	-	-	-	4.6721
$K_1$	$1.74 \times 10^5$	-	-	-
$K_2$	$1.84 \times 10^4$	-	-	-

Titration curves for carboxylate anion of aspartic acid with  $14 \cdot Na^+$  in  $CD_3CN$



Job's plots for carboxylate anion of aspartic acid with  $14 \cdot Na^+$  in  $CH_3CN$



aq) NMR titration data for carboxylate anion of glutamic acid with **14**·Na<sup>+</sup> in CD<sub>3</sub>CN

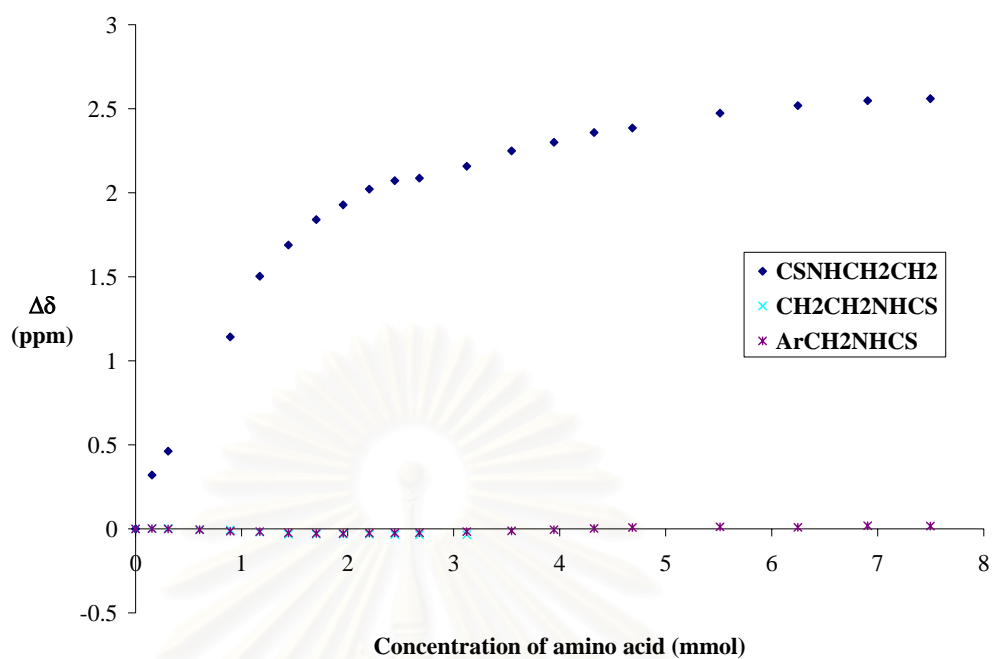
Solvent: CD<sub>3</sub>CN  
 Starting volume of host solution: 600 μL  
 Concentration of host solution: 1.87 mM  
 Concentration of guest solution: 18.7 mM  
 Association constant: 5.37x10<sup>3</sup> M<sup>-1</sup> (ave)

Volume added /μL	-NH <sup>b</sup> CH <sub>2</sub> - /ppm	-CONH <sup>c</sup> - /ppm	-CH <sub>2</sub> <sup>e</sup> NH- /ppm	-CH <sub>2</sub> <sup>d</sup> NH- /ppm
0	6.9068	6.7122	3.6375	4.6785
5	6.9073	7.0323	3.6390	4.6796
10	6.9149	7.1742	3.6410	4.6778
20	6.9445	-	3.6333	4.6732
30	-	7.8545	3.6310	4.6644
40	-	8.2152	3.6175	4.6620
50	8.0461	8.4008	3.6062	4.6542
60	8.1176	8.5522	3.6059	4.6520
70	8.2265	8.6403	3.6055	4.6512
80	8.3135	8.7335	3.6053	4.6534
90	8.3497	8.7842	3.6035	4.6543
100	8.3530	8.7986	3.6029	4.6556
120	8.4233	8.8699	3.6025	4.6620
140	8.4728	8.9613	-	4.6665
160	8.5138	9.0122	-	4.6738
180	8.5399	9.0703	-	4.6810
200	8.5620	9.0978	-	4.6868
250	8.5961	9.1858	-	4.6904
300	8.6169	9.2312	-	4.6873
350	8.6277	9.2598	-	4.6969
400	8.6312	9.2718	-	4.6951
<b>K<sub>I</sub></b>	<b>6.30x10<sup>3</sup></b>	<b>4.44x10<sup>3</sup></b>	-	-

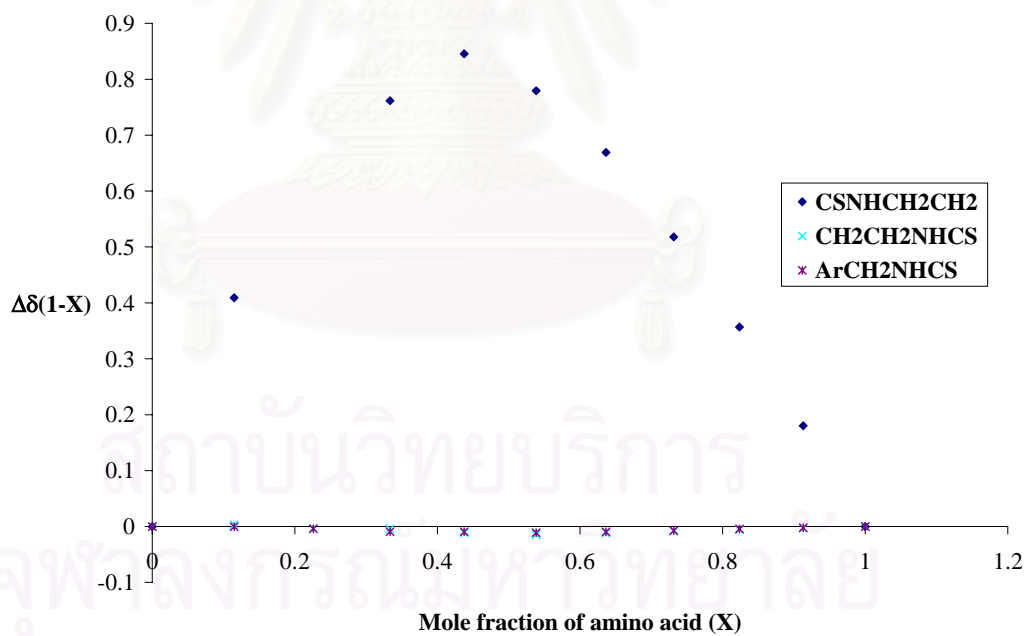
จุฬาลงกรณ์มหาวิทยาลัย



Titration curves for carboxylate anion of glutamic acid with  $14 \cdot \text{Na}^+$  in  $\text{CD}_3\text{CN}$



Job's plots for carboxylate anion of glutamic acid with  $14 \cdot \text{Na}^+$  in  $\text{CH}_3\text{CN}$

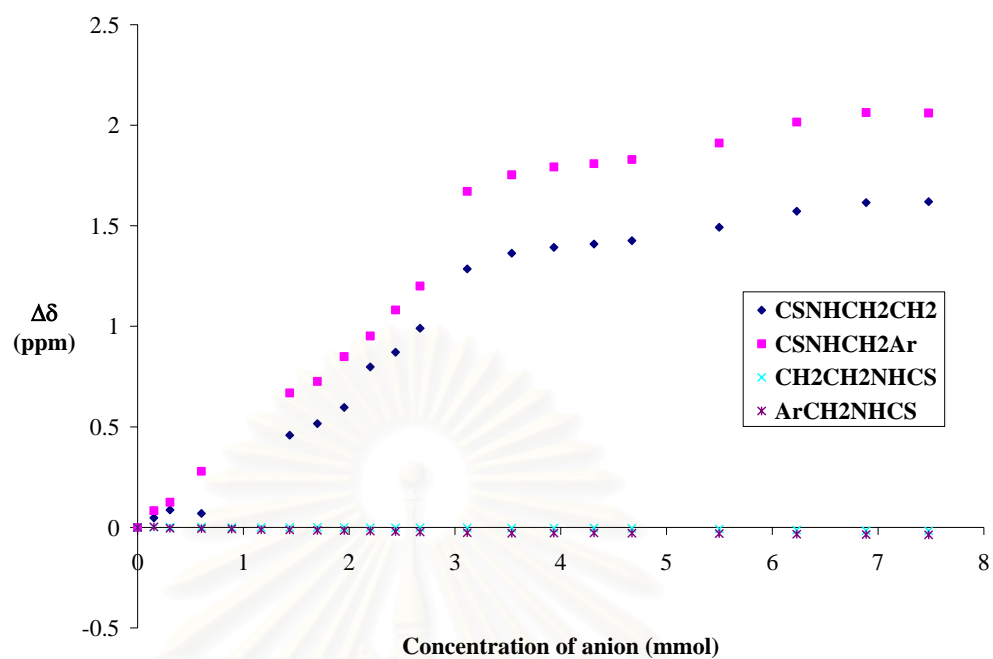
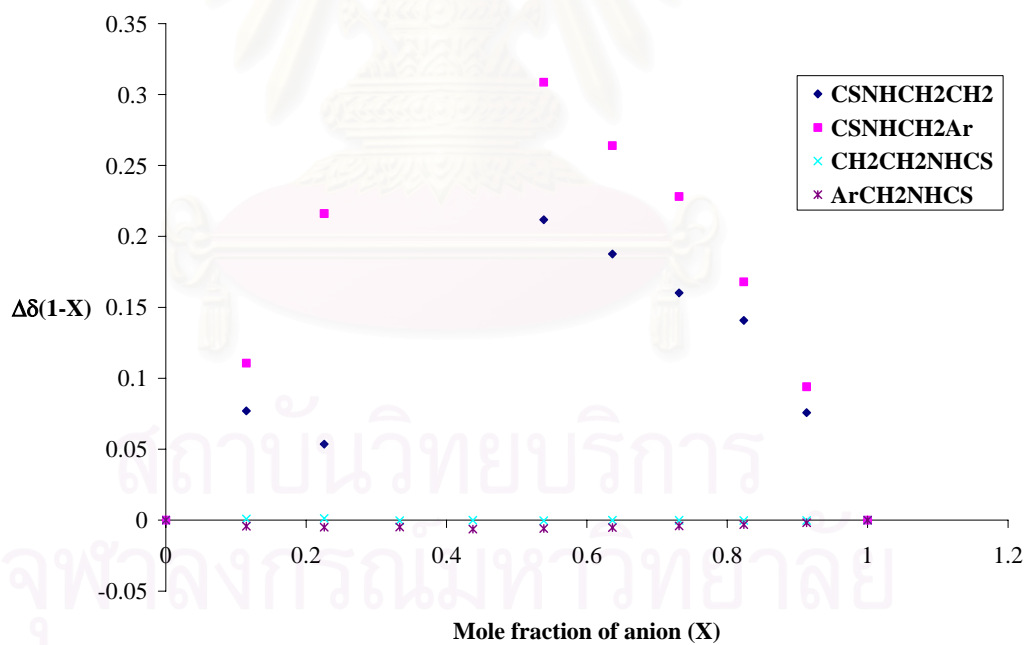


ar) NMR titration data for acetate with  $15\cdot\text{Na}^+$  in  $\text{CD}_3\text{CN}$

Solvent:	$\text{CD}_3\text{CN}$
Starting volume of host solution:	600 $\mu\text{L}$
Concentration of host solution:	1.87 mM
Concentration of guest solution:	10.7 mM
Association constant:	$2.80\times 10^4 \text{ M}^{-1}$ (ave)

Volume added / $\mu\text{L}$	$-\text{NH}^{\text{b}}\text{CH}_2-$ /ppm	$-\text{NH}^{\text{a}}\text{CH}_2-$ /ppm	$-\text{CH}_2^{\text{c}}\text{NH}-$ /ppm	$-\text{CH}_2^{\text{d}}\text{NH}-$ /ppm
0	7.0325	6.8226	3.6622	4.6833
5	7.0800	6.9059	3.6632	4.6858
10	7.1195	6.9476	3.6632	4.6785
20	7.1017	7.1017	3.6638	4.6768
30	-	-	3.6617	4.6761
40	-	-	3.6621	4.6721
50	7.4914	7.4914	3.6614	4.6705
60	7.5485	7.5485	3.6620	4.6688
70	7.6289	7.6717	3.6620	4.6682
80	7.8304	7.7744	3.6608	4.6652
90	7.9038	7.9038	3.6598	4.6627
100	8.0228	8.0228	3.6605	4.6606
120	8.3177	8.4938	3.6597	4.6567
140	8.3957	8.5761	3.6585	4.6548
160	8.4248	8.6150	3.6588	4.6549
180	8.4420	8.6313	3.6592	4.6553
200	8.4582	8.6519	3.6582	4.6546
250	8.5247	8.7338	3.6544	4.6524
300	8.6049	8.8382	3.6492	4.6494
350	8.6478	8.8855	3.6462	4.6475
400	8.6521	8.8832	3.6452	4.6466
<b><math>K_I</math></b>	<b><math>3.65\times 10^4</math></b>	<b><math>3.82\times 10^4</math></b>	-	<b><math>9.28\times 10^3</math></b>

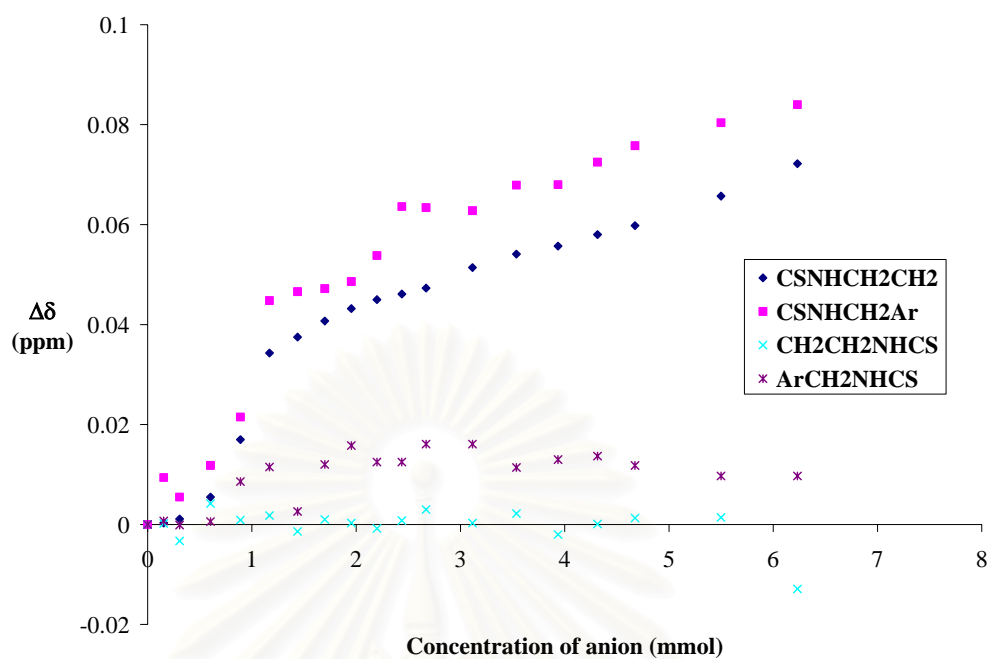
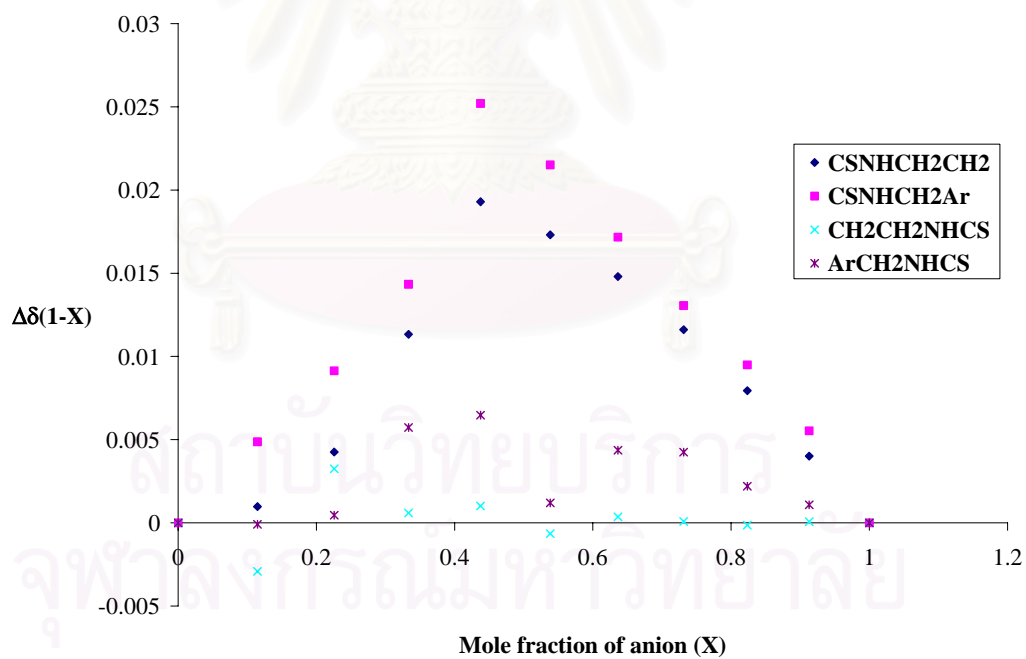
จุฬาลงกรณ์มหาวิทยาลัย

Titration curves for acetate with  $15\cdot\text{Na}^+$  in  $\text{CD}_3\text{CN}$ Job's plots for acetate with  $15\cdot\text{Na}^+$  in  $\text{CH}_3\text{CN}$ 

as) NMR titration data for benzoate with  $15\cdot\text{Na}^+$  in  $\text{CD}_3\text{CN}$

Solvent:	$\text{CD}_3\text{CN}$
Starting volume of host solution:	600 $\mu\text{L}$
Concentration of host solution:	1.87 mM
Concentration of guest solution:	10.7 mM
Association constant:	$9.82 \times 10^2 \text{ M}^{-1}$ (ave)

Volume added / $\mu\text{L}$	$-\text{NH}^{\text{b}}\text{CH}_2-$ /ppm	$-\text{NH}^{\text{a}}\text{CH}_2-$ /ppm	$-\text{CH}_2^{\text{c}}\text{NH}-$ /ppm	$-\text{CH}_2^{\text{d}}\text{NH}-$ /ppm
0	6.8561	6.5929	3.6766	4.6841
5	6.8564	6.6023	3.6768	4.6848
10	6.8572	6.5984	3.6733	4.6840
20	6.8616	6.6047	3.6808	4.6847
30	6.8731	6.6144	3.6775	4.6927
40	6.8904	6.6377	3.6784	4.6956
50	6.8936	6.6395	3.6752	4.6867
60	6.8968	6.6401	3.6776	4.6961
70	6.8993	6.6415	3.6769	4.6999
80	6.9011	6.6467	3.6758	4.6966
90	6.9022	6.6565	3.6774	4.6966
100	6.9034	6.6563	3.6796	4.7002
120	6.9075	6.6557	3.6769	4.7002
140	6.9102	6.6608	3.6788	4.6955
160	6.9118	6.6609	3.6746	4.6971
180	6.9141	6.6654	3.6767	4.6978
200	6.9159	6.6687	3.6779	4.6959
250	6.9218	6.6733	3.6780	4.6938
300	6.9283	6.6769	3.6637	4.6938
350	-	-	-	-
400	-	-	-	-
$K_I$	-	$9.82 \times 10^2$	-	-

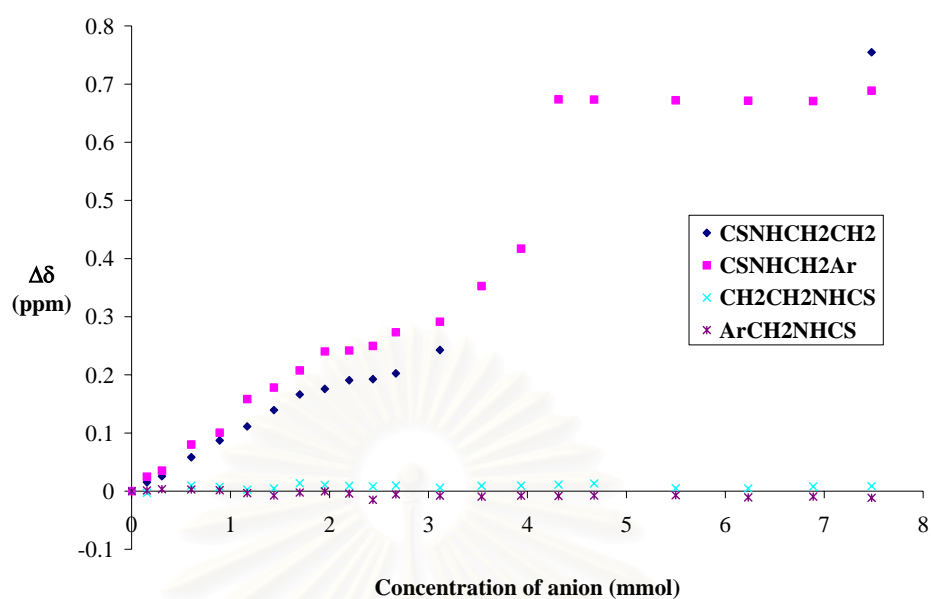
Titration curves for benzoate with  $15 \cdot \text{Na}^+$  in  $\text{CD}_3\text{CN}$ Job's plots for benzoate with  $15 \cdot \text{Na}^+$  in  $\text{CH}_3\text{CN}$ 

at) NMR titration data for dihydrogen phosphate with  $15 \cdot \text{Na}^+$  in  $\text{CD}_3\text{CN}$

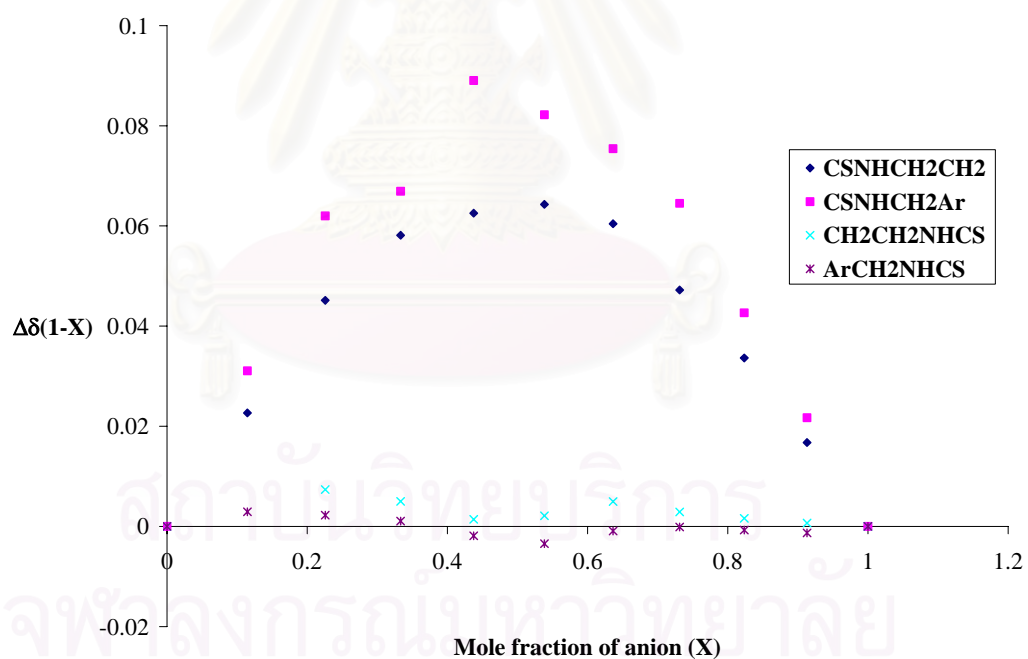
Solvent:	$\text{CD}_3\text{CN}$
Starting volume of host solution:	600 $\mu\text{L}$
Concentration of host solution:	1.87 mM
Concentration of guest solution:	10.7 mM
Association constant:	$5.39 \times 10^4 \text{ M}^{-1}$ (ave)

Volume added	$-\text{NH}^{\text{b}}\text{CH}_2-$	$-\text{NH}^{\text{a}}\text{CH}_2-$	$-\text{CH}_2^{\text{c}}\text{NH}-$	$-\text{CH}_2^{\text{d}}\text{NH}-$
/ $\mu\text{L}$	/ppm	/ppm	/ppm	/ppm
0	6.9222	6.6846	3.6784	4.6845
5	6.9375	6.7094	3.6755	4.6857
10	6.9478	6.7197	-	4.6878
20	6.9805	6.7647	3.6879	4.6874
30	7.0094	6.7850	3.6859	4.6861
40	7.0334	6.8429	3.6809	4.6812
50	7.0615	6.8627	3.6830	4.6770
60	7.0884	6.8920	3.6921	4.6820
70	7.0979	6.9247	3.6892	4.6841
80	7.1128	6.9263	3.6875	4.6803
90	7.1148	6.9342	3.6863	4.6696
100	7.1247	6.9578	3.6879	4.6787
120	7.1648	6.9757	3.6842	4.6766
140	-	7.0371	3.6875	4.6750
160	-	7.1016	3.6879	4.6766
180	-	7.3583	3.6896	4.6762
200	-	7.3579	3.6917	4.6770
250	-	7.3566	3.6834	4.6774
300	-	7.3558	3.6830	4.6737
350	-	7.3554	3.6863	4.6750
400	7.6769	7.3732	3.6871	4.6729
$K_I$	$2.95 \times 10^4$	$7.82 \times 10^4$	-	-

Titration curves for dihydrogen phosphate with  $15 \cdot \text{Na}^+$  in  $\text{CD}_3\text{CN}$



Job's plots for dihydrogen phosphate with  $15 \cdot \text{Na}^+$  in  $\text{CH}_3\text{CN}$



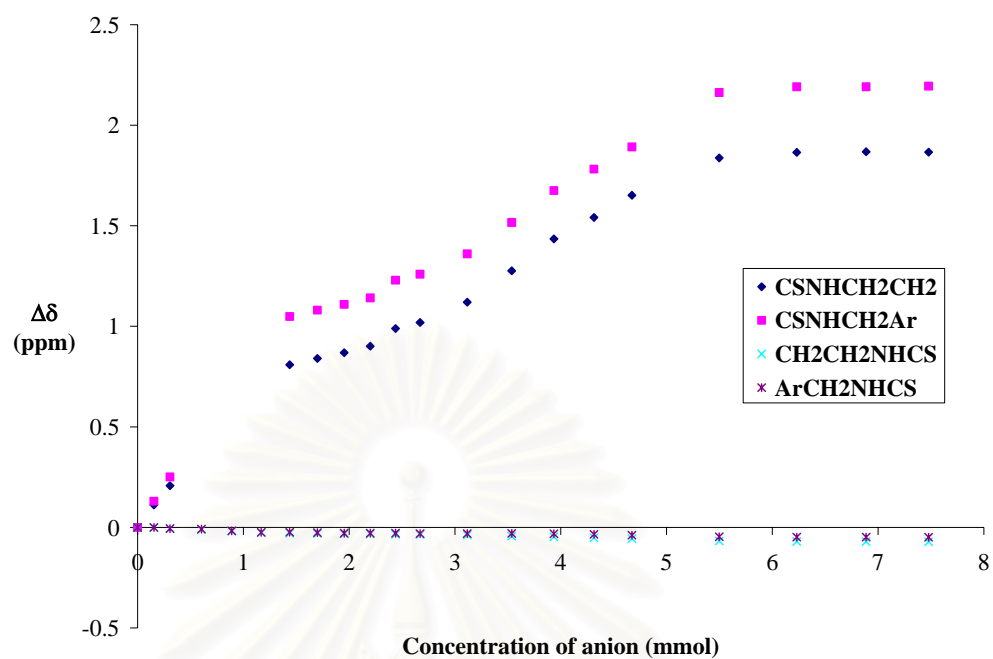
au) NMR titration data for phenylphosphinate with **15**·Na<sup>+</sup> in CD<sub>3</sub>CN

Solvent:	CD <sub>3</sub> CN
Starting volume of host solution:	600 μL
Concentration of host solution:	1.87 mM
Concentration of guest solution:	22.7 mM
Association constant:	4.58x10 <sup>4</sup> M <sup>-1</sup> (ave)

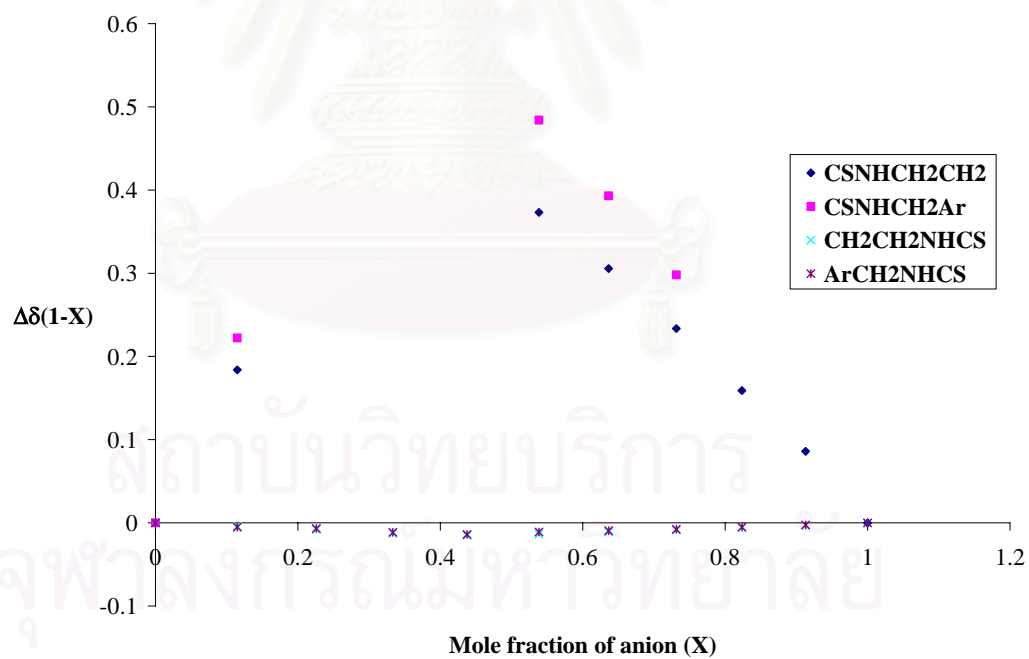
Volume added /μL	-NH <sup>b</sup> CH <sub>2</sub> - /ppm	-NH <sup>a</sup> CH <sub>2</sub> - /ppm	-CH <sub>2</sub> <sup>e</sup> NH- /ppm	-CH <sub>2</sub> <sup>d</sup> NH- /ppm
0	6.9072	6.6669	3.6769	4.6843
5	7.0189	6.7969	3.6769	4.6843
10	7.1149	6.9179	3.6725	4.6785
20	-	-	3.6667	4.6755
30	-	-	3.6582	4.6672
40	-	-	3.6500	4.6596
50	7.7157	7.7157	3.6477	4.6604
60	7.7477	7.7477	3.6466	4.6585
70	7.7762	7.7762	3.6450	4.6554
80	7.8081	7.8081	3.6442	4.6554
90	7.8960	7.8960	3.6418	4.6554
100	7.9258	7.9258	3.6413	4.6532
120	8.0271	8.0271	3.6395	4.6536
140	8.1834	8.1834	3.6337	4.6543
160	8.3418	8.3418	3.6299	4.6527
180	8.4486	8.4486	3.6255	4.6497
200	8.5587	8.5587	3.6208	4.6453
250	8.7448	8.8295	3.6093	4.6378
300	8.7722	8.8580	3.6073	4.6362
350	8.7755	8.8580	3.6067	4.6358
400	8.7733	8.8613	3.6056	4.6357
<b>K<sub>I</sub></b>	<b>3.90×10<sup>4</sup></b>	<b>1.25×10<sup>5</sup></b>	<b>9.61×10<sup>3</sup></b>	<b>9.56×10<sup>3</sup></b>



Titration curves for phenylphosphinate with  $15\cdot\text{Na}^+$  in  $\text{CD}_3\text{CN}$



Job's plots for phenylphosphinate with  $15\cdot\text{Na}^+$  in  $\text{CH}_3\text{CN}$



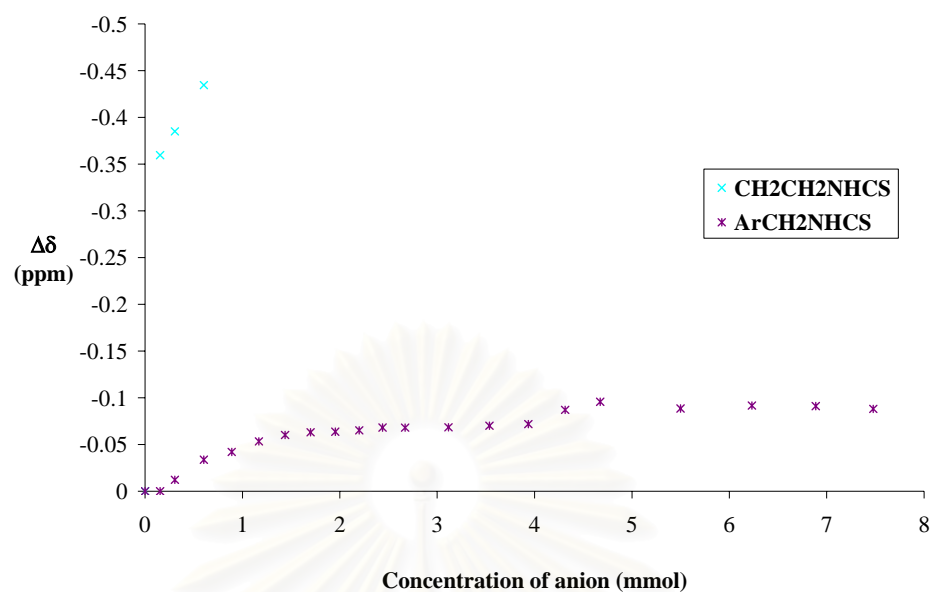
av) NMR titration data for diphenylphosphate with  $15 \cdot \text{Na}^+$  in  $\text{CD}_3\text{CN}$

Solvent:	$\text{CD}_3\text{CN}$
Starting volume of host solution:	600 $\mu\text{L}$
Concentration of host solution:	1.17 mM
Concentration of guest solution:	18.7 mM
Association constant:	$1.11 \times 10^4 \text{ M}^{-1}$ (ave)

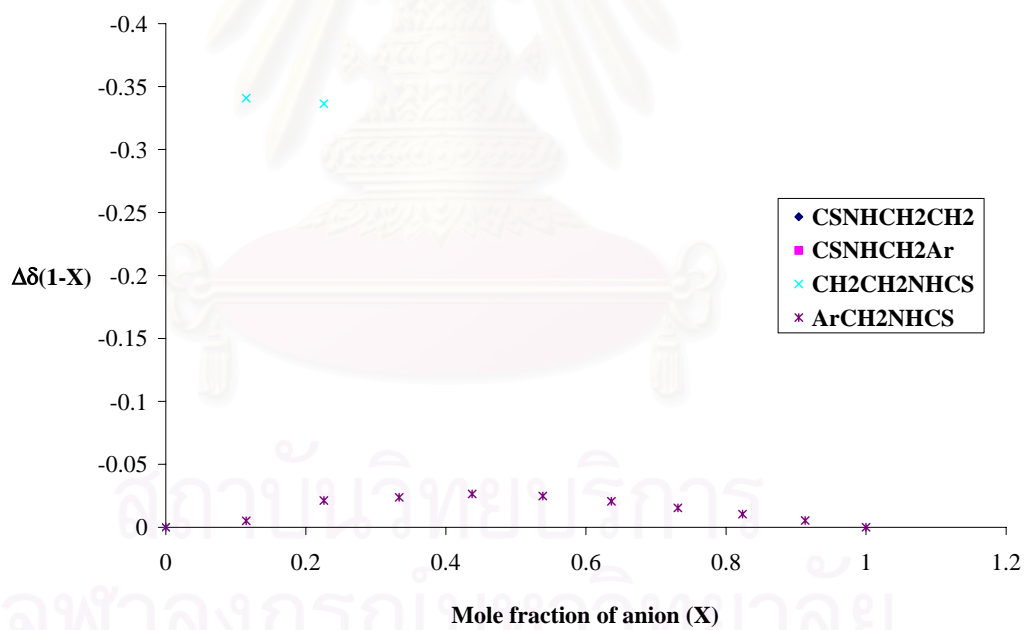
Volume added / $\mu\text{L}$	$-\text{NH}^b\text{CH}_2-$ /ppm	$-\text{NH}^a\text{CH}_2-$ /ppm	$-\text{CH}_2^e\text{NH}-$ /ppm	$-\text{CH}_2^d\text{NH}-$ /ppm
0	-	-	3.9935	-
5	-	-	3.6339	4.6909
10	-	-	3.6085	4.6787
20	-	-	3.5590	4.6571
30	-	-	-	4.6488
40	-	-	-	4.6375
50	-	-	-	4.6307
60	-	-	-	4.6278
70	-	-	-	4.6272
80	-	-	-	4.6257
90	-	-	-	4.6227
100	-	-	-	4.6228
120	-	-	-	4.6225
140	-	-	-	4.6208
160	-	-	-	4.6190
180	-	-	-	4.6039
200	-	-	-	4.5952
250	-	-	-	4.6024
300	-	-	-	4.5992
350	-	-	-	4.5998
400	-	-	-	4.6028
<b><math>K_I</math></b>	-	-	-	<b><math>1.11 \times 10^4</math></b>

สถาบันวิจัยบริการ  
จุฬาลงกรณ์มหาวิทยาลัย

Titration curves for diphenylphosphate with  $15 \cdot \text{Na}^+$  in  $\text{CD}_3\text{CN}$



Job's plots for diphenylphosphate with  $15 \cdot \text{Na}^+$  in  $\text{CH}_3\text{CN}$

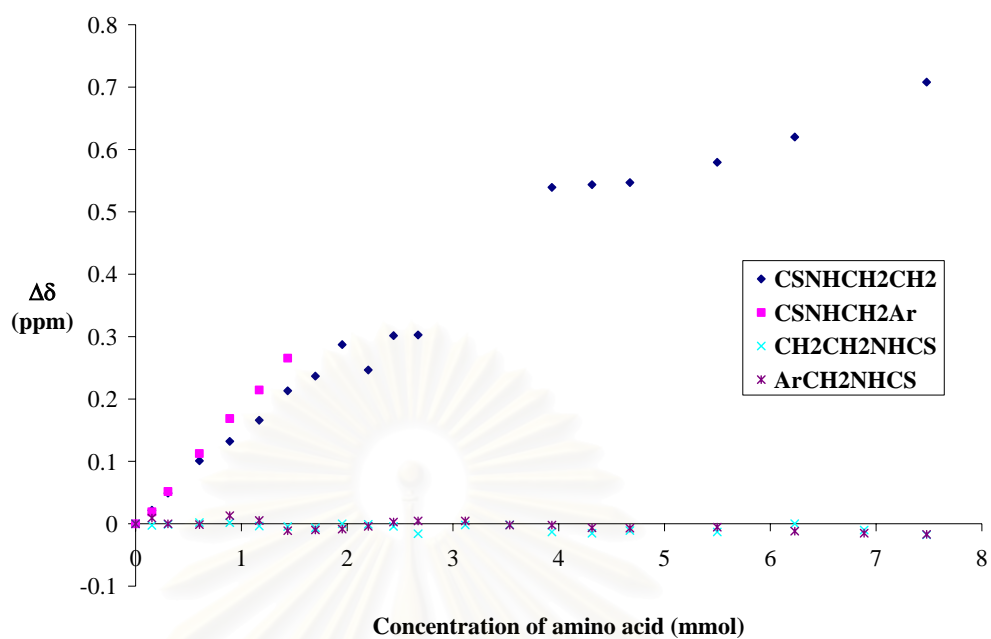


aw) NMR titration data for carboxylate anion of aspartic acid with  $15\cdot\text{Na}^+$  in  $\text{CD}_3\text{CN}$

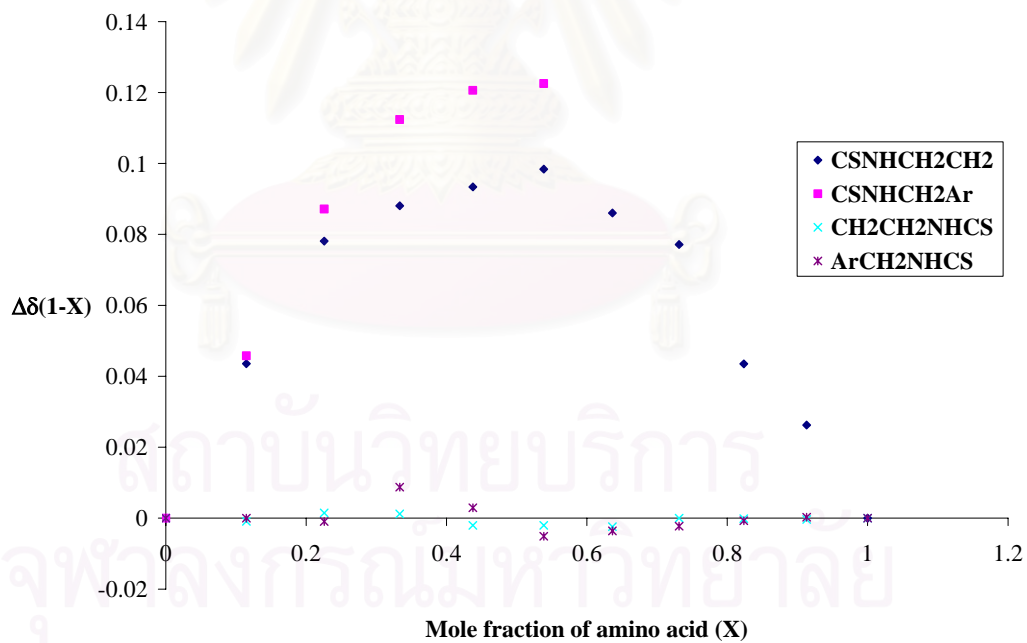
Solvent:	$\text{CD}_3\text{CN}$
Starting volume of host solution:	600 $\mu\text{L}$
Concentration of host solution:	1.87 mM
Concentration of guest solution:	10.7 mM
Association constant:	$1.62 \times 10^2 \text{ M}^{-1}$ (ave)

Volume added	$-\text{NH}^{\text{b}}\text{CH}_2-$	$-\text{NH}^{\text{a}}\text{CH}_2-$	$-\text{CH}_2^{\text{c}}\text{NH}-$	$-\text{CH}_2^{\text{d}}\text{NH}-$
/ $\mu\text{L}$	/ppm	/ppm	/ppm	/ppm
0	6.8641	6.6163	3.6783	4.6797
5	6.8859	6.6355	3.6757	4.6889
10	6.9133	6.6680	3.6773	4.6797
20	6.9650	6.7289	3.6802	4.6785
30	6.9962	6.7849	3.6801	4.6928
40	7.0301	6.8307	3.6747	4.6849
50	7.0773	6.8818	3.6739	4.6687
60	7.1007	-	3.6717	4.6698
70	7.1513	-	3.6783	4.6712
80	7.1106	-	3.6775	4.6756
90	7.1657	-	3.6740	4.6825
100	7.1668	-	3.6622	4.6844
120	-	-	3.6764	4.6842
140	-	-	3.6768	4.6777
160	7.4034	-	3.6652	4.6776
180	7.4077	-	3.6631	4.6733
200	7.4110	-	3.6675	4.6727
250	7.4435	-	3.6652	4.6742
300	7.4840	-	3.6785	4.6679
350	-	-	3.6683	4.6647
400	7.5720	-	3.6605	4.6627
<b><math>K_I</math></b>	<b><math>1.62 \times 10^2</math></b>	-	-	-

Titration curves for carboxylate anion of aspartic acid with  $15 \cdot \text{Na}^+$  in  $\text{CD}_3\text{CN}$



Job's plots for carboxylate anion of aspartic acid with  $15 \cdot \text{Na}^+$  in  $\text{CH}_3\text{CN}$



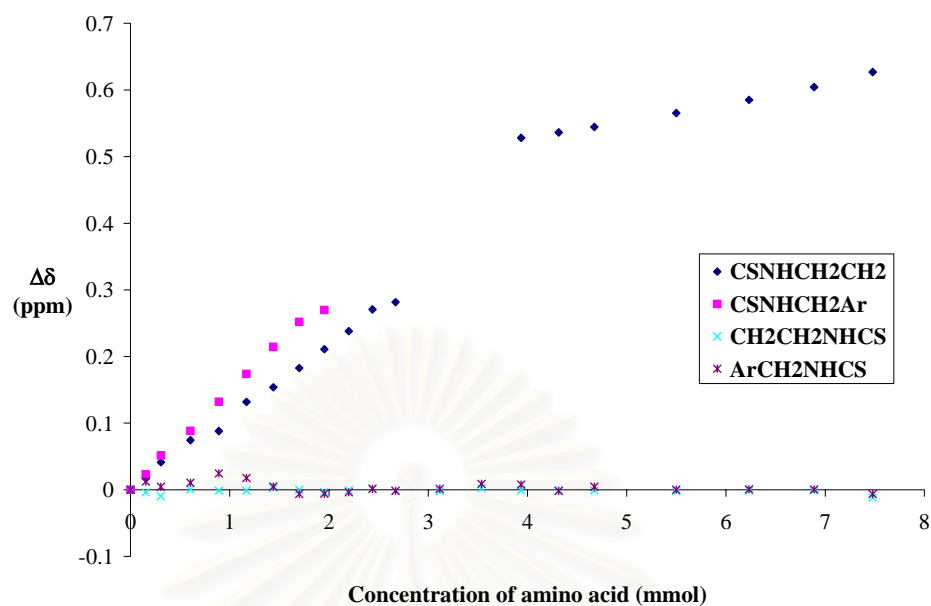
ax) NMR titration data for carboxylate anion of glutamic acid with  $15\cdot\text{Na}^+$  in  $\text{CD}_3\text{CN}$

Solvent:	$\text{CD}_3\text{CN}$
Starting volume of host solution:	600 $\mu\text{L}$
Concentration of host solution:	1.87 mM
Concentration of guest solution:	10.7 mM
Association constant:	$9.36 \times 10^1 \text{ M}^{-1}$ (ave)

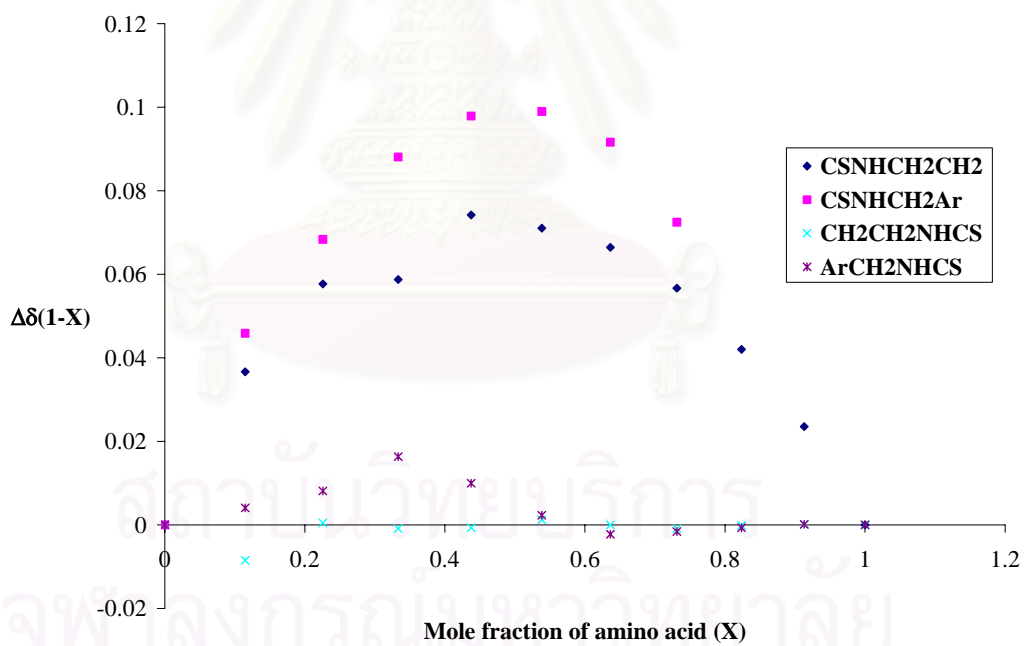
Volume added	$-\text{NH}^{\text{b}}\text{CH}_2-$	$-\text{NH}^{\text{a}}\text{CH}_2-$	$-\text{CH}_2^{\text{c}}\text{NH}-$	$-\text{CH}_2^{\text{d}}\text{NH}-$
$/\mu\text{L}$	$/\text{ppm}$	$/\text{ppm}$	$/\text{ppm}$	$/\text{ppm}$
0	6.8767	6.6201	3.6799	4.6766
5	6.8939	6.6433	3.6762	4.6889
10	6.9181	6.6719	3.6703	4.6812
20	6.9512	6.7084	3.6805	4.6871
30	6.9648	6.7522	3.6786	4.7011
40	7.0086	6.7941	3.6787	4.6943
50	7.0306	6.8345	3.6826	4.6816
60	7.0594	6.8720	3.6799	4.6704
70	7.0877	6.8898	3.6765	4.6706
80	7.1148	-	3.6791	4.6728
90	7.1473	-	3.6813	4.6781
100	7.1583	-	3.6785	4.6750
120	-	-	3.6779	4.6781
140	-	-	3.6823	4.6854
160	7.4048	-	3.6791	4.6844
180	7.4130	-	3.6792	4.6749
200	7.4212	-	3.6788	4.6811
250	7.4421	-	3.6780	4.6769
300	7.4618	-	3.6786	4.6774
350	7.4809	-	3.6788	4.6771
400	7.5035	-	3.6684	4.6702
<b><math>K_I</math></b>	<b><math>9.36 \times 10^1</math></b>	-	-	-

จุฬาลงกรณ์มหาวิทยาลัย

Titration curves for carboxylate anion of glutamic acid with  $15 \cdot \text{Na}^+$  in  $\text{CD}_3\text{CN}$



Job's plots for carboxylate anion of glutamic acid with  $15 \cdot \text{Na}^+$  in  $\text{CH}_3\text{CN}$



## VITA

Miss Gamolwan Tumcharern was born on January 2, 1975 in Udonthanee, Thailand. She was a student under “The Development and Promotion of Science and Technology Talent Project (DPST)” from 1989 till 1998. She received her Bachelor’s and Master’s degree of Science in Chemistry from Chulalongkorn University in 1995 and 1998, respectively. Since then, she has been a postgraduate student studying inorganic chemistry and become a member of Supramolecular Chemistry Laboratory under the supervision of Assist. Prof. Thawatchai Tuntulani. During this period, her financial support is granted by “Royal Golden Jubilee (RGJ)”, the Thailand Research Fund (TRF). This scholarship gave her an opportunity to do the research under the supervision of Prof. Jeremy D. Kilburn at University of Southampton, United Kingdom during 2001-2002. She graduated with a doctorate degree in chemistry in the academic year 2003.

### Publications

1. “A Novel Ditopic Receptor and Reversal of Anion Binding Selectivity in the Presence and Absence of Bound Cation”  
Tumcharern, G.; Tuntulani, T.; Coles, S. J.; Hursthouse, M. B.; Kilburn, J. D.  
*Org. Lett.* **2003**, 5(26), 4971-4974.
2. “Recognition Studies of a Pyridine-Pendant Calix[4]arene with Neutral Molecules: Effects of Non-Covalent Interactions on Supramolecular Structures and Stabilities”  
Tuntulani, T.; Tumcharern, G.; Ruangpornvisuti, V.  
*J. Inclu. Phenom.* **2001**, 39, 47-53.
3. “S- and NH- Bridging Pyridine- and Pyrimidine-Based Ligands for 2x2, 3x3 and 4x4 Molecular grids: Evidence of [2x2]Zn(II) Grids”  
Tuntulani, T.; Tumcharern, G.; Volkmer, D.  
*Bull. Kor. Chem. Soc.* **2000**, 21, 1245-1248.
4. “Synthesis and characterisation of polyaza crown ether derivatives of calix[4]arene and their role as anion receptors”  
Rojsajakul, T.; Veravong, S.; Tumcharern, G.; Seangprasertkij-Magee, R.; and Tuntulani, T.  
*Tetrahedron*, **1997**, 53(13), 4669-4680.